CONTENTS

(Abstracts/Contents Lists published in Analytical Abstracts, Biochemical Abstracts, Biological Abstracts, Chemical Abstracts, Chemical Titles, Chromatography Abstracts, Current Contents/Life Sciences, Current Contents/Physical, Chemical & Earth Sciences, Deep-Sea Research/Part B: Oceanographic Literature Review, Excerpta Medica, Index Medicus, Mass Spectrometry Bulletin, PASCAL-CRNS, Referativnyi Zhurnal, Research Alert and Science Citation Index)

REGULAR PAPERS

(Continued overleaf)

Contents (continued)

Gas Chromatography

(Continued overleaf)

Contents (continued)

Planar Chromatography

JOURNAL

of

CHROMATOGRAPHY

INCLUDING ELECTROPHORESIS AND OTHER SEPARATION METHODS

CHROM. 23 474

Unusual effect of temperature on the retention of enantiomers on a chiral column

WILLIAM H. PIRKLE

School of Chemical Sciences, University of Illinois, Urbana, IL 61801 (USA)

(First received April 3rd, 1991; revised manuscript received May 14th, 1991)

ABSTRACT

The Van 't Hoff plots of data obtained by chromatographing the enantiomers of a conformationally rigid spirolactam on a commercial high-performance liquid chromatographic column packed with a stationary phase derived from (R)-N-(3,5-dinitrobenzoyl)phenylglycine are non-linear. The extent and sense of the curvature of these plots depends not only on the temperature but also on the concentration of 2-propanol in the hexane mobile phase. With low concentrations of 2-propanol, retention is seen to decrease, then increase, then decrease again as the temperature is raised. This unusual behavior is ascribed to the temperature-dependent interaction of 2-propanol with the stationary phase and/or the analyte.

INTRODUCTION

Plots of the natural logarithms of chromatographic retention factors against the reciprocal of absolute temperature are termed Van 't Hoff plots and are usually linear. In the brief explorations by ourselves and others [1–3] into the effect of temperature upon chiral recognition during liquid chromatography, non-linear Van 't Hoff plots had not been reported until rather recently when Papadopoulou-Mourkidou [4] described such non-linear behavior for the enantiomers of two pesticides.

Many of the causes of non-linear Van 't Hoff behavior are addressed in papers by Horváth and co-workers [5–7]. Basically, any reversible process which alters the enthalpy or entropy of adsorption can, in principle, give rise to non-linear Van 't Hoff plots. These processes may involve the analyte, the stationary phase, or the mobile phase. Dissociative processes such as ionization, changes in conformation, or changes in the extent to which the mobile phase interacts with either the analyte or stationary phase are examples of such reversible processes. Additionally, the presence of multiple types of retention mechanisms or multiple types of binding sites may also lead to non-linear Van 't Hoff plots. In view of the importance of conformation and solvation to chiral recognition, the frequency with which multiple retention processes can be expected, and the occurrence of multiple types of binding sites on many chiral stationary phases (CSPs), the marvel is not that an instance of non-linear Van 't Hoff behavior has been found, but that such behavior had not been reported previously. Because Papadopoulou-Mourkidou [4] used a hexane mobile phase containing but 0.2% 2-propanol as a polar modifier, we immediately suspected that this might be a

contributing factor to her observation. We also suspected that the narrow temperature range over which prior studies were conducted might also have led to the observed linear Van 't Hoff plots.

In this paper, we report an instance of extreme non-linear Van 't Hoff behavior and rationalize its occurrence.

EXPERIMENTAL

The chromatographic system used consists of a Rainin Rabbit HPX pump, a Rheodyne Model 7125 injector, a Regis covalent 250 × 4.6 mm I.D. (R)-N-(3,5-dinitrobenzoyl)phenylglycine column, a Milton Roy UV monitor D operating at 254 nm and a Shimadzu CR1A integrating recorder. Column temperature was controlled by immersing the column in either a stirred constant-temperature bath containing ethylene glycol or a large dewar flask filled with ice and either water or methanol. In the heated bath, temperature was controlled to ± 0.2°C; in the ice–methanol baths, temperatures were held to ± 0.5°C of the recorded value. Void volumes were determined at each temperature from the detector response to a trace amount of 1,3,5-tri-tert.-butylbenzene spiked into the analyte and were fitted to a linear plot. Values obtained from the plot were used in computing capacity factor k' and in k' values, the computation being performed by the "Enantiotherm" program written by C. J. Welch of this laboratory for the Apple Macintosh computer. The preparation and characterization of this analyte are reported elsewhere [8].

RESULTS AND DISCUSSION

The conformationally rigid spirolactam 1 [8] was chromatographed at different temperatures on a commercial covalent (R)-N-(3,5-dinitrobenzoyl)phenylglycine CSP using mobile phases of hexane containing either 20, 10 or 5% (v/v) 2-propanol. Void volumes were determined using 1,3,5-tri-tert.-butylbenzene as a marker. Retention times were recorded to 0.01 min by a recording integrator. Plots of the natural
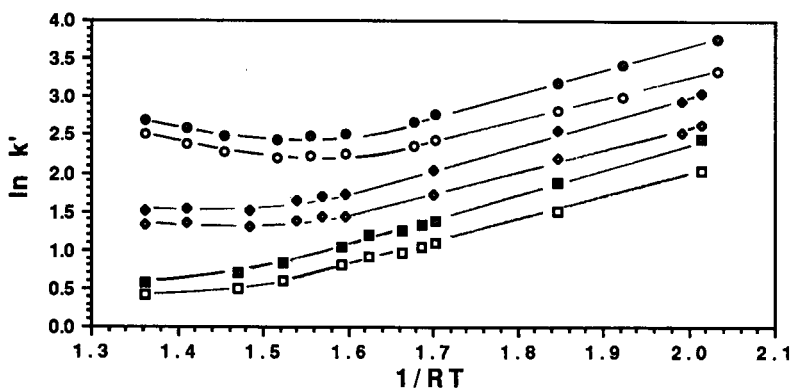
Fig. 1. Non-linear Van 't Hoff plots for the enantiomers of 1 on the chiral phase using respectively: ○ and ● = 5% 2-propanol in hexane; ◇ and ◆ = 10% 2-propanol in hexane; □ and ■ = 20% 2-propanol in hexane as an eluent.

logarithms of the capacity factors *versus* $1/RT$ (R is the gas constant; T is absolute temperature) are shown in Fig. 1.

As one normally expects, increasing the 2-propanol concentration in the mobile phase hastens the elution of the analyte enantiomers. Starting at subambient temperatures, one finds that an increase in column temperature causes a reduction in retention, linear Van 't Hoff behavior being observed *up to a point*. The temperature at which the deviation from linear Van 't Hoff behavior begins is found to decrease as the 2-propanol concentration is reduced. Note that, with the 5% 2-propanol mobile phase, retention begins to increase as the temperature is raised above *ca.* 55°C. It seems likely that similar retention increases might have been encountered, had sufficiently high temperatures been used, with the 10 and 20% 2-propanol mobile phases. However, there is so little retention with these mobile phases at the higher temperatures that the experiments were not conducted. Instead, the 2-propanol concentration was reduced to 2.5% so as to increase retention and to make possible the use of an extended temperature range. Fig. 2 shows the Van 't Hoff plots resulting from these experiments.

From Fig. 2, one may note, progressing from low to high temperature, an initial linear Van 't Hoff segment, deviation from linearity followed by an increase in retention until a maximum is reached at *ca.* 110°C, followed by a subsequent decrease in retention as the temperature is increased further. The last portion of the high-temperature segment is again (approximately) linear. How might one rationalize such a plot?

Thermodynamic data such as reported herein include contributions from many sources, contributions which are not readily segregated. Even so, plausible rationalization of the observations can be offered and finds considerable precedent in some achiral systems. At low temperatures, residual silanol groups and strands of bonded phase adsorb the 2-propanol. Since analyte adsorption requires loss of associated 2-propanol by the stationary phase and by the analyte, the determined enthalpies and entropies of adsorption contain the enthalpies and entropies of the 2-propanol loss and are accordingly reduced in magnitude. Note that below 25°C, the slopes of the ln k' *versus* $1/RT$ plots at each enantiomer are similar for each of the four 2-propanol
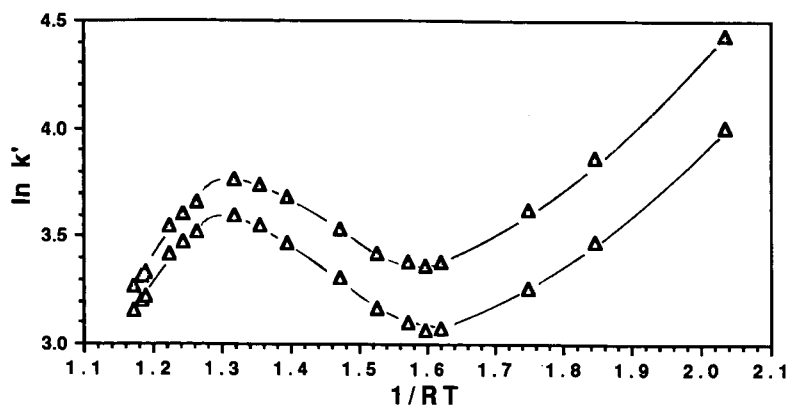
Fig. 2. Non-linear Van 't Hoff plot for the enantiomers of **1** on the CSP using 2.5% 2-propanol in hexane as an eluent.

concentrations. These slopes are the ΔH values of adsorption and are, proceeding from 20 to 2.5% 2-propanol, -3.07 ± 0.032, -2.83 ± 0.28, -2.72 ± 0.10 and -2.64 ± 0.18 kcal/mol for the least-retained enantiomer and -3.46 ± 0.036, -3.19 ± 0.30, -3.01 ± 0.08 and -2.90 ± 0.16 kcal/mol for the most-retained enantiomer. The lack of a strong dependence of ΔH on 2-propanol concentration suggests that the stationary phase and analytes are "saturated" with 2-propanol below 25°C even when but 2.5% 2-propanol is present. Analyte adsorption thus "displaces" essentially the same quantity of 2-propanol at each of the concentrations used. Note that the enthalpy of adsorption becomes slightly more exothermic as the 2-propanol concentration increases. This can be rationalized by the reasonable assumption that the return of adsorbed 2-propanol to the bulk mobile phase becomes more exothermic as the 2-propanol concentration increases. Thus, of the three processes, analyte adsorption, 2-propanol desorption, and 2-propanol "resolvation", only the ΔH of the latter is dependent upon the 2-propanol concentration. Note that the loss in entropy upon analyte adsorption also increases as the propanol concentration increases. In the same order as before, the ΔS values are -8.23 ± 0.12, -6.11 ± 1.06, -4.36 ± 0.37 and -2.71 ± 0.66 entropy units (e.u., cal mol^{-1} degree^{-1}) for the least-retained enantiomer and -8.95 ± 0.07, -6.69 ± 0.56, -4.70 ± 0.15 and -2.88 ± 0.29 e.u. for the most-retained enantiomer. This trend is consistent with the view that analyte adsorption returns essentially the same quantity of 2-propanol to the bulk mobile phase at each of the 2-propanol concentrations used. Since the ΔS value of the return of 2-propanol to the bulk mobile phase is determined in part by the change in the mobile phase's 2-propanol concentration, these ΔS values might be expected to be more positive at the lower 2-propanol concentrations. Here, return of a given quantity of 2-propanol procedures the greatest change in concentration. A greater positive ΔS of 2-propanol return more effectively reduces the magnitude of the large negative ΔS of analyte adsorption, thus explaining the overall trend of the observed ΔS values with a decrease in 2-propanol concentration. The correlation coefficients for the data leading to these four linear plots are 0.998 or greater.

   As the temperature increases, thermal desorption of 2-propanol leads to the formation of sites at which analyte adsorption is more exergonic owing to the reduced need to displace 2-propanol. This can increase retention of the analyte provided the magnitude of the effect is sufficiently great. Such effects were noted some years ago by Maggs [9], Scott and Lawrence [10] and by Gilpin and Sisco [11] on achiral systems. At a given temperature, the number of "desolvated" sites increases as the 2-propanol concentration is reduced. Hence, as the temperature is increased, the point at which an increase in retention is first noted is found to decrease as the 2-propanol concentration is reduced. However, analyte retention can only increase until the thermal desorption of 2-propanol nears completion. Beyond this temperature, the decrease in retention expected with an increase in temperature is again observed. The enthalpies of analyte adsorption, -5.12 ± 0.90 and -5.45 ± 0.87 kcal/mol, obtained from the linear high-temperature segment of the Van 't Hoff plots exceed those obtained from the linear low-temperature segments, since there is less of the offsetting contribution from displacement of 2-propanol from the stationary phase (or the analytes) upon analyte adsorption.

   Severely non-linear Van 't Hoff plots have been noted by Gilpin and Sisco [11] using polar stationary phases (silica, 2-carbomethoxyethyl, cyanopropyl) and hexane

saturated with water as a mobile phase. These concave plots were explained on the basis of "changes in modifier concentration in the mobile phase and on the surface as a function of temperature". This is in line with the views of Maggs [9] and Scott and Lawrence [10]. The explanation of the present data is simply an elaboration on this theme. Since most CSPs are rather polar, non-linear Van 't Hoff plots will doubtless be the rule when non-polar mobile phases containing polar modifiers are used and extended temperature ranges are investigated.

We hasten to add that other factors may also be involved in producing non-linear Van 't Hoff plots. Self-association of the bonded-phase strands, were it to occur, could be disrupted by increasing either the temperature or the 2-propanol concentration. Amides of N-(3,5-dinitrobenzoyl)amino acids do indeed associate in solution. This interaction is thought to favor a "head to tail" orientation [12] whereas the adjacent strands are more or less confined to a head-to-head orientation. Self-association is still conceivable, however. In any event, differential scanning calometric experiments with the dry adsorbent show no transition (up to 200°C) which would suggest thermal disruption of such self-association. Even so, such self-association of the strands of bonded phase cannot be totally discounted as a contributing factor to the observed effect. Under identical conditions, several other analytes do not afford the complex curves noted herein for the enantiomers of 1. Hence, the unusual behavior cannot be attributed solely to the CSP–mobile phase combination. Evidently, there is some domain into which the various equilibrium constants must fall if the Van 't Hoff plots are to resemble those described herein. Depending upon the values of the ΔH and ΔS values of the various processes, thermally promoted "desolvation" can cause Van 't Hoff plots to be concave or convex.

Three interesting points remain to be made. First, plots of the natural logarithm of the separation factor for the enantiomers against the reciprocal of absolute temperature (Fig. 3) are essentially linear for all four 2-propanol concentrations even though the 2.5% 2-propanol mobile phase produces the very non-linear Van 't Hoff plot of the retention parameter, k'. This indicates that whatever the unusual occurrence is, it affects both enantiomers equally and that chiral recognition is little influenced by the 2-propanol concentration. This seemingly rules out either a mechanism change (such
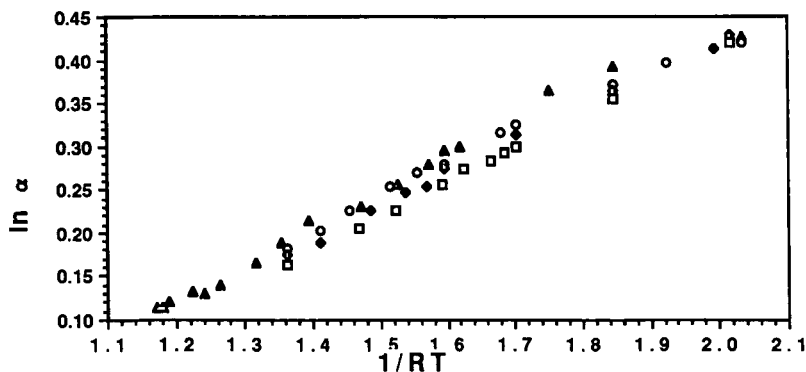
Fig. 3. Plots of ln α *versus* $1/RT$ for the enantiomers of 1 on the CSP using, respectively: ▲ = 2.5; ○ = 5; ◆ = 10 and □ = 20% 2-propanol in hexane as an eluent.

as a change in the proportion of achiral *vs.* chiral retention processes) or the population of higher energy conformers which afford a different enantioselectivity. This behavior is to be contrasted with the non-linear natural logarithm of the separation factor, ln α, *versus* $1/T$ behavior noted recently during the gas chromatographic separation of the enantiomers of several amino acid derivatives on a CSP [13]. Second, the demonstrated difference in the thermodynamic parameters determined in the 2-propanol-desorbed region and the 2-propanol-saturated region should be given heed by those who formulate computer models for chiral recognition systems. Computer models have as yet taken no explicit cognizance of the role played by the solvent. For that reason, thermodynamic parameters calculated from these models should perhaps be compared with experimental values obtained from high-temperature "desolvated" experiments rather than those determined at ambient temperature in the presence of strongly interactive mobile phases. Finally, the ability of the chiral column to separate enantiomers is unimpaired after its use at more than 150°C for several hours, thus indicating that neither racemization nor loss of bonded phase has occurred to any significant extent. Such durability is not expected of all CSPs (*e.g.*, protein or cellulosic CSPs). Although the higher temperatures are well above the boiling point of the mobile phase at atmospheric pressure, the pressure within the system is great enough to prevent boiling in either the column or the flow cell, considerable cooling of the eluent having occurred before the latter was reached.

ACKNOWLEDGEMENTS

REFERENCES

1 W. H. Pirkle and J. L. Schreiner, *J. Org. Chem.*, 46 (1981) 4988.
2 J. N. Akarya and D. R. Taylor, *Chromatographia*, 25 (1988) 639.
3 W. H. Pirkle, C. J. Welch, J. A. Burke III and P. G. Murray, unpublished results.
4 E. Papadopoulou-Mourkidou, *Anal. Chem.*, 61 (1989) 1149.
5 W. R. Melander, A. Nahum and Cs. Horváth, *J. Chromatogr.*, 185 (1979) 129.
6 A. Nahum and Cs. Horváth, *J. Chromatogr.*, 203 (1981) 53.
7 K. E. Bij, Cs. Horváth, W. R. Melander and A. Nahum, *J. Chromatogr.*, 203 (1981) 65.
8 W. H. Pirkle and J. V. Gruber, *J. Org. Chem.*, 54 (1989) 3422.
9 R. S. Maggs, *J. Chromatogr. Sci.*, 7 (1969) 145.
10 R. P. W. Scott and J. G. Lawrence, *J. Chromatogr. Sci.*, 8 (1970) 619.
11 R. K. Gilpin and W. R. Sisco, *J. Chromatogr.* 194 (1980) 185.
12 W. H. Pirkle and T. C. Pochapsky, *J. Am. Chem. Soc.*, 109 (1987) 5975.
13 K. Watabe, R. Charks and E. Gil-Av, *Angew. Chem.*, 101 (1989) 195.

Retention prediction of analytes in reversed-phase high-performance liquid chromatography based on molecular structure

VII[a]. Separations using tetrahydrofuran–buffer eluents

ROGER M. SMITH* and RUI WANG

Department of Chemistry, Loughborough University of Technology, Loughborough, Leics. LE11 3TU (UK)

(First received March 11th, 1991; revised manuscript received May 6th, 1991)

ABSTRACT

As part of the development of a technique to predict retention in high-performance liquid chromatography from the molecular structure of analytes by the summation of contributions representing the parent skeleton and functional groups, the retention index values for benzene and the substituent indices for 21 aromatic and 4 aliphatic substituent groups, based on the alkyl aryl ketone scale, have been determined in 20:80 to 60:40 tetrahydrofuran–pH 7.0 buffer eluents on a Spherisorb ODS-2 column. The results have been compared with index values obtained with eluents based on methanol and acetonitrile.

INTRODUCTION

In recent years there has been considerable interest in the application of computer-based systems to predict retention times and relative retention times in high-performance liquid chromatography (HPLC) [1]. Previous studies from these laboratories have examined predictions based on the components of the molecular structure of the analyte [2–4]. To increase the applicability of the system the calculations were based on the alkyl aryl ketone retention index scale. The retention index (I) of the analyte is given by the summation of a series of terms:

$$I = I_P + I_{S,R} + \sum I_{S,R-X} + \sum I_{S,Ar-X} + \sum I_{I,Y-Z} \tag{1}$$

These represent the retention index of a parent compound (I_P), a contribution for saturated alkyl chains ($I_{S,R}$), contributions for substituents on saturated aliphatic carbons ($I_{S,R-X}$), contributions for aromatic substituents ($I_{S,Ar-X}$), and terms to account for any interactions between substituents ($I_{I,Y-Z}$) caused by electronic, hydro-

---

[a] For part VI, see ref. 4.

gen bonding and steric effects. Each of these terms will be sensitive to eluent composition and the organic modifier in the eluent and will be related to the percentage of modifier using a quadratic equation ($I = ax^2 + bx + c$ in which x = % organic modifier and a, b and c are index coefficients). So far in this study [3,4] the coefficients for benzene as a parent compound and for the substituent and interaction indices of a wide range of aromatic and aliphatic functional groups have been determined for separations carried out using methanol–pH 7 buffer and acetonitrile–pH 7 buffer eluents. The terms have been included in an expert systems program CRIPES ("chromatographic retention index prediction expert system") which has been tested with a range of substituted analytes [3].

In studies to improve or optimise the selectivity of a separation, tetrahydrofuran (THF) has frequently been proposed as a useful alternative organic modifier, instead of methanol or acetonitrile, with different interaction and retention properties [5,6]. It would therefore be expected that the index values of the parent compound and the different substituents should differ when determined in each of the three eluents. An understanding of these relative changes for compounds containing different groups should make possible the prediction of the optimum conditions for the separation of the components of a mixture.

In the present work the parent and substituent index coefficients for a number of aromatic and aliphatic functional groups are reported for separations carried out using THF–pH 7.0 buffer eluents over the range 20–60% THF and are compared with the indices determined earlier for methanol and acetonitrile–buffer eluents. The potential application of the alkyl aryl ketone retention index scale in THF–water eluents has been demonstrated in a preliminary study [7], which examined the effect of different eluent compositions on a small set of model compounds.

EXPERIMENTAL

Chemicals, equipment and procedures were as described previously [2]. THF was HPLC grade from FSA Scientific Apparatus (Loughborough, UK).

The retention indices were calculated by linear interpolation of the retentions of the model compounds between the log k' of the alkyl aryl ketones, which were assigned retention index values of carbon number × 100. Retention index $I = 100\,n + 100(\log k'_x - \log k'_n)/(\log k'_{n+1} - \log k'_n)$ in which k'_x = capacity factor of model compound and k'_n and k'_{n+1} = the capacity factors of the alkyl aryl ketones, containing n and $n + 1$ carbon atoms, respectively, which were eluted immediately before and after the analyte. For compounds which eluted more rapidly than acetophenone the scale was extrapolated from the results for acetophenone and propiophenone.

RESULTS AND DISCUSSION

The retention times and capacity factors were determined for a series of alkyl aryl ketones from acetophenone to heptanophenone and for three sets of model compounds, alkylbenzenes from benzene to butylbenzene (five compounds), substituted benzenes (nineteen compounds) and terminal substituted propylbenzenes (four compounds). The last set was used as model for aliphatic substitution as previously it has been demonstrated that there were no significant interactions between

TABLE I

CAPACITY FACTORS OF MODEL COMPOUNDS ON ELUTION WITH THF–BUFFER ELUENTS

Compound	k'				
	THF (%)				
	20	30	40	50	60
Acetophenone	7.22	3.48	1.87	1.12	0.69
Propiophenone	19.25	7.59	3.39	1.73	0.96
Butyrophenone	45.50	14.35	5.35	2.38	1.20
Valerophenone	112.42	27.28	8.33	3.21	1.47
Hexanophenone	–	51.31	12.72	4.26	1.78
Heptanophenone	–	93.37	18.90	5.54	2.13
Benzene	27.63	11.86	5.21	2.54	1.37
Toluene	64.54	21.24	7.74	3.38	1.68
Ethylbenzene	–	38.37	11.31	4.34	1.98
n-Propylbenzene	–	68.23	16.86	5.61	2.38
n-Butylbenzene	–	124.08	24.16	7.21	2.80
Acetanilide	–	1.45	0.82	0.53	0.33
Aniline	3.87	2.43	1.51	0.95	0.61
Anisole	24.75	9.71	4.16	2.04	1.12
Benzaldehyde	6.89	3.56	1.97	1.16	0.72
Benzamide	1.11	0.65	0.45	0.37	0.23
Benzenesulphonamide	1.89	1.21	0.81	0.54	0.35
Benzonitrile	9.64	4.56	2.29	1.26	0.74
Biphenyl	–	53.28	12.40	4.11	1.76
Bromobenzene	99.11	24.87	7.83	3.14	1.52
Chlorobenzene	79.50	21.91	7.29	3.01	1.51
N,N-Dimethylbenzamide	1.07	0.63	0.46	0.35	0.25
N-Ethylaniline	27.77	12.32	5.20	2.38	1.21
Fluorobenzene	35.75	13.61	5.38	2.48	1.30
Methyl benzoate	18.40	6.87	3.02	1.55	0.88
N-Methylbenzamide	1.25	0.71	0.50	0.35	0.25
Naphthalene	–	29.50	8.39	3.23	1.51
Nitrobenzene	20.43	8.35	3.49	1.68	0.91
Phenyl acetate	–	4.78	2.44	1.36	0.80
Phenol	8.84	4.23	2.07	1.10	0.62
1-Bromo-3-phenylpropane	–	69.26	15.59	4.94	2.00
1-Chloro-3-phenylpropane	–	58.99	13.83	4.57	1.89
4-Phenylbutyronitrile	–	9.88	3.86	1.77	0.92
3-Phenyl-1-propanol	–	3.97	1.76	0.92	0.54

functional groups in this position and the phenyl ring [8]. A range of THF–pH 7.0 phosphate buffers eluents (20:80 to 60:40) gave capacity factors in the range 0.2–100 (Table I). As with the previous studies [2], it was impractical to measure the retentions of carboxylic acids or of aliphatic amines as these compounds were often partially or completely ionised in the pH 7.0 buffer. The stationary phase was Spherisorb ODS-2 from the same batch as the earlier work [2] to ensure a uniform set of retention data.
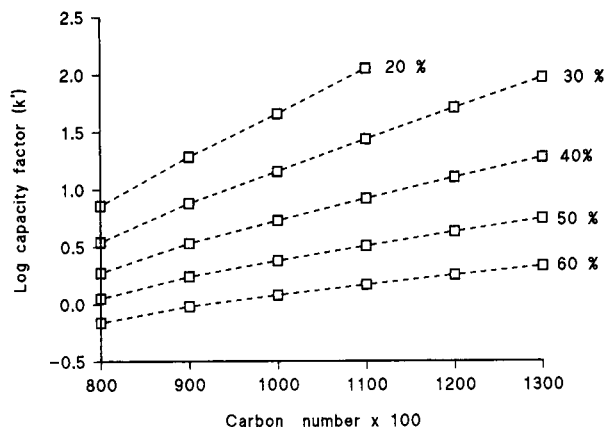
Fig. 1. Relationship between log k' and carbon number × 100 for the alkyl aryl ketones at different % of THF.

Unlike the previous studies [2] using methanol or acetonitrile as the organic modifier, the relationships between the logarithms of the capacity factors of the alkyl aryl ketones and their carbon numbers was not linear as acetophenone was eluted more rapidly than predicted in each eluent (Fig. 1). A similar but less pronounced effect was also observed in the preliminary studies [7] on a Spherisorb ODS column. This effect might be caused by a difference between the empirical value for the column void volume, measured using aqueous sodium nitrate solution, and the effective void volume experienced by the alkyl aryl ketones. A linear interpolation between the logarithms of the capacity factors of the alkyl aryl ketones was therefore used to calculate the retention indices of the model compounds (Table II). The retention indices were similar to those obtained previously [7] on a Spherisorb ODS column (e.g., at 30% THF, previous values in parenthesis: methyl benzoate, I = 887 (896); nitrobenzene, I = 915 (931); toluene, I = 1061 (1049). However, the differences in the index values were greater than the expected experimental error of ±10 units [2] indicating a small but significant difference in the retention properties of the two stationary phases.

In order to determine the coefficients of the parent index value for benzene (I_P), the experimental retention indices were related to the percentage of THF (x) using a quadratic least-squares correlation to give the equation $I_P = 0.0243x^2 + 1.037x + 913$ over the composition range 20–60% THF. As in the earlier studies, extrapolation outside the empirically determined range is likely to be inaccurate. Using this equation the predicted retention indices of benzene in the different eluent compositions were calculated (Table II). They showed a close correspondence to the empirical values and will be used as the reference values to calculate the effects of the substituents on retention. The values of the parent indices in the THF–buffer eluents (I_p = 944–1063) are generally higher than those found earlier for the parent indices of benzene in methanol–buffer (I_P = 888–999) or acetonitrile–buffer eluents (I_P = 910–963) [2].

The rentention indices for the alkylbenzenes (benzene, toluene, ethylbenzene and n-propylbenzene) increased with the chain length as expected (Table II) but the

TABLE II

RETENTION INDICES OF MODEL COMPOUNDS ON ELUTION WITH THF–BUFFER ELUENTS

Compound	I				
	THF (%)				
	20	30	40	50	60
Benzene	942	970	994	1022	1065
Calculated I_P	944	966	994	1026	1063
Toluene	1039	1061	1083	1118	1165
Ethylbenzene	–	1153	1172	1207	1259
n-Propylbenzene	–	1247	1271	1304	1361
Calculated I_{R-H}[a]		1252	1280	1312	1349
n-Butylbenzene	–	1347	1362	1400	1452
Acetanilide	–	688	661	627	577
Acetophenone[b]	800	800	800	800	800
Aniline	736	753	764	762	762
Anisole	929	939	945	952	969
Benzaldehyde	795	803	809	808	812
Benzamide	609	585	560	545	467
Benzenesulphonamide	663	665	659	632	594
Benzonitrile	829	835	834	827	821
Biphenyl	–	1206	1195	1187	1195
Bromobenzene	1086	1086	1086	1093	1117
Chlorobenzene	1062	1066	1070	1078	1114
N,N-Dimethylbenzamide	605	581	564	532	493
N-Ethylaniline	943	976	994	1000	1004
Fluorobenzene	972	992	1001	1014	1039
N-Methylbenzamide	621	596	578	532	493
Methyl benzoate	895	887	881	875	873
Naphthalene	–	1112	1101	1102	1114
Nitrobenzene	907	915	906	893	884
Phenol	821	825	817	795	767
Phenyl acetate	–	841	845	845	813
1-Bromo-3-phenylpropane	–	1250	1251	1256	1265
1-Chloro-3-phenylpropane	–	1227	1221	1227	1233
4-Phenylbutyronitrile	–	934	928	905	887
3-Phenyl-1-propanol	–	817	789	755	726

[a] Calculated as $I_P + I_{I.PhCH_2R} + 3 \times 100$.
[b] Defined as carbon number $\times$ 100.

increases for each additional methylene unit were often smaller than the theoretical value of 100 units expected for the increments between homologues (Table III). The mean value for the addition of a methylene group to the benzylic carbon was significantly smaller (91 units) than the increment for the other methylene groups (95–98 units). A similar effect was observed earlier in studies with methanol- and acetonitrile-containing eluents, when the increments were in the range 92–112 units, except for the addition of a methylene group to a benzylic carbon, 87–95 units [9]. These results suggest that the methylene increment for the alkylbenzenes in a THF–buffer eluent

TABLE III

RETENTION INDEX INCREMENTS FOR THE ADDITION OF A METHYLENE GROUP TO AN ALKYLBENZENE

Compound	Retention index increment					
	THF (%)					Mean
	20	30	40	50	60	
I_P (Benzene)	944	966	994	1026	1063	
Benzene–toluene	95	95	89	92	102	95
Toluene–ethylbenzene		92	89	89	94	91
Ethylbenzene–n-propylbenzene		94	99	97	102	98
Propylbenzene–n-butylbenzene		100	91	96	91	95

differs from that of the alkyl aryl ketones. From the Martin equation, the methylene increment should be constant irrespective of the functional groups. However, similar differences have been observed previously, particularly between aliphatic and aromatic homologous series, as in a recent study comparing homologous nitroalkanes with 2-alkanones and alkyl aryl ketones [10]. In the present study, an interaction index term was therefore included for the addition of a methylene group to a benzylic carbon ($I_{1,PhCH_2R} = -14$) similar to the correction in methanol and acetonitrile eluents ($I_{1,PhCH_2R} = -12$) [9]. This interaction value ignores the low value for alkyl substitution on benzene but would compensate by slightly over-correcting for substitution of toluene. Using this interaction value the predicted retention indices can be calculated for n-propylbenzene (Table II) and these will be used as the reference point for aliphatic substitution.

The differences in the effect of methylene groups on retention could pose problems for retention prediction systems and imply that additional correction factors might be required for precise results on different homologous series. However, the discrepancies are small compared to the effects of many of the substituents and are similar to the uncertainty in the empirical measurement of retention indices. Thus, they can probably be safely ignored in most predictions.

Substituent index increments

Using the calculated parent index values for benzene (I_P) and n-propylbenzene ($I_{R-H} = I_P + I_{1,PhCH_2R} + 3 \times 100$) the changes in the retention caused by the presence of each aromatic and aliphatic substituent were calculated as the retention index increments between the substituted model compound and the corresponding parent hydrocarbon ($\delta I = I_{Ar-X} - I_{Ar-H}$ or $\delta I = I_{R-X} - I_{R-H}$) (Table IV). In each case the increments changed systematically with eluent composition. As with the other eluent modifiers, there were large differences between the same group as an aliphatic or aromatic substituent (*e.g*, in 40% THF, δI for Ar–Br = 92 and R–Br = −29).

Although, as expected, the difference between the amino group (–NH$_2$) and the N-ethyl group (–NHEt) in THF–buffer (20:80) was about 200 units, the difference

TABLE IV

RETENTION INDEX INCREMENTS FOR SUBSTITUENTS ON AN AROMATIC RING IN THF–BUFFER ELUENTS

Substituent	Hansch constant, π [12]	Retention index increment THF (%)				
		20	30	40	50	60
$Ar-X$ ($\delta I = I_{Ar-X} - I_{Ar-H}$)						
SO_2NH_2	−1.82	−281	−301	−335	−394	−469
$CONH_2$	−1.49	−335	−381	−434	−481	−596
$CONHCH_3$	−1.27	−323	−370	−416	−494	−570
$CON(CH_3)_2$	−	−339	−385	−430	−494	−570
NH_2	−1.23	−208	−213	−230	−264	−301
$NHCOCH_3$	−0.97	−−	−278	−333	−399	−486
OH	−0.67	−123	−141	−177	−231	−296
CHO	−0.65	−149	−163	−188	−218	−251
$OCOCH_3$	−0.64	−	−125	−149	−181	−250
CN	−0.57	−115	−131	−160	−199	−242
$COCH_3$[a]	−0.55	−144	−166	−194	−222	−263
NO_2	−0.23	−37	−51	−88	−133	−179
OCH_3	−0.02	−15	−27	−49	−74	−94
CO_2CH_3	−0.01	−49	−79	−113	−151	−190
H	0.00	0	0	0	0	0
$NHCH_2CH_3$	0.08	−1	10	0	−26	−59
F	0.14	28	26	7	−12	−24
CH_3	0.56	95	95	89	92	102
Cl	0.72	118	100	76	52	51
Br	0.86	142	120	92	67	54
Ph	1.96	−−	240	201	161	132
(Naphthalene)	−−	−	146	107	76	51
$R-X$ ($\delta I = I_{R-X} - I_{R-H}$)						
OH	−1.64	−	−435	−491	−557	−623
CN	−1.27	−	−318	−352	−407	−462
Cl	0.06	−	−25	−59	−85	−116
Br	0.20	−	2	−29	−56	−84

increased to 250 units at higher proportions of modifier, suggesting that the influence of the eluent on primary and secondary amino groups differed and that different substituent index coefficients are necessary. A comparison of the increments for the carboxamide (–CONH$_2$), N-methylcarboxamide (–CONHMe) and N,N-dimethyl-carboxamide [CON(Me)$_2$] groups showed an even more marked effect. At each eluent composition the increments for all three functional groups were very similar (i.e., THF–buffer (20:80), $I_{S,Ar-X}$ = − 335, − 323 and − 339 units, respectively, and at THF–buffer (60:40), $I_{S,Ar-X}$ = − 596, − 570 and − 570 units) despite the presence of the additional methyl and dimethyl groups, which might have been expected to make the subsituted carboxamide groups more hydrophilic. The retention prediction system will therefore have to regard primary, secondary and tertiary amides as different groups (with different substituent index coefficients), rather than simply considering them as primary amides, which have been altered by alkyl substitution. During the

evaluation of the retention index expert system (CRIPES) this simpler approach was used for the prediction of the indices of N,N-dimethylbenzamide and N-methylbenzamide in methanol and acetonitrile eluents [3]. However, there were large differences between the predicted and experimental values and it was clear that the substituted amides would also need to be distinguished in those eluents.

Using the retention index increments for each substituent the coefficients of the quadratic relationship between the increment and the percentage of THF in the eluent

TABLE V

COEFFICIENTS OF SUBSTITUENT INDEX EQUATIONS FOR SUBSTITUENTS

I_{Ar-X} or $I_{R-X} = ax^2 + bx + c$, $x = \%$ THF in eluent.

Substituent	Index coefficients		
	a	b	c
$Ar-X$			
SO_2NH_2	-0.0964	3.024	-303
$CONH_2$	-0.1228	4.009	-389
$CONHCH_3$	-0.0643	-1.037	-277
$CONH-R^a$	-0.0643	-1.037	-377
$CON(CH_3)_2$	-0.0564	-1.196	-294
$CON-R_2{}^a$	-0.564	-1.196	-496
NH_2	-0.0721	3.601	-259
$NHCOCH_3$	-0.0800	0.300	-215
$NHCO-R^a$	-0.0800	0.300	-315
OH	-0.0800	2.040	-131
CHO	-0.0307	-0.133	-133
$OCOCH_3$	-0.1125	6.055	-207
$OCO-R^a$	-0.1125	6.055	-307
CN	-0.0457	0.437	-105
$COCH_3$	-0.0271	-0.769	-118
$CO-R^a$	-0.0271	-0.769	-218
NO_2	-0.0514	0.454	-23
OCH_3	-0.0121	-1.099	14
$O-R^a$	-0.0121	-1.099	-86
CO_2CH_3	-0.0157	-2.283	3
CO_2-R^a	-0.0157	-2.283	-97
H	0.0	0.0	0
$NHCH_2CH_3$	-0.0743	4.423	-58
$NH-R^a$	-0.0743	4.423	-258
F	-0.0429	2.409	-18
CH_3	0.0	0.0	100
Cl	0.0243	-3.763	186
Br	0.0150	-3.490	208
Ph	0.0250	-5.890	395
(Naphthalene)	0.0350	-6.310	304
$R-X$			
OH	-0.0250	-4.050	-290
CN	-0.0520	-0.145	-265
Cl	0.0075	-3.665	76
Br	0.0075	-3.535	101

[a] Values of core functional groups excluding alkyl groups (methyl $= 100$, ethyl $= 200$).
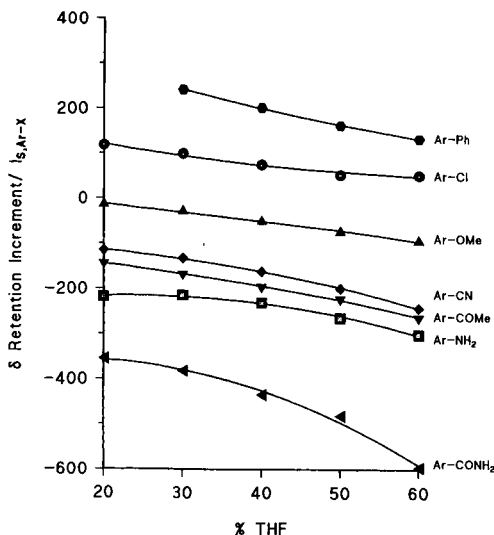
Fig. 2. Relationship between retention increments or calculated substituent indices for selected aromatic substituents and the proportion of THF in the eluent. Points indicate experimental values (retention index increment, δI) and the lines are calculated substituent indices ($I_{S,Ar-X}$) based on the coefficients in Table V.

were calculated (Table V). For substituents containing aliphatic, methyl or ethyl groups (such as –COMe, –CONMe$_2$ and –NHEt) the corresponding coefficients for the core functional group (–CO–, –CON= and –NH–) were determined by subtracting 100 or 200 units as appropriate. These coefficients can then be used as general terms for the prediction of the retention indices of substituted functional groups (such as –NHbutyl) by adding the appropriate alkyl chain substituent contribution ($I_{S,R}$). From the coefficients in Table V the substituent indices ($I_{S,Ar-X}$ and $I_{S,R-X}$) can be calculated and these corresponded closely with the empirical retention increments (for examples see Fig. 2).

The substituents indices in the three different modifiers can now be compared to identify those groups which are particularly susceptible to differences in the properties of the eluents (Table VI). As in a typical optimisation procedure approximately isoeluotropic conditions were selected for comparison. These were chosen to give similar capacity factors for acetophenone (methanol–buffer (50:50), $k' = 3.23$; acetonitrile–buffer (40:60), $k' = 2.91$; THF–buffer (30:70), $k' = 3.48$). The parent index values for benzene differed in each eluent ($I_P = 913$, 927 and 966, respectively). In contrast, the value for the phenyl substituents decreased ($I_{S,Ar-Ph} = 305$, 271 and 241, respectively). For many of the substituents the differences between the eluents were less than 30 units and the aromatic nitro ($I_{S,Ar-NO_2} = -54$, -54 and -56) and chloro groups ($I_{S,Ar-Cl} = 105$, 98 and 92) had almost identical indices. However, these comparisons are not general and would alter with the strength of the eluents. For example, the substituent index of the chloro group (Fig. 3) changed markedly with THF composition, whereas in methanol and acetonitrile eluents it was almost constant with eluent composition [2].

The largest differences between modifiers was found for the phenolic hydroxy group ($I_{S,Ar-OH}$, methanol–buffer $= -229$; acetonitrile–buffer $= -243$ and THF–

TABLE VI

COMPARISON OF SUBSTITUENT INDICES IN METHANOL-, ACETONITRILE- AND THF-BUFFER-CONTAINING ELUENTS

$I_{S,Ar-X}$ and $I_{S,R-X}$ based on coefficients in [2,8] and Table V.

Eluents selected to give similar capacity factors for acetophenone; 50:50 methanol–buffer, $k' = 3.23$; 40:60 acetonitrile–buffer, $k' = 2.91$; 30:70 THF–buffer, $k' = 3.48$

Substituent	Substituent index		
	MeOH–Buffer (50:50)	MeCN–buffer (40:60)	THF–buffer (30:70)
Benzene I_p	913	927	966
Ar–X			
CONH$_2$	−321	−392	−381
NH$_2$	−254	−230	−216
OH	−229	−243	−142
CHO	−138	−141	−165
CN	−134	−111	−133
COCH$_3$	−113	−127	−165
NO$_2$	−54	−54	−56
OCH$_3$	−11	−19	−30
CO$_2$CH$_3$	−10	−34	−80
Cl	105	98	95
Br	135	127	117
Ph	305	271	241
R–X			
OH	−362	−459	−434
CN	−300	−280	−316
Cl	−39	−49	−27
Br	3	−13	2

buffer $= -142$). In contrast, the aliphatic hydroxyl group behaved very differently ($I_{S,R-OH} = -362$, -459 and -434, respectively). Although the values for the carbomethoxyl substituent (CO$_2$CH$_3$) were relatively similar in the three isoeluotropic eluents the values became markedly different in eluents with higher proportions of modifier (Fig. 3). These changes emphasise that differences in the elution order between modifiers may be significantly dependent on the composition of each eluent and it may not be sufficient to rely on comparisons of a single set of isoeluotropic eluents to achieve the optimisation of a separation.

However, even relatively small differences of less than 50 units in different eluents can have a marked influence on the relative retentions of the components of a mixture. A typical pair of compounds, *e.g.*, methyl benzoate and nitrobenzene, have predicted retention indices of 903 and 859 units, respectively, in a methanol–buffer (50:50) eluent but their elution would be reversed to $I = 886$ and 910 units in THF–buffer (30:70). This predicted change would mirror changes reported previously for these compounds by Tanaka *et al.* [11] on an ODS-bonded Hypersil column.

Many workers have used HPLC retentions for the approximate determination of octanol–water distribution constants (log P) and close correlations have often been
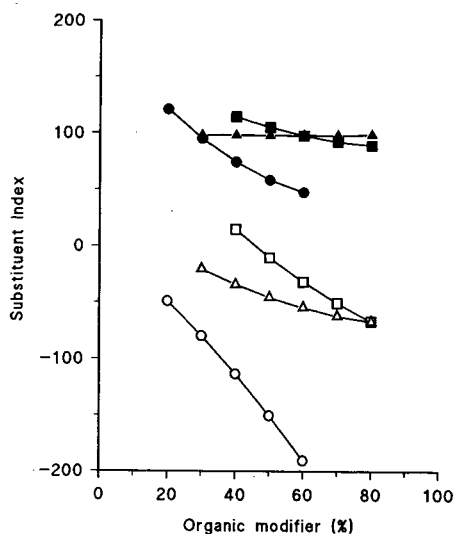
Fig. 3. Comparison of the substituent indices of the aryl chloro group (Ar–Cl, solid symbols) and the carbomethoxy group (Ar–CO$_2$CH$_3$, open symbols) in THF–buffer eluents (○ and ●), methanol–buffer eluents (□ and ■) and acetonitrile eluents (△ and ▲) (values from ref. 2).

found, particularly amongst members of a homologous or pseudohomologous group of compounds (such as the alkylsubstituted barbiturates). The substituent indices were therefore compared with the corresponding Hansch substituent constants (π values [12], see Table IV). Across the range of aromatic substituents there was a close correlation (Fig. 4). Unlike the corresponding comparison in methanol and acetonitrile eluents [2], the value for the aromatic hydroxyl group in THF–buffer correlated with its π value. However, the carboxamide (as with the other eluent modifiers) and sulphonamide groups were outliers, although in different directions.
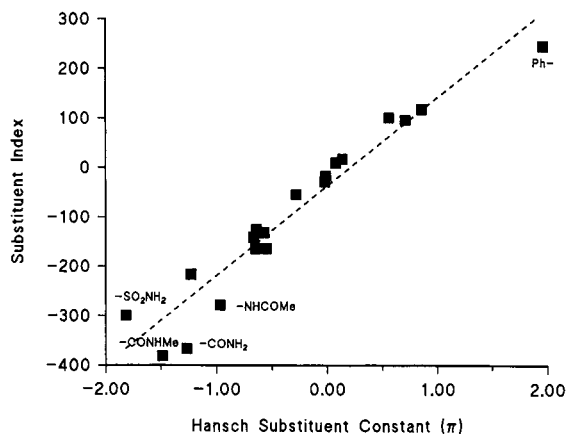
Fig. 4. Relationship between the magnitude of the calculated substituent indices of aromatic substituents in THF–buffer (30:70) eluent and Hansch π values (from Table IV).

CONCLUSIONS

The parent retention indices for benzene and substituent indices for 21 aromatic substituents and 4 aliphatic substituents have been determined and expressed as the coefficients of quadratic equations covering an eluent composition range from 20 to 60% THF. The magnitude of the substituent indices corresponded closely to the Hansch π values for the groups.

REFERENCES

1 G. L. Glach and L. R. Snyder (Editors) *Computer-Assisted Method Development for High-Performance Liquid Chromatography*, Elsevier, Amsterdam, 1990; *J. Chromatogr.*, 485 (1989).
2 R. M. Smith and C. M. Burr, *J. Chromatogr.*, 475 (1989) 57.
3 R. M. Smith and C. M. Burr, *J. Chromatogr.*, 485 (1989) 325.
4 R. M. Smith and C. M. Burr, *J. Chromatogr.*, 550 (1991) 335.
5 J. C. Berridge, *Techniques for the Automated Optimisation of HPLC Separations*, Wiley, Chichester, 1985.
6 A. Ahuja, *Selectivity and Detectability Optimisations in HPLC*, Wiley, New York, 1989.
7 R. M. Smith, G. A. Murilla and C. M. Burr, *J. Chromatogr.*, 388 (1987) 37.
8 R. M. Smith and C. M. Burr, *J. Chromatogr.*, 481 (1989) 71.
9 R. M. Smith and C. M. Burr, *J. Chromatogr.*, 481 (1989) 85.
10 R. M. Smith and N. Finn, *J. Chromatogr.*, 518 (1991) 75.
11 N. Tanaka, H. Goodell and B. L. Karger, *J. Chromatogr.*, 158 (1978) 223.
12 C. Hansch and A. Leo, *Substituents Constants for Correlation Analysis in Chemistry and Biology*, Wiley, New York, 1979.

Effect of stationary phase structure on retention and selectivity of restricted-access reversed-phase packing materials

KAZUHIRO KIMATA, KEN HOSOYA, NOBUO TANAKA* and TAKEO ARAKI

Kyoto Institute of Technology, Department of Polymer Science and Engineering, Matsugasaki, Sakyo-ku, Kyoto 606 (Japan)

RIYOU TSUBOI

Nacalai Tesque, Kaide-cho, Mukoh 617 (Japan)

and

JUN HAGINAKA

Mukogawa Women's University, Faculty of Pharmaceutical Sciences, 11-68, Koshien Kyuban-cho, Nishino-miya 663 (Japan)

(First received January 4th, 1991; revised manuscript received April 9th, 1991)

ABSTRACT

Various restricted-access reversed-phase (RARP) packing materials, including alkyl-, alkyl ether- and alkylamide-type stationary phases, were compared with a commercially available peptide-bonded internal surface reversed-phase material and a shielded-type RARP material. Alkyl-type RARP materials were found to be more hydrophobic than ether or amide-type phases, which in turn were more hydrophobic than the materials commercially available at present. The contribution of polar as well as ionic groups in the stationary phase structure to retention selectivity was noted with some materials. The advantages of having a variety of RARP materials in terms of retention and selectivity were shown for separation of various drugs with a limited range of mobile phases.

INTRODUCTION

Restricted-access reversed-phase (RARP) packing materials were developed for the high-performance liquid chromatographic (HPLC) analysis of body fluids, namely serum, in which proteins co-exist with the analytes. Pretreatment of biological samples can be simplified by using these materials, because high-molecular-weight solutes can be excluded from the pores of RARP materials which possess hydrophilic external and hydrophobic internal surfaces.

Two types of RARP materials have been reported in terms of the preparation procedure. The first method is a three-step procedure; (1) introduction of hydrophobic groups on all the surfaces of porous silica particles; (2) removal of hydrophobic groups from the external surface; (3) introduction of hydrophilic groups onto the external surface.

Hagestam and Pinkerton [1] prepared a glycylphenylalanylphenylalanine (GFF)-bonded internal surface reversed-phase (ISRP) material [abbreviated to ISRP-peptide (GFF)] [1–6], and Haginaka and co-workers [7,8] prepared alkyl amide-bonded ISRP material (ISRP-amide) following this scheme by utilizing enzyme-catalyzed cleavage of external hydrophobic groups. The packing materials prepared by these methods necessarily include a functional group such as an amide group in the hydrophobic part of the stationary phase which can be cleaved by an enzyme.

RARP materials can also be prepared from ordinary alkylsilylated silica gels such as silica-C_{18}. Sudo *et al.* [9] used oxygen plasma, and Kimata *et al.* [10] used aqueous hydrochloric acid to remove alkylsilyl groups from the external surface of packing materials designed for reversed-phase liquid chromatography (RPLC).

The second type of RARP materials are mixed-type materials, which possess both hydrophobic and hydrophilic groups on all surfaces of the porous silica gel. Gisch and co-workers [11,12] reported an RARP material with phenyl groups bonded with polyoxyethylene chains, currently available as LC-HISEP. Haginaka and Wakai reported a C_{18} phase bonded together with diol groups [13]. They also reported an RARP material with chiral groups for the separation of enantiomers [14]. In these RARP materials, the hydrophobic properties of alkyl or aryl groups were controlled by the presence of hydrophilic groups so that proteins are not retained under the separation conditions for low-molecular-weight compounds.

The RARP materials prepared by different methods are expected to show different retention characteristics, depending upon the solute accessibility to and the chemical structure of the hydrophobic groups on the internal surface in relatively small pores of *ca.* 8 nm or less. In RPLC, a variety of packing materials, such as alkyl- or aryl-bonded silica gel [15], polymer-based materials [16] and carbon packing materials [17] have been used to meet various separation needs. The characterization of C_{18} packing materials from various manufacturers would allow one to select a proper column for a particular application [18]. Such characterization of RARP materials would be similarly useful for column selection as well as for designing new RARP materials, because a limited range of mobile phases can be used with RARP materials which should not denature proteins in a column.

Here we report the comparison of retention characteristics of various RARP materials with respect to the effect of hydrophobicity and the contribution of ionizable groups in the stationary phase.

EXPERIMENTAL

Equipment

The HPLC system consisted of an LC-6A pump, an SIL-6A automatic sample injector, an SPD-6A UV detector and a C-R5A data processor (all from Shimadzu, Kyoto, Japan). Column temperature was maintained at 30°C by using a thermostated water bath.

Materials

An ISRP column (15 cm × 4.6 mm I.D.) of glycylphenylalanylphenylalanine-bonded phase [ISRP-peptide (GFF)], originally prepared by Hagestam and Pinkerton [1], was purchased from Kohken (Tokyo, Japan). An LC-HISEP column (15 cm × 4.6

Internal   External
Surface   Surface

$-OH$ $-O-\overset{|}{\underset{|}{Si}}-R$ $-OH$ $-O-\overset{|}{\underset{|}{Si}}-(CH_2)_3-O-CH_2-CH-CH_2$

$HO-$ $R-\overset{|}{\underset{|}{Si}}-O-$ $R-\overset{|}{\underset{|}{Si}}-O-$ $R-\overset{|}{\underset{|}{Si}}-O-$ OH OH

alkylsilylation   decomposition   introduction of
in conc. HCl   diol functionality
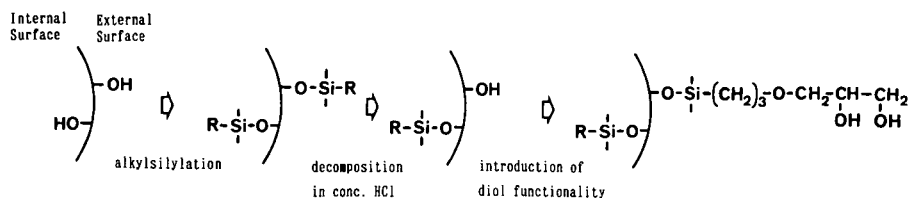
Fig. 1. Preparation method of SHRP packing materials by acid decomposition, and stationary phase structure. R: $C_{18}H_{37}$ (SHRP-C_{18}), C_8H_{17} (SHRP-C_8), $C_6H_5CH_2CH_2$ (SHRP-PE), $CH_3OCH_2CH_2OCH_2CH_2CH_2$ (SHRP-E2), $CH_3O(CH_2CH_2O)_2CH_2CH_2CH_2$ (SHRP-E3).

mm I.D.) was purchased from Supelco (Bellefonte, PA, USA). A size-exclusion chromatography column (30 cm × 7.5 mm I.D.), TSK G2000SW, was purchased from Tosoh (Tokyo, Japan). A Cosmosil 5-C_{18} column was obtained from Nacalai Tesque (Kyoto, Japan).

ISRP-amide packing material was prepared according to a previously reported procedure [7]. Superficially hydrophilic reversed-phase (SHRP) packing materials with alkyl groups, SHRP-C_{18}, SHRP-C_8 and SHRP-phenylethyl (SHRP-PE), as well as alkyl ether-type materials, SHRP-E2 and SHRP-E3 (see Fig. 1 for structures), were prepared by acid decomposition of bonded phases followed by the introduction of diol groups, as reported previously [10]. Acid decomposition of the precursor of SHRP-E2 and -E3 phases with concentrated hydrochloric acid was performed in the presence of stearyl alcohol (10% of the weight of packing material). The carbon contents of these packing materials at each stage of preparation are listed in Table I. The packing materials were packed into stainless-steel columns (150 mm × 4.6 mm I.D.).

Silica particles (Develosil; particle size = 5 μm; pore size = 6 nm; surface area = 500 m^2/g) were purchased from Nomura (Seto, Japan). Alkylsilylating reagents were either purchased from Petrarch System (Bristol, PA, USA) or prepared by standard methods. Bovine serum albumin (BSA) and drug standards were obtained commercially.

TABLE I

CARBON CONTENTS OF RARP PACKING MATERIALS

Packing material	Carbon content (%)		
	Before decomposition[a]	After decomposition	Alkyl/diol
SHRP-C_{18}	20.08	12.29	14.95
SHRP-C_8	14.01	6.79	9.06
SHRP-PE	14.33	5.85	8.62
SHRP-E2	5.76	4.38	5.37
SHRP-E3	5.76	4.05	7.29
ISRP-amide	–	–	5.44

[a] End-capped.

Chromatographic measurement

All chromatographic measurements were carried out at 30°C. The recovery of BSA was calculated based on the peak area by taking the area obtained without a column as 100%.

RESULTS AND DISCUSSION

Hydrophobicity

The hydrophobicity of RARP materials was compared in terms of the retention increase with the addition of one methylene group in the solute structure in 10% acetonitrile and in 60% methanol. The slopes of the plots of log k' (k' = capacity factor) values of phenylalkyl alcohols in 10% acetonitrile, and those of alkylbenzenes in 60% methanol, against the carbon number of the alkyl portion of the solutes were calculated according to eqn. 1 and are listed in Table II. The correlation coefficients were always greater than 0.99 for alkylbenzenes, and greater than 0.98 for phenylalkyl alcohols.

$$\log k' = aC_n + b \qquad\qquad (1)$$

TABLE II

HYDROPHOBICITY OF RARP PACKING MATERIALS

Packing material	a value in 60% methanol[a]	k'^b	a value in 10% acetonitrile[c]	k'^d
SHRP-C$_{18}$	0.277	11.62	0.407	31.39
SHRP-C$_8$	0.255	9.19	0.376	29.74
SHRP-PE	0.201	5.92	0.322	14.24
SHRP-E2	0.164	3.65	0.292	11.56
SHRP-E3	0.158	2.95	0.270	8.58
ISRP-peptide (GFF)	0.031	0.95	0.113	1.70
LC-HISEP	0.076	1.22	0.187	2.17
ISRP-amide	0.168	2.29	0.262	5.66
C$_{18}$-60[e]	0.295	19.90	0.422	67.84
C$_{18}$-60-D[f]	0.282	10.31	0.418	39.20
C$_{18}$-100[g]	0.278	15.24	0.410	63.79
C$_{18}$-300[h]	0.266	4.34	0.397	23.54
C$_{12}$-300[h]	0.257	4.12	0.401	20.16
C$_8$-300[h]	0.236	3.45	0.386	16.31
C$_6$-300[h]	0.220	2.75	0.370	14.14
C$_4$-300[h]	0.196	1.78	0.336	8.57
C$_3$-300[h]	0.187	1.57	0.323	7.07
C$_1$-300[h]	0.170	1.35	0.293	3.53

[a] Calculated according to the equation, $\log k' = aC_n + b$; solute: alkylbenzene, $C_6H_5\text{–}C_nH_{2n+1}$.
[b] Solute = methyl benzoate; mobile phase = 40% methanol.
[c] Solute = benzyl alcohol; 2-phenylethanol, 3-phenylpropanol; mobile phase = 10% acetonitrile.
[d] Solute = 3-phenylpropanol; mobile phase = 10% acetonitrile.
[e] Precursor of SHRP-C$_{18}$, before decomposition.
[f] Precursor of SHRP-C$_{18}$, after decomposition, before the introduction of diol groups.
[g] Prepared from silica gel with 10-nm pores.
[h] Prepared from silica gel with 30-nm pores.

Generally the longer the alkyl group of stationary phase, the greater the hydrophobicity. Commercially available ISRP-peptide (GFF) and LC-HISEP showed very low hydrophobicity. The a values obtained with the ISRP-amide phase were similar to those with SHRP-E2 and SHRP-E3 at an intermediate range. Alkyl-type SHRP materials gave a values which were closely related to the carbon contents of the packing materials prior to the introduction of the diol groups.

Also listed in Table II are the a values obtained with the precursor of SHRP-C_{18} and ordinary RPLC materials with end capping. The similar a values found with the precursors of SHRP-C_{18}, C_{18}-60 and C_{18}-60-D, as well as SHRP-C_{18} suggest that the acid decomposition of alkylsilylated phase proceeded preferentially at the external surface, leaving the C_{18} groups on the internal surface at relatively high surface densities [10]. C_{18} phases with lower surface coverages are known to give much smaller a values [10]. Note that the effect of pore size on a value, or on the hydrophobicity, is smaller than that of alkyl chain length.

Small-pore materials generally resulted in greater retention, because of their large surface areas, accompanied by slightly larger a values. A slight increase in retention was seen with the introduction of the diol function to the decomposed alkyl phase. These results suggest that the solute retention is determined not only by the hydrophobicity but also by the microscopic environment in the bonded phase composed of hydrophobic and hydrophillic groups, in addition to the availability of such surfaces, or the surface area of the packing materials.

Contribution of ionic groups in the stationary phase

Fig. 2 shows the dependence of retention of benzoic acid on the pH of the mobile phase. As shown in Fig. 3, the retention of the acid on LC-HISEP and ISRP-amide showed a clear decrease at low pH. The ISRP-amide phase possesses an alkylamine structure [7]. The pK_a of the amine structure in the stationary phase is expected to be around 9. As the protonation of the amino groups in the stationary phase increases from pH 8 to pH 6, the retention of ionized benzoic acid with a pK_a of *ca.* 4.2 [19]
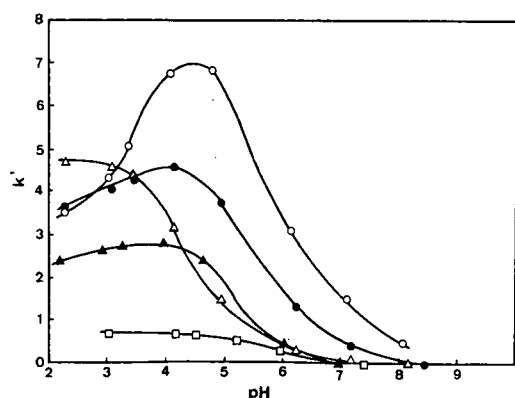
Fig. 2. The pH dependence of the k' value of benzoic acid. $\bigcirc$ = LC-HISEP; $\bullet$ = ISRP-amide; $\triangle$ = SHRP-E3; $\blacktriangle$ = ISRP-peptide (GFF); $\square$ = SHRP-C_{18}. Methanol concentration of mobile phase: LC-HISEP = 10%; SHRP-amide and SHRP-E3 = 15%; SHRP-peptide (GFF) = 5%, SHRP-C_{18} = 60%; each mobile phase containing 0.02 M phosphate buffer.
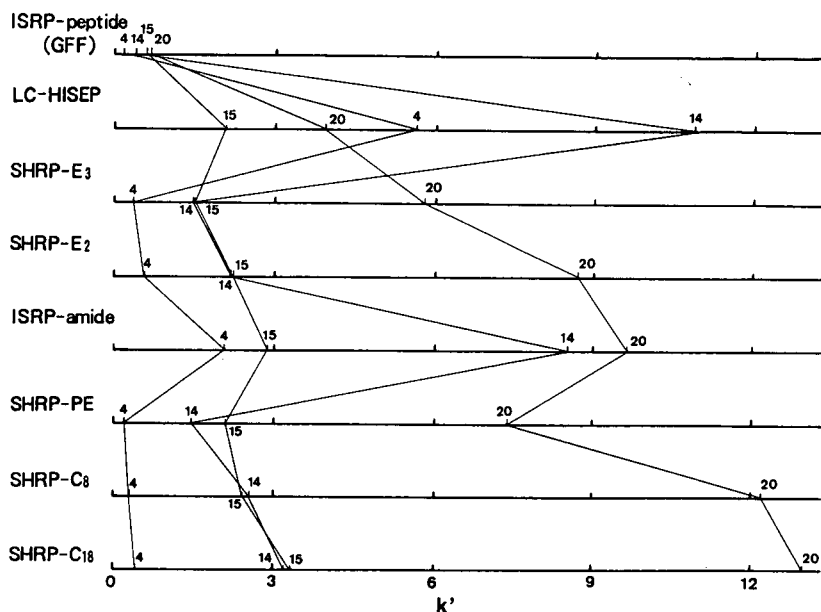
Fig. 3. Difference in selectivity of various RARP materials. Mobile phase: 30% acetonitrile–0.02 M phosphate buffer containing 0.1 M sodium sulfate (pH 7). Solutes: 4 = furosemide; 14 = indomethacin; 15 = carbamazepine; 20 = nifedipine.

increases. With the decrease in the extent of ionization of benzoic acid below pH 5, the retention decreases at relatively constant ionization state of the amine. A similar observation with LC-HISEP suggests the presence of an amine function on this stationary phase. Other packing materials showed normal retention behavior for benzoic acid for the pH range studied.

Recovery of BSA from RARP materials

Table III shows the recovery of BSA from the RARP columns. All the stationary phases gave nearly complete recovery of BSA with less than 40% acetonitrile in the

TABLE III

RECOVERY OF BSA FROM RARP COLUMNS

Packing material	Acetonitrile content (%) of mobile phase[a]					
	0	10	20	30	40	50
ISRP-peptide (GFF)	94	89	103	100	89	50
SHRP-C_{18}	85	85	96	96	93	64
LC-HISEP	101	94	100	103	115	73
ISRP-amide	98	91	90	84	89	47
TSK gel G2000SW	107	99	97	102	75	47

[a] Mobile phase = acetonitrile–0.02 M phosphate buffer + 0.1 M sodium sulfate (pH 7).
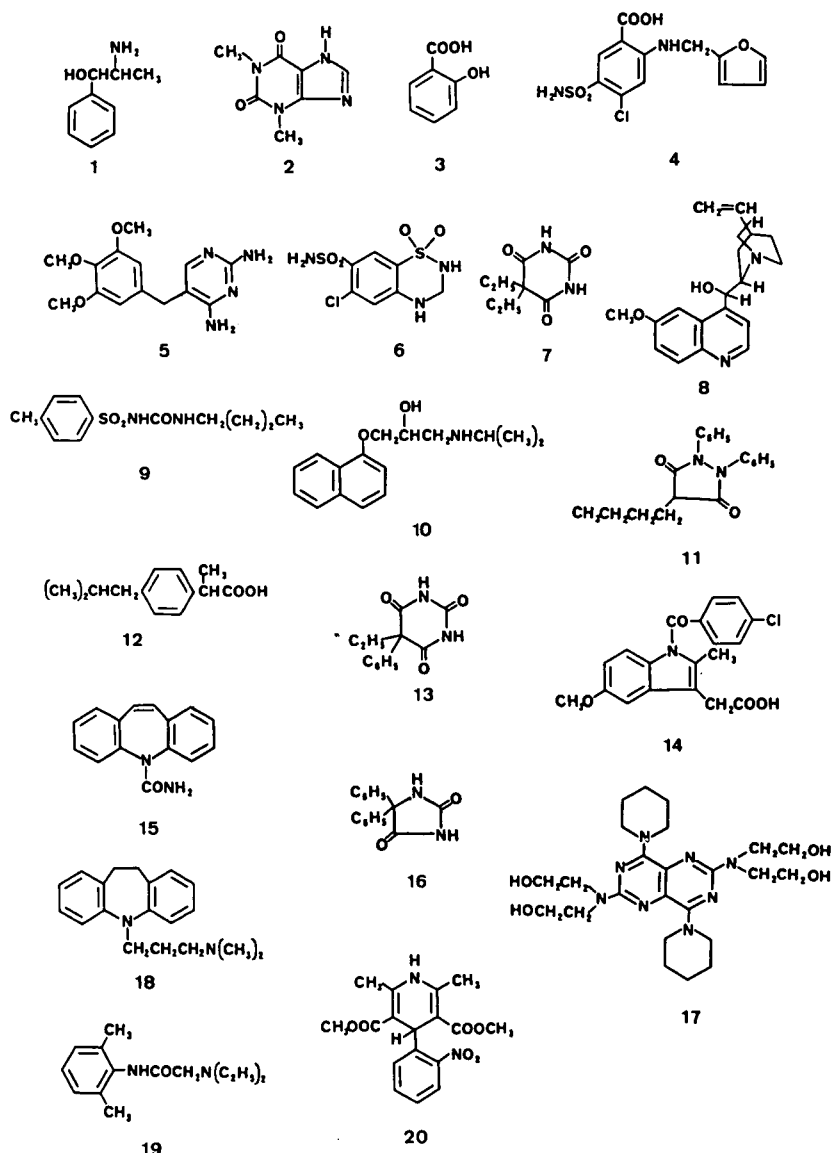
Fig. 4. Structure of drugs. 1 = Phenylpropanolamine; 2 = theophylline; 3 = salicylic acid; 4 = furosemide; 5 = trimethoprim; 6 = hydrochlorothiazide; 7 = barbital; 8 = quinidine; 9 = tolbutamide; 10 = propranolol; 11 = phenylbutazone; 12 = ibuprofen; 13 = phenobarbital; 14 = indomethacin; 15 = carbamazepine; 16 = phenytoin; 17 = dipyridamole; 18 = imipramine; 19 = lidocaine; 20 = nifedipine.

mobile phase. The recovery of BSA in 40% acetonitrile was noticeably lower, and the column for aqueous size-exclusion chromatography, TSK G20000SW, was not an exception. This suggests that the denaturation of BSA was not caused by a particular stationary phase structure, but by the mobile phase. The results indicate that the organic solvent content in mobile phase should be limited to be 30% or less, if

acetonitrile is to be used as an organic solvent. Pinkerton *et al.* [2] suggested that the organic solvent content should not exceed 25% acetonitrile, 20% isopropanol and 10% tetrahydrofuran. The mobile phase composition is limited when RARP materials are to be used for serum analysis.

Retention selectivity for drugs

Fig. 3 shows the retention of drugs on the RARP columns (The structures of the drugs are shown in Fig. 4). The stationary phases are arranged in order of increasing hydrophobicity. The stationary phase with greater hydrophobicity generally gives the larger retention for neutral compounds (Nos. 15 and 20), with SHRP-PE being an exception. Compounds with a carboxyl group (Nos. 4 and 14), however, were retained on LC-HISEP and on ISRP-amide much more than expected on the basis of hydrophobicity.
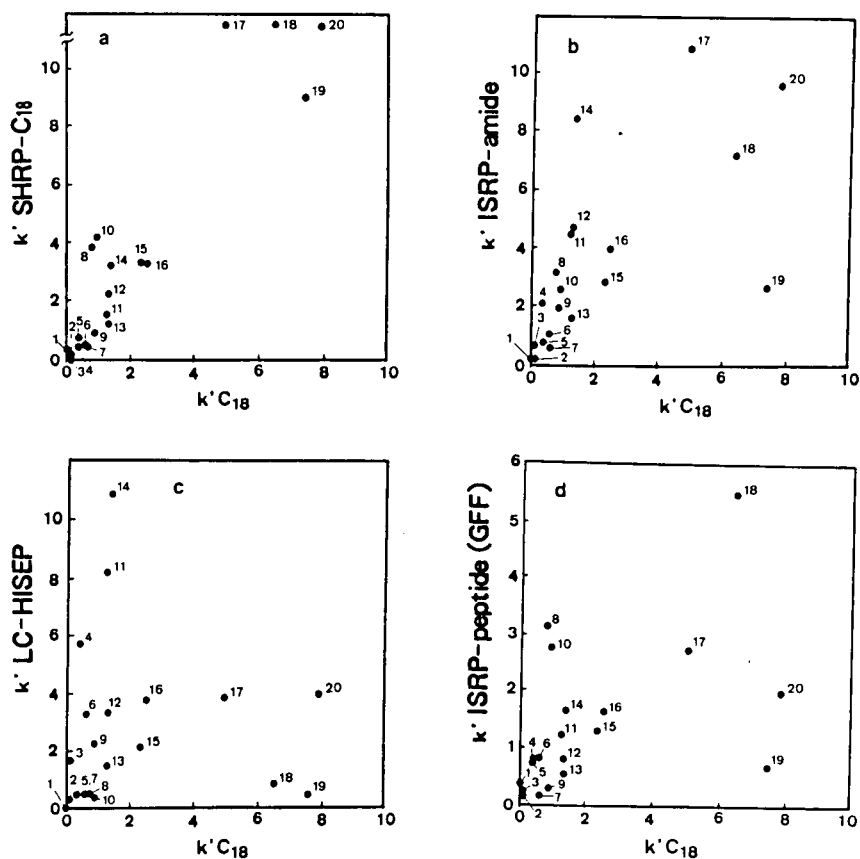
Fig. 5. Selectivity of RARP materials relative to C_{18} packing material. Acetonitrile concentration of mobile phase: $C_{18} = 40\%$; ISRP-peptide (GFF) = 20%; other RARP packing materials = 30%. The mobile phase contained 0.02 M phosphate buffer and 0.1 M sodium sulfate (pH 7). Solute number as indicated in Fig. 4.

The log k' values on SHRP-C$_{18}$, ISRP-peptide (GFF), LC-HISEP and ISRP-amide are compared with those on an ordinary C$_{18}$ column in Fig. 5. The retention selectivities of RARP materials prepared via acid decomposition of the bonded phase, SHRP-C$_{18}$, as well as C$_8$, E2 and E3, were relatively similar to that of ordinary C$_{18}$, as shown in Fig. 5a.

ISRP-amide and LC-HISEP showed preferential retention of solutes with a carboxyl group (Nos. 14 and 4), as shown in Fig. 5b and c, while relatively little retention was seen with amino compounds (Nos. 8, 10, 18 and 19). The contribution of amino groups in the stationary phase should be responsible for these results. In contrast, the ISRP-peptide (GFF) phase showed selective retention of amino compounds (Nos. 8 and 10). This packing material is known to contain a carboxyl group in the peptide-bonded stationary phase, which exists as an anion at this pH [4–6]. These RARP materials showed widely different retention selectivity indicated by the scattered plots in Fig. 5b–d from ordinary C$_{18}$, presumably due to the presence of hydrophilic groups in the stationary phase. The difference in the range of k' value as well as the difference in selectivity provided by these RARP materials can increase the capability of RARP materials, because a limited range of mobile phases can be used with these packing materials to retain the native state of proteins in a sample, as mentioned earlier.

It has been pointed out that hydrophilic compounds were not well resolved from the early-eluting protein peak by using commercial ISRP-peptide (GFF) [7]. Fig. 6 shows the chromatograms for theophylline, phenylpropanolamine and barbital on ISRP-peptide (GFF), LC-HISEP, SHRP-C$_{18}$ and C$_8$. ISRP-peptide (GFF) and LC-HISEP gave very small retention for these drugs under the present conditions. Although the quantification of theophylline and caffeine has been successfully achieved by using ISRP-peptide (GFF) [20,21], the optimization of the separation conditions would be easier with stationary phases showing greater retention. A newer peptide-bonded ISRP phase, ISRP-peptide (GFF)-II, has been reported to be more retentive than ISRP-peptide (GFF) [22]. As shown in Fig. 6, SHRP-C$_8$ and C$_{18}$ gave adequate retention for these compounds in the presence of 5% acetonitrile, although the peaks were somewhat broader on these phases.

When hydrophobic drugs were chromatographed, the ISRP-peptide (GFF) column gave fast separation of dipyridamole, nifedipine and imipramine in 20% acetonitrile, while SHRP-C$_{18}$ showed prolonged retention, as shown in Fig. 7. Because the recovery of proteins tend to decrease with acetonitrile content at 40% or higher, the RARP materials with high hydrophobicity cannot conveniently be used for these drugs. These are just a few examples of the advantages of having a variety of RARP materials with different retention properties.

Fig. 8 shows another example to illustrate the advantage of the availability of various types of stationary phases. The two RARP columns with similar hydrophobicity can provide different selectivity. When one phase fails to give separation, still another phase is available. These RARP materials with intermediate hydrophobicity seem to be applicable for a wide range of compounds. The acid decomposition method for the preparation of RARP materials can produce a variety of phases from RPLC phases currently available.
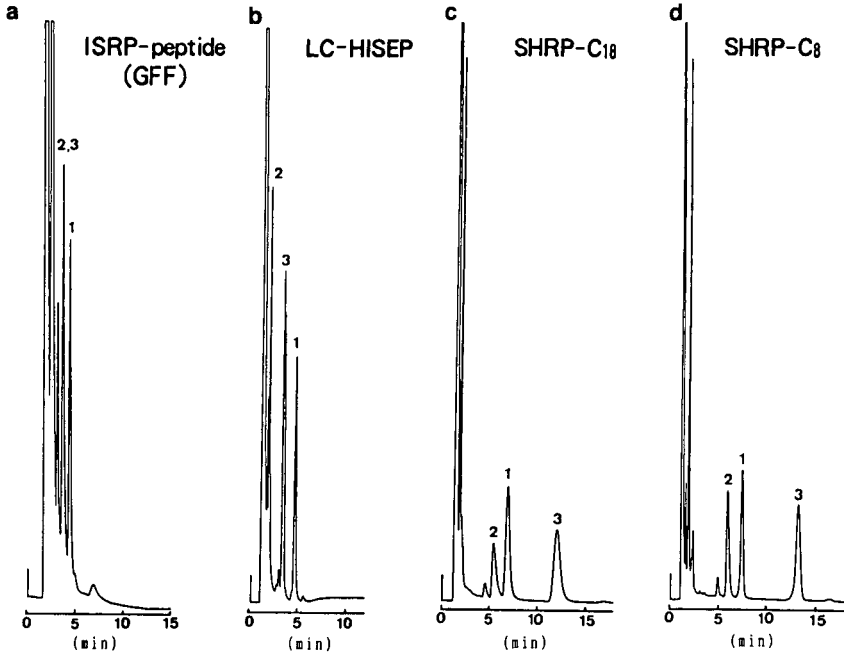
Fig. 6. Chromatograms of hydrophilic drugs injected with 20 μl of human serum. (a) ISRP-peptide (GFF), (b) LC-HISEP, (c) SHRP-C_{18}, (d) SHRP-C_8. Solute: 1 = theophylline; 2 = phenylpropanolamine; 3 = barbital. Mobile phase: (a) and (b), 0.02 M phosphate buffer + 0.1 M sodium sulfate (pH 7); (c) and (d), mobile phase for (a) and (b) + 5% acetonitrile. Flow-rate: 1.0 ml/min. Wavelength: 254 nm.
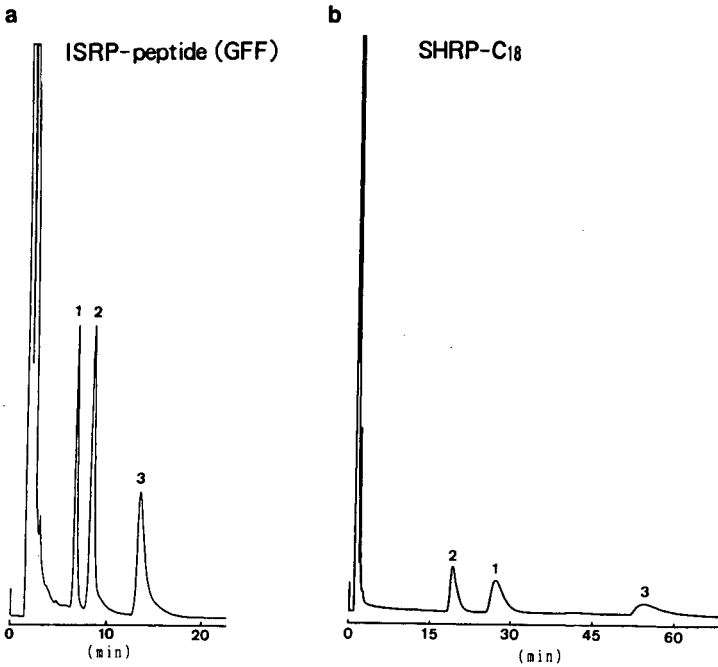
Fig. 7. Chromatograms of hydrophobic drugs injected with 20 μl of human serum. (a) ISRP-peptide (GFF), (b) SHRP-C_{18}. Mobile phase: (a) = 20% acetonitrile–0.02 M phosphate buffer + 0.1 M sodium sulfate; (b) = 30% acetonitrile–0.02 M phosphate buffer + 0.1 M sodium sulfate. Solute: 1 = dipyridamole; 2 = nifedipine; 3 = imipramine. Flow-rate: 1.0 ml/min. Wavelength: 254 nm.
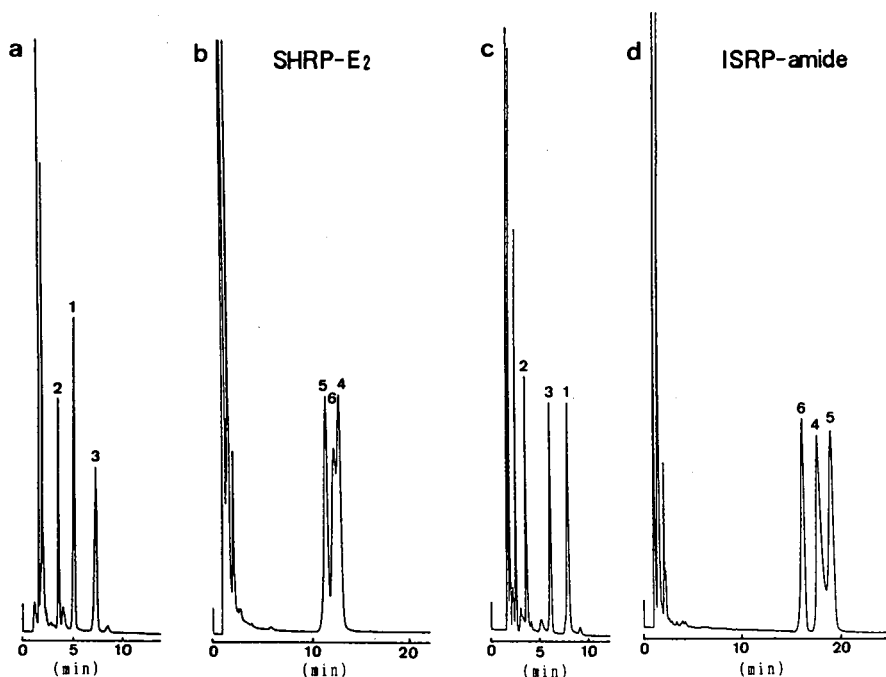
Fig. 8. Drug separation using (a and b) SHRP-E2 and (c and d) ISRP-amide. Mobile phase: (a) 5% acetonitrile–0.02 M phosphate buffer + 0.1 M sodium sulfate, (b and d) 30% acetonitrile–0.02 M phosphate buffer + 0.1 M sodium sulfate, (c) 0.02 M phosphate buffer + 0.1 M sodium sulfate. Solutes (injected with 20 µl of human serum): 1 = theophylline; 2 = phenylpropanolamine; 3 = barbital; 4 = dipyridamole; 5 = nifedipine; 6 = imipramine. Flow-rate: 1.0 ml/min. Wavelength: 254 nm.

CONCLUSIONS

The hydrophobicity of RARP materials was found to be as follows: SHRP-C_{18} > SHRP-C_8 > SHRP-E2 ≈ E3 ≈ ISRP-amide > LC-HISEP > ISRP-peptide (GFF). The order of extent of retention was roughly the same. In order to achieve complete recovery of proteins, and also to elute analytes in a proper k' range, hydrophobic RARP materials should be used for the separation of hydrophilic drugs, and hydrophilic stationary phases for hydrophobic drug analysis. Those with intermediate hydrophobicity can be used for both hydrophobic and hydrophilic compounds. The availability of RARP materials with a wide range of hydrophobicity and with different selectivity will increase the separation capability of RARP stationary phases in the analysis of biological samples. Further addition of RARP materials is expected [22].

ACKNOWLEDGEMENT

REFERENCES

1 I. H. Hagestam and T. C. Pinkerton, *Anal. Chem.*, 57 (1985) 1757.
2 T. C. Pinkerton, T. D. Miller, S. E. Cook, J. A. Perry, J. D. Rateike and T. J. Szczerba, *Biochromatography*, 1 (1986) 96.
3 S. E. Cook and T. C. Pinkerton, *J. Chromatogr.*, 368 (1986) 233.
4 T. Nakagawa, A. Shibukawa, N. Shimoto, T. Kawashima, H. Tanaka and J. Haginaka, *J. Chromatogr.*, 420 (1987) 397.
5 T. C. Pinkerton and K. A. Koeplinger, *J. Chromatogr.*, 458 (1988) 129.
6 J. A. O. Meriluoto, K. Isaksson, H. Soini, S. E. Nygard and J. E. Eriksson, *Chromatographia*, 30 (1990) 301.
7 J. Haginaka, N. Yasuda, J. Wakai, H. Matsunaga, H. Yasuda and Y. Kimura, *Anal. Chem.*, 61 (1989) 2445.
8 J. Haginaka, J. Wakai, N. Yasuda, H. Yasuda and K. Kimura, *J. Chromatogr.*, 515 (1990) 59.
9 Y. Sudo, R. Miyagawa and Y. Takahata, *Chromatography*, 9 (1988) 179.
10 K. Kimata, R. Tsuboi, K. Hosoya, N. Tanaka and T. Araki, *J. Chromatogr.*, 515 (1990) 73.
11 D. J. Gisch, B. T. Hunter and B. Feibush, *J. Chromatogr.*, 422 (1988) 264.
12 D. J. Gisch, B. Feibush, B. T. Hunter and T. L. Ascah, *Biochromatography*, 4 (1989) 206.
13 J. Haginaka and J. Wakai, *Chromatographia*, 29 (1990) 223.
14 J. Haginaka and J. Wakai, *Anal. Chem.*, 62 (1990) 997.
15 L. C. Sander and S. A. Wise, *CRC Crit. Rev. Anal. Chem.*, 18 (1987) 299.
16 N. Tanaka and M. Araki, *Adv. Chromatogr.*, 30 (1989) 81.
17 J. H. Knox, B. Kaur and G. R. Millward, *J. Chromatogr.*, 352 (1986) 3.
18 K. Kimata, K. Iwaguchi, S. Onishi, K. Jinno, R. Eksteen, K. Hosoya, M. Araki and N. Tanaka, *J. Chromatogr. Sci.*, 27 (1989) 721.
19 R. C. Weast (Editor), *CRC Handbook of Chemistry and Physics*, CRC Press, Boca Raton, FL, 66th ed., 1985, pp. D 161–163.
20 S. J. Rainbow, C. M. Dawson and T. R. Tickner, *Ann. Clin. Biochem.*, 26 (1989) 527.
21 F. Tagliaro, R. Dorizzi, A. Frigerio and M. Marigo, *Clin. Chem. (Winston-Salem, N.C.)*, 36 (1990) 113.
22 J. A. Perry, L. J. Glunz, T. J. Szczerba and J. D. Rateike, *LC·GC*, 8 (1990) 932.

Diffusion of sorbed pyrene in the bonded layer of reversed-phase silicas

Effect of alkyl chain length and pore diameter

A. Yu. FADEEV* and G. V. LISICHKIN

Laboratory of Petrochemical Synthesis, Department of Chemistry, Lomonosov State University, Leninskye Gory, 119 899 Moscow (USSR)

V. K. RUNOV

Laboratory of Preconcentration, Department of Chemistry, Lomonosov State University, Leninskye Gory, 119 899 Moscow (USSR)

and

S. M. STAROVEROV

Laboratory of Petrochemical Synthesis, Department of Chemistry, Lomonosov State University, Leninskye Gory, 119 899 Moscow (USSR)

(First received May 29th, 1990; revised manuscript received December 19th, 1990)

ABSTRACT

The processes of lateral diffusion of solutes in the bonded layer of *n*-alkylchlorosilane-modified silicas were studied using pyrene as a luminescence probe. It was shown that all bonded-chain carbon atoms interact with the solute for supports of pore diameter 40-50 nm. The reduction of the average pore diameter results in partial permeation of the solute into the bonded layer, which in turn leads to a decrease in apparent viscosity of the bonded layer. The presence of accessible silanol groups causes a strong decrease in pyrene mobility in the bonded layer.

INTRODUCTION

The most informative method for the investigation of the state and dynamics of surface-adsorbed molecules is high-sensitivity luminescence. This method considers the diffusion-limited processes of probe molecules: luminescence quenching, non-radiating energy transfer of electronic excitation and formation of exciplexes (excited complexes) and excimers (excited dimers) [1–5].

The most successfully applied luminescence probe material is pyrene: it provides quantitative data on diffusion of adsorbed molecules [6–8] and allows study of conformational organization of the bonded layer of reversed-phase packings in liquid chromatography [9–11]. Knowledge of the dynamic behaviour of molecules adsorbed in the bonded layer allows prediction of the properties of reversed-phase packings and more understanding of their chromatographic non-reproducibility.

This paper deals with the study of pyrene lateral diffusion in the bonded layer of *n*-alkylsilane-modified silicas. Emphasis is placed on the effect of the bonded alkyl chain length and average pore diameter.

EXPERIMENTAL

Silica supports

The relevant characteristics of the silica supports used in this work are given in Table I. The specific surface area was determined by benzene adsorption [13].

Modification of silica surfaces

Modification was carried out using absolute octane as solvent and absolute pyridine as activator [14].

Additional silanization (end-capping)

Silanization was effected with a trimethylchlorosilane–hexamethyldisilazane (1:2) mixture.

Surface concentration of bonded alkyl groups

The surface concentration of bonded alkyl groups was determined through carbon content analysis and eqn. 1 [14]:

$$P \; (\mu mol/m^2) \; = \; \frac{10^6 P_c}{(1200 n_c - P_c M)S} \tag{1}$$

TABLE 1

CHARACTERISTICS OF THE MODIFIED SILICAS

Sample	Initial support			Modifier	Carbon content (%)	Bonding density ($\mu mol/m^2$)	Sample symbol[a]
	Type	Specific surface area (m^2/g)	Pore diameter (nm)				
1	Silochrom C-80	67	45	$ClSi(CH_3)_3$	1.1	4.0	MC_1
2	Silochrom C-80	67	45	$ClSi(CH_3)_2C_6H_{13}$	2.3	4.0	MC_6
3	Silochrom C-80	67	45	$Cl_3SiC_8H_{17}$	2.0	2.7	$TC_{8/S}$
4	Silochrom C-80	67	45	$Cl_3SiC_8H_{17}$	1.9	2.7	TC_8
5	Silochrom C-80	67	45	$Cl_3SiC_{12}H_{25}$	4.0	3.67	$TC_{12/S}$
6	Silochrom C-80	67	45	$Cl_3SiC_{16}H_{33}$	5.3	3.67	$TC_{16/S}$
7	Silochrom C-80	67	45	$Cl_3SiC_{16}H_{33}$	5.1	3.67	TC_{16}
8	Silochrom C-80	67	45	$Cl_3SiC_{18}H_{37}$	5.7	3.67	$TC_{18/S}$
9	A-300	166	25	$ClSi(CH_3)_2C_{16}H_{33}$	10.3	3.33	MC_{16}
10	KCK-2	186	13.5	$ClSi(CH_3)_2C_{16}H_{33}$	11.4	3.33	MC_{16}
11	Si-100	283	11.5	$ClSi(CH_3)_2C_{16}H_{33}$	15.3	3.16	MC_{16}
12	Si-60	476	5.4	$ClSi(CH_3)_2C_{16}H_{33}$	17.6	2.21	MC_{16}

[a] S = Sample end-capped by trimethylchlorosilane–hexamethyldisilazane; M, T = treatment with mono- and trichlorosilanes, respectively.

where P is the surface concentration of the bonded alkyl group, n_c is the number of carbon atoms in the modifier molecule, M is the corrected molecular weight of organosilicon modifier, P_c is the carbon content (%) of the sample and S is the specific surface area of initial silica. The surface concentrations of the bonded alkyl groups for synthesized silicas are listed in Table I.

Introduction of pyrene onto the support surface

Pyrene was introduced from a solution in hexane; this was then followed by solvent removal *in vacuo* (10 Torr) at 35–40°C for 15–20 min. For wide-pore modified silicas (samples 1–8, Table I), the surface concentration of pyrene was determined from eqn. 9 (see below) and varied between $8.3 \cdot 10^{-4}$ and $0.16 \ \mu mol/m^2$. This range corresponds to 0.1–20% of surface monolayer coverage given a pyrene adsorption area on silica of $1.5 \ nm^2$ [4].

For narrow-pore modified silicas (samples 9–12, Table I), the surface concentration of pyrene was determined from eqns. 10 and 11 and varied between $2.2 \cdot 10^{-3}$ and $0.20 \ \mu mol/m^2$.

Fluorescence excitation and fluorescence spectra

Fluorescence was measured with a Perkin-Elmer LS-5 spectrofluorimeter; solid samples in cuvettes (2.5-nm bandpass).

RESULTS AND DISCUSSION

The synthesized adsorbents may be classified into three types on the basis of their potential interaction with pyrene:

(I) Samples obtained by modification with alkyltrichlorosilanes ($RSiCl_3$). The interaction of such modifiers with the silica surface affords the following structure [14,15]:
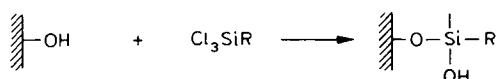
Consequently, a significant amount of accessible silanol groups is present on the sample surface [14,15].

(II) Samples prepared by modification with alkyltrichlorosilanes and additionally silanized (end-capped) by a trimethylchlorosilane (TMS)–hexamethyldisilazane (HMDS) mixture. Such treatment leads to shielding of residual silanol groups [14,15]:
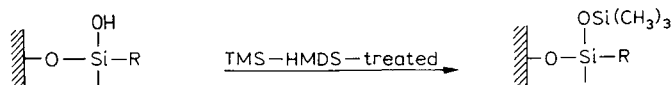
(III) Samples treated with alkyldimethylchlorosilanes of the general formula $ClSi(CH_3)_2R$. After such treatment residual silanol groups on the surface are mainly shielded [14,15]:

$$\text{—OH} \quad + \quad \text{ClSi(CH}_3)_2\text{R} \quad \longrightarrow \quad \text{—O—Si—R}$$
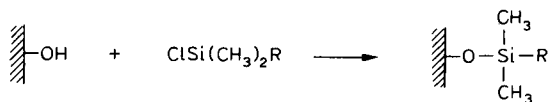
It would be expected that adsorbents having shielded residual silanol groups (types II and III) will show weak adsorbate–adsorbent dispersion interactions (Fig. 1a). Increasing the bonded alkyl chain length may intensify these interactions due to pyrene dissolution in the bonded hydrocarbon layer.

For adsorbents with accessible silanol groups (type I) specific interaction of pyrene with silanol groups is possible (Fig. 1b).

Reduction of the silica support average pore diameter leads to the formation of a "conformationally rigid" bonded layer structure [16] which should also affect the behaviour of adsorbed molecules (Fig. 1c).

Formation of pyrene excimers on the support surface. Calculation of the coefficient of lateral diffusion

Effect of alkyl chain length and end-capping. The excitation fluorescence and fluorescence spectra of the various wide-pore silica samples (samples 1–8, Table I) were measured over a wide range of pyrene concentration.

Electronic-vibration bands typical of pyrene monomer were observed in fluorescence excitation and fluorescence spectra at low degrees of surface coverage (Fig. 2). The increase of pyrene surface concentration results in fluorescence of excimers, as has been found for solutions [17,18], with a maximum at 460 nm. However, the excitation fluorescence spectra coincides with that of pyrene monomer (Fig. 3).

Excimer formation depends on both bonded alkyl chain length and the presence of accessible silanol groups. The minimum concentration required for supports of types II and III for formation of pyrene excimers increases with increasing bonded alkyl chain length (Table II). The formation of pyrene excimers was not observed on silicas with accessible surface silanol groups (Type I) at up to 20% pyrene monolayer surface coverage (Table II, last two lines).
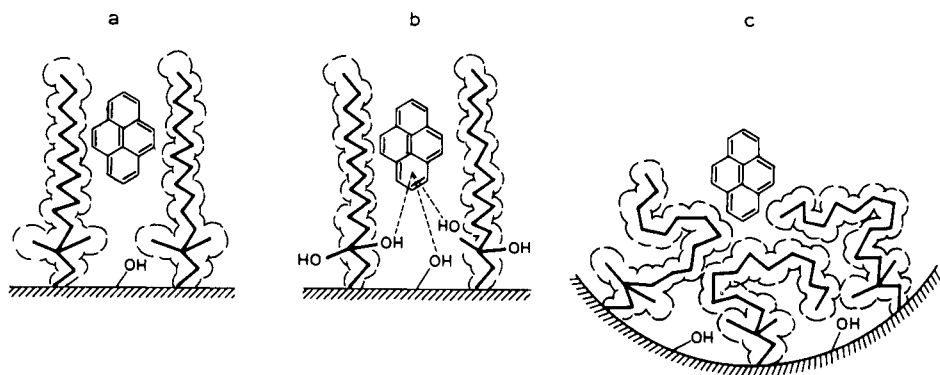
Fig. 1. Interaction of pyrene with the bonded layer of modified silicas.
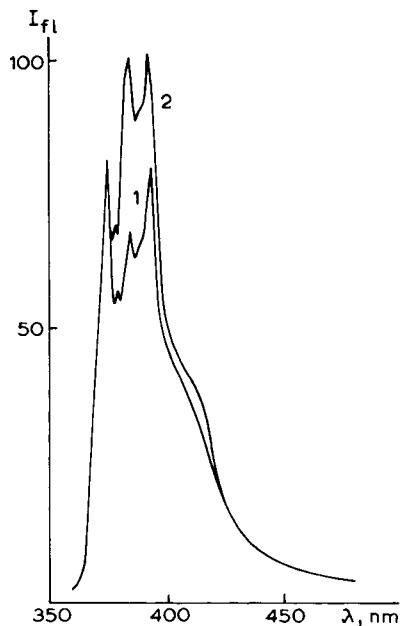
Fig. 2. Normalized fluorescence spectra of pyrene sorbed on (1) octyltrichlorosilane-modified silica and (2) the same sample after end-capping. Surface concentration of pyrene in both cases: $2.5 \cdot 10^{-2}$ $\mu mol/m^2$.

The surface formation of pyrene excimers is a diffusion-limited process. A qualitative description of the observed effects can be obtained using the Einstein–Smolukhovsky equation:

$$D = \langle \Delta x \rangle^2 / 4t \tag{2}$$
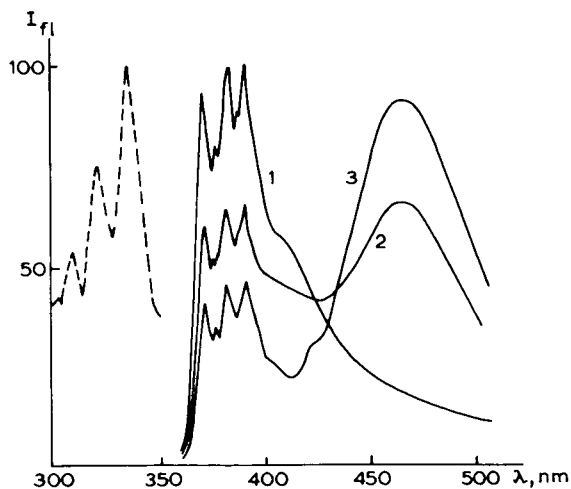
Fig. 3. Normalized excitation (broken line) and emission (solid line) fluorescence spectra of pyrene sorbed on hexyldimethylchlorosilane-modified silica. Surface concentration of pyrene: $1 = 0.83 \cdot 10^{-3}$; $2 = 4.20 \cdot 10^{-3}$; $3 = 8.30 \cdot 10^{-3}$ $\mu mol/m^2$.

TABLE II

STATE OF PYRENE IN THE BONDED LAYER OF ALKYLSILANE-MODIFIED SILICAS

M = Monomer; E = excimer; P = phase. Support C-80.

Sample[a]	Surface concentration of pyrene (μmol/m^2 $\cdot$ 10^3)										
	0.83	2.5	4.4	4.2	5.0	8.3	16	25	33	130	160
MC$_1$	E	E	E	E	E	P	P	P	P	—	––
MC$_6$	M	M	E	E	E	E	E	P	P	P	—
TC$_{8/S}$	M	M	E	E	E	E	E	E	P	P	—
TC$_{12/S}$	M	M	M	M	M	M	M	E	E	P	P
TC$_{16/S}$	M	M	M	M	M	M	M	M	E	E	E
TC$_{18/S}$	M	M	M	M	M	M	M	M	M	E	E
TC$_8$	M	M	M	M	M	M	M	M	M	M	M
TC$_{16}$	M	M	M	M	M	M	M	M	M	M	M

[a] Notations as in Table I.

where D is the diffusion coefficient, and Δx and t are the length and time of the molecule jump, respectively. Considering t as the lifetime of the pyrene monomer in an excited state (680 ns [18]) and Δx as the mean distance between pyrene molecules (l), given by the equation $l = 1.075/\sqrt{C_0}$, where C_0 is the surface pyrene concentration in molecules per nm^2 at which the intensity of excimer fluorescence at 460 nm is three times the noise level, it is possible to estimate (using eqn. 2) the diffusion coefficient of pyrene in bonded layer of the modified silicas. The results are given in Table III.

Such an approach is only applicable for a qualitative description of diffusion in the bonded layer, as pyrene molecules may not be uniformly distributed on the surface, $\Delta x \neq l$, and t depends on the nature of the support.

TABLE III

PHYSICO-CHEMICAL CHARACTERISTICS OF LATERAL DIFFUSION PROCESSES OF PYRENE IN BONDED LAYER OF ALKYLSILANE-MODIFIED SILICAS

Sample No.	Sample[a]	n_C (atoms/nm^2)	$C_0 \cdot 10^3$ (μmol/m^2)	Diffusion coefficient $\cdot$ 10^6 (cm^2/s) according to		η (cP)	$k_{DM} \cdot 10^{-12}$ (m^2/mol $\cdot$ s)	E_a (kJ/mol)
				Eqn. 2	Eqn. 5			
1	MC$_1$	6.9	0.41	5.28	2.60	1.7	1941	2.59
2	MC$_6$	17.6	0.82	2.64	0.72	6.2	540	6.60
3	TC$_{8/S}$	13.5	1.16	1.88	0.44	10.2	327	5.05
5	TC$_{12/S}$	26.4	5.25	0.20	0.06	76.6	43	9.90
6	TC$_{16/S}$	33.6	8.20	0.18	0.03	162.5	21	12.62
8	TC$_{18/S}$	38.1	9.16	0.12	0.02	231.7	14	14.33
13	C$_6$H$_{14}$					0.29		
14	C$_{18}$H$_{38}$					3.81		
15	Glycerol					1480		

[a] Notations as in Table I.

The diffusion coefficients can be more accurately determined if the kinetics of pyrene excimer formation are considered [19,20]:

--------► = radiating process

─wwww─► = non-radiating process
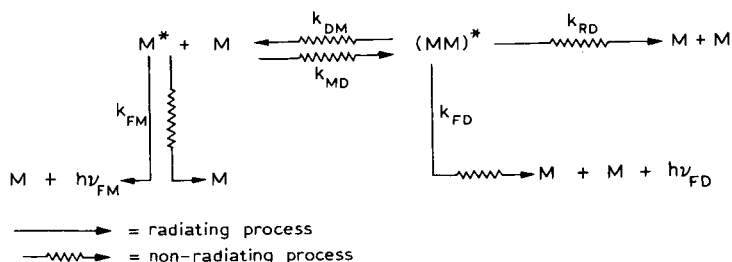
M and M* are pyrene monomers in ground and excited states, respectively, (MM)* is an excimer, and the k values are the rate constant of the corresponding radiating and non-radiating processes. Solving the steady-state equation and introducing the total surface concentration of pyrene, C, enables the ratio of excimer, I_{FD}, and monomer, I_{FM}, fluorescene intensities to expressed thus:

$$I_{FD}/I_{FM} = k_{FD}k_{DM}C/k_{FM}k_D \tag{3}$$

where $k_D = k_{FD} + k_{RD}$.

The literature values [21] of k_{FD} $(1.3 \cdot 10^7 \text{ s}^{-1})$, k_{FM} $(1.5 \cdot 10^6 \text{ s}^{-1})$ and k_D $(7.1 \cdot 10^7 \text{ s}^{-1})$ are almost independent of the solvent nature and can be used to determine the bimolecular reaction rate constant of excimer formation, k_{DM}, on the basis of the relationship $I_{460 \text{ nm}}/I_{393 \text{ nm}} = F(C)$ thus derived from eqn. 3. The application of Smolukhovsky equation for diffusion-limited bimolecular reactions

$$k_{DM} = 2\pi D N_A \tag{4}$$

where N_A is Avogadro's number, allows calculation of the diffusion coefficients of pyrene, and the viscosity of the bonded layer (η) when combined with the Stokes–Einstein equation

$$D = kT/6\pi b \eta \tag{5}$$

where k is the Boltzmann constant, T is the absolute temperature and b is the Stokes radius.

Diffusion coefficients calculated according to eqns. 2 and 5 are given in Table III. As expected, diffusion coefficient values decrease with increasing bonded alkyl chain length. This dependence is described by eqn. 6:

$$D = \text{constant} \cdot \exp(-0.13n) = \text{constant} \cdot \exp(-0.37n/RT) \tag{6}$$

where n is the number of carbon atoms per nm^2 of surface and R is the universal gas constant. The diffusion coefficient can also be expressed thus:

$$D = \text{constant} \cdot \exp(-E_a/RT) \tag{7}$$

This indicates that the activation energy (E_a) of diffusion in the bonded layer is linearly related to the number of carbon atoms on the surface and to the bonded alkyl chain length. Eqn. 8:

$$E_a = 0.13nRT = 0.37n \tag{8}$$

obtained from eqns. 6 and 7 allows the determination of the activation energy values for pyrene diffusion in the bonded layer of modified silicas; these are given in Table III.

The results given in Table III show that the bonded alkyl layers have markedly higher viscosities than the corresponding liquid alkanes. This is due to the reduction in the degree of freedom after alkyl chain fixation on the silica surface. The diffusion of sorbed molecules in the bonded layer of reversed-phase silicas corresponds to that in viscous fluids.

Effect of the support pore structure. Fadeev and Staroverov [16] showed that the conformation structure of bonded long chain alkyl layers depends on the support pore structure. Reduction in average support pore diameter produces a bonded layer of "rigid structure" in contrast to the "flexible structure" found in wide-pore modified silicas.

This section considers the effect of support pore diameter on the physico-chemical characteristics of pyrene diffusion in a bonded silica layer modified by hexadecyldimethylchlorosilane. The samples used are described in Table I.

A similar procedure is used for investigating pyrene diffusion on both bonded layer and wide-pore samples. Using eqns. 3–5, the rate constants of excimer formation diffusion coefficients and bonded-layer viscosity were determined; the results are given in Table IV.

The only difference between the procedures involves the determination of the surface concentration of pyrene. Thus for wide-pore silica samples (type C-80, Table I) the surface areas accessible to benzene (specific surface area measurement) and pyrene are practically the same. C-80 is an aerosilogel, synthesized from aerosil and subjected to hydrothermal treatment. This leads to silicas which have a surface fractal dimension close to 2 [24]. The surface concentration of pyrene for samples 1–8 (Table I) may be defined [22,24] as follows:

$$C = m_{pyr}/S_{benz} \tag{9}$$

TABLE IV

EFFECT OF AVERAGE SILICA SUPPORT PORE DIAMETER ON PHYSICO-CHEMICAL CHARACTERISTICS OF PYRENE DIFFUSION IN THE BONDED LAYER OF HEXADECYL-DIMETHYLCHLOROSILANE-MODIFIED SILICAS

Sample No.	Average pore diameter (nm)	Surface fractal dimension	S_{pyr}/S_{benz}	Diffusion coefficient (cm^2/s) according to eqn. 4	η (cP)	$k_{DM} \cdot 10^{-12}$ (m^2/mol $\cdot$ s)	%R (share of rigid structure [16])
9	25	2.3	0.84	0.036	117.3	30.4	2
10	13.5	2.4	0.79	0.120	44.3	76.8	60
11	11.5	2.6	0.71	0.061	81.2	46.7	30
12	5.4	2.8	0.64	0.135	36.0	94.1	100

where m_{pyr} is the amount of sorbed pyrene and S_{benz} is the specific surface area as determined by benzene adsorption [22].

In the case of a narrow-pore support, part of the surface accessible to benzene is inaccessible to large pyrene molecules [22]:

$$S_{pyr}/S_{benz} = (\sigma_{pyr}/\sigma_{benz})^{(2-d)/2} \tag{10}$$

where σ_{pyr} and σ_{benz} are cross-sectional areas for pyrene (1.5 nm^2) and benzene (0.49 nm^2) [4,13] and d is the surface fractal dimension. The surface concentration of pyrene for samples 9–12 (Table I) has been determined according to

$$C = m_{pyr}/S_{pyr} \tag{11}$$

It was found [22–24] that in general pore diameter and d are related. For non-porous and wide-pore silica, d values are low (2.0–2.2.); whereas d values of narrow-pore silicas, e.g., type Si-60, are high (2.8–3.0) and S_{pyr}/S_{benz} may be much less than 1 (Table IV). The d values for Si-60, Si-100, KCK-2 (as for Si-200) and A-300 (as for Si-250) silicas were taken from ref. 23.

The results show that the efficient viscosity of the bonded hexadecyl layer reduces as the average pore diameter of the silica support decreases. This may be explained through the concept of a "rigid structure" of the bonded layer [16]. The reduction in viscosity (or increase in diffusion coefficient) reflects the decrease in dispersion interaction of the pyrene-bonded layer. The "rigid structure" of the bonded layer —formed by tightly interwoven alkyl chains— does not permit adsorbed pyrene molecules to permeate completely into the bonded layer (Fig. 1c). The bonded layer is much less accessible than wide-pore samples with "flexible structures" which are totally permeable to solute molecules. The smaller the average support pore diameter, the greater the rigid stucture and the greate the difference in diffusion parameters (Table IV).

From this point of view sample 10 (Table IV) is of interest. It has an asymmetric pore size distribution curve and a significant "tail" in the small-pore region —in contrast to the symmetric distribution curves of other supports. The rigid structure of sample 10 is higher than, for example, of sample 11 (Table IV) and only loses a monotonic order of decreasing bonded-layer viscosity with reduction of average support pore diameter.

Thus, the decrease in average pore diameter results in only partial permeation of pyrene in the bonded layer. A narrow-pore silica such as Si-60 is not able to interact with silanol groups in spite of a low bonding density (only 2.2 μmol/m^2, Table I, sample 12). For a wide-pore sample (such as C-80), modified by hexadecyltrichlorosilane with a bonding density of 3.7 μmol/m^2 (sample 7, Table I), pyrene interacts with silanol groups, leading to a sharp decrease in its mobility and an absence of excimer formation (Table II). The same result was reported by Avnir et al. [7]. It was shown that a relatively low viscosity corrseponds to a densely packed layer, in contrast to partially modified silicas with accessible silanol groups.

Aggregation of pyrene on the surface of modified silicas

Increasing the surface concentration of pyrene results in the formation of
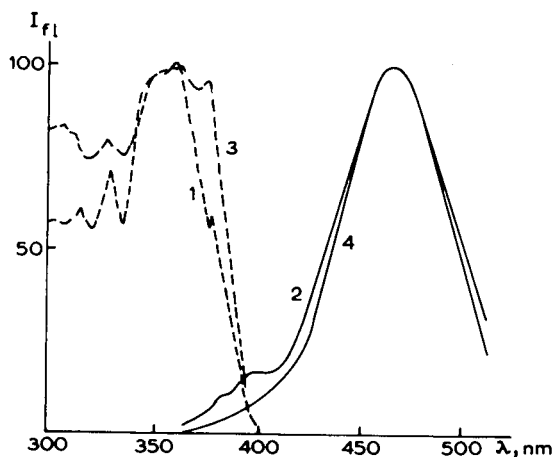
Fig. 4. Normalized excitation (broken line) and emission (solid line) fluorescence spectra of pyrene sorbed on silica modified by butyldimethylchlorosilane (1 and 2) and crystalline pyrene (3 and 4). Surface concentration of pyrene (1 and 2) $1.60 \cdot 10^{-2}$ μmol/m^2.

a pyrene phase that is revealed as new bands in excitation and emission fluorescence spectra, typical of pyrene crystals (Fig. 4). This is unusual since the pyrene phase formation occurs at a very low degree of surface coverage (Table II). As a rule, formation of a phase on the surface is observed at close-to-monolayer coverage.

As with excimer formation, the minimum concentration required to produce this pyrene phase increase with increasing modifier chain length. In the case of samples modified by hexa- and octadecylsilanes, the formation of the phase was not observed even up to 20% surface coverage (Table II).

In our opinion, the formation of a pyrene phase on modified surfaces depends on the ratio of interaction energies between pyrene–pyrene and pyrene-bonded alkyl chains. For samples modified by short-chain silanes the formation of the phase is observed at 0.7–1.0% surface coverage. Increasing the bonded alkyl chain length leads to a growth in the dispersion interaction between pyrene and the bonded layer and thus to an increase in the minimum pyrene concentration at which the phase is formed (Table II).

Silicas treated with trichlorosilane without end-capping (type I) have increased surface–pyrene interaction energies due to specific interactions with accessible silanol groups (Fig. 1a). The presence of such interactions is confirmed by the change in vibrational structure of fluorescence spectra of pyrene adsorbed on the alkylchloro-silane-modified samples without end-capping in comparison with end-capped samples (Fig. 2). Interaction of pyrene with silanol groups results in a lack of pyrene phase formation, even at 20% surface monolayer coverage for a sample with bonded octyl groups (Table II, penultimate line).

CONCLUSIONS

The experimental results presented here allow some general conclusions to be made about the dependence of the properties of silicas with bonded alkyl groups on chain length, pore diameter and accessibility of silanol groups.

Comparison of the samples with a large number of accessible silanol groups with the end-capped samples reveals the important role of silanol groups, which may exceed the role of the bonded alkyl chain length (Table II). The effect of the chain length and pore size on the character of solute bonded layer interaction can only be seen for samples with shielded silanol groups.

The linear relationship between activation energy of diffusion and the number of carbon atoms per unit of surface (eqn. 8) for wide-pore supports (pore diameter 40–50 nm) indicates that in this case all bonded carbon atoms participate in solute interaction.

For narrow-pore silicas, not all bonded alkyl chain atoms interact with the solute, as indicated by the decrease in apparent viscosity of the bonded layer. In case of the support with pore diameter 25 nm with bonded hexadecyl chains the bonded layer viscosity decreases 1.5 times comparing to the viscosity of the hexadecyl layer bonded to the support with pore diameter 45 nm. For supports with pore diameters $ca.$ 10 nm or less the viscosity of the bonded layer corresponds to that of wide-pore samples with a bonded chain length of $ca.$ 10–12 carbon atoms (Tables III and IV). In our opinion the results explain an observed [25] dependence of log k' (k' = capacity factor) on the bonded chain length, which forms a plateau at the 12–14 carbon atoms chain length for supports with pore diameter 10–12 nm. For short bonded chains, pores of 10–12 nm are rather wide and all the bonded atoms interact with the sample molecule. Increasing the bonded chain length results in steric hindrance and only some of the bonded chain atoms participate in interaction.

It should also be mentioned that solute (pyrene) mobility within the bonded layer of hexadecyl groups varies with average pore diameter (Table IV). The chromatographic properties of even similar reversed-phase silicas should therefore be unalike due to the differences in their pore sizes. This is one reason for the discrepancy in properties between reversed-phase packings of various manufacturers and those obtained from various samples of the same silica.

Our results show that the most widely applied reversed-phase packings leave much to be desired. Further study is needed to optimize the modifier chain length and the strutural and geometrical composition of the support. Problems with the reproducibility of reversed-phase packings should also be addressed.

REFERENCES

1 R. J. Hurtubise, Solid surface luminescence analysis: theory, instrumentation and application, Marcel Dekker, New York, 1981, 274 p.
2 H. Birenbaum, D. Avnir and M. Ottolenghi, Langmuir, 5 (1989) 48.
3 C. H. Lochmuller, M. T. Kersey and M. L. Hunnicutt, Anal. Chim. Acta, 175 (1985) 267.
4 R. K. Bauer, P. de Mayo, W. R. Ware and K. C. Wu, J. Phys. Chem., 86 (1982) 3781.
5 R. K. Bauer, R. Borenstein, P. de Mayo, K. Okada, M. Rafalska, W. R. Ware and K. C. Wu, J. Am. Chem. Soc., 104 (1982) 4635.
6 R. Bogar, J. C. Thomas and J. B. Callis, Anal. Chem., 56 (1984) 1080.
7 D. Avnir, R. Busse, M. Ottolenghi, E. Wellner and K. A. Zachariasse, J. Phys. Chem., 89 (1985) 3521.
8 E. Wellner, M. Ottolenghi, D. Avnir and D. Huppert, Langmuir, 2 (1986) 616.
9 C. H. Lochmuller, A. S. Colborn, M. L. Hunnicutt and J. M. Harris, J. Am. Chem. Soc., 106 (1984) 4077.
10 C. H. Lochmuller and M. L. Hunnicutt, J. Phys. Chem., 90 (1986) 4318.
11 J. W. Carr and J. M. Harris, Anal. Chem., 58 (1986) 626.
12 J. W. Carr and J. M. Harris, Anal. Chem., 59 (1987) 2546.

13 A. V. Kiselev and V. P. Dreving (Editors), *Eksperimenntalnye metody v adsorbtsii i khromatografii (Experimental methods in adsorption and chromatography)*, Moscow State University Press, Moscow, 1973.

14 G. V. Lisichkin (Editor), *Modifitsirovannye kremnezemy v sorbtsii, katalize i khromatografii (Modified silicas in adsorption, catalysis and chromatography)*, Khimia, Moscow, 1986.

15 L. C. Sander and S. A. Wise, *CRC Crit. Rev. Anal. Chem.*, 4 (1987) 299.

16 A. Yu. Fadeev and S. M. Staroverov, *J. Chromatogr.*, 447 (1989) 103.

17 Th. Forster and K. Kasper, *Z. Electrochem.*, 59 (1955) 977.

18 Th. Forster and K. Kasper, *Z. Phys. Chem. (Frankfurt)*, 1 (1954) 275.

19 K. Kasper, *Z. Phys. Chem. (Frankfurt)*, 12 (1959) 52.

20 E. Doleer and Th. Forster, *Z. Phys. Chem. (Frankfurt)*, 34 (1962) 132.

21 J. B. Birks, *Photophysics of Aromatic Molecules*, Wiley-Interscience, London, 1970, Ch. 7.

22 D. Avnir, *J. Am. Chem. Soc.*, 109 (1987) 2931.

23 D. Pines-Rojansky, D. Huppert and D. Avnir, *Chem. Phys. Lett.*, 139 (1987) 109.

24 D. Farin and D. Avnir, *J. Chromatogr.*, 406 (1987) 317.

25 K. D. Lork and K. K. Unger, *Chromatographia*, 26 (1988) 115.

Modification of reversed-phase columns with dyed surfactants

Preparation of mechanically resistant efficient immobilized dyes for protein purification

YOUNE LIE KONG SING, ETIENNE ALGIMAN and YOLANDE KROVIARSKI
INSERM U 160, Hopital Beaujon, 92118 Clichy (France)
CHRISTIAN MASSOT
INSERM SC 5, 16 Av. P.V. Couturier, 94807 Villejuif (France)
and
DIDIER DHERMY and OLIVIER BERTRAND*
INSERM U 160, Hopital Beaujon, 92118 Clichy (France)
(First received September 24th, 1990; revised manuscript received April 12th, 1991)

ABSTRACT

The properties of reversed-phase chromatographic supports can be substantially altered by saturating the hydrophobic sites at their surface with easily prepared dyed non-ionic surfactants. The dissociation constants governing the interaction between a reversed-phase support and a model dyed surfactant were found to be in the micromolar range under several mobile phase conditions. The total amount of modified surfactant immobilized on the reversed-phase support was also measured and found to be as great as that usually immobilized on agarose supports (expressed as micromoles per millilitre of support). A reversed-phase column saturated with dyed surfactant can be used with the same aqueous mobile phases as used with immobilized dye columns prepared with agarose as a supporting matrix, but the mechanical sturdiness of the silica matrix allows the use of higher flow-rates. This methodology was used to screen several dyes to find the one best suited for a given purification. A convenient procedure (with affinity elution) was devised for the purification of pancreatic ribonuclease and chymotrypsinogen.

INTRODUCTION

Surfactants have, for several years, been added to the mobile phase for chromatography on reversed-phase supports in techniques such as ion-pair chromatography [1] and micellar liquid chromatography [2]. In both techniques, the surfactants are present at defined concentrations in the mobile phases and organic solvents are used to control the retention of injected solutes.

Surfactants can also be used to modify the surface properties of a reversed-phase column so as to be able to use it thereafter with purely aqueous mobile phases

(with no free surfactant added to the mobile phase). Ionic surfactants can be used to prepare columns from reversed-phase supports, which perform essentially as ion exchangers [3]. An affinity chromatography support can be prepared by grafting a suitable ligand onto the polar end of a non-ionic surfactant [4].

We have used the latter approach to prepare immobilized dye columns which can withstand high flow-rates. There are several ways of preparing mechanically resistant immobilized dye columns: dyes or derivatives thereof can be directly covalently grafted onto covalently modified silica [5,6], polymer-coated silica [7,8] or mechanically resistant polymeric supports [8].

The use of dyed non-ionic surfactants to prepare immobilized dye columns is not conceptually very different from another approach in which dyes grafted onto perfluorinated alkane tails are immobilized on polytetrafluoroethylene beads [9].

EXPERIMENTAL

Materials

The non-ionic surfactants Brij 76 (decaethylene glycol *n*-octadecyl ether) and Triton X-100 were purchased from Sigma (St. Louis, MO, USA). The reactive dyes were a generous gift from ICI France (Clamart, France). The list of dyes used and abbreviations (taken from ref. 10) used to identify them in the text are given in Table II. Bovine pancreas acetone powder and yeast RNA were purchased from Sigma. Sep-Pak C_{18} cartridges and preparative C_{18} reversed-phase packing material (55–105-μm particle size, 60 Å pore diameter; ref. No. 51 922) were purchased from Waters Assoc. (Milford, MA, USA). All other chemicals and solvents were purchased from Merck (Darmstadt, Germany).

Synthesis of dyed surfactants

A modification of the method developed by Johansson and Joelsson [11] for the synthesis of dyed polyoxyethylene derivatives was used. Dye (0.4 g) was added to Brij 76 (12.5 g) dissolved in 100 ml of 0.2 *M* potassium hydroxide solution and the mixture was stirred overnight at 50°C.

Purification of Procion Navy HE-R150-dyed Brij 76 (B4-Brij 76)

The crude synthesis mixture was passed at 3.0 ml/min through a Sephadex LH-20 column (100 cm × 5 cm I.D.) equilibrated with 5 m*M* ammonium hydrogencarbonate buffer (pH 8.3). The modified surfactant B4-Brij 76 together with unreacted Brij 76 were eluted in the void volume of the column. Deactivated and reactive B4 were washed from the column with distilled water.

The excluded peak (250 ml) from the Sephadex LH-20 column was chromatographed in 50-ml batches on a 100-ml column of specially prepared low-capacity anion exchanger (see below). The column was washed extensively with water to remove unmodified (hence uncharged) Brij 76 (the efficiency of column washing was checked by monitoring the column effluent for non-foaming when vigorously stirred, as described [4]). The B4-Brij 76 derivative was then eluted with 2 *M* sodium chloride solution, desalted by chromatography on a 6-cm bed of preparative C_{18} reversed-phase packing settled in a 1.5-cm diameter Buchner funnel: the dyed derivative was loaded onto the reversed-phase material, washed extensively with water and the dyed

Brij 76 eluted with methanol–isopropanol (3:2, v/v). The product was dried by rotary evaporation, dissolved in a small amount of water and lyophilized.

Low-capacity anion exchanger was prepared by reacting cyanogen bromide-activated Sepharose 4B [12] with 0.1 M ammonium chloride solution (0.046 mequiv. titratable groups per millitre of gel was found by automatic titration).

Dyed surfactants were analysed by chromatography on a Nucleosil C_{18} (100 Å) (Macherey, Nagel & Co., Düren, Germany) column (25 cm × 0.46 cm I.D.) obtained from Interchim (Montluçon, France). A 35-min linear gradient from 100% A to 100% B was used: eluent A was 0.05 M triethylamine containing 0.15 M acetic acid and eluent B was methanol–isopropanol (3:2, v/v). The absorbance of the column effluent was monitored at 607 nm and the flow-rate was 1.0 ml/min. The elution volume of unmodified surfactant was established by monitoring the ability of evaporated eluate fractions to foam after addition of water. Unmodified surfactant eluted after the dyed surfactant.

Quantitative analysis of the interaction between stationary phase and B4-Brij 76

We used a method described elsewhere [13]. A 150-mg amount of Waters preparative C_{18} reversed-phase material was packed into a Pharmacia FPLC HR 5/2 column. The mobile phase was 25 mM sodium phosphate–25 mM sodium acetate adjusted to pH 5.5, plus 0, 1 or 2 M sodium chloride. B4-Brij 76, dissolved in the mobile phase at $4.5 \cdot 10^{-6}$–$6.3 \cdot 10^{-5}$ mol/l, was loaded onto the column at 2.0 ml/min. When the effluent absorbance was equal to the absorbance of the incoming solution, the tubing upstream of the column was carefully rinsed with methanol–isopropanol (3:2, v/v). Dyed surfactant was stripped from the column with the same mixture. The amount of eluted dyed surfactant was determined spectrophotometrically after evaporating the organic solvents under reduced pressure and was corrected for the dead volume of the column. The dead volume was determined with tritiated water. The results were used to determine dissociation constants and the maximum amount of dyed surfactant retained by the column using the procedures of Kasai and Oda [14]. Data Desk and SAS software were used for statistical analysis of the experimental data.

Preparation of bovine pancreas acetone powder extract

Bovine pancreas acetone powder was suspended (10 mg/ml) in buffer A (25 mM sodium phosphate–25 mM sodium acetate, pH 5.5) containing 5% (w/v) PEG 6000 and shaken overnigth at 4°C. The extract was clarified by centrifugation.

Screening of dyed surfactants for ribonuclease (RNAse) purification

Crude synthesis mixtures of the dyed polyoxyethylene derivatives were diluted 15-fold with buffer A and 10 ml of each solution were injected on to Sep-Pak C_{18} cartridges with a syringe. Each cartridge was then connected to a pump and a sample injector (fitted with a 7-ml loop). Buffer A was flushed through the cartridge at 1 ml/min until no colour was eluted from the cartridge. Extract (1 ml) was then injected (note: some color was always desorbed during this first sample loading) and the cartridge was developed with 7 ml of buffer C (same composition as buffer A but adjusted at pH 7 and containing 2 M sodium chloride) and re-equilibrated with buffer A. A second injection of extract was done and the cartridge treated likewise (no

further dye bleeding was ever observed). The cartridge was then connected to a fraction collector and a third aliquot of pancreas extract was loaded onto it. The cartridge was developed successively with 5 ml of buffer A, 7 ml of buffer B (of the same composition as buffer A but adjusted to pH 7), 7 ml of buffer B containing 5 mM cytidine 5'-monophosphate (CMP) and 7 ml of buffer C. RNAse activity and protein concentration were assayed in the fractions of the column eluate.

Purification of RNAse A

Preparative C_{18} reversed-phase packing material was packed to a height of 2 · cm in a 1.5-cm I.D. glass column and the column was washed extensively with methanol and deionized water. Dye-modified surfactant (0.18 mM in buffer A) was pumped through the column at 4 ml/min. When the effluent dyed surfactant concentration reached a constant value, the column was washed extensively with buffer A.

The column was loaded with 4 ml of bovine pancreas extract. Some colour was desorbed during this initial sample loading. The column was then washed with buffer C, re-equilibrated with buffer A and used for RNAse purification as follows: the flow-rate was 4 ml/min, 4 ml of crude extract were loaded at a time and then the column was washed with buffer A (5 min) followed by buffer B (4 min). Thereafter RNAse A was specifically eluted with 5 mM CMP dissolved in buffer B, then column was rinsed with buffer C, re-equilibrated with buffer A and subsequently reused in the same way several times.

Purification was also performed using a column loaded with 15-fold diluted crude synthesis mixture. The conditions for column pretreatment and for RNAse chromatography were identical with those given above.

Partially purified RNAse eluted from the immobilized dye column was loaded on a Nucleosil 100 C_4 (Macherey, Nagel & Co.) column (250 mm × 4.6 mm I.D.) equilibrated with 0.1% trifluoroactic acid (TFA) in water and the column was developed at 1 ml/min with a 1-h linear gradient between this latter mobile phase and 0.1% TFA in acetonitrile–water (1:1, v/v).

Other procedures

The activity of RNAse A was determined by the spectrophotometric method of Kunitz [15]. An activity unit is defined as the amount of enzyme causing a change of 1.0 absorbance unit/min. Chymotrypsinogen was assayed after trypsin activation using the chromogenic substrate benzyltyrosyl p-nitroanilide [16]. Proteins were assayed by the Bradford method [17]. Eluate fractions were analysed by sodium dodecyl sulphate polyacrylamide gel electrophoresis (SDS-PAGE) according to Laemmli [18] in 15% slab gels and stained with Coomassie Brilliant Blue. Elemental analyses were performed by the Centre de Microanalyse (CNRS, Vernaison, France).

RESULTS AND DISCUSSION

Purification and characterization of dyed surfactant

Most of the dyed surfactants were used as crude synthesis mixtures without further purification. B4-Brij 76 was purified by a combination of hydrophobic and ion-exchange chromatographic steps. The specially prepared ion exchanger with a low concentration of ion-exchange groups was used because B4-Brij 76 could not be eluted from several commercial anion exchangers.

The formula of Procion Navy HE-R150 is given in ref 19. As it contains two monochlorotriazine rings, dyed surfactants can conceivably be produced containing either one or two surfactant molecules. B4-Brij 76 was synthesized under different reaction conditions and the products were analysed by reversed-phase liquid chromatography (RPLC). The RPLC results for several molar ratios of dye and surfactant showed two species of dyed surfactants. The derivative with a single surfactant molecule per dye molecule largely predominates under the reaction conditions given above. Purified B4-Brij 76 was free from unmodified surfactant as appreciated from results of the analytical high-performance liquid chromatographic procedure described above.

Adsorption of purified dyed surfactant molecules on the preparative C_{18} support

Fig. 1 shows a double reciprocal plot which is similar to that described by Kasai and Oda [14]. The intercept with the ordinate gives the reciprocal of the maximum amount, Q_m, of dyed surfactant retained by the column. The intercept with the abscissa is the reciprocal of the dissociation constant between the dyed surfactant and sites which interact with it.

Statistical treatment of the experimental data indicated that K_d values measured with B4-Brij 76 are not significantly different. Even though interactions between the organic coverage of the reversed-phase support and the dyed surfactant are undoubtly hydrophobic in nature, the experimental results failed to prove any influence of the mobile phase ionic strength on the dissociation constant values. Dissociation constants are in the micromolar range.

The calculated values for Q_m (the amount of surfactant bound to the column from a mobile phase containing an infinite concentration of surfactant) are shown in Table I. The observed values for Q_m were compared with the amount of alkyl chains grafted onto the silica support. Assuming that all the carbon present in the reversed-
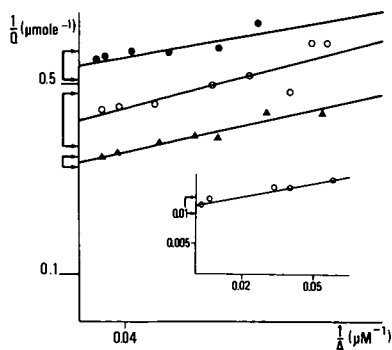
Fig. 1. Double reciprocal plot of the interaction between dyed surfactant and reversed–phase chromatographic support. Ordinate, reciprocal of the amount of dyed surfactant retained by the column; abscissa, reciprocal of incoming dyed surfactant concentration. Results in the main figure were obtained with Procion Navy HE-R150-Brij 76 and those in the inset with Triton X-100. Mobile phases for loading were ($\bullet$) buffer A ($\bigcirc$) buffer A plus 1 *M* NaCl and ($\blacktriangle$) buffer A plus 2 *M* NaCl. The double arrows on the ordinate indicate the 0.95 confidence intervals for $1/Q_m$ values.

TABLE I

VALUES OF Q_m AND K_d OBTAINED BY GRAPHICAL ANALYSIS OF THE CURVES SHOWN IN FIG 1

Q_m is the total amount of dyed surfactant retained by the reversed-phase support. Results for Q_m are given with 0.95 confidence limits. K_d is the dissociation constant of the interaction between B4-Brij 76 and the reversed-phase support.

Parameter	Procion Navy HE-R150-Brij 76 dissolved in			Triton X-100 dissolved in buffer A
	Buffer A	Buffer A + 1 M NaCl	Buffer A + 2 M NaCl	
Q_m (μmol retained by the column)	1.85 ± 0.10	2.36 ± 0.36	2.99 ± 0.23	83.6 ± 7.7
Q_m (μmol/ml of reversed-phase support)	6.17 ± 0.33	7.87 ± 1.20	9.97 ± 0.77	278.7 ± 25.6
K_d (M)	$0.45 \cdot 10^{-6}$	$1.46 \cdot 10^{-6}$	$1.41 \cdot 10^{-6}$	$6.6 \cdot 10^{-6}$

phase support is derived from the alkyl chains, the microanalysis data indicate that there are 288 μmol of C_{18} chain per millitre of support. The value obtained with Triton X-100 is similar, suggesting that all the alkyl chains are involved in binding to Triton X-100 molecules, presumably via hydrophobic interactions with the hydrophobic tail of the non-ionic surfactant. A similar situation probably existed in the experiments described by Torres *et al.* [4], who obtained a very high level of adsorbed modified surfactant.

The Q_m values measured with B4-Brij 76 were much lower, 6.17–9.97 μmol/ml of support. This is probably because the substituent grafted onto the polar end of the surfactant is bulky compared with the pyridinium ring of the modified surfactant of Torres *et al.* [4] or the polar head of Triton X-100. Some steric hindrance would preclude crowding of dye molecules at a density similar to that of the alkyl chains grafted onto the reversed-phase support.

The composition of the mobile phase influenced the amount of dyed surfactant retained by the reversed-phase support (observed differences are significant, $p < 0.05$). A high ionic strength allowed more dyed surfactant molecules to be retained on the reversed-phase support. A similar effect was observed in the interaction of reversed-phase supports with ionic surfactants [20] and was attributed to a diminution of electrostatic repulsion between like charges at high ionic strength. The same explanation probably holds for dyed surfactants. The stacking of dyes is known to be favoured at high ionic strength [21].

When the amount of retained dye is expressed as micromoles per millitre of column volume, as is usually done for dyed soft gels, the figures are in the range considered satisfactory for agarose-based immobilized dyes (1–10 μmol/ml of gel [22]).

Rapid screening of dyed surfactant-loaded Sep-Pak cartridges for purification of RNAse (Table II)

B4-Brij 76 is satisfactory for RNAse purification: no enzyme was eluted during sample loading or during washing with buffer B. The enzyme is eluted with CMP at a

TABLE II

RESULTS WITH SEP-PAK C_{18} CARTRIDGES LOADED WITH SEVERAL DIFFERENT DYED SURFACTANTS

Abbreviations used to identify the different dyes are the same as used before [10]; i = irrelevant.

Dye	Unretained RNAse		RNAse eluted with buffer B		RNAse eluted with buffer B + 5 mM CMP	
	Purification factor	Yield (%)	Purification factor	Yield (%)	Purification factor	Yield (%)
Procion Navy HE-R150 (B4)	i	0	i	0	25.6	98
Procion Blue MX-R (B8)	0.9	53	11.5	50	i	0
Procion Blue HE-GN (B16)	1.1	69	5.2	32	i	0
Procion Brown H-3R (C3)	1.9	42	6.1	14	i	0
Procion Orange HE-R (O3)	0.6	40	27.3	71	i	0
Procion Red HE-3B (R1)	0.9	90	i	0	i	0
Procion Turquoise P-GX (T4)	1.3	47	5.7	46	2.5	4
Procion Green HE-4BD G1	1.3	71	2.1	14	2.5	13
Procion Yellow MX-GR (Y13)	1.4	100	i	0	i	0

satisfactory yield. O3-Brij 76 is also adequate as the enzyme is eluted from the column under mild conditions (pH 7) with a fairly high specific activity, but the capacity of the dyed column is lower than that of B4-Brij 76.

Other dyes were much less satisfactory. The cumulative yield obtained with the C3-Brij 76 column was low (an additional 5% of the total deposited activity could be eluted with buffer C).

The screening procedure was conducted with only a small number of dyes, which is probably why no immobilized dye suitable as a negative column for RNAse purification i.e., absorbing most of the unwanted proteins but not RNAse, was identified [23].

Purification of RNAse

A representative chromatogram of the purification of RNAse on a dyed surfactant-loaded reversed-phase column is shown in Fig. 2. Fig. 3 shows the SDS-PAGE patterns of the eluate. Yields and purification factors are shown in Fig. 4.

The yield was almost quantitative after the column had been used six times (column prepared with purified B4-Brij 76) or four times (column prepared with crude synthesis mixture).

The low yields obtained during early use of the columns suggest that some
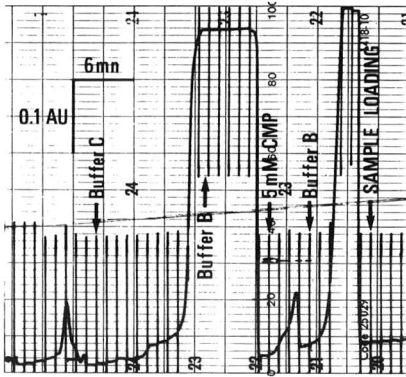
Fig. 2. Chromatography of extract of bovine pancreas acetone powder on a B4-Brij 76-loaded reversed-phase column. The dyed surfactant was loaded as a crude synthesis mixture. Column, 2.5 cm × 1.5 cm I.D.; flow-rate, 4.0 ml/min; chart speed, 12 cm/h.
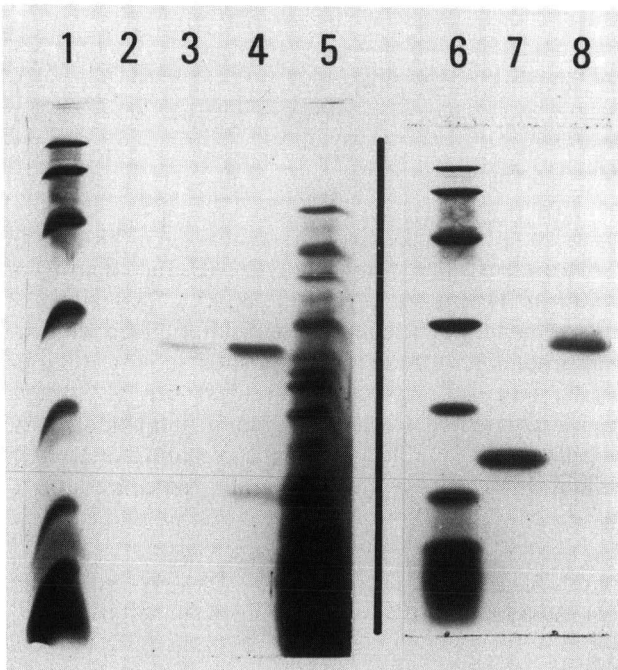
Fig. 3. SDS-PAGE on a 15% polyacrylamide gel [17]. Lanes 1 and 6 contain molecular weight standards (from top to bottom, 94, 67, 43, 30, 20.1, 14.4 and 6.6; lane 5 contains bovine pancreas acetone powder extract (prepared without PEG); lanes 3 and 4 contain aliquots of the proteins eluted from a B4-Brij 76-loaded reversed-phase column with 5 m*M* CMP; lanes 7 and 8 contain RNAse and chymotrypsinogen purified by subsequent reversed–phase chromatography.
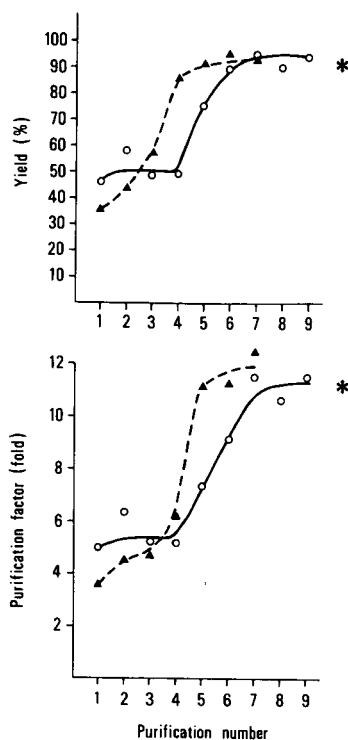
Fig. 4. Yields (top) and purification factors (bottom) for successive purifications of RNAse on (○) a purified B4-Brij 76-loaded column or (▲) a crude synthesis mixture-loaded column. The yield and purification factor obtained with a B4 agarose column are indicated by the asterisks.

RNAse is retained by interactions that are not reversed either by adding a ligand for the enzyme to the mobile phase or by increasing the ionic strength. These sites are quickly saturated, especially if the column is prepared using a crude synthesis mixture. These unwanted affinity sites are probably of a reversed-phase nature. Non-ionic surfactants are retained by the reversed-phase support and the crude synthesis mixture of dyed surfactant contains unmodified surfactant. Hence, a significant proportion of the alkyl chains of the reversed-phase support which cannot interact with the dyed surfactant (for the reasons given above) will interact with unmodified surfactant molecules, lowering the amount of reversed-phase sites later available to RNAse. Dyed surfactant-loaded columns were stripped of their modified surfactant layer by methanol–isopropanol (3:2, v/v) after several uses. Although the dyed surfactant molecules in the eluate precluded direct assay of RNAse activity, RNAse was detected in the eluate by SDS-PAGE (data not shown).

Although the yield of RNAse is not quantitative in the early runs with a dyed surfactant-loaded column, RNAse could be eluted by a known ligand of the enzyme (CMP has been used in the past to elute RNAse from a Cibacron Blue F3GA agarose column [24]). CMP-eluted enzyme was retained on the dyed surfactant loaded column only by a biospecific mechanism.

Purification factors also increased to a plateau during the first few uses of the column (Fig. 4). Thus RNAse probably contributes more than other proteins in the crude extract to coverage of the suspected remaining reversed-phase sites. The purification factor plateau values are equal to values obtained with the same dye immobilized on an agarose matrix (Fig. 4).

The SDS gels (Fig. 3) show that another protein was eluted from the dyed column by CMP. This protein was found to be chymotrypsinogen by specific assay using a chromogenic substrate after activation with trypsin.

Elution of chymotrypsinogen from an immobilized dye column by a phosphorylated nucleotide is not surprising. It has been shown [25] that it is worth trying many different eluents to elute a protein retained on an immobilized dye, without limiting such a screening to the known natural ligands of the protein. The two proteins were readily separated by reversed-phase chromatography: RNAse was pure, chymotrypsinogen was contaminated by a small amount of impurities which are barely visible on the gel (Fig. 3).

Because unmodified dye is retained on a reversed-phase material from a purely aqueous mobile phase, we checked the behaviour of RNAse injected onto a reversed-phase column loaded with unmodified or only deactivated Procion Navy HE-R150. When crude pancreatic extract was loaded on such a column large amounts of dye were desorbed, and no RNAse could be eluted with CMP. Hence the satisfactory results obtained with dyed surfactant-loaded reversed-phase columns were obtained because the non-polar part of the surfactant moiety anchored the dyed surfactant to the reversed-phase silica and the polar part acts as a spacer arm presenting proteins in the mobile phase with a ligand molecule free from other interactions with the support.

General comments and conclusion

This work has demonstrated that reversed-phase material can be modified by loading it with dyed surfactants and used in the same way as a conventional immobilized dye column with agarose as the supporting matrix. The flow-rates which can be used with these columns are fairly high because of the mechanical strength of the silica. Reversed-phase materials are readily available in a range of porosities and particle sizes, in contrast to the polytetrafluoroethylene beads used in a similar application [9]. Dyes can be very easily grafted onto non-ionic surfactants, and unfractionated synthesis mixtures can be used to screen rapidly several dyes to find the one best suited to a purification using ready-to-use reversed-phase cartridges. Also, one can plan to load successively the same reversed-phase column with different dyed surfactants, each suitable for purifying one given protein.

Nevertheless, the use of reversed-phase supports to immobilize dyed surfactants is not free from problems. First, the reversed-phase nature of the packing is not totally suppressed by the dyed surfactant-loading, which may explain the low yield of RNAse from a newly loaded column.

Second, although it had been claimed [4] that this approach allows the preparation of chromatographic supports with a very high density of immobilized affinity ligands, our data show that this is not so if the ligands are as bulky and charged as the reactive dyes. Nevertheless, the amounts of B4-Brij 76 retained by the reversed-phase material are about the same as amounts of dye grafted onto agarose-based supports. It should be remembered that an increased ligand loading is not always associated

with an increased column capacity, as soon as a limit value is reached [26], and it may be difficult to elute proteins from highly substituted affinity chromatographic supports [27]. Hence a very high level of substitution is not necessarily desirable.

Third, the dye derivative is not covalently bound to the reversed-phase material. Its affinity for the stationary phase is high, but dye is retained on the column packing because of a dynamic equilibrium. Thus, when incoming mobile phase contains no dissolved dyed surfactant, some dyed surfactant will be desorbed from the column, even though the loss may be too low to be seen by the naked eye or by standard spectrohotometric measurements (this was checked by adsorbance readings at 607 nm). Changing the mobile phase composition from one which strongly promotes hydrophobic interactions to one which is less favourable may speed up dye leakage, and dyed surfactant should therefore be loaded using the mobile phase of the purification process, which favours hydrophobic interactions less strongly.

Despite its limitations, this approach successfully allows the purification of proteins by immobilized dye chromatography at high flow-rates. It has two great advantages: straightforward chemistry is all that is needed to prepare the dyed surfactants, and the satisfactory results obtained with columns loaded with crude synthesis mixtures make the preparation of efficient immobilized dye columns simple and rapid.

ACKNOWLEDGEMENTS

REFERENCES

1 E. Tomlinson, T. M. Jefferies and C. M. Riley, *J. Chromatogr.*, 159 (1978) 315–358.
2 M. R. Borgerding, R. L. Williams, Jr., W. L. Hinze and F. H. Quina, *J. Liq. Chromatogr.*, 12 (1989) 1367–1406.
3 D. E. Keller, J. L. Torres, R. G. Carbonell and P. K. Kilpatrick, *Anal. Biochem.*, 176 (1989) 191–198.
4 J. L. Torres, R. Guzman, R. G. Carbonell and P. K. Kilpatrick, *Anal. Biochem.*, 171 (1988) 411–418.
5 C. R. Lowe, M. Glad, P. O. Larsson, S. Ohlson, D. A. P. Small, T. Atkinson and K. Mosbach, *J. Chromatogr.*, 215 (1981) 303–316.
6 R. Ledger and E. Stellwagen, *J. Chromatogr.*, 299 (1984) 175–183.
7 Y. Kroviarski, X. Santarelli, S. Cochet, D. Muller, T. Arnaud, P. Boivin and O. Bertrand, in M. A. Vijayalakshmi and O. Bertrand (Editors), *Protein–Dye Interactions*, Elsevier, Amsterdam, 1989, pp. 115–120.
8 E. Algiman, Y. Kroviarski, S. Cochet, Y. L. Kong Sing, D. Muller, D. Dhermy and O. Bertrand, *J. Chromatogr.*, 510 (1990) 165–175.
9 C. R. Lowe, N. Burton, S. Dilmaghanian, S. McLoughlin, J. Pearson, D. Stewart and Y. D. Clonis, in M. A. Vijayalakshmi and O. Bertrand (Editors), *Protein–Dye Interactions*, Elsevier, Amsterdam, 1989, pp. 11–20.
10 Y. Kroviarski, S. Cochet, C. Vadon, A. Truskolaski, P. Boivin and O. Bertrand, *J. Chromatogr.*, 449 (1988) 403–412.
11 G. Johansson and M. Joelsson, *Biotechnol. Bioeng.*, 27 (1985) 621–625.
12 J. Porath, R. Axen and S. Ernback, *Nature (London)*, 215 (1967) 1491–1492.
13 A. Berthod, I. Girard and C. Gonnet, *Anal. Chem.*, 58 (1986) 1356–1358.
14 K. I. Kasai and Y. Oda, *J. Chromatogr.*, 376 (1986) 33–47.
15 M. Kunitz, *J. Biol. Chem.*, 164 (1946) 563–568.
16 P. E. Wilcox, *Methods Enzymol.*, 19 (1970) 64–108.

17 M. M. Bradford, *Anal. Biochem.*, 141 (1976) 248–254.
18 U. K. Laemmli, *Nature (London)*, 227 (1970) 680–685.
19 C. V. Stead, *J. Chem. Tech. Biotechnol.*, 37 (1987) 55–71.
20 M. M. Federici, P.B. Chock and E. R. Stadtman, *Biochemistry*, 24 (1985) 647–660.
21 A. Berthod, I. Girard and C. Gonnet, *Anal. Chem.*, 58 (1986) 1362–1367.
22 C. R. Lowe and J. C. Pearson, *Methods Enzymol.* 104 (1984) 97–113.
23 R. K. Scopes, *J. Chromatogr.*, 376 (1986) 131–140.
24 S. T. Thompson, K. H. Cass and E. Stellwagen, *Proc. Natl. Acad. Sci. U.S.A.*, 72 (1975) 669–672.
25 Y. Kroviarski, S. Cochet, C. Vadon, A. Truskolaski, P. Boivin and O. Bertrand, *J. Chromatogr.*, 449 (1988) 413–422.
26 J. Turkova, K. Blaha and K. Admova, *J. Chromatogr.*, 236 (1982) 375–383.
27 M. J. Holroyde, J. M. E. Chesher, I. P. Trayer and D. G. Walker, *Biochem. J.*, 153 (1976) 351–361.

Comparison of the performance of immunosorbents prepared by site-directed or random coupling of monoclonal antibodies

CAROLYN L. ORTHNER*, FRANK A. HIGHSMITH and JOHN THARAKAN[a]

Plasma Derivatives Laboratory, American Red Cross, Jerome H. Holland Laboratory for the Biomedical Sciences, 15601 Crabbs Branch Way, Rockville, MD 20855 (USA)

and

RAPTI D. MADURAWE, TULIN MORCOL and WILLIAM H. VELANDER

Department of Chemical Engineering, Virginia Polytechnic Institute and State University, Blacksburg, VA 24061 (USA)

(First received January 17th, 1991; revised manuscript received April 26th, 1991)

ABSTRACT

The majority of methods used to prepare immunosorbents immobilize antibodies through their reactive amino acid residues. The bound antibody activity of these immunosorbents is low. Hydrazide-based matrices couple antibodies through carbohydrate chains frequently located in the Fc region. This paper reports a comparative study of the performance of immunosorbents prepared by cyanogen bromide or hydrazide immobilization methods. The experiments utilized murine monoclonal antibodies to the human plasma proteins Factor IX or Protein C. The antibodies were immobilized at low densities to beaded agarose matrices which had similar properties. The hydrazide immunosorbents had binding efficiencies which were lower (anti-Factor IX) or up to 1.6-fold higher (anti-Protein C) than comparable cyanogen bromide coupled gels. However, there was no improvement in performance due to lower recoveries of bound protein from the hydrazide gels. Control experiments demonstrated that oxidation of antibody which is required for its coupling to hydrazide gels had no effect on antibody binding to antigen. Our results indicate that, as with cyanogen bromide coupling methods, site-directed immobilization through carbohydrate residues results in a restricted ability to bind to antigen. Both monoclonals were found to contain carbohydrate in their Fab' regions through which coupling may have occurred. The frequency of carbohydrate in the Fab region and the ability to control glycosylation at these sites are factors which may impact the utility of carbohydrate-directed immobilization of antibodies.

INTRODUCTION

Covalent attachment of monoclonal or polyclonal antibodies (Ab) to matrices has long been employed to create highly specific sorbents for haptens or proteins. However once immobilized, a significant reduction in antigen binding capacity occurs. For example the antigen binding capacities (efficiencies) based on divalent Ab activity have been reported to be 30% or less for immunosorbents containing 1 mg or

---

[a] Present address: Department of Chemical Engineering, Howard University, Washington, DC 20059, USA.

more bound Ab per ml of gel [1–5]. This is true for monoclonal or polyclonal antibodies. The application of immunosorbents to large-scale purification is to a large extent constrained by the high cost of Ab. Increasing the acitivty of an immunosorbent would reduce the Ab requirement and significantly lower the cost of the immunosorbent, thus increasing the feasibility of its use in large-scale purification processes.

Changes in immunoaffinity interactions which occur because of Ab immobilization are not well understood. However, it has been suggested that steric hindrance, improper orientation, and alterations of the antigen-binding site contribute to the low bound Ab activity observed for most immunosorbents [6]. Both direct chemical modification of a critical amino acid residue(s) in the antigen-binding site during coupling or indirect distortion of its conformation resulting from multipoint attachment in a nearby region of the molecule, for example, may adversely affect antigen binding.

Several approaches have been used to maximize the efficiency of immunosorbents. Coupling parameters such as the concentration of reactive groups on the gel, pH and reaction time have been varied to minimize multipoint attachment of Ab [7]. It is likely that a uniform and appropriately spaced distribution of reactive sites on the gel is important in optimizing the performance of an immunosorbent [4]. Lower surface densities of Ab have been found to result in greater antigen binding capacity relative to bound Ab, which is thought to be due to decreased steric hindrance between Ab molecules [3,8,9]. In addition, steric hindrance of Ab due to unfavorable interaction with the matrix is thought to be minimized if an adequately long hydrophilic spacer arm is employed [10–12]. An extension of approximately 1–2 nm has been shown to increase the bound activity of immobilized enzymes and co-factors using alkylamines [11] and polyglycine [12] as spacer arms. However, the orientation of antibodies and alteration of their antigen-binding sites have been more difficult to control due to the random nature of the coupling chemistries most frequently utilized. For example, the reactive groups formed by cyanogen bromide (CNBr), N-hydroxysuccinimide, carbonyldiimidazole and toluene sulphonylchloride activation methods immobilize the protein through accessible primary amino groups [7]. Because many such groups are present on the surface of a protein, its site(s) of covalent attachment is thought to be random [6]. This would result in a distribution ranging from coupled antibodies having lowered activity to those which are completely inactive.

Immunoglobulin G (IgG) is an approximately 160 000 molecular weight glycoprotein consisting of two identical heavy and two identical light chains. Each chain consists of several domains which are highly conserved among species (see ref. 13 for review). The CH_2 domain of the heavy chain contains an asparagine residue in the recognition sequence –Asn–X–Thr(Ser) which is glycosylated in human, rabbit, and murine IgG [14–20]. Hence, coupling chemistry specific for carbohydrate has been utilized for site-directed coupling of Ab through the oligosaccharide chain in the Fc region (consisting of the CH_2 and CH_3 domains of the heavy chains) of the Ab. This has been accomplished by oxidation of the vicinal hydroxyl groups of the carbohydrate residues to form aldehydes which are then reacted with the hydrazine groups of a solid support to obtain a covalent hydrazone linkage (Fig. 1). Affinity sorbents prepared using hydrazide-activated solid supports have been reported to have increased binding efficiency compared to random coupling methods [21–25]. In a variation of this approach, the carbohydrate moieties of Ab were selectively biotinylated with hydrazine-biotin [22] and then adsorbed on avidin- or streptavidin-coupled supports [26].
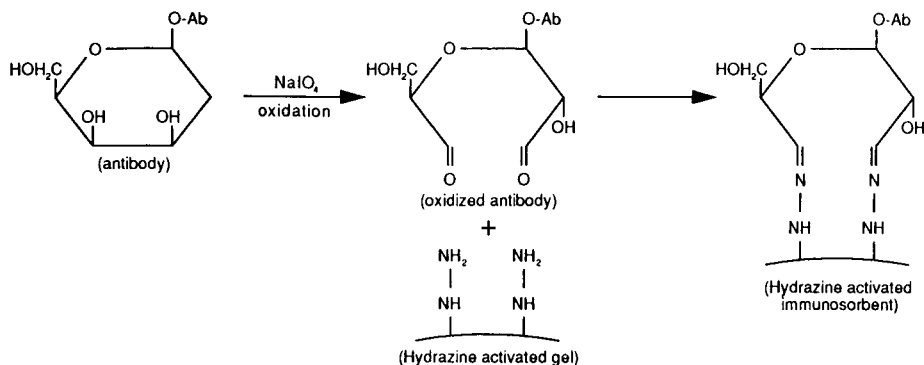
Fig. 1. Schematic representation of antibody attachment to hydrazide-activated gels (adapted from ref. 23). Carbohydrate residues in the oligosaccharide chains of the antibody are oxidized at the vicinal hydroxyls to form aldehydes. The aldehyde groups are coupled with the hydrazine groups of the gel to form the hydrazone-linked immunosorbent.

However, the performance of carbohydrate-linked immunosorbents has not been well documented. Previous studies have examined the effect of hydrazide vs. conventional coupling on the binding efficiency of immunosorbents, while little data has been presented on the ability to recover the bound antigen. Furthermore, most published data relates to polyclonal antibodies with little information available on monoclonal antibodies (Mabs), which are more relevant for large scale immunosorbent processes.

In the present study, we compared the performance of immunosorbents prepared by either hydrazide- or CNBr-coupling methods. The matrices for both types of immunosorbents were beaded, cross-linked agarose gels of similar bead size and porosity [27–29]. Two different murine Mabs directed against the human plasma proteins Factor IX (FIX) or Protein C (PC) were used. These Mabs bind to the corresponding antigens in the presence or absence of divalent cations, respectively [30–32]. The resulting antigen–antibody complexes are easily disrupted by chelation or addition of low concentrations of divalent cations. This unique property makes it possible to elute the immunosorbents prepared using these Mabs under mild elution conditions.

METHODS

Materials and reagents

Assera Protein C, a specific rabbit anti-human Protein C antiserum and horseradish peroxidase (HRP)-conjugated anti-human Protein C rabbit antiserum were purchased from American Bio-Products, Parsippany, NJ, USA. Affinity-purified, HRP-conjugated, goat anti-mouse immunoglobulins (IgA + IgG + IgM) antibody was from Cappel, West Chester, PA, USA. o-Phenylenediamine (OPD) was from Dakopatts, Denmark. Immulon II microtiter plates were from Dynatech Labs., Chantilly, VA, USA. Protac was from American Diagnostica, New York, NY, USA. S-2366 was from Helena Labs., Beaumont, TX, USA. Aquasil, a water-soluble siliconizing fluid, and Protein A-agarose were from Pierce, Rockford, IL, USA. Papain

(25 mg protein/ml, 27 units/mg) was from Sigma, St. Louis, MO, USA. $NaIO_4$ (certified A.C.S. grade) and glutaraldehyde were from Fisher Scientific, Fair Lawn, NJ, USA. Amicon columns were from Amicon, Danvers, MA, USA. Polypropylene Econo-Columns and Econo-Pac 10DG desalting columns were from Bio-Rad Labs., Richmond, CA, USA and Sepharose CL-2B was from Pharmacia, Piscataway, NJ, USA. Hydrazide derivatized agarose gels were purchased from two manufacturers, BioProbe International, Tustin, CA, USA (Manufacturer A) and Bio-Rad Labs. (Manufacturer B). All other chemicals were reagent grade or better.

Protein purification

Mabs. The murine metal-dependent anti-FIX Mab 1H5B7 was purified from cultured cell supernatant as described by Wang *et al.* [30]. The murine "ethylenediaminetetraacetic acid (EDTA)-dependent" anti-PC Mab 7D7B10 [31] was purified from cultured cell supernatant as follows. The cell supernatant was filtered and concentrated by precipitation with saturated ammonium sulphate at room temperature. The precipitate was dissolved in 0.05 M Tris–HCl, 0.1 M sodium chloride, pH 7.5 and reprecipitated with 45% ammonium sulphate at 4°C. This precipitate was dissolved in 0.05 M Tris–HCl, 0.1 M sodium chloride, pH 7.5 and dialyzed extensively against 0.15 M sodium chloride. The purity of this material by sodium dodecyl sulphate (SDS)-polyacrylamide gel electrophoresis (PAGE) was greater than 90%. Both Mabs were of the IgG_1 subtype with κ light chains. Mab concentrations were determined by absorbance at 280 nm (A_{280}) using an absorption coefficient ($A_{2\%}^{1\%}$) of 15.5 and assuming a molecular weight of 160 000 [7].

Fab′ fragments were prepared by treatment of the Mab with papain followed by affinity chromatography of the digest on Protein A–agarose using methods as described in ref. 7. The Fab′ fragment preparations contained 10% or less contamination by Fc fragment and no detectable whole IgG, as analyzed by SDS-PAGE. The concentration of Fab′ was calculated from the A_{280} using an absorption coefficient of 10.0 for a 1% solution and a molecular weight of 50 000 [7].

Antigens. Human FIX was purified from cryo (cryoprecipitated antihemophilic factor)-poor plasma by immunoaffinity chromatography using Mab 1H5B7 as described by Tharakan and co-workers [33,34]. The final product was 95% pure by SDS-PAGE and had a specific activity of 202 units/mg. FIX concentrations were determined by A_{280} using an $A_{2\%}^{1\%}$ of 13.2 and assuming a molecular weight of 57 000 [35]. Human PC was purified from cryo-poor plasma using an immunosorbent based upon the murine anti-human PC Mab 8861. Bound PC was eluted with a pH 10.0 buffer [36]. The final product was 92% pure by SDS-PAGE and had a specific activity of 200 units/mg. PC concentration was determined by A_{280} using an $A_{2\%}^{1\%}$ of 14.5 and a molecular weight of 62 000 [37]. Purified PC and FIX were used in the experiments described herein to evaluate the performance of the various immunosorbents.

Immunosorbent preparation

Anti-FIX hydrazide immunosorbent A. The coupling was performed by Manufacturer A according to their standard protocol, briefly described as follows. A 20–30 mg/ml solution of anti-FIX Mab in 0.05 M sodium acetate, pH 5.0 was oxidized by gently agitating with 0.1 M $NaIO_4$ in a 10:1 volumetric ratio (64-fold molar excess $NaIO_4$) for 1 h at room temperature in the dark. $NaIO_4$ was removed by desalting.

An 8–10 mg/ml solution of oxidized Mab was mixed with the hydrazide gel A in a 1:1 volumetric ratio at 4°C overnight. The gel was sequentially washed with 0.05 M sodium acetate, pH 5.0, distilled water, and 1 M sodium chloride. The coupling efficiency and the immunosorbent density were reported to be 98% and 1.87 mg/ml, respectively. The amount of Mab coupled to the gel was calculated as the difference between total Mab added to the gel and uncoupled Mab recovered in the coupling supernatant and wash pools, as measured by A_{280}. The coupling efficiency was calculated as the ratio of (coupled Mab/total Mab) · 100%.

Anti-PC hydrazide immunosorbents. The anti-PC immunosorbent A(i) was prepared in our laboratory using hydrazide gel from Manufacturer A by a modification of the procedure described above because preliminary experiments resulted in a low coupling efficiency. A 17 mg/ml solution of anti-PC Mab was gently agitated with 0.05 M NaIO$_4$ in a 3:1 volumetric ratio (157-fold molar excess NaIO$_4$) for 1 h at room temperature in the dark. NaIO$_4$ was removed by desalting. A 2.5 mg/ml solution of oxidized Mab was gently agitated with hydrazide gel A in a 1:2 volumetric ratio for 48 h at 4°C. The gel was washed with 0.05 M sodium acetate, pH 5.0. The coupling efficiency was 90% and the immunosorbent density was 1.0 mg/ml. Anti-PC hydrazide immunosorbent A(ii) was prepared by Manufacturer A according to their standard protocol outlined above for anti-FIX. A 100-fold molar excess of NaIO$_4$ was used in the Mab oxidation step. The coupling efficiency and the immunosorbent density were reported to be 98% and 2.3 mg/ml, respectively. Anti-PC hydrazide immunosorbent B was prepared in our laboratory from hydrazide gel from Manufacturer B using the protocol recommended by the manufacturer. A 2.7 mg/ml solution of anti-PC Mab in 0.05 M sodium acetate, pH 5.5 was mixed with 0.1 M NaIO$_4$ in a 12:1 volumetric ratio (494-fold molar excess NaIO$_4$) for 1 h at room temperature in the dark. NaIO$_4$ was removed by desalting. A 1.8 mg/ml solution of oxidized Mab was mixed with hydrazide gel B in a 1:1 volumetric ratio for 48 h at room temperature. The gel was washed with 0.05 M sodium acetate, pH 5.5. The coupling eficiency was 71% and the immunosorbent density was 1.5 mg/ml. For control experiments to determine the amount of nonspecific binding in the absence of Mab, hydrazide gel from manufacturer A was incubated for 20 h at 4°C with a 3.5-fold molar excess of glutaraldehyde relative to the total hydrazine groups on the gel under conditions as described above.

CNBr-activated immunosorbents. Anti-FIX Mab was coupled to CNBr-activated Sepharose CL-2B according to the method of March *et al.* [38]. The activated gel was coupled to Mab in 0.1 M NaHCO$_3$, 0.5 M sodium chloride, pH 8.5 and blocked with 1 M glycine ethylester pH 8.5. The coupling efficiency was 94% and the immunosorbent density was 1.0 mg/ml. Anti-PC Mab was coupled to CNBr-activated Sepharose CL-2B as described above. The coupling efficiency was 88% and the immunosorbent density was 1.7 mg/ml.

Chromatography

Anti-FIX immunosorbents. The immunosorbents were packed in Aquasil-treated, Amicon G 150 × 10 mm I.D. columns. The columns were equilibrated in 10 mM MgCl$_2$, 110 mM sodium chloride, 20 mM imidazole, pH 7.5. Purified FIX at a concentration of 0.44 mg/ml in 20 mM sodium citrate, 110 mM sodium chloride, pH 6.8 containing 40 mM MgCl$_2$ was loaded onto the columns, rinsed with 10 mM MgCl$_2$, 1

M sodium chloride, 20 m*M* imidazole, pH 7.2 and eluted with 20 m*M* sodium citrate, 110 m*M* sodium chloride, pH 6.8 [33,34]. The columns were then washed with 2 *M* sodium chloride, 0.1 *M* sodium citrate, pH 7.2. All column operations were performed at a flow-rate of 1.0 ml/min at 4°C. The corrected absorbance of the effluent fractions was measured as $A_{280} - A_{320}$ and used to calculate the protein concentration. The amount of protein in the load, fall-through and rinse, eluate, and wash pools was determined by summation of the protein in the fractions consituting each pool.

Anti-Protein C immunosorbents. All immunosorbents were packed in 12 ml polypropylene Econo-column with the exception of the anti-PC hydrazide immunosorbent A(i), which was packed in an Aquasil-treated Amicon G 250 × 10 mm I.D. column. The columns were equilibrated in 0.025 *M* Tris–HCl, 0.05 *M* sodium chloride, pH 7.5 [Tris-buffered saline (TBS)]. Purified PC, at a mean concentration of 0.42 ± 0.03 mg/ml (range 0.40–0.47 mg/ml) equilibrated in TBS, was loaded, rinsed with TBS and eluted with 20 m*M* $CaCl_2$ in TBS. The columns were then successively washed with 100 m*M* $CaCl_2$, 2 *M* sodium chloride and 2 *M* NaSCN, each in TBS. Column fractions of 3.0 ml were collected and the A_{280} was measured. All column operations were performed at a flow-rate of 0.5 ml/min at 4°C.

Assays

FIX. FIX activity was measured by a clotting assay according to the method of Biggs [39] as modified by Miekka [40]. A unit is defined as 4 μg of FIX, the amount present in 1 ml of normal pooled human plasma.

PC. The assay was performed according to the method of Odegaard *et al.* [41]. PC was activated by Protac and the chromogenic substrate S-2366 was used to measure the activity of the resulting activitated PC, determined from the rate of change of absorbance at 410 nm using a Vmax kinetic microtiter plate reader (Molecular Devices). A unit of PC is defined as 4 μg, the amount present in 1 ml of normal pooled human plasma.

Enzyme-linked immunosorbent assay (ELISA) of oxidized and native anti-PC Mab. Immulon II microtiter plates were coated with a 1:200 dilution of rabbit anti-PC antisera in 0.1 *M* $NaHCO_3$, pH 9.6 for 1 h at 37°C. Wells were blocked with 1% BSA, 0.1 *M* $NaHCO_3$, pH 9.6 for 1 h at 37°C ad washed with TBS, 0.1% Tween-20. Serially diluted PC samples in TBS, 10 m*M* EDTA, 0.1% BSA were incubated with 32 n*M* oxidized ($NaIO_4$-treated) or native (untreated) anti-PC Mab for 1 h at room temperature. The PC-Mab mixtures were added to the coated wells and incubated for 1 h at room temperature. The wells were washed and incubated with 1:1000 dilution of HRP-conjugated goat anti-mouse IgG in TBS, 10 m*M* EDTA, 0.1% BSA for 1 h at room temperature. The wells were washed and HRP activity was detected with OPD substrate by absorbance at 490 nm using a Vmax plate reader. The results were calculated as a percentage of the signal obtained at saturation.

ELISA of PC purified by different methods. Serially diluted PC samples from a conventional purification [31], and from immunoaffinity purifications using the anti-PC Mabs 8861 or 7D7B10 [32] were preincubated with 32 n*M* native 7D7B10 Mab and assayed by the ELISA procedure outlined above.

SDS-PAGE

SDS-PAGE was performed according to the method of Laemmli [42] using a 12.5% polyacrylamide gel, and stained with 2% Coomassie Brilliant Blue R-250.

Carbohydrate analysis

Sialic acid. Anti-PC and anti-FIX Mabs were heated with 0.05 M H_2SO_4 for 1 h at 80°C to liberate sialic acid residues which were quantitated by colorimetric analysis using thiobarbituric acid [43].

Reducing sugars. The reducing sugar content of the parent IgGs and purified Fab' fragments were analyzed by the *o*-toluidine high-performance thin-layer chromatographic (HPTLC) method [44]. Briefly described, proteins or reference sugars in carbohydrate-free bovine serum albumin (BSA) were hydrolyzed in an identical manner in 6 M hydrochloric acid (HCl) at 110°C for 14 h or in 2 M trifluoroacetic acid (TFA) at 110°C for 2 and 6 h. The hydrolysates were applied to HPTLC plates. The sugars were resolved by the sequential migration of two solvent systems: *n*-butanol–pyridine–water (16:5:4) followed by ethylacetate–methanol–acetic acid–water (4:1:1:1). The plates were sprayed with *o*-toluidine in acetic acid and allowed to react at 100°C for 25 min and then scanned at 295 nm using a Shimadzu CS 9000 diffuse reflectance densitometer. A linear signal extending from 0.050–1.0 μg was obtained for each reducing sugar standard (data not shown). A 2–4% coefficient of variation was obtained for quadruplicate applications of each sample and reference sugar.

RESULTS

Experiments were performed to directly compare the performance of immunosorbents prepared by coupling purified Mab to hydrazide *vs.* CNBr-activated agarose supports. For each experiment the immunosorbent efficiency, defined as the percent of the theoretical maximum binding capacity assuming a 2:1 molar ratio of protein antigen to Mab, was calculated in two ways: (1) based upon the amount of protein (PC or FIX) that bound to the immunosorbent and (2) based upon the amount of protein (PC or FIX) that was specifically eluted under the mild elution conditions.

Table I summarizes the results of experiments with immunosorbents prepared by immobilizing the anti-PC Mab 7D7B10 to hydrazide or CNBr-activated gels. The hydrazide-coupled immunosorbents utilized were from two manufacturers. Five experimental runs were performed with the anti-PC immunosorbent prepared from the hydrazide gel of Manufacturer A in our laboratory [A(i)]. The efficiency of this immunosorbent remained essentially unchanged through three consecutive uses by dynamic loading (runs 1–3). Despite the fact that these three runs were column-loaded with less than saturating amounts of PC, almost half of the loaded material was recovered in the fall-through fraction. This immunosorbent was also batch loaded with saturating amounts of PC for 1 h with gentle, end-over-end agitation (runs 4 and 5). Similar results were obtained with batch loading under saturating conditions suggesting that the efficiencies observed with dynamic loading were not limited by kinetic phenomena. Table I also contains the results of experiments using the following anti-PC immunosorbents: A(ii), hydrazide immunosorbent prepared by Manufacturer A; B, hydrazide immunosorbent prepared in our laboratory using hydrazide gel from Manufacturer B; CNBr, Sepharose CL-2B immunosorbent prepared in our

TABLE I

PERFORMANCE OF ANTI-PC IMMUNOSORBENTS

Immunosorbents were prepared and operated as described in the Methods section. Hydrazide gels from two manufacturers (A and B) were evaluated. Immunosorbent A(i), prepared from hydrazide gel of Manufacturer A, had a Mab density of 1.0 mg Mab/ml gel and a bed volume of 6.0 ml. Immunosorbent A(ii), prepared by Manufacturer A, had a Mab density of 2.3 mg Mab/ml and a bed volume of 3.2 ml. Immunosorbent B, prepared using hydrazide gel from Manufacturer B had a Mab density of 1.5 mg Mab/ml of gel and a bed volume of 5.0 ml. Immunosorbent CNBr was prepared from Sepharose CL-2B following CNBr activation [38]. It had a Mab density of 1.7 mg Mab/ml gel and a bed volume of 2.0 ml. The immunosorbents were prepared in our laboratory, with the exception of A(ii). All runs utilized dynamic loading, except for runs 4 and 5 with immunosorbent A(i), in which batch loading was performed. Efficiency is defined as the percent of theoretical maximum binding capacity, assuming a 2:1 molar ratio of PC to Mab.

Immunosorbent	Run No.	Load (mg PC)	Fallthrough and rinse (mg PC)	Efficiency[a] (%)	Efficiency[b] (%)
A(i)	1	2.00	0.99	21	15
	2	1.88	0.73	24	13
	3	2.00	0.79	25	13
	4	4.90	4.14	16	10
	5	5.64	4.07	33	15
A(ii)	1	4.51	1.59	51	27
	2	5.29	2.59	47	26
B	1	6.59	3.67	49	26
	2	6.18	3.01	53	23
	3	6.67	4.03	44	28
CNBr	1	2.80	1.78	37	26
	2	2.00	1.45	20	17
	3	2.00	1.14	32	24

[a] Efficiency based upon PC bound to the immunosorbent.
[b] Efficiency based upon PC recovered in the eluate.

laboratory by the CNBr activation method of March [38]. Approximately saturating amounts of PC were column-loaded in these experiments. The immunosorbent efficiencies based upon bound PC were higher for hydrazide immunsorbents A(ii) and B as compared to hydrazide immunsorbents A(i) and the CNBr immunosorbent. However, the higher PC binding efficiencies of these gels did not result in improved performance. This is seen by examining the efficiencies based upon PC recovered in the eluates, which were similar for the CNBr and hydrazide immunosorbents and in all cases lower than efficiencies based upon bound PC.

Table II presents the results of experiments with immunosorbents prepared by immobilizing the anti-FIX Mab 1H5B7 to hydrazide or CNBr-activated gels. In these experiments, 59% of a saturating amount of FIX was column-loaded under identical conditions. The immunosorbent efficiency based upon bound FIX was higher for the CNBr gel (48–51%) compared to the hydrazide gel (29–33%). This was also true for the efficiency based upon recovered FIX, which ranged from 36–40% for the CNBr gel and 17–20% for the hydrazide gel. As was the case with the anti-PC immunosor-

TABLE II

PERFORMANCE OF ANTI-FIX IMMUNOSORBENTS

Immunosorbent A was prepared from hydrazide gel by Manufacturer A and operated as described in the text. The Mab density was 1.87 mg Mab/ml gel and the bed volume was 4.9 ml. Immunosorbent CNBr, prepared from CNBr-activated Sepharose CL-2B, had a Mab density of 1.0 mg Mab/ml gel and a bed volume of 5.0 ml. Efficiency is as in the legend to Table I.

Immunosorbent	Run No.	Load (mg FIX)	Fallthrough and rinse (mg FIX)	Efficiency[a] (%)	Efficiency[b] (%)
A	1	3.84	1.86	29	17
	2	3.69	1.44	33	20
	3	3.81	1.83	29	20
CNBr	1	2.12	0.31	49	37
	2	2.10	0.35	48	40
	3	2.01	0.23	48	38
	4	2.08	0.21	51	36

[a] Efficiency based upon FIX bound to the immunosorbent.
[b] Efficiency based upon FIX recovered in the eluate.

bents, the immunosorbent efficiencies were lower based upon recovered as compared to bound FIX.

Table III summarizes the mean efficiency data for the experiments listed in Table I and II. For the anti-PC immunosorbents, the efficiencies based upon bound PC for hydrazide immunosorbents A(ii) and B were $49 \pm 3\%$ and $49 \pm 5\%$, significantly higher than the efficiency of the CNBr gel of $30 \pm 9\%$. However, this 1.6-fold increase in PC binding efficiency of the hydrazide gels did not result in a comparable increase in efficiency based upon PC that could be eluted from these immunosorbents. The efficiency based upon PC recovered in the eluates was $27 \pm 1\%$ and $26 \pm 2\%$ for

TABLE III

SUMMARY OF MEAN EFFICIENCIES OF IMMUNOSORBENTS

The mean efficiencies for the experiments listed in Table I and II were calculated. Efficiency is as defined in the legend to Table I.

Immunosorbent[a]	Efficiency (%)			
	(Based on protein bound)		(Based on protein recovered)	
	PC	FIX	PC	FIX
A(i)	$24 \pm 6 (5)^b$	N.A.[c]	$13 \pm 2 (5)$	N.A.
A(ii)	$49 \pm 3 (2)$	$30 \pm 2 (3)$	$27 \pm 1 (2)$	$19 \pm 2 (3)$
B	$49 \pm 5 (3)$	N.A.	$26 \pm 2 (3)$	N.A.
CNBr	$30 \pm 9 (3)$	$49 \pm 1 (4)$	$22 \pm 4 (3)$	$38 \pm 2 (4)$

[a] Immunosorbents are as given in the legends to Tables I and II.
[b] Mean $\pm$ S.D. with the number of experiments in parentheses.
[c] Not applicable.
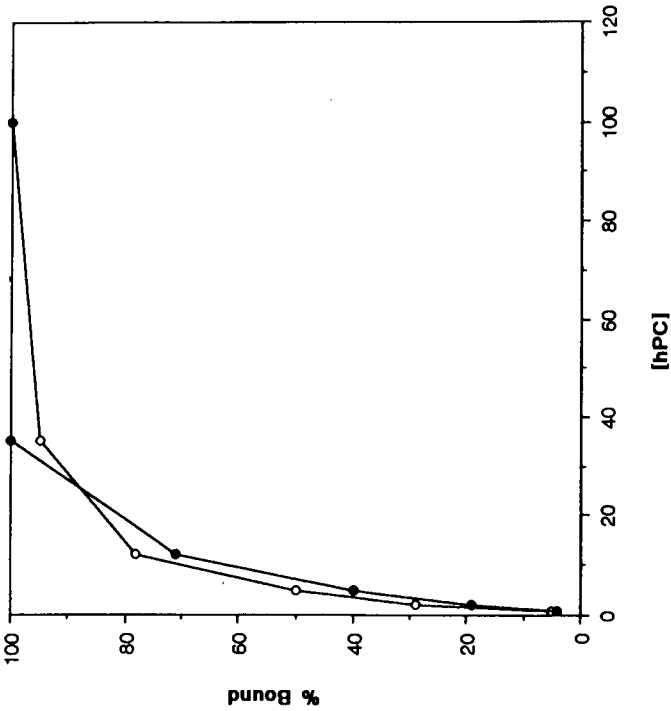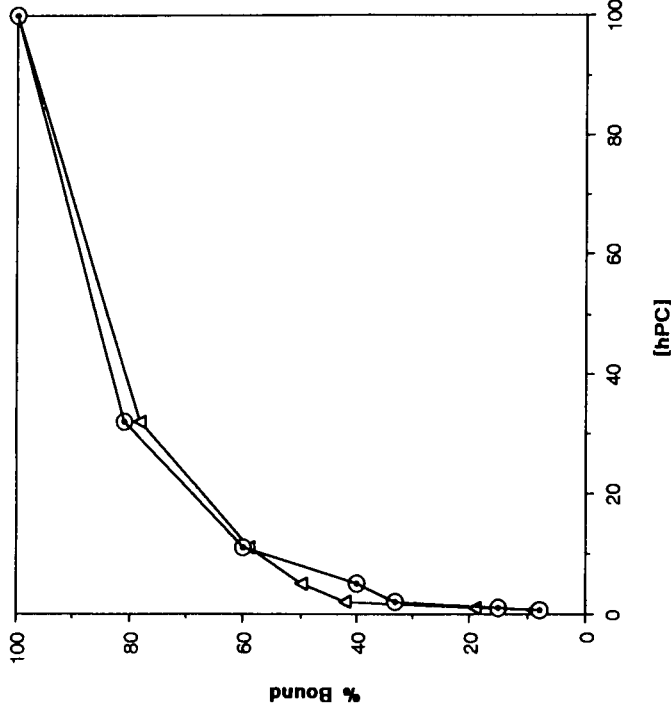
Fig. 2. Comparison of PC binding by native and oxidized anti-PC Mab. Native (untreated) and oxidized (periodate-treated) Mab was incubated with varying concentrations of PC, as indicated. The resulting PC–Mab complex was quantitated by ELISA as described in the Experimental section. ● = native Mab; ○ = oxidized Mab. The concentration of Protein C ([hPC]) is given in n*M*.

Fig. 3. Comparison of anti-PC Mab binding to PC purified by different methods. Anti-PC Mab (7D7B10) was incubated with increasing concentrations of PC, purified by conventional methods (△), by immunoaffinity chromatography using anti-PC Mab 7D7B10 (○), or anti-PC Mab 8861 (●). The resulting PC–Mab complex was quantitated by ELISA.

TABLE IV

SUMMARY OF MEAN RECOVERIES OF IMMUNOSORBENTS

The mean recoveries for the experiments listed in Tables I and II are tabulated. Recovery was calculated based upon the amount of bound protein recovered in the eluate (no brackets) or recovered in the eluate plus subsequent washes (in brackets).

Immunosorbent[a]	Recovery (%)	
	PC	FIX
A(i)	55 ± 12 (5)[b]	N.A.[c]
	[55 ± 12]	
A(ii)	52 ± 1 (2)	61 ± 5 (3)
	[52 ± 1]	[77 ± 6]
B	60 ± 9 (3)	N.A.
	[60 ± 9]	
CNBr	75 ± 8 (3)	75 ± 5 (4)
	[85 ± 5]	[85 ± 9]

[a] Immunosorbents are as given in the legends to Tables I and II.
[b] Mean ± S.D. with the number of experiments indicated in parentheses.
[c] Not applicable.

hydrazide gels A(ii) and B, respectively, compared to 22 ± 4% for the CNBr gel representing approximately a 20% increase in immunosorbent efficiency. The efficiency of hydrazide immunosorbent A(i) was less than that of the CNBr gel based upon both bound and eluted PC. For the anti-FIX immunosorbents, the efficiency of the CNBr gel was 49 ± 1% compared to 30 ± 2% for the hydrazide gel prepared by Manufacturer A based upon bound FIX and 38 ± 2% compared to 19 ± 2% for CNBr and hydrazide gels, respectively, based upon eluted FIX.

Table IV summarizes the mean recovery data for the immunosorbents. For each experiment, both protein specifically recovered in the eluate (specific recovery) as well as total protein recovered in the eluate plus subsequent wash pools (total recovery) was calculated as a percentage of the bound protein. For the anti-PC immunosorbents, the mean specific recovery of PC for the CNBr-coupled gel was 75% which was higher than found for the hydrazide immunosorbents which ranged from 52 to 60%. Likewise for the anti-FIX immunosorbents, the mean specific recovery of FIX was 75% for the CNBr gel as compared to 61% for the hydrazide gel. For both CNBr immunosorbents as well as for the anti-FIX hydrazide immunosorbent, additional protein was recovered in the buffered 2 M sodium chloride wash such that the total protein recovery was 77–85%. The anti-PC hydrazide immunosorbents were the exception, however, in that no additional PC was recovered following successive washes with buffered 2 M sodium chloride and buffered 2 M NaSCN.

In order to determine whether $NaIO_4$ treatment of the anti-PC Mab affected its ability to bind to PC, oxidized anti-PC Mab ($NaIO_4$-treated) and native anti-PC Mab (untreated) were compared by an ELISA (Fig. 2). The dose-response curves of PC binding to both oxidized and native Mab were very similar indicating that the periodate oxidation step did not impair the activity of the Mab.

In further experiments, the binding of 7D7B10 Mab to varying concentrations

TABLE V

CARBOHYDRATE COMPOSITION OF MURINE Mab AND Fab′ FRAGMENTS

Data from 14 h hydrolysis with 6 M hydrochloric acid, except for mannose data which is from 2 and 6 h hydrolysis with 2 M trifluoroacetic acid.

Sample	NAG (mol/mol)[a]	Galactose (mol/mol)	Mannose (mol/mol)	Sialic acid (mol/mol)
7D7B10 Mab	23.3	4.2	7.0	1-2
7D7B10 Fab′ (nc)[b]	4.1	0.5	nd[b]	na[b]
7D7B10 Fab′ (c)[b]	3.1	nd	nd	na
1H5B7 Mab	16.7	11.7	3.6	1–2
1H5B7 Fab′ (nc)	4.1	1.8	nd	na
1H5B7 Fab′ (c)	2.4	0.6	nd	na

[a] Molecular weights of 160 000 for Mab and 50 000 for Fab′ were assumed. NAG = N-acetylglucosamine.
[b] nc = Not corrected for Fc contamination; c = corrected for Fc contamination (5% in 7D7B10 Fab′ and 10% in 1H5B7 Fab′ as judged by desitometry of SDS-PAGE); nd = none detected; na = not analyzed.

of conventionally purified PC, or PC purified using either 7D7B10 or 8861 Mab was measured by ELISA. As shown in Fig. 3, the binding curves for purified PC from all three sources were indistinguishable. Conversely, similar ELISA experiments verified that an excess of PC was able to bind 100% of a limiting amount of 7D7B10 Mab, indicating that the anti-PC Mab preparation did not contain a subpopulation of Mab molecules that lacked the ability to bind PC (data not shown).

Because hydrazide immunosorbents are formed through the coupling of oligosaccharide chains, the carbohydrate content of the anti-PC and anti-FIX Mabs as well as their Fab′ fragments were analyzed. The results are presented in Table V. N-acetylglucosamine (NAG) was the predominant reducing sugar detected in either Mab with 23 residues per 7D7B10 IgG and 17 residues per 1H5B7 IgG using hydrochloric acid hydrolysis. Similar results were obtained using TFA hydrolysis (data not shown). The galactose content was considerably higher in the 1H5B7 Mab with 12 mol/mol compared to 4 mol/mol of 7D7B10 Mab. Mannose was only detected in the hydrochloric acid hydrolysates of the 7D7B10 Mab (5 mol/mol) and not the 1H5B7 Mab. However, when TFA hydrolysis was used which is less destructive to mannose, 7 mol/mol 7D7B10 was found and 4 mol/mol 1H5B7 Mab. No fucose was detected in either Mab when hydrochloric acid or TFA hydrolyzed samples were analyzed. Both Mabs contained 1–2 residues of sialic acid. Importantly, significant amounts of NAG were also found in the purified Fab′ fragments from either Mab. Correction for the small amount of Fc contamination in the Fab′ preparations (5% Fc contamination in the 7D7B10 Fab′ and 10% Fc contamination in the 1H5B7 Fab′) yielded 3.1 and 2.4 residues of NAG per Fab′ fragment from the 7D7B10 and 1H5B7 Mabs, respectively. Little or no galactose, mannose or fucose was detected in the Fab′ preparations.

DISCUSSION

The hydrazide- and CNBr-activated matrices used in the present studies were beaded agaroses which had similar porosities and particle sizes [27–29] and were

found to have minimal nonspecific adsorptive properties under the conditions used in these experiments. Therefore, these two systems should be sufficiently similar for a direct comparison of the effects of hydrazide and CNBr immobilization chemistry upon immunosorbent performance.

The concentration, distribution, and accessibility of reactive groups (such as hydrazides) on the agarose matrix may be of importance in determining the binding efficiency of a given immunosorbent. These reactive sites should have a uniform distribution and accessibility to achieve proper spacing of Mabs on the matrix and thus avoid clustering which could result in steric hindrance and lower efficiencies. Clustering of Mab for either the hydrazide- or CNBr-activated gels was likely to have been minimal because the total reactive groups on the matrix were in approximately a 1000-fold molar excess over that needed to couple Mabs at the low densities used in these experiments. These calculations are based upon the hydrazide linker concentrations given by the manufacturers [28,29] and the minimum concentration of CNBr-activated groups from the data of March et al. [38]. The Mab densities used in these experiments varied from 1.0 to 2.3 mg Mab/ml of gel. While the efficiency of immunosorbents on porous supports has been shown to decrease with increasing Mab densities, these effects were found to occur at considerably higher Mab densities than used in the present experiments [3,8]. In fact, varying the Mab density over the 1-2 mg/ml range had little effect on the efficiency of the CNBr-activated anti-FIX immunosorbent used in the present studies [9,45].

Both hydrazide- and CNBr-activated gels immobilize proteins under mild conditions which do not irreversibly denature or are non-denaturing to the antibodies evaluated in this study. While the hydrazide coupling was performed at a lower pH than the CNBr coupling procedure (pH 5.0–5.5 vs. pH 8.5), immobilization through the carbohydrate should preserve the conformational flexibility of the peptide backbone of the molecule thus allowing it to resume its normal conformation under antigen binding conditions at neutral pH. The Mabs used to form the hydrazide immunosorbents were oxidized in a 64- to 494-fold molar excess of $NaIO_4$ for 1 h at room temperature. Although these mild conditions are generally insufficient to oxidize amino acids of proteins [22], it seemed possible that the efficiencies of the hydrazide immunosorbents may have been adversely affected by loss of activity of the Mab as a result of $NaIO_4$ treatment. However, this was not the case as seen for the anti-PC Mab, where the oxidized and native Mab had indistinguishable PC binding curves.

The anti-FIX/FIX and the anti-PC/PC systems behaved similarly in these studies in that essentially quantitative recoveries of bound protein were obtained using the CNBr-coupled immunosorbents. For both the anti-FIX/FIX and anti-PC/PC CNBr-coupled immunosorbents, 75% of bound protein was recovered under specific mild elution conditions (millimolar concentrations of EDTA or $CaCl_2$, respectively). These mild conditions are thought to destabilize a conformation which is recognized by the Mab. In both cases, small amounts of additional protein were eluted in the 2 M sodium chloride was pool, such that 85% of the bound protein could be accounted for. For both systems, 52–61% of bound protein was recovered from the hydrazide-coupled immunosorbents under mild elution conditions. For the anti-FIX immunosorbent, additional FIX was recovered with the high salt wash such that 77% of the bound protein could be accounted for. In contrast, for the anti-PC hydrazide immunosorbent, no additional protein was recoverd with 2 M sodium chloride of 2 M

NaSCN. Because nonspecific protein adsorption was not observed with the glutar-aldehyde-blocked hydrazide matrix, it is likely that the lower recovery of PC can be attributed to the presence of covalently attached Mab. The possibility that this was due to a population of immobilized antibodies with higher avidity seems unlikely because further treatment with harsh elution conditions (2 M NaSCN) did not result in a desorption of PC not previously recovered by CaCl$_2$ elution. The reason for the lower recoveries of PC from the hydrazide gels is unknown.

Hydrazide-activated gels couple Abs through their carbohydrate residues. This offers several *potential* advantages. First, Ab coupling occurs through residues that are not involved in antigen-binding, thus providing a peptide-sparing effect. In contrast, CNBr-activated gels are linked to the matrix through reactive amino acids. As many such groups are present on a macromolecule like an Ab, linkage can occur through many sites on the protein including peptide regions that may be vital to the Ab-antigen interaction, thus compromising the acitivity of the bound Ab. Second, the carbohydrate groups on the Ab have the potential advantage of being able to act as a linker to space the molecule away from the matrix and thus improve its accessibility to the antigen. Conversely, the Abs of CNBr-activated gels can be expected to be located closer to the surface of the matrix giving rise to steric hindrance effects [10]. Third, linkage through the carbohydrate moieties is expected to give a higher degree of Ab orientation compared to coupling through amino acids, as the coupling is thought to involve only the Fc region of the molecule [21–25].Therefore, the hydrazide immunosorbents were expected to have higher bound Ab activities and efficiencies than CNBr-coupled immunosorbents.

Despite the *potential* advantages of site-directed coupling via carbohydrate residues, both the anti-PC and anti-FIX hydrazide immunosorbents failed to perform better than conventional CNBr-activated gels. In the case of the anti-FIX hydrazide immunosorbent, the efficiency was approximately one-half that of the comparable CNBr-coupled gel whether based upon bound FIX or specifically recovered FIX. In the case of the anti-PC immunosorbents, 2 out of 3 hydrazide gels had a 1.6-fold increase in PC binding efficiency compared to the CNBr-coupled gel. However, this increase was not translated into improved performance, because the efficiencies based upon specifically recovered PC were only 1.2-fold higher. It is interesting to note that 3- to 5-fold increases in antigen binding efficiency have been reported for hydrazide immobilized polyclonal antibodies relative to CNBr immunosorbents [22–25], while no increase [23,24] or at most a 2-fold increase [25] was found for hydrazide immobilized monoclonal antibodies. In most cases, the amount of bound antigen that could be eluted from the hydrazide immunosorbents was not reported in these studies.

Our results indicate that monoclonal antibodies immobilized to agarose matrices by site-directed coupling via carbohydrate residues on the Mab still have a restricted ability to bind to antigen. It is apparent that the presentation of carbohydrate is such that it does not result in significant changes in binding capacity relative to that seen with CNBr-coupled Mabs. Apparently, coupling through the well-conserved carbohydrate chains located in the Fc region [14–20] does not benefit antigen binding, albeit that these carbohydrate moieties could potentially impart several nm greater extension than the 1 nm spacer-arms used to increase the bound activity of β-galactosidase on a similar agarose matrix [10]. This may indicate that despite this site-directed coupling, there is still a considerable degree of variation in orientation of Ab in

terms of the spatial relationship, for example, between the Fab antigen-binding region and the matrix.

The presence of oligosaccharide in the CH_2 domain of the Fc fragment of immunoglobulins has been in part a reason for the development of carbohydrate-directed immobilization chemistry. However, N-linked glycosylation is dictated by the peptide sequence Asn–X–Ser which has also been shown to occur in the variable regions of the antigen-binding domain of rabbit, murine and human immunoglobulins [46–48]. For this reason, we analyzed the carbohydrate composition of the Mabs used in the present study, as well as the purified Fab' fragments derived from them. The sugar composition of both Mabs was consistent with the dibranched complex structure of N-linked oligosaccharides of murine IgG reported by others [19]. Importantly, both Mabs employed in this study had significant amounts of NAG in the Fab' fragment. Thus, some coupling via the Fab antigen-binding domain may have occurred which may have abrogated the potential advantage of site-directed coupling through the carbohydrate in the Fc region. The frequency of carbohydrate in the Fab region of monoclonal antibodies and the ability to control glycosylation at these sites, for example, by cell culture growth conditions [49] are additional factors which may impact the utility of carbohydrate-directed immobilization of antibodies.

CONCLUSION·

There was no advantage in terms of improved efficiency in the use hydrazide-activated immunosorbents over the more conventional CNBr-activated immunosorbents. Furthermore, the heavier protein losses observed with the hydrazide gels were an added disadvantage.

REFERENCES

1 S. J. Tarnowski, S. K. Roy, R. A. Liptak, D. K. Lee and R. Y. Ning, *Methods Enzymol.*, 119 (1986) 153.
2 S. J. Tarnowski and R. A. Liptak, *Adv. Biotechnol. Processes*, 2 (1983) 271.
3 J. W. Eveleigh and D. E. Levy, *J. Solid Phase Biochem.*, 2 (1977) 45.
4 M. T. W. Hearn, *J. Chromatogr.*, 376 (1986) 245.
5 M. Wilchek, T. Miron and J. Kohn, *Methods Enzymol.*, 104 (1984) 3.
6 H. A. Chase, *Chem. Eng. Sci.*, 39 (1984) 1099.
7 J. W. Goding, *Monoclonal Antibodies: Principles and Practice*, Academic Press, New York, 1983, Ch. 6, p. 188.
8 J. W. Eveleigh, in T. C. J. Gribnau, J. Visser and R. J. F. Nivard (Editors), *Affinity Chromatography and Related Techniques (Analytical Chemistry Symposium Series*, Vol. 9), Elsevier, Amsterdam, 1982, p. 293.
9 J. Tharakan, D. B. Clark and W. N. Drohan, *J. Chromatogr.*, 522 (1990) 153.
10 P. Cuatrecasas, *J. Biol. Chem.*, 245 (1970) 3059.
11 E. Steers, Jr., P. Cuatrecasas and H. B. Pollard, *J. Biol. Chem.*, 246 (1971) 196.
12 C. R. Lowe, M. J. Harvey, D. B. Craven and P. D. G. Dean, *Biochem. J.*, 133 (1973) 499.
13 D. R. Davies, E. A. Padlan, and S. Sheriff, *Ann. Rev. Biochem.*, 59 (1990) 439.
14 H. L. Spiegelberg, C. A. Abel, B. G. Fishkin and H. M. Grey, *Biochemistry*, 9 (1970) 4217.
15 T. Taniguchi, T. Mizuochi, M. Beale, R. A. Dwek, T. W. Rademacher and A. Kobata, *Biochemistry*, 24 (1985) 5551.
16 R. B. Parekh, R. A. Dwek, B. J. Sutton, D. L. Fernandes, A. Leung, D. Stanworth and T. W. Rademacher, *Nature (London)*, 316 (1985) 452.
17 F. Melchers, *Biochemistry*, 10 (1971) 653.
18 F. Melchers, *Biochem. J.*, 119 (1970) 765.

19   T. Mizuochi, J. Hamako and K. Titani, *Arch. Biochem. Biophys.*, 257 (1987) 387.

20   F. Mizuochi, T. Taniguchi, A. Shimizu and A. Kobata, *J. Immunol.*, 129 (1982) 2016.

21   D. J. O'Shannessy and W. L. Hoffman, *Biotechnol. Appl. Biochem.*, 9 (1987) 488.

22   D. J. O'Shannessy and R. H. Quarles, *J. Immunol. Methods*, 99 (1987) 153.

23   M. C. Little, C. J. Siebert and R. S. Matson, *BioChromatogr.*, 3 (1988) 156.

24   R. S. Matson and M. C. Little, *J. Chromatogr.*, 458 (1988) 67.

25   M. C. Cress and T. T. Ngo, *Am. Biotechnol. Lab.*, 7 (1989) 16.

26   J. V. Babshak and T. M. Phillips, *J.Chromatogr.*, 444 (1988) 21.

27   *Data Sheet: Sepharose and Sepharose CL Gel Filtration Media*, Pharmacia, Uppsala, 1985.

28   *Data Sheet: Affi-Gel Hz Agarose Gel*, Bio-Rad, Richmond, CA, 1989.

29   *Data Sheet: Hydrazide Avid Gel AX*, BioProbe International, Tustin, CA, 1989.

30   H. L. Wang, J. Steiner, F. Battey and D. Strickland, *Fed. Proc.*, 46 (1987) 2119.

31   C. L. Orthner, R. D. Madurawe, W. H. Velander, W. N. Drohan, F. D. Battey and D. K. Strickland, *J. Biol. Chem.*, 264 (1989) 18781.

32   W. H. Velander, C. L. Orthner, J. P. Tharakan, R. D. Madurawe, A. H. Ralston, D. K. Strickland and W. N. Drohan, *Biotechnol. Prog.*, 5 (1989) 119.

33   J. Tharakan, S. I. Miekka, H. E. Behre, B. D. Kolen, D. M. Gee, W. N. Drohan and D. B. Clark, *Thromb. Haemostas.*, 62 (1989) 56.

34   J. Tharakan, D. Strickland, W. Burgess, W. Drohan and D. B. Clark, *Vox Sang.*, 58 (1990) 21.

35   R. G. DiScipio, M. A. Hermodson, S. G. Yates and E. W. Davie, *Biochemistry*, 16 (1977) 698.

36   C. L. Orthner, A. H. Ralston, J. D. McGriff, D. M. Gee and W. N. Drohan, in preparation.

37   W. Kisiel, *J. Clin. Invest.*, 64 (1979) 761.

38   S. C. March, I. Parikh and P. Cuatrecasas, *Anal. Biochem.*, 60 (1974) 149.

39   R. Biggs, *Human Blood Coagulation, Haemostasis and Thrombosis*, Blackwell Scientific, Oxford, 1st ed., 1972, p. 614.

40   S. I. Miekka, *Thromb. Haemostas.*, 58 (1987) 349.

41   O. R. Ødegaard, K. Try and T. R. Anderson, *Haemostas.*, 17 (1987) 109.

42   U. K. Laemmli, *Nature (London)*, 227 (1970) 680.

43   L. Wiñen, *J. Biol. Chem.*, 231 (1959) 1971.

44   T. Mrcol and W. H. Velander, *Anal. Biochem.*, 195 (1991) 153.

45   J. Tharakan, presented at the *International Chemical Congress of Pacific Basin Societies*, Honolulu, HI, December 1989.

46   R. Melchers, *Biochemistry*, 8 (1969) 938.

47   Wood, *Cold Spring Harbor Symp. Quant. Biol.*, 32 (1967) 262.

      . W. Fanger and D. G. Smyth, *Biochem. J.*, 127 (1972) 757.

49   C. F. Goochee and T. Monica, *BioTechnol.*, 8 (1990) 421.

Diffusion of proteins in the chromatographic gel AcA-34

MOHSEN MOUSSAOUI, MOHAMED BENLYAS and PHILIPPE WAHL*

Centre de Biophysique Moléculaire, C.N.R.S., 1A Avenue de la Recherche Scientifique, 45071-Orléans Cedex 2 (France)

(First received February 18th, 1991; revised manuscript received May 3rd, 1991)

ABSTRACT

The reduced diffusion of globular proteins in the gel AcA-34 was measured. The proteins were labelled with fluorescein isothiocyanate. The partition coefficient of the labelled proteins in the gel was equal to that of the native proteins. This result means that the fluorescein residues do not induce any specific interaction between the macromolecules and the gel matrix. The D/D_0 value was measured by alternately determining the fluorescence recovery after photobleaching curves of the labelled protein solution either in the free state or included in a gel bead. Both values of D/D_0, as a function of the Stokes radius of the proteins and the partition coefficient of the proteins in the gel, agree with the values predicted previously. These results suggest that the retardation of the diffusion of the proteins in the AcA-34 gel is due to the obstruction effect of the gel matrix.

INTRODUCTION

One of the factors determining the efficiency of the separation of macro-molecules by gel chromatography is the diffusion coefficient of the solute in the gel beads which fill the chromatographic column [1]. There are some similarities between diffusion in the gel and other transport properties which operate in separation methods such as sedimentation in polymer solutions and electrophoresis [2]. Measurements of diffusion in chromatographic gels are still scarce [3,4] and the physical basis of the retardation of diffusion by a gel matrix is not yet firmly established [5]. For these reasons, measurements of diffusion in gels are needed.

In previous work, these authors measured the reduced coefficient of diffusion D/D_0 (where D and D_0 are the diffusion coefficients of the solute in the gel and in the free solvent, respectively) of fluorescein-labelled dextran fractions in Sephadex gel beads [6]. The technique used was fluorescence recovery after photobleaching (FRAP) [7].

In this method, a small region of a volume containing a mobile fluorescent molecule is exposed to a brief intense pulse of light, thereby causing an irreversible photochemical bleaching of the fluorophores. The diffusion coefficient is determined by measuring the rate of recovery of fluorescence which results from transport into the bleached region from the unirradiated surroundings.

In this work, the same method was used to measure the diffusion of

fluorescein-labelled globular proteins in the gel AcA-34. The variation of D/D_0 was studied as a function of the Stokes radius of the protein molecules. The partition coefficient of these proteins in the gel was also determined and the variation of D/D_0 as a function of the partition coefficient was measured.

MATERIALS AND METHODS

Origin of the products

Bovine pancreas ribonuclease (ref. B-5112S), bovine pancreas chymotrypsinogen A (ref. C-4879), hen egg albumin (ref. A-2512), bovine serum albumin (BSA) (ref. A-7638), rabbit muscle aldolase (ref. A-7145) and bovine thyroid thyroglobulin (ref. T-1001) were purchased from Sigma. Catalase and ferritin were used from a gel filtration calibration kit from Pharmacia. Fluorescein isothiocyanate isomer I (FITC) was purchased from Molecular Probes (ref. F-143) and Sigma (ref. 7250). Dextran blue 2000 was from Pharmacia.

The Ultrogel AcA-34 was from Industrie Biologique Française (IBF) (lot 8379).

Macromolecule labelling

The proteins were labelled as follows: 50 mg of protein were dissolved in 2 ml of sodium hydrogencarbonate buffer solution at pH 9. A 2.6-ml volume of 1 mg/ml FITC in buffer solution A (10 mM sodium phosphate, 0.15 M sodium chloride, 1 mM sodium azide pH 8) was added. The mixed solution was stored at room temperature, away from light, for 5 h. The labelled protein was then dialysed against buffer A (pH 8) for 1–2 weeks in a cold room (4°C) with frequent changes of the dialysate. In the case of BSA, the following additional treatment was applied: the labelled protein was eluted on a Sephadex G-25 column with 20 mM acetic acid at pH 3 [8]. The solution was then dialysed for 24 h against buffer A with frequent changes of the dialysate.

The absence of free fluorescein in the preparations was checked by chromatography on a silica gel 60 plate (Merck ref. N-5724) with an eluent consisting of n-butanol–water–ethanol–acetic acid (50:20:20:10).

The labelling ratio was determined by spectrophotometry. The absorption coefficients of the fluorescein residues at 495 and 280 nm were taken as equal to 72 000 cm^{-1} M^{-1} and 16 500 cm^{-1} M^{-1}, respectively [8]. The absorption coefficient of the proteins at 280 nm was taken from Fasman [9].

Dextran 2000 from Pharmacia (molecular weight 2 000 000) was labelled with FITC by the method of De Belder and Granath [10]. Fractions of fluorescein dextran, excluded from the AcA-34 gels, were obtained by chromatography on the gel Sepharose Cl-2B.

Gel chromatography

Native and labelled proteins were chromatographed on a column (90 × 1.35 cm) filled with the AcA-34 gel. The column was equilibrated with buffer A. A 2-ml volume of a solution of a protein at a concentration of 5 mg/ml in the same buffer solution was injected onto the column. The volume of a fraction collected at the bottom of the column was about 2 ml; the exact volume was determined by weight. The flow-rate was 5–7 ml/h. The void volume, V_0, was determined by the elution of Dextran blue 2000 and absorption measurements at 305 nm. The elution diagrams of

the native and labelled proteins were obtained by measuring the absorbance of each fraction at 280 and 495 nm, respectively.

The partition coefficient of a protein sample (K_{AV}) was determined according to the formula of Laurent and Killander [11]:

$$K_{AV} = \frac{V_e - V_0}{V_t - V_0}$$ (1)

where V_t is the volume of the gel bed in the column and V_e the elution volume of the fraction situated at the peak of the elution diagram. V_t was determined from the height and diameter of the column.

Measurements of the reduced coefficient of diffusion

For these measurements the labelled protein solution was obtained by eluting the main chromatographic fraction of the AcA-34 column in a Sephadex G-25 column.

These measurements were performed with the FRAP apparatus previously described [6]. The laser beam was horizontal and crossed the vertical microscope axis at right-angles, in the object plane.

The gel beads were immersed in a solution of fluorescent macromolecules contained in a small glass cuvette. The FRAP curves were measured with the laser beam crossing a single gel bead and the surrounding solvent alternately. Both measurements were repeated from seven to twenty times.

The FRAP curves were fitted with the function of Yguerabide et al. [12]:

$$F(t) = \frac{F_0 + F_\infty t/t_{1/2}}{1 + t/t_{1/2}}$$ (2)

where F_0, F_∞, are, respectively, the fluorescence intensities emitted immediately after the bleaching pulse and at an infinite time after bleaching. $t_{1/2}$ is the half-time of recovery and t is time.

Eqn. 2 was fitted by the non-linear least-squares method of Marquardt [23] on an IBM-PS2 computer.

The fraction of freely diffusing molecules (or recovery fraction), L, was calculated by the following formula:

$$L = (F_\infty - F_0)/(F_i - F_0)$$ (3)

where F_i is the intensity before bleaching.

The bleaching fraction (B) is defined as:

$$B = (F_i - F_0)/F_i$$ (4)

Eqn. 2 is an approximation of the function of Axelrod et al. [7] which correctly describes that function when the bleaching fraction is smaller than 0.85 [12].

The reduced diffusion coefficient of a protein in a gel was obtained by applying the following relationship [6]:

$$\left(\frac{D}{D_0}\right) = \left(\frac{(t_{1/2})_0}{t_{1/2}}\right) \cdot \left(\frac{\beta}{\beta_0}\right)$$ (5)

where D and D_0 are the coefficients of diffusion in the gel and in the free solvent, respectively; $t_{1/2}$, $(t_{1/2})_0$ are the half-times of recovery measured on the bead and on the surrounding solution, respectively; and the factor β or β_0 depends on the bleaching fraction of the molecules included in the bead or in the solvent, respectively. The values of β and β_0 have been determined by comparing the function of Axelrod et al. [7] with eqn. 2 [12].

It has already been noted that the fluorescence was not zero for fluorescein dextran fractions excluded from a gel [6]. This stray fluorescence came from the fluorescence track of the laser beam in the free solution surrounding the bead. This stray fluorescence did not influence the value of D/D_0 measured for the protein samples, except for the thyroglobulin sample which had a very low partition coefficient in the gel.

In the thyroglobulin sample the fluorescence of the macromolecules included in a bead was small and the stray fluorescence was therefore relatively important. To take this contribution into account, the FRAP measured on the bead immersed in a thyroglobulin solution was analysed with a sum of two terms, as follows:

$$F(t) = \frac{F_0^1 + F_\infty^1 t/t_1}{1 + t/t_1} + \frac{F_0^2 + F_\infty^2 t/t_2}{1 + t/t_2} \tag{6}$$

where the sub- and superscripts 1 and 2 refer to the molecules surrounding the bead (stray fluorescence) and to the fluorescence of the molecules included in the gel, respectively.

Eqn. 6 is equivalent to eqn. 7:

$$F(t) = C_1\left(\frac{F_0 + F_\infty t/t_1}{1 + t/t_1}\right) + (1 - C_1)\left(\frac{F_0 + F_\infty t/t_2}{1 + t/t_2}\right) \tag{7}$$

where

$$F_0 = F_0^1 + F_0^2$$

$$F_\infty = F_\infty^1 + F_\infty^2$$

$$C_1 = \frac{L_1}{L}\frac{B_1}{B}\frac{F_i^1}{F_i} \tag{8}$$

F_i^1, L_1 and B_1 are the prebleaching intensity, the recovery fraction and the bleaching fraction of the stray fluorescence.

It was found experimentally that L_1 and L were equal to 1 and that B_1 was approximately equal to B. Therefore eqn. 8 becomes:

$$C_1 = F_i^1/F_i \tag{9}$$

t_2 is the parameter which allows the calculation of D/D_0 (eqn. 5). t_2 was obtained by fitting eqn. 7 to the experimental FRAP. C_1 and t_1 were considered as fixed parameters and were determined as follows.

Gel beads were immersed in a solution of a fluorescent dextran fraction of high molecular weight which was excluded from the gel. The prebleaching fluorescences F_B on a bead and F_f in the free solution were measured successively. The same measurements were made on a bead immersed in a labelled thyroglobulin solution. C_1 was then given by the following relationship:

$$C_1 = \left(\frac{F_B}{F_f}\right)_e \bigg/ \left(\frac{F_B}{F_f}\right)_p \tag{10}$$

where e and p refer to the dextran and protein solutions, respectively.

To obtain t_1 the half-time of recovery of FRAP curves measured on a bead and in the free solution of the high-molecular-weight dextran were measured successively. If α is the ratio of these half-times, t_1 is equal to the product of α by the $t_{1/2}$ value measured in the free solution of the labelled thyroglobulin.

RESULTS

Chromatography of proteins on a gel column

Eight native proteins, namely ribonuclease A, α-chymotrypsinogen A, ovalbumin, BSA, aldolase, catalase, ferritin and thyroglobulin were chromatographed on a column of AcA-34 gel. The partition coefficients, K_{AV}, of these proteins were calculated according to eqn. 1.

The proteins were labelled with FITC and purified. The study of labelled ferritin and catalase was not continued as a denaturation of the proteins occurring during the preparation.

Five of these labelled samples were also chromatographed on the same column. Table I shows that the partition coefficients of the labelled and native proteins were equal within the range of experimental accuracy.

For a macromolecule which does not bind to the gel matrix, the partition coefficient between the gel and the surrounding solution is equal to the volume fraction available to the macromolecule in the gel [11]. In the Ogston model the gel is made up

TABLE I

COMPARISON OF THE PARTITION COEFFICIENTS OF THE NATIVE AND LABELLED PROTEINS

Proteins	Labelling ratio	K_{AV}	
		Native	Labelled
Ribonuclease A	0.56	0.91	0.89
Chymotrypsinogen A	1.86	0.81	0.79
Ovalbumin	1.39	0.63	0.62
Serum albumin	1.9	0.52	--
Aldolase	4.8	0.40	0.37
Thyroglobulin	17	0.08	0.1

of a random network of straight fibres, and the partition coefficient of a spherical molecule can be written as [11,13]:

$$K_{AV} = \exp[-\pi l (R + R_f)^2] \tag{11}$$

where l is the total length of fibres per unit volume, R is the radius of the molecule and R_f is the radius of a fibre.

Eqn. 11 was fitted to the variation of the K_{AV} value of proteins in the AcA-34 gel as a function of the protein Stokes radius R_S (see Fig. 1). The values of R_S were taken from ref. 14. The following parameter values were obtained by the method of non-linear least-squares:

$$l = 1.05 \pm 0.16 \, \text{nm}^{-2}$$

$$R_f = 0.5 \pm 0.3 \, \text{nm} \tag{12}$$

The AcA-34 gel consists of 3% polyacrylamide and 4% agarose gels [15]. Its sieving properties are expected to be those of the polyacrylamide component, the agarose component essentially giving the rigidity to the gel beads [16]. This is confirmed by comparing the l and R_f values of eqn. 12 to those obtained by protein chromatography on polyacrylamide [17]. This comparison shows that the AcA-34 gel has the sieving properties of a polyacrylamide gel with a low bisacrylamide content.

Determination of the reduced diffusion coefficient of proteins in a AcA-34 gel bead
This was performed by FRAP as described under Materials and methods. Eqn. 2 satisfactorily reproduced the experimental curves after curve-fitting. In every case it was found that the fraction of fluorescence recovery L was equal to 1. This showed that
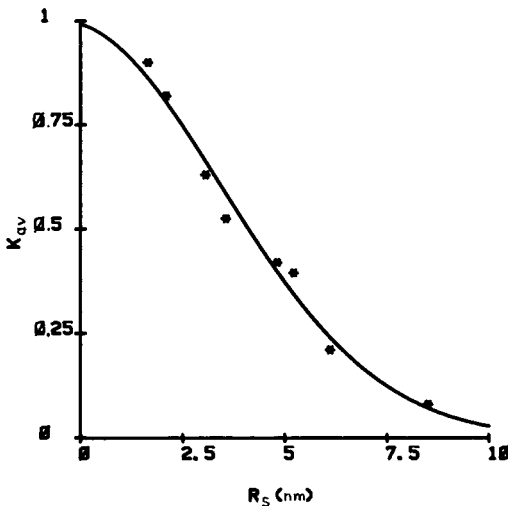
Fig. 1. Partition coefficient of globular proteins in the AcA-34 gel as a function of the Stokes radius of the protein. The continuous line represents eqn. 11 after curve-fitting.
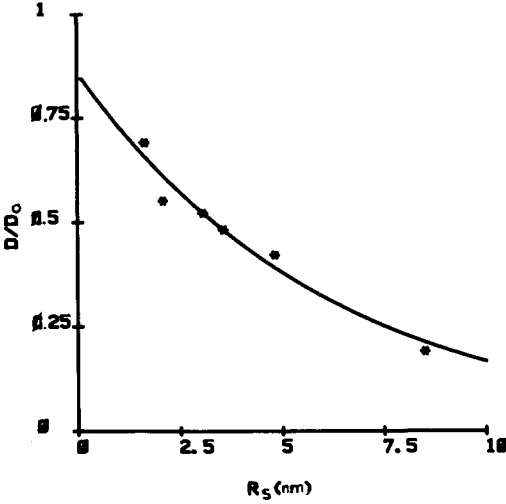
Fig. 2. Reduced diffusion coefficient of fluorescein-labelled proteins in the AcA-34 gel as a function of the Stokes radius of the protein. The continuous line represents eqn. 13 after curve-fitting.

there was no interaction between the proteins and the gel matrix, leading to a slow exchange between the free and the bound species. The reduced coefficient of diffusion was determined by eqn. 5.

In the case of thyroglobulin, which had a small K_{AV} value, there was a significant contribution of the stray fluorescence, and consequently the FRAP curves were fitted by eqn. 7.

The variation of D/D_0 as a function of R_S is plotted in Fig. 2, and as a function of K_{AV} in Fig. 3.
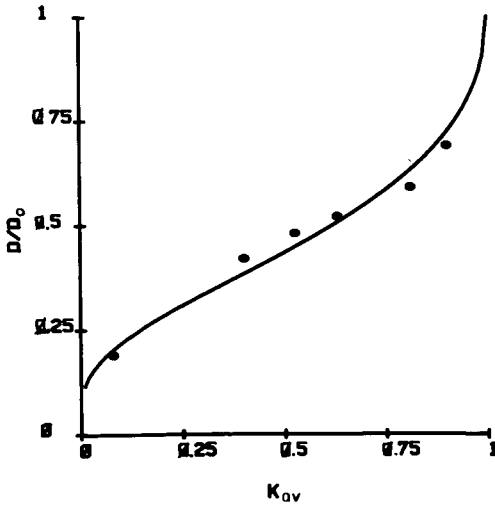
Fig. 3. Reduced diffusion coefficient of fluorescein-labelled proteins in AcA-34 gel as a function of the protein partition coefficient in the same gel. The continuous line represents eqn. 15.

DISCUSSION

The FRAP method is a convenient and relatively simple method for measuring the diffusion of fluorescent molecules in a single gel bead. This method was previously used to measure the diffusion of fluorescein dextran fractions in Sephadex gels [6]. The diffusion of labelled proteins in Sepharose was also measured [18].

It is necessary to label the macromolecules with covalently linked fluorescent residues. The diffusion coefficient of the parent non-labelled molecules in the gel will be equal to that of the labelled molecules if the fluorescent residues do not induce additional interactions with the gel matrix. This condition may be checked by chromatography as described earlier.

The fluorescent track produced by the laser beam in the free solution surrounding the bead brings about a stray fluorescence which becomes relatively important when the partition coefficient of the macromolecules in the gel is small (<0.1). Consequently the determination of the diffusion coefficient in the gel of such macromolecules becomes complicated and inaccurate.

It was found that the stray fluorescence decreased when the diameter of the bead increased. This stray fluorescence can also be decreased by reducing the diameter of the microscope-photometer diaphragm. The volume of the illuminated region in the bead must be small compared to the total volume of the bead to avoid boundary effects on the diffusion [19].

From these considerations, it is concluded that there is a minimum diameter under which the diffusion coefficient in the gel becomes difficult to measure. This limiting size depends on the optical configuration of the laser beam and of the fluorescence measurement system. With this optical arrangement the bead diameter should not be smaller than 50 μm.

It was found that the partition coefficient of the fluorescein-labelled proteins in AcA-34 was equal to the partition coefficient of the native proteins. This shows that the fluorescein residues did not induce any interaction of the macromolecules with the gel matrix. As already discussed, the chromatographic properties of the protein in AcA-34 are explained by the sieve properties of its polyacrylamide component which does not contain charged groups. Furthermore, the salt concentration used in the elution buffer will decrease the electrostatic interactions. Fig. 2 shows that there was a regular decrease of D/D_0 as R_S increased, which cannot be explained by hydrophobic or hydrogen bonding. Such interactions are expected to depend on the primary, secondary and tertiary structure of the protein molecules and not on their molecular size. Two main effects may cause this behaviour [5]: (1) the hydrodynamic effect, in which the gel fibres increase the hydrodynamic drag exerted by the solvent on the solute molecule; and (2) the obstruction effect, in which the presence of impenetrable, immobile polymer molecules increases the path length of the solute diffusion. Several theoretical works deal with these physical principles and provide mathematical expressions of D/D_0 as a function of the radius of the solute molecules [20–22].

The parameters of these expressions were fitted to the experimental variation of D/D_0 as a function of the Stokes radius of the protein molecules. These calculations were performed by the non-linear least-squares method of Marquardt [23]. In this method the parameter values are determined which minimize χ_2, the sum of the square of the differences between the predicted and experimental D/D_0 values.

None of these theoretical formulae were satisfactory. After fitting them to the data the value of χ_2 remained high. In addition, the values of the parameters were not in agreement with their physical meanings. These discrepancies may be partly ascribed to the crudeness of the matrix models on which the calculations were based.

The matrix model of Ogston [13], which was used to derive eqn. 9 [11], appears to be more realistic. The same model supplied the basis of the theory of diffusion in gels [2]. According to this theory, the reduced diffusion coefficient may be written as follows:

$$\frac{D}{D_0} = A\exp(-BR) \tag{13}$$

where

$$A = \exp[-(\pi l/R_f)^{1/2}]$$
$$\tag{14}$$
$$B = (\pi l)^{1/2}$$

The curve representing eqn. 13 with A and B fitted to these experimental data is represented in Fig. 2. The χ_2 value is better than any value obtained with the other theoretical expressions quoted earlier. The values of A and B are in fairly good agreement with the values calculated from eqn. 14 when replacing l and R_f by the values obtained from the K_{AV} data (eqn. 12).

Combining eqns. 13 and 14 leads to the relationship [2]:

$$\frac{D}{D_0} = \exp[(-\ln K_{AV})^{1/2}] \tag{15}$$

As seen in Fig. 3, this function describes the experimental results reasonably well. It may be concluded that:

(1) The partition coefficient of globular proteins in the AcA-34 gel is described well by the Laurent and Killander equation (eqn. 11).

(2) The variation of the reduced diffusion coefficient of the proteins in this gel, as a function of R_S, agrees with the prediction of Ogston et al. [2] (eqns. 13 and 14). The variation of D/D_0 as a function of K_{AV} is also in agreement with the theory (eqn. 15).

According to this theory the diffusion coefficient of a solute is decreased by the obstruction effect exerted by the gel matrix. Therefore these results suggest that the obstruction effect is an important cause of the diffusion retardation of the globular proteins in the AcA-34 gel.

REFERENCES

1 J. C. Giddings, Dynamics of Chromatography, Marcel Dekker, New York, 1965.
2 A. Ogston, B. N. Preston and J. D. Wells, Proc. R. Soc. London Ser. A., 333 (1973) 297.
3 P. Y. Key and D. B. Sellen, J. Polym. Sci. Polym. Phys., 20 (1982) 659.
4 I. Noshio, J. C. Reina and R. Bansil, Phys. Rev. Lett., 59 (1987) 684.
5 A. H. Muhr and J. M. U. Blanshard, Polymer, 23 (1982) 1012.

6 E. Poitevin and Ph. Wahl, *Biophys. Chem.*, 31 (1988) 247.

7 D. Axelrod, D. E. Koppel, J. Schlessinger, E. Elson and W. W. Webb, *Biophys. J.*, 16 (1976) 1055–1069.

8 R. R. Chen, *Arch. Biochem. Biophys.*, 133 (1969) 263.

9 G. Fasman (Editor), *Handbook of Biochemistry and Molecular Biology —Proteins*, Vol. II, CRC Press, Boca Raton, FL, 3rd ed., 1976.

10 A. N. De Belder and K. Granath, *Carbohydr. Res.*, 30 (1973) 375.

11 T. C. Laurent and J. Killander, *J. Chromatogr.*, 14 (1964) 317.

12 J. Yguerabide, J. A. Schmidt and E. E. Yguerabide, *Biophys. J.*, 40 (1982) 69–75.

13 A. G. Ogston, *Trans. Faraday Soc.*, 54 (1958) 1754–1757.

14 *Gel Filtration Calibration Kit Instruction Manual*, Pharmacia, Uppsala, 1985.

15 *Ultrogel AcA and Ultrogel A —Product Information Sheet No. 200908*, Reactifs Industrie Biologique Française, Villeneuve-la Garenne.

16 E. Boschetti, R. Tixier and R. Garelle, *Sci. Tools*, 21 (1974) 35.

17 J. S. Fawcett and C. J. O. R. Morris, *Sep. Sci.*, 1 (1966) 9.

18 M. Moussaoui, M. Benlyas and P. Wahl, in preparation.

19 H. Quian and E. L. Elson, *J. Cell Biol.*, 106 (1988) 1921–1923.

20 F. Renkin, *J. Gen. Phys.*, 38 (1954) 225.

21 R. F. Cukier, *Macromolecules*, 17 (1984) 252–255.

22 A. R. Altenberger and M. Tirrel, *J. Chem. Phys.*, 80 (1984) 2208.

23 D. W. Marquardt, *J. Soc. Ind. Appl. Math.*, 11 (1963) 431–441.

CHROMSYMP. 2361

Retention data for five ketotrichothecenes in reversed-phase high-performance liquid chromatography with different eluent systems[a]

S. N. LANIN* and Yu. S. NIKITIN

Department of Chemistry, Lomonosov State University of Moscow, 119899 Moscow (USSR)

(First received August 21st, 1989; revised manuscript received April 1st, 1991)

ABSTRACT

The effect of the eluent composition (nature of the modifier and its mole fraction in the mobile phase) on the retention of trichothecene mycotoxins of group B (derivatives of 12,13-epoxytrichothecene-9), *i.e.*, desoxynivalenol (DON), nivalenol, DON-3-acetate, DON-15-acetate and 7-desoxy-DON was studied. Ethanol, acetonitrile or tetrahydrofuran were used as the organic component (modifier) of the binary water–organic mobile phases. The retention mechanism and separation selectivity of the trichothecene mycotoxins in reversed-phase high-performance liquid chromatography (RP-HPLC) on Nucleosil C-18 is discussed. Optimum conditions were determined for the separation of the five trichothecene mycotoxins with the use of RP-HPLC under isocratic conditions.

INTRODUCTION

Trichothecene mycotoxins are a group of chemically similar secondary metabolites of the *Fusarium* mould fungus. Structurally they belong to derivatives of 12,13-epoxytrichothecene-9 and can be classed into two groups: group B with the carbonyl oxygen atom in position 8 and group A without this atom (Fig. 1) [1].

The purpose of this work was to optimize the conditions for determining trichothecene mycotoxins of group B in grain samples by reversed-phase high-performance liquid chromatography (RP-HPLC) using a Milichrome microcolumn chromatograph (USSR).

EXPERIMENTAL

Instruments and reagents

A liquid microcolumn chromatograph (Milichrome) equipped with a syringe pump (eluent flow-rate 2–600 μl/min) and a spectrophotometric detector (spectral

---
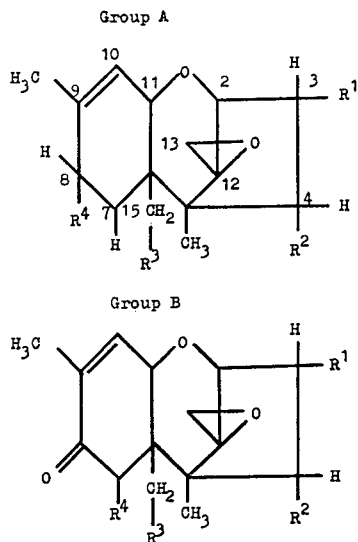
Fig. 1. Structures of trichothecene mycotoxins. Group A: T-2 tetraol, $R^1 = R^2 = R^3 = R^4 = OH$; DAS, $R^1 = OH$, $R^2 = R^3 = OAc$, $R^4 = H$; HT-2 toxin, $R^1 = R^2 = OH$, $R^3 = OAc$, $R^4 = -OC(O)C_4H_9$; T-2 toxin, $R^1 = OH$, $R^2 = R^3 = OAc$, $R^4 = -OC(O)C_4H_9$. Group B: nivalenol, $R^1 = R^2 = R^3 = R^4 = OH$; DON, $R^1 = R^3 = R^4 = OH$, $R^2 = H$; 7-desoxy-DON, $R^1 = R^3 = OH$, $R^2 = R^4 = H$; DON-3-acetate, $R^1 = OAc$, $R^2 = H$, $R^3 = R^4 = OH$; DON-15-acetate, $R^1 = R^4 = OH$, $R^2 = H$, $R^3 = OAc$. OAc = acetate.

range 190–360 nm) was used. The steel column (62 × 2 mm I.D.) was packed with Nucleosil C_{18} (specific surface area 300 m^2/g, mean particle diameter 5 μm) using the suspension technique. The retention volume of a non-sorbed substance (V_0) was measured by using sodium nitrite and was 89 μl; the column efficiency with respect to desoxynivalenol was 2500–3000 theoretical plates. The UV spectra of the substances were recorded in the range 190–360 nm with a 2-nm spacing in the detector cell where the flow of the mobile phase was preliminarily stopped. The reference cell was filled with the eluent.

The following retention parameters were determined using the chromatograms: the adsorbate capacity factor $k' = (V_R - V_0)/V_0$, where V_R is the adsorbate retention volume, and the relative retention volume (selectivity) for pairs of components, $\alpha_{i/j} = k'_i/k'_j$, where k'_j and k'_i are the capacity factors of substances j and i.

Ethanol, acetonitrile (ACN) and tetrahydrofuran (THF) were purified by distillation; acetonitrile was preboiled with potassium permanganate and THF was distilled over potassium hydroxide. Solutions of desoxynivalenol (DON), nivalenol, DON-3-acetate, DON-15-acetate and mixtures of DON with 7-desoxy-DON in methanol were used. In addition, samples of grain extracts purified and evaporated to dryness were used. The extraction mixture was water–acetonitrile (1:5) and adsorption purification of the extracts was performed on glass columns packed with AGN-type active carbon and Celite-545. The solutions and purified extracts were provided by the Laboratory of Mycotoxicology, All-Union Research Institute of Veterinary Sanitation.

Chromatographic measurements

DON solutions with concentrations of 1, 5, 10, 20, 40 and 200 μg/ml were prepared by sequential dilution of the initial solution (10 mg/ml) with water–THF (76:24). Evaporated samples of grain extracts were also dissolved in 1 ml of this mixture, which was then used as the eluent for the determination of DON. A test sample of the solution investigated (5 μl) was taken with the needle of the eluent feeder of the chromatograph (0.5–20 μl range with 0.1-μl spacing). The eluent flow-rate was 50 μl/min. The detection wavelength was 224 nm.

RESULTS AND DISCUSSION

The most difficult pairs to separate are DON–7-desoxy-DON and DON-3-acetate–DON-15-acetate. Separation of the latter using HPLC has not been described in literature. Separation of the former has been attained by using much more polar eluents (containing 10% of methanol [2]). In this case, k' increases to 15 and higher [3], which makes the analysis longer and more complicated and the simultaneous determination with DON in mixtures with more hydrophobic trichothecenes (such as acetates) under isocratic conditions impossible. For this reason, we investigated less polar organic modifiers for the optimization of the eluent composition in order to determine simultaneously all five mycotoxins investigated.

The following requirements were established for choosing the modifier: unlimited solubility in water, low viscosity, ready availability, low absorption threshold in the UV range and classification with various groups of selectivity according to Snyder and Kirkland [4,5]. Ethanol, acetonitrile and tetrahydrofuran were chosen. We employed the strategy of De Galan and co-workers [6–8] to find the optimum composition of the eluent. The investigation of the dependence of the retention of trichothecene mycotoxins on the composition of binary aqueous eluents was carried out first. The data (capacity factors, k', and relative retention volumes, α) for three binary systems are given in Table I.

Fig. 2 and Table I show that the retention of trichothecene mycotoxins increases with increasing hydrophobity. Fig. 2 shows that dependence of $1/k'$ on N_b is linear. For this reason, the dependence of the capacity factor on the eluent composition (the nature of the modifier and its mole fraction in the mobile phase) for DON-3-acetate, the most retained sorbate of those studied, was considered for the optimization of the duration of analysis. Fig. 3 shows that large amounts of polar modifier compared with the less polar modifier should be introduced into the eluent in order to attain the same retention value for mycotoxins, *e.g.*, $CH_3CN > C_2H_5OH > C_4H_8O$. The dependence of the mole fraction of the mobile phase modifier (N_b) corresponding to the retention of DON-3-acetate ($k' = 10$; see Fig. 3) on the polarity, P', of the modifier is linear (Fig. 4).

When ethanol is employed as a modifier, the separation selectivity is low: DON and 7-desoxy-DON are not separated at all ($\alpha_{3/2} = 1.0$) and DON-3- and -15-acetate are poorly separated ($\alpha_{5/4} = 1.05$) (see Fig. 5 and Table I).

The selectivity of the trichothecene separation with the use of acetonitrile-containing mobile phases is higher than that with ethanol-containing mobile phases, although it remains insufficient for complete separation of DON and 7-desoxy-DON and particularly of DON-3- and -15-acetate. The separation selectivity of the pair

TABLE I

DEPENDENCE OF CHROMATOGRAPHIC PARAMETERS OF TRICHOTHECENE SEPARATION ON THE MOBILE PHASE COMPOSITION

Mobile phase	Composition (%, v/v, of organic component)	Capacity factor (k')					Relative retention volume (α)					
		Nivalenol (1)	DON (2)	7-desoxy-DON (3)	DON-3-acetate (4)	DON-15-acetate (5)	2/1	3/1	3/2	2/3	5/4	4/5
Ethanol–water	10	2.16	4.92	4.92	21.47	21.47	2.27	2.27	1.00	1.00	—	—
	15	1.57	3.16	3.16	14.40	15.20	2.01	2.01	1.00	1.00	1.06	0.95
	20	1.15	2.17	2.17	7.31	7.66	1.89	1.89	1.00	1.00	1.05	0.95
	25	0.85	1.58	1.58	5.07	5.29	1.85	1.85	1.00	1.00	1.04	0.96
	30	0.66	1.16	1.16	3.93	3.93	1.75	1.75	1.00	1.00	1.00	1.00
Acetonitrile–water	18	2.46	7.46	8.38	21.47	21.47	3.03	3.40	1.12	0.89	—	—
	25	1.76	5.68	6.45	21.47	21.47	3.23	3.66	1.14	0.88	—	—
	33	1.40	2.83	3.09	16.29	17.98	2.02	2.20	1.09	0.92	1.10	0.91
	36	1.36	2.40	2.61	13.72	13.72	1.76	1.92	1.09	0.92	1.00	1.00
	40	1.25	1.92	2.08	9.39	8.86	1.54	1.66	1.08	0.92	0.94	1.06
	50	1.06	1.48	1.62	5.52	5.06	1.40	1.53	1.09	0.91	0.92	1.09
Tetrahydrofuran–water	15	1.63	3.00	2.52	13.56	13.35	1.84	1.55	0.84	1.19	0.98	1.02
	18	1.30	2.22	1.85	8.11	7.49	1.71	1.42	0.83	1.20	0.92	1.08
	20	1.26	2.16	1.81	7.79	7.17	1.71	1.43	0.84	1.19	0.92	1.09
	25	1.08	1.88	1.54	6.08	5.37	1.74	1.42	0.82	1.22	0.88	1.13
	30	1.01	1.70	1.43	4.52	3.85	1.68	1.42	0.84	1.19	0.85	1.17
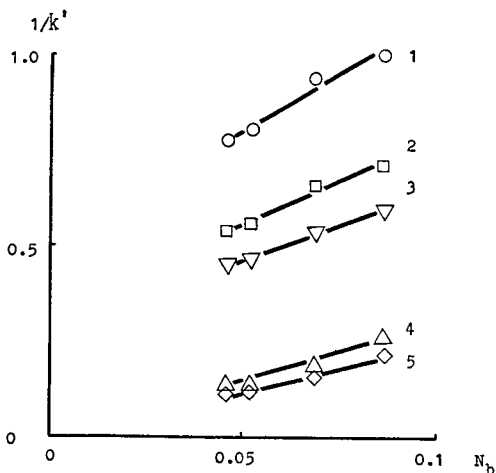
Fig. 2. Dependence of $1/k'$ for trichothecene mycotoxins on the composition of the mobile phase (N_b) modified with THF. 1 = Nivalenol; 2 = 7-desoxy-DON; 3 = DON; 4 = DON-15-acetate; 5 = DON-3-acetate.

7-desoxy-DON–DON is virtually constant $(\alpha_{3/2} \approx 1.10)$ over the entire concentration range of acetonitrile (18–50%). The highest selectivity for the pair DON-3-acetate–DON-15-acetate $(\alpha_{5/4} = 1.10)$ was observed at an acetonitrile concentration of 33% when the retention of acetates (and, consequently, the separation of peaks and the duration of analysis) are too high $(k' > 15$; see Fig. 3). A concentration of acetonitrile of 40% is considered to be the optimum, as the retention of all the components remains
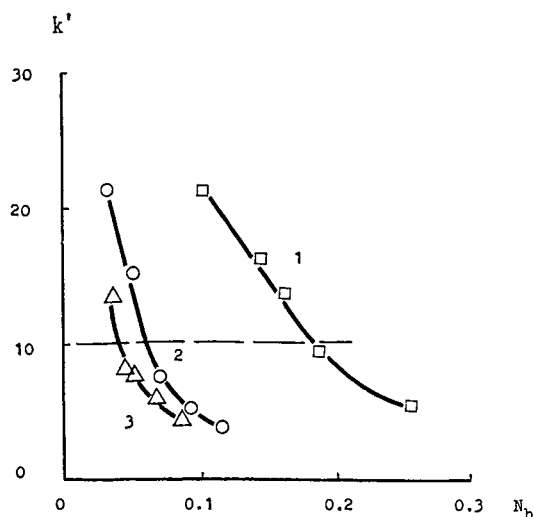
Fig. 3. Dependence of the capacity factor k' of DON-3-acetate on the mole fraction (N_b) of the organic component in the eluent. 1 = Acetonitrile; 2 = ethanol; 3 = tetrahydrofuran.
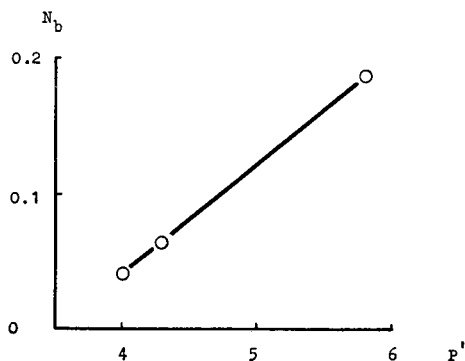
Fig. 4. Dependence of the mole fraction of the mobile phase modifier (N_b) corresponding to the retention of DON-3-acetate ($k' = 10$) on the polarity (P') of the modifier.

in the k' range 1.25–8.86 and the selectivity for the 7-desoxy-DON–DON pair is $\alpha_{3/2} = 1.08$ and for the DON acetates $\alpha_{4/5} = 1.06$.

The best separation selectivity among the binary mobile phases investigated was observed with the THF–water system. As a less polar modifier capable of forming hydrogen bonding with C–OH groups, THF provides for separations due both to the difference in the number of hydroxyl groups in the toxin molecule and to the different positions of the acetyl groups. The increase in selectivity of the separation DON-3- and -15-acetate on increasing the THF content, the selectivity of the pair 7-desoxy-DON– DON remaining constant, indicates that the effect of THF on the separation of more hydrophobic adsorbates is stronger.

Fig. 5 shows that an increasing amount of THF in the eluent increases the separation selectivity of the components of the mixture and decreases the duration of
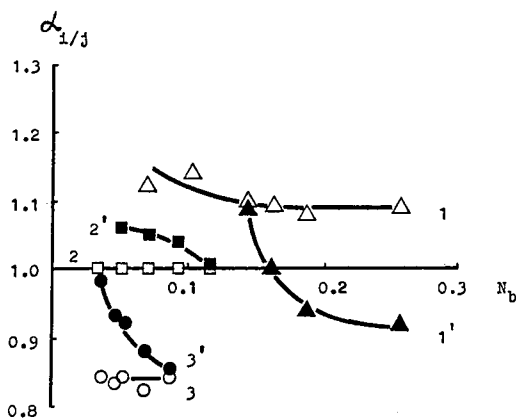
Fig. 5. Dependence of the relative retention volume ($\alpha_{i/j}$) on the mole fraction (N_b) of the organic component in the eluent for poorly separated pairs of substances: open symbols, 7-desoxy-DON–DON; closed symbols, DON-15-acetate–DON-3-acetate. 1,1' = Acetonitrile; 2,2' = ethanol; 3,3' = tetrahydrofuran.
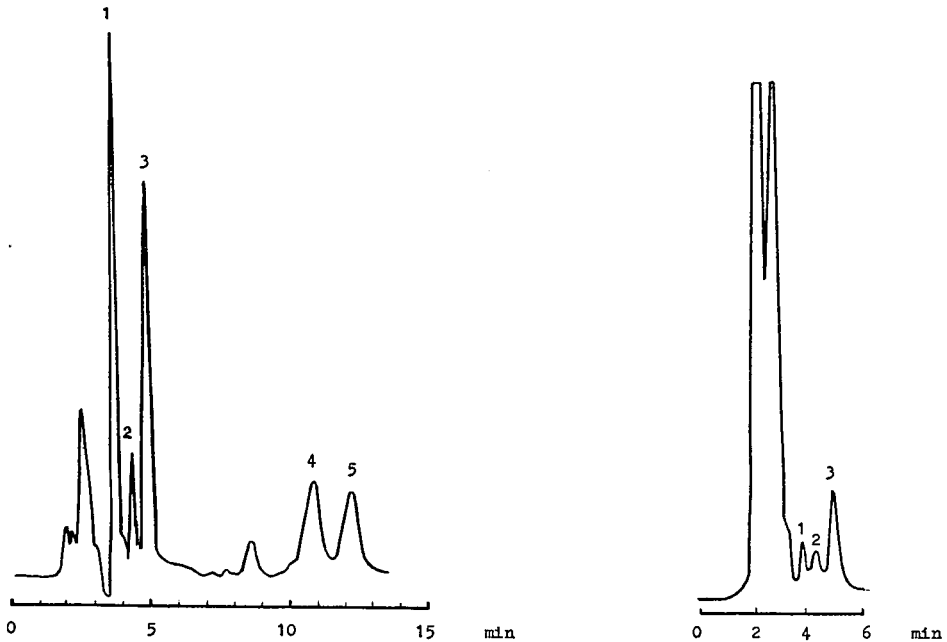
Fig. 6. Chromatogram of trichothecene separation with the optimized composition of the eluent, water–tetrahydrofuran (76:24). Nucleosil C_{18} column (62 × 2 mm I.D.); flow-rate, 50 μl/min; λ, 224 nm. 1 = Nivalenol; 2 = 7-desoxy-DON; 3 = DON; 4 = DON-15-acetate; 5 = DON-3-acetate.

Fig. 7. Chromatogram of an extract from wheat meal. 1 = Nivalenol; 2 = 7-desoxy-DON; 3 = DON. Conditions as in Fig. 6.

analysis (see Fig. 3). However, when the THF content is 30% (N_b = 0.087), the retention of nivalenol and 7-desoxy-DON decreases to such an extent that their peaks begin to overlap with those of polar impurities present in the samples. However, when the THF content decreases, the separation of the DON acetates deteriorates. A compromise (optimum) composition of mobile phase with 24% of THF provides both a good separation of all the components of the mixture (Fig. 6) and an acceptable duration of analysis (14 min). The substances elute from column in the sequence nivalenol < 7-desoxy-DON < DON < DON-15-acetate < DON-3-acetate. The selectivity for the pair DON–7-desoxy-DON was 1.18 and for the pair DON-3-acetate–DON-15-acetate it was 1.13. The separation of DON acetates has not been reported previously.

Fig. 7 shows the chromatographic analysis of an extract from wheat meal.

CONCLUSIONS

Optimum conditions are determined for the separation of five trichothecene mycotoxins (nivalenol, 7-desoxy-DON, DON, DON-3-acetate and DON-15-acetate) using RP-HPLC under isocratic conditions. The chromatographic system was shown to exhibit high selectivity when using an eluent containing THF.

REFERENCES

1 R. J. Cole and R. H. Cox (Editors), *Handbook of Toxic Fungal Metabolites*, Academic Press, New York, 1981.
2 G. A. Bennet, *J. Am. Oil Chem. Soc.*, 58 (1981) 1002A.
3 M. W. Witt, L. P. Hart and J. J. Pestka, *J. Agric. Food Chem.*, 33 (1985) 745.
4 L. R. Snyder, *J. Chromatogr. Sci.*, 16 (1978) 223.
5 L. R. Snyder and J. J. Kirkland, *Introduction to Modern Liquid Chromatography*, Wiley, New York, 2nd ed., 1979.
6 P. J. Schoenmakers, H. A. Billet and L. de Galan, *J. Chromatogr.*, 205 (1981) 13.
7 P. J. Schoenmakers, H. A. Billet and L. de Galan, *J. Chromatogr.*, 218 (1981) 261.
8 A. C. Drouen, H. A. Billet and L. de Galan, *J. Chromatogr.*, 352 (1986) 127.

CHROM. 23 438

Carbohydrate separation by ligand-exchange liquid chromatography

Correlation between the formation of sugar–cation complexes and the elution order

H. CARUEL, L. RIGAL and A. GASET*

Laboratoire de Chimie des Agroressources / CATAR, Ecole Nationale Supérieure de Chimie de Toulouse, 118 Route de Narbonne, 31077 Toulouse Cedex (France)

ABSTRACT

Carbohydrate separation (hexoses, pentoses and corresponding polyols) was studied by liquid chromatography using ligand exchange on cation-exchange resin column with water as eluent. Seven cations (Ca^{2+}, Sr^{2+}, Ba^{2+}, Pb^{2+}, Y^{3+}, La^{3+} and Pr^{3+}) were tested. The carbohydrate elution order is considered in connection with the complexing sites likely to be involved for each sugar or polyol molecule and with the exclusion processes.

INTRODUCTION

Extraction of sugars from plants by diffusion or pressing and by acid or enzymatic hydrolysis yields sugar mixtures. Catalytic or enzymatic hydrogenation gives polyol mixtures which may contain some residual sugars, the separation of which is required. Liquid chromatography with ligand exchange on ion-exchange resins and water as eluent seems to be the most efficient method. Techniques for the analytical separation of sugars developed over the last 15 years [1–3] are now being used for industrial carbohydrate separations, especially glucose–fructose separation [4–6]. This type of separation was studied by Angyal *et al.* [7] and Goulding [6]. The formation of a donor–acceptor complex between the cations immobilized on the ion-exchange resin and the carbohydrate hydroxyl groups is the mechanism effecting the separation [7–9]. Some water molecules of cation hydration are thus displaced and replaced by the carbohydrate [8]. The movement of the latter through the column is caused by the water molecules of the eluent, which in turn replace sugar or polyol molecules. Their separation is directly proportional to the stability of the complex formed with the cation: the more stable the complex, the more immobilized the molecule will remain [8,10]. The influence of the cation fixed on the resin constitutes one of the major parameters of the separation process.

This study was aimed at selecting the most appropriate resin counter ion to

achieve the separation of carbohydrate compounds produced by treatment of plants. The components of the mixtures studied were D-glucose, D-xylose, D-galactose, D-mannose, L-arabinose, mannitol, arabinitol, galactitol, xylitol and sorbitol. Seven cations (Ca^{2+}, Sr^{2+}, Pb^{2+}, Y^{3+}, La^{3+} and Pr^{3+}) were selected according to their characteristics and the literature [7,8,11–16]. In order to form a bidentate complex (less stable, $K_{stab} = 0.1$ mol^{-1}) or a tridentate complex (more stable, $K_{stab} = 1–5$ mol^{-1}), with two or three sequences of hydroxyl groups supported by adjacent carbons, the cation must have an octahedrial structure—in solution the hydration of non-octahedral cations of Group 1A in the Periodic Table causes a structural change allowing complex formation [8]; the highest possible electronic deficit [11]; and an optimum size with respect to the complexing site, $i.e.$, a 1 Å ionic radius [17] for the tridentate complex produced on adjacent hydroxyl sequences, in axial–equatorial–axial (a–e–a) on a pyranose ring, in $cis–cis$ on a furanose ring and on a so-called M–P sequence on an open carbonated chain where the first and second carbon are $gauche$ clockwise and the second and third carbons are $gauche$ anticlockwise or $vice$ $versa$ [18]. This sequence is analogous to the a–e–a pyranose sequence on an open chain. Below 1 Å, the small cation will tend to produce axial–equatorial (a–e) bidentate complexes. Above 1 Å, the large cations will tend to produce 1–3 diaxial (1–3 a–a) or equatorial–equatorial (e–e) bidentate complexes [8].

Concerning complex formation, one may observe a difference between sugars and polyols. Sugars will yield complexes with cations function as their own immobilized sites whereas polyols can all achieve the M–P configuration by rotation around carbon–carbon bonds. The formation of more or less stable complexes will largely depend on the energy supplied to obtain this M–P configuration. When the energy consumption averages 1–2 kcal/mol, complexing occurs but weakly. With a greater energy no complexing occurs [17]. The complex stability is linked to the polyol structure. It decreases in the following structural order: $threo–threo$ (t–t) a pair of $threo$ adjacent to a primary hydroxyl (w–t) $erythro–threo$ (e–t) a pair of $erythro$ adjacent to a primary hydroxyl (w–e) [18].

EXPERIMENTAL

A 200 cm × 1.67 cm I.D. glass column, thermostated at 50°C by fluid circulation in the jacket, was packed with Duolite C204/2078 resin (6.4% divinylbenzene, 0.15–0.3 mm diameter) in the appropriate form by the sedimentation method. The counter ions used for resin permutation were supplied by Prolabo (calcium, strontium and barium chloride), Degussa (lead nitrate) and Rhone-Poulenc Rare Earth Unit (yttrium, lanthanum, praseodymium nitrates).

The products used to reconstitute the carbohydrate mixtures were supplied by Fluka (glucose, xylitol, mannitol), Prolabo (xylose, galactose, galactitol) Jansen (mannose, arabinose), Aldrich (sorbitol) and Extrasynthese (arabinitol).

The mixtures were reconstituted in deionized water with a resistivity higher than 10 MΩ/cm and from 45 to 75 g/l of each component.

The injection of 1.5 cm^3 of separating solution was performed by direct deposition on the resin. In order to prevent dilution of the injected solution, elution water with was initiated only after complete penetration of the solution into the resin. A Gilson Minipuls 2 peristaltic pump fed the system with water as eluent at 50°C. An
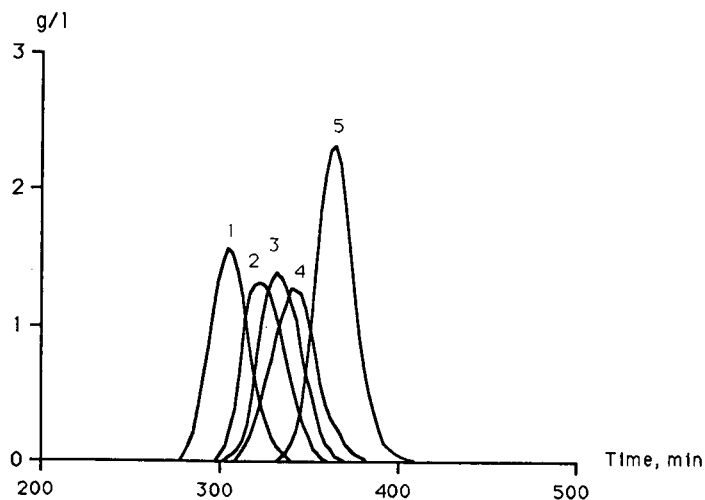
Fig. 1. Chromatogram of sugars on Ca^{2+} ion-exchange resin. Flow-rate, 0.83 ml/min. In Figs. 1–14 the numbers on the peaks correspond to the carbohydrates listed in Table I.

MTDC Gilson automated fraction collector recovered the effluent at the column output. When the separation procedure was completed, the collected fractions were analysed by high-performance liquid chromatography (HPLC) on an LDC Milton Roy III apparatus with refractometric detection.
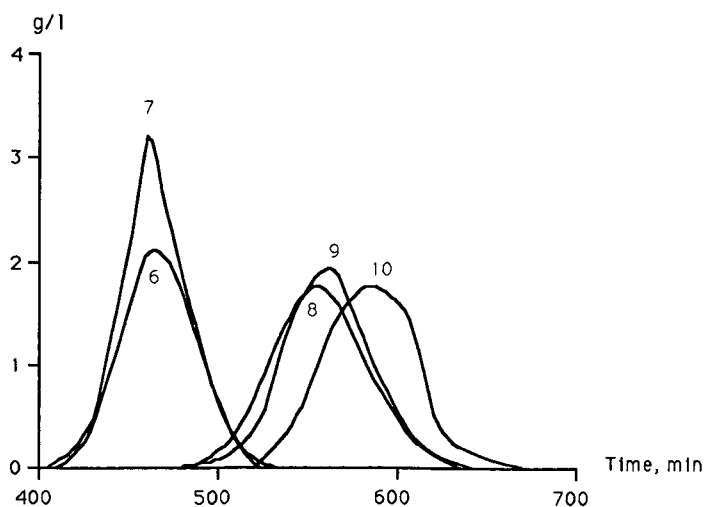
Fig. 2. Chromatogram of polyols on Ca^{2+} ion-exchange resin. Flow-rate, 0.83 ml/min.
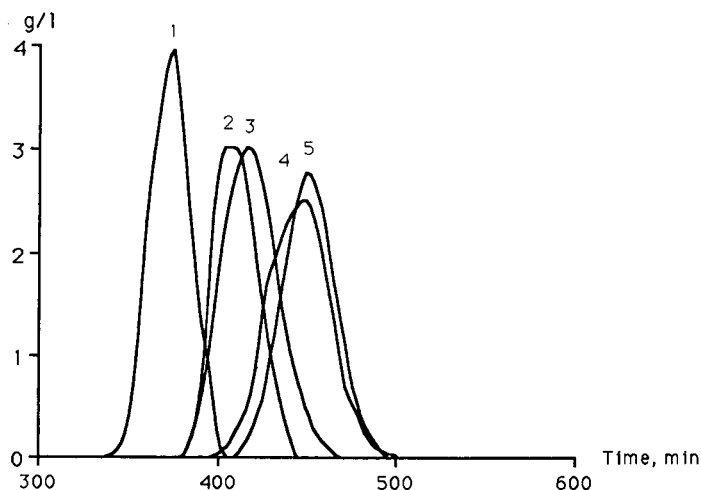
Fig. 3. Chromatogram of sugars on Sr^{2+} ion-exchange resin. Flow-rate, 0.69 ml/min.

RESULTS

Fig. 1–14 illustrate the chromatograms for each of the seven cations. The capacity factor (k') was calculated (Table I) for each monosaccharide, polyol and cation. The k' order corresponds to the elution order of the monosaccharides and polyols. It should be noted that the values of k' are similar to those determined by Goulding [8].

One can observe that sugars always elute before polyols whatever the cation used. The separation of the two groups is complete with lanthanum, praseodymium,
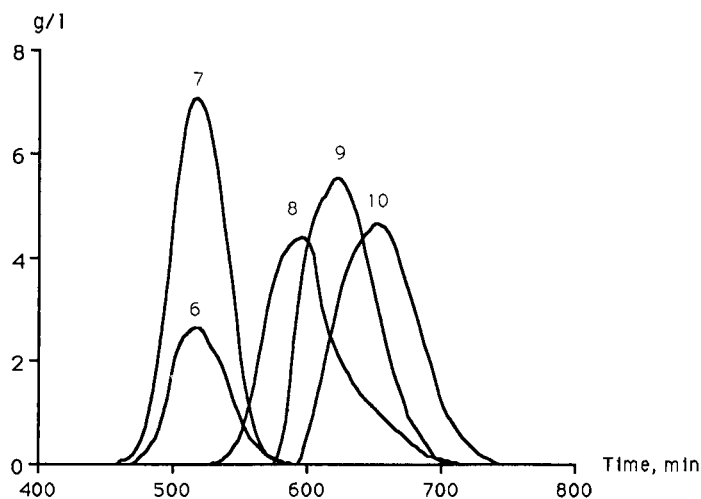
Fig. 4. Chromatogram of polyols on Sr^{2+} ion-exchange resin. Flow-rate, 0.69 ml/min.
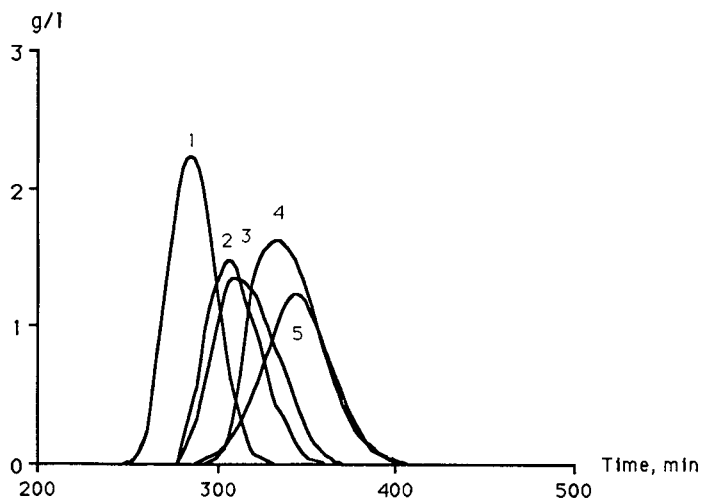
Fig. 5. Chromatogram of sugars on Ba^{2+} ion-exchange resin. Flow-rate, 0.90 ml/min.

calcium and lead cations and almost complete with the yttrium cation. This is not the case for strontium (Figs. 3 and 4) and barium (Figs. 5 and 6), although the overlapping remains minor and restricted to the mannose–arabinose and mannitol–arabinitol pairs. These results are in agreement with the theoretical data available on the stability of the sugar–cation complexes [3,8,17]. All the polyols are likely to form tridentate complexes. This is not the case for the monosaccharides studied.

One can also say that in general the elution order is (1) glucose, (2) xylose, (3) galactose, (4) mannose, (5) arabinose, (6) mannitol, (7) arabinitol, (8) galactitol, (9)
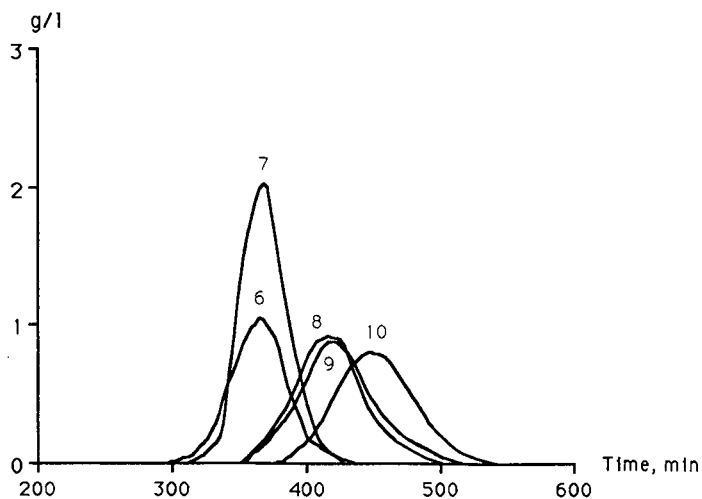
Fig. 6. Chromatogram of polyols on Ba^{2+} ion-exchange resin. Flow-rate, 0.90 ml/min.

TABLE I

CAPACITY FACTORS (k') FOR THE DIFFERENT SEPARATED COMPONENTS ON DUOLITE C204/2078 RESIN WITH WATER AS ELUENT

$$k' = \frac{t_{ri} - t_0}{t_0} = t_{ri} \cdot \frac{D}{LS\varepsilon} - 1$$

where t_{ri} = retention time of component i measured at the maximum of the chromatographic peaks (min), t_0 = residence time of the mobile phase in the column, t_0 = L/μ (min), L = length of the column (cm), μ = linear flow-rate of the eluent, $\mu = D/S\varepsilon$ (cm/min), D = eluent flow-rate (ml/min), S = column cross-section (cm²) and ε = void volume = volume of the eluting phase contained in the column/volume of the column ($\varepsilon = 0.4$).

Counter ion	(1) Glucose	(2) Xylose	(3) Galactose	(4) Mannose	(5) Arabinose	(6) Mannitol	(7) Arabinitol	(8) Galactitol	(9) Xylitol	(10) Sorbitol
Ca²⁺	0.46	0.54	0.57	0.61	0.73	1.24	1.202	1.65	1.67	1.78
Sr²⁺	0.48	0.61	0.65	0.76	0.78	1.04	1.06	1.36	1.46	1.60
Ba²⁺	0.49	0.57	0.63	0.73	0.79	0.89	0.89	1.15	1.17	1.32
Pb²⁺	0.59	0.66	0.83	1.09	0.95	2.10	2.09	3.14	3.02	3.69
Y³⁺	0.29	0.36	0.36	0.39	0.50	0.84	1.03	1.23	1.50	1.52
La³⁺	0.34	0.43	0.43	0.53	0.54	1.52	1.81	2.69	3.36	3.69
Pr³⁺	0.41	0.48	0.50	0.56	0.61	2.66	3.31	6.16	6.03	7.96
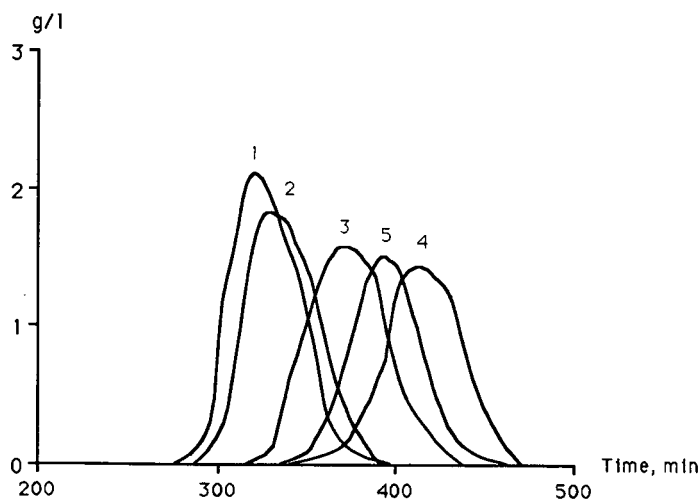
Fig. 7. Chromatogram of sugars on Pb^{2+} ion-exchange resin. Flow-rate, 0.88 ml/min.

xylitol and (10) sorbitol. There are several exceptions with Pb^{2+}. For mannose–arabinose, mannitol–arabinitol and xylitol–galactitol (Figs. 7 and 8), three inversions were observed. These results, already reported by Baker and Himmel [13] for mannose and arabinose, were corroborated by HPLC on Pb^{2+} and Ca^{2+} analytical columns (Table II).

Ca^{2+} seems to be the most suitable cation for obtaining an efficient separation of the components of sugar–polyol, glucose–galactose, –mannose or –arabinose, ara-
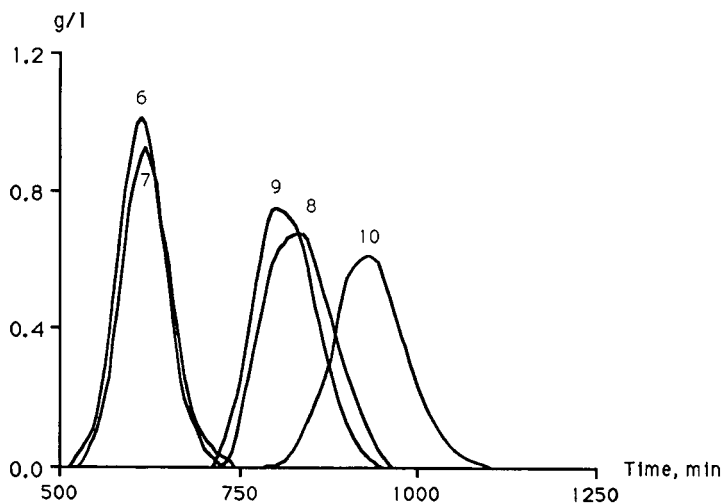
Fig. 8. Chromatogram of polyols on Pb^{2+} ion-exchange resin. Flow-rate, 0.88 ml/min.
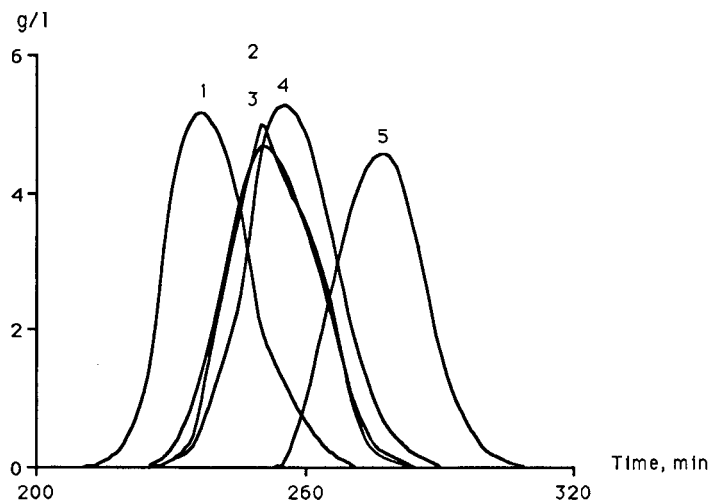
Fig. 9. Chromatogram of sugars on Y^{3+} ion-exchange resin. Flow-rate, 0.95 ml/min.

binose–xylose, –galactose or –mannose, mannitol–galactitol, –xylitol –sorbitol and arabinitol–galactitol, –xylitol –sorbitol mixtures.

In some instances, separation can be improved by using other cations (Table III). For example, the glucose–xylose separation is more efficient with Sr^{2+} (Figs. 1 and 3) and the arabinitol–galactitol, –xylitol or –sorbitol separation is better with La^{3+} (Figs. 1 and 12). Pr^{3+} leads to capacity factors that are sharply higher for polyols. For the separation of alditols, a Pr^{3+} column considerably smaller than one
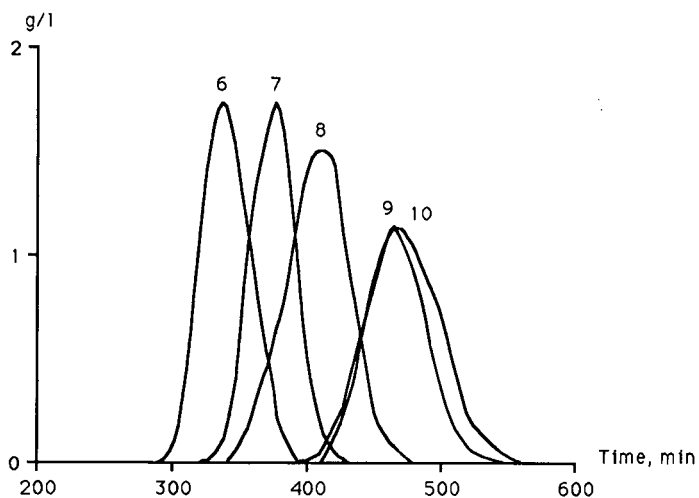
Fig. 10. Chromatogram of polyols on Y^{3+} ion-exchange resin. Flow-rate, 0.95 ml/min.
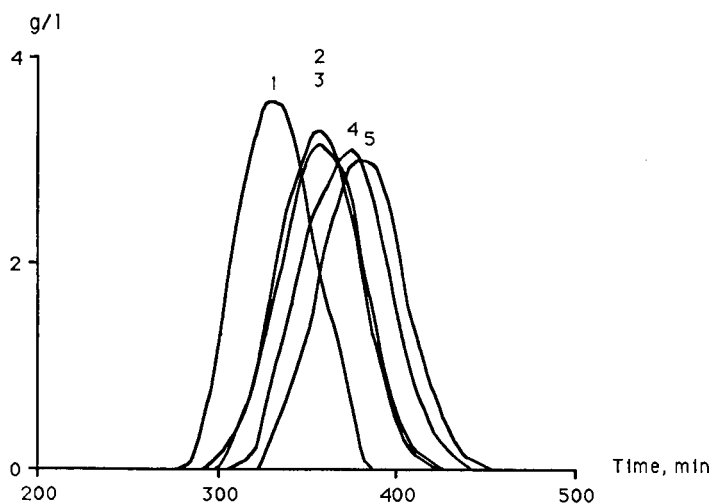
Fig. 11. Chromatogram of sugars on La^{3+} ion-exchange resin. Flow-rate, 0.70 ml/min.

made with La^{3+} could be used. Lastly, separation on Ca^{2+} resin is almost or completely impossible in certain situations. Table IV reports unsolved separations with Ca^{2+} and suggests the use of other cations. Although Ba^{2+} allows a satisfactory separation of D-tagatose and D-talose [19], in our study it did not yield better results than the other cations tested.
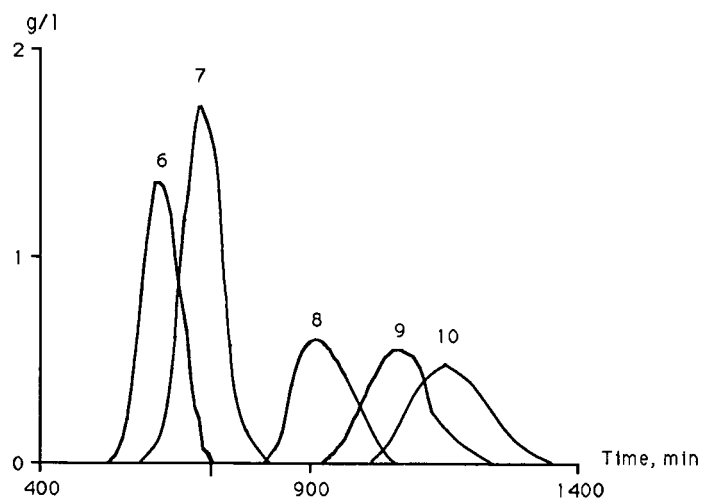
Fig. 12. Chromatogram of polyols on La^{3+} ion-exchange resin. Flow-rate, 0.70 ml/min.

TABLE II

RETENTION TIMES (min) ON ANALYTICAL COLUMNS FOR THE THREE PAIRS WITH IN-
VERTED ELUTION ORDER BETWEEN CALCIUM AND LEAD

Carbohydrate	Brownlee Labs. Cartridge, 20 cm, 0.3 ml/min, 85°C (Ca^{2+})	Bio-Rad Labs. HPX 87P 30 cm, 0.6 ml/min, 85°C (Pb^{2+})	Bio-Rad Labs. HPX 87C, 30 cm, 0.6 ml/min, 85°C (Ca^{2+})	Interaction CHO-682, 30 cm, 0.4 ml/min, 90°C (Pb^{2+})
Mannose	6.97	16.44	12.47	25.44
Arabinose	7.59	15.48	13.75	24,27
Mannitol	9.57	--	—	40.72
Arabinitol	9.74	—	—	40.42
Galactitol	10.94	--	~	53.07
Xylitol	11.24	—	—	51.32

TABLE III

COMPARATIVE QUALITATIVE RESULTS FOR POSSIBLE SEPARATIONS FOR CALCIUM
AND OTHER CATIONS

The separation obtained with the cation is equal to ($=$) greater than ($>$) or much better than ($\gg$) that obtained with Ca^{2+}.

Mixture	Ca^{2+}	Sr^{2+}	Pb^{2+}	Y^{3+}	La^{3+}	Pr^{3+}
Sugar–polyol	+		>		>	>
Glucose–galactose	+	>				
Glucose–mannose	+	>				
Glucose–arabinose	+	>				
Xylose–arabinose	+	=				
Galactose–arabinose	+				>	$\gg$
Mannose–arabinose	+			>	$\gg$	$\gg$
Mannitol–galactitol	+				>	$\gg$
Mannitol–xylitol	+			>	>	>
Mannitol–sorbitol	+	>	>			>
Arabinitol–galactitol	+	>			>	
Arabinitol–xylitol	+				>	
Arabinitol–sorbitol	+	>			>	

TABLE IV

CATION SELECTION WHEN SEPARATION IS IMPOSSIBLE WITH CALCIUM

Mixture	Sr^{2+}	Pb^{2+}	Y^{3+}	La^{3+}	Pr^{3+}
Glucose–xylose	Fig. 3				
Xylose–galactose		Fig. 7			
Xylose-mannose		Fig. 7			
Galactose–mannose		Fig. 7			
Mannitol-arabinitol			Fig. 10	Fig. 12	Fig. 14
Galactitol–xylitol			Fig. 10	Fig. 12	
Galactitol–sorbitol				Fig. 12	
Xylitol–sorbitol		Fig. 8			Fig. 14
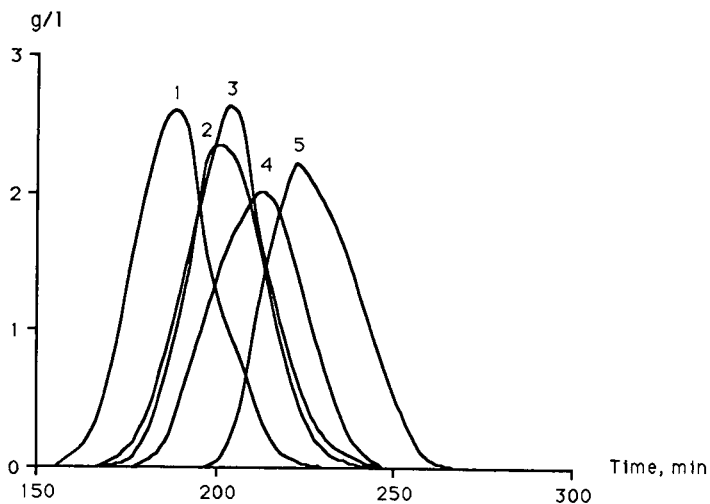
Fig. 13. Chromatogram of sugars on Pr^{3+} ion-exchange resin. Flow rate, 1.30 ml/min.

DISCUSSION

The results obtained illustrate the different behaviours of monosaccharides and polyols. Both will be considered separately in order to check whether the complex formation theory is consistent with the elution order in both groups. The contribution of the exclusion phenomena related to the use of ion-exchange resins as chromatographic supports will be discussed according to the separation efficiency.
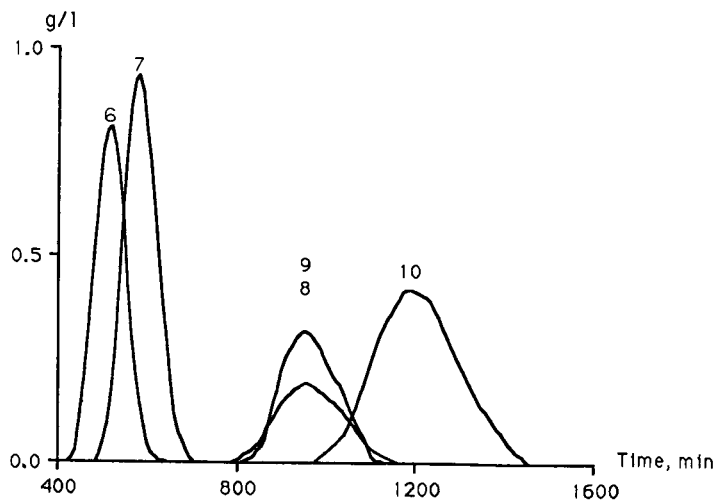
Fig. 14. Chromatogram of polyols on Pr^{3+} ion-exchange resin. Flow-rate, 1.30 ml/min.

Monosaccharides

Contribution of complex formation. According to theory, the sugar and related configuration sites (a–e–a, a–e, e–e, 1–3 a–a) allow the formation of more or less strong complexes. Although there are no available current data, to our knowledge, on the formation speed of sugar–cation complexes, the kinetics of mutarotation seem to be a restrictive factor compared with those of sugar–cation complexes formation. In order to substantiate this observation, we may add that the mutarotation equilibrium is achieved slowly [20,21]; the separation of some sugar anomers by HPLC on cation–exchange resins with calcium or lead columns has already been completed [8,13]; and sugar analysis by NMR spectroscopy identifies the five anomeric forms (α- and β-py-ranose, α- and β-furanose and open-chain) whenever they exist in sufficient amounts. The kinetics of exchanges between the different forms are slow compared with the NMR time scale. However, when there is a cation, only a average spectrum corre-sponding to the free sugar and to the sugar-cation complex will be observed [17]. The kinetics of the complex formation are very fast compared with the NMR time scale.

The contributions of the sites likely to form a complex with a cation will be proportional to each tautomeric form of dissolved sugars. All the monosaccharides are present in water solution in several forms at equilibrium. For the five sugars studied, the α- and β-pyranose forms prevail [22]. According to Angyal *et al.* [23], apart from β-L-arabinose, which has the two confirmation, $^1C_4$ and $^4C_1$, the prevail-ing conformation of the studied aldopyranoses is $^4C_1$. The energy to change confor-mation is always greater than 2 kcal/mol.

Although there are no direct data on the energies generated by the formation of a bi- or tridentate sugar–cation complex, the stabilization energy brought about by the formation of a tridentate complex does not seem to be sufficient to reach the level required to induce a conformation change. According to Angyal [17], with polyols and when the conformation change requires very little energy (1–2 kcal/mol), the tridentate complex will occur but its stability will be weak. Beyond this level, it will no longer occur. This is even more true for bidentate complexes. Symons *et al.* [24] related some sugar NMR spectroscopic changes with variation in calcium chloride concentration to the shift of conformation equilibrium, $^1C_4 \rightleftharpoons {}^4C_1$. However, and in compliance with Goulding's observation [8], only the complexes likely to occur with the $^4C_1$ prevailing conformations will be studied, except for β-L-arabinose. The part played by the a–e–a complex of the β-D-mannopyranose $^1C_4$ conformation in the separation will be discounted. In the same way, no 1–3 a–a complex will be taken into account as they could only occur with D-glucose and D-xylose in the $^1C_4$ forms. The contribution of the open-chain forms will also be discounted because they only occur as trace components [25]. As far as the furanose forms of sugars are concerned, their proportion is small [26,27]. The contribution of the bidentate complex which they may generate remains negligible. This is also the case for the tridentate complex of β-D-mannofuranose [8].

The a–e complexes will form preferentially the e–e forms proportionally to the equilibrium obtained at 50°C. Table V summarizes the contribution of each complex for each sugar.

The chromatographic elution order of the monosaccharides is linked to the proportion of a–e bidentate complexes likely to form. With calcium the contribution of the weaker e–e bidentate complexes seems to be minor with this small-sized cation

(*ca.* 1 Å). In contrast, this contribution can be higher [1] with strontium and barium, whose ionic radii are larger (1.12 and 1.34 Å, respectively). This might account for the poor xylose–galactose and mannose–arabinose separations observed with these cations (Figs. 3 and 5). However, the elution order of sugars remains identical with that obtained with Ca^{2+}. The same applies to the yttrium, lanthanum and praseodymium cations. However, the total lack of xylose–galactose separation demonstrated by identical capacity factors (0.36 for Y^{3+}, 0.43 for La^{3+}) or close capacity factors (0.48–0.5 for Pr^{3+}) cannot only be accounted for by the ionic radius of the cations (0.89, 1.02 and 1.1 Å, respectively). In the same way, although the contributions of the a–e and e–e complexing sites are identical for glucose and xylose, these sugars are always clearly separated by all the cations.

Contribution of exclusion phenomena. Another factor limiting the contribution of sugar–cation complexes in the separation process will have to be taken into account. The comparison of cation structures or of their electronic deficit is not sufficient to explain the separation. However, the contribution of exclusion phenomena linked to the differences in steric crowding between hexoses and pentoses might clarify the interpretation of the observed phenomena.

For all the cations described, xylose and glucose on the one hand and galactose and arabinose on the other are always clearly separated. These hexose–pentose pairs do not differ from a structural viewpoint except for the presence of the hydroxymethyl group on the pyranose ring. As far as xylose and glucose are concerned, the complexing site contributions are equivalent but the exclusion phenomenon remains prevalent.

TABLE V

CONTRIBUTION TO THE SEPARATION OF EACH SUGAR COMPLEX

Sugar	Form[a]	Proportion at 50°C (%)	Complexation sites	
			a–e	e–e
D-Glucose	α-P	37	1	1
[26,27]	β-P	63	0	2
	Total	100	0.37	1.63
D-Xylose	α-P	40	1	1
[3]	β-P	60	0	2
	Total	100	0.4	1.6
D-Galactose	α-P	33	2	0
[26,27]	β-P	57	1	1
	Total	90[b]	1.23	0.56
D-Mannose	α-P	62	1	0
[3]	β-P	38	2	0
	Total	100	1.38	0
L-Arabinose	α-P	63	2	0
[31]	β-P	34	1	1
	Total	97[c]	1.60	0.34

[a] P = pyranose.
[b] 10% of furanose forms.
[c] 3% of furanose forms.

The permutation of the exchanger by trivalent ions is shown by the moderate swelling of the resin, which will increase the exclusion penomena. The capacity factors observed with Y^{3+}, La^{3+} and Pr^{3+} are weaker for the sugars than for those observed with Ca^{2+}, Sr^{2+} and Ba^{2+}. Nevertheless the glucose–xylose and galactose–arabinose separations, for which the exclusion contribution to the separation is important, remain effective. However, the penetration of galactose and mannose into the cation-exchange resin in their Y^{3+}, La^{3+} or Pr^{3+} forms is less extensive. This restricts the contribution of complex formation and accounts for the weaker retention and poor separation with xylose.

Lead

The situation is even more complex for lead. Glucose, galactose and mannose are separated as with calcium. Xylose is no longer separated from glucose, and arabinose is eluted between galactose and mannose. It seems as if hexoses were more immobilized than pentoses. This phenomenon might be linked to the increase in the contribution of complex formation compared with the exclusion phenomena. This assumption is substantiated by the observation of the capacity factors: they are much higher for most of the sugars with Pb^{2+} than those obtained with other cations. Pb^{2+} is located at the hard and soft acid limit owing to its partially vacant $5d$ orbital ($4f^{14}$, $5d^8$, $6s^2 6p^2$) [28,29]. The association with oxygen free pairs of hydroxyl groups which are soft bases are therefore stronger (soft acid–soft base association) than those obtained with alkaline earth metal cations (hard acid). The prevailing contribution of complexing phenomena levels off the different xylose and glucose behaviours which have the same contributions on complexing sites, and in smaller proportions than those for arabinose and galactose. Also, the larger ionic radius of the Pb^{2+} cation (1.2 Å) could lead to a modification in relation to the contribution on the a–e and e–e sites. This cation accelerates the speed of mutarotation of sugars [13], which could alter the proportions of α- and β-forms.

To conclude, without totally leaving aside the complexing tridentate site contribution, the elution order of the investigated monosaccharides can thus be correlated with a–e or e–e bidentate complex formation. Depending on the type of cation, the phenomena will be more or less affected by exclusion factors linked to the size of resin pores.

Polyols

In contrast to monosaccharides, polyols in aqueous solution have an acyclic form, the prevailing conformation being [18,19] either planar or "zig-zag" when there is no 1–3 diaxial interaction between the oxygen atoms, or bent or sickle form in the opposite case. By rotating round carbon–carbon bonds, all the alditols studied can form tridentate M–P-type complexes with a cation. These complexes are strong. It would appear reasonable to assume that the contribution of the exclusion phenomena to separation will be minor compared with that of complex formation. This assumption is confirmed by the following observation: for the same ionic radius (Ca^{2+} and La^{3+}, for instance), passing from two to three load units does not entail any decrease in capacity factors as occurs with monosaccharides (Table II). In the same way, the sharp increase in capacity factors observed with Pr^{3+} corroborated the predominant role of the complex formation. The formation of strong complexes with lanthanide ions is widely used in NMR spectroscopy [12,18,32].

The elution order observed on rare earths, *i.e.*, mannitol, arabinitol, galactitol, xylitol, sorbitol, appears to be consistent with the work of Angyal *et al.* [18] on ^{1}H NMR chemical shifts induced by the addition of lanthanum ions (Table VI). The best separation pattern is obtained with La^{3+} (Fig. 12), whose ionic radius averages 1 Å. The sorbitol–xylitol separation could be explained by the fact that in addition to the sequence t–t formed on O_2–O_3–O_4, sorbitol can also lead to the formation of two other M–P complexes from the sequences w–t formed on O_1–O_2–O_3 and w–e formed on O_4–O_5–O_6. Such an alternative does not occur with xylitol, which can only yield one M–P complex from either of the w–t sequences formed O_2–O_3–O_4 or on O_3–O_4–O_5.

Moreover, in addition to the O_1–O_2–O_3 and O_2–O_3–O_4 complexing sites similar to those of arabinitol, galactitol can form another M–P complex from the w–t sequence of O_4–O_5–O_6 oxygen atoms; this second complex is independent of the first. With the Pr^{3+} cation whose ionic radius averages 1 Å, this alternative induces a higher galactitol retention with no xylitol separation (Fig. 14).

A decrease in the ionic radius of the cation (Y^{3+}, 0.89 Å) results in a lack of xylitol–sorbitol separation (Fig. 10) together with a 50% decrease in the capacity factors of the polyol group (Table I). This result is in agreement with the hypothesis of a 1 Å cation for the formation of M–P complexes [8,17]. On the other hand, this prerequisite does not appear to be applicable for alkaline earth metal cations. Despite the optimum 1 Å ionic radius, the calcium ion does not lead to an efficient separation of the mannitol–arabinitol and galactitol–xylitol pairs (Fig. 2). The situation is identical for Sr^{2+}, Ba^{2+} and Pb^{2+} for the mannitol–arabinitol pair (Figs. 4, 6 and 8).

The results tend indicate that 2+ cations do not carry enough energy to compensate for the energy needed to modify the conformation by rotation around a C–C axis facilitating the formation of sequences yielding complexes formation. As is the case for monosaccharides, the phenomena ruling the polyol separation involve the capacity to form complexes. The strength of these complexes stimulated by a 1 Å ionic radius cation and a three unit loading deficit allows for a larger retention of aditols and a efficient separation of each component. Exclusion phenomena appear to play a minor role.

TABLE VI

COMPLEXATION IDENTIFIED BY NMR ANALYSIS

^{1}H chemical shifts induced by the addition of lanthanum [18].

Polyol	Complexation sites		
	t–t	w–t	e–t
Mannitol			O_2–O_3–O_4
Arabinitol		O_1–O_2–O_3	O_2–O_3–O_4
Galactitol		O_1–O_2–O_3	O_2–O_3–O_4
Xylitol	O_2–O_3–O_4		
Sorbitol	O_2–O_3–O_4		

CONCLUSIONS

The contribution of carbohydrate–cation complex formation appears to be directly correlated with the elution order of sugars and polyols in ligand-exchange chromatography. In the former instance, the complexes are of the weak bidentate type and the exclusion phenomena leading to steric crowding of the different sugars can also result in chromatographic separation. In the latter, the complexes are of the tridentate type and the separation occurs as a function of the energy needed for the polyols to have the appropriate configuration. In both instances, a suitable choice of the cation improves the separation process, the quality of which also depends on the characteristic of the support (granulometry, cross-linking, swelling, etc.). The study of the influence of these different factors is in progress.

ACKNOWLEDGEMENTS

REFERENCES

1 A. Meunier, M. Caude and R. Rosset, *Analusis*, 14 (1986) 363.
2 P. Jandera and J. Churacek, *J. Chromatogr.*, 98 (1974) 55.
3 T. Carillon, *Thèse de Docteur Ingénieur*, Institut National Polytechnique, Toulouse, 1987.
4 Colonial Sugar Refining, *Br. Pat.*, 1 083 500 (1967).
5 V. S. H. Liu, N. E. Lloyd and K. Khaleeluding, *US Pat.*, 4 096 036 (1978).
6 H. Ishikawa, H. Tanabe and K. Usui, *US Pat.*, 4 182 633 (1980).
7 S. J. Angyal, G. S. Bethell and R. J. Beveridge, *Carbohydro. Res.*, 73 (1979) 9.
8 R. W. Goulding, *J. Chromatogr.*, 103 (1975) 229.
9 F. Helfferich, *Ion Exchange*, McGraw-Hill, New York, 1962.
10 B. Porch, *J. Chromatogr.*, 253 (1982) 49.
11 S. J. Angyal, *Aust. J. Chem.*, 25 (1972) 1957.
12 S. J. Angyal and J. A. Mills, *Aust. J. Chem.*, 38 (1985) 1279.
13 J. O. Baker and M. E. Himmel, *J. Chromatogr.*, 357 (1986) 161.
14 S. J. Angyal and R. J. Hickamn, *Aust. J. Chem.*, 28 (1975) 1279.
15 S. J. Angyal and D. Greeves, *Aust. J. Chem.*, 29 (1976) 1223.
16 R. M. Saunders, *Carbohydr. Res.*, 7 (1968) 76.
17 S. J. Angyal, *Tetrahedron*, 30 (1974) 195.
18 S. J. Angyal, D. Greeves and J. A. Mills, *Aust. J. Chem.*, 37 (1974) 1447.
19 J. K. N. Jones and R. A. Wall, *Can. J. Chem.*, 38 (1960) 2290.
20 A. de Grandchamp-Chaudun, *C. R. Acad. Sci.*, 258 (1964) 6564.
21 A. de Grandchamp-Chaudun, *C. R. Acad. Sci. Ser. C*, 262 (1966) 1441.
22 S. J. Angyal, *Angew. Chem. Int. Ed. Engl.*, 8 (1969) 157.
23 S. J. Angyal, *Aust. J. Chem.*, 21 (1968) 2737.
24 M. C. R. Symons, J. A. Benbow and H. Pelmore, *J.Chem. Soc., Faraday Trans. 1*, 80 (1984) 1999.
25 L. D. Hayward and S. J. Angyal, *Carbohydr. Res.*, 53 (1977) 13.
26 S. J. Angyal and V. A. Pickles, *Aust. J. Chem.*, 25 (1972) 1695.
27 L. Rigal, *Thèse de Doctorat d'Etat*, Institut National Polytechnique, Toulouse, 1987.
28 R. G. Pearson, *J. Am. Chem. Soc.*, 85 (1963) 3533.
29 J. Seyden-Penne, *Bull. Soc. Chim. Fr.*, 9 (1968) 3871.
30 J. A. Mills, *Aust. J. Chem.*, 27 (1974) 1433.
31 S. J. Angual and V. A. Pickles, *Carbohydr. Res.*, 4 (1967) 269.
32 P. Girard, H. Kagan and S. David, *Tetrahedron*, 27 (1971) 5911.

CHROM. 23 439

Liquid chromatographic method for the determination of the carbohydrate moiety of glycoproteins

Application to α_1-acid glycoprotein and tissue plasminogen activator

M. TAVERNA* and A. BAILLET

Centre d'Études Pharmaceutiques, Laboratoire de Chimie Analytique, Tour D2, 3ème Étage, Rue J.B. Clément, 92290 Chatenay Malabry (France)

R. WERNER

Dr. Karl Thomae GmbH, P.O. Box 1755, 7950 Biberach an der Riss (Germany)

and

D. BAYLOCQ-FERRIER

Centre d'Études Pharmaceutiques, Laboratoire de Chimie Analytique, Tour D2, 3ème Étage, Rue J.B. Clément, 92290 Chatenay Malabry (France)

(First received February 5th, 1991; revised manuscript received May 1st, 1991)

ABSTRACT

A rapid procedure is described for the qualitative and quantitative analysis of the carbohydrate composition of glycoproteins by liquid chromatography with light-scattering detection. The analysis was carried out in three steps. First, the glycoprotein samples were purified by a two-step purification on a Sephadex G-25 column with a 90% yield. Second, the selectivity of the separation and the sensitivity of detection of monosaccharides, as methyl glycosides obtained by direct methanolysis of glycoproteins, were improved by modified simplex optimization of the methanolysis parameters (temperature, methanolic hydrochloric acid strength and reaction time) determined at 66°C, 1.2 M and 8.1 h for α_1-acid glycoprotein (α-AGP) and 73°C, 1.5 M and 12.5 h for tissue plasminogen activator (tPA). Finally, the method was applied to the determination of the carbohydrate moiety of the two N-glycosylated glycoproteins α-AGP and tPA.

INTRODUCTION

Many methods have been proposed for the determination of the carbohydrate moieties of glycoproteins after acid hydrolysis [1–3] or methanolysis [4,5]. Methanolysis of glycoconjugates produces methylglycosides in a one-step procedure. However, gas chromatographic methods require other cumbersome derivatization steps and direct liquid chromatographic techniques are limited by the poor detectability of the methylglycosides.

We have described previously a rapid method for the determination of neutral and amino sugars present in polysaccharides and glycoproteins [6]. A light-scattering detector, which is more sensitive than a refractive index detector, was used and was suitable for the detection of methylglycosides having weak UV absorption bands. Using this procedure, quantitative analysis was possible as the calibration graphs obtained for various methylglycosides showed a linear response in double logarithmic coordinates.

The purpose of this work was to improve this method to allow the determination of the carbohydrate moieties of various glycoproteins using methanolysis. The first step was to develop a purification method for the glycoproteins to allow a suitable methanolysis procedure. The second step was to determine the optimum conditions of methanolysis as numerous conditions have been reported for the determination of carbohydrates in glycoproteins [4,7,8]. This scatter of values suggests that different glycoproteins would probably need differing optimum conditions of methanolysis. The choice of the internal standard and the reproducibility of the method were also investigated. Finally, this method was applied to the determination of the carbohydrate moieties of α_1-acid glycoprotein (α-AGP) and tissue plasminogen activator (tPA).

EXPERIMENTAL

Apparatus and chromatographic conditions

The chromatographic separation was carried out using a Shimadzu LC 6A pump equipped with a Cunow DDL 11 light-scattering detector and a Spectra-Physics Chromjet integrator.

The column effluent was nebulized by a stream of nitrogen. The particles formed were passed through a heated evaporation tube to evaporate the solvent. The particles then crossed a light beam and the scattered light was collected at an angle of 120° by a photomultiplier. The optimal nebulization pressure of 25 p.s.i. and the evaporative setting temperature of 30°C were determined previously [6].

The chromatographic column was Spherisorb ODS 2, 5 μm (250 × 4.6 mm I.D.) (SFCC). Methylglycosides were eluted with water–methanol (97:3) at 0.5 ml min^{-1}.

Reagents

Methanolic hydrochloric acid (3 M) was purchased from Supelco and methanolic hydrochloric acid (8.4 M) was provided by Dr. Doussin (Laboratoire de Biochimie, Hôpital Intercommunal de Creteil, France).

Human α-AGP, monosaccharides and standards of methylglycosides were obtained from Sigma. Plasminogen activator in solution was kindly donated by Dr. Schluter (Karl Thomae). All other chemicals were of analytical reagent grade.

Glycoprotein purification

In order to remove irrelevant products such as salts, buffers or contaminants from the sample, glycoprotein solutions were applied to a Sephadex G-25 PD10 column (Pharmacia) and eluted with 10% acetic acid. Gel filtration was performed twice. Eluted fractions (800 μl) were monitored by Lowry assay [9] and phenol–sulphuric acid assay [10].

Thin-layer chromatography (TLC) of the eluted fractions was performed on silica gel G-60 plates (Merck) with n-butanol–acetic acid–water (60:20:20, w/w/w) as eluent and ninhydrin solution as the spray reagent.

Methanolysis procedures

The glycoprotein-containing fractions were lyophilized for 18 h and the lyophilizates were used to prepare 1 mg ml^{-1} solutions. Aliquots of glycoprotein solution (250 μl) together with the internal standard (lyxose) were then lyophilized and dried over P_2O_5 under vacuum. A mixture of 500 μl of methanolic hydrochloric acid and 125 μl of methyl acetate was then added. To avoid decomposition of the reagent during storage, fresh methanolic hydrochloric acid stored at $-20°C$ in sealed ampoules was used for each methanolysis. Dry distilled methanol was used to prepare the methanolic hydrochloric acid reagent at various strengths.

Samples were heated at various temperatures and durations according to the modified simplex procedure described below. Thereafter, the acid was removed under a stream of nitrogen at room temperature for 30 min. Samples were either freshly dissolved in distilled water or stored at $-20°C$ without no significant destruction of the monosaccharide derivatives.

A modified simplex procedure [11] was used to optimize the methanolysis parameters. Three parameters were investigated: temperature, methanolic hydrochloric acid strength and reaction time. The boundaries of each parameter were defined according to previous published data on methanolysis [8,12]: temperature 50–120°C, methanol hydrochloric acid strength 0.2–4.2 M and reaction time 1–30 h. Each experiment was evaluated by a criterion C_R which was designed to assess the quality of the chromatogram:

$$C_R = \prod_{i=1}^{i=n} H_i$$

where H_i is the height of the main peak for each derivatized monosaccharide.

RESULTS AND DISCUSSION

Glycoprotein purification

The presence of buffer salts or other contaminants in the glycoprotein samples does not interfere with methanolysis [12]. Nevertheless, the additives present in the tPA solution disturbed the chromatographic separation of the first-eluted methyl glycosides released by methanolysis.

As shown in Fig. 1, contaminants could be removed from the glycoprotein solution by means of two consecutive gel filtrations on Sephadex G-25 with 10% acetic acid.

The elution of the glycoprotein was monitored both by the Lowry assay (for the peptidic fraction) and phenol–sulphuric acid reaction (for the glycan moiety); it was observed between the third and sixth eluted fractions.

Some interference with arginine, used in the buffer medium, was noted in the Lowry assay and allowed us to follow the elimination of arginine. The presence of
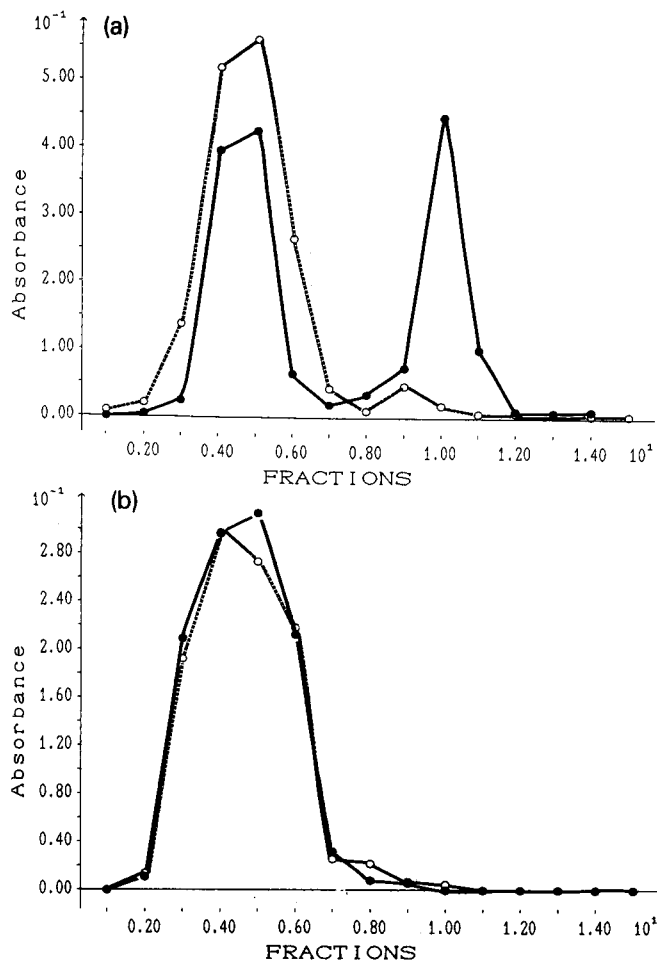
Fig. 1. Purification by gel filtration of tPA: (a) = step 1; (b) = step 2. Injected volume: 2 ml of a 1 mg ml^{-1} glycoprotein solution. Glycoprotein was monitored by ($\bullet$) Lowry assay and by ($\bigcirc$) phenol-sulphuric acid reagent.

residual arginine in the eluted fractions was checked by TLC and it was found to be present from fraction 9 to fraction 12.

The absorbance of the ninth fraction could be attributed to the presence of Tween 80 which interfered, to a minor extent, in the phenol–sulphuric acid assay.

The proposed two-step purification on Sephadex G-25 led to purified glycoprotein in 90% yield.

Simplex procedure

Methanolysis of a sugar produces a mixture of anomeric forms of methylglycosides and the anomer ratio is a function of the conditions used in the methanolysis step [13]. To obtain both good selectivity and sensitivity of the method, it was necessary to determine the methanolysis conditions which gave a main chromatographic peak per sugar.

To assess the quality of each chromatogram, we used the criterion C_R, which incorporates the product of the height of the main peak for each derivatized sugar. The product of H_i shows a better performance than the sum of H_i in which a small value for one peak can be compensated for by a great response of another peak. This product reflects an equal importance for each sugar as one bad response can lead to a dramatic decrease in the criterion.

The simplex procedure was stopped after five and seven steps for α-AGP and tPA, respectively. In the initial step of the experiments, the 50°C–0.2 M–1 h point was the first rejected point for both glycoproteins as these conditions were not sufficient to allow the methanolysis reaction. The extreme values for the three parameters studied, except the 4.1 M methanolic acid strength with α-AGP, were successively eliminated during the simplex evolution, leading to intermediate parameter values. This evolution causes the simplex to diminish in size (Fig. 2).
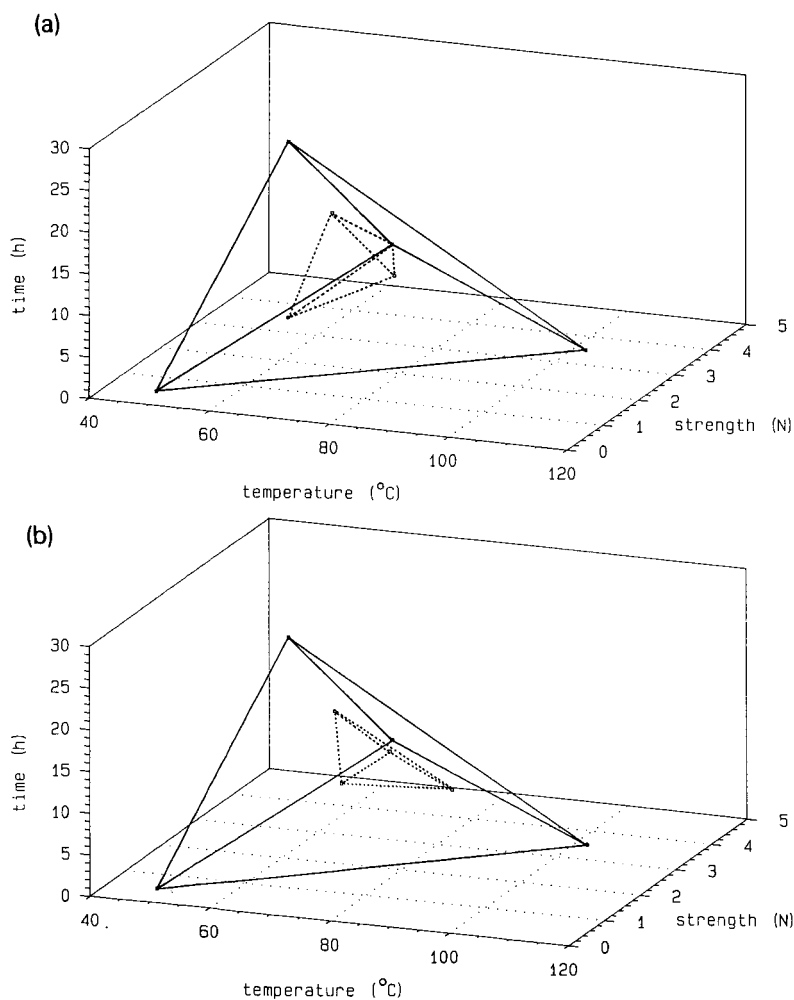
Fig. 2. Progress of the three-dimensional simplex towards the optimum for (a) α-AGP and (b) tPA.

Based on the results and the feasibility of the process, the optimum conditions established are reported in Table I. In order to compare the optimum conditions for α-GPA with those already published [8], a methanolysis of α-AGP was also carried out at 70°C with 0.6 *M* acid for 16 h. The criterion was improved by 50% with the new conditions.

Assuming that these two glycoproteins have similar N-glycan chains (high mannose, hybrid and complex types), the differences in the optimum point could be assigned to a dissimilarity in their spatial configuration rather than a different resistance of the glycosidic bonds to the methanolic hydrochloric acid. These results provide further evidence that optimum methanolysis conditions should be determined for each glycoprotein. The modified simplex procedure could be a simple approach for the optimization of these parameters in which variables such as temperature, reagent strength and reaction time, interact.

TABLE I

OPTIMUM CONDITIONS FOR THE METHANOLYSIS OF α-AGP AND tPA

Regression data in logarithmic coordinates for methylglycosides released from the glycoproteins by methanolyses under optimum conditions.

Methylglycoside	Methanolysis conditions					
	73°C, 1.5 *M*, 12.5 h			66°C, 1.2 *M*, 8.15 h		
	Slope	Intercept	Correlation coefficient	Slope	Intercept	Correlation coefficient
Galactose	1.264	4.548	0.997	1.448	3.783	0.999
Mannose	1.166	4.173	0.999	1.448	3.738	0.998
N-Acetylglucosamine	1.088	3.425	0.999	1.348	3.375	0.998
Fucose	1.050	3.506	0.996	1.422	2.712	0.998

Chromatographic application

A typical chromatogram of the separation of all methylglycosides including neutral and amino sugars is presented in Fig. 3. All the compounds are eluted within 16 min with good repeatability of the retention times [relative standard deviation (R.S.D.) ranging from 0.16 to 0.71%].

In order to choose an appropriate internal standard, we studied the repeatability of the chromatographic method with two different compounds, mesoinositol and lyxose. Two mixtures of methylglycosides containing either mesoinositol or lyxose as internal standards were analysed. The repeatibility of the method was evaluated by measuring the ratio of the peak height of each sugar to that of the internal standard with nine consecutive injections. The results obtained with both internal standards are reported in Table II. The average R.S.D. for all sugar derivatives was 3.9% with mesoinositol and 3.3% with lyxose. The R.S.D. values were scattered when mesoinositol was used as the internal standard. This could be attributed to its fast elution (retention time, t_R = 5.8 min), leading to a worse repeatability of peak heights for the last peaks. Moreover, mesoinositol has the disadvantage of being an underivatizable compound. In fact, the use of a methylglycoside for standardization provides a more
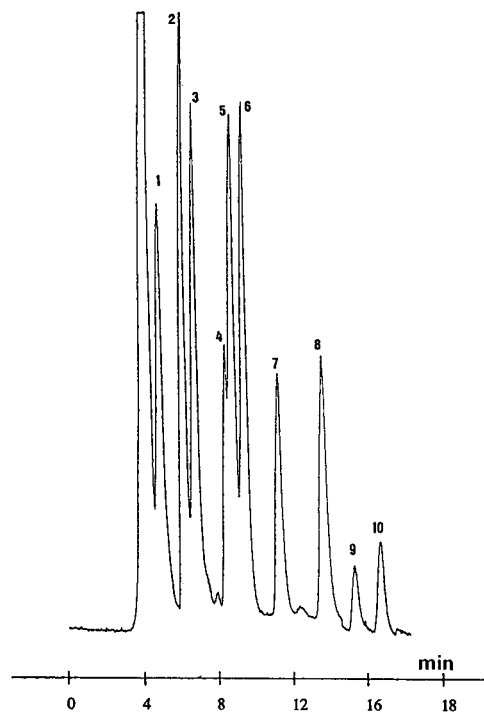
Fig. 3. Chromatographic separation of a mixture of methylglycosides. Detector parameters: atomiser inlet pressure, 25 p.s.i.; temperature, 30°C. Peaks: 1 = mesoinositol; 2 = methyl α-D-galactopyranoside; 3 = methyl α-D-glucopyranoside; 4 = methyl β-D-xylopyranoside; 5 = methyl α-D-mannopyranoside; 6 = methyl-D-lyxose; 7 = methyl α-D-N-acetylgalactosamine; 8 = methyl α-D-N-acetylglucosamine; 9 = methyl α-L-fucopyranoside; 10 = methyl α-L-rhamnopyranoside. Injections: 20 μl of 50 μg/ml of each solute. Attenuation: 256.

TABLE II

REPEATABILITY OF PEAK HEIGHT USING EITHER MESOINOSITOL OR LYXOSE AS INTERNAL STANDARD

Methylglycoside	R.S.D. (%)[a]	
	Lyxose as internal standard	Mesoinositol as internal standard
Galactose	3.7	4.7
Glucose	3.0	2.4
Mannose	3.5	1.3
N-Acetylglucosamine	3.6	3.3
Fucose	3.9	6.5
Rhamnose	2.4	5.2
Average	3.3	3.9

[a] $n = 9$.
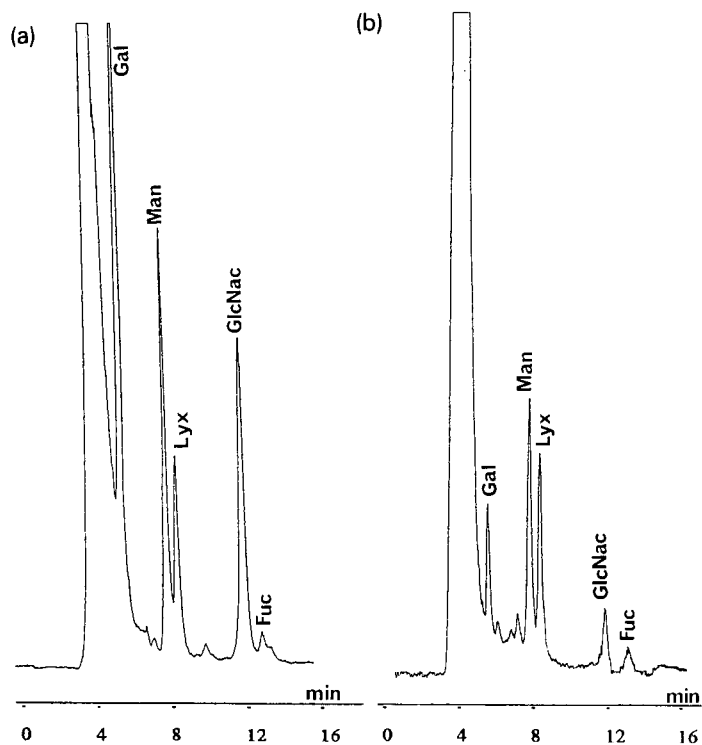
Fig. 4. Chromatograms of methylglycosides released from (a) α-AGP and (b) tPA by methanolysis using optimum methanolysis conditions. Detector parameters: atomiser inlet pressure, 25 p.s.i.; temperature, 30°C, injected volume: 20 μl, corresponding to 100 μg of the glycoprotein. Gal = galactose; Man = mannose; Lyx = lyxose; GlcNac = N-acetylglucosamine; Fuc = fucose. Attenuation: (a) 512, (b) 256.

rigorous test for the methanolysis procedure than the use of a free sugar. In contrast, lyxose seemed to be a more suitable internal standard in terms of repeatability. Methanolysis could be carefully monitored with respect to lyxose which was derivatized simultaneously with the glycoprotein sample. Lyxose gave rise to main peak which

TABLE III

MONOSACCHARIDIC COMPOSITION OF α-AGP AND tPA DETERMINED BY METHANOLYSIS FOLLOWED BY CHROMATOGRAPHIC ANALYSIS

Values expressed as mean ± S.D. in mole of sugar/mole of glycoprotein. tPA: MW = 66 000; α-AGP: MW = 44 000.

Component	Plasminogen activator[a]	α-AGP[b]
Galactose	3.9 ± 0.3	18.5 ± 1.4
Mannose	11.0 ± 0.5	15.9 ± 0.9
N-Acetylglucosamine	5.9 ± 0.7	26.1 ± 2.7
Fucose	2.1 ± 0.1	2.3 ± 0.1

[a] n = 6.
[b] n = 3.

was eluted intermediately (t_R = 8.25 min) just after methylmannose. A secondary anomer was also formed (t_R = 7.5 min) but it did not interfere with other sugars.

The method was applied to the determination of carbohydrate moiety of the two glycoproteins α-AGP and purified tPA using the conditions of methanolysis established above. Galactose, mannose, N-acetylglucosamine and fucose were readily identified in both glycoproteins (Fig. 4). In both glycoproteins, no significant amount of N-acetylgalactosamine was found, suggesting the absence of O-linked oligosaccharide. The results showed that tPA contained a high proportion of mannose, which points to the presence of mainly oligomannosidic or hybrid-type N-glycosidic chains. Moreover, the high content of N-acetylglucosamine in α-AGP indicates that N-linked oligosaccharides consist mainly of the N-acetyllactosamine type.

The reproducibility was investigated by carrying out the entire procedure (methanolysis followed by chromatographic analysis) nine times for the α-AGP and five times for the plasminogen activator. The results, expressed as the peak height of each derivative relative to that of methyllyxose, were satisfactory for all the monosaccharides present in the two glycoproteins, the R.S.D. ranging from 8.1 to 9.4% and from 4.6 to 11.2% for α-AGP and tPA, respectively.

Quantitative analysis was performed with a calibration using four concentrations (5–40 μg per 100 μl) of each monosaccharide. The peak heights were related to a constant lyxose peak height. As shown in Table I, the plots of peak height *versus* sample concentration in double logarithmic coordinates are linear. A four-point calibration graph is more accurate when dealing with unknown glycoproteins, but a two-point method would be sufficient when some data on monosaccharidic composition are already known.

The results obtained from the quantitative analysis are summarized in Table III and the quantification of each monosaccharide was found to be in a reasonable agreement with previously published data [2–4, 14–16].

This method, if applied more specifically to purified glycopeptides, could provide interesting information on the nature of the glycosidic chains attached to each glycosylation site of a glycoprotein.

CONCLUSIONS

It has been shown that the modified simplex procedure could be useful for optimizing rapidly the parameters involved in methanolysis such as temperature, reaction time and methanolic hydrochloric acid strength, as these factors are numerous and interdependent.

The entire technique, which involves the cleavage of glycosidic linkages by methanolysis of a purified glycoprotein and the determination of the released methylglycosides by liquid chromatography, is a rapid, sensitive and reproducible method for the determination of monosaccharidic maps from glycoproteins. The carbohydrate compositions of α-AGP and tPA obtained by this method closely match the compositions previously reported with other analytical techniques.

REFERENCES

1 R. J. Kraus, F. L. Shinnic and J. A. Marlett, *J. Chromatogr.*, 513 (1990) 71–81.
2 H. Takemoto, S. Hase and T. Ikenaka, *Anal. Biochem.*, 145 (1985) 245–250.
3 M. R. Hardy, R. R. Townsend and Y. C. Lee, *Anal. Biochem.*, 170 (1988) 54–62.
4 P. C. Elwood, W. R. Reid, P. D. Marcell, R. H. Allen and J. F. Kolhouse, *Anal. Biochem.*, 175 (1988) 202–211.
5 J. L. Jentoft, *Anal. Biochem.*, 148 (1985) 424–433.
6 M. Taverna, A. E. Baillet and D. Baylocq-Ferrier, *J. Chromatogr.*, 514 (1990) 70–79.
7 J. P. Zanetta, W. C. Breckenridge and G. Vincendon, *J. Chromatogr.*, 69 (1972) 291–304.
8 M. F. Chaplin, *Anal. Biochem.*, 123 (1982) 336–341.
9 R. H. Lowry, N. J. Rosenbrough, A. L. Farr and R. Randall, *J. Biol. Chem.*, 193 (1951) 265–273.
10 J. G. Beeley, *Glycoprotein and Proteoglycan Techniques*, Vol. 16, Elsevier, New York, 1985.
11 S. N. Deming and S. L. Morgan, *Anal. Chem.*, 45 (1973) 278A–283A.
12 R. E. Chambers and J. R. Clamp, *J. Biochem.*, 125 (1971) 1009–1018.
13 N. W. H. Cheetham and P. Sirimanne, *J. Chromatogr.*, 208 (1981) 100–103.
14 G. Pohl, L. Kenne, B. Nilsson and M. Einarsson, *Eur. J. Biochem.*, 170 (1987) 69–75.
15 D. C. Rijken, J. J. Eimeis and G. J. Gerwig, *Thromb. Haemostasis*, 54 (1985) 788–791.
16 F. M. Eggert and M. Jones, *J. Chromatogr.*, 333 (1985) 123–131.

Comparative studies on the high-performance liquid chromatographic determination of thiamine and its phosphate esters with chloroethylthiamine as an internal standard using pre- and post-column derivatization procedures

S. SANDER, A. HAHN, J. STEIN and G. REHNER*

Institute of Nutrition, Justus-Liebig-University, Wilhelmstrasse 20, D-6300 Giessen (Germany)

(First received February 8th, 1991; revised manuscript received May 6th, 1991)

ABSTRACT

Two improved reversed-phase high-performance liquid chromatographic procedures for the rapid separation and sensitive fluorimetric quantification of thiamine and its phosphate esters are presented using pre-column and post-column derivatiziation. Further, for the first time chloroethylthiamine has been introduced into thiamine determination as an internal standard which allows the analytical procedure to be controlled. Complete separation and sensitive detection can be achieved by both methods within 15 min. The pre-column derivatization technique is easier to perform but is sometimes accompanied by technical problems caused by the derivatization reagent. In the post-column derivatization procedure the chromatographic system was not attacked but a chemically inert derivatization pump was essential. Analysis of rat intestinal tissue by both methods including a simplified extraction scheme yielded the same results, indicating that the techniques are interchangeable.

INTRODUCTION

Early methods for the analysis of thiamine derivatives such as animal experiments [1] or microbiological assays [2,3] were based on the biological function of the vitamin. These tests are often sensitive but time-consuming, expensive and difficult to standardize and therefore sometimes less reliable. Further, they are not specific for single derivatives and therefore do not allow differentiation between the different forms of thiamine which is necessary in metabolic studies.

The most common procedure in thiamine analysis is the alkaline oxidation of thiamine and its phosphate esters to highly fluorescent thiochromes [4]. This reaction has frequently been combined with conventional column chromatography [5–7] as well as with high-performance liquid chromatography (HPLC) [8–25] to separate the thiochromes from other fluorescent compounds present in the sample.

Some of the HPLC procedures described are suitable for determining thiamine only [8–14], *i.e.* the phosphate esters must be hydrolyzed prior to chromatography.

Thus they do not allow different derivatives to be quantified. Of the systems capable of separating all thiamine derivatives, some have only been applied to standard solutions [15–17]. Therefore their suitability for the analysis of biological materials is not proven.

Moreover, only one successful attempt to integrate an internal standard has been described using amprolium [25], although several thiamine derivatives such as chloroethylthiamine might be suitable for this purpose.

The present work was aimed at establishing two rapid HPLC procedures for the quantification of thiamine and its phosphate esters as well as chloroethylthiamine as an internal standard. The systems are based either on chromatography of the intact thiamines and post-column derivatization to thiochromes or on pre-column oxidation of the vitamers to thiochromes with subsequent chromatography of the latter. A simplified scheme for the extraction of thiamine compounds from biological materials will be shown. Both methods were applied to rat intestinal tissue.

EXPERIMENTAL

Chemicals

Thiamine-chloride-hydrochloride (T), thiamine monophosphate (TMP) and thiamine pyrophosphate (TPP) were purchased from Sigma (Deisenhofen, Germany), thiamine triphosphate (TTP) from Wako (Osaka, Japan) and 5-chloroethylthiamine (CET) was provided by courtesy of Dr. Saeki (Kyoto, Japan). All substances were diluted in 0.01 N hydrochloric acid and kept at $-80°C$. All other chemicals and solvents were obtained from Merck (Darmstadt, Germany) and were of the highest purity available. Water was purified with a Millipore Q system (Waters, Eschborn, Germany).

Chromatography

Separations were carried out on a Merck–Hitachi HPLC system consisting of an L-5000 gradient former, a 655A-11 solvent metering pump, an F-1000 fluorescence detector, a D-2000 integrator and a loop injector (Rheodyne, Model 7125) with a 20-μl syringe. All analyses were performed at room temperature. Excitation and emission maxima of the different thiochromes were determined by recording fluorescence spectra during the analysis using the stop-flow technique. Quantification was performed on the basis of peak area. Calibration graphs were constructed for each compound by plotting the peak area *versus* the amount injected, and calculations were made by least-square regression analysis.

The analytical columns were filled by the upward slurry technique [26] using 2-propanol for preparing the slurry. In both methods the analytical columns were connected with a C-135 B pre-column kit (Upchurch Scientific, Oak Harbour, WA, USA) containing dry-packed Shandon ODS Hypersil (10 μm). All the solvents were freshly prepared on the day of use, filtered through 0.45-μm filters (Schleicher & Schüll, Dassel, Germany) and degassed ultrasonically under vacuum.

Pre-column derivatization technique

Oxidation of thiamine and its derivatives to fluorescent thiochromes was peformed with the help of a 0.1% solution of potassium ferricyanide in 15% sodium

hydroxide. The solution was freshly prepared from an aqueous stock solution (1%) of potassium ferricyanide every 2 h. For derivatization 80 μl of the samples were mixed with 50 μl of the reagent. A 20-μl sample of this solution was injected exactly 1 min after adding the reagent.

Thiochrome derivatives were separated on a 5-μm ODS Hypersil (Shandon) analytical column (250 × 4.6 mm I.D.). The mobile phase consisted of a gradient of 25 mM potassium hydrogenphosphate and methanol (Table Ia), which was pumped at a flow-rate of 1.2 ml/min. The pH of the buffer was adjusted to 8.4 with orthophosphoric acid. Fluorescence was recorded at excitation and emission wavelengths of 365 and 450 nm, respectively.

TABLE I

GRADIENT COMPOSITION DURING THE HPLC ANALYSIS OF THIAMINE DERIVATIVES APPLYING PRE- OR POST-COLUMN DERIVATIZATION PROCEDURES

(a) Pre-column derivatization technique				(b) Post-column derivatization technique				
Component[a]	time (min)			Component[b]	time (min)			
	0	6	11		0	2	5	8
A (%)	85	50	50	C (%)	100	100	0	0
B (%)	15	50	50	D (%)	0	0	100	100

[a] A = 25 mM potassium phosphate (pH 8.4); B = methanol.
[b] C = 50 mM sodium citrate (pH 4.0)–5 mM sodium hexane sulfate–5% methanol; D = 50 mM sodium citrate (pH 4.0)–5 mM sodium hexane sulfate–50% methanol.

Post-column derivatization technique

Thiamine and its derivatives were separated on a 3-μm ODS Hypersil (Shandon) column (125 × 4.6 mm I.D.) with a gradient of methanol and 50 mM sodium dihydrogenphosphate (Table Ib) whose pH had been adjusted to 4.0 with orthophosphoric acid. The flow-rate was 0.8 ml/min.

The derivatization reagent (0.02% postassium ferricyanide in 10% sodium hydroxide) was pumped into the eluent stream leaving the column through a T-junction with a laboratory-constructed perfusor pump at a flow-rate of 0.4 ml/min. The solution was replaced every 2 h. After a reaction zone consisting of a 2-m PTFE tube (0.8 mm I.D.), three-dimensionally coiled to minimize peak broadening [27], the fluorescence of the resulting thiochromes was measured at the wavelengths mentioned above.

Extraction procedure

To extract thiamine and its derivatives from biological materials, tissue was removed from the animals and immediately frozen in liquid nitrogen. About 1 g of tissue was homogenized in a glass–PTFE homogenizer in ice-cold 10% trichloroacetic acid (TCA) at 4°C, after 10 nmol of CET had been added. The homogenate was

brought to an end volume of 3 ml and was centrifuged for 20 min at 10 000 g. The resulting pellet was re-extracted with 10% TCA twice more, and the combined supernatants were brought to a pH of 4.5 by adding solid sodium acetate. This solution was either directly injected (post-column derivatization method) or used for derivatization (pre-column derivatization technique).

Extraction efficiency was determined by an endogenous labeling technique: Rat intestinal tissue was incubated *in vivo* for 1 h using the "ligated loop" technique [28] with 1 ml of Krebs' bicarbonate solution containing 5 mM glucose and 2 μM (thiazole-2-[^{14}C])thiamine-chloride-hydrochloride ([^{14}C]T, specific activity 0.85 GBq/mmol, Amersham, Braunschweig, Germany). The radiochemical purity of thiamine was examined by HPLC and found to be 98%. When incubations were terminated the segments were removed from the animals and extracted as described above. The radioactivity in the supernatant was measured by liquid scintillation counting and compared with that in the untreated homogenate. Pretests revealed that no measurable interconversion or loss of different thiamine derivatives resulted from the TCA treatment.

Application of the method to biological materials

The thiamine content of rat intestinal tissue was determined by both methods. Quantification was performed using an external standard graph and results were corrected for the incomplete extraction as determined in extraction efficiency studies.

RESULTS AND DISCUSSION

Pre-column derivatization technique

Fig. 1A shows a typical chromatogram of thiochromes using pre-column conversion of the thiamine derivatives. All substances were completely separated within 14 min and the next sample could be injected after approximately 15 min as the initial elution conditions can be restored at 11 min, *i.e.* before the analysis is terminated. Table IIa gives the quantitative chromatographic parameters for thiamine analysis by reversed-phase HPLC after pre-column conversion of the analyte. Only a few of the various methods for thiamine analysis using pre-column derivatization are capable of separating all vitamers [17–19,22], which is essential for metabolic studies. One of these methods was only used to separate standard solutions [17].

Although the chromatographic system described here is the first pre-column technique to integrate an internal standard, the separation is as fast as in other pre-column techniques capable only of separating natural thiamine derivatives [17,22]. In one case applying post-column derivatization, amprolium was used as an internal standard [25]. We prefer to use CET which has a greater structural similarity to thiamine and its derivatives than amprolium. We propose introducing an internal standard in thiamine analysis when the vitamers are quantified by the thiochrome reaction. Pretests revealed that the pre-column derivatization may produce varying results if it is not exactly standardized.

In contrast to other authors [22] who have reported that derivatized samples can be stored in the dark for three days, we observed that reproducibility decreased even 1 h after adding the derivatization solution. Therefore oxidation was performed just before HPLC analysis, taking into account the fact that complete oxidation is achieved within 15 s [10].
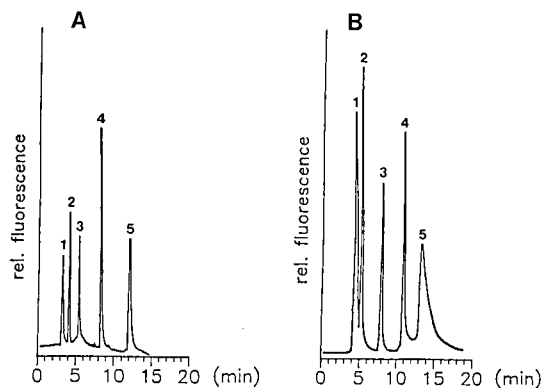
Fig. 1. Chromatographic separation of thiochromes and thiamine derivatives. (A) Separation of thiochromes after pre-column conversion of different thiamine derivatives. Conditions: column, Shandon Hypersil ODS (5 μm, 250 × 4.6 mm I.D.); mobile phase, gradient (Table Ia) consisting of 25 mM potassium phosphate (pH 8.4) and methanol at a flow-rate of 1.2 ml/min; ambient temperature; fluorimetric detection at excitation and emission wavelengths of 365 and 450 nm, respectively; 20–30 pmol of each compound were injected. Peaks: 1 = TTP-thiochrome; 2 = TPP-thiochrome; 3 = TMP-thiochrome; 4 = T-thiochrome; 5 = CET-thiochrome. (B) Separation of intact thiamines and subsequent derivatization to the corresponding thiochrome derivatives by a post-column derivatization arrangement. Conditions: column, Shandon Hypersil ODS (3 μm, 125 × 4.6 mm I.D.); mobile phase, gradient (Table Ib) consisting of 50 mM sodium citrate (pH 4.0)–5 mM sodium hexane sulfate–5% methanol and 50 mM sodium citrate (pH 4.0)–5 mM sodium hexane sulfate–50% methanol at a flow-rate of 0.8 ml/min; derivatization reagent (0.02% potassium ferricyanide in 10% sodium hydroxide) was pumped into the eluent stream leaving the column at a flow-rate of 0.4 ml/min; detection and peaks as described under (A).

TABLE II

QUANTITATIVE CHROMATOGRAPHIC PARAMETERS FOR HPLC ANALYSIS OF THIA-MINE DERIVATIVES

Compound	Retention time (min)	Range of linearity (pmol)	Detection limit (pmol)	Standard curve parameters[a]			Precision[b]
				a	b	r	
(a) After pre-column derivatization procedure to the corresponding thiochromes							
TTP	2.85	0.5 – 200	0.1	21.3	−11.3	0.994	6.8
TPP	4.11	0.2 – 200	0.05	23.6	−10.8	0.995	4.2
TMP	5.20	0.2 – 200	0.05	27.6	−19.8	0.996	5.9
T	9.01	0.1 – 200	0.02	59.6	−19.8	0.998	2.7
CET	12.3	0.1 – 200	0.02	6.1	5.3	0.993	3.3
(b) After separation of intact thiamines and subsequent derivatization to the corresponding thiochrome derivatives							
TTP	3.99	0.4 – 200	0.1	24.4	−58.0	0.996	5.4
TPP	4.95	0.2 – 200	0.05	36.0	−33.1	0.998	5.5
TMP	6.33	0.2 – 200	0.05	35.1	−42.1	0.999	3.5
T	10.64	0.1 – 200	0.03	44.6	16.6	0.998	3.4
CET	13.54	0.6 – 200	0.1	15.2	12.6	0.994	2.6

[a] Parameters were determined using the equation $y = ax + b$, with x = pmol injected and y = peak area.
[b] Precision is the percentage deviation of the mean as it has been obtained by repeated analysis of the same sample ten times; sample contained 62.5 pmol per injection of each compound.

Nevertheless, the addition of a constant amount of an internal standard like CET to each sample makes it possible to control the reproducibility of the analytical procedure and allows possible deviations within the derivatization step to be corrected. One group analyzing thiamine with a post-column derivatization technique reported the use of salicylamide as an internal standard [10], but it is evident that this substance, which is structurally dissimilar to the thiamine molecule, is not suitable for this purpose.

As Table IIa indicates, the pre-column technique is highly reproducible and enables us to detect subpicomolar quantities of thiamine and its derivatives. The detection limits, which were determined at a signal-to-noise ratio of 3:1, are in the same range as those observed by other authors [20–24].

A disadvantage of the pre-column derivatization technique is the fact that aggressive solutions have to be applied to the chromatographic system. We noted that parts of the loop's injector were rapidly destroyed. This can only be prevented by using special, i.e. chemically inert, materials. Moreover, in spite of using a pre-column the analytical column was attacked within several days during routine analysis, leading to worse resolution and peak symmetry. This could be prevented when the system was flushed with distilled water for 5 min after each analysis.

Post-column derivatization technique

As Fig. 1B and Table IIb clearly indicate, chromatographic separation of intact thiamine derivatives on reversed-phase HPLC with post-column conversion of the vitamers to the corresponding thiochromes also allows the fast and sensitive quantification of these substances. Separation was terminated after 16 min and the next sample could be injected immediately because the gradient program was terminated after 8 min and therefore the column was re-equilibrated by the time the analysis was finished. Detection limits were comparable to the pre-column derivatization technique and thus to other methods proposed [20–24]. Concerning the reproducibility of both chromatographic procedures presented here, it should be mentioned that we injected very low quantities of substrate. As can be seen from the results of others [29], reproducibility increases when higher amounts are chromatographed.

Several techniques for the HPLC separation of thiamine with post-column derivatization to thiochromes have been proposed [10–12,15,16,21,23,25], but some authors separated thiamine itself but not its phosphate esters [10–12]. The application of post-column HPLC analysis of thiamine and its derivatives to biological material was shown in two cases only [23,25]. As mentioned, one of these techniques integrated amprolium as an internal standard [25].

In contrast to the pre-column procedure described above, separation of intact thiamine derivatives obviously did not present any technical problems, but delivery of the oxidation reagent by a conventional HPLC system attacked the equipment. Therefore we used a laboratory-constructed perfusor-like pump which was chemically inert and guaranteed a continuous flow without pulsation. Unlike the commercially available derivatization systems this pump was cheap to acquire.

Extraction procedure

As can be seen from Fig. 2, practically no impurities were found in the chromatograms of rat intestine, indicating that extraction is highly specific. This could also
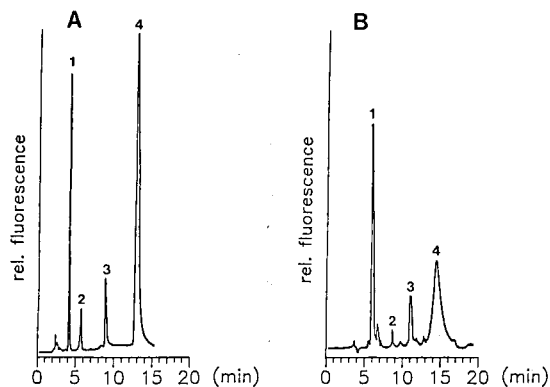
Fig. 2. Typical chromatograms of thiamine derivatives from rat intestinal tissue; separation conditions as in Fig. 1. Peaks: 1 = TPP-thiochrome; 2 = TMP-thiochrome; 3 = T-thiochrome; 4 = CET-thiochrome.

be confirmed by recording fluorescence spectra of the different peaks, which were compared with those of standards and found to be identical. Compared with other extraction methods using TCA with subsequent removal of the acid by extraction with ethyl ether [19,22,24], the procedure described here is much easier and faster to perform.

The extraction efficiency is one important factor responsible for the precision of a method, but it is difficult to determine [30]. We chose an endogenous labeling technique to evaluate the extraction efficiency using intestinal tissue as a model matrix. Chromatographic studies revealed that the relation of radiolabeled thiamine derivatives after incubation (Fig. 3) was identical to the endogenous substrates (Table III), thus indicating that [14C]T had equilibrated with the endogenous metabolites. Extraction efficiency as judged by this technique was 86.4 ± 3.7% (n = 12).

We favor the endogeneous labeling technique over the generally given "recovery rates", which are easier to determine but which involve several problems. For example they do not reflect the efficiency with which protein bonds are cracked because substrates given to tissue homogenate just before the extraction cannot be expected to behave like the endogenous substances. Our results confirm this assumption. For comparison we also determined the recovery rates, which were found to be about 95–100% and thus in the same range as those found by several authors [8,14,23–25], whereas extraction efficiency was lower.

Analysis of rat intestinal tissue

Table III gives the amount of different thiamine metabolites as determined by the two methods, and Fig. 2 shows typical chromatograms. Both procedures led to similar results concerning the total content of thiamine as well as the relation between the different metabolites. Differences were within the deviation of the thiamine contents and not statistically significant. TTP could not be detected in rat intestinal tissue, which is not surprising considering that there is probably no function for this derivative in the gut wall. On the other hand, most of the thiamine was found as TPP,
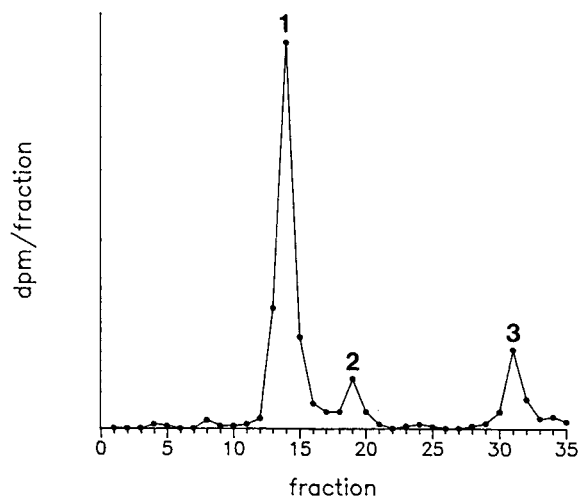
Fig. 3. Separation of radiolabeled thiamine derivatives from "ligated loops" of rat small intestine. Intestinal tissue was incubated with 2 μM [^{14}C]T and extracted as described under Experimental; separation conditions as in Fig. 1B; the solvent stream was collected in fractions of 0.3 ml and assayed by liquid scintillation counting. Peaks were identified by comparison with standard chromatograms. Peaks and percentage relation of total thiamine: 1 = TPP-thiochrome (74.3%); 2 = TMP-thiochrome (7.6%); 3 = T-thiochrome (18.1%).

which is because of its biological role and the mechanism of intestinal absorption of thiamine, which involves rapid conversion to TPP as can ben seen from the incubation experiments (Fig. 3) as well as from the results of others [31,32].

Table IV shows the reproducibility of the overall methods as determined by five-fold analysis of the same samples emphasizing that the technique is easily reproducible. When interpreting these small variations it should not be overlooked that these discrepancies might even be due to an inhomogeneity of the sample itself because five small pieces of gut were analyzed separately.

The results clearly indicate that both methods presented in this paper allow the

TABLE III

THIAMINE CONTENT AND THIAMINE DERIVATIVES OF RAT INTESTINAL TISSUE AS DETERMINED BY PRE-COLUMN DERIVATIZATION AND POST-COLUMN DERIVATIZATION TECHNIQUE, RESPECTIVELY (nmol/g ± S.D.); PERCENTAGE OF TOTAL THIAMINE DERIVATIVES

	T	Percentage	TMP	Percentage	TPP	Percentage	Total
Pre-column[a]	2.31 ± 0.87	16.5	1.25 ± 0.63	8.9	10.46 ± 2.96	74.6	14.02
Post-column[b]	2.05 ± 0.96	16.6	0.79 ± 0.71	6.4	9.52 ± 0.97	77.0	12.36

[a] Pre-column derivatization of thiamine derivatives to the corresponding thiochromes with subsequent separation of these compounds as shown in Fig. 1A and Table Ia.

[b] Separation of intact thiamines with post-column derivatization to thiochromes as shown in Fig. 1B and Table Ib.

TABLE IV

PRECISION OF THE OVERALL METHOD AS DETERMINED BY FIVE-FOLD ANALYSIS OF THE SAME GUT SAMPLE

Extraction and HPLC analysis were carried out with five small intestinal segments obtained from the same rat. Values given are the means ± S.D. (nmol/g tissue)

	T	TMP	TPP
Pre-column[a]	2.15 ± 0.16	1.08 ± 0.09	10.38 ± 1.06
Post-column[b]	2.23 ± 0.13	0.77 ± 0.08	9.66 ± 1.03

[a] Pre-column derivatization of thiamine derivatives to the corresponding thiochromes with subsequent separation of these compounds as shown in Fig. 1A and Table Ia.
[b] Separation of intact thiamines with post-column derivatization to thiochromes as shown in Fig. 1B and Table Ib.

fast separation and quantification of thiamine and its phosphate esters from biological samples. There can be no general answer to the question of which method is preferable, this must be decided individually depending on the purpose and technical possibilities of each laboratory. For routine analysis we propose post-column derivatization with a perfusor-like derivatization pump which is less expensive, whereas determination of single samples is easier to perform by the pre-column technique.

ACKNOWLEDGEMENTS

REFERENCES

1 E. F. Cook, *J. Am. Pharm. Assoc.*, 28 (1939) 267.
2 C. F. Niven and K. L. Smiley, *J. Biol. Chem.*, 150 (1943) 1.
3 H. Sobotka, H. Baker and O. Frank, *Proc. Soc. Exp. Bull. Med.*, 103 (1960) 801.
4 B. C. P. Jansen, *Rec. Trav. Chim. Pays Bas*, 55 (1936) 1046.
5 G. Rindi and L. De Giuseppe, *Biochem. J.*, 78 (1961) 602.
6 H. Koike, T. Wada and H. Minakami, *J. Biochem.*, 62 (1967) 492.
7 T. Matsuda and J. R. Cooper, *Anal. Biochem.*, 117 (1981) 203.
8 R. L. Roser, A. H Andrist, W. H. Harrington, H. K. Naito and D. Londsdale, *J. Chromatogr.*, 146 (1978) 43.
9 C. Y. W. Ang and F. A. Moseley, *J. Agric. Food Chem.*, 28 (1980) 486.
10 J. P. M. Wielders and C. J. K. Mink, *J. Chromatogr.*, 277 (1983) 145.
11 R. L. Wehling and D. L. Wetzel, *J. Agric. Food Chem.*, 32 (1984) 1326.
12 H. Ohta, H. Baba, Y. Suzuki and E. Okada, *J. Chromatogr.*, 284 (1984) 281.
13 W. Weber and H. Kewitz, *Eur. J. Clin. Pharmacol.*, 28 (1985) 213.
14 B. Bötticher and D. Bötticher, *Int. J.Vit. Nutr. Res.*, 56 (1986) 155.
15 B. C. Hemming and C. J. Gubler, *J. Liq. Chromatogr.*, 3 (1980) 1697.
16 M. Kimura, T. Fujita, S. Nishida and Y. Itokawa, *J. Chromatogr.*, 188 (1980) 417.
17 J. Bontemps, L. Bettendorff, J. Lombet, C. Grandfils, G. Dandrifosse, E. Schoffeniels, F. Nevejans and J. Crommen, *J. Chromatogr.*, 295 (1984) 486.
18 K. Ishii, K. Sarai, H. Sanemori and T. Kawasaki, *Anal. Biochem.*, 97 (1979) 191.

19 K. Ishii, K. Sarai, H. Sanemori and T. Kawasaki, *J. Nutr. Sci. Vitaminol.*, 25 (1979) 517.
20 H. Sanemori, H. Ueki and T. Kawasaki, *Anal. Biochem.*, 107 (1980) 451.
21 M. Kimura, B. Panijpan and Y. Itokawa, *J. Chromatogr.*, 245 (1982) 141.
22 J. Bontemps, P. Philippe, L.Bettendorff, J. Lombet, G. Dandrifosse, E. Schoffeniels and J. Crommen, *J. Chromatogr.*, 307 (1984) 283.
23 M. Kimura and Y. Itokawa, *J. Chromatogr.*, 332 (1985) 181.
24 L. Bettendorff, C. Grandfils, C. de Rycker and E. Schoffeniels, *J. Chromatogr.*, 382 (1986) 297.
25 J. T. Vanderslice and M. H. Huang, *J. Micronutr. Anal.*, 2 (1986) 189.
26 P. A. Bristow, P. N. Brittain, C. M. Riley and B. F. Williamson, *J. Chromatogr.*, 131 (1977) 57.
27 H. Engelhardt and U. D. Neue, *Chromatographia*, 15 (1982) 403.
28 A. Sols and F. Ponz, *Rev. Esp. Fisiol.*, 3 (1947) 207.
29 C. Wegner, M. Trotz and H. Nau, *J. Chromatogr.*, 378 (1986) 55.
30 J. F. Gregory, *Food Technol.*, 13 (1983) 75.
31 G. Ferrari, G. Sciorelli, P. Del Poggio, U. Ventura and G. Rindi, *Pflügers Arch (Eur. J. Physiol.)*, 356 (1975) 111.
32 G. Ferrari, C. Patrini and G. Rindi, *Pflügers Arch. (Eur. J. Physiol.)*, 393 (1982) 37.

Column liquid chromatographic determination of carbadox and olaquindox in feeds

FERNANDO JORGE DOS RAMOS* and IRENE NORONHA DA SILVEIRA

Laboratório de Bromatologia e Nutrição, Faculdade de Farmácia da Universidade de Coimbra, 3000 Coimbra (Portugal)

and

GERRIT DE GRAAF

Central Veterinary Institute, Department of Biochemistry and Toxicology, P.O. Box 65, 8200 AB Lelystad (Netherlands)

(First received November 6th, 1990; revised manuscript received April 3rd, 1991)

ABSTRACT

A column liquid chromatographic method for simultaneous determination of carbadox and olaquindox in swine feeds is described. The drugs were extracted from feeds with carbon tetrachloride–dimethylformamide (80:20) at 60°C for 30 min. The extract was mixed with water (25:45). After centrifugation the aqueous layer was chromatographed on a reversed-phase column using gradient elution and ultraviolet detection at wavelengths of 305 and 262 nm. Recoveries from samples fortified at levels of 20–50 ppm were $92 \pm 9\%$ for carbadox and $93 \pm 6\%$ for olaquindox (means $\pm$ standard deviations, $n = 71$).

INTRODUCTION

Growth promoters are widely used in the production of animal protein. The additives carbadox [methyl-3-(2-quinoxalinylmethylene)-N^1,N^4-dioxide] and olaquindox[2-(N-2'-hydroxyethylcarbamoyl)-3-methylquinoxaline-N^1,N^4-dioxide] are used as such in swine feeds in the European Community. It is recommended that there should not exceed 50 mg per kg of complete feed, except that olaquindox can reach 100 mg/kg in milk substitutes [1,2].

The published methods concern the determination of either carbadox [3-13] or olaquindox [14-18] in feeds. High-performance liquid chromatography (HPLC) is chosen because this technique permits the detection of low-level concentrations of carbadox (10-24 μg/kg) [3-5] as well as olaquindox (0.3-1 mg/kg) [14,15].

The present study aims to offer a view of the use of these additives by Portuguese enterprises and, at the same time, to present a method that permits the simultaneous determination of the two growth promoters.

EXPERIMENTAL

Chemicals and reagents

Carbadox and olaquindox were kindly provided by Pfizer (Lisbon, Portugal) and Lusifar (Lisbon, Portugal), respectively. N,N-Dimethylformamide (DMF) and carbon tetrachloride were reagent grade from Merck (Darmstad, Germany). Methanol (LiChrosolv, Merck)–water purified via Milli-Q (Millipore, Bedford, MA, USA) was used as the mobile phase.

Apparatus

A Gilson liquid chromatograph (Villiers-le-Bel, France) equipped with two Model 302 pumps, a mixing chamber, Model 116 a UV dual-wavelength detector set at 305 nm for carbadox and 262 nm for olaquindox, a Model 7125 injection valve (Rheodyne, Cotati, CA, USA) with a 20-μl loop, and a Versapack C_{18} reversed-phase column, 250 $\times$ 4.1 mm I.D., 10 μm particle size (Alltech, Deerfield, IL, USA), were used. The chromatographic system was controlled by an Apple II_e personal computer (Cupertino, CA, USA) with proper software and data registration. The mobile phase was degassed by ultrasonication (Bandelin Sonorex RK 100, Berlin, Germany). A Moulinex blender (Lisbon, Portugal) with a steel blade and a 40-mesh tammy was used to grind and to sieve the sample. The extraction process was performed with a Selecta Agimatic N magnetic mixer (Barcelon, Spain), a G_1 glass filter (100 μm porosity), and a Selecta Macrotronic centrifuge.

Standard solutions

Weigh accurately 50.0 mg of carbadox into a 100-ml volumetric flask and dissolve in DMF (Solutions of carbadox and olaquindox are light-sensitive. Protect standard solutions and sample extracts from direct sunlight or artificial light. Conduct the analytical process under diffused lighting or use brown glass.) This stock solution is stable for several months when kept in the dark at 4°C. To 100-, 50-, 25- and 20-ml volumetric flasks, introduce 2 ml of stock solution and complete the volume with DMF. Then add 10 ml of each previous solution to a 50-ml volumetric flask and adjust the volume with carbon tetrachloride. These solutions contain respectively 2, 4, 8 and 10 μg of carbadox per ml.

To prepare standard solutions of olaquindox, proceed as for carbadox.

Sample preparation

Weigh 10.0 g of a sample, previously ground and sieved by the Moulinex blender, into a 250-ml flask and add a magnetic bar, 20 ml of DMF and 60 ml of carbon tetrachloride. Adapt an air condensator and put in the magnetic mixer set to 500 rpm at 60°C for 30 min. Then cool, filter through G_1 under vacuum and wash the residue with a minimum of carbon tetrachloride. Transfer to a 100-ml volumetric flask and adjust the volume with carbon tetrachloride [19]. Introduce 25 ml of the filtered extract into a centrifuge tube, add 45 ml of water, stir vigorously for 2 min, and centrifuge for 5 min at 320 *g*.

Chromatography

Inject the anterior aqueous layer into the chromatographic system. Elution was

performed by gradient, starting with methanol–water (15:85) until $t = 4$ min, increasing linearily to 50:50 until $t = 6$ min, maintaining 50:50 till $t = 10$ min, and returning linearly to 15:85 till $t = 12$ min. Flow-rate was 1.5 ml/min.

Peak areas were interpolated in a calibration curve obtained from similarly treated standard solutions. Calibration curves had coefficients of correlation of 0.997 and 0.998 for carbadox and olaquindox, respectively.

RESULTS AND DISCUSSION

Chromatograms of carbadox and olaquindox samples are presented in Figs. 1 and 2, respectively. Fig. 3 presents chromatograms of a sample without carbadox and olaquindox (Fig. 3A) and the same sample supplemented with 20 mg/kg of the two growth promoters (Fig. 3B), showing good separation of the compounds and the absence of interfering components, while the sensitivity is quite satisfactory.

The recoveries of carbadox and olaquindox from fortified feed samples, based on peak areas, are given in Table I. In this table it can be seen, for instance, that a sample without carbadox (quantity existent $= 0.00$ mg/kg) spiked with 20.00 mg/kg (quantity added $= 20.00$ mg/kg) has a recovery of 100% (mean recovery of carbadox, $n = 3$). The precision of the method was analysed by repeated determinations of carefully prepared feed samples. The intra-assay coefficient of variation (C.V.) of three samples ranged from 1.3 to 3.9% for carbadox and from 1.0 to 3.6% for olaquindox. Interassay C.V. at the different concentrations ranged from 4.9 to 9.1% for carbadox and from 2.2 to 6.5% for olaquindox.

Apparently, at the concentration levels studied, the recovery is independent both of the quantity with which the samples were supplemented and of the concentration of
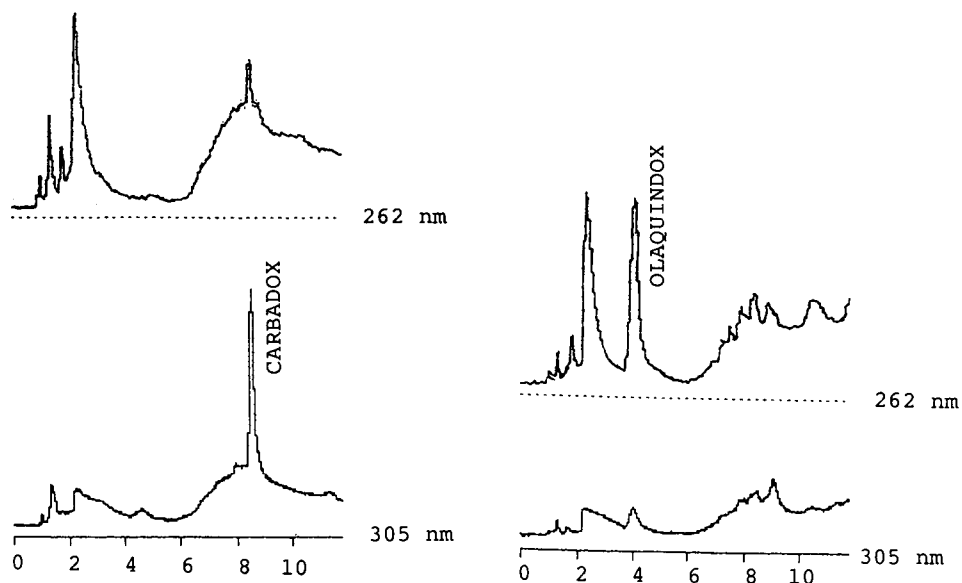
Fig. 1. Chromatograms of a sample with carbadox (22.58 mg/kg).

Fig. 2. Chromatograms of a sample with olaquindox (32.85 mg/kg).
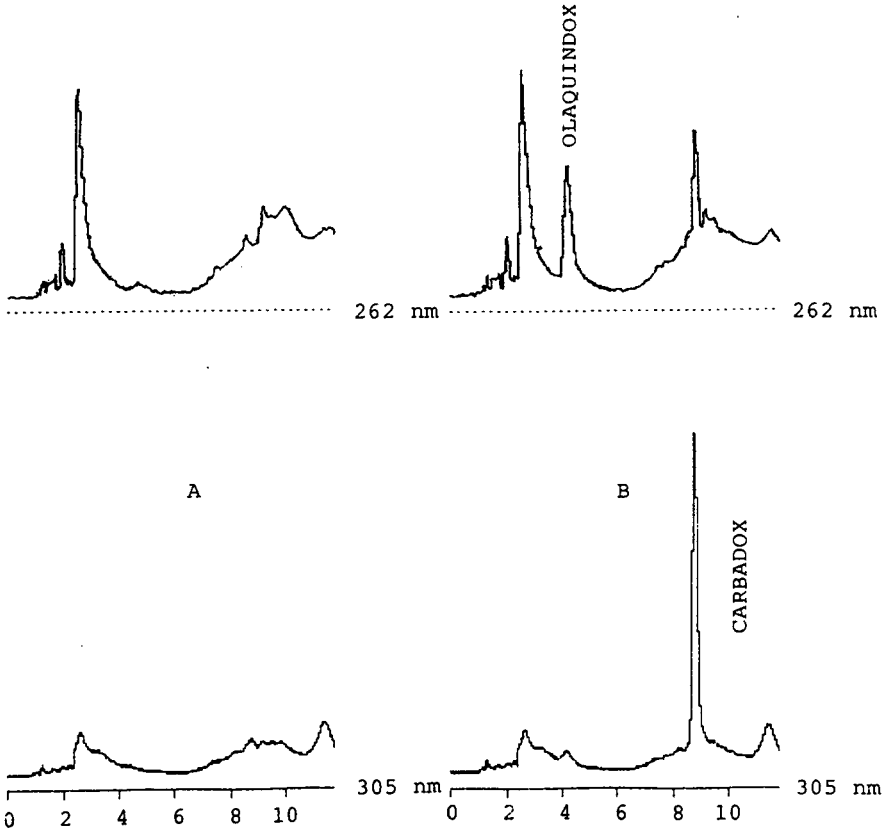
Fig. 3. Chromatograms of a representative sample without carbadox or olaquindox (A), and the same sample supplemented with 20 mg/kg of the two growth promoters (B).

TABLE I

MEAN RECOVERIES (%) OF CARBADOX AND OLAQUINDOX IN SPIKED FEED SAMPLES ($n = 3$)

Growth promoters	Quantity existent (mg/kg)	Quantity added (mg/kg)			
		20.00	30.00	40.00	50.00
Carbadox	0.00	100	99	94	94
	20.37	100	95	103	98
	49.66	72	81	84	85
Olaquindox	0.00	100	89	88	91
	15.94	99	95	101	101
	44.62	93	84	89	94
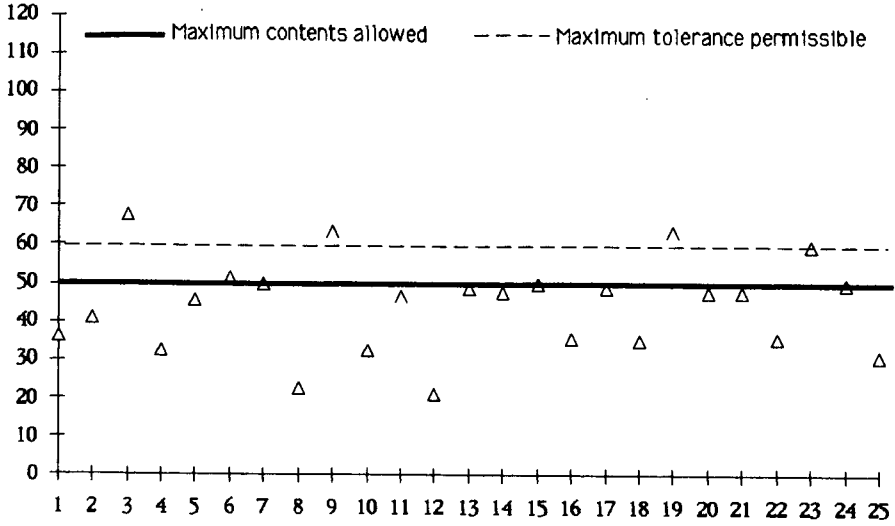
Fig. 4. Distribution of carbadox concentrations in feed samples. *y*-axis: concentration in mg/kg; *x*-axis: samples.

the additives previously determined in the samples. The results also indicate that this method is quite acceptable for routine determination of carbadox and olaquindox in feeds.

Various commercial swine feeds were sampled as random and analysed for their carbadox and olaquindox content of the 71 samples obtained, 25 contained carbadox,
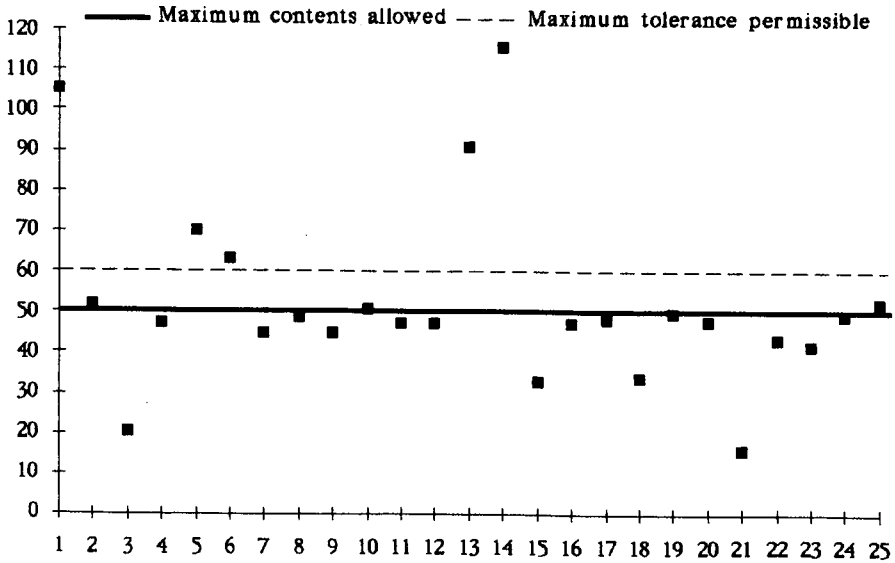
Fig. 5. Distribution of olaquindox concentrations in feed samples. *y*-axis: concentration in mg/kg; *x*-axis: samples.

25 contained olaquindox, and 20 contained neither. Only one sample contained both promoters, which under Portuguese law is not permitted [20].

Figs. 4 and 5 show the contents of carbadox and olaquindox in 50 samples containing at least one of the additives, verifying that the samples do not exceed either the maximum limit allowed or the tolerance of 20%. In general, it can be concluded that the use of carbadox as a growth promoter in Portuguese feeds obeys Portuguese rules. However, the use of olaquindox should be subjected to rigid vigilance since the limit is frequently trespassed.

REFERENCES

1 Directive 87/316/EEC, *Off. J. Eur. Communities*, L160, 1987.
2 Directive 87/317/EEC, *Off. J. Eur. Communities*, L160, 1987.
3 J. E. Roybal, R. K. Munns and W. Shimoda, *J. Assoc. Off. Anal. Chem.*, 68 (1985) 635.
4 G. J. de Graaf and T. J. Spierenburg, *J. Assoc. Off. Anal. Chem.*, 68 (1985) 658.
5 R. G. Luchtefeld, *J. Assoc. Off. Anal. Chem.*, 60 (1977) 279.
6 J. T. Goras, D. A. Gonci, K. Murai, J. E. Curley and P. N. Gordon, *J. Assoc. Off. Anal. Chem.*, 57 (1974) 982.
7 V. A. Thorpe, *J. Assoc. Off. Anal. Chem.*, 59 (1976) 1290.
8 V. A. Thorpe, *J. Assoc. Off. Anal. Chem.*, 61 (1978) 88.
9 J. T. Goras, *J. Assoc. Off. Anal. Chem.*, 62 (1979) 982.
10 V. A. Thorpe, *J. Assoc. Off. Anal. Chem.*, 63 (1980) 981.
11 D. M. Lowie, R. T. Teague, F. E. Quick and C. L. Foster, *J. Assoc. Off. Anal. Chem.*, 66 (1983) 602.
12 R. M. L. Aerts and G. A. Werdmuller, *J. Assoc. Off. Anal. Chem.*, 71 (1988) 484.
13 E. D. McGary, *Analyst (London)*, 111 (1988) 1341.
14 K. Thente and B. Andersson, *J. Sci. Food Agric.*, 33 (1982) 945.
15 T. J. Spierenburg, H. Van Lenthe, G. J. de Graaf and L. P. Jager, *J. Assoc. Off. Anal. Chem.*, 71 (1988) 1106.
16 Analytical Methods Committee, *Analyst (London)*, 110 (1985) 75.
17 N. Botsoglou, D. Kufidis, A. B. Spais and V. Vassilopoulos, *J. Agric. Food Chem.*, 33 (1985) 907.
18 G. F. Bories, *J. Chromatogr.*, 172 (1979) 505.
19 P. Hocquellet, *Ind. Aliment. Anim.*, 6 (1975) 7.
20 Portaria 1103/89, *Diário da República*, I série (1989) 296.

Highly sensitive determination of photosynthetic pigments in marine *in situ* samples by high-performance liquid chromatography

KUNIO KOHATA* and MASATAKA WATANABE

Laboratory of Marine Environment, National Institute for Environmental Studies, 16-2 Onogawa, Tsukuba, Ibaraki 305 (Japan)

and

KAZUO YAMANAKA

Department of Industrial Chemistry, Science University of Tokyo, 1-3 Kagurazaka, Shinjuku-ku, Tokyo 162 (Japan)

(First received February 20th, 1989; revised manuscript received April 24th, 1991)

ABSTRACT

A reversed-phase high-performance liquid chromatographic (HPLC) method was developed by optimizing a solvent system for the highly sensitive determination of photosynthetic pigments in marine *in situ* samples. The proposed HPLC system can handle injection volumes greater than 400 μl without a significant loss in the resolution between chlorophyllide a and chlorophyll $c_1 + c_2$. The system also reduces the sample volumes required for the analysis of typical pigments of oligotrophic sea water to 500 ml. The elution time for all pigments is 24 min at a flow-rate of 1 ml/min and 12 min at a flow-rate of 2 ml/min using a 250 mm × 4.6 mm I.D. column.

INTRODUCTION

The determination of photosynthetic pigments and their degradation products is one of most reliable methods of estimating phytoplankton biomass in marine samples [1,2]. The chromatographic analysis of photosynthetic pigments is a powerful technique for the characterization of phytoplankton communities to provide the relative abundance of each phytoplankton class in a particular sample [3–5]. Analysis of the pigments by high-performance liquid chromatography (HPLC) has been applied successfully to samples from marine ecosystems [2–9]. However, large volumes (up to several tens of liters) of oligotrophic or tropical samples (*e.g.* chlorophyll a concentrations less than 1 μg l^{-1}) are required for pigment analysis by this method [2–8]. The time-consuming filtration of such large sample volumes has presented problems in analyses in the field. This paper shows how this problem can be overcome by using a large injection volume.

EXPERIMENTAL

Algal culture

Clonal axenic strains of *Heterosigma akashiwo* (NIES-6), *Gephyrocapsa ocean-ica* (NIES-353), *Thalassiosira rotula* (NIES-328), *Skeletonema costatum* (NIES-323), *Heterocapsa triquetra* (NIES-7) and *Pyramimonas parkeae* (NIES-254), maintained in the Microbial Culture Collection of the National Institute for Environmental Stud-ies (NIES), were used. The algal cultures were maintained on a 12:12 h light:dark cycle at 23°C in f/2 medium. Illumination was provided by daylight fluorescent lamps at a quantum flux density of 80 $\mu E \ m^{-2} \ s^{-1}$. The cultures were harvested 2–3 weeks after inoculation and were filtered onto GF/C filters (Whatman International, Maid-stone, UK). The filters were refrigerated at $-20°C$ until analysis.

Oceanic samples

Samples were taken with a 10-l Van Dorn-type bottle in the Seto Inland Sea on 20 July 1987 [10]. For the chromatographic analysis of chlorophyll (Chl) and carote-noids, 2000 ml of sea water were filtered through a Whatman CF/C filter at a field station. For preparing alloxanthin, 6000 ml of sea water were filtered in the same way. The filters were stored at $-20°C$ until analysis at NIES.

Pigment extraction

The filtered samples were extracted in 10 ml of ice-cold 90% acetone, which had been degassed with nitrogen. The extraction was performed in the dark. Pigment extracts were obtained after homogenization of the filter with a glass grinder followed by centrifugation. The extract (25–400 μl) of the pigments was injected directly into an HPLC system after filtration with a Millipore FH filter (0.5 μm pore size, Nihon Millipore, Tokyo, Japan).

Column liquid chromatographic analysis

The HPLC system was essentially the same as that described previously (LC-6A pumps controlled by SCL-6A, Shimadzu, Kyoto, Japan) [11] except for a solvent system for linear-gradient elution. The gradient-elution was performed as follows: from 100% solvent A (ion-pairing solution–water–acetone–acetonitrile, 5:25:20:50) to 100% solvent B (acetone–ethyl acetate, 50:50) in a 20 min, followed by an isocratic hold at 100% B over 5 min at a flow-rate of 1.0 ml min^{-1}. In a fast-flow mode, each time period of gradient elution was shortened to half of the original period, and the flow-rate was maintained at 2.0 ml min^{-1}. The ion-pairing solution [1] consisted of tetrabutylammonium hydroxide (10 ml of a 0.5 M solution) and ammonium acetate (7.7 g) made up to 100 ml with distilled water. The solution was neutralized with acetic acid to pH 7.1. The solvent system was chosen to allow a large injection volume (up to 400 μl) to reduce the sampling volume in the field. The two solvents were degassed by helium throughout the analyses. The HPLC column used in this work was a 250 mm × 4.6 mm I.D. Whatman Partisil ODS-3, 5 μm (packed by Chemco Scientific, Osaka, Japan) column protected by a CSK I guard column with ODS packing (Whatman, Clifton, NJ, USA).

The absorbance was measured at 440 nm (Shimadzu, SPD-6AV) and fluo-rescence detection (Shimadzu RF-540 spectrofluorophotometer) was used to aid in

the identification of the chloropigments. The spectrofluorophotometer was set at an excitation wavelength of 440 nm (20 nm slit width) and an emission wavelength of 660 nm (40 nm slit width). Peak heights and peak area were measured (Shimadzu C-R3A Chromato-data processor) on the absorbance trace. Supplemental identification of pigments was carried out from absorbance spectra (every 2 nm from 350 to 668 nm) obtained with a photo-diode array detector (Shimadzu, SPD-M6A) and a data-processing system (PC9801RA5, NEC, Tokyo, Japan).

Pigment standards and solvents

Authentic chlorophyll (Chl) *a*, Chl *b*, and β-carotene were purchased from Sigma (St. Louis, MO, USA). Standard samples of carotenoids other than alloxanthin were obtained from the axenic cultures described earlier. Alloxanthin was obtained from the oceanic sample. Pigment extracts of the algal cultures and the oceanic sample were obtained in the same way as for the HPLC samples. The extract was transferred to diethyl ether and concentrated under a nitrogen gas stream. The pigments were isolated on reversed-phase C_8 thin-layer chromatography (TLC) plates (20 × 5 cm, KC8, Whatman) developed with 98–80% aqueous methanol in a saturated-type TLC box (Model HPS-204, hanging plate type, Advantec Toyo Kaisha, Tokyo, Japan) at room temperature. The pigments were scraped from the plates and redissolved in 90% acetone or ethanol. The standard solutions of pigments, the absorption spectra of which had been recorded with a Hitachi 220A spectrophotometer and standardized using reported specific absorption coefficients [12], were injected into the HPLC system to provide pigment identification and quantitative data from the HPLC chromatogram (Table I).

Chlorophyllide *a* was obtained from the enzymatic degradation of Chl *a* [13] with chlorophyllase extracted from the acetone powder of *Citrus unshiu* fruits [14]; the powder was a gift from Dr. K. Shimokawa. Phaeophytin *a* was prepared by acidification of Chl *a* [2].

Acetone, acetonitrile, ethanol and ethyl acetate were HPLC-grade reagents (Wako, Osaka, Japan) and were used without purification other than filtration and degassing. Water was purified using a Millipore Milli-Q system.

RESULTS AND DISCUSSION

The chromatographic and spectroscopic properties of the algal pigments are listed in Table I and compared with those reported previously. The purities of the peaks in Table I were calculated by averaging two correlation factors at the upslope and downslope; the correlation factor was defined as [15]:

$$\text{Correlation factor} = \frac{[\sum x \cdot y - (\sum x \cdot \sum y)]^2}{\left[\sum x^2 - \frac{(\sum x \cdot \sum x)}{n}\right]\left[\sum y^2 - \frac{(\sum y \cdot \sum y)}{n}\right]}$$

The values x and y are the measured absorbances in the peak-top and upslope (or downslope) spectrum at the same wavelength; n is the number of data points and $\sum$ is the sum of the data.

TABLE I

CHROMATOGRAPHIC AND SPECTROSCOPIC PROPERTIES OF ALGAL PIGMENTS

No.	Pigment	Retention time (min)	Solvent	Maximum wavelengths (nm)			Peak ratio[a]	Purity[b]	Ref.
				I	II	III			
1	Chlorophyllide a	7.03	Eluent[c]	429	616	664	1.1	0.9999	TW[e]
			Diethyl ether	429	615	662	1.2		
			Eluent[d]	430	616	664	1.3		2
			Diethyl ether	428		662		29	
2	Chl c^f	8.71	Eluent	442	580	630	7.5	0.9999	TW
			Acetone	446	580	630	8.1		
			Eluent	442	580	630	9.8		2
			Acetone	444	581	630	6.7		30
3	Peridinin	11.34	Eluent		472			1.0000	TW
			Ethanol		471				
			Eluent		470				2
			Ethanol		472				31
4	Neoxanthin	11.85	Eluent	413	437	465	87	0.9999	TW
			Ethanol	413	437	466	88		
			Eluent	412	437	466	91		2
			Ethanol	410	436	464	93		2
5	Fucoxanthin	12.40	Eluent		447	(466)		1.0000	TW
			Acetone		446	467	5.4		
			Eluent		446	(468)			2
			Acetone		446	470	3.3		20
6	Loroxanthin	12.77	Eluent		445	474	51	0.9999	TW
			Ethanol	(420)	446	474	47		21
7	19'-Hexanoyloxy-fucoxanthin	13.30	Eluent		444	467	28	1.0000	TW
			Acetone		445	470	36		
			Acetone		445	471	44		20
8	Violaxanthin	13.45	Eluent	416	440	468	91	0.9999	TW
			Ethanol	417	441	471	96		
			Eluent	417	440	470	89		2
			Ethanol	417	440	470	93		32
9	Diadinoxanthin	14.46	Eluent	(422)	446	475	63	1.0000	TW
			Ethanol	424	448	478	55		
			Eluent	424	448	478	74		2
			Ethanol	(424)	446	476	39		2
10	Antheraxanthin	14.92	Eluent	426	445	471	54	1.0000	TW
			Ethanol	422	445	474	49		
			Eluent	(421)	448	475	62		2
			Ethanol	422	444	472	54		33
11	Alloxanthin	15.33	Eluent	(426)	452	481	41	0.9996	TW
			Ethanol	427	454	484	45		
			Eluent	(430)	452	481	50		2
			Ethanol	(430)	453	483			34
12	Diatoxanthin	15.78	Eluent		453	481	57	0.9989	TW
			Ethanol	(427)	453	481	28		
			Eluent	424	448	476	25		2
			Ethanol	428	452	479			12

TABLE I *(continued)*

No.	Pigment	Retention time (min)	Solvent	Maximum wavelengths (nm)			Peak ratio[a]	Purity[b]	Ref.
				I	II	III			
13	Lutein	16.22	Eluent	(421)	445	473	58	0.9999	TW
			Ethanol	(421)	447	475	55		
			Eluent	(422)	446	474	65		2
			Ethanol	422	445	474	62		33
14	Zeaxanthin	16.23	Eluent	(425)	450	477	29	1.0000	TW
			Ethanol	426	452	480	52		
			Eluent	(426)	452	480	32		2
			Ethanol	(428)	450	478	26		33
15	Chl *b*	19.64	Eluent	456	597	646	2.9	0.9999	TW
			Acetone	458	596	646	2.9		
			Eluent	456	598	646	3		2
			Acetone	453	598	645			35
16	Chl *a*	20.50	Eluent	429	616	663	1.2	0.9999	TW
			Acetone	430	618	665	1.2		
			Eluent	430	617	664	1.2		2
			Acetone	430	618	665			36
17	Phaeophytin *a*	22.30	Eluent	407	504	666	2.4	1.0000	TW
			Acetone	409	506	667	2.3		
			Eluent	408	504	666	2.2		2
			Diethyl ether	408	503	667	2.1		37
18	*β*-Carotene	23.07	Eluent		451	476	17	0.9993	TW
			Ethanol	(425)	448	475	21		
			Eluent	(426)	452	478	20		2
			Ethanol	(425)	450	477			38

[a] For chlorophylls and their derivatives, the peak ratio is that of the Soret band absorbance divided by the maximum absorbance in the red region. For carotenoids, the peak ratio refers to the percentage III/II ratio [39].
[b] The purity of the peaks was calculated by averaging two correlation factors at the up- and downslopes.
[c] The pigments were eluted using a linear gradient from 100% solvent A (ion-pairing solution–water–acetone–acetonitrile, 5:25:20:50) to 100% solvent B (acetone–ethyl acetate, 50:50) in a 20-min period.
[d] The pigments were eluted using a linear gradient from 90% acetonitrile to ethyl acetate over 20 min.
[e] This work.
[f] Chlorophyl $c_1 + c_2$.

It has been elucidated that there are many types of Chl c whereas Chl c_2 and/or c_1 are commonly observed in marine algae [16,17]. This system was not able to resolve Chl c_1 from c_2. The sum of Chl c_1 and c_2 is represented as Chl c in this work (Table I).

Chromatograms of the pigment extracts from various algal classes are shown in Fig. 1. The chlorophyllide *a* (peak 1) was resolved well from the Chl *c* peak (peak 2). The carotenoids of major significance in ecological studies, peridinin (peak 3), fucoxanthin (peak 5), diadinoxanthin (peak 9) and lutein (peak 13), were all completely

ABSORBANCE

RETENTION TIME (Min)
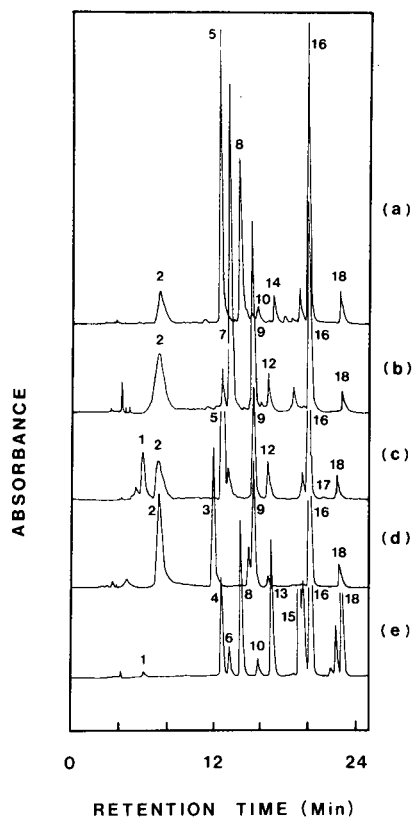
.Fig. 1. HPLC absorbance (440 nm) chromatograms of various algae: (a) *Heterosigma akashiwo* (Raphi-dophyceae); (b) *Gephyrocapsa oceanica* (Haptophyceae); (c) *Thalassiosira rotula* (Bacillariophyceae); (d) *Heterocapsa triquetra* (Dinophyceae); (e) *Pyramimonas parkeae* (Prasinophyceae). Peak identities are given in Table I.

resolved. Neoxanthin (peak 4) of *Pyramimonas parkeae* was presumably in a *cis*-form [18], according to the maximum wavelength [19]. Alloxanthin and 19′-hexanoyloxy-fucoxanthin had the same absorbance spectra as those reported previously [2,20]. Most peaks on the chromatogram of the oceanic sample were identified (Fig. 2c). Several HPLC systems have been reported to provide better pigment separation for green algae and higher plants than that in this work [21–23]. However, less attention has been paid in these systems to the separation of chlorophyllide *a* from Chl *c*, because green algae and plants lack Chl *c*. This separation is essential for analyzing marine aquatic ecosystems [1–7], large parts of which consist of many algal classes containing Chl *c*. In this system, the separation was taken into account even with a large sample injection volume (Fig. 2, Table II).

    For dilute samples, concentration by ether partitioning has been necessary de-spite its serious disadvantages. It has been reported that improved resolution and sensitivity are obtained by this procedure, but also that there is a significant increase in the proportions of *cis*-fucoxanthin and phaeophytin *a* [2]. For quantitative work,
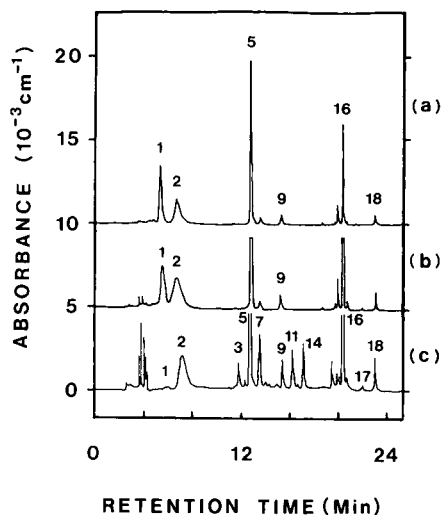
Fig. 2. Effect of injection volume on resolution of pigments on an absorbance (440 nm) chromatogram. (a) 20 μl injection of a *Skeletonema costatum* extract; (b) 400 μl injection of a *S. costatum* extract; (c) 400 μl injection of a field sample from the Seto Inland Sea. The chromatograms (a) and (b) are shifted by 10 and 5 × 10^{-3} cm^{-1}, respectively, for convenience. Peak identities are the same as those in Fig. 1.

the final extract was used without concentration, as the ether partitioning method gave an incomplete recovery and promoted the degradation of Chl *a* to phaeophytin *a* [2,24].

To minimize the loss of pigments during analytical procedures, it is recommended to inject the final extract directly into an HPLC system. Previous carotenoid analyses by HPLC have required sea water samples of more than 10 l, which is inconvenient for handling during field surveys. To increase the sensitivity of carote-

TABLE II

COMPARISON OF THE RESOLUTION BETWEEN CHLOROPHYLLIDE *a* AND CHLOROPHYLL $c_1 + c_2$ ACCORDING TO INJECTION VOLUMES

The resolution of each separation was calculated by $R_s = 2(t_{R2} - t_{R1})/(w_1 + w_2)$, where t_R and w are the retention times and peak widths of each pigment, respectively.

Solvent A composition[a]	Resolution				Ref.
	Injection volumes (μl)				
	100	200	300	400	
P[b]–DW[c]–acetone–CH$_3$CN (5:25:20:50)	1.32	1.33	1.23	1.12	This work
P–DW–methanol (5:5:90)	1.72	1.13	0.69	0.63	11
P–DW–methanol (10:10:80)	1.54	NC[d]	NC	NC	1

[a] Other experimental conditions were the same as those of this work.
[b] Ion-pairing solution (see text).
[c] Distilled water.
[d] Peak leading is too large to calculate the resolution.
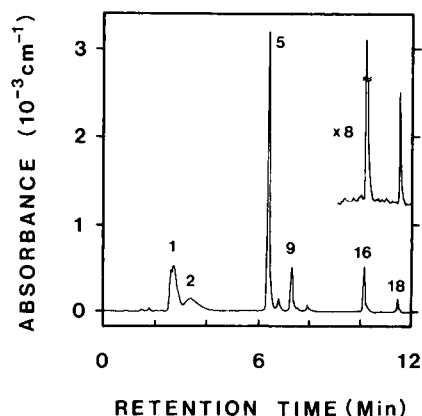
Fig. 3. HPLC absorbance (440 nm) chromatogram of an injection of a 400 μl sample of diluted *S. costatum* extract in the fast-flow mode. Peak identities are the same as those in Fig. 1. Content of β-carotene (peak 18) is 0.23 ng.

noid analysis by HPLC, one choice is to increase the sensitivity of the UV detector. However, it will probably be many years before the sensitivity of the detector is improved sufficiently, unless completely different procedures are developed.

Another way to increase the sensitivity is to increase the injection volume. With the usual analytical column of 250 × 4.6 mm I.D. packed with 5-μm ODS-bonded silica gel, the pigment extract injection volume chosen has been 20–50 μl [1–7] at a flow-rate of 1.0 ml min^{-1}. This HPLC system allows an injection volume of greater than 400 μl (Fig. 2) without a significant loss of resolution between chlorophyllide *a* and Chl *c* (Table II).

Peak spreading was commonly observed at an early retention time on the chromatogram and depended on the difference in solvent strength [25] between the extracts and mobile phases. Acetone has been used as an extract solvent because it reduces the chlorophyllase activity [23,26]. The mobile phases were therefore pre-

TABLE III

DETECTION LIMITS AND REQUIRED SAMPLE VOLUME OF THIS HPLC ANALYSIS

Pigment	Detection limit[a] (ng)	Concentration in sea water (μg l^{-1})	Least required sample[b] volume (ml)
Chl *a*	0.2	(i) 0.20[c]	25
		(ii) 0.67[d]	7
Chl *c*	0.5	(ii) 0.20	63
Fucoxanthin	0.4	(i) 0.02	500
		(ii) 0.14	71
β-Carotene	0.2	(i) 0.02	250
		(ii) 0.02	250

[a] Corresponds to $S/N = 10$ on an HPLC chromatogram.
[b] 400 μl injection of 10 ml extract.
[c] Oligotrophic sea water (from Gieskes and Kraay [6]).
[d] Oceanic sample of this work.

pared to permit the simultaneous separation of the pigments, allowing a large injection volume of the 90% acetone extracts without only significant decay in the shape of the peaks at early retention times.

The viscosities of acetone, acetonitrile and ethyl acetate, which are used in this HPLC system, are lower than that of methanol. Thus the flow-rate of this system could be twice that of methanol systems. The HPLC chromatogram, which was obtained at twice the flow-rate and half the gradient elution time, was similar to that obtained under the original conditions (Fig. 3). The column pressure with the fast-flow mode was less than 160 kgf cm^{-2} (1.6 · 10^7 N m^{-2}). The higher flow-rate requires a shorter elution time without significant peak spreading. This makes it potentially suitable for field work and continuous surveys.

Simultaneous and rapid separation of pigments by HPLC has been achieved in gradient-elution modes. However, gradient elution sometimes causes a marked baseline drift, which prevents the measurement of small peaks on the chromatogram [27,28]. In this analysis, the baseline of the absorbance trace at 440 nm remained constantly low, thus allowing highly sensitive observations to be made (Fig. 3). The rise in sensitivity reduces the sample volumes needed for field surveys (Table III). Thus this solvent system ensures rapid and highly sensitive analyses and is convenient for use in the field, especially for oceanic samples.

REFERENCES

1 R. F. C. Mantoura and C. A. Llewellyn, *Anal. Chim. Acta*, 151 (1983) 297.
2 S. W. Wright and J. D. Shearer, *J. Chromatogr.*, 294 (1984) 281.
3 W. W. C. Gieskes and G. W. Kraay, *Mar. Biol. (Berlin)*,75 (1983) 179.
4 B. Klein and A. Sournia, *Mar. Ecol. Prog. Ser.*, 37 (1987) 265.
5 D. A. Everitt, S. W. Wright, J. K. Volkman, D. P. Thomas and E. J. Lindstrom, *Deep-Sea Res.*, 37 (1990) 975.
6 W. W. Gieskes and G. W. Kraay, *Mar. Biol. (Berlin)*, 91 (1986) 567.
7 H. W. Paerl, J. Tucker and P. T. Bland, *Limnol. Oceanogr.*, 28 (1983) 847.
8 P. S. Ridout and R. J. Morris, *Mar. Biol. (Berlin)*, 87 (1985) 7.
9 S. Roy, R. P. Harris and S. A. Poulet, *Mar. Ecol. Prog. Ser.*, 52 (1989) 145.
10 Y. Nakamura, J. Takashima and M. Watanabe, *J. Oceanogr. Soc. Jpn.*, 44 (1988) 113.
11 K. Kohata and M. Watanabe, *J. Phycol.*, 24 (1988) 58.
12 F. H. Foppen, *Chromatogr. Rev.*, 14 (1971) 133.
13 Y. Shioi, M. Doi and T. Sasa, *J. Chromatogr.*, 298 (1984) 141.
14 K. Shimokawa, *Phytochemistry*, 21 (1982) 543.
15 L. Huber, *Application of Diode-Array Detection in High Performance Liquid Chromatography; Publication Number 12-5953-2330*, Hewlett-Packard, Waldbronn, 1989, p. 134.
16 S. W. Jeffrey and S. W. Wright, *Biochim. Biophys. Acta*, 894 (1987) 180.
17 S. W. Jeffrey, in J. C. Green, B. S. C. Leadbeater and W. L. Diver (Editors), *The Chromophyte Algae: Problems and Perspectives, Systematics Association Special Volume No. 38*, Clarendon Press, Oxford, 1989, p. 13.
18 T. Bjørnland, in N. I. Krinsky, M. M. Mathews-Roth and R. F. Taylor (Editors), *Carotenoids: Chemistry and Biology*, Plenum Press, New York, 1990, p. 21.

19 S. W. Wright, personal communication.
20 S. W. Wright and S. W. Jeffrey, *Mar. Ecol. Prog. Ser.*, 38 (1987) 259.
21 K. Kohata and M. Watanabe, *J. Phycol.*, 25 (1989) 377.
22 D. Siefermann-Harms, *J. Chromatogr.*, 448 (1988) 411.
23 R. K. Juhler and R. P. Cox, *J. Chromatogr.*, 508 (1990) 232.
24 S. W. Jeffrey and G. M. Hallegraeff, *Mar. Ecol. Prog. Ser.*, 35 (1987) 293.
25 L. R. Snyder and J. W. Dolan, *J. Chromatogr.*, 165 (1979) 3.
26 Y. Shioi and T. Sasa, *Methods Enzymol.*, 123 (1986) 421.
27 R. J. Carter, D. J. Flett and C. F. Gibbs, *J. Chromatogr. Sci.*, 26 (1988) 121.
28 E. Hoque, *J. Chromatogr.*, 448 (1988) 417.
29 S. R. Brown, *J. Fish. Res. Board Can.*, 25 (1968) 523.
30 S. W. Jeffrey, *Biochim. Biophys. Acta*, 177 (1969) 456.
31 S. W. Jeffrey, M. Sielicki and F. T. Haxo, *J. Phycol.*, 11 (1975) 374.
32 H. Stransky and A. Hager, *Arch. Mikrobiol.*, 71 (1970) 164.
33 A. Hager and H. Stransky, *Arch. Mikrobiol.*, 72 (1970) 68.
34 J. Y. Cheng, M. Don-Paul and N. J. Antia, *J. Protozool.*, 21 :1974) 761.
35 P. H. Hynninen, *Acta Chem. Scand.*, 27 (1973) 1487.
36 S. W. Jeffrey, *Biochem. J.*, 80 (1961) 336.
37 P. H. Hynninen and N. Ellfolk, *Acta Chem. Scand.*, 27 (1973)1463.
38 N. J. Antia and J. Y. Cheng, *Br. Phycol. J.*, 17 (1982) 39.
39 B. Ke, F. Imsgard, H. Kjøsen and S. Liaaen-Jensen, *Biochim. Biophys. Acta*, 21; (1970) 139.

Liquid chromatographic method for the determination of calcium cyanamide using pre-column derivatization

S. CHEN, A. P. OCAMPO* and P. J. KUCERA

Analytical Development, Lederle Laboratories, Pearl River, NY 10965 (USA)

(First received December 10th, 1990; revised manuscript received May 13th, 1991)

ABSTRACT

A specific and stability-indicating high-performance liquid chromatographic (HPLC) method has been developed for the analysis of calcium cyanamide in bulk material and dosage form. Calcium cyanamide in samples was converted into dansyl cyanamide. A μBondapak C_{18} column was employed for HPLC with 0.01 M sodium phosphate (pH 6.3)–acetonitrile (75:25, v/v) as the mobile phase. The proposed HPLC method was validated for linearity, specificity, accuracy and reproducibility.

INTRODUCTION

Calcium cyanamide in the citrated form (Temposil, Dipsan) was introduced into medicine in 1956 as a pharmacological adjunct in the treatment of chronic alcoholism [1]. The drug blocks ethanol metabolism by inhibition of aldehyde dehydrogenase which increases both hepatic and blood acetaldehyde levels after ingestion of ethanol [2,3]. Increased acetaldehyde levels result in a number of undesirable effects such as tachycardia, hypotension, flushing and disnea [4,5].

A limited number of analytical procedures are available in the literature for the quantitation of calcium cyanamide. These methods involve spectrophotometric, paper chromatographic and gas–liquid chromatographic assays [6–9]. A liquid chromatographic procedure for the determination of cyanamide in biological fluids has recently been published in the literature [10]. The method currently used in industry requires a titrimetric assay consisting of an ammonia–silver nitrate reagent precipitation followed by a titration of the silver in the reagent.

Calcium cyanamide is one of many compounds that cannot be readily analyzed directly by high-performance liquid chromatography (HPLC) using spectrophotometric detection. This problem can be overcome by derivatization to introduce a chromophore or fluorophore. The present paper describes the application of dansyl chloride as a pre-column derivatization agent for cyanamide. The assay is a more reliable analytical method for calcium cyanamide in bulk material and dosage form. The method also offers the advantage of monitoring the stability of the citrated formulation with reasonable simplicity, selectivity and specificity.

EXPERIMENTAL

Chemicals and reagents

Calcium cyanamide and Temposil were obtained from American Cyanamid Company (Baie d'Urfe, Canada). Sodium acetate, glacial acetic acid, sodium carbonate, dibasic potassium phosphate (all ACS reagent grade) were purchased from J. T. Baker (Phillipsburg, NJ, USA). Dansyl chloride was purchased from Aldrich (Milwaukee, WI, USA). All organic solvents were of HPLC grade and were obtained from Burdick & Jackson Labs. (Muskegon, MI, USA). The water used was purified through a Milli-Ro-Milli-Q system (Millipore, Bedford, MA, USA). All chemicals and solvents were used as received without any further purification.

Apparatus and chromatographic conditions

Chromatographic separations were carried out on an HPLC system consisting of an SSI 222B pump (State Scientific Instruments, State College, PA, USA), a Waters WISP 712 automatic injector (Waters Assoc., Milford, MA, USA), and a Kratos 783 (Applied Biosystems, Foster City, CA, USA) variable-wavelength UV detector set at 254 nm. The detector's 0–10 mV analog signal was recorded with a Model 1200 chart recorder (Linear Instruments, Reno, NV, USA) and the 0–1 V signal was digitized and recorded with a Nelson Analytical Data system at a sampling rate of one point per second.

All chromatographic procedures were performed at ambient temperature. Injections were made onto a Waters μBondapak C_{18} analytical column (150 mm $\times$ 39 mm I.D., 10 μm particle size). The column was equilibrated with mobile phase at a flow-rate of 1 ml/min. The relative standard deviation (R.S.D.) of six replicate injections of a standard was not more than 2%, as defined in the USP XXII under "System suitability for HPLC" [11]. The detection wavelength and the sensitivity were set at 254 nm and at 0.05 a.u.f.s., respectively.

Standard preparation

A 25-mg weight of calcium cyanamide of known purity was accurately weighed and quantitatively transferred to a 100-ml volumetric flask. To it were added 20 ml of buffer solution for extraction. The buffer solution was made by dissolving 12.0 g of anhydrous sodium acetate in a mixture of 980 ml of water and 20 ml of glacial acetic acid. The calcium cyanamide mixture was sonicated for 10 min for complete dissolution and then diluted to volume with 0.2 M sodium carbonate. The flask was allowed to stand at room temperature for 15 min. The clear part of the solution was withdrawn for derivatization.

Sample preparation

Bulk material. A 25-mg calcium cyanamide sample was accurately weighed and transferred to a 100-ml volumetric flask. The sample was treated subsequently in the same manner as standard.

Tablets. Twenty tablets were accurately weighed and the average tablet weight was determined. The tablets were ground to a fine powder and a portion of the tablet powder equivalent to one-half tablet weight was weighed and transferred quantitatively to a 100-ml volumetric flask. The powder was treated in the same manner as the standard.

Derivatization reaction

   With a pipettor, 200 μl of the clear part of the solution described in *Standard preparation* and *Sample preparation* were accurately withdrawn and transferred to a screw-cap vial (7.4 ml capacity, Supelco, Bellefonte, PA, USA). Using a pipettor, 200 μl of the derivatizing agent was added and the solution was mixed well. The derivatizing agent was prepared by dissolving 100 mg of dansyl chloride in 10 ml of acetone. The vial was heated in a heating block at 40°C for 30 min and cooled the vial to room temperature. A 4-ml volume of mobile phase was accurately added to the vial and mixed. An aliquot of the solution was transferred to an HPLC vial and 10 μl were injected onto the column.

RESULTS AND DISCUSSION

   A selective, sensitive, and specific reversed-phase HPLC assay was developed for the determination of calcium cyanamide in bulk raw material and in its citrated formulation. Calcium cyanamide is dissolved in a sodium acetate buffer (pH $\approx$ 4.3) solution and subsequently hydrolyzed to cyanamide. The cyanamide in a basic solution is reacted with dansyl chloride to form dansyl cyanamide which can be analyzed quantitatively by reversed-phase HPLC (Fig. 1).

   A pure dansyl cyanamide was synthesized and evaluated using spectroscopic techniques. The synthesized dansyl cyanamide was characterized by the following spectroscopic data: UV λ_{max} 326 nm (ε 4800), 246 nm (ε 15 000); Fourier transform IR v 3060 (aromatic H), 2960 (CH$_3$), 2180 (sharp s, $-C \equiv N$), 1600, 1540 (aromatic); ^{1}H NMR (in [^{2}H$_6$]dimethyl sulfoxide, d$_6$-DMSO) δ 3.15 (s, 6H, N–(CH$_3$)$_2$, 7.7 (m, 3H, aromatic), 8.15 (d, J = 7.2, 1H, aromatic), 8.39 (d, J = 8.5, 1H, aromatic), 8.72 (d, J = 7.9, 1H, aromatic); chemical ionization mass spectrometry (ammonia) m/z 293 (M + NH$_4$), 276 (M + H), 251 (M $-$ CH$_3$ + H). The elemental analysis of dansyl cyanamide confirmed its composition: C 56.35%, H 4.68%, N 15.12%, S 11.64% (theoretical: C 56.71%, H 4.76%, N 15.24%, S 11.65%). The material is also fluorescent with excitation wavelength at 324 nm and emission wavelength at 520 nm. The material was found to be pure (HPLC purity of 97.2% by area percent).

   The chemical shift of the N-methyl group of dansyl cyanamide in d$_6$-DMSO was at relatively low-field (3.18 ppm) as compared to the N-methyl absorption (2.82 ppm) of the model compound, dansylamide. When one drop of NaO^{2}H was added to the

CaNCN   H$_3$NCN

   (I)   (II)
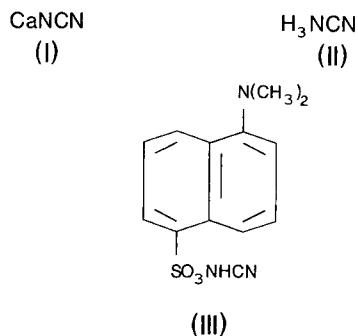
Fig. 1. Structures for calcium cyanamide (I), cyanamide (II) and dansyl cyanamide (III).

NMR tube, the N-methyl absorption of dansyl cyanamide shifted from 3.18 to 2.82 ppm. On the other hand, when one drop of trifluoroacetic acid was added to the NMR tube of dansylamide, the N-methyl absorption shifted from 2.82 to 3.08 ppm. The NMR data thus indicate the formation of a zwitterion in the solution of dansyl cyanamide.
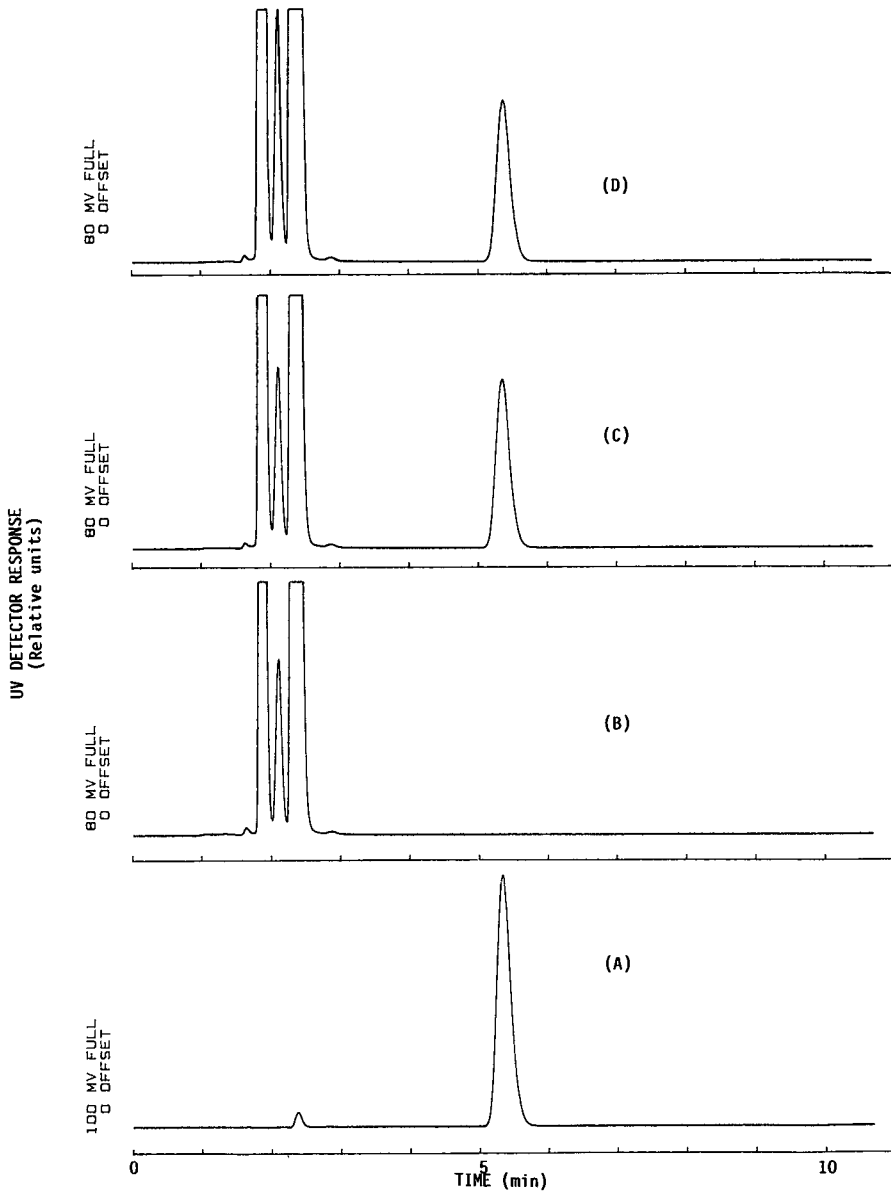
Fig. 2. HPLC chromatograms for synthesized dansyl cyanamide (A), Temposil tablet placebo (B), Temposil tablet (C), and calcium cyanamide bulk material (D).

To evaluate the yield of the derivatization process, calcium cyanamide of known purity was assayed according to the procedure above against the synthesized dansyl cyanamide. HPLC results showed the derivatization process *in situ* to be quantitative (99.9%). The peak purity of dansyl cyanamide was verified by the UV scan of the peak of interest using a diode-array UV detector.

Chromatographic conditions

Fig. 2 shows a typical standard and sample chromatograms obtained using the above procedure. The method proposed here proved suitable to the determination of calcium cyanamide in bulk material and citrated tablet formulation. Since dansyl cyanamide exhibits features of amphoterism as indicated by its ^{1}H NMR in d$_6$-DMSO, the retention time of dansyl cyanamide was found to be very sensitive to pH as well as the organic modifier in the mobile phase. The mobile phase or the pH was modified to obtain optimum separation. An increase in the acetonitrile concentration decreased the retention time. An increase in pH reduced the retention of dansyl cyanamide. However, it is not recommended to increase the pH of the mobile phase above 7.0.

Linearity, precision, accuracy and sensitivity

Aliquots of calcium cyanamide solution (10–50 mg/100 ml) were taken and derivatized as described under *Derivatization procedure*. Calibration graphs were constructed of peak area *versus* concentration. The results of linear regression analysis were slope 0.0036, intercept 0.5066 and correlation coefficient $r = 0.9999$ ($n = 11$).

The precision of the proposed method was evaluated by ten replicate injections of solution of bulk material (225 μg/ml). For replicate analyses of a sample (50 mg/tablet) were taken to calculate the assay precision in the dosage form. The intra-day assay variation (% R.S.D.) for the bulk material and tablet were 0.20% and 0.67%, respectively. The inter-assay variation was determined by replicate analyses of a 50 mg/tablet of Temposil over a three-day period in two laboratories with the mean inter-assay coefficient of variation (%) calculated to be 1.13%.

The accuracy of the proposed method was examined by preparing tablet placebo samples containing different amounts of calcium cyanamide equivalent to 50, 100 and 150% of label strength. No interference was observed from the tablet excipients. The overall % recovery of calcium cyanamide was 99.43 ± 1.33%.

The limit of detection is $1 \cdot 10^{-9}$ dansyl cyanamide with a signal-to-noise ratio of 2.0.

Stability

The stability of calcium cyanamide was demonstrated by replicate injections at different time intervals against freshly prepared derivatized standard solution. The dansyl derivative solution was found to be stable for up to 24 h. Calcium cyanamide was stable in either the buffer solution or 0.2 M sodium carbonate. Calcium cyanamide in 0.1 M hydrochloric acid lost 16% of its potency after 20 h at room temperature.

Forced degradation by UV light, heat, acid, base and oxidation were also performed. The calcium cyanamide solution dissolved in buffer (1 ml) was exposed to UV light for 2 h. Similarly, another 1-ml aliquot of calcium cyanamide solution was heated on a steam bath for 2 h. In addition, 1-ml aliquots were treated with 2 ml of

1 M sodium hydroxide, 2 ml of 1 M hydrochloric acid and 0.5 ml of 30% hydrogen peroxide. All the degradation solutions were kept at room temperature for 2 h. A 0.5-ml portion of 10 M sodium hydroxide was added to the calcium cyanamide–peroxide solution to remove excess peroxide. After degradation, all solutions were diluted with 0.2 M sodium carbonate and then derivatized for the HPLC assay. One flask containing calcium cyanamide was set aside as the control. Results of the study showed that calcium cyanamide was stable after UV, acid and base treatment. However, it lost 20% and 100% of its potency after its reaction with heat and hydrogen peroxide, respectively.

Assays

The results of the HPLC analysis indicate that the new method can be used for the quantitation of calcium cyanamide in both bulk material and tablet formulation. Comparison of the results obtained by the HPLC method with the titrimetric assay showed that both sets of the results are comparable. Two lots of bulk material were determined to have an HPLC mean potency value of 92.65% ($n = 10$) *versus* 92.85% potency value by titration. Three lots of Temposil tablets had a mean % label strength of 95.00% ($n = 36$). Titrimetric data for the same three lots yielded a mean % label strength of 94.96%.

CONCLUSIONS

A simple stability-indicating assay for the quantitation of calcium cyanamide has been successfully developed, validated and applied to the bulk material of calcium cyanamide and its tablet formulation. The proposed method is an excellent alternative to the ammonium thiocyanate method for the determination of calcium cyanamide. The assay is specific, separating the drug from the excipients and the degradation products. With minor modifications, the assay could also be used for dissolution studies.

ACKNOWLEDGEMENTS

REFERENCES

1 K. J. W. Ferguson, *Can. Med. Assoc. J.*, 74 (1956) 793.
2 R. A. Deitrich, P. A. Troxell, W. S. Worth and V. G. Erwin, *Biochem. Pharmacol.*, 25 (1976) 2733.
3 J. F. Brien and C. W. Loomis, *Drug Metab. Rev.*, 14 (1983) 113.
4 J. F. Brien, J. E. Peachy, B. J. Rogers and C. W. Loomis, *Eur. J. Clin. Pharmacol.*, 14 (1978) 133.
5 J. F. Brien, J. E. Peachy, C. W. Loomis and B. J. Rogers, *Clin. Pharmacol. Ther.*, 25 (1979) 454.
6 D. A. Buyske and V. Downing, *Anal. Chem.*, 32 (1960) 1798.
7 T. A. Neiman, F. J. Holler and C. G. Enke, *Anal. Chem.*, 48 (1976) 899.
8 J. E. Milks and R. H. Janes, *Anal. Chem.*, 28 (1956) 846.
9 C. W. Loomis and J. F. Brien, *J. Chromatogr.*, 222 (1981) 421.
10 J. Prunonosa, R. Obach and J. M. Valles, *J. Chromatogr.*, 377 (1986) 253.
11 *The United States Pharmacopeia*, Mack Publishing, Easton, PA, 22nd revision, 1990, pp. 1565–1566.

Determination of benzocaine, dextromethorphan and cetylpyridinium ion by high-performance liquid chromatography with UV detection

P. LINARES, M. C. GUTIÉRREZ, F. LÁZARO, M. D. LUQUE DE CASTRO* and M. VALCÁRCEL

Department of Analytical Chemistry, Faculty of Sciences, University of Córdoba, E-14004 Córdoba (Spain)

(First received February 12th, 1991; revised manuscript received April 16th, 1991)

ABSTRACT

A high-performance liquid chromatographic method for the determination of benzocaine, cetylpyridinium ion and dextromethorphan based on the use of an end-capped Ultrabase C_{18} column and an ion-pair formation reaction in a water–chloroform–methanol (10:50:40, v/v/v) mobile phase containing dioctyl sulphosuccinate is proposed. The use of a conventional or diode-array spectrophotometer resulted in calibration graphs with very different features. The determination ranges for benzocaine, cetylpyridinium and dextromethorphan provided by the diode-array detector were 10–100, 250–2000 and 250–2000 μg/ml, respectively, with relative standard deviations smaller than 3.0% for peak-height measurements and less than 1.40% for peak-area measurements. The conventional detector provided poorer results as a compromise wavelength must be chosen for measurements. The method was applied to the resolution of mixtures of the three analytes in pharmaceutical tablets. No interferences from other components of the tablets such as sorbitol, mint flavour and magnesium stearate were observed.

INTRODUCTION

There are several methods for the determination of benzocaine, cetylpyridinium ion and dextromethorphan, both alone and in mixtures with other drugs, some of which involve a prior separation of the analytes. Thus, dextromethorphan was determined individually after high-performance liquid chromatographic (HPLC) separation in syrup [1] and blood [2] samples. However, it is more frequently determined in mixtures with other pharmaceuticals on the basis of different principles depending on the nature of the remainder of the analytes involved and the sample matrix itself. Thus, pseudoephedrine hydrochloride, chlorpheniramine malate and dextromethorphan hydrobromide were determined simultaneously by second-derivative photodiode-array spectroscopy [3] and guaiphenesin, dextromethorphan and diphenhydramine by capillary gas chromatography [4]; however, most of these simultaneous determinations involve HPLC [5–8]. Conversely, methods for benzocaine normally rely on potentiometric (ion-selective electrode) [9] or photometric [10] measurements and on the use of HPLC for mixtures [11]. There are relatively few methods for the determination of cetylpyridinium ion. One of them involves its

separation using ion-interaction chromatography with methanol–water mobile phases containing an ion-pairing agent [12].

A Spanish pharmaceutical manufacturer (Calmante Vitaminado) is soon to release a new pharmaceutical that includes dextromethorphan as cough supressant, benzocaine as local anaesthetic and cetylpyridinium ion as disinfectant. A method for the determination of these three drugs in mixtures will therefore be needed.

The proposed method relies on the separation of the analytes by HPLC using an end-capped Ultrabase C_{18} column and on measuring their intrinsic absorbances. Two types of detectors (conventional and diode-array) were used to monitor the eluate from the column. The sensitivity achieved depended on whether a single wavelength was used for measurement of all three analytes (conventional spectrophotometer) or whether each was monitored at its maximum absorption wavelength (diode-array spectrophotometer).

EXPERIMENTAL

Standards

Aqueous solutions of benzocaine (1.000 g/l), cetylpyridinium chloride (5.000 g/l) and dextromethorphan hydrobromide (5.000 g/l) solutions were prepared in the medium used as mobile phase. All the standards were supplied by Calmante Vitaminado.

Columns

Nucleosil C_{18} (5-μm) and end-capped Ultrabase C_{18} (5-μm) columns, both 25 cm $\times$ 4.6 mm I.D., were supplied by Scharlau (Barcelona, Spain).

Apparatus

An HP 1040A diode-array spectrophotometer equipped with an HP1040 DAD flow-cell (inner volume 2 μl) coupled to an HP 9000 Chem Station (all from Hewlett-Packard) or a Pye Unicam SP500 spectrophotometer furnished with a Hellma 178.2QS flow cell (inner volum 18 μl) was connected to an HP 1050 system (high-pressure quaternary gradient pump and a Rheodyne Model 7125 manual injection system).

RESULTS AND DISCUSSION

The absorption spectra of the analytes are shown in Fig. 1. The method was implemented in two ways: (a) by selecting a compromise wavelength for measurements and using a conventional spectrophotometer; and (b) by connecting the chromatograph to a diode-array detection (DAD) system to monitor each component at its maximum absorption wavelength. The results obtained in each instance are compared below.

Study of variables

The experimental variables optimized to accomplish adequate separation in eluting the analytes were the composition of the mobile phase, the ion-pairing reagent, the flow-rate, the injection volume and the type of column.
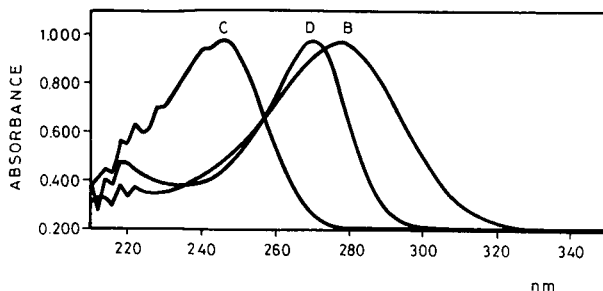
Fig. 1. Absorption spectra of (B) benzocaine, (C) cetylpyridinium ion and (D) dextromethorphan. Absorption maxima: 278, 244 and 270 nm, respectively. Concentrations: B, 10; C, 500; D, 250 μg/ml.

Among the different mobile phase tried, 0.03 M KH_2PO_4–acetonitrile–methanol (50:10:40, v/v/v) at different pH values (3.7, 4.0 and 5.3) was found to elute benzocaine alone, as also did 10 mM ammonium nitrate–acetonitrile–0.05 M dioctyl sulphosuccinate (25:50:25, v/v/v). The presence of chloroform was found to be essential for the three components to be eluted reasonably fast. The different water–chloroform–methanol ratios tried eluted benzocaine very fast, while dextromethorphan and cetylpyridinium were eluted slowly and with very long tails. Addition of an ion-pairing reagent to this mobile phase in the optimal proportions (10:50:40) was also examined. Sodium lauryl sulphate at different concentrations from 0.05 to 0.1 M ensured elution of the three analytes, but benzocaine and dextromethorphan overlapped, whereas 0.01 M sodium dioctyl sulphosuccinate provided acceptable resolution for all three compounds.

Of the different flow-rates studied over the range 0.6–1.2 ml/min, the best resolution of the mixture was achieved at 0.9 ml/min.

An injection volume of 20 μl resulted in adequate sensitivity.

The above experiments were performed by using a 25-cm Nucleosil C_{18} column (5-μm, pore diameter 120 Å). Despite the absence of overlapping peaks in the chromatogram obtained under the optimum working conditions, the tailing of dextromethorphan and especially cetylpyridinium resulted in long analysis times (about 15 min). To expedite the analyses and to improve the peak shapes we used an end-capped Ultrabase C_{18} column. Undesirable solute–stationary phase interactions were eliminated by this column, in which surface groups were first capped and then deactivated [13]. The time required to obtain a chromatogram was reduced to less than 6 min. Fig. 2 shows a typical chromatogram of an equimolar mixture of the analytes, obtained by using DAD and monitoring at 240, 270 and 278 nm for cetylpyridinium, dextromethorphan and benzocaine, respectively, and Fig. 3 shows a three-dimensional recording.

A sampling frequency of up to 10 h^{-1} was achieved under the optimum working conditions.

Features of the proposed method

Calibration graphs were obtained by using both the conventional and the diode-array spectrophotometer. Measurements were performed at 254 nm with

TABLE I

FEATURES OF THE CALIBRATION GRAPHS

Detection	Parameter measured	Wavelength (nm)	Analyte[a]	Intercept (absorbance)	Slope [absorbance/ (μg/ml)]	Linear range (μg/ml)	r^2	R.S.D.[b] (%)
Conventional	Peak height	254	B	0.015	$5.8 \cdot 10^{-3}$	15–110	0.999	5.02
			C	−0.114	$6.5 \cdot 10^{-4}$	250–2100	0.995	4.10
			D	−0.003	$9.6 \cdot 10^{-5}$	600–2500	0.998	4.82
DAD	Peak height	278	B	0.054	$14.8 \cdot 10^{-3}$	10–75	0.995	2.84
		244	C	0.016	$6.2 \cdot 10^{-4}$	250–1500	0.998	1.70
		270	D	0.063	$2.8 \cdot 10^{-4}$	250–2500	0.989	1.45
DAD	Peak area	278	B	616.713	149.610	10–100	0.997	1.33
		244	C	1372.219	12.770	250–2500	0.996	1.37
		270	D	544.632	5.965	250–2500	0.997	1.05

[a] B = Benzocaine; C = cetylpyridinium ion; D = dextromethorphan.

[b] n = 11. Concentrations for R.S.D. determination: benzocaine = 50, cetylpyridinium ion = 1000 and dextromethorphan = 1000 μg/ml.
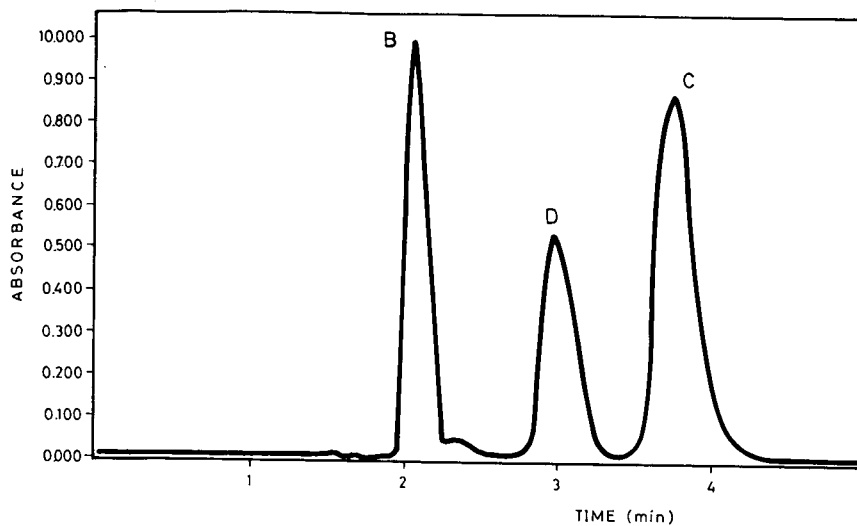
Fig. 2. Chromatogram of (B) benzocaine (25 µg/ml), (D) dextromethorphan (1000 µg/ml) and (C) cetylpyridinium ion (500 µg/ml). Mobile phase, water–chloroform–methanol (10:50:40, v/v/v) containing 0.1 M sodium lauryl sulphate; flow-rate, 0.1 ml/min; volume injected, 20 µl; column, end-capped Ultra-base C_{18}.
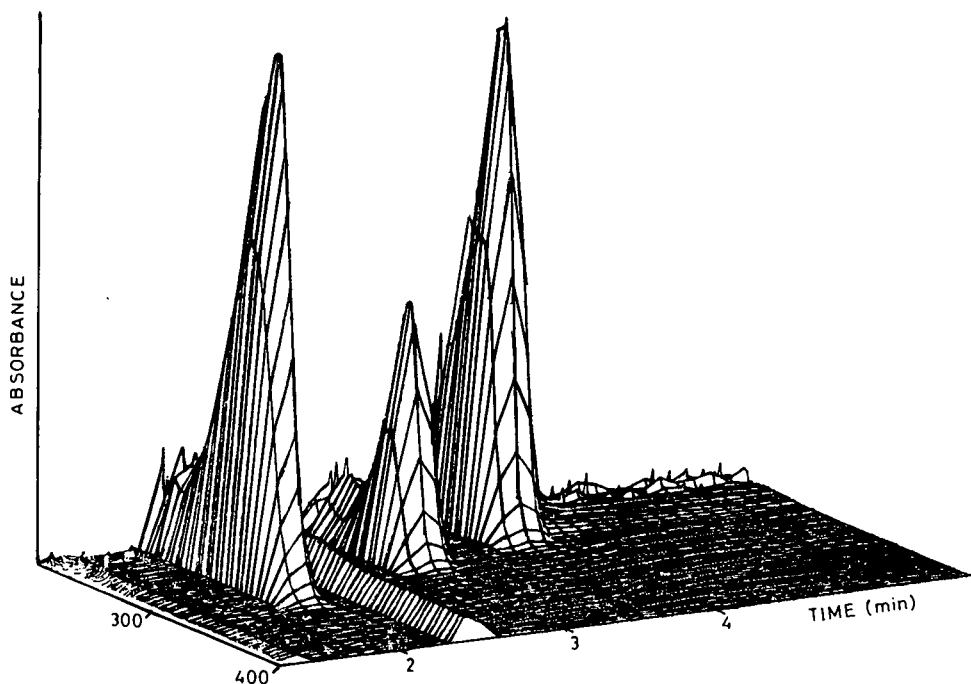
Fig. 3. Three-dimensional chromatogram of benzocaine, dextromethorphan and cetylpyridinium ion obtained using the conditions specified in Fig. 2.

conventional detection and at 278, 244 and 270 nm for benzocaine, cetylpyridinium and dextromethorphan, respectively, with DAD. Both peak-height and peak-area measurements were made in the latter instance. Table I summarizes the results obtained. The detection limits calculated as the ratio of the peak height to three times the baseline noise were 3.5, 80 and 175 μg/ml for benzocaine, dextromethorphan and cetylpyridinium, respectively.

On comparing the calibration graphs based on peak-height measurements obtained by using the two detectors, it is seen that the sensitivity achieved with DAD was higher than that provided by the conventional detector. The limit of determination for benzocaine was slightly improved by using DAD, but the gains were more significant for cetylpyridinium and dextromethorphan. The reproducibility of the method was studied by using eleven different samples containing concentrations of the analytes in the middle of the linear range (50, 1000 and 100 μg/ml for benzocaine, cetylpyridinium and dextromethorphan, respectively). Excellent relative standard deviation (R.S.D.) values were obtained with DAD (less than 3.0% in all instances), but they were higher than 4.0% with conventional detection. The explanation of this behaviour could be the data collection procedure (by a data station and manually, respectively).

Of the two types of measurements made on the data from the chromatogram obtained with DAD, those based on peak areas provided better sensitivity (slopes at least ten times greater), a similar linear range (except for cetylpyridinium, for which the range was wider) and better reproducibility (R.S.D. less than 1.40%).

Application of the proposed method to real samples

Applicability of the proposed method to the analysis of pharmaceutical tablets was tested in two ways. The manufacturer provided the composition of the tablets. We analysed synthetic samples containing the analytes plus additional compounds present in the tablets (sorbitol, mint flavour and magnesium stearate) in several proportions. Then, the tablets supplied by the manufacturer were dissolved in the mobile phase and injected directly into the chromatograph. The chromatogram thus obtained showed no interference from any of the components of the sample matrix in the synthetic or the real samples.

CONCLUSIONS

The proposed method for the chromatographic separation and determination of benzocaine, cetylpyridinium ion and dextromethorphan allows the determination of these drugs in pharmaceuticals. This is the first reported method for the resolution of this type of mixture, which only occurs in a still commercially unavailable pharmaceutical that will require a procedure for monitoring tablet production and for quality control.

As the concentration of the active substances in the tablets is high enough, a conventional spectrophotometer can be used for the routine control method. Future determination of these drugs at lower concentrations in biological fluids will require DAD in order to obtain better sensitivity and precision.

REFERENCES

1 E. J. Kubiak and J. W. Munson, *J. Pharm. Sci.*, 69 (1980) 1380.
2 R. Gillilan, R. C. Lanman and W. D. Mason, *Anal. Lett.*, 13 (1980) 381.
3 J. L. Murtha, T. N. Julian and G. W. Radebaugh, *J. Pharm. Sci.*, 77 (1988) 715.
4 M. Bambagiotti-Alberti, S. Pinzauti and F. F. Vincieri, *Pharm. Acta Helv.*, 62 (1987) 175.
5 D. R. Heidemann, K. S. Groon and J. M. Smith, *LC · GC*, 5 (1987) 422.
6 S. S. Yang and R. K. Gilpin, *J. Chromatogr. Sci.*, 26 (1988) 416.
7 T. Chen, J. R. Pacifico and R. E. Daly, *J. Chromatogr. Sci.*, 26 (1988) 636.
8 S. I. Sa'sa, K. A. Momani and I. M. Jalal, *Microchem. J.*, 36 (1987) 391.
9 A. F. Shoukry, Y. M. Issa, R. El-Sheik and M. Zareh, *Microchem. J.*, 37 (1988) 299.
10 M. E. El-Kommos and K. M. Emara, *Analyst (London)*, 112 (1987) 253.
11 L. Gagliardi, A. Amato, A. Basili, G. Cavazzutti, E. Gattavecchia and D. Tonelli, *J. Chromatogr.*, 362 (1986) 450.
12 R. C. Meyer and L. T. Takahashi, *J. Chromatogr.*, 280 (1983) 159.
13 R. B. Moore, J. E. Wilkerson and C. R. Martin, *Anal. Chem.*, 56 (1984) 2572.

Determination of sulfonamides by liquid chromatography, ultraviolet diode array detection and ion-spray tandem mass spectrometry with application to cultured salmon flesh[a]

S. PLEASANCE[*,b], P. BLAY[b] and M. A. QUILLIAM

Institute for Marine Biosciences, National Research Council of Canada, 1411 Oxford Street, Halifax, Nova Scotia B3H 3Z1 (Canada)

and

G. O'HARA

Syndel Laboratories Ltd., 9211 Shaughnessy Street, Vancouver, British Columbia V6P 6R5 (Canada)

(First received January 25th, 1991; revised manuscript received April 16th, 1991)

ABSTRACT

Ion-spray mass spectrometry was investigated for the analysis of 21 antibacterial sulfonamide drugs. All of the sulfonamides analyzed gave positive ion mass spectra with abundant protonated molecules and no fragmentation. Tandem mass spectrometry (MS–MS) using collision-induced dissociation provided structural information, allowing the identification of common fragmentation pathways and the differentiation of isomeric and isobaric sulfonamides. A reversed-phase high-performance liquid chromatographic method was developed, using gradient elution and ultraviolet diode-array detection (DAD), enabling the separation of 16 of the sulfonamides. Combined liquid chromatography (LC)–MS was accomplished using the ion-spray interface. Analyses of a mixture of sulfonamide standards were performed with gradient elution and the mass spectrometer configured for full-scan acquisition, selected-ion monitoring, or selected-reaction monitoring.

Procedures for the analysis of sulfadimethoxine (SDM), a representative sulfonamide used in the aquaculture industry, are described. The presence of SDM in cultured salmon flesh was confirmed at levels as low as 25 ng/g by a combination of LC–DAD and LC–MS–MS.

INTRODUCTION

Sulfonamides are antibacterial compounds commonly used for the prevention and treatment of diseases in livestock production. A major concern with the use of these compounds is that residues may be present in food products if proper withdrawal times for treated animals have not been strictly enforced. Such residues may pose a health threat to consumers through allergic or toxic reactions, or through induction of antibiotic resistance in pathogenic organisms. For this reason, regulatory agencies

---

[a] NRCC No. 31957.

[b] Under contract from SCIEX, 55 Glen Cameron Road, Thornhill, Ontario L3T 1P2, Canada.

have established tolerance levels (0.1 ppm in most countries) for these drugs in food products.

Concerns over these issues in Canada have recently focused public attention on the aquaculture industry, where antibiotics are used to control bacterial infections in farmed fin-fish such as salmon. Some of the sulfonamides currently used to treat salmon include sulfamerazine, Romet-30 (a potentiated sulfonamide containing sulfadimethoxine and ormetoprim) and Tribrissen (sulfadiazine and trimethoprim). Sulfonamide residues may be monitored by a variety of analytical techniques such as bioassay, colorimetric assays, thin-layer chromatography, gas chromatography (GC), high-performance liquid chromatography (LC) and mass spectrometry (MS) [1]. Instrumental methods provide the advantages of ease of automation, high sensitivity and increased specificity. Spectroscopic methods are particularly important for confirmation of structures.

GC and GC–MS have been used for confirmatory analyses of antibiotics such as sulfonamides. However, due to their low volatility and thermally labile nature, chemical derivatization is usually required. Several methods have been reported that are based on derivatization followed by GC with detection either by electron capture [2] or MS with selected-ion monitoring in the electron ionization (EI) [3] and chemical ionization (CI) [4] modes. GC–MS and tandem mass spectrometry (MS–MS) have also been used for the confirmation of methylated sulfonamides in bovine and porcine tissue [5]. Unfortunately, such analyses are time-consuming as they require extensive sample clean-up prior to the additional derivatization step.

The mass spectral behaviour of underivatized sulfonamides under EI and more recently CI has been well documented [6–7]. Chemical ionization with isobutane as the reagent gas has also been used for the tandem MS of protonated sulfonamides by collision-induced dissociation with mass-analyzed ion kinetic energy spectrometry (CID–MIKES) [7]. In a more recent investigation [8], very similar CID spectra of sulfonamides were obtained using ammonia as CI reagent gas, on a hybrid instrument. While both of these studies demonstrated that direct confirmation of sulfonamide residues in animal tissue at a level of 0.1 ppm could be achieved by MS–MS without chromatography, the authors stressed the problems of possible interferences. Due to the complex nature of the matrices involved, even after clean-up procedures, the most reliable method will likely be one combining chromatographic separation prior to spectroscopic detection.

LC is the most commonly used instrumental method for the analysis of antibiotics and antimicrobial agents in biological matrices [9,10]. Several authors have reported multi-residue LC methods with UV detection for the determination of sulfonamides, other antibiotics and growth promoters in feed stuffs [11], animal tissue [12,13] and other food products [14–16]. Sensitive LC methods for the determination of sulfonamides in cultured fish tissue have also been described previously [17–20].

Despite the selectivity of the extraction and cleanup methods employed, LC with UV detection at single wavelengths is still prone to interferences which can result in reduced confidence in analyses. The combination of LC with UV diode-array detection (DAD) [21] and with MS have tremendous potential for this type of analysis. In 1982, Henion *et al.* [22] described the use of an atmospheric pressure ionization (API) source for the LC–MS analysis of five sulfonamides in racehorse urine and plasma by LC–MS. While clearly demonstrating the potential of LC–MS and also of

LC–MS–MS, the prototype heated nebulizer interface used in this investigation provided full-scan detection limits only in the μg range.

Ion spray (ISP) is a recently developed API technique [23] that is proving to be well suited to the LC–MS analysis of trace levels of polar and thermally labile compounds [24,25]. The mechanism of both ISP and electrospray, a related technique [26] is believed to involve ion evaporation [27] although nebulization plays an important role in the former process [23]. A recent review has detailed the use of API-MS as a detection system for the separation sciences [28]. This paper will present LC–DAD and LC–MS–MS methods that have been developed for the analysis of sulfonamides and related agents, and demonstrate their application to the determination of sulfadimethoxine (SDM) in salmon flesh.

EXPERIMENTAL

Chemicals

All of the sulfonamide standards listed in Table I were obtained from Sigma (St. Louis, MO, USA) and used as received, without purification. Trifluoroacetic acid (TFA) and formic acid were obtained from BDH (Poole, UK). HPLC-grade acetonitrile was purchased from Anachemia (Lachine, Canada). A Milli-Q water purification system (Millipore, Bedford, MA, USA), equipped with ion-exchange and carbon filters, was used to further purify glass-distilled water.

Extraction of sulfadimethoxine from salmon flesh

The extraction procedure used in this investigation was based on those reported by Weiss *et al.* [17] and Nose *et al.* [20], Salmon flesh (40 g) was mixed with acetone (200 ml) and homogenized with a Brinkmann Polytron for 3 min. After addition of sufficient quantities of Celite (10 g) and sodium sulphate (20 g) the homogenate was again blended for a further 2 min. This mixture was vacuum-filtered and the filter cake was washed with acetone (3 × 15 ml). After transferring the filtrate to a round-bottomed flask, the acetone was removed on a rotary evaporator at 40°C. The residue was re-dissolved in 100 ml of dichloromethane; 50 ml of this solution was mixed with 100 ml of 0.1 *M* sodium hydroxide and shaken vigorously. This mixture was transferred to a 250-ml centrifuge jar and centrifuged for 20 min at 12 *g* and 10°C. The aqueous layer was transferred to a round-bottomed flask and neutralized with hydrochloric acid. This aqueous extract was freeze-dried overnight. The remaining water was removed on a rotary evaporator at 40°C the following day. The residue was dissolved in 5.0 ml of aqueous 25% methanol, and the solution was filtered through a 0.45-μm nylon syringe filter.

Liquid chromatography

Analyses were performed on a Hewlett-Packard Model HP1090M liquid chromatograph equipped with a variable-volume (1–25 μl) injector and autosampler, a ternary DR5 solvent-delivery system, a built-in HP1040A diode-array detector and a HP79994A data system. For the analysis of sulfonamide mixtures, separations were achieved on a 25 cm × 2.1 mm I.D. column packed with 5-μm Vydac 201TP stationary phase (Separations Group, Hesperia, CA, USA). Aqueous acetonitrile containing 0.1% TFA was used as the mobile phase at a flow-rate of 200 μl/min with

TABLE I

NAMES, STRUCTURES, RETENTION TIMES, UV AND PARTIAL MS–MS SPECTRAL DATA FOR SULFONAMIDES EXAMINED IN THIS STUDY
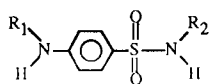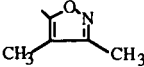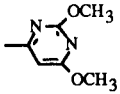
Name	Code	R_1	R_2	Mol.wt.	$t_R{}^a$ (min)
Sulfaguanidine	SGN	H		214	3.60
Sulfanilamide	SNL	H	H	172	3.74
Sulfacetamide	SMD	H	—COCH$_3$	214	6.49
Sulfadiazine	SDZ	H		250	6.50
Sulfapyridine	SPR	H		249	7.36
Sulfamerazine	SMR	H		264	7.51
Sulfathiazole	STH	H		255	7.97
Sulfamethazine	SMT	H		278	8.51
Sulfamoxole	SMX	H		267	8.63
Sulfisomidine	SID	H		278	9.24
Sulfamethoxypyridazine	SMP	H		280	10.59
Sulfamethizole	SMZ	H		270	10.77
Sulfameter	SME	H		280	10.89
Succinylsulfathiazole	SRTZ	HOOC(CH$_2$)$_2$CO$^-$		355	12.08
Sulfachloropyridazine	SCP	H		284	12.98

$\lambda_{max}{}^b$	f	c	a	b	d	e	Other
263	122(1)	156(75)	60(12)	108(32)	92(38)		
261	—	—	—	156(8)	NA	92(11)	139(2)
272	149(1)	—	156(61)	60(1)	108(16)	92(23)	173(60) 65(1)
270	185(2)	158(5)	156(100)	96(9)	108(21)	92(16)	
245 264 312	184(21)	—	156(88)	95(8)	108(18)	92(13)	232(3) 167(4)
245 265	199(3)	172(22)	156(100)	110(40)	108(28)	92(15)	
260(S)^c 285	190(1)	—	156(100)	101(6)	108(19)	92(15)	139(1)
245 265(WS)^c 310(WS)^c	213(7)	186(42)	156(100)	124(85)	108(25)	92(20)	
272	—	—	156(100)	113(36)	108(21)	92(12)	
260 285(S)^c	—	186(22)	156(60)	124(100)	108(13)	92(1)	
270	215(3)	188(3)	156(60)	126(30)	108(15)	92(10)	
255(WS)^c 275	—	178(1)	156(100)	116(8)	108(19)	92(14)	
270	215(12)	188(8)	156(100)	126(45)	108(21)	92(12)	
260 285	—	—	256(100)	—	208(1)	192(41)	156(16) 108(7)
270	—	—	156(100)	130(8)	108(12)	92(9)	

TABLE I (*continued*)

Name	Code	R$_1$	R$_2$	Mol.wt.	$t_R{}^a$ (min)
Sulfamethoxazole	SMO	H		253	14.86
Sulfisoxazole	SIX	H		267	15.57
Phthalylsulfathiazole	PST			403	15.65
Sulfabenzamide	SBD	H		276	16.79
Sulfadimethoxine	SDM	H		310	18.48
Sulfaquinoxaline	SQO	H		300	18.05

[a] Retention time on Vydac 201TP52 column with a linear gradient of the aqueous mobile phase from 5–40% acetonitrile (containing 0.1% TFA) in 20 min; flow-rate of 200 μl/min.

[b] λ_{max} obtained under isocratic conditions with a mobile phase of aqueous acetonitrile (80%) containing 0.1% TFA.

[c] S = Shoulder; WS = weak shoulder.

a linear gradient of 5–40% acetonitrile in 20 min. An injection volume of 5 μl was used. Detection was at 270 nm (10-mm bandwidth) with acquisition of UV spectra in the peak-triggered mode. For the determination of SDM in salmon extracts, isocratic separations were achieved on a 25 cm × 4.6 mm I.D. column packed with 5-μm Supelcosil LC 18DB stationary phase (Supelco, Santa Clara, CA, USA), using an injection volume of 20 μl. Aqueous 35% acetonitrile containing 0.1% formic acid was used as the mobile phase at a flow-rate of 1 ml/min. Multi-wavelength detection with the DAD system was used at the following wavelengths (and bandwidths): 250 (4), 260 (4), 265 (10), 270 (4), 280 (4) and 290 (4) nm.

LC–MS–MS

All LC–MS experiments were performed on a SCIEX API III triple quadrupole mass spectrometer (Thornhill, Canada), equipped with an API source and an IonSpray interface. A Macintosh IIx computer was used for instrument control, data acquisition and data processing. Polypropylene glycols were used to calibrate the mass scale and to adjust the resolution to unity (40% valley definition) over the mass range 50–500 dalton. For LC–MS experiments the column effluent was connected to the fused-silica transfer line (50–75 μm I.D.) of the ISP interface via a Valco sub-μl injection valve with interchangeable loops. This injector was used to optimize the LC–MS system (0.1-μl loop) and for all flow-injection experiments (1.0 μl loop). For

$\lambda_{max}{}^{b}$	f	c	a	b	d	e	Other
270	188(6)	159(4)	156(100)	99(9)	108(24)	92(18)	
270	—	—	156(100)	113(59)	108(19)	92(18)	139(1) 175(1)
285 260	—	—	304(24)	—	256(27)	—	149(70) 156(100) 386(26)
235	— —	—	156(100)	—	108(9)	92(7)	174(12)
269	245(4)	218(4)	156(100)	156(0)	108(9)	92(5)	173(4)
249 269 395(WS)^c	235(1)	208(1)	156(100)	146(18)	108(9)	92(5)	

simultaneous LC–DAD–MS acquisitions the column effluent was split using a zero-dead-volume "T" connector, with approximately one quarter of the flow being fed to the mass spectrometer (again via the post-column injector). The split ratio was determined by the length of a fused-silica capillary (50 μm I.D.) connecting the "T" to the DAD flow cell. Identical LC conditions to those described above were used for the analysis of sulfonamide mixtures. For the confirmation of SDM in salmon flesh by LC–MS, the 2.1 mm I.D. (201TP) column was used with 100 μl/min aqueous 35% acetonitrile containing 0.1% formic acid and with the end of the column connected directly to the ISP interface.

The ISP voltage was maintained at approximately 5.6 kV for all LC–MS analyses. High-purity air at an operating pressure of 90 p.s.i. (approximately 2 l/min) was used as the nebulizing gas. A dwell time of 5 ms/dalton was used for full-scan LC–MS analyses. For single- and multiple-ion monitoring LC–MS experiments dwell times of 200 and 100 ms/dalton were employed, respectively. MS–MS measurements were based on CIDs within the r.f. only quadrupole at a collision energy of 35 eV (aboratory frame). Both parent- and daughter-ion LC–MS–MS scans were performed. Argon was used as the target gas at an indicated thickness of $2.5 \cdot 10^{14}$ molecules/cm^2. For comparative MS–MS work, CID product ion spectra of the standards were acquired over a range of collision energies (0–50 eV) and at several target-gas thicknesses $(0.1–5.0 \cdot 10^{14}$ molecules/cm$^2)$. Preliminary MS–MS experiments with the

standards indicated that the masses of the product ions were well separated; it was possible therefore to obtain an appreciable gain in sensitivity, for the less-intense product ions, by operating at peak widths on the third quadrupole (Q_3) corresponding to more than 1 dalton wide. The first quadrupole (Q_1), however, was maintained at unit mass resolution. Selected fragmentation pathways were confirmed by grand-daughter-ion experiments, whereby dissociations of the protonated molecules were induced in the source region, prior to entering the mass analyzer, by increasing the declustering voltage applied to the sampling orifice. Product ions generated in this way were then subjected to further fragmentation in conventional parent/daughter MS–MS experiments.

RESULTS AND DISCUSSION

ISP-MS

Table I gives the names, abbreviations and structures of the 21 sulfonamides examined in this study. All of these compounds provided very simple ISP mass spectra, containing only a protonated molecule, $[M + H]^+$, and no fragment ions of significant intensity. Good-quality spectra could be obtained by flow-injection analysis (FIA) in the full-scan mode with as little as 1 ng of compound injected. Fig. 1a presents the full-scan, background-subtracted ISP mass spectrum obtained from flow injection of 50 ng SDM into a 50-μl/min flow of aqueous acetonitrile (50%) containing 0.1% TFA. The fact that most of the iron current is associated with the $[M + H]^+$ ion suggests that ISP should be ideal for trace-level determinations using selected-ion monitoring (SIM). This is demonstrated in Fig. 1b, which shows the response obtained from duplicate injections of standard solutions of SDM. These results indicate a FIA–SIM detection limit of around 10 pg (signal-to-noise ratio = 3). Very similar sensitivities
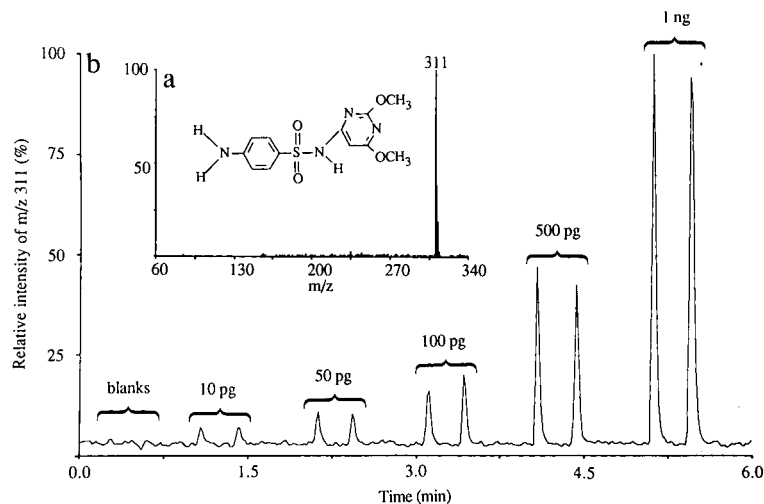
Fig. 1. Flow-injection ISP–MS analysis of sulfadimethoxine (SDM). (a) Positive ion, background-subtracted ISP mass spectrum of 50 ng of SDM; (b) duplicate 1-μl injections of a series of dilutions using SIM of the protonated molecule (*m/z* 311). Conditions: 50 μl/min aqueous acetonitrile (50%) containing 0.1% TFA.
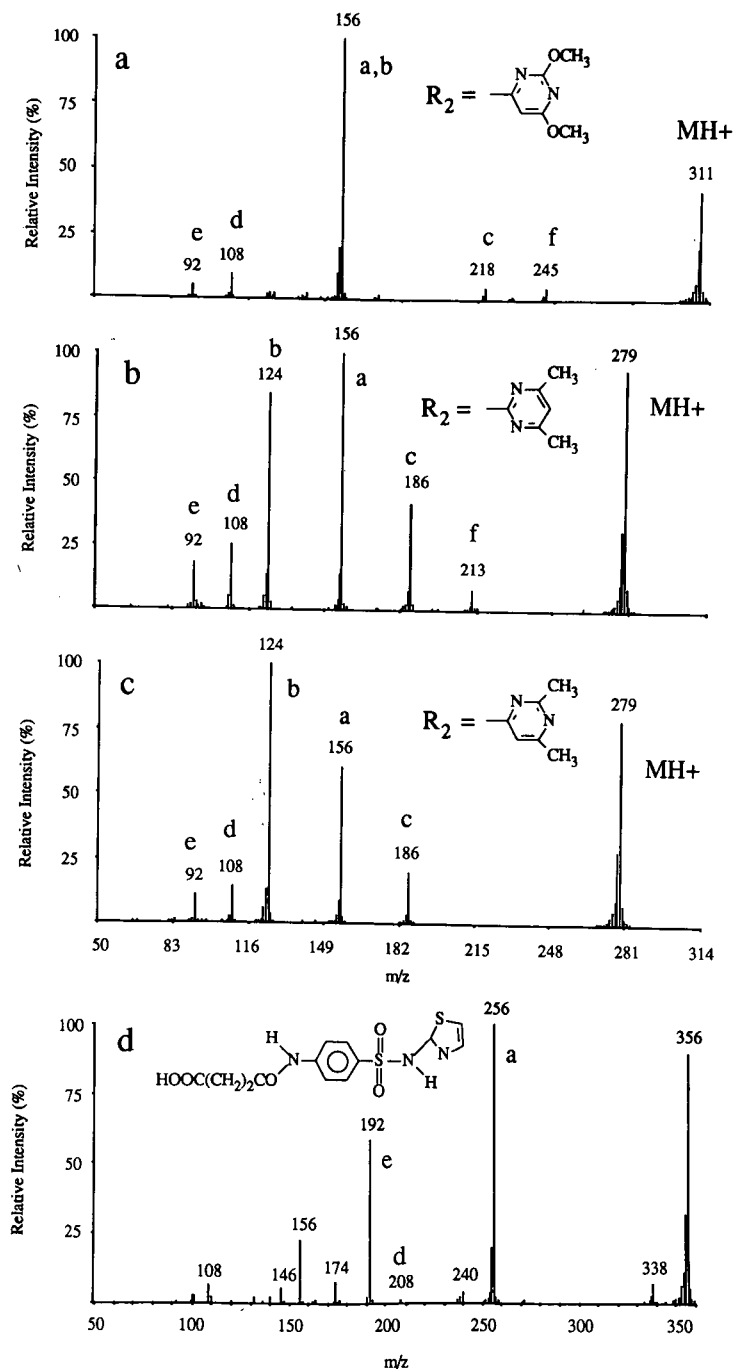
Fig. 2. Positive-ion ISP-MS–MS product ion spectra of the protonated molecules of standard compounds obtained by flow injection. (a) SDM (m/z 311); (b) SID (m/z 279); (c) SMT (m/z 279); and (d) STZ (m/z 356). Conditions: as Fig. 1 except with a collision energy of 35 eV (laboratory frame) and using argon as the collision gas at an indicated thickness of $3.0 \cdot 10^{14}$ molecules/cm^2.
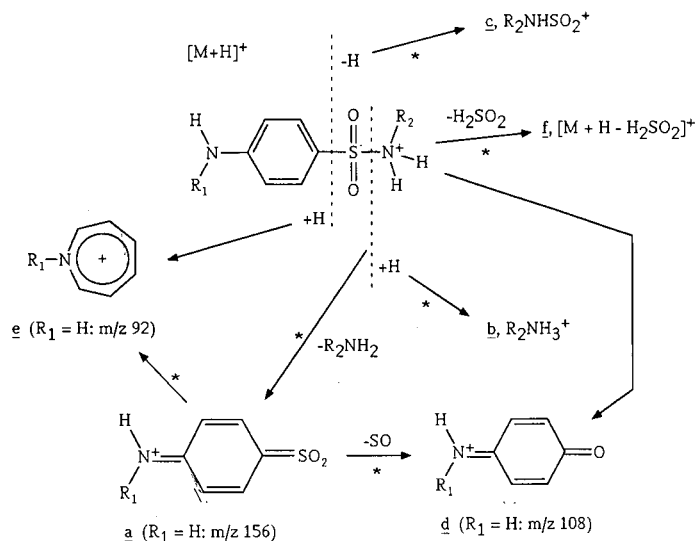
Fig. 3. Proposed fragmentation scheme for the collison-induced dissociation of the protonated sulfon-amides. Pathways denoted with an asterisk are supported by granddaughter-ion experiments using SDM, SID and SMT (see Experimental section).

were obtained for the other sulfonamides in Table I, with the exception of the parent sulfonamide, sulfanilamide (SNL), the response of which was approximately 5 times lower.

The lack of structural information provided by the simple ISP mass spectra can be remedied by the use of MS–MS techniques. Table I lists the most abundant product ions observed for the 21 standard sulfonamides using the triple quadrupole API III mass spectrometer, all under identical CID conditions. The resolution on Q_3 was reduced to provide additional sensitivity for the less-abundant product ions. It should be noted that this results in a somewhat fragmented appearance of peaks in the CID spectra presented; the latter is also due, in part, to the nature of the detection system used, which performs ion counting instead of the more usual continuous analog acquisition. In general, the ISP product ion spectra are less complex than those previously reported on sector instruments using CI [7,8]. Some representative product ion spectra of sulfonamides obtained by FIA–ISP are shown in Fig. 2. These spectra are similar to the CID spectra reported by Henion *et al.* [22], generated by corona discharge atmospheric pressure CI using a prototype heated nebulizer interface.

Fig. 3 illustrates fragmentation mechanisms proposed to rationalize the CID spectra of the sulfonamides. Charge localization in the $[M+H]^+$ ion through protonation of the sulfonamide nitrogen helps to explain the observed fragmentations. The abundant product ion *a* (m/z 156 for $R_1 = H$) is characteristic of all the sulfonamides analyzed and likely arises from the cleavage of the sulfur–nitrogen bond and loss of the neutral species R_2NH_2. Charge retention on the nitrogen with hydrogen abstraction results in ion *b*, corresponding to $R_2NH_3^+$, *i.e.*, $[M+H-155]$. In the case of SDM, ions *a* and *b* both coincidentally appear at m/z 156 (see Fig. 2a). For the isomeric sulfonamides SMT and SID (Fig. 2b and c), ion *b*, due to the protonated

pyrimidyl moiety, appears at m/z 124. Two other product ions, d and e observed at m/z 108 and 92, are common to all of the sulfonamides and may be rationalized by the losses of SO and of SO_2 from the ion at m/z 156, with the latter assigned to a ring-expanded azatropylium ion. An additional characteristic product ion at m/z 65, which presumably results from the loss of HCN from m/z 92, was also reported in the heated nebulizer CID spectra [22]. However, under the present conditions, this ion was observed only occasionally. Fragment ion c, at m/z 218 in the spectrum of SDM and at m/z 186 in the spectra of both SMT and SID, is assigned to the loss of neutral aniline (93 dalton) from $[M + H]^+$. This loss is also observed in the majority of the sulfonamides (Table I). It should be noted that while SMT and SID, and another isomeric pair SMP and SME, can be differentiated by the relative intensities of the ions described above, an additional ion at m/z 213 is observed in the spectrum of SMT which does not appear in that of SID. This ion, designated as f, has been reported previously in the CID–MIKES spectra of protonated sulfonamides generated with CI, where it was assigned to $[M + H - H_2SO_2]$ [7]. Selected-fragmentation pathways indicated in Fig. 3 were confirmed by granddaughter-ion experiments in which dissociations of the protonated molecules were induced in the source region, prior to conventional MS–MS experiments in the triple quadrupole.

Additional evidence for the above assignments was obtained from CID of the ^{37}Cl isotope peak of the protonated molecule of the chlorinated sulfonamide SCP, at m/z 287. The product ion spectrum was identical to that obtained for the ^{35}Cl protonated molecule, indicating that the R_2 group is not involved in the major fragmentation pathways discussed above. The two sulfonamides which contain an R_1 group, STZ and PST, also show analogous product ions and losses. The product ion spectrum of STZ is presented in Fig. 2d, and product ion from the corresponding loss of H_2NR_2 is seen at m/z 256 with those from the subsequent losses of SO and SO_2 at m/z 208 and 192, respectively.

The identification of the common fragmentation pathways shown in Fig. 3 opens up the possibility of using MS–MS techniques to screen extracts for putative sulfonamides, and this approach is discussed later. Although isomer distinction could be enhanced to some degree by proper selection of target-gas thickness and collision energy, the use of combined LC–MS should provide the necessary additional selectivity via retention time.

LC–MS

While we have found excellent sensitivity and quantitation for standard solutions of sulfonamides using FIA (Fig. 1b), the technique has a number of drawbacks in the analysis of real-world complex extracts containing salts and other endogenous material. The simultaneous introduction of many possible sources of interferences into the ion source with the analyte effectively prevents the use of FIA for quantitative analyses. Although the use of MS–MS techniques in conjunction with FIA can provide additional selectivity to filter out many potential interferences, there still remains the problem of other components influencing the ionization efficiency. Effective sample clean-up is necessary for quantitative work, and the easiest way to accomplish this without introducing additional sample handling steps is to provide a chromatographic separation prior to ionization.

Recent advances in bonded stationary phase technology have resulted in the
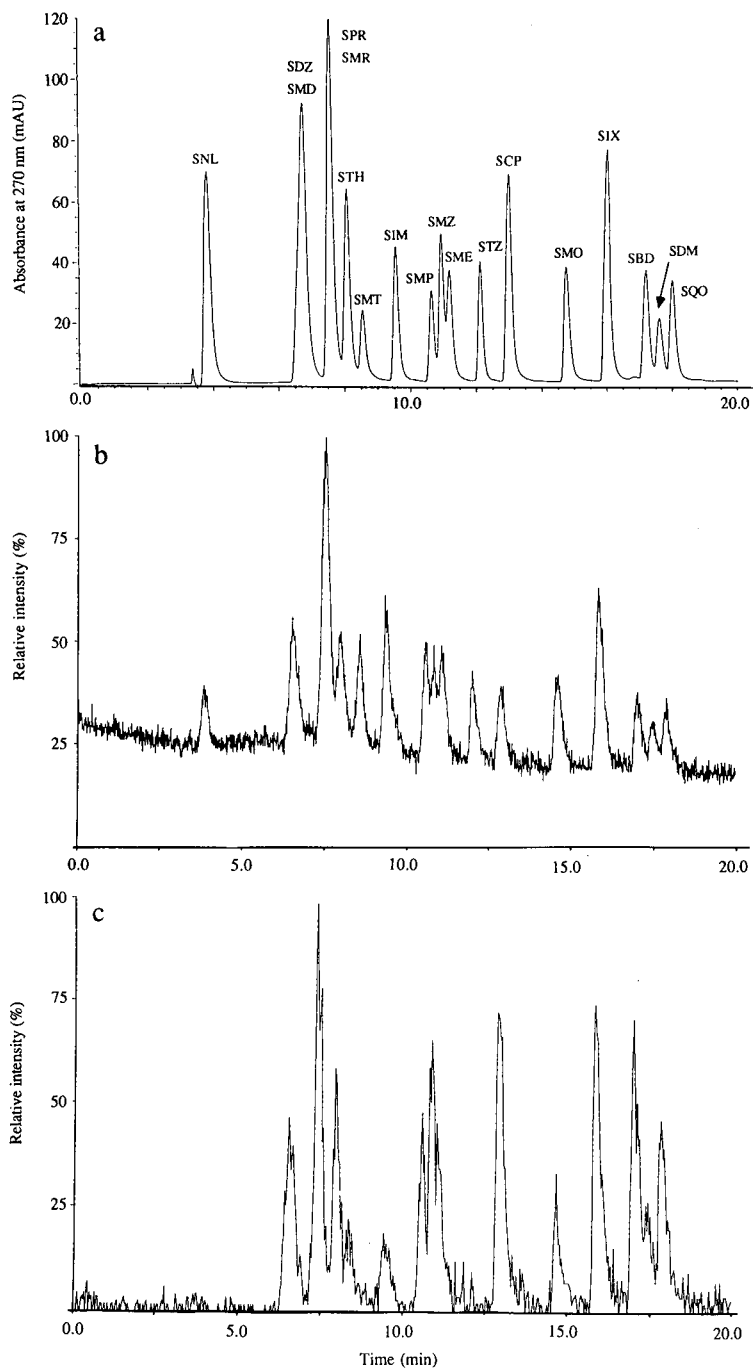
Fig. 4. Separation of a mixture of 18 sulfonamides by reversed-phase HPLC with simultaneous detection using (a) DAD with 270 nm (bandwidth = 4 nm) and (b) ISP-MS with multiple-ion monitoring of protonated molecules. A separate LC–MS–MS parent-ion scan experiment was conducted to produce the data in (c) where Q_1 was scanned from 160 to 400 dalton with Q_3 set at m/z 156. Conditions: 25 cm × 2.1 mm I.D. Vydac 201 TP52 column and a mobile phase of aqueous acetonitrile containing 0.1% TFA, with a linear gradient of 5–40% acetonitrile in 20 min and a flow-rate of 200 μl/min split 1:4 post-column between DAD and MS, respectively; 5-μl injection volume.

development of a number of multi-residue, reversed-phase LC methods for the analysis of several classes of antibiotics [9]. One recent study reported the separation of a wide range of sulfonamides using a small-particle-size (3 μm) C_{18} stationary phase packed in a capillary column (30 cm × 0.35 mm I.D.). Although 20 sulfonamides could be resolved adequately, peak tailing was evident for the late-eluting drugs and the analysis required more than 1 h [10].

For the present study, several commercially available columns packed with different stationary phases (aminopropylsilica and octadecylsilica) were examined as potential candidates for a general LC method. It quickly became apparent that, for such a complex mixture of closely related compounds, gradient elution in conjunction ·with a C_{18} stationary phase would be required. Mass spectral detection can also reduce the reliance on the complete resolution of all individual components, provided that these are not isobaric. In the present study complete baseline resolution remained an objective, but greater emphasis was placed on the development of an LC method capable of presenting a wide range of sulfonamides in suitable form to the ISP interface.

The sensitivity of the ISP process is directly related to the degree of ionization of the analyte in solution. The nitrogen of the central sulfanilamide bond is amenable to protonation which can be enhanced by increasing the acidity of the analyte solution. Lowering the pH of the mobile phase can also improve peak shape of basic compounds in reversed-phase LC by reducing adsorption on silica-based stationary phases, although this does lead to lower capacity factors, k', values. Both formic and trifluoroacetic acids were evaluated as modifiers in the aqueous acetonitrile mobile phase. The latter has the added advantage of being an effective ion-pairing agent, thus compensating for the lower pH by increasing retention.

Fig. 4a shows LC–UV analysis of a mixture of 18 sulfonamide standards on a 2.1 mm I.D. column, using 0.1% TFA and a linear-gradient elution profile. Only 16 peaks were observed in the trace due to the coelution of SDZ with SMD and SPR with SMR. The retention times of all of the 21 sulfonamides analyzed under this elution profile are listed in Table I. Using DAD, complete UV spectra of the individual sulfonamides were obtained to help confirm peak identities. The observed maximum wavelength, λ_{max} values for each of the sulfonamides examined are given in Table I. SPR and SMR could not be differentiated in this way as they possessed almost identical UV spectra.

The LC–MS reconstructed-ion chromatogram (RIC), acquired simultaneously using multiple-ion monitoring of 16 protonated molecules (two isobaric pairs), is presented in Fig. 4b. The correspondence between the UV and RIC traces is excellent, and this close correspondence allows the rapid confirmation of individual chromatographic peaks by mass as well as retention time.

The ability to screen samples for putative sulfonamides by selective LC–MS–MS techniques is demonstrated in Fig. 4c, which shows the full-scan total-ion current (TIC) trace from an analysis of the same mixture of sulfonamides using a parent-ion scan mode. For this analysis, the post-column split was removed and the 200-μl/min flow from the column was fed directly to the ISP interface. In this experiment Q_3 was adjusted to transmit only m/z 156 product ions, formed from the CID (in Q_2) of parent ions scanned by Q_1 (160–400 dalton), $i.e.$, only those protonated molecules which give rise to an m/z 156 product ion gave a response at the detector. Not all of the sulfonamides provided an intense m/z 156 product ion, and this is shown by the lack of

a response for SNL and also for STZ, which contains an R_2 group. The neutral-loss mode is another MS–MS mode in which the triple quadrupole mass spectrometer may be used. In this configuration Q_1 and Q_3 are scanned together, with Q_1 leading Q_3 by some neutral mass loss characteristic of the compound(s) of interest. In the case of the sulfonamides this was achieved using the $[M + H - 155]^+$ fragmentation discussed earlier, although fewer of the sulfonamides give this particular fragmentation than that yielding the product at m/z 156.

The sensitivity of the more selective LC–MS–MS method can be increased by using selected-reaction monitoring (SRM). In this configuration, both Q_1 and Q_3 may be linked to monitor individual parent/daughter CID reactions. The LC–MS–MS detection limit for SDM, monitoring the dissociation of m/z 311 to m/z 156, was found to be approximately 200 pg on-column. This is approximately an order of magnitude less sensitive than by LC–MS with SIM.

As mentioned above, trimethoprim (TMP) and ormetoprim (OMP) are commonly used as potentiators in commercial formulations with sulfonamides, and it would be useful if LC–MS could be used in a multi-residue approach for the determination of both classes of compound. Fig. 5a shows the SIM LC–MS response obtained from the analysis of a 1:1 mixture of TMP and OMP, with 50 ng of each injected on-column, under the same gradient conditions as used for the sulfonamides. The two compounds gave approximately equal molar responses under the ISP ionization process, with TMP eluting slightly before OMP. As for the sulfonamides, only protonated molecules are observed in their ISP spectra. Good-quality CID spectra with abundant product ions were obtained for both compounds, and these are presented in Fig. 5b and c. The product ion at m/z 123, which is assigned to a product
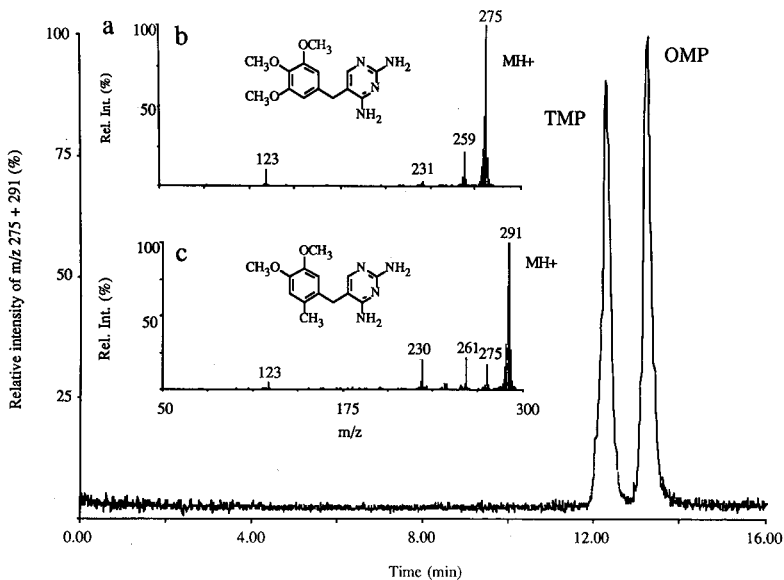
Fig. 5. (a) Analysis of a 1:1 mixture of trimethoprim (TMP) and ormetoprim (OMP) (50 ng each injected) by LC–MS using selected-ion monitoring of protonated molecules (m/z 291 and 275, respectively). The insets show the positive-ion ISP-MS–MS product ion spectra of OMP (b) and TMP (c). LC–MS and MS–MS conditions as in Figs. 4b and 2, respectively.

ion containing the pyrimidine moiety plus the bridging carbon atom, appears in the spectra of both TMP and OMP and could be used as a target dissociation in an SRM methodology.

Determination of SDM in salmon flesh

An opportunity to test the effectiveness of the LC–DAD and LC–MS methods, described above, arose when samples of farmed Coho salmon suspected of containing SDM were made available for analysis. Initial measurement of suspect flesh extracts, using LC with single-wavelength UV detection, showed a peak at the correct retention time for SDM and indivated levels in the different samples ranging from 25 to 1800 ng/g (ppb). The main objective of our subsequent analyses was to confirm the peak identity with DAD and MS.

A specific extraction method for SDM could be used in this case. The method selected is similar to those reported in the literature and is detailed in the Experimental section. Recoveries of SDM spiked into control flesh samples over the 100–1000 ng/g level were approximately 60% (unpublished results). These results are consistent with those previously reported by other workers, who have suggested that the poor recoveries may be due to the higher levels of cholesterol found in salmonids than in other species of fish [18]. Clearly there is a need to improve the extraction and cleanup procedures, and these are currently under investigation.

For the present experiments, a rapid isocratic procedure was developed which gave a retention time of 7.3 min ($k' = 3$) for SDM. Excellent peak shape and separation of SDM from other endogenous substances was achieved, using a base-deactivated column (Supelcosil LC18DB) and a mobile phase of aqueous 35% acetonitrile with 0.1% formic acid. Fig. 6a shows the analysis of a control salmon flesh extract spiked with 83 ng/g SDM, using UV absorption detection at 265 nm with a 10-nm bandwidth. This method gave an excellent detection limit of 0.03 μg/ml in salmon flesh extract. This corresponds to approximately 13 ng/g in the flesh with correction for a 60% recovery factor. The quantitation aspects were not investigated further at this stage since the primary objective at present was qualitative analysis.

At trace residue levels the DAD is not sufficiently sensitive in the full-scan mode to provide useful UV spectra for confirmation of identity. However, by acquiring at several characteristic wavelengths simultaneously, it is possible to conform that a compound has the correct spectral features in a broad sense. The UV spectrum of SDM is given in Fig. 6b, and indicates the six additional wavelengths that were selected for acquisition: 240, 250, 260, 270 and 290 nm (all with 4-nm bandwidths). Fig. 6c shows the multi-wavelength data set for the same spiked control flesh sample (83 ng/g) as in Fig. 6a. The peak area ratios in the six traces match exactly the absorbance ratios measured in the UV spectrum in Fig. 6b, at the different wavelengths indicated.

An LC–MS method was then established for the rapid analysis of SDM. Fig. 7a shows the LC–ISP–MS analysis of an SDM standard solution (1.1 μg/ml) using similar isocratic conditions, with SIM of the protonated molecule at m/z 311. The inset in Fig. 7a shows a typical calibration curve for standard solutions over the 0.08–80 μg/ml range. A detection limit of 0.04 μg/ml was estimated.

Fig. 7b and c shows the LC–MS and LC–DAD analyses, respectively, of an extract of a salmon flesh sample estimated by the latter technique to contain 25 ng/g (ppb). Confirmation of the SDM was clear and unequivocal with the LC–MS data.
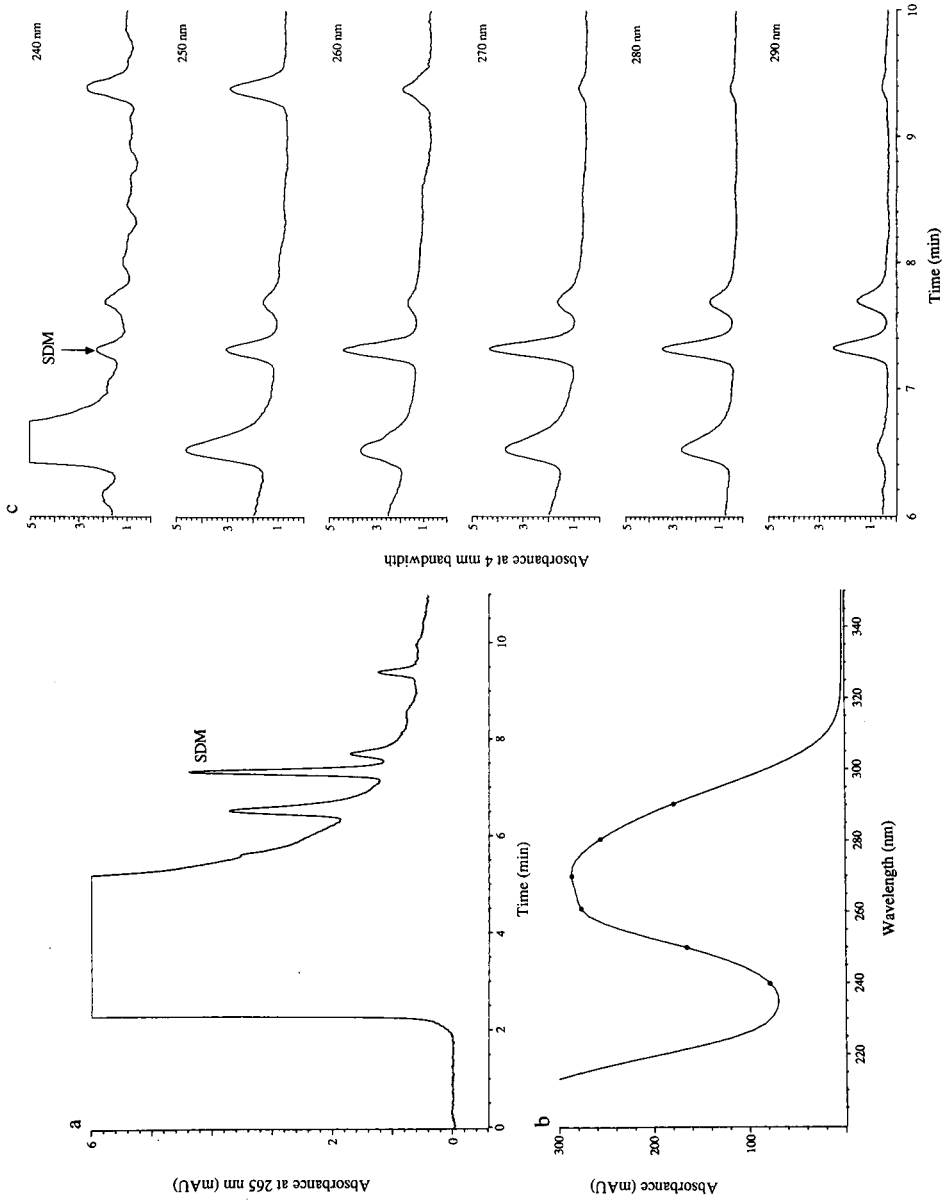
Fig. 6. Isocratic LC–DAD analysis of an extract of salmon flesh spiked at the 83 ng/g level with SDM. The first trace (a) shows the chromatogram with detection at 265 nm using a 10-nm bandwidth. The UV spectrum of SDM acquired for a standard is given in (b) to indicate the wavelengths (designated by dots) selected for the acquisition of the multi-wavelength data set (c) [acquired simultaneously with the trace in (a)]. Conditions: 25 cm × 4.6 mm I.D. Supelcosil LC18DB column: 1 ml/min aqueous acetonitrile (35%) containing 0.1% formic acid; 20-μl injection volume.
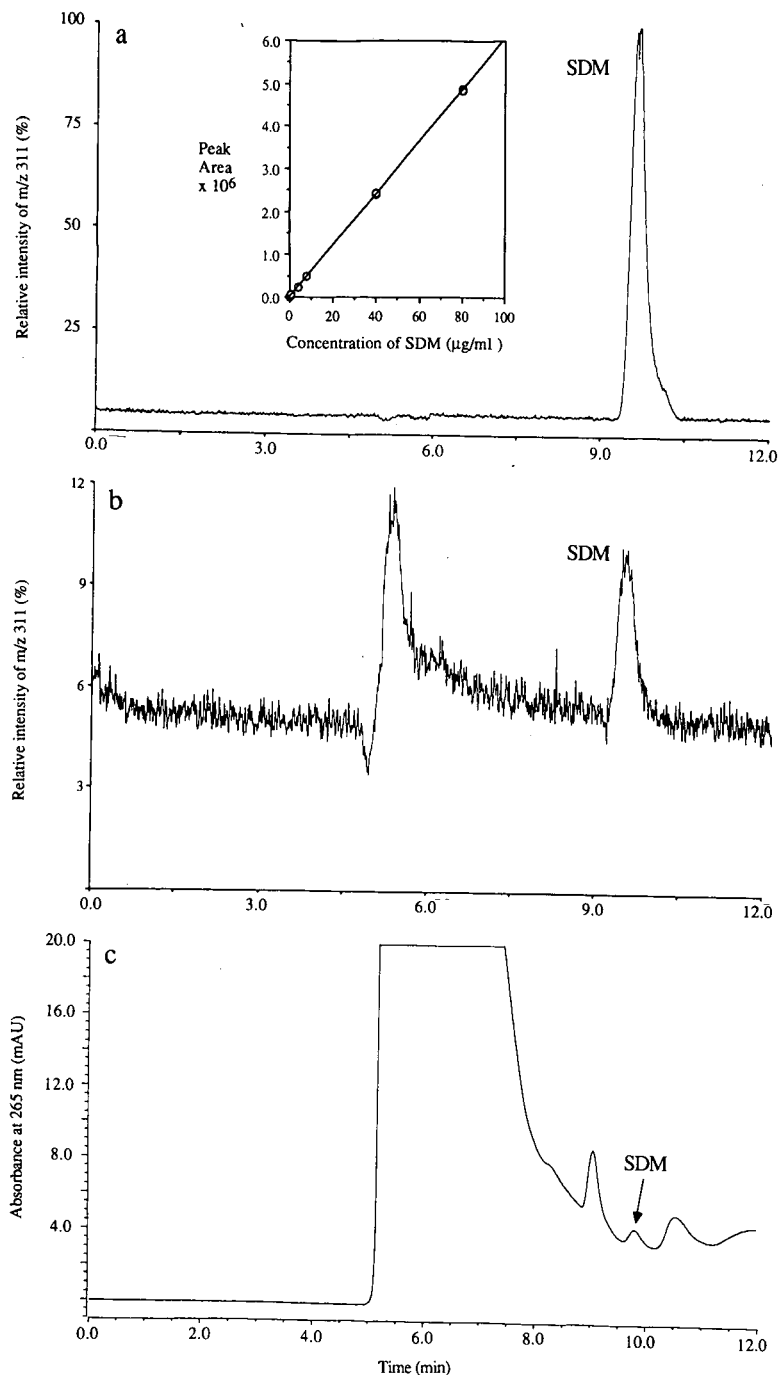
Fig. 7. (a) Analysis of SDM standard (1.1 μg/ml) by LC–MS with selected-ion monitoring of the protonated molecule, m/z 311; (b) analysis of suspect salmon flesh extract by LC–MS; (c) LC–DAD analysis of salmon flesh extract confirming the presence of SDM. The inset in (a) shows the linear relationship between LC–MS peak area and concentration of SDM. Conditions: 25 cm × 2.1 mm I.D. Vydac 201TP52 column; 100 μl/min aqueous acetonitrile (35%) containing 0.1% formic acid; 10-μl injection volume.

With the present extraction and cleanup procedure, it is possible to confirm SDM in flesh at the 10 ppb level. At these low levels the LC–DAD analysis was complicated by closely eluting endogenous substances, but the multi-wavelength data set did provide additional conformatory evidence for the presence of SDM. Improvements in the extraction procedure, together with the use of gradient elution, should provide significantly lower detection limits. Both of these improvements are under development.

CONCLUSIONS

There is considerable urgency for the development of reliable instrumental methods of analysis for antibiotics in the flesh of farmed fish. Since LC is the tool most widely used for routine monitoring of these compounds, it is important to develop confirmatory methods based on the combination of LC with spectroscopic methods. Mass spectrometry is a preferred method due to its inherent sensitivity and selectivity. It has been shown here that LC–ISP–MS–MS provides the key to confidant detection and identification of trace level sulfonamides in fish tissue. It has also been shown that UV DAD, in either the full-scan or the multiwavelength acquisition modes, is a useful technique for additional confirmation of sulfonamide identity. The combination of LC, DAD, and ISP–MS–MS techniques, provides a powerful approach to the analysis of sulfonamides and other antibiotics in fish tissue.

ACKNOWLEDGEMENTS

REFERENCES

1 W. Horwitz, *J. Assoc. Off. Anal. Chem.*, 64 (1981) 104.
2 D. P. Goodspeed, R. M. Simpson, R. B. Ashworth, J. W. Shafer and H. R. Cook, *J. Assoc. Off. Anal. Chem.*, 61 (1978) 1050.
3 R. M. Simpson, F. B. Suhre and J. W. Shafer, *J. Assoc. Off. Anal. Chem.*, 68 (1985) 23.
4 W. Garland, B. Miwa, G. Weiss, G. Chen, R. Saperstein and A. MacDonald, *Anal. Chem.*, 52 (1980) 842.
5 J. E. Matusik, R. S. Sternal, C. J. Barnes and J. A. Sphon, *J. Assoc. Off. Anal. Chem.*, 73 (1990) 529.
6 E. Dynesen, S. O. Lawesson, G. Schroll, J. H. Bowie and R. G. Cooks, *J. Chem. Soc.*, (B) 1 (1968) 15.
7 W. C. Brumley, Z. Min, J. E. Matusik, J. A. G. Roach, C. J. Barnes, J. A. Sphon and T. Fazio, *Anal. Chem.*, 55 (1983) 1405.
8 E. M. H. Finlay, D. E. Games, J. R. Startin and J. Gilbert, *Biomed. Environ. Mass Spec.*, 13 (1986) 633.
9 W. A. Moats, *J. Assoc. Off. Anal. Chem.*, 73 (1990) 343.
10 R. F. Cross, *J. Chromatogr.*, 478 (1989) 42.
11 M. K. Cody, G. B. Clark, B. O. B. Conway and N. Crosby, *Analyst (London)*, 115 (1990) 1.
12 A. R. Long, L. C. Hsieh, M. S. Malbrough, C. R. Short and S. A. Barker, *J. Agric. Food Chem.*, 38 (1990) 423.
13 K. Takatsuki and T. Kikuchi, *J. Assoc. Off. Anal. Chem.*, 73 (1990) 886.
14 A. R. Long, L. C. Hsieh, M. S. Malbrough, C. R. Short and S. A. Barker, *L. Liq. Chromatogr.*, 12 (1989) 1601.
15 A. R. Long, C. R. Short and S. A. Barker, *J. Chromatogr.*, 502 (1990) 87.
16 M. D. Smedley and J. D. Weber, *J. Assoc. Off. Anal. Chem.*, 73 (1990) 875.
17 G. Weiss, P. D. Duke and L. Gonzales, *J. Agric. Food Chem.*, 35 (1987) 905.

18 J. A. Waliser, H. M. Burt, T. A. Valg, D. D. Kitts and K. M. McErlane, *J. Chromatogr.*, 518 (1990) 179.
19 A. R. Long, L. C. Hsieh, M. S. Malborough, C. R. Short and S. A. Barker, *J. Assoc. Off. Anal. Chem.*, 73 (1990) 868.
20 N. Nose, Y. Hoshino, Y. Kikuchi, M. Horie, K. Saitoh, T. Kawachi and H. Nakazawa, *J. Assoc. Off. Anal. Chem.*, 70 (1987) 714.
21 M. Horie, K. Saito, Y. Hoshino, N. Nose, N. Hamada and H. Nakazawa, *J. Chromatogr.*, 502 (1990) 371.
22 J. D. Henion, B. A. Thompson and P. H. Dawson, *Anal. Chem.*, 54 (1982) 451.
23 A. P. Bruins, T. R. Covey and J. D. Henion, *Anal. Chem.*, 59 (1987) 2642.
24 M. A. Quilliam, B. A. Thompson, G. J. Scott and K. W. M. Si, *Rapid Commun. Mass Spectrom.*, 3 (1989) 145.
25 S. Pleasance, M. A. Quilliam, A. S. W. deFreitas, J. C. Marr and A. D. Cembella, *Rapid Commun. Mass Spectrom.*, 4 (1990) 206.
26 C. M. Whitehouse, R. M. Dreyer, M. Yamashita and J. B. Fenn, *Anal. Chem.*, 57 (1985) 675.
27 B. A. Thompson and J. V. Iribarne, *J. Chem. Phys.*, 71 (1979) 4451.
28 E. C. Huang, T. Wachs, J. J. Conboy and J. D. Henion, *Anal. Chem.*, 62 (1990) 713A.

·

Pre-column derivatization of sulfa drugs with fluorescamine and high-performance liquid chromatographic determination at their residual levels in meat and meat products

NOBUYUKI TAKEDA* and YUMI AKIYAMA

Food and Drug Division, Hyogo Prefectural Institute of Public Health, Arata-cho, Hyogo-ku, Kobe 652 (Japan)

(First received February 25th, 1991: revised manuscript received May 8th, 1991)

ABSTRACT

A rapid, sensitive and selective high-performance liquid chromatographic method is described for simultaneous determination of eight sulfa drugs in meat and meat products using pre-column derivatization with fluorescamine. The drugs are sulfisomidine, sulfadiazine, sulfamerazine, sulfadimidine, sulfamonomethoxine, sulfamethoxazole, sulfadimethoxine and sulfaquinoxaline. The method includes blender extraction of 3-g samples with chloroform, partition with 3 M hydrochloric acid, derivatization with fluorescamine at pH 3.0 and subsequent high-performance liquid chromatographic analysis on a C_{18} column with fluorescence detection at an excitation wavelength of 405 nm and an emission wavelength of 495 nm. The drugs were separated with a mobile phase of acetonitrile–2% acetic acid (3:5) at 55°C. The average recovery from samples fortified at 0.1 ng/g was 92.6% with a coefficient of variation of 6.2%. The detection limit was 0.01 ng/g for sulfaquinoxaline and 0.005 ng/g for the other seven drugs. The method was field-tested in a survey of 37 samples including beef (five), pork (seven), chicken (seven), ham (five), sausage (eight), bacon (two) and roast beef (three). Sulfadimidine was detected in one pork sample at the level of 0.295 ng/g and in ham at 0.178 ng/g.

INTRODUCTION

Sulfa drugs are popular antibacterial agents for livestock, however their residues in meat products are a potential danger to human health. Tolerances in feed and withdrawal periods for the drugs have been established to minimize their residual levels in the meat, nevertheless claims of food contamination have often been made. A recent report showed that 11% of pork meat imported into Japan had been contaminated with sulfadimidine at levels in the range of 0.05–1.05 ng/g [1].

Several simultaneous assay procedures for sulfa drugs have been reported [2,3], however they generally include time-consuming extraction and clean-up steps to obtain the desired sensitivity. In addition, high-performance liquid chromatographic (HPLC) determination with UV detection is not selective for sulfa drugs. Although a photodiode-array detection system or post-column derivatization has been adopted to achieve selectivity for sulfa drugs, these require expensive equipment or additional apparatus and involve setting up and optimizing the system [1,4,5].

We applied a pre-column derivatization system with fluorescamine to develop a rapid and selective assay for sulfa drugs in meat and its products, since such a system requires no additional equipment in the post-column system and the reagent seems to be suitable for HPLC determination. Fluorescamine is specific for sulfonamide analogue in the acidic pH range and produces highly fluorescent fluorophores having essentially similar excitation–emission spectral characteristics. Also, the reagent and its hydrolysis products are non-fluorescent [6,7].

EXPERIMENTAL

Samples

A total of 37 samples, from three items of meat cut (pork, beef and chicken) and four items of meat products (ham, sausage, bacon and roast beef) was taken in the winter of 1990–1991. The products were purchased from three retailers in the Kobe area of Japan and stored in the refrigerator until analysis. Meat samples containing adipose and connective tissue were cut into small pieces with a kitchen knife and mixed manually in a beaker.

Reagents and apparatus

Sulfisomidine (ID), sulfadiazine (DZ) and sulfamethoxazole (XZ) were purchased from Sigma (St. Louis, MO, USA), sulfamonomethoxine (MX) and sulfadimethoxine (DX) from Daiichi-Seiyaku (Tokyo, Japan) and sulfaquinoxaline (SQ) from Dainihon-Seiyaku (Osaka, Japan). Sulfamerazine (MR) and sulfadimidine (DM) were generous gifts from Dr. T. Hamano of the Public Health Research Institute of Kobe City, Japan. The standard stock solution (100 μg/ml) was prepared by accurately weighing *ca.* 10 mg and dissolving in 100 ml of methanol. Fluorescamine reagent (0.2%) was prepared by dissolving 10 mg of Fluram (F. Hoffman-La Roche, Switzerland) in 50 ml of acetone. HPLC-grade methanol, acetonitrile, acetone and chloroform, and reagent-grade hydrochloric acid, acetic acid and sodium acetate were used (Wako Pure Chemicals, Japan). Water was purified by Milli-Q SP TOC (Millipore, Bedford, MA USA).

A liquid chromatograph was composed of an LC-6AD pump, an RF-535 fluorescence monitor (Shimadzu, Kyoto, Japan) and a Chemcosorb 5-ODS-H column (150 × 4.6 mm I.D., 5 μm particle size, Chemco Scientific, Osaka, Japan). The column was put in a water bath kept a 55°C. HPLC separation was performed in a mobile phase of acetonitrile–2% acetic acid (5:3) at a flow-rate of 1 ml/min.

Extraction

A 3-g portion of the meat sample was weighed into a 50-ml centrifuge tube and blended in 30 ml of chloroform for 2 min with a Polytron homogenizer (Brinkman Instruments, Westbury, USA), then the mixture was shaken for 10 min. After centrifugation at 1600 g for 5 min, the chloroform phase was filtered through No. 5A filter paper (Toyo Roshi Kaisha, Japan), and 5 ml of the extract was transferred into a 10-ml test tube. A 1-ml portion of 3 *M* hydrochloric acid was added and the tube was shaken for 10 min, then centrifuged at 1600 g for 5 min. This acid concentration has previously been shown to give the highest recoveries for some sulfa drugs using this extraction method [2].

Derivatization with fluorescamine

For optimizing reaction conditions (pH and incubation period), a flow injection (FI) technique was used by eliminating a column from the LC system. The standard solutions of DM, MR, MX, DX and SQ were evaporated under a nitrogen gas stream and redissolved in 3 *M* hydrochloric acid to give a concentration of 1 µg/ml. Derivatization was performed by modifying the method of Sakano *et al.* [6] as follows: 2.5 ml of the standard solution were mixed with the same volume of sodium acetate solution, the concentration of which ranged from 2.5 *M* to 5.0 *M*, then with 1.0 ml of 0.2% fluorescamine acetone solution. The pH of the content was measured by a Beckman Φ 12 pH/ISE meter (Beckman Instruments, Fullerton, USA). The content was incubated for various lengths of time at room temperature. The incubate, 10 µl, was injected into the FI system and the fluorophore was detected at an excitation wavelength of 405 nm and an emission wavelength of 495 nm.

For HPLC analysis, a volume of the acidic sample extract, 3.5 *M* sodium acetate solution and the fluorescent reagent was scaled down to one-tenth, that is 250 µl of both the sample and alkaline solutions and 100 µl of the reagent were mixed in this order with a vortex mixer. The sample was ready for HPLC injection after standing for 20 min at room temperature. A 10-µl sample was injected into the system, and was equivalent to a 0.08-g sample.

RESULTS AND DISCUSSION

Optimization for fluorescamine derivatization

The first approach was to optimize pH for the derivatization in our system. Five sulfa drugs (DM, MR, MX, DX and SQ) were individually dissolved in 3 *M* hydrochloric acid and pH of the solution was varied by adding serially diluted sodium acetate-solution. Fig. 1 shows that the fluorescence intensities of the derivatives varied with the variation in pH ranging from 0.42 to 4.23. Optimal reactivity was obtained at pH 3.00 (sodium acetate concentration of 3.5 *M*) for all the drugs tested, while the intensity was very low in the strong acid range (pH 0.42 and 0.55) and decreased with an increase in pH. The pH profiles for the fluorophore were similar to those reported in the literature [6,7]. The optimal incubation period was also examined at the above buffer concentration and found to be 20–60 min (Fig. 2). In later
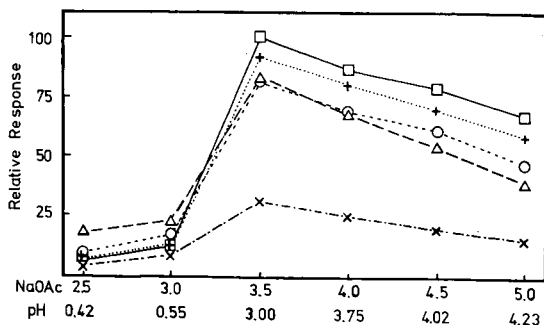
Fig. 1. Effect of pH on fluorescence intensity of fluorescamine derivatives of sulfa drugs. □ = DM; + = MR; O = MX; △ = DX, × = SQ. NaOAc = sodium acetate concentration in *M*.
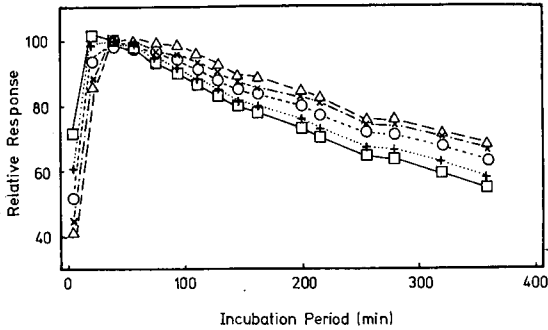
Fig. 2. Effect of incubation period on fluorescence intensity of fluorescamine derivatives of sulfa drugs. □ = DM; + = MR; ○ = MX; △ = DX; × = SQ.

experiments the reaction was performed for 20 min, since much longer incubation lowered the intensity. In practice, a reproducible reaction period was achieved as follows: the stop time of the integrator was set at 20 min (HPLC separation was completed within the time) and the sample solution for the next injection was prepared immediately after the previous sample had been injected for HPLC. In such a manner, the interval was measured for twelve injection and found to be 19.98 ± 0.95 min.

HPLC separation

HPLC conditions for separating eight sulfa drugs were examined by varying column temperature and the ratio of acetonitrile to 2% acetic acid in the mobile phase. As shown in Fig. 3A, the best separation was obtained within 20 min at 55°C
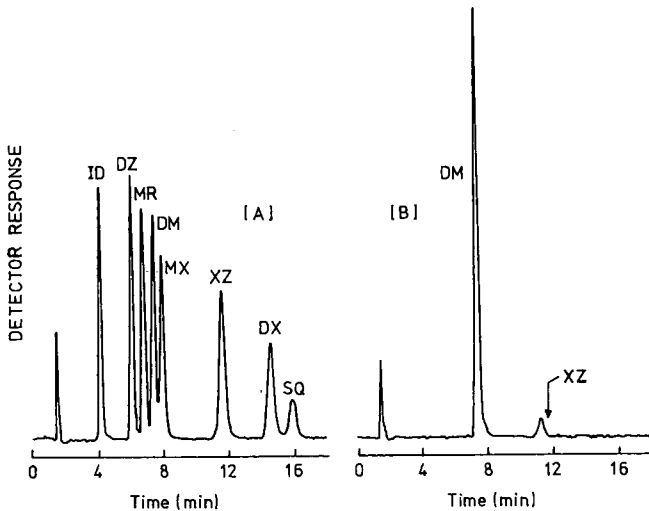
Fig. 3. Chromatograms of standard sulfa drugs (A) and positive pork sample (B). ID = Sulfisomidine; DZ = sulfadiazine; MR = sulfamerazine; DM = sulfadimidine; MX = sulfamonomethoxine; XZ = sulfamethoxazole; DX = sulfadimethoxine; SQ = sulfaquinoxaline.

and at a composition ratio of 3:5 (37.5% acetonitrile in 2% acetic acid). A dose–response relation was tested at the above optimal reaction conditions with the highest HPLC detector sensitivity, and found to be linear over the range tested (16.6–167 ng per milliter of final solution). The fluorescent peak height of the derivative of SQ was the lowest of the drug compounds examined, giving a detection limit of 0.05 ng on the chromatogram. Those of other derivatives were as low as 0.02 ng. These values correspond to 0.006 ng/g and 0.003 ng/g, respectively. In a practical analysis, the detection limit was set at 0.01 ng/g for SQ and 0.005 ng/g for the other seven sulfa drugs.

Sample analysis

The method was applied to residue analysis for sulfa drugs in 37 samples of meat and meat products including beef, pork, chicken, ham, sausage, bacon and roast beef. The results are summarized in Table I. Sulfadimidine (DM) was detected in two samples: pork at 0.30 ng/g (Fig. 3B) and ham at 0.18 ng/g. No sulfa drug was detected in beef, chicken, sausage, bacon or roast beef (Table I), however all the samples showed a fluorscent peak at retention time 11.2 min, which cause ambiguity of identification of XZ (11.6 min) (Fig. 3B). The peak (equivalent to 0.003–0.011 ng/g XZ) may be derived from some usual but unidentified meat component. Although the other seven sulfa drugs except DM were not detected in all the samples tested, a large peak having retention time 8.6 min appeared in one of the eight sausage samples. This could not be identified in a limited number of our authentic standards but may be a sulfa drug, since other sausage samples exhibited no fluorescent peak at this retention time.

TABLE I

ANALYSIS OF SULFA DRUGS IN COMMERCIAL MEATS AND MEAT PRODUCTS

Sample analyzed		Sulfadimidine (DM)	
Item	Number	Detected	Level (ng/g)
Beef	5	n.d.[a]	
Chicken	7	n.d.	
Pork	7	1	0.295 ± 0.011[b]
Ham	5	1	0.180
Sausage	8	n.d.	
Bacon	2	n.d.	
Roast beef	3	n.d.	

[a] n.d. = Not detected (<0.005 ng/g).
[b] Average ± S.D. of four determinations.

Recovery test

The recovery study was done at the level of 0.1 ng/g through the entire procedure using samples which had not showed any peak. The percentage recoveries are summarized in Table II. The highest recovery was 102% with a coefficient of variation (C.V.) of 2.6% for DM and the lowest 82.3% with a C.V. of 3.6% for DZ.

TABLE II

RECOVERY (%) OF EIGHT SULFA DRUGS FROM MEAT AND MEAT PRODUCTS FORTI-
FIED AT 0.1 ng/g

Sample	Sulfa drug										
	ID	DZ	MR	DM	MX	XZ	DX	SQ	Mean	S.D.	C.V.(%)
Beef	87.9	83.4	94.8	98.8	90.6	89.0	89.5	79.3	89.2	5.7	6.4
Chicken	89.8	77.8	97.6	102.9	88.9	107.3	92.9	85.2	92.7	9.0	9.7
Pork	91.1	80.0	102.4	105.2	93.1	90.8	97.2	91.7	93.9	7.3	7.8
Ham	87.4	85.0	97.2	104.1	93.4	101.0	94.7	92.3	94.4	6.0	6.4
Sausage	88.3	85.4	96.8	99.0	91.6	94.5	93.9	94.4	93.0	4.1	4.5
Mean	88.8	82.3	97.7	102.0	91.5	96.5	93.6	88.6	92.6	5.6	6.2
S.D.	1.3	3.0	2.5	2.6	1.7	6.8	2.5	5.6			
C.V.(%)	1.5	3.6	2.6	2.6	1.8	7.0	2.7	6.3			

Every meat sample gave high recoveries for the eight drugs ranging from 89.2% in the beef sample to 94.4% in ham. The average mean recovery was 92.6% with a C.V. of 6.2%. The contaminated pork sample had the level of 0.295 ± 0.011 ng/g with a C.V. of 3.8%.

The high recovery rate and low C.V. value indicate that the method is reproducible and accurate. The method is also rapid and simple, since it requires little glassware and solvent and no laborious clean-up and solvent evaporation. In conclusion, the method is applicable to a highly specific and sensitive routine analysis for sulfa drugs in various kinds of meat and meat products.

REFERENCES

1 M. Horie, K. Saito, Y. Hoshino, N. Nose, N. Hamada and H. Nakazawa, *J. Food Hyg. Soc. Japan*, 31 (1990) 171.
2 H. Terada, M. Asanoma, H. Tsubouchi, T. Ishihara and Y. Sakabe, *Eisei Kagaku*, 29 (1983) 226.
3 T. Nagata and M. Saeki, *J. Food Hyg. Soc. Japan*, 29 (1988) 13.
4 R. L. Smallidge, E. J. Kentzer, K. R. Stringham, E. H. Kim, C. Lehe, R. W. Stringham and E. C. Mundell, *J. Asoc. Off. Anal. Chem.*, 71 (1988) 710.
5 M. N. L. Aerts, W. M. J. Beek and U. A. Th. Brinkman, *J. Chromatogr.*, 435 (1988) 97.
6 T. Sakano, S. Masuda, A. Yamaji, T. Amano, H. Oikawa and K. Nakamoto, *Yakugaku Zasshi*, 97 (1977) 464.
7 J. A. F. de Silva and N. Strojny, *Anal. Chem.*, 47 (1975) 714.

Separation of metal complexes of ethylenediaminetetraacetic acid in environmental water samples by ion chromatography with UV and potentiometric detection

W. BUCHBERGER[a], P. R. HADDAD* and P. W. ALEXANDER

Department of Analytical Chemistry, University of New South Wales, Kensington, NSW 2033 (Australia)

(First received March 14th, 1991; revised manuscript received April 29th, 1991)

ABSTRACT

An ion chromatographic method is described for the analysis of several metal complexes of ethylenediaminetetraacetic acid (EDTA) in water samples. Separations are achieved on C_{18} bonded silica, typically using a mobile phase comprising 1% (w/v) cetrimide–1.2 mM phosphate buffer (pH 7)–25% (v/v) acetonitrile–15% (v/v) methanol, as well as on a polymer-based anion exchanger using 2 mM phosphate buffer (pH 7) as eluent. Direct UV detection at 250 nm is employed for EDTA complexes of Fe(III), Cu(II), Pb(II) and Ni(II), whilst UV detection at 250 nm after post-column reaction with copper ions is utilized for EDTA complexes of Zn(II), Cd(II), Co(II), Pb(II), Ni(II) and Cu(II). Detection limits are in the range 1.5–4.0 ng for direct UV detection and 30–50 ng for post-column reaction detection. Indirect potentiometric detection after post-column reaction with copper ions is utilized with metallic copper as the indicator electrode, giving detection limits in the range 1.0–1.5 μg. These separations are applied to the determination of metal–EDTA complexes in river water at the ppb[b] level and to remobilization studies of metal ions in sediment.

INTRODUCTION

Aminopolycarboxylic acids are widely used in industrial processes and in particular as substitutes for phosphates in detergents. After release to the environment these chelating agents may affect the distribution of metals within aquatic ecosystems. Reliable analytical methods for monitoring metal complexes of aminocarboxylic acids in natural water are still lacking. In this paper the use of ion chromatography is investigated for the analysis of metal complexes of ethylenediaminetetraacetic acid (EDTA), which is one of the most widely used aminopolycarboxylic acids.

Some information on the ion chromatographic behaviour of several metal–EDTA complexes is already available. On the one hand, total EDTA has been determined by formation of the copper complex [1,2] or the iron complex [3–5] before

---

[a] Permanent address: Department of Analytical Chemistry, Johannes-Kepler-University, A-4040 Linz, Austria.
[b] Throughout this article, the American billion (10^9) is meant.

separation using ion-interaction chromatography; on the other hand, various metal ions have been separated by *in situ* formation of metal–EDTA complexes using a mobile phase which contains EDTA [6–11]. From this literature it can be concluded that both anion-exchange chromatography and ion-interaction chromatography should be adequate for the determination of metal–EDTA complexes in water samples.

For the analysis of environmental water samples a detection mode with a certain degree of selectivity is necessary in order to avoid extensive sample cleanup. In this work we have employed UV detection at 250 nm, including a post-column reaction for those metal–EDTA complexes which do not give a direct UV response at this wavelength. Furthermore, we have also investigated the application of a potentiometric detector with a copper electrode, since this has already proved useful for the analysis of free aminocarboxylic acids [12].

EXPERIMENTAL

The ion-chromatographic instrumentation consisted of a Millipore Waters (Milford, MA, USA) M510 pump, a Rheodyne (Berkeley, CA, USA) 7010 injection valve with a 120-μl loop, a Waters M484 UV absorbance detector and finally a Waters NRC-1094 mixing device for post-column mixing of the reagent delivered by a Waters M45 pump. The cell of a Waters 464 electrochemical detector equipped with a metallic copper working electrode and a Ag/AgCl (3 M KCl) reference electrode was used for potentiometric detection. This cell was connected to a Beckman (Fullerton, CA, USA) Φ34 pH meter. Chromatograms were recorded using a homemade analog-to-digital converter, interfaced with an Apple IIe computer.

Stock solutions of EDTA complexes were prepared by mixing equimolar solutions of EDTA and the metal ion. These solutions were diluted as required. Ion-interaction chromatography of the Fe(III)–EDTA complex was performed on a metal-free Waters Deltapak C_{18} column (250 × 4 mm I.D.). The mobile phase consisted of a 10-mM tetrabutylammonium chloride solution in 10 mM sodium acetate containing 10% acetonitrile and adjusted to pH 4.5 using acetic acid. Ion-interaction chromatography of all the other metal–EDTA complexes investigated in this study was carried out on a stainless-steel Waters μBondapak C_{18} column (250 × 4 mm I.D.). The mobile phase was prepared by dissolving 10 g of cetyltrimethylammoniumbromide (cetrimide) in 600 ml of 2 mM phosphate buffer pH 7 and diluting to 1000 ml with a mixture of methanol and acetonitrile of varying ratio. A Waters IC Pak A (50 × 4.6 mm I.D.) column was used for ion-exchange chromatography with 2 mM phosphate buffer pH 7 as the mobile phase.

The post-column reagent was a solution of 0.1 mM copper sulphate solution in 0.3 M acetic acid. The flow-rates of the mobile phase and of the post-column reagent were 0.9 ml/min each.

River water samples from Lane Cove River, Sydney, were passed through a Millipore (Bedford, MA, USA) 0.45-μm Millex filter and then through a Waters C_{18} SepPak cartridge before injection.

RESULTS AND DISCUSSION

Separation of EDTA complexes

During this study we restricted ourselves to the determination of EDTA complexes of Fe^{3+}, Cu^{2+}, Pb^{2+}, Zn^{2+}, Cd^{2+}, Ni^{2+} and Co^{2+}. Because of its versatility we employed ion-interaction chromatography on C_{18} bonded silica with tetraalkylammonium salts as ion-interaction reagents. Mobile phases in the neutral pH range were considered to be advantageous for our purposes because mobile phases of low or high pH could lead to severe disturbances of the equilibria between metal ions and EDTA in the samples during the chromatographic separation.

All the above-mentioned metal–EDTA complexes gave well-shaped peaks in eluents of pH 7, except the Fe(III)–EDTA complex. For this complex, it was necessary to use a mobile phase of pH 4.5 in order to obtain satisfactory peak shape. Unfortunately, at any pH below 5 severe problems were encountered when using stainless-steel columns for the analysis of Fe(III)–EDTA in the presence of an excess of free EDTA. Fe(III) released from the stainless-steel frits of the column tended to react with free EDTA leading to erroneously high results for Fe(III)–EDTA. These interferences could be overcome by employing a metal-free column (Waters Deltapack C_{18}), which was used for all further analytical work on Fe(III)–EDTA.

Optimization experiments for separation of all other metal–EDTA complexes at pH 7 revealed that sufficient selectivity of the mobile phase could be achieved only by using very hydrophobic ion-interaction reagents (such as cetrimide), together with relatively high amounts of organic modifier in the mobile phase. Acetonitrile, methanol and tetrahydrofuran were tested as organic modifiers. The selectivity of mobile phases containing methanol or tetrahydrofuran was practically the same so that only methanol and acetonitrile were used as organic modifiers for further experiments.

UV detection of EDTA complexes

UV detection at 250 nm was found adequate for the determination of Fe(III)–EDTA in the river water samples examined. In cases where the detection selectivity is insufficient at this wavelength, higher wavelengths in the range between 280 and 300 nm can be utilized without severe loss of sensitivity. The detection limit (measured with standards for a signal-to-noise ratio of 3) was about 1.5 ng Fe(III)–EDTA injected. Linear response was observed up to at least 200 ng injected ($r = 0.9998$, $n = 7$). A typical chromatogram of a spiked river water sample is shown in Fig. 1.

Direct UV detection at 250 nm is also possible for Cu–EDTA, Pb–EDTA and Ni–EDTA, although the sensitivity for Ni–EDTA is only about a tenth of that for Cu–EDTA or Pb–EDTA. A mobile phase with only acetonitrile as organic modifier (40%, v/v) was used for this separation, giving capacity factor, k', values of 2.3, 3.0 and 4.3 for Pb–EDTA, Ni–EDTA and Cu–EDTA, respectively. Detection limits (measured with standards for signal-to-noise ratios of 3) were about 4 ng injected for Pb–EDTA and Cu–EDTA and about 40 ng for Ni–EDTA. Linear response was obtained over at least two orders of magnitude ($r > 0.9995$, $n = 7$). A series of experiments was carried out to illustrate the applicability of this chromatographic separation to remobilization studies of heavy metals in river water. A 100-ml sample of river water was spiked with 2 ppm of free EDTA and left in contact with 50 g sediment for a certain time. A typical
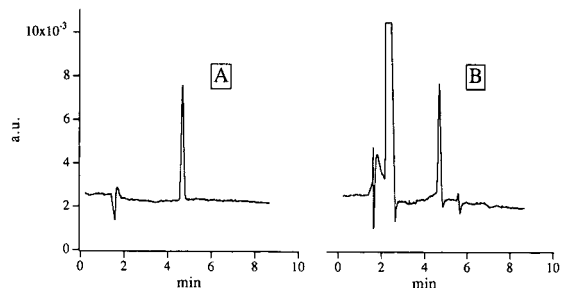
Fig. 1. Chromatograms for the determination of Fe(III)–EDTA in river water. (A) Standard containing 130 ppb Fe(III)–EDTA; (B) river water sample spiked with 130 ppb Fe(III)–EDTA. UV detection at 250 nm.

chromatogram obtained using this method is given in Fig. 2, which shows that Pb–EDTA and Cu–EDTA were detectable at ppb levels.

Zn–EDTA, Cd–EDTA and Co–EDTA show a major UV absorption only at rather low wavelengths but can be detected at 250 nm after conversion to the Cu–EDTA in a post-column reaction using 0.1 mM copper sulphate in 0.3 M acetic acid as reagent. Under these conditions Pb–EDTA is also converted to Cu–EDTA, whereas Ni–EDTA could not be converted, probably due to slow kinetics. A complete separation of Zn–EDTA, Cd–EDTA, Co–EDTA, Pb–EDTA, Ni–EDTA and Cu–EDTA in a single run could not be achieved, but the methanol/acetonitrile ratio of the organic modifier can be optimized to meet the requirements of specific separation problems. A typical mobile phase containing 25% (v/v) acetonitrile and 15% (v/v) methanol resulted in k' values of 3.3, 3.4, 4.3, 4.4, 5.2 and 6.0 for Pb–EDTA, Cd–EDTA, Co–EDTA, Zn–EDTA, Ni–EDTA and Cu–EDTA, respectively. The limits of detection for metal–EDTA complexes after post-column conversion to Cu–EDTA were between 30 and 50 ng injected. Linearity of response was checked up to 5 μg injected and in all cases the correlation coefficient was better than 0.9995 (n = 7). Fig. 3 shows a chromatogram of a river sample spiked with 1.3 ppm of Cd–EDTA, 1.4 ppm of Zn–EDTA and 11 ppm free EDTA. The peak eluted just prior to Cd–EDTA could be attributed to alkaline earth metal–EDTA complexes, which had been formed in the sample by the excess of free EDTA.
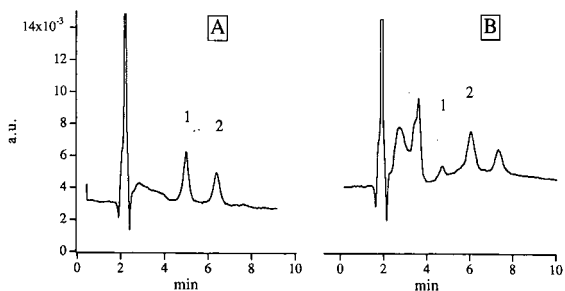
Fig. 2. Chromatograms of (A) standard containing 230 ppb Pb–EDTA and 220 ppb Cu–EDTA; (B) river water, 1 h after spiking the sample in contact with sediment with 2.2 ppm EDTA. Peaks: 1 = Cu–EDTA; 2 = Pb–EDTA. UV detection at 250 nm.
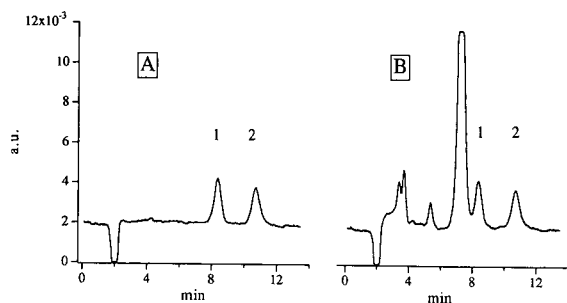
Fig. 3. Chromatograms for the determination of Zn–EDTA and Cd–EDTA in river water. (A) Standard containing 1.3 ppm Cd–EDTA and 1.4 ppm Zn–EDTA; (B) river water spiked with 1.3 ppm Cd–EDTA and 1.4 ppm Zn–EDTA. Peaks: 1 = Cd–EDTA; 2 = Zn–EDTA. UV detection at 250 nm after post-column reaction with copper ions.

Potentiometric detection of EDTA complexes

As an alternative to UV detection we investigated the applicability of a potentiometric detector using metallic copper as the indicator-electrode [13–15]. The potential of the electrode is governed by the concentration of free copper ions at the electrode surface. This concentration depends on, among other things, the oxygen content and the complexation properties of the eluent. Eluted solutes which form very strong complexes with copper ions will cause a change in the level of copper ions at the electrode surface, thereby producing a decrease in the electrode potential. Therefore, all metal–EDTA complexes with stability constants lower than that for Cu–EDTA should be possible candidates for this detection mode, provided the kinetics of the ligand-exchange reaction between copper ions at the electrode surfacde and the eluted EDTA complexes are suitable. Unfortunately, in our experiments no response could be obtained at the electrode, suggesting that there was insufficient time for the ligand-exchange reaction to occur. As an alternative, we decided to apply the same post-column reagent used above for UV detection to potentiometric detection. In this case, the electrode responds to the changes in the copper concentration of the post-column reagent during elution of metal–EDTA complexes. Co–EDTA, Zn–EDTA, Cd–EDTA and Pb–EDTA could be detected in this way.

When this approach was coupled with the ion-interaction separation used above, the high amount of organic modifier in the mobile phase resulted in extremely high noise levels of the electrode response. Therefore, we combined the potentiometric detection mode with anion-exchange chromatography using a totally aqueous mobile phase. Naturally, this introduced the drawbacks that separation efficiency was poorer and the possibilities of mobile phase optimization more limited than in ion-interaction chromatography. When 2 mM phosphate buffer at pH 7 was used as the mobile phase, k' values of 7.6, 8.6, 10.0 and 10.6 were obtained for Cd–EDTA, Pb–EDTA, Co–EDTA and Zn–EDTA, respectively. Detection limits (measured for a signal-to-noise ratio of 3) were between 1.0 and 1.5 μg injected. A typical chromatogram of a river water sample spiked with Zn–EDTA and Cd–EDTA is given in Fig. 4 (potential values given in this figure indicate relative mV changes only and the actual baseline potential was -9.5 mV). The response was non-linear, as could be expected from the Nernst equation and from previous studies with this detector [13–15].
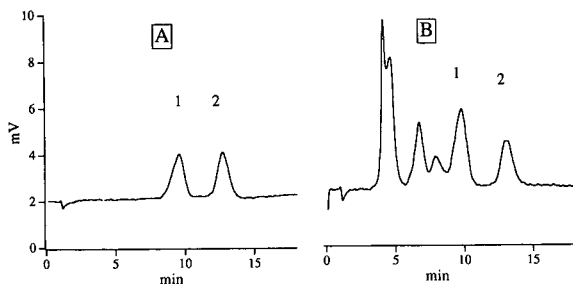
Fig. 4. Chromatograms for the determination of Zn–EDTA and Cd–EDTA in river water with potentiometric detection. (A) Standard containing 109 ppm Cd–EDTA and 98 ppm Zn–EDTA; (B) river water spiked with 128 ppm Cd–EDTA and 88 ppm Zn–EDTA. Peaks: 1 = Cd–EDTA; 2 = Zn–EDTA. Potentiometric detection after post-column reaction with copper ions.

The relatively high detection limits obtained with potentiometric detection indicate that unless appropriate preconcentration techniques are employed, this technique is less suited for environmental samples but may be more advantageous due to its selectivity when difficult matrices, such as waste water, are to be analyzed. In such cases, UV detection is likely to result in complex chromatograms.

An advantage of all the ion chromatographic methods described in this paper is the requirement for simple sample cleanup only, which avoids risks of disturbing the equilibria existing between free and complexed metal ions, leading to quantitative recoveries.

REFERENCES

1 G. A. Perfetti and C. R. Warner, J. Assoc. Off. Anal. Chem., 62 (1979) 1092.
2 C. C. T. Chinnick, Analyst (London), 106 (1981) 1203.
3 J. Harmsen and A. van den Toorn, J. Chromatogr., 249 (1982) 379.
4 D. L. Venezky and W. E. Rudzinski, Anal. Chem., 56 (1984) 315.
5 C. Retho and L. Diep, Z. Lebensm. Unters. Forsch., 188 (1989) 223.
6 S. Matsushita, J. Chromatogr., 312 (1984) 327.
7 T. Tanaka, Fresenius' Z. Anal. Chem., 320 (1985) 125.
8 M. L. Marina, J. C. Diez-Masa and M. V. Dabrio, J. High Res. Chromatogr. Chromatogr. Commun., 9 (1986) 300.
9 W. Lien, B. K. Boerner and J. G. Tarter, J. Liq. Chromatogr., 10 (1987) 3213.
10 G. Schwedt and B. Kondratjonok, Fresenius' Z. Anal. Chem., 332 (1989) 855.
11 A. Nitsch, K. Kalcher and U. Posch, Fresenius' Z. Anal. Chem., 338 (1990) 618.
12 W. Buchberger, P. R. Haddad and P. W. Alexander, J. Chromatogr., 546 (1991) 311.
13 P. W. Alexander, P. R. Haddad and M. Trojanowicz, Anal. Chem., 56 (1984) 2417.
14 P. W. Alexander, P. R. Haddad and M. Trojanowicz, Anal. Chim. Acta, 171 (1985) 151.
15 P. W. Alexander, P. R. Haddad and M. Trojanowicz, Chromatographia, 20 (1985) 179.

CHROM. 23 449

Thermoanalytical and chromatographic studies of copper(II), nickel(II) and oxovanadium(IV) complexes of tetradentate Schiff bases derived from β-diketones and 2,3-diaminopentane

M. Y. KHUHAWAR* and A. G. BHATTI

Institute of Chemistry, University of Sindh, Jamshoro, Sindh (Pakistan)

(First received July 20th, 1990; revised manuscript received May 2nd, 1991)   .

ABSTRACT

Differential thermal analysis and thermogravimetric analysis of copper(II) and nickel(II) complexes of [4,4'-(1-ethyl-2-methyl-1,2-ethanediyl)dinitrilo]bis(1,1,1-trifluoro-2-pentanone) [bis(trifluoroacetylacetone)ethylmethylethylenediimine]($H_2F_3A_2$EMen) and [4,4'-(1-ethyl-2-methyl-1,2-ethanediyl)dinitrilo]bis(1,1,1-trifluoro-6-methyl-5-hepten-2-one) [bis(trifluoroacetylmesityl oxide)ethylmethylethylenediimine] ($H_2F_3AM_2$EMen) and copper(II), nickel(II) and oxovanadium(IV) complexes of [4,4'-(1-ethyl-2-methyl-1,2-ethanediyl)dinitrilo]bis(2-pentanone) [bis(acetylacetone)ethylmethylethylenediimine] (H_2A_2EMen) were carried out and losses in weight between 78 and 100% occurred at temperatures up to 300°C. The copper, nickel and oxovanadium complexes of H_2A_2EMen are adequately separated by gas chromatographic (GC) columns, but the copper and nickel complexes of $H_2F_3A_2$EMen and $H_2F_3AM_2$EMen could not be resolved. The copper and nickel complexes of $H_2F_3A_2$EMen and $H_2F_3AM_2$EMen and the copper, nickel and oxovanadium complexes of H_2A_2EMen were separated on normal- and reversed-phase high-performance liquid chromatographic (HPLC) columns. The elution of copper and nickel complexes on GC and HPLC columns was compared in order to evaluate the effects of substituents on elution.

INTRODUCTION

Tetradentate Schiff bases have proved to be promising reagents for the gas chromatographic (GC) and high-performance liquid chromatographic (HPLC) separation of copper and nickel [1–6], copper, nickel and palladium [7–9], copper, nickel and cobalt [10,11], copper, nickel and oxovanadium [12–14] and copper, nickel, palladium and oxovanadium [15,16] as metal chelate compounds. The reagents react with a limited number of metal ions quantitatively at all concentrations. Therefore, in this work the copper(II) and nickel(II) complexes of [4,4'-(1-ethyl-2-methyl-1,2-ethanediyl)dinitrilo]bis(1,1,1-trifluoro-2-pentanone) [bis(trifluoroacetylacetone)ethylmethylethylenediimine] ($H_2F_3A_2$EMen) and [4,4'-(1-ethyl-2-methyl-1,2-ethanediyl)dinitrilo]bis(1,1,1-trifluoro-6-methyl-5-hepten-2-one) [bis(trifluoroacetylmesityl oxide)-ethylmethylethylenediimine] ($H_2F_3AM_2$EMen) and copper(II), nickel(II) and oxovanadium(IV) complexes of [4,4'-(1-ethyl-2-methyl-1,2-ethanediyl)dinitrilo]bis(2-
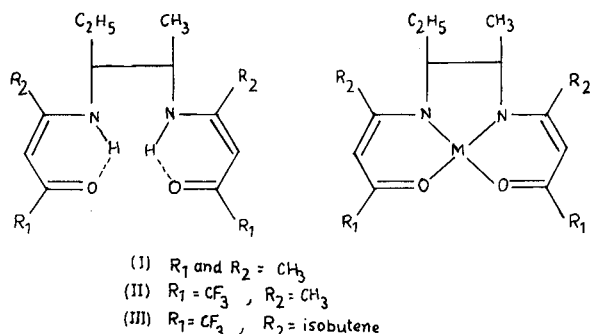
Fig. 1. Structures of reagents and metal chelates. The metal (M) is Ni(II), Cu(II) or VO(IV).

pentanone) [bis(acetylacetone)ethylmethylethylenediimine] (H₂A₂EMen) (Fig. 1) were examined on GC and HPLC columns for their possible separations and to examine the effect of substituents on their relative elution.

EXPERIMENTAL

The reagents H$_2$A$_2$EMen, H$_2$F$_3$A$_2$EMen and H$_2$F$_3$AM$_2$EMen and their copper and nickel complexes were prepared as reported [17]. The reagents were prepared by condensation of acetylacetone (0.01 M), trifluoroacetylacetone (0.01 M) or trifluoroacetylmesityl oxide (1,1,1-trifluoro-6-methyl-5-hepten-2,4-dione) with 2,3-diaminopentane (0.005 M) in ethanol and chloroform as solvent. The copper and nickel complexes were prepared by refluxing together an equimolar solution of reagent (0.001 M) and nickel acetate or copper acetate (0.001 M) in methanol. The results of elemental analysis agreed with the expected values and the mass spectra of the reagents indicated the molecular ion peak corresponding to the expected molecular weight.

Preparation of oxovanadium complex of [4,4'-(1-ethyl-2-methyl-1,2-ethanediyl)-dinitrilo]bis(2-pentanone) [bis(acetylacetone)ethylmethylethylenediimine] (H$_2$A$_2$EMen)

The oxovanadium (IV) complex of H$_2$A$_2$EMen is conveniently prepared by a ligand-exchange method [18]. An equimolar amount · of the reagent H$_2$A$_2$EMen (0.133 g, 0.0005 M) and bis(acetylacetone)oxovanadium(IV) (0.13 g, 0.0005 M) were placed together in a 10-cm^3 round-bottomed flask connected to a high-vacuum pump. The mixture was heated and maintained within the range 220–230°C for 2 h at 3 mmHg. The residue was washed with diethyl ether and recrystallized from n-hexane, m.p. 195°C. Calculated for C$_{15}$H$_{24}$N$_2$O$_3$V, C 55.22, H 7.23, N 8.43%; found, C 54.34, H 6.54, N 9.03%. IR (KBr), cm^{-1}: 1580(s), 1510(sb), 1400(s), 990(vs). UV–visible spectra (methanol), λ_{max}, nm (molar absorptivity ε, l mol^{-1} cm^{-1}, in parentheses): 630 (522), 546 (46), 433 (67), 355 (4100), 315 (16 000), 240 (sh) (8000), 208 (16 000).

Bis(acetylacetone)oxovanadium(IV) was prepared as reported [19]. Elemental analysis was carried out by Elemental Micro-Analysis, UK. IR and spectrophoto-

metric studies were carried out on a Perkin-Elmer Model 1430 IR spectrophotometer using potassium bromide discs and a Hitachi Model 220 spectrophotometer. Differential thermal analysis (DTA) and thermogravimetric analysis (TGA) of metal complexes were carried out on Shimadzu TG 30 and DTA 30 thermal analysers at the Department of Chemistry, Quaid-e-Azam University, Islamabad, at heating rates of 10 and 15°C min^{-1} for TGA and DTA, respectively, and a nitrogen flow-rate of 40 cm^3 min^{-1}. DTA and TGA were carried out between room temperature and 500°C with 5–12-mg samples in aluminium cups against alumina as a reference material.

A Hitachi Model 163 gas chromatograph equipped with a flame ionization detector and a Model 056 recorder was used. Stainless-steel columns (6 ft. × 0.085 in. I.D. and 3 m × 3 mm I.D. packed with 3% OV-101 and 3% OV-17 on Chromosorb W HP (80–100 mesh) were used.

A Hitachi Model 655A liquid chromatograph equipped with a variable-wavelength UV detector, a Rheodyne Model 7125 injector and a Model 561 recorder and a Shimadzu LC-5 liquid chromatograph equipped with an SPD-2A spectrophotometric detector, a SIL-1A LC injector and a Chromatopac C-RIB were used. A stainless-steel column (250 mm × 4 mm I.D.) was packed with LiChrosorb Si 100 (5 μm) (Merck) as reported earlier [5] and a Zorbax ODS (5 μm) column (250 mm × 4.6 mm I.D.) DuPont with an ODS guard column obtained from a commercial source were used.

Solutions of 1 mg cm^{-3} for GC and normal- and reversed-phase HPLC were prepared with acetone, chloroform and methanol respectively. Samples of 1–5 μl was injected for GC and HPLC separations. Calibration graphs were constructed by plotting average peak height *versus* amount of complex injected.

RESULTS AND DISCUSSION

The IR spectrum of the oxovanadium complex shows the expected pattern and a band is observed at 990 cm^{-1} due to V = O stretching vibrations. A spectrophotometric study of the oxovanadium complex in methanol indicated three bands in the visible region due to d–d transitions in the d^1 system of oxovanadium(IV). The complex also shows fairly high molar absorptivities in the UV region, ideally suited for HPLC separations with UV detection.

In order to determine the volatility and thermal stability of metal chelates to assess their possible elution and separation on GC columns, DTA and TGA of the metal chelates were studied. The TGA results (Fig. 2) indicate that nickel complexes are more thermally stable and lose more weight, in the range 94–100%, between 150 and 285°C than copper and oxovanadium complexes, which lose 83–96% and 78% weight between 130 and 310°C and 170 and 285°C, respectively. The copper and nickel complexes of fluorinated ligands are more thermally stable and lose more weight, in the range 94–100%, than corresponding copper and nickel complexes of the non-fluorinated ligand H$_2$A$_2$EMen, which lose 83–94% weight within a similar temperature range. DTA (Fig. 3) shows mostly a melting endotherm, followed by vaporization/decomposition endotherms and exotherms, but exotherms observed above 300°C could be assigned to decomposition exotherms of non-volatile residues.

The complexes were examined on different GC columns to assess the elution and possible separation of metal complexes and it was observed that the metal com-
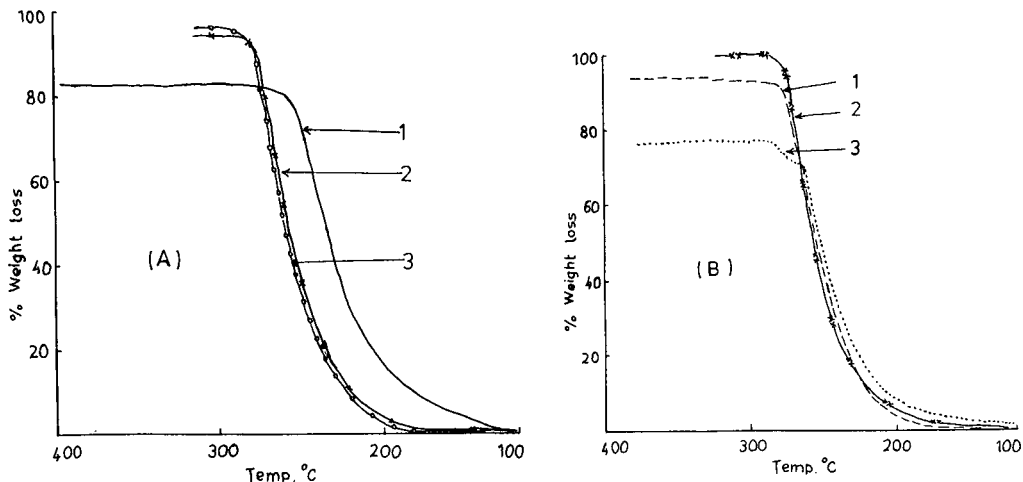
Fig. 2. (A) TGA of copper(II) complexes at a heating rate of $10°C$ min^{-1} and a nitrogen flow-rate of 40 cm^3 min^{-1}. 1, A$_2$EMenCu; 2, F$_3$A$_2$EMenCu; 3, F$_3$AM$_2$EMenCu. (B) TGA of nickel and oxovanadium complexes at a heating rate of $10°C$ min^{-1} and a nitrogen flow-rate 40 cm^3 min^{-1}. 1, A$_2$EMenNi; 2, F$_3$A$_2$EMenNi; 3, A$_2$EMenVO.
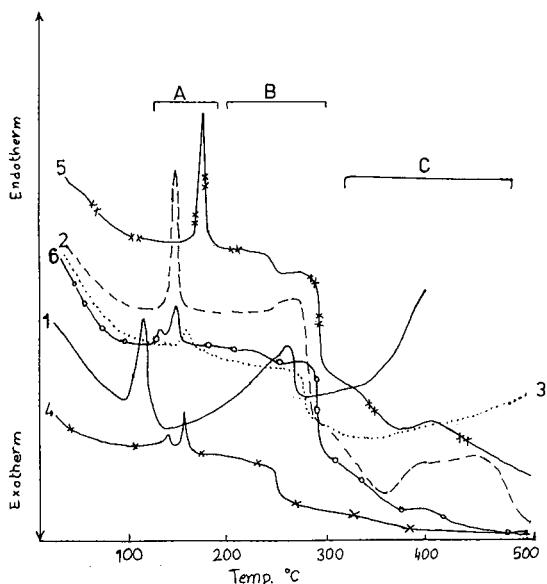
Fig. 3. DTA of metal complexes at a heating rate of $15°C$ min^{-1} and a nitrogen flow-rate 40 cm^3 min^{-1}. 1 = A$_2$EMenCu; 2 = A$_2$EMenNi; 3 = A$_2$EMenVO; 4 = F$_3$A$_2$EMenCu; 5 = F$_3$A$_2$EMenNi; 6 = F$_3$AM$_2$EMenCu. (A) Melting endotherms; (B) vaporization/decomposition endotherms and exotherms; (C) decomposition exotherm of non-volatile residue.

plexes were eluted at column temperatures of 220–250°C. Attemps were made to separate the copper and nickel complexes of $H_2F_3A_2EMen$ and $H_2F_3AM_2EMen$, but no separation was obtained on the columns tested. However, there was an adequate separation of the reagent from the complexes. The detection limits, measured as three times background noise, on the 6 ft. × 0.085 in. I.D. column packed with 3% OV-101 on Chromosorb W HP (80–100 mesh) were 15–30 ng for the complex.

Similarly, when copper, nickel and oxovanadium complexes of H_2A_2EMen were investigated for their separation and the conditions were optimized, a complete separation between the copper, nickel and oxovanadium complexes was obtained on the 3 m × 3 mm I.D. column packed with 3% OV-17 on Chromosorb W HP (80–100 mesh) at a column temperature of 250°C, with retention times of 11.2, 13.7 and 24.4 min for the copper, nickel and oxovanadium complexes, respectively (Fig. 4). When an excess of the reagent was added to the metal complex solution and the mixture was injected under the optimized separation conditions, no interference by the reagent on the separation of copper, nickel and oxovanadium was observed. Linear calibration graphs for copper, nickel and oxovanadium complexes were obtained at microgram
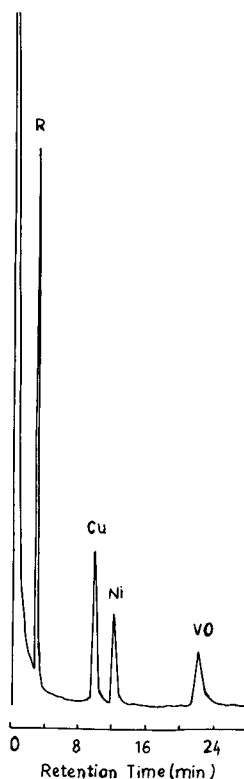
Fig. 4. GC separation of H_2A_2EMen and its Cu, Ni and VO complexes on a stainless-steel column (3 m × 3 mm I.D.) packed with 3% OV-17 on Chromosorb W HP (80–100 mesh). Column temperature, 250°C; injection port temperature, 270°C; nitrogen flow-rate, 30 cm³ min⁻¹.
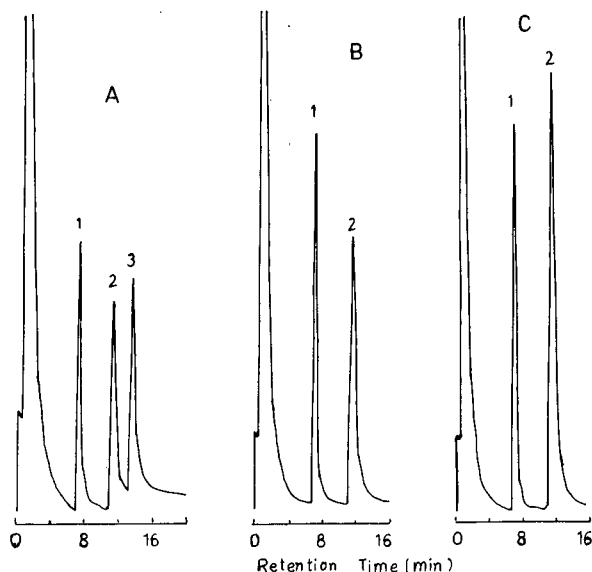
Fig. 5. Relative GC elution of (A) (1) $F_3A_2EMenNi$, (2) $F_3AM_2EMenNi$ and (3) $A_2EMenNi$; (B) (1) $F_3A_2EMenCu$ and (2) $A_2EMenCu$; (C) (1) $F_3A_2EMenCu$ and (2) $F_3AM_2EMenCu$. Column, 3 m × 3 mm I.D., 3% OV-17 on Chromosorb W HP (80–100 mesh). Column temperature, 250°C; injection port temperature, 270°C; nitrogen flow-rate, 30 cm^3 min^{-1}.

levels of the complexes injected with detection limits of 50, 40 and 50 ng of copper, nickel and oxovanadium complexes, respectively.

In order to determine the effects of substituents on the GC elution of copper and nickel complexes, mixtures of copper and nickel complexes of all three reagents were injected onto the 3 m × 3 mm I.D. column packed with 3% OV-17 on Chromosorb W HP (80–100 mesh) at a column temperature of 250°C, injection port temperature 270 °C and nitrogen flow-rate 30 cm^3 min^{-1}. Complete separations between all three nickel complexes and separation of the copper complex of $H_2F_3A_2EMen$ from those of H_2A_2EMen and $H_2F_3AM_2EMen$ were obtained (Fig. 5). It is concluded from the separations that CF_3 substitution decreases and alkyl (isobutene) substitution increases the retention of metal complexes.

The reagent H_2A_2EMen gave a highly promising GC separation of copper, nickel and oxovanadium complexes, but shows no separation between copper and nickel complexes of $H_2F_3A_2EMen$ and $H_2F_3AM_2EMen$. Normal- and reversed-phase HPLC were thus investigated for the separation of metal complexes, the separation of GC with flame ionization detection was compared with that of HPLC with UV detection.

When mixtures of copper and nickel complexes of $H_2F_3AM_2EMen$ and $H_2F_3A_2EMen$ were injected onto a 250 mm × 4 mm I.D. column packed with LiChrosorb Si 100 (5 μm), the complexes were easily eluted with chloroform–n-hexane. However, optimum separations between copper and nickel complexes of $H_2F_3AM_2EMen$ and $H_2F_3A_2EMen$ were obtained when eluted with chloroform–n-hexane (10:90) and chloroform–1,2-dichloroethane–n-hexane (15:3:82), respectively
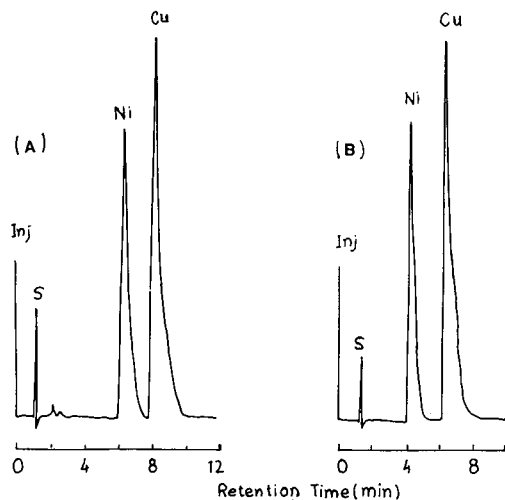
Fig. 6. HPLC separation of copper and nickel complexes of (A) $H_2F_3A_2EMen$ and (B) $H_2F_3AM_2EMen$. Column, 250 mm × 4 mm I.D., Si 100 (5 μm). (A) Eluent, chloroform–1,2-dichloroethane–n-hexane (15:3:82); flow-rate, 2.2 cm³ min⁻¹; detection, UV at 295 nm. (B) Eluent, chloroform–n-hexane (10:90); flow-rate, 2.0 cm³ min⁻¹; detection, UV at 300 nm.

(Fig. 6). The retention volumes of the copper and nickel complexes of $H_2F_3AM_2EMen$ were 8.56 and 12.66 cm³ and for $H_2F_3A_2EMen$ 14.12 and 18.44 cm³, respectively, with flow-rates of 2.0 and 2.2 cm³ min⁻¹, respectively.

Linear calibration graphs for the copper and nickel complexes of $H_2F_3AM_2EMen$ and $H_2F_3A_2EMen$ using UV detection at 300 nm were obtained over the range 0.5–6.0 μg of complex and the detection limits were 10–15 ng of metal.

Similarly, when the copper, nickel and oxovanadium complexes of H_2A_2EMen were investigated for HPLC separation on the Zorbax ODS column, optimum sep-
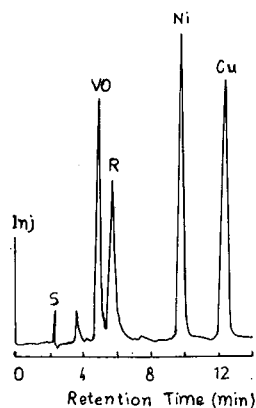
Fig. 7. HPLC separation of H_2A_2EMen and its Cu, Ni and VO complexes on a Zorbax ODS (5 μm) column. Eluent, water–methanol (25:75); flow-rate, 1 cm³ min⁻¹; detection, UV at 260 nm.
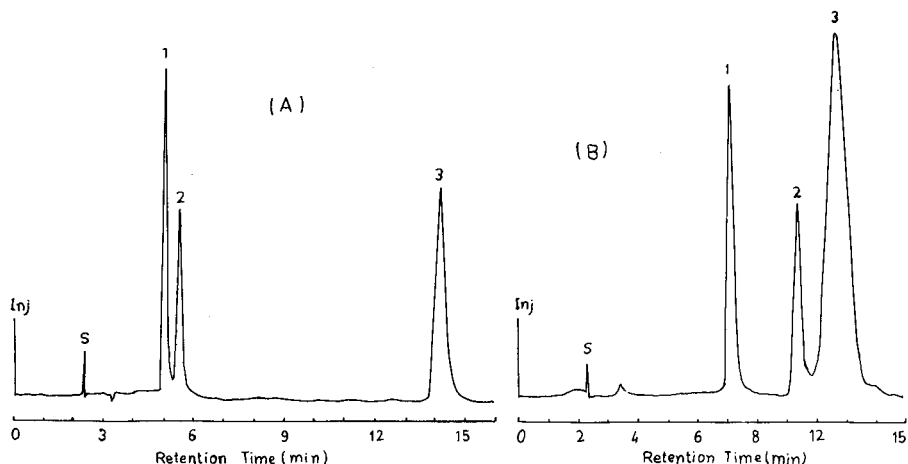
Fig. 8. (A) Relative elution of nickel complexes on a Zorbax ODS (5 μm) column. (1) F_3A_2EMenNi; (2) A_2EMenNi; (3) F_3AM_2EMenNi. Eluent, methanol–water (80:20); flow-rate, 1 cm^3 min^{-1}; detection, UV at 260 nm. (B) Relative elution of (1) F_3A_2EMenCu, (2) A_2EMenCu and (3) F_3AM_2EMenCu on a Zorbax ODS (5 μm) column. Eluent, methanol–water (75:25); flow-rate, 1 cm^3 min^{-1}; detection, UV at 260 nm.

aration was obtained when the complexes were eluted isocratically with methanol–water (75:25), with retention volumes of 4.93, 9.75 and 12.3 cm^3 for the oxovanadium, nickel and copper complexes, respectively, at a flow-rate of 1 cm^3 min^{-1}. The reagent solution was also added to the mixture to determine its effect on the HPLC separation of metal the complexes, and it was found that the reagent eluted with a retention volume of 5.67 cm^3 and interfered with the response for the oxovanadium complex (Fig. 7).

The response of the detector at 260 nm was checked under the optimized conditions of separation, and linear calibration graphs were obtained over the range 0.5–3.5 μg of the complex and the detection limit was 10 ng of complex.

Finally, the relative elution of the copper and nickel complexes of all the three reagents was investigated on the Zorbax ODS column. The copper or nickel complexes of the ligands were mixed, injected onto the column and eluted with methanol–water (80:20 and 75:25, respectively). Separations between the nickel and copper complexes were obtained (Fig. 8A and B), with elution of the copper and nickel complexes of $H_2F_3A_2$EMen, followed by H_2A_2EMen and $H_2F_3AM_2$EMen. The results also suggest that the CF$_3$ group slightly decreases and an alkyl (isobutane) group increases the retention in reversed-phase HPLC, as was observed in GC.

CONCLUSIONS

The work demonstrated the applicability of GC and HPLC for the separation of copper, nickel and oxovanadium complexes of tetradentate ketoamine Schiff bases at microgram to nanogram levels. GC provides easy separations of copper, nickel and oxovanadium complexes of H_2A_2EMen without any interference from excess of the reagent. Similar separations were also obtained by reversed-phase HPLC, with the reverse order of elution to that observed in GC, but the reagent interfered with

elution of the oxovanadium complex. The separation of copper and nickel complexed of fluorinated ligands, which was unsuccesful using GC, was easily achieved by normal-phase HPLC. HPLC with UV detection gave a greater sensitivity than GC with flame ionization.

REFERENCES

1 R. Belcher, A. Khalique and W. I. Stephen, *Anal. Chim. Acta*, 100 (1978) 503.
2 O. W. Lan and W. I. Stephen, *Anal. Chim. Acta*, 180 (1986) 417.
3 M. Y. Khuhawar, *Arab Gulf J. Sci. Res.*, 4 (1986) 463.
4 P. C. Uden, D. M. Parees and F. H. Walters, *Anal. Lett.*, 8 (1975) 795.
5 M. Y. Khuhawar, Z. Tanwari and S. A. Memon, *J. Chem. Soc. Pak.*, 9 (1987) 419.
6 M. Y. Khuhawar and A. G. Bhatti, *J. Chem. Soc. Pak.*, 11 (1989) 246.
7 P. C. Uden and D. E. Henderson, *J. Chromatogr.*, 99 (1974) 301.
8 P. C. Clark, I. E. Trable and P. C. Uden, *Polyhedron*, 1 (1982) 789.
9 M. Y. Khuhawar and G. Q. Khaskheli, *J. Chem. Soc. Pak.*, 11 (1989), 1631.
10 H. Veening and R. B. Willford, *Rev. Inorg. Chem.*, 1 (1979) 281.
11 E. Gaetani, C. F. Laurei, A. Mangla and G. Parolari, *Anal. Chem.*, 48 (1976) 1725.
12 S. Dilli and A. M. Maitra, *J. Chromatogr.*, 254 (1983) 133.
13 S. Dilli and E. Patsalides, *J. Chromatogr.*, 134 (1977) 477.
14 S. Dilli, A. M. Maitra and E. Patsalides, *Inorg. Chem.*, 21 (1982) 2832.
15 M. Y. Khuhawar, A. I. Soomro and A. G. M. Vasandani, *J. Chem. Soc. Pak.*, 12 (1990) 201.
16 P. C. Uden, *J. Chromatogr.*, 313 (1984) 3.
17 M. Y. Khuhawar and A. G. Bhatti, *J. Chem. Soc. Pak.*, submitted for publication.
18 D. F. Martin and K. Ramiah, *J. Inorg. Nucl. Chem.*, 27 (1965) 2027.
19 J. Selbin, G. Maus and D. L. Johnson, *J. Inorg. Nucl. Chem.*, 29 (1967) 1735.

CHROMSYMP. 2337

Reversed-phase separation of transition metals, lanthanides and actinides by elution with mandelic acid[a]

STEVE ELCHUK*, KERRY I. BURNS, RICHARD M. CASSIDY[b] and CHARLES A. LUCY

AECL Research, General Chemistry Branch, Chalk River Laboratories, Chalk River, Ontario K0J 1J0 (Canada)

ABSTRACT

Mandelic acid was investigated as an eluent for the determination of inorganic cations via dynamic ion-exchange and 'hydrophobic interaction' chromatography. Mandelic acid displays similar complexation chemistry to α-hydroxyisobutyric acid, but it is a more hydrophobic ligand and thus the resultant metal–ligand complexes are retained more strongly by the reversed phase surface. The retention behaviour of transition metals, lanthanides and actinides was studied. Retention of the actinides depends on the concentration and pH of the mandelic acid eluent, the column temperature and the concentration of organic modifier. Increasing either the column temperature or the eluent pH above 3.5 altered the selectivity between the actinides. Near-baseline separation was achieved for U, Am, Pu, Np and Th with mandelic acid eluent using isocratic conditions.

INTRODUCTION

One of the key advantages of "dynamic ion-exchange chromatography" is the ability to rapidly alter the column ion-exchange capacity and selectivity. With α-hydroxyisobutyric acid (HIBA) as eluent, thorium and uranium can either be eluted amongst the lanthanides or well after them, depending on the concentration of the 1-octanesulphonate in the mobile phase [1]. This selectivity change results from differences in the complexation chemistries and the ion-exchange equilibria of the two classes of metal ions. Under typical HIBA eluent concentrations the lanthanides should be predominantly in the MI_2^+ form (based on stability constants) and are retained largely through ion-exchange reactions with the 1-oxtanesulphonate sorbed on the reversed-phase surface. Uranium and thorium are also retained by an ion-exchange mechanism. However, previous studies have shown that if HIBA is used as

---

[b] Present address: Department of Chemistry, University of Saskatchewan, Saskatoon, Saskatchewan S7N 0W0, (Canada).

eluent with no 1-octanesulphonate present, Th(IV) and U(VI) are selectively sorbed onto the reversed-phase support [2]. Lanthanides and a number of transition metal ions [Cu(II), Zn(II), Fe(II), Fe(III), Mn(II), Co(II), Pb(II) and Ni(II)] are not significantly retained and virtually elute at the solvent front [2]. This selective sorption of U(VI) and Th(IV) apparently results from hydrophobic interaction of the metal–HIBA complex with the reversed-phase surface. The mechanism could be referred to as an "ion-pair" separation; however, this term would downplay the complexation chemistry which is integral to the system. Therefore, the more generic term "hydrophobic interaction" will be used to refer to the selective sorption. This interaction has been used to determine U and Th in samples from ore refineries [2], to selectively preconcentrate U from ground waters [3] and to determine uranium in mixed uranium–aluminium nuclear fuels [4].

Mandelic acid (phenylhydroxyacetic acid) complexes metals in a similar manner to HIBA. However, since it also contains a phenyl group, it is much more hydrophobic than HIBA. Thus, the interaction of the mandelic acid–metal complexes with the reversed phase would be expected to be much stronger than that for HIBA. Given the great utility of the reversed-phase effect in the HIBA system from metal separations, this paper reports on studies of the separation chaacteristics of mandelic acid.

EXPERIMENTAL

Apparatus

Isocratic elutions were performed with a M6000A pump (Waters Assoc., Milford, MA, USA), while gradient elutions were carried out on a Shimadzu LC610 solvent delivery system. The inlet tubing and column were thermostatted using a Haake G refrigerating water bath. Samples were injected using a 7125 valve (Rheodyne, Berkeley, CA, USA) equipped with a 100-μl sample loop. The post-column reagent was delivered with a syringe pump (Model M314, ISCO, Lincoln, NE, USA) and mixed with the column effluent at a screen-tee mixer [5]. The metal complexes were monitored using a fixed-wavelength detector (Model 441, Waters Assoc.) at wavelengths of 546 nm for 4-(2-pyridylazo)resorcinol (PAR) and 658 nm for 2,7-bis(*o*-arsenophenylazo)-1,8-dihydroxynaphthalene-3,6-disulphonic acid (Arsenazo III). The output from the detector was recorded on a Spectra Physics computing integrator (Model SP4100).

Initial studies performed with inactive standards (transition metals, lanthanides, U and Th) were performed using stainless-steel tubing for all connections. For studies of the actinides, the tubing in the sample flow path was replaced with poly(etherether)ketone tubing (Upchurch Scientific, Oak Harbor, WA, USA) to minimize losses of actinides to metal surfaces.

Reagents and materials

Water used for solutions and eluents was freshly distilled and purified in a Milli-Q deionizing unit (Millipore, Bedford, MA, USA). Acetonitrile was high-performance liquid chromatographic (HPLC) grade (Fisher). DL-Mandelic acid was obtained from Fluka and was used as received. Mandelic acid eluents were protected from light to prevent decomposition. Stock solutions of sodium 1-octanesulphonate

(0.1 mol l^{-1}, $C_8SO_3^-$) and $1.5 \cdot 10^{-3}$ mol l^{-1} Arsenazo III were purified using a Dowex 50W-X8 cation exchanger in the NH_4^+ form. The Arsenazo III solution contained 0.1 mol l^{-1} urea to prevent oxidation, and was diluted to the desired concentration ($1.5 \cdot 10^{-4}$ mol l^{-1}) with 0.1 mol l^{-1} HNO_3 prior to use. The PAR post-column reagent ($2 \cdot 10^{-4}$ mol l^{-1}) also contained 2 mol l^{-1} ammonia and 1 mol l^{-1} acetic acid. All HPLC eluents were filtered through 0.45-μm filters. Other chemicals were reagent grade.

Transition metal and lanthanide standards were prepared from SPEX Industries (Metuchen, NJ, USA) standards. Plutonium, neptunium-237 and americium-241 standards were prepared in 8 mol l^{-1} HNO_3 and were obtained at the Chalk River Laboratories. Their concentrations were determined by α-spectrometry.

Preliminary studies were performed using a 150 mm × 4.6 mm I.D. stainless-steel column packed with 5-μm Supelcosil C_{18} packing (Supelco, Oakville, Canada). A 100 m × 4 mm glass-lined column packed with 3-μm Spherisorb was used for all other work. This latter column was slurry-packed at 5000 p.s.i. from a solvent mixture of methanol–isopropanol–cyclohexanol–cyclohexane–1,1,1-trichloroethane (10:5:10:5:70, v/v) [6].

RESULTS AND DISCUSSION

Lanthanides

Since HIBA is most commonly used for the separation of the lanthanides [7–9], this application of mandelic acid was studied. Using a mandelic acid gradient containing 0.01 mol l^{-1} $C_8SO_3^-$ all fourteen lanthanides can be separated (Fig. 1). Unlike the comparable gradient using HIBA, Th(IV) and U(VI) are well separated from the lanthanides. The cause of the baseline shift evident in Fig. 1 is not known. Passage of the stock mandelic acid solution through a Dowex 50W × 8 cation-exchange column did not affect the baseline.
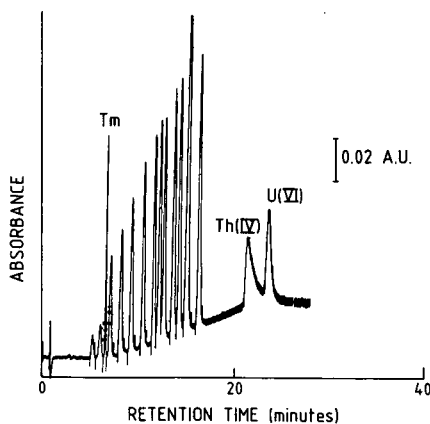
Fig. 1. Gradient separation of lanthanides, Th(IV) and U(VI) using mandelic acid and 1-octanesulphonate. Column 3-μm Spherisorb C_{18}, 100 × 4.0 mm I.D.; eluent 0.14 mol l^{-1} mandelic acid (pH 4.1) to 0.50 mol l^{-1} mandelic acid (pH 4.1) over 15 min, [$C_8SO_3^-$] constant at 0.01 mol l^{-1}; flow-rate, 1.0 ml min^{-1}; Temperature, 23°C; injection, 100 μl of 1 mg l^{-1} each of Lu, Yb, Tm, Er, Ho, Dy, Tb, Gd, Eu, Sm, Nd, Pr, Ce and La plus 2.5 mg l^{-1} U and Th; detection, post-column reaction with Arsenazo III.

While the separation shown in Fig. 1 is excellent, the chromatographic efficiencies (H = 0.009 mm for La) and the separation of the lanthanides are inferior to those obtained with HIBA [1,5]. With HIBA, the lanthanides are retained solely through ion exchange within the charged double layer which is formed when the hydrophobic 1-octanesulphonate modifier sorbs onto the reversed-phase surface. However, with mandelic acid, metal ions may be retained through either an ion-exchange or hydrophobic interaction mechanism. The degree to which the lanthanides retention is dictated by each mechanism is shown in Fig. 2 where the retention times under isocratic conditions are plotted *versus* eluent pH. As the pH is increased from pH 3.0 to 4.2, the proportion of mandelic acid which is ionized increases (pK_a = 3.19 [10]). For a pure ion-exchange mechanism, the retention times should decrease with increasing pH in proportion to the concentration of ionized mandelic acid present (about two-fold increase in ionized mandelic acid over the pH range 3.2 (pK_a) to 4.2). Alternatively, for the hydrophobic interaction mechanism retention should increase, as illustrated by U(VI) and Th(IV) in Fig. 2. The retention of La and Sm decreases with increasing pH indicating that the mandelic acid system lanthanide retention is largely due to ion exchange with the sorbed 1-octanesulphonate. Nonetheless, the change in retention time observed for La and Sm is smaller than would be expected for pure ion exchange, and Sm shows a small increase in retention at the higher pH values studied. Thus, some retention is believed to be due to the hydrophobic interaction of the lanthanide–mandelic acid complex with the surface, in addition to the dynamic ion exchange.

This conclusion is supported by the results obtained when mandelic acid alone is used as eluent (*i.e.*, no $C_8SO_3^-$ modifier in the eluent). A separaration of the rare-earth elements is still possible (Fig. 3c). Interestingly, the order of elution of the lanthanides is the same as observed with the ion-exchange modifier; however, only the first seven heavy lanthanides are well separated; the lighter lanthanides essentially co-elute.
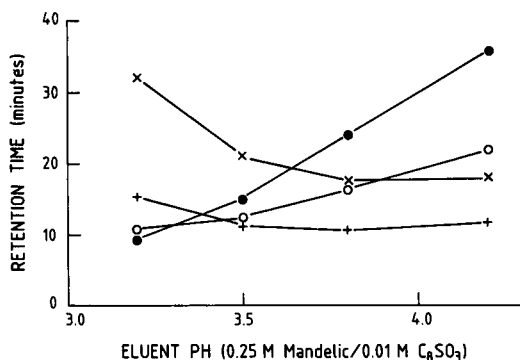
Fig. 2. Effect of pH of mandelic acid eluent on lanthanide and actinide separation in the presence of 1-octanesulphonate. Column, same as Fig. 1; eluent, 0.25 mol l^{-1} mandelic acid with 0.01 mol l^{-1} $C_8SO_3^-$; flow-rate, 0.8 ml min^{-1}; column temperature, 23°C; injection, 100 μl of 1.0 mg l^{-1} La and Sm and 2.5 mg l^{-1} U and Th; detection, post-column reaction with Arsenazo III. ● = U; ○ = Th; × = La; + = Sm.
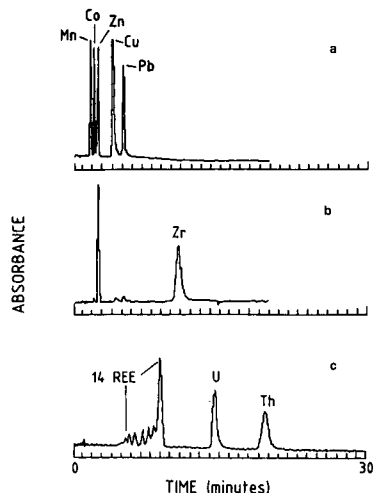
Fig. 3. Metal-ion separation with mandelic acid alone. (a) Transition metals; (b) zirconium; and (c) lanthanides, Th and U(VI). Column, 5-μm Supelcosil C$_{18}$, 150 × 4.6 mm I.D.; Eluent, 0.5 mol l^{-1} mandelic acid at pH 3.2; flow-rate, 1.0 ml min^{-1}; column temperature, room temperature; injection, 1–2.5 mg l^{-1} of each metal; detection, post-column reaction with PAR for the transition metals and Zr and with Arsenazo III for the lanthanides, Th and U(VI).

Transition metals

If HIBA is used without an organic ion-exchange modifier, the transition metals are unretained and coelute [2]. Using mandelic acid alone, however, a number of transition metals can be separated, as shown in Fig. 3. The transition metals elute prior to the lanthanides and actinides, although there is some overlap with the heavier lanthanides. For Mn(II), Co(II), Ni(II) (not shown in figure), Zn(II) and Cu(II) the retention order is opposite to that observed using HIBA with an ion-exchange column [3], reflecting the opposite effect of complex formation in the two modes of chromatotgraphy. Pb(II), however, shows unexpected behaviour. Normally, Pb(II), elutes between Zn(II) and Ni(II) in the HIBA ion-exchange system and yet in the mandelic acid system it elutes later. Unfortunately, stability constants for the Pb(II)–mandelic acid system are not available, so its is not known whether the retention behaviour results from differences in complexation reactions of HIBA and mandelic acid towards Pb(II), or if the retention mechanism is different for this metal.

Cu(II) also displayed interesting behaviour in the mandelic acid system. The retention of Cu(II) relative to the other transition metals varied with eluent concentration and pH, while no other changes in selectivity for the other transition metal studied were observed. Increases in the concentration of the mandelic acid in the eluent improved the symmetry of the Cu(II) peak, but changes in eluent pH did not.

Fig. 3b shows the retention of Zr under the same chromatographic conditions as for the transition metal separation shown in Fig. 3a. In order to prevent hydrolysis of Zr prior to complexation with mandelic acid, it was necessary to react Zr directly from a strong acid (8 mol l^{-2} HNO$_3$) solution with the mandelic acid. The pH was subsequently adjusted to match the eluent conditions. Standards were stable only at

concentrations less then 10 mg l^{-1}. More concentrated standards would precipitate upon standing. Hydrolyzed Zr eluted in the void volume. The Hf–mandelic acid peak could not be identified in this system. Subsequent test-tube experiments showed that the HF–PAR complex does form, but the kinetics of the complex formation is slow and so no significant colour formation occurred in the low dead-volume post-column reactor [5].

Fe(II) and Fe(III) were also separated using this system. Fe(III) eluted in the same time region as the heavy lanthanides, but the mandelic acid reduced Fe(III) *in situ*, resulting in Fe being distributed between the Fe(II) and Fe(III) peaks. Ca(II) was found to elute at a similar retention time to that of Mn(II).

Actinides

Previous studies have shown that HIBA, in the presence of 1-octanesulphonate, elutes the higher oxidation states of the actinides ahead of the lanthanides [1,11,12]. Significant retention of actinides such as Pu has only been achieved in the HIBA–C$_8$SO$_3^-$ system by reducing the actinides to their +3 oxidation state [11]. Unfortunately, under these conditions the +3 state is not stable for either Pu or Np. In addition, Am(III) and Pu(III) elute in close proximity to one another (resolution, R_s = 1.1) leading to difficulties in their subsequent determination by α-spectrometry since Pu-238 and Am-241 emit α particles of very similar energy.

The use of HIBA alone (*i.e.*, no C$_8$SO$_3^-$ present) has been shown to be a selective means of separating uranium from other metal ions [2–4]. Unfortunately, similar success is not possible for the other actinides using HIBA. Fig. 4 shows the separation of Th, U, Np, Pu and Am using HIBA alone. U(VI) and Th(IV) are strongly retained as has been reported previously [2–4]. However, Am(III) is only weakly retained and Pu(IV) co-elutes with Th(IV). The Np(IV) is separated from Th(IV), but some Np
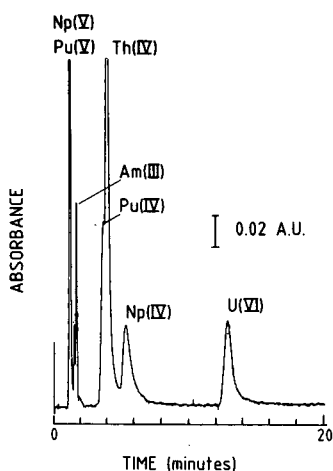
Fig. 4. Separation of actinides using HIBA in the absence of 1-octanesulphonate present. Column, 5-μm Supelcosil C$_{18}$, 150 × 4.6 mm I.D.; eluent; 0.16 mol l^{-1} HIBA (pH 4.5) with 4% methanol; flow-rate, 2.0 ml min^{-1}; column temperature, room temperature; injection, 0.3 mg l^{-1} Am and 3.0 mg l^{-1} each U, Th, Pu and Np; detection: post-column reaction with Arsenazo III.
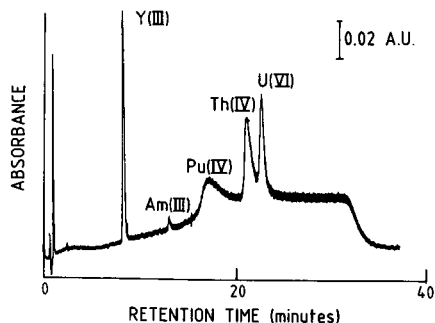
Fig. 5. Gradient elution of actinides using mandelic acid and 1-octanesulphonate. Column, 3-μm Spherisorb C_{18}, 100 × 4.0 mm I.D.; Eluent, 0.19 mol l^{-1} mandelic acid (pH 4.1) to 0.50 mol l^{-1} mandelic acid (pH 4.1) over 15 min, $[C_{18}SO_3^-]$ constant at 0.01 mol l^{-1}; flow-rate, 1.0 ml min^{-1}; temperature, 23°C; injection, 100 μl of 1.0 mg l^{-1} Y, 2.5 mg l^{-1} of Th(IV) and U(VI), 0.3 mg l^{-1} Am and 2.5 mg l^{-1} Pu.

also exists as NpO_2^+, and elutes at the solvent front. Furthermore, some changes in the Np and Pu oxidation states were observed when standards were allowed to stand in HIBA for a few days.

Use of mandelic acid–1-octanesulphonate as the mobile phase results in greater retention of the actinides than is possible with HIBA, as seen in Fig. 5. Under these conditions Am(III) elutes at the same retention time as would Sm, while Pu(IV) elutes as a broad peak just after the lanthanides (Fig. 1) and is followed by Th(IV) and U(VI). Interestingly, the elution order of Th(IV) and U(VI) reverses when 1-octanesulphonate is removed from the mandelic acid eluent. This differs from the behaviour observed with HIBA, where U(VI) is more strongly retained than Th(IV), regardless of the presence or absence of 1-octanesulphonate.

Unfortunately, the strong retention of mandelic acid on the reversed-phase support results in slow re-equilibration of the column to the initial gradient conditions, and thus limits the usefulness of mandelic acid to isocratic chromatography. Nevertheless, an excellent separation of the actinides can be achieved using mandelic acid alone under isocratic conditions (Fig. 6). Pu(IV) is stable for indefinite periods in mandelic acid solutions and can be quantitatively recovered from the system (Table I). Some tailing of the Pu-239 peak is evident in Table I, but this is believed to result from Pu retention on metal surfaces present in our fraction collection line. Am-241 was also quantitatively recovered (105% for a 84-ng injection), with 93% being present in the expected fraction. Np was recovered in two fractions, corresponding to the +4 and +5 oxidation states, with the latter eluting at the solvent front. Np can be reduced quantitatively to the +4 state by addition of Fe(II) to the sample; however, this also causes some reduction of the Pu(IV). The poor recovery of Np in Table I is believed to result from the increased background in the α-spectrum from Pu present in the Np fraction. Similar difficulties made the determination of Np-237 in the original mixed actinide standard impossible.

In order to achieve the separation shown in Fig. 6 a number of factors must be optimized or controlled. The temperature of the eluent strongly affected the selectivity, as can be seen in Fig. 7. While both enthalpic and entropic behaviour was observed upon altering the temperature, the most marked temperature dependence,
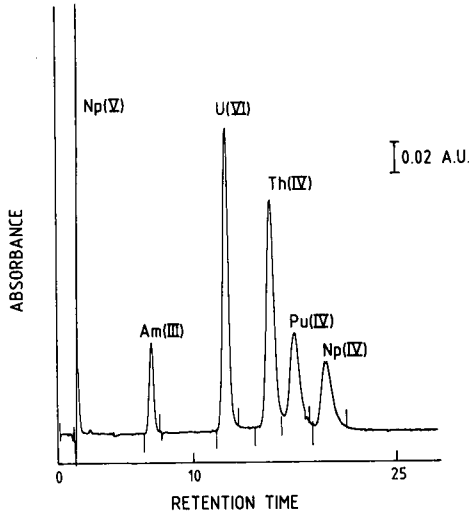
Fig. 6. Separation of actinides using mandelic acid alone. Column, 3-μm Spherisorb C$_{18}$, 100 × 4.0 mm I.D., eluent, 0.50 mol l^{-1} mandelic acid (pH 3.2) with 5% acetonitrile; flow-rate, 0.8 ml min^{-1}; temperature; 23°C; injection, 100 μl of 3.0 mg l^{-1} of Th and U(VI), 0.3 mg l^{-1} Am, 3.0 mg l^{-1} Pu and 3.0 mg l^{-1} Np; detection, post-column reaction with Arsenazo III.

TABLE I

DISTRIBUTION OF Pu, Np AND Am IN VARIOUS FRACTIONS COLLECTED DURING ISO-CRATIC ELUTION WITH MANDELIC ACID ALONE

Chromatographic conditions: column, 3-μm Spherisorb C18, 100 × 4.0 mm I.D.; eluent, 0.50 mol l^{-1} mandelic acid (pH 3.2); flow-rate, 0.75 ml min^{-1}; temperature, 25°C; injection, 100 μl of 2.5 mg l^{-1} of Th, Y and U(VI), 100 mg l^{-1} Sr and Ca and actinides as indicated in table; detection, fraction collection and subsequent α-spectrometry on 100 μl of fraction (precision is ±10% due to variability in plate preparation).

Fraction collection times (min)	Weight of Pu-239 (ng)	Weight of Np-237 (ng)	Weight of Am-241 (ng)
0–4	0.8	69	0.02
4–8	1.0	—	0.02
8–12	—	—	82
12–18	—	—	5
18–22	—	—	0.9
22–27	20	—	—
27–32	710[a]	—	—
32–36	75	360	—
36–40	13	—	—
40–44	9	—	—
44–48	7	—	—
48–52	4	—	—
Total mass recovered (ng)	840	429	88
Mass injected (ng)	860	830[b]	84
Recovery (%)	97	52	105

[a] Possibly Pu-240 present.

[b] Np-237 was not detected in the mixed standard by α-spectrometry due to the presence of plutonium. Quantity indicated is from analysis of pure Np-237 standard used to prepare the solution injected.
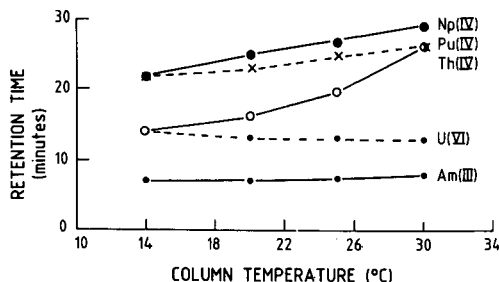
Fig. 7. Effect of temperature on separation of actinides using only mandelic acid. Conditions as in Fig. 6, except that the column temperature is varied.

and the only one which actually resulted in a selectivity change amongst the actinides was that for Th(IV). Above 27°C Th(IV) will overlap with the Pu(IV), so a temperature of 23°C was used for the actinide separations.

Increasing the pH of the eluent over the range 2.0–4.2 resulted in an increase in the actinide retention (Fig. 8), as would be expected from the increasing hydrophobicity of the metal ligand complexes. At low pH the actinides elute in two groups: the early-eluting group consisting of U(VI) and Am(III) and the later group of Pu(IV), Th(IV) and Np(IV). As the pH is increased up to a pH of 3.6 the order of elution is as shown in Fig. 6, but at pH 3.8 Pu(IV) elutes before Th(IV). Extension of this study to higher values of pH was precluded by the long retention times. Nevertheless, studies using lower mandelic acid concentrations have shown that at pH > 4 Pu(IV) will elute prior to U(VI). Unfortunately, Np(IV) also shows reduced retention relative to Th(IV) and U(IV) at pH > 4, resulting in poor separations between Th(IV) and Np(IV).

Increasing the mandelic acid concentration in the eluent showed an unexpected effect. Previously, it had been observed that increases in the HIBA concentration in the eluent results in small increases in the retention times of U(VI) and Th(IV) [2]. In the mandelic acid system (Fig. 9), increases in the concentration of mandelic acid (pH
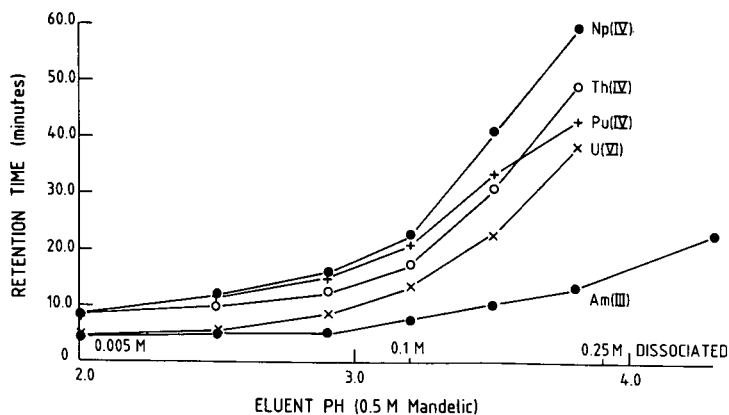
Fig. 8. Effect of eluent pH on separation of actinides using only mandelic acid. Conditions as in Fig. 6, except for eluent pH.
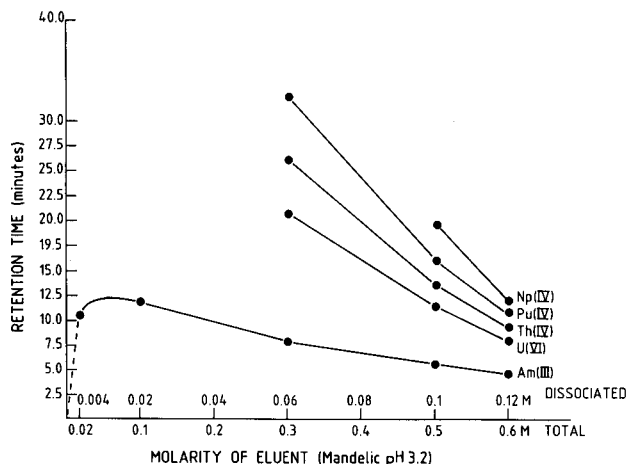
Fig. 9. Effect of mandelic acid concentration on retention of actinides. Conditions as in Fig. 6, except for the mandelic acid concentration.

3.2) from 0.3 to 0.6 mol l^{-1} resulted in significant decreases in the retention time. Only the retention of Am(III) was studied below eluent concentrations of 0.3 mol l^{-1} due to the long retention times under these conditions. Below a mandelic acid concentration of 0.1 mol l^{-1} the retention of Am(III) was observed to decrease with decreasing concentration. However, under these conditions the Am(III) peak was extremely broad and displayed poor peak shape.

Two explanations are possible for the results in Fig. 9. First, increases in the mandelic acid concentration result in the formation of anionic metal–ligand complexes which have a lower retention than cation complexes. However, if this were the case, then a similar decrease in retention should be observed for increases in the eluent pH (Fig. 8) but the opposite was actually observed, *i.e.*, the retention increased with pH. Furthermore, if formation of anionic complexes were the cause of the decreased retention, then some selectivity changes should be observed as a result of the different formation constants for the metal–ligand complexes. Again this effect was not observed. Therefore the formation of anionic metal–ligand complexes is not believed to be responsible for the reduced retention observed for increased eluent concentration.

A second explanation is that the protonated mandelic acid is competing with the actinide–mandelate complex for adsorption onto the reversed-phase surface. Essentially, the protonated mandelic acid is believed to act like an organic modifier. Additions of a more conventional organic modifier, *e.g.*, acetonitrile, over the range 0–20% (v/v) also resulted in reduced retention of the actinides without alteration of the selectivities. This is analogous to the behaviour previously observed with the U(VI)–HIBA system [2]. Unlike the U(VI)–HIBA system, however, no significant improvements in peak shape were observed using methanol rather than acetonitrile [4]. Nevertheless, these results do suggest that the primary effect of increased mandelic acid concentration is to act as an organic modifier, resulting in more rapid elution of the actinides.

CONCLUSIONS

Mandelic acid is not as efficient an eluent for dynamic ion-exchange separations of transition metals and lanthanides as is HIBA. This is due to the more hydrophobic character of mandelic acid causing increased hydrophobic interaction with the stationary phase, resulting in poorer efficiences than those obtained with the dynamic ion exchange.

Nevertheless, the hydrophobic interaction of the mandelic acid–metal ion complexes with reversed-phase surfaces displays useful selectivities for the separation of actinides, both from each other and from other metals. Use of mandelic acid alone as the eluent results in the separation of metal ions primarily based on the charge on the cation: +2 transition metals elute early, followed by +3 species such as the lanthanides, and finally the +4 species such as many of the actinides.

Actinide retention is enhanced by increasing the eluent pH or by decreasing the concentration of either the mandelic acid or the organic modifier (acetonitrile) in the mobile phase. Selectivity can be altered either by changing the eluent pH over the range 3.5–4.5 or by changing the column temperature.

Studies are now underway to investigate the suitability of this system for the determination of actinides in low-level radioactive waste, and of lanthanides in uranium fuels.

REFERENCES

1 C. H. Knight, R. M. Cassidy, B. M. Recoskie and L. W. Green, *Anal. Chem.*, 56 (1984) 474.
2 D. J. Barkley, M. Blanchette, R. M. Cassidy and S. Elchuk, *Anal. Chem.*, 58 (1986) 2222.
3 A. Kerr, W. Kupferschmidt and M. Attas, *Anal. Chem.*, 60 (1988) 2729.
4 R. M. Cassidy, S. Elchuck, L. W. Green, C. H. Knight, F. C. Miller and B. M. Recoskie, *J. Radioanal. Nucl. Chem.*, 139 (1990) 55.
5 R. M. Cassidy, S. Elchuk and P. K. Dasgupta, *Anal. Chem.*, 59 (1987) 85.
6 K. Kuwata, M. Uebori and Y. Yamazaki, *J. Chromatogr.*, 211 (1981) 378.
7 M. Marhol, *Ion Exchangers in Analytical Chemistry –Their Properties and Use in Inorganic Chemistry, (Comprehensive Analytical Chemistry*, Vol. XIV) Elsevier, Amsterdam, 1982 p. 214.
8 Y. Shuheng, L. Fa, Z. Hongdi, L. Xueliang and Z. Shulan, *J. Radioanal. Nucl. Chem.*, 124 (1988) 187.
9 D. Ishii, A. Hirose and Y. Iwasaki, *J. Radioanal. Chem.*, 46 (1978) 41.
10 A. E. Martell and R. M. Smith, *Critical Stability Constants, Vol. 3 Other Organic Ligands*, Plenum Press, New York, 1977, p. 47.
11 R. M. Cassidy, C. H. Knight, B. M. Recoskie, S. Elchuk and L. W. Green, in G. R. Choppin, J. D. Navratil and W. W. Schultz (Editors), *Actinide/Lanthanide Separations*, World Scientific, Singapore, 1985, p. 1.
12 R. M. Cassidy, S. Elchuk, N. L. Elliot, L. W. Green, C. H. Knight and B. M. Recoskie, *Anal. Chem.*, 58 (1986) 1181.

CHROM. 23 406

Ion chromatographic determination of anions, especially sulphur-containing anions, with conductimetric and kinetic detection

O. N. OBREZKOV*, O. A. SHPIGUN and Yu. A. ZOLOTOV

Department of Analytical Chemistry, Faculty of Chemistry, M. V. Lomonosov Moscow State University, Lenin Hills, Moscow 119899 (USSR)

and

V. I. SHLYAMIN

Vernadsky Institute of Geochemistry and Analytical Chemistry, Kosygin Str. 19, Moscow 117975 (USSR)

(First received January 8th, 1991; revised manuscript received April 22nd, 1991)

ABSTRACT

A new mode of detection in ion chromatography called "kinetic detection" is suggested. The technique uses an ion chromatograph with a conductimetric detector and a multichannel flow mounting with a spectrophotometric detector. The potassium bromate degradation reaction in hydrochloric acid accelerated by reducing anions, is used as a model indicator system. The sensitive determination of S^{2-}, SO_3^{2-}, $S_2O_3^{2-}$, SCN^- and NO_2^- has been performed. The simultaneous determination of weak and strong inorganic acid anions is shown to be possible.

INTRODUCTION

The determination of anions of weak inorganic acids, in particular sulphur-containing anions, is an important analytical problem. Ion chromatography is a convenient method for the determination of sulphur as anions [1–4], and can be used to determine S^{2-}, SO_3^{2-}, SO_4^{2-}, $S_2O_3^{2-}$, $S_2O_4^{2-}$, $S_2O_6^{2-}$, $S_2O_8^{2-}$, $S_4O_6^{2-}$ and SCN^- in the presence of other inorganic anions [5–8]. However, it is difficult, in most instances, to ensure the selective and sensitive determination of all such components of complicated samples by conventional ion chromatographic techniques. It seems reasonable to use a chromatograph with several detectors, each of which is selective for one or a number of anions.

The authors' laboratory uses a conventional ion chromatograph with a conductimetric detector in combination with a so-called "kinetic detector". The latter is a multichannel post-column kinetic reaction with spectrophotometric detection. The degradation of potassium bromate in hydrochloric acid is accelerated by S^{2-}, SCN^-, SO_3^{2-}, $S_2O_3^{2-}$, NO_2^- or AsO_2^- [9,10] and has been used as an indicator reaction. This method makes it possible to determine small concentrations of weak acidic anions and other inorganic anions (F^-, Cl^-, NO_3^-, HPO_4^{2-}, SO_4^{2-}) simultaneously, because the

former are not recorded by the conductimetric detector and the latter do not affect the indicator reaction.

EXPERIMENTAL

A Biotronik IC-5000 ion chromatograph with a 100×3 or 100×4 mm separator column and a 150×6 mm suppressor column, a conductimetric detector, and a Chromatopac CR 2A integrator were used. Oka-1 and Anieks N were used as the separator resins. Sodium carbonate solutions of various concentrations were used as eluents. The flow system for kinetic detection consisted of two Zalimp PP-2-15 peristaltic pumps, several reaction coils and pipelines, and a Biotronik BT-3030 spectrophotometric detector with a recorder. The inner diameter of all the pipelines was 0.7 mm and that of the reaction coils was 1 mm. The pH was controlled with a glass electrode using an EV-74 ionometer.

All solutions were prepared from dry analytical reagent-grade chemicals using doubly deionized water. Solutions containing S^{2-}, SO_3^{2-}, $S_2O_3^{2-}$ and SCN^- were prepared daily.

RESULTS AND DISCUSSION

Kinetic detection

Kinetic detection was accomplished in a multichannel flow system which was coupled to an ion chromatograph connected to a conductimetric detector. The indicator kinetic reaction, which is accelerated by the sample components, is performed; the sample components are detected spectrophotometrically after separation on a column.
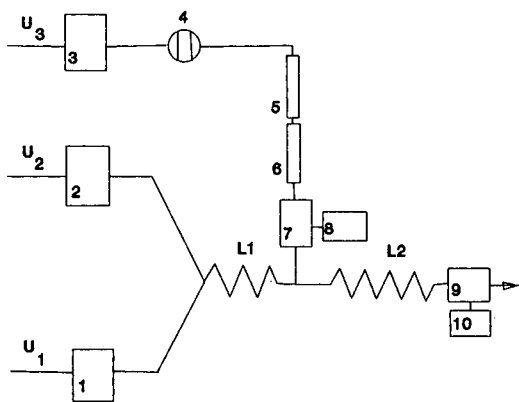
Fig. 1. Schematic diagram of an ion chromatographic experimental arrangement with kinetic detection. U_1 = Flow of methyl orange solution in hydrochloric acid; U_2 = potassium bromate flow; U_3 = eluent flow; 1,2 = peristaltic pumps; 3 = ion chromatograph pump; 4 = injection valve; 5 = separator column; 6 = suppressor column; 7 = conductimetric detector; 8 = integrator; 9 = spectrophotometric detector; 10 = recorder; L_1, L_2 = reactors.

Ion chromatograph with kinetic detection

The degradation of potassium bromate in hydrochloric acid, one version of the Landolt system, was used as the indicator reaction, the catalysts being S^{2-}, SO_3^{2-}, NO_2^-, SCN^-, $S_2O_3^{2-}$, Br^-, I^- and AsO_2^- [9,10]. The study was carried out using the arrangement shown in Fig. 1.

The sample was injected into the eluent flow stream (U_3). After separation, the sample components were detected conductimetrically, then the eluent was mixed with the flows of potassium bromate (U_2) and methyl orange in hydrochloric acid (U_1). Through the reaction coil (L_2) the flow was driven into the flow cell of a spectrophotometric detector, where the absorption of the solution was measured (as a result of the reaction, the methyl orange became colourless, and the determination was accomplished over negative peaks).

Choice of flow system parameters

To provide sensitive detection with effective separation and minimum sample dispersion in the flow, the optimum experimental conditions were determined. It is known that the rate of the indicator reaction is proportional to $[KBrO_3]$ and $[H^+]$ [2]; however, the rate of the non-catalysed process increases considerably with increasing concentrations of the reactants. The determination of the sensitivity depends on the concentration of the indicator substance. However, at the same time, a high concentration of methyl orange causes noise and drift of the baseline. The results of the experiments have shown that the optimum parameters are as follows: flow-rates, $U_1 = U_2 = 0.5$ ml/min, $U_3 = 1.5$ ml/min; reactor lengths, $L_1 = 40$ cm, $L_2 = 1500$ cm, initial concentration, $c_{(initial)}$ [methyl orange] $= 10^{-4}$ M, $c_{(initial)}$ [HCl] $= 2.5 \cdot 10^{-1}$ M, $c_{(initial)}$ [KBrO$_3$] $= 1.5 \cdot 10^{-2}$ M, sample volume $= 100$ μl, time of sample in the system $= 4.5 - 7.5$ min, spectrophotometric detector wavelength $= 522$ nm.

A dual-column variant of ion chromatography has been used. It was found that the suppressor column does not affect the spectrophotometric determination of the
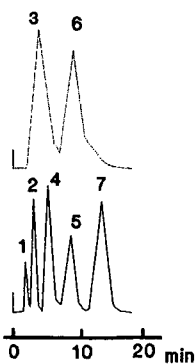
Fig. 2. Chromatogram of a solution of 2 ppm F^- (1), 5 ppm Cl^- (2), 3 ppm S^{2-} (3), 25 ppm NO_3^- (4), 50 ppm HPO_4^{2-} (5), 6 ppm SO_3^{2-} (6) and 50 ppm SO_4^{2-} (7). Column, 100 × 3 mm (Oka-1). Eluent, 0.0025 M sodium carbonate (1 ml/min). Solid line = conductimetric detector output; dotted line = spectrophotometric detector output.
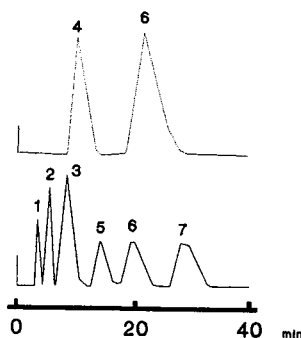
Fig. 3. Chromatogram of a solution of 2 ppm F^- (1), 5 ppm Cl^- (2), 25 ppm NO_3^- (3), 1 ppm NO_2^- (4), 20 ppm HPO_4^{2-} (5), 12 ppm SO_3^{2-} (6) and 20 ppm SO_4^{2-} (7). Eluent, 0.0015 M sodium carbonate (1 ml/min).
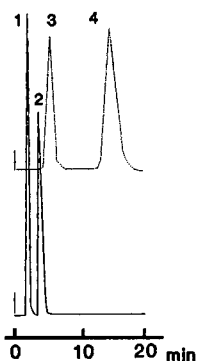
Fig. 4. Chromatogram of a solution of 5 ppm Cl⁻ (1), 50 ppm SO_4^{2-} (2), 0.2 ppm S^{2-} (3) and 1 ppm SCN⁻ (4). Column, 100 × 4 mm (Oka-1). Eluent, 0.006 M sodium carbonate (1.5 ml/min).
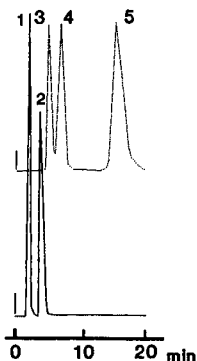
Fig. 5. Chromatogram of a solution of 5 ppm Cl⁻ (1), 50 ppm SO_4^{2-} (2), 1 ppm S^{2-} (3), 2 ppm SO_3^{2-} (4) and 5 ppm $S_2O_3^{2-}$ (5). Column, 100 × 3 mm (Oka-1). Eluent, 0.005 M sodium carbonate (1.5 ml/min).

catalyst anions. In addition, it decreases the conductimetric signal of the weak acid anions, and these anions do not affect the conductimetric determination of other sample components.

Determination of inorganic anions

The determination of weak inorganic acid anions simultaneously with strong acid anions is a complicated analytical task. The described experimental arrangement allows such a determination. Figs. 2–5 show chromatograms of mixtures containing F⁻, S^{2-}, Cl⁻, NO_2^-, NO_3^-, HPO_4^{2-}, SO_3^{2-}, SO_4^{2-}, $S_2O_3^{2-}$ and SCN⁻, separated using the sorbent Oka-1. Figs. 2 are 3 are examples of the simultaneous determination of F⁻, Cl⁻, S^{2-}, NO_3^-, HPO_4^{2-}, SO_3^{2-} and SO_4^{2-}, and of F⁻, Cl⁻, NO_2^-, NO_3^-, HPO_4^{2-}, SO_3^{2-} and SO_4^{2-}, respectively. Examples of the simultaneous determination of weakly and strongly retained anions are shown by the chromatograms of Figs. 4 and 5. The reducing anions are detected kinetically; the other anions are detected
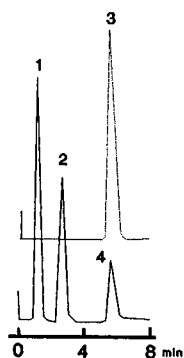
Fig. 6. Chromatogram of a solution of 2 ppm F⁻ (1), 5 ppm Cl⁻ (2), 0.2 ppm S^{2-} (3) and 5 ppm SO_4^{2-} (4). Column, 100 × 4 mm (Anieks N). Eluent, 0.004 M sodium carbonate (1.5 ml/min).

conductimetrically. Using two detectors provides a rapid determination; for example, the determination of a mixture of F^-, S^{2-}, Cl^- and SO_4^{2-} can be achieved in 7 min (Fig. 6).

The detection limits calculated for a signal-to-noise ratio of 3:1 are (in ppm): 0.01 (S^{2-}), 0.05 (SO_3^{2-}), 0.05 ($S_2O_3^{2-}$) and 0.06 (SCN^-). These are essentially lower than the detection limits for conductimetric detection in single-column (direct and indirect methods) ion chromatography. The determination of the maximum concentration for each anion depends on the conditions of each individual task. The upper limit of the linear operating range of the calibration graphs is 50 ppm for each anion. The relative standard deviation in the determination of 1 ppm of S^{2-}, SO_3^{2-}, $S_2O_3^{2-}$ and SCN^- is 6%. The determination of 1 ppm of S^{2-}, SO_3^{2-}, SO_4^{2-}, $S_2O_3^{2-}$, SCN^- and NO_2^- is influenced by the presence of 0.01 ppm Br^-, 0.1 ppm I^-, 1000 ppm F^-, 1000 ppm Cl^-, 500 ppm NO_3^-, 500 ppm SO_4^{2-}, 500 ppm HPO_4^{2-} and 500 ppm CO_3^{2-}. All anions with reducing properties also affect the determination.

CONCLUSIONS

A new mode of detection in ion chromatography called "kinetic detection" has been proposed. The approach demonstrated makes it possible to solve a number of ion chromatographic problems, including the sensitive determination of sulphur-containing inorganic anions and the simultaneous determination of weak acid anions and strong inorganic acid anions.

ACKNOWLEDGEMENTS

REFERENCES

1 J. Weis and M. Gobl, *Fresenius Z. Anal. Chem.*, 320 (1985) 439.
2 C. O. Moses, D. K. Nordstrom and A. L. Mills, *Talanta*, 31 (1984) 331.
3 T. Sunden, M. Lindgren, A. Cedergren and D. D. Seimer, *Anal. Chem.*, 55 (1983) 2.
4 F. J. Irujillo, M. M. Miller, R. K. Shogerbol, H. E. Taylor and C. L. Grant, *Anal. Chem.*, 53 (1981) 1944.
5 J. G. Tarter, *Anal. Chem.*, 56 (1984) 1264.
6 R. D. Rocklin and E. L. Johnson, *Anal. Chem.*, 55 (1983) 4.
7 A. M. Bond, I. D. Heritage, G. G. Wallace and M. J. McCormick, *Anal. Chem.*, 54 (1982) 582.
8 L. D. Hansen, B. E. Richter, D. K. Rollins, J. D. Lamb and D. J. Eatough, *Anal. Chem.*, 51 (1979) 633.
9 L. M. Tamarchenko, *Zh. Anal. Khim.*, 33 (1978) 824.
10 V. F. Toropova and L. M. Tamarchenko, *Zh. Anal. Khim.*, 22 (1967) 576.

Capillary gas chromatography–mass spectrometry of unusual and very long-chain fatty acids from soil oligotrophic bacteria

T. ŘEZANKA*

Institute of Microbiology, Vídeňská 1083, 14220 Prague (Czechoslovakia)

I. V. ZLATKIN

Institute of Microbiology, Prosp. 60-letia Oktiabrya 7/2, 117811 Moscow (USSR)

I. VÍDEN

Institute of Chemical Technology, 16628 Prague (Czechoslovakia)

and

O. I. SLABOVA and D. I. NIKITIN

Institute of Microbiology, Prosp. 60-letia Oktiabrya 7/2, 117811 Moscow (USSR)

(First received March 15th, 1991; revised manuscript received May 6th, 1991)

ABSTRACT

More than 60 fatty acids (as oxazolines) were identified in soil oligotrophic bacteria by capillary gas chromatography–mass spectrometry. The fatty acids covered the whole range from enanthic to cerotic acid and included both saturated and, to lesser extent, even monoenoic acids. Linear non-hydroxy and/or 3-hydroxy and branched-chain acids (iso- or anteiso) were also detected. Palmitic and stearic acid were major acids. Some species were found to contain unusual fatty acids; *e.g.*, *Arcocella flava* contained almost 20% of caprinic acid and *Blastobacter novus* more than 6% of 3-hydroxyisopentadecanoic acid (i-3-OH-15:0). Very unusual hydroxy fatty acids, *e.g.*, 3-hydroxy-5-dodecenoic acid, were identified in three strains.

INTRODUCTION

The study of oligotrophic soil bacteria is very complicated, *e.g.*, because of their difficult cultivation. Only a few papers have therefore dealt with these unique bacteria [1,2].

Gram negative bacteria are characterized by a variable content of fatty acids (FAs). In addition to their typical representatives (*e.g.*, *Escherichia coli*), much attention has been paid to the structure of lipopolysaccharides of clinically important pathogens, such as *Salmonella* and *Legionella* [3–5]. This structure is very complicated, the unifying component being the type of fatty acids present. Straight-chain fatty acids are saturated or monoenoic and are often observed. Branched-chain fatty acids may also be found, most frequently iso- and/or anteiso. In both types, the acids are often substituted by a hydroxy group at C-2 or -3.

Identification of fatty acids in oligotrophic soil bacteria has been carried out several times [6,7]. Unfortunately, in these attempts many peaks remained unidentified, even though capillary gas chromatography–mass spectrometry (GC–MS) was used. In another publication on soil bacteria [8], some FAs were identified by using reversed-phase high-performance liquid chromatography (RP-HPLC) and GC–MS on packed columns.

Based on our previous results, we performed also this identification using capillary GC–MS [9,10]; the number of FAs identified showed a tenfold increase compared with similar published data. The fatty acid analysis was carried out even in unique soil oligotrophic bacteria.

EXPERIMENTAL

Bacterial isolates and growth conditions

All the bacteria used were from the collection of the Institute of Microbiology, Moscow, USSR. *Arcocella aquatica* NO.502, *Hyphobacter diversus* NP-802, *Pedodermatophilus paradoxus* NP-801, *Flectobacillus major* and *Spirosoma linguale* No. 1 were grown on PYG medium [peptone–yeast extract–glucose, 0.1% (w/v) each]. *Geodermatophilus obscurus* NP-800 was grown on yeast extract (0.5%), glycerol (5%) and calcium carbonate solution (0.1%). *Blastobacter novus* NP-141, *Renobacter vacuolatum* strains NP-300-W, NP-300-G and VZ-9, *Methylbacterium* sp. No. 5 were grown on medium [11] No. 337 with 1% or 0.3% (strain NP-141) methanol. All the strains were grown aerobically to the stationary phase (5–8 days at 28°C). The cells were harvested by low-speed centrifugation, washed with 0.1 M sodium chloride solution and stored at $-25°C$.

Derivatization and GC–MS identification

Methyl esters of corresponding fatty acids were prepared by alkaline hydrolysis and reaction of free acids with boron trifluoride–methanol [9]. The oxazolines and/or their trimethylsilyl (TMS) ethers were prepared using a modification of published methods [12,13] (method b, *e.g.*, lower temperature method): 5 mg of dicyclohexylcarbodiimide (Sigma, St. Louis, MO, USA) were added to a solution of 5 mg of FAs (free form) in 1 ml of dichloromethane. After stirring (10 min), 5 mg of 2-amino-2-methylpropanol (Sigma) were added (20°C, 4 h). The evaporated mixture was dissolved in 1 ml of diethyl ether and treated with 0.5 ml of thionyl chloride (20°C, 1 h), washed with ice-cold water and dried (anhydrous sodium sulphate). The eluate was evaporated, dissolved in pyridine (0.5 ml) and heated with trimethylsilyl chloride (50°C, 4 h).

Methyl esters were identified and quantified (by total ion current) in a Shimadzu (Kyoto, Japan) QP-1000 apparatus equipped with a fused-silica capillary column (60 m × 0.32 mm I.D.) coated with a 0.25-μm layer of SPB-1 (Supelco, Gland, Switzerland); splitless injection was used, with helium as carrier gas. Replacement of helium by hydrogen improved the elution and resolution only slightly (*ca.* 5–7%). The oven temperature was programmed from 100 to 320°C at 4°C/min. The mass spectrometer was operated with an ionization energy of 70 eV and an electron multiplier voltage of 2.5 kV.

TMS ethers of oxazolines were identified under similar conditions to the methyl

esters, except that the column temperature was programmed from 150 to 330°C at 5°C/min.

RESULTS AND DISCUSSION

The separation and identification of more than 60 peaks representing FAs typical of oligotrophic bacteria is shown in Table I. About half of the FAs had not previously been described in these microorganisms. Straight-chain FAs, iso-, anteiso- and monoenoic acids were identified.

The amount of straight- and branched-chain FAs (iso- and anteiso-) was large. Fewer than 15 of the total of 32 peaks were identified in a previous study [6] on soil bacteria. Therefore, the presence of almost 35 non-hydroxy saturated FAs is not so striking. The major fatty acids were, as usual, saturated with an even number of carbon atoms in the molecule (e.g., 14:0, 16:0, 18:0). Other FAs were much more variable; for example, the series i, ai and/or n FAs were present, from C_{13} up to C_{20}.

Monounsaturated FAs were separated on a capillary column and, in some instances, two positional isomers were identified. Only one positional isomer has previously been identified [6,8] in oligotrophic soil bacteria. On the basis of the mass spectra of 2-alkenyl-4,4-dimethyloxazolines, two possible structures ($n-9$ and $n-7$) were detected; the former was markedly prevalent. By using these derivatives [12,14] we were able to identify monoenoic acids even in the complex mixture obtained from oligotrophic bacteria. The derivatization of FAs to their oxazolines has a great advantage because, as reported by Yu et al. [15], their elution temperature is only 5°C higher than that for fatty acid methyl esters (FAMEs). Fig. 1 shows one of the most interesting parts of the chromatogram, i.e., that including the range from 12:0 to 14:0. Also, part of the mass spectrum of tentative 3-OH-12:1 is depicted (see caption of Fig. 1).

Another interesting group of FAs found in soil bacteria are hydroxy acids. In some work they have been neglected, probably because of their poor identification by GC (lack of standards). In keeping with literature data [4,6], most hydroxy acids exhibited a chain length of C_9–C_{16}. In this study the majority were C_{11}–C_{15}. Both normal and iso-hydroxy acids have been observed [3,4], albeit in other genera of Gram negative bacteria. We detected a higher content of FAs with an odd number of carbon atoms in the molecule, in contrast to the previous work [4,6].

Also, a 3-hydroxymonoenoic acid was identified, in the molecule of which the position of the double bond was thought to be between C-5 and -6 (see also the caption to Fig. 1). In the only work known [16], the position of the double bond in monoenoic 3-OH-FA was shown to be between the C-5 and -6 (determined by means oxidative splitting with potassium permanganate).

To our knowledge, FAs longer than C_{20} have not been detected in soil oligotrophic bacteria. The presence of very long-chain fatty acids (VLCFAs), i.e., acids having more than 24 carbon atoms in the molecule, is unusual and these acids have not yet been found in oligotrophic bacteria, although they are described in a report on FAs in soil [17]. As mentioned by Nikitin et al. [18], oligotrophic bacteria represent a major part of soil biomass and, therefore, the presence of VLCFAs in these microorganisms is not surprising. C_{24} acids dominated; 24:0 was always present with the exception of the genus Methylobacterium. In the strains NO-300-G and VZ-9 of the

TABLE I

FATTY ACID COMPOSITION OF SELECTED OLIGOTROPHIC BACTERIA (IN MOL. %)

Fatty acid[a]	*Arcocella aquatica*	*Blastobacter novus*	*Flectobacillus major*	*Geodermatophilus obscurus*	*Hyphobacter diversus*
7:0	1.10	0	0.75	0	0.12
8:0	0.98	0	0.46	0	0.61
9:0	0.28	0	0.31	0.07	0.11
10:0	17.23	0.13	10.58	0.12	0.79
3-OH-9:0	0.56	0.59	0.42	0	0.30
11:0	3.37	2.01	0.98	0.08	1.09
i-5-12:1	0	0	0	0.21	0
3-OH-10:0	0	0	0	0.13	0.24
i-12:0	0	0	0	0.11	0
12:0	6.45	9.44	8.71	0.53	2.49
i-3-OH-11:0	0	0	0	0.12	1.46
3-OH-11:0	0.56	0.15	0.63	0.41	5.64
i-13:0	0	0	0	0.26	0
ai-13:0	0	0	0	0.93	0
13:0	1.54	2.42	2.31	0.25	1.03
i-3-OH-12:0	0.29	0-10	0.15	0	1.44
3-OH-5-12:1	0	0	0	0	1.33
3-OH-12:0	0	0	0.12	0	1.21
i-14:0	0.98	1.17	0.31	3.52	0
7-14:1	0	0	0	0.41	0.31
14:0	4.49	8.57	8.21	5.38	2.61
i-3-OH-13:0	0	0	0	0	1.10
3-OH-13:0	0.30	0.42	0.25	0	0.29
i-15:0	2.52	6.21	3.52	0.57	0.67
ai-15:0	1.26	0.56	0.76	7.31	1.34
8-15:1	0	0.86	0	0.90	0.49
15:0	2.38	8.74	1.91	5.46	10.92
3-OH-14:0	4.35	3.12	3.58	0	0.36
i-7-16:1	0	0.26	0	0.15	0
i-16:0	1.19	3.37	1.39	7.65	1.58
7-16:1	3.09	4.52	3.55	4.18	0.85
16:0	21.04	12.63	17.21	10.31	13.95
i-3-OH-15:0	6.31	6.27	5.68	0	0.55
3-OH-15:0	0.42	0.69	0.59	0	0.30
i-17:0	0.58	0.13	0.63	3.84	0.36
8-17:1	0	0	0	0	3.64
ai-17:0	0	0	0	9.16	0
10-17:1	0	0.17	0	1.28	2.91
17:0	0.84	0.38	0.25	0.54	20.83
3-OH-16:0	0.41	0.42	0.63	0	0
9-18:1	3.92	9.25	8.28	9.56	3.22
i-18:0	0	0	0	1.24	0
11-18:1	0	4.13	3.42	3.50	0
18:0	8.09	11.62	9.39	7.32	8.49
i-10-19:1	0	0	0	0	1.03
i-19:0	0	0	0	3.12	0.28
ai-19:0	0	0	0	6.18	0
10-19:1	0	0	0	0.20	2.90
19:0	0.15	0	0	0.17	0.92
i-20:0	0	0	0	1.46	0

Methylobacterium sp. No. 5	Pedodermatophilus paradoxus	Renobacter vacuolatum			Spirosoma linguale
		NP-300-W	NP-300-G	VZ-9	
0	0	0	0	0.21	0.56
0	0	0	0.17	0.14	0.75
0.42	0.13	0.13	0.24	0	0.31
0.84	0.10	0.29	0.35	1.46	15.46
0.88	0	0.17	0	0.21	0.31
0.42	0.14	2.28	0.17	0.95	3.85
0.09	0.22	0	0	0.37	0
0	0.12	0.16	0	0.24	0
0	0.11	0.24	0	0	0.13
3.10	0.62	3.98	1.62	3.71	6.92
0	0.15	0.34	0	0.22	0.12
3.81	0.11	0	0.08	0.26	0.63
0.89	0.21	0	0	0.58	0
0.22	0.71	0.34	0	0.94	0
1.98	0.31	2.03	2.08	1.39	1.85
0.74	0	0	0	0.36	0.31
0	0	0	0	0.95	0.17
0	0.13	1.28	0	0.55	0
3.48	5.33	1.64	0.63	0.76	1.46
0.98	0.11	1.77	0.17	0.33	0
8.19	3.60	3.67	2.64	2.38	5.15
0	0	1.19	0	0	0
1.41	0	0	0	0.42	0.25
2.67	0.27	3.23	3.11	1.74	4.47
0.90	14.06	3.54	4.37	2.73	3.28
0	0.32	0	0.42	0.31	0.07
7.51	3.46	6.67	5.15	8.44	3.56
0.86	0	0	0.24	1.41	6.17
2.37	0.36	1.24	0	0	0
4.35	8.00	6.82	3.46	2.18	3.74
3.16	1.38	1.96	1.41	0.92	4.07
21.14	6.65	18.62	18.68	15.37	17.42
0	0	0.14	2.47	2.15	3.29
0.35	0	0.67	0.80	0.48	0.24
0.51	5.31	0.18	0.31	0.94	0.84
1.43	0	0.05	0	0	0.15
0.83	11.76	1.46	0	0.43	0
0.17	0.75	0.18	0.39	0.31	0
0.29	3.34	1.25	0.17	0.24	0.56
0	0	0	0.56	0.85	0.93
12.39	1.73	6.57	1.41	0.86	1.48
0.18	2.53	0	0.91	0	0
1.46	0.32	0	0.27	0.30	0
9.43	6.30	17.32	21.23	29.08	8.57
0	0	0	0	0	0
0	4.35	2.89	0.15	0.42	0
0	5.41	3.38	0.91	0.66	0
1.15	0.80	0	0	0	0
0.96	1.02	1.07	1.37	2.28	0
0	1.38	0.58	0	0	0

Fatty acid[a]	Arcocella aquatica	Blastobacter novus	Flectobacillus major	Geodermatophilus obscurus	Hyphobacter diversus
11-20:1	0	0	0.58	0.28	0
20:0	1.96	0.67	1.35	1.31	0.97
i-21:0	0	0	0	0.08	0
21:0	0	0	0	0.59	0
i-22:0	1.14	0.46	0.98	0	0
13-22:1	0.15	0	0.12	0	0
22:0	0.30	0.13	0.48	0.47	0.42
i-24:0	0.32	0	0.19	0.12	0.07
15-24:1	0.84	0	0.90	0	0.42
24:0	0.61	0.41	0.34	0.45	0.36
i-26:0	0	0	0	0	0
17-26:1	0	0	0	0	0
26:0[b]	0	0	0.08	0.07	0

[a] First number, number of carbon atoms in the chain; second number, number of double bonds; number before the hyphen, position of double bond or hydroxy group; i = iso-acid; ai = anteiso-acid; OH = hydroxy acid.

[b] By means of SIM (m/z = 55 and 74) some peaks were identified that have retention times corresponding to 28:1 and 28:0.

genus *Renobacter*, the presence of 28:1 and 28:0 acids was suggested on the basis of the occurrence of ions of m/z 55 and 74 (base peaks for saturated and monounsaturated FAMEs). By using single ion monitoring (SIM), we were able to detect the acids up to C_{28} in two strains, which is nine carbon atoms higher than previously reported.
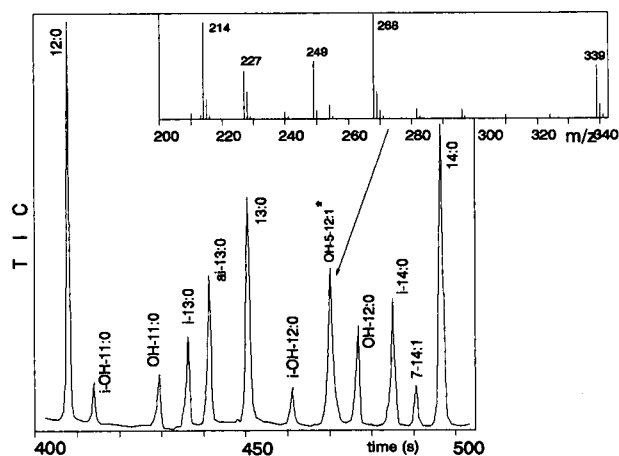
Fig. 1. Partial GC–MS of TMS-oxazolines from *R. vacuolatum* VZ-9. Mass spectrum of tentative FA (3-OH-5-12:1) is shown at the top. Proposed structures of ions from the mass spectrum: m/z 339, M^+; m/z 324, $M - CH_3$; m/z 310, $M - C_2H_5$; m/z 296, $M - C_3H_7$; m/z 282, $M - C_4H_9$; m/z 268, M − chain from C_8 to C_{12}, e.g., C_5H_{11}; m/z 254, M − chain from C_7 to C_{12}; m/z 249, M − TMSOH; m/z 240 M − chain from C_6 to C_{12}; m/z 228, M − chain from C_5 to C_{12}; m/z 227, chain from C_3 to C_{12}; m/z 214, M − chain from C_4 to C_{12}. On the basis of the above fragmentation pattern of the derivatized FA the structure 3-hydroxy-5-dodecenoic acid is proposed.

Methylobacterium sp. No. 5	Pedodermatophilus paradoxus	Renobacter vacuolatum			Spirosoma linguale
		NP-300-W	NP-300-G	VZ-9	
0	0.11	0.07	0.74	0	0
0.37	5.09	0.95	8.85	2.65	1.01
0	0.71	0	0	0	0
0	1.51	0	0	0	0
0	0	0.13	0.55	0.91	0.23
0	0	0.14	0.33	0.58	0.07
0.07	0.53	0.84	6.42	0.52	0.44
0	0.11	0.17	0.91	0.31	0.25
0	0	0	1.14	1.88	0.49
0	0.27	0.37	3.15	3.01	0.35
0	0	0	0.36	0.48	0
0	0	0	0.85	0.20	0
0	0.07	0	0.76	0.83	0.09

In conclusion, the most important feature of this work is the detailed description of new FAs, exceeding several times the number of FAs identified previously in oligotrophic bacteria. No significant differences in either the separation or the proportion of the compounds were observed on comparing the chromatographic properties of FAMEs and oxazolines.

REFERENCES

1 P. Hirsch, *Annu. Rev. Microbiol.*, 28 (1974) 391.
2 J. M. Poindexter, *Microbiol. Rev.*, 76 (1981) 123.
3 E. Fautz, G. Rosenfelder and L. Grotjahn, *J. Bacteriol.*, 140 (1979) 852.
4 W. R. Mayberry, *J. Bacteriol.*, 147 (1981) 373.
5 A. Sonesson, E. Jantzen, K. Bryn, L. Larsson and J. Eng, *Arch. Microbiol.*, 153 (1989) 72.
6 Y. Suwa and T. Hattori, *J. Gen. Appl. Microbiol.*, 32 (1986) 451.
7 Y. Suwa, and T. Hattori, *Soil. Sci. Plant. Nutr.*, 33 (1987) 235.
8 L. V. Andreev, V. N. Akimov and D. I. Nikitin, *Folia Microbiol.*, 31 (1986) 144.
9 T. Řezanka, M. Yu. Sokolov and I. Viden, *FEMS Microbiol. Ecol.*, 73 (1990) 231.
10 T. Řezanka and M. Yu. Sokolov, *J. Chromatogr.*, 508 (1990) 275.
11 P. Hirsch and S. F. Conti, *Arch. Microbiol.*, 48 (1964) 339.
12 Q. T. Yu, B. N. Liu, J. Y. Zhang and Z. H. Huang, *Lipids*, 23 (1988) 804.
13 A. P. Tulloch, *Lipids*, 20 (1985) 652.
14 J. Y. Zhang, Q. T. Yu, Y. M. Yang and Z. H. Huang, *Chem. Scr.*, 28 (1988) 357.
15 Q. T. Yu, B. N. Liu, J. Y. Zhang and Z. H. Huang, *Lipids*, 24 (1989) 79.
16 E. A. Bishop and K. Still, *Biophys. Res. Commun.*, 7 (1962) 337.
17 J. F. Dormaar, *Can. J. Soil Sci.*, 62 (1982) 487.
18 D. I. Nikitin, O. Yu. Vishnewetskaya, K. M. Chumakov and I. V. Zlatkin, *Arch. Microbiol.*, 153 (1990) 123.

Characterization of nitrogen-containing aromatic compounds in soil and sediment by capillary gas chromatography–mass spectrometry after fractionation

WILLIAM C. BRUMLEY*, CYNTHIA M. BROWNRIGG and GEORGE M. BRILIS

US Environmental Protection Agency, Environmental Monitoring Systems Laboratory, P.O. Box 93478, Las Vegas, NV 89193–3478 (USA)

(First received February 19th, 1991; revised manuscript received May 3rd, 1991)

ABSTRACT

Nitrogen-containing aromatic compounds (NCACs) are characterized in soil and sediment by full-scan capillary gas chromatography–mass spectrometry under electron ionization. The approach makes use of fractionation of methylene chloride extracts based first on partitioning of the basic compounds into acid. The neutral NCACs are then isolated by preparative thin-layer chromatography which serves to separate them from the bulk of the polynuclear aromatic hydrocarbons. NCACs can then be determined using deuterated internal standards to 100 μg/kg or below. Examples of determinations in sediment and creosote-contaminated soil are given. An advantage of the two-step fractionation scheme is the chemical separation of azaarenes and cyanoazaarenes of the same elemental composition which facilitates identification of compound class and simplifies chromatographic separations.

INTRODUCTION

The occurrence of nitrogen-containing aromatic compounds (NCACs) as environmental pollutants has been the subject of growing concern [1–3]. Interest in NCACs parallels interest in polynuclear aromatic hydrocarbons (PNAs) [4–6] because many of these compounds are mutagenic, carcinogenic [7] and toxic, especially to marine biota [8].

The presence of NCACs in sediments and soils can often be attributed to creosote contamination [3]. Indeed, many designated Superfund sites are a result of wood treatment activities involving creosote [9]. Of 1207 recent sites listed by category, about 5% were concerned with wood preservation. Creosote itself has been the subject of analytical investigation by several workers [1,3,6]. In the context of determining NCACs in sediments of Eagle Harbor, Puget Sound, Krone *et al.* [3] compared analyses of sediment directly to analyses of creosote extracts. Wright *et al.* [1] compared NCACs in synthetic fuels to those found in creosote. Nestler [10] characterized the major compounds of creosote, a coal tar distillate, which included PNAs, NCACs, and oxygen-containing and sulfur-containing aromatic compounds.

Sediments have been the focus of investigation in the U.S. and in Canada [2,3].

The analytical problem presented by NCACs is their determination in the presence of hunderds of other compounds including PNAs and alkyl hydrocarbons. This problem has been approached by using column chromatography to produce fractions enriched in the NCACs [11]. Thus, Wright *et al.* [1] and Krone *et al.* [3] have employed silica and alumina columns to afford enriched fractions. The disadvantage of column chromatography is the time-consuming need to standardize the column and the large volume of solvents used [12]. Onuska and Terry [2] employed a simple chemical separation based on partitioning of the basic compounds into acid.

Identification and quantitation usually rely on capillary gas chromatography–mass spectrometry (GC–MS) with appropriate internal standards. Levels of NCACs in the range of 10 μg/kg to 20 mg/kg have been reported for sediments [2,3] with levels 10^2–10^3 times greater in creosote itself [3]. Typically, three classes of functional groups are found among NCACs in the environment: (a) tertiary nitrogen in the aromatic ring (*e.g.*, acridine); (b) secondary nitrogen derived from indole/carbazole; and (c) nitrile-containing aromatics (*e.g.*, cyanonaphthalene). Primary amines such as anilines do not occur appreciably in the context of these investigations, and this is possibly due to their appreciable water solubility and to their low initial concentration in sources of contamination such as creosote.

Other instrumental and chromatographic methods have been applied to the determination of NCACs. GC–nitrogen-phosphorous detection has been effectively employed as a screening tool [2]. An alternative element-specific detection can be used that is based on atomic emission spectroscopy with a microwave-induced plasma (GC–AES or GC–MIP, respectively) [13]. High-performance liquid chromatography with UV–visible or fluorescent detection can also serve to quantitate PNAs and NCACs [14]. Thin-layer chromatography (TLC) has long been employed in monitoring PNAs and NCACs [15–17], and Snook *et al.* [18] have isolated NCACs from tobacco smoke using silicic acid and gel chromatographies.

Current methods promulgated in the US Environmental Protection Agency (EPA) SW-846 manual [14] do not address most of the NCACs routinely encountered in contaminated sediments and soils. In order to address this need, development and evaluation of methodology to determine NCACs is needed [9].

In this paper we present the results of the analyses of sediments and soils for NCACs. After Soxhlet or sonication extraction, a separation scheme yielding two fractions is used. The basic fraction (class a) is prepared by extraction of the methylene chloride extract with HCl and subsequent repartitioning into methylene chloride after adjusting to a basic pH. The remaining neutral fraction (classes b and c) is isolated by preparative TLC and recovered into methylene chloride. The choice of internal standards is presented as well as compound structures likely to be encountered.

EXPERIMENTAL

Sample preparation

Sediments. Sediment samples from Eagle Harbor, Puget Sound, WA, were subjected to standard US EPA methodology, *i.e.*, SW-846 [14]. Briefly, this involves a hexane—acetone Soxhlet extraction and a gel permeation chromatography cleanup step. Final concentration of extracts of 20–100 g samples was to 0.5 ml methylene chloride.

Soils. Soil samples from Spotsylvania, VA (L. A. Clark site) were subjected to standard US EPA methodogy, *i.e.*, SW-846 [14]. Briefly, 2-g samples were extracted using either Soxhlet or sonication methods. Final concentration of methylene chloride extracts was to 5.0 ml.

Fractionation

Methylene chloride extracts (0.5 ml) were extracted three times with 0.5 ml of 6 *M* HCl. The HCl fraction was taken to pH 14 with 6 *M* NaOH and extracted three times with methylene chloride. This methylene chloride fraction was dried by passing it through a column of Na_2SO_4 and was then concentrated to 100 μl using nitrogen, and was fortified with internal standards. The neutral fraction was applied to a preparative TLC plate (1-mm film thickness, 20 × 20 cm, E. Merck) with preconcentration layer. Developing solvent was methylene chloride–hexane (30:70) after pre-equilibrating the tank. The appropriate R_F range was defined by standards of 1,4-dicyanobenzene and 9-methylcarbazole as R_F = 0.05–0.32 and scraped after evaporation of solvent. The scrapings were extracted with methylene chloride, filtered, and concentrated to 100 μl under a nitrogen steam. Internal standards were added to the final extract.

Internal standards and response factors

A spiking solution of nominally 20–40 ng/μl consisted of [$^2H_7$] 3-picoline, [$^2H_7$]quinoline, [$^{13}C_1$]indole, [$^2H_9$]acridine, [$^2H_8$]naphthalene and [$^2H_{10}$]phenanthrene. Response factors for available standards were determined using a series of standard solutions *versus* a spiking solution. Response factors for tentatively identified compounds not confirmed by standards were estimated using the available data and chemical reasoning based on similar structures.

Chemicals

[$^2H_7$]3-Picoline, [$^2H_7$]quinoline, [$^{13}C_1$]indole and [$^2H_9$]acridine were obtained from Cambridge Isotope Laboratories. [$^2H_8$]Naphthalene, [$^2H_{10}$]phenanthrene were obtained from the US EPA repository. The following compounds were obtained from Aldrich: quinoline, isoquinoline, 2-methylquinoline, benzonitrile, indole, 3-picoline, 2,4,6-collidine, 8-methylquinoline, 4-methylquinoline, 6-methylquinoline, 2,4-dimethylquinoline, 2,8-dimethylquinoline, 1-methylisoquinoline, 2-phenylpyridine, 3-methyl-2-phenylpyridine, 7,8-benzoquinoline, phenanthridine, carbazole, 9-cyanophenanthene, 2-phenylquinoline 2,4-lutidine, 2,6-lutidine, 1-cyanonaphthalene and 1,4-dicyanobenzene.

GC–MS

Electron impact mass spectra were obtained on a Finnigan-MAT 4023 repetitively scanned from m/z 50 to 450 in 1 s under data system control of a INCOS 2300 (Nova 4X, software Rev. 6.1). Gas chromatography was accomplished with a DB-5 (J & W) column (30 m × 0.32 mm I.D.) programmed from 60 to 300°C at 20°C/min using splitless injection at 220°C. Emission current was 0.50 mA at 70 eV, temperature of the source was 270°C, while that of the transfer line and separator was 250°C; conversion dynode voltage was 3 kV, multiplier was set at 1000 V and preamplifier set at 10^{-8} A/V. Flow-rate was 38 cm/s He at 60°C oven temperature.

Accurate mass measurements

A 1.0-μl sample was introduced by capillary GC–MS using a 30 m × 0.25 mm I.D. SPB-5 Supelco column with 0.25 μm film thickness operated at 60°C for 3 min followed by temperature programming at 20°C/min to 300°C; flow-rate was 40 cm/s He at 60°C; sample was injected on column using a deactivated 1 m × 0.53 mm I.D. column as a retention gap. Accurate mass measurements were made on a VG 7070 EQ operated at 3000 resolution (15% valley) scanned from 250 to 150 at 3 s/dec under data system control (11–250, 11/24 based system, version 3.0, B22 tasks) and the following conditions: emission current, 0.1 mA; electron energy, 70 eV; source temperature, 180°C.

RESULTS AND DISCUSSION

GC–MS

Fig. 1 and 2 illustrate the chromatograms of total-ion current for the HCl and neutral fractions of NCACs from a soil heavily contaminated by creosote. Selected compound classes are labeled in order to facilitate comparison of retention behavior and relative amounts of NCACs present. The major components of the HCl fraction are benzoquinoline, acridine, 2-methylquinoline, azapyrenes or isomers, methyl acridines or isomers and azachrysenes or isomers. The major component of the neutral fraction is carbazole with lesser amounts of 1-cyanonaphthalene, methylcarbazoles and cyanophenanthrenes or isomers.
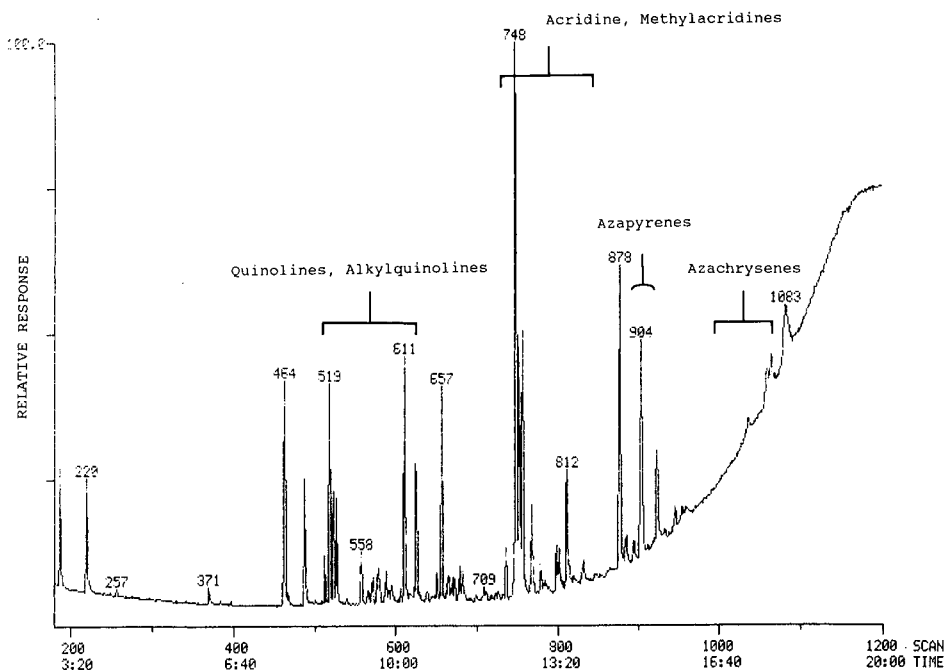
Fig. 1. GC–MS total-ion current chromatogram of the HCl fraction from a creosote-contaminated soil. Retention time in min:s.
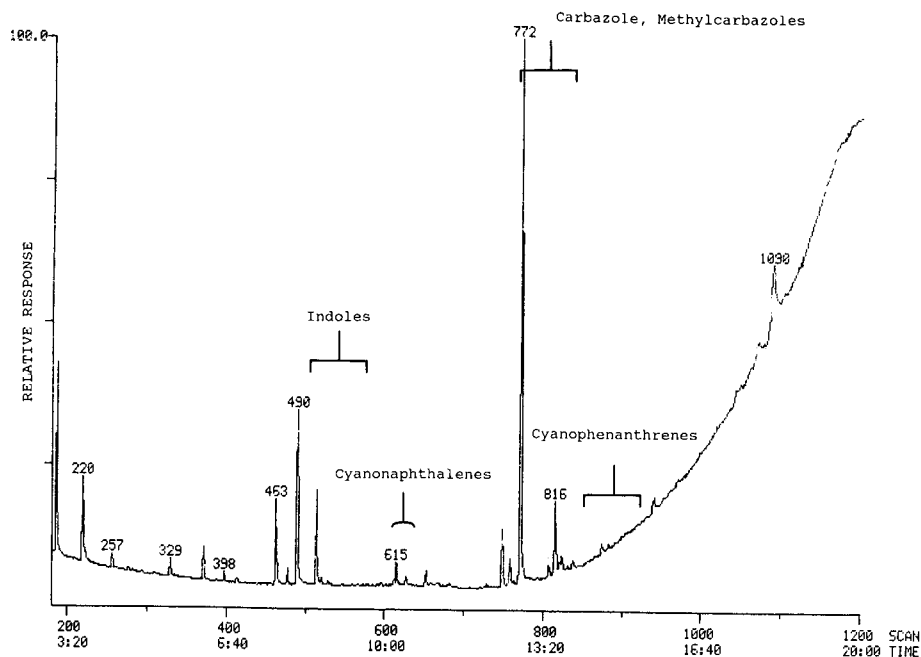
Fig. 2. CG–MS total-ion current chromatogram of the neutral fraction of a creosote-contaminated soil. Retention time in min:s.

A broad spectrum of NCACs was considered in characterizing samples. Table I summarizes compound classes divided into the HCl fraction and the neutral fraction. A minor number of NCACs containing sulfur or oxygen are included. One advantage of the fractionation is the ability to chemically separate isobaric and isotopic ions such as cyanophenanthene and azapyrene (molecular mass, M_r = 203). Not all of these classes are found as significant components in samples. A routine monitoring program will likely be limited to representative compounds or to those that are of special interest because of their extreme toxicity.

Quantitative results

Table II presents quantitative results for the compounds monitored using a contaminated soil sample as an example. These data are again divided into the HCl and neutral fractions.

In the HCl fraction quinoline and isoquinoline (M_r = 129) were found. About eight isomers of methylquinolines, six isomers of dimethylquinolines and eight isomers of trimethylquinolines (M_r = 171) were observed. Four compounds of M_r = 179 were observed including 7,8-benzoquinoline, acridine, phenanthridine, and presumably, another benzoquinoline. Usually, three isomers of M_r = 203 and two isomers of M_r = 229 were observed in sample extracts. Azafluorene, azabenzofluorenes, phenylpyridine and methylphenylpyridines, and phenylquinolines were found. Quinolinol and methylquinolinol were oxygen-containing NCACs discovered.

In the neutral fraction, 1-cyanonaphthalene and 2-cyanonaphthalene were found. Benzothiazole was observed in this fraction as well. Usually, three isomers of

TABLE I

KINDS OF NCACs CONSIDERED FOR TARGETS OF GC–MS

Representative compounds are given. Other isomers are implicit.

HCl fraction	M_r (with alkyl derivatives)	Neutral fraction
Pyridine	79 (93, 107, 121)	
Quinoline	129 (143, 157, 171)	
Benzoquinoline, acridine, phenanthridine,	179 (193, 207)	Cyanobiphenyl
Azapyrene, azafluoranthene	203 (217)	Cyanophenanthrene
Azachrysene	229 (243)	Cyanophenylnaphthalene
Phenylpyridine	155 (169)	
Phenylquinoline	205 (219)	
Diphenylpyridine	231	
Azafluorene	167 (181, 195)	Carbazole
Dibenzoacridine	279	
Quinolinol	145 (159)	
Acridone	195	
	103 (117, 131)	Benzonitrile
	153 (167)	Cyanonaphthalene
	227	Cyanopyrene
	253	Cyanochrysene
	117 (131)	Indole
	217 (231)	Benzocarbazole
	267	Dibenzocarbazole
	135	Benzothiazole
	185	Dibenzothiazole
	235	Naphthobenzothiazole
	191	Benzo[def]carbazole, cyanofluorene

methylcarbazole were present in sample extracts but no 9-methylcarbazole. In addition, cyanophenanthrene/anthracenes, cyanopyrenes and cyanofluorene compounds were observed. Benzocarbazole responses were noted as well as a $M_r = 229$ compound of unknown structure not expected in this fraction (*i.e.*, an azachrysene would be in the HCl fraction). This M_r could represent a cyanophenylnaphthalene for example. On a weight basis, these responses are individually about 1–10% relative to carbazole.

The retention time and internal standard reference are also included in Table II. In general, response factors for available standards exhibited relative standard deviations of less than 15%. A typical response factor plot of analyte *versus* internal standard is shown in Fig. 3 for acridine [$^2H_9$]acridine. In all cases, the area of the molecular ion was used for quantitation. Additional internal standards would be useful for late-eluting NCACs as additional analyte standards become available for further study. For example, an azachrysene standard and labeled compound would be expected to improve quantitation of similar compounds.

NCACs with similar chemical structures were found in some sediment samples from Eagle Harbor. Levels were generally 10–100 times lower than those in the con-

TABLE II

THE GC–MS DETERMINATION OF NCACs IN A CREOSOTE-CONTAMINATED SOIL

Compound	M_r	Retention time (min:s)	Amount detected ($\mu g/g$)	I.S.[a]
HCl fraction				
3-Picoline	93	3:40	−	1
2,4-Lutidine	107	5:09	0.603	1
2,6-Lutidine	107[b]	5:17	0.296	1
2,4,6-Collidine	121[b]	5:48	0.149	1
Quinoline	129	8:10	0.624	2
Isoquinoline	129	8:22	0.699	2
Methylquinoline	143	8:39	2.30	2
2-Methylquinoline	143[b]	8:44	13.3	2
Methylquinoline	143	8:48	1.74	2
8-Methylquinoline	143[b]	8:54	0.262	2
1-Methylisoquinoline	143[b]	9:00	0.816	2
6-Methylquinoline	143[b]	9:06	0.212	2
2,8-Dimethylquinole	157[b]	9:17	1.71	2
Dimethylquinoline	157	9:29	1.27	2
2,6-Dimethylquinoline	157[b]	9:37	4.43	2
2,4-Dimethylquinoline	157[b]	9:48	3.83	2
Dimethylquinoline	157	9.52	1.66	2
Dimethylquinoline	157	9:57	0.595	2
Trimethylquinoline	171	10:06	0.622	2
Trimethylquinoline	171	10:18	1.06	2
Trimethylquinoline	171	10:23	0.399	2
Trimethylquinoline	171	10:27	0.201	2
Trimethylquinoline	171	10:38	0.634	2
Trimethylquinoline	171	10:44	0.548	2
Trimethylquinoline	171	10:52	0.106	2
Trimethylquinoline	171	10:58	0.313	2
2-Phenylpyridine	155[b]	9:55	2.25	2
Methylphenylpyridine	169	10:21	2.16	2
Methylphenylpyridine	169	10:48	1.22	2
Methylphenylpyridine	169	11:11	2.19	2
Quinolinol	145	11:40	1.49	4
Methylquinolinol	159	11:58	0.307	4
7,8-Benzoquinoline	179	12:32	20.5	4
Acridine	179	12:37	30.8	4
Phenanthridine	179	12:48	1.94	4
Benzoquinoline/isomer	179	13:04	2.49	4
Methylacridine/isomer	193	12:59	4.67	4
Methylacridine/isomer	193	13:07	1.49	4
Methylacridine/isomer	193	13:18	9.63	4
Methylacridine/isomer	193	13:32	6.14	4
Methylacridine/isomer	193	13:42	3.57	4
Azafluorene	167	11:22	6.84	4
Azapyrene/isomer	203	14:46	3.11	4
Azapyrene/isomer	203	14:55	2.23	4
Azapyrene/isomer	203	15:24	10.8	4
Phenylquinoline	205	13:51	0.387	4
2-Phenylquinoline	205[b]	14:07	0.497	4
Azachrysene/isomer	229	17:16	7.53	4
Azachrysene/isomer	229	17:38	6.36	4

TABLE II *(continued)*

Compound	M_r	Retention time (min:s)	Amount detected (μg/g)	I.S.[a]
Benzoazafluorene/isomer	217	15:51	1.96	4
Benzoazafluorene/isomer	217	15:59	2.66	4
Acridone	195	–	–	4
Diphenylpyridine	231	–	–	4
Benzothiazole	135	8:04	0.119	3
Dibenzothiazole	185	12:24	1.04	4
Neutral fraction				
Benzonitrile	103	5:53	–	1
Methylbenzonitrile	117	7:06	–	1
Benzothiazole	135	8:05	0.079	3
1-cyanonaphthalene	153	10:15	3.54	2
2-Cyanonaphthalene	153	10:28	1.51	2
Carbazole	167	12:52	34.8	6
Methylcarbazole	181	13:28	0.924	6
Methylcarbazole	181	13:44	2.02	6
Methylcarbazole	181	13:51	0.433	6
Cyanophenanthrene/isomer	203	15:00	0.404	4
Cyanophenanthrene/isomer	203	15:05	0.402	4
Cyanopyrene/isomer	227	17:00	0.567	4
Cyanopyrene/isomer	227	17:05	0.790	4
Cyanobiphenyl	179	12:44	0.182	4
Dibenzothiazole	185	12:24	1.01	4
Benzo[*def*]carbazole, cyanofluorene	191	15:40	1.63	6
Benzocarbazole	217	15:53	0.117	6
Benzocarbazole	217	16:02	0.184	6
Cyanophenylnaphthalene	229	17:23	2.81	4

[a] Internal standards (I.S.): 1 = [$^2H_7$]3-picoline; 2 = [$^2H_7$]quinoline; 3 = [$^{13}C_1$]indole; 4 = [$^2H_9$]acridine; 5 = [$^2H_8$]naphthalene; 6 = [$^2H_{10}$]phenanthrene.

[b] Since not all isomers were available to us for investigation, the possibility exists that another isomer could coelute with the assigned compound. These identifications, therefore, must be considered tentative.
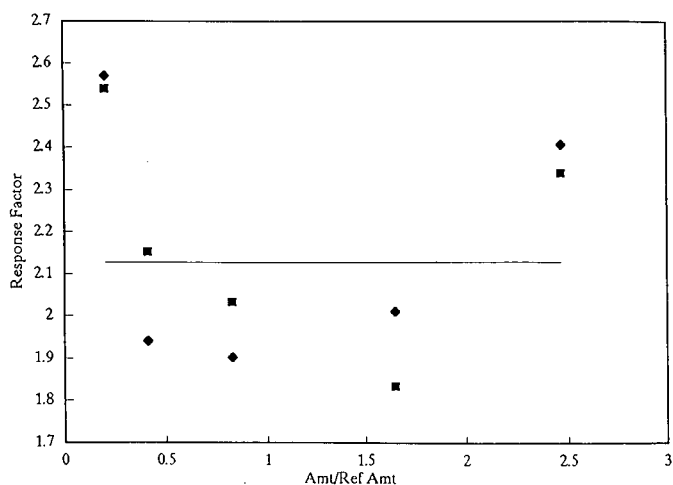
Fig. 3. Calibration plot of acridine response *versus* response of its internal standard ([$^2H_9$]acridine). Relative standard deviation = 11.9%. Amt/Ref Amt = ng of analyte/ng of I.S. ◆ and ■ are duplicate injections of the same solution.

taminated soils. As a typical example of contamination levels in one of these sediments, the following major components are reported in μg/kg: acridine (43.7), methylacridine (6.0), azapyrene (12.0), carbazole (463.0) and methylcarbazole (61.5). Other compounds were often below 5 μg/kg. Results varied depending on sampling site.

Interferences

The removal of PNAs is complete enough to allow concentration of fractions to below 100 μl. In heavily contaminated samples, the methylene chloride solution afforded by the HCl fractionation procedure (with subsequent repartitioning to organic phase) may be taken through a second round of HCl fractionation to remove any PNAs that had appreciable aqueous solubility in 6M HCl due to their initial high concentration.

The neutral fraction afforded by preparative TLC is satisfactorily free of interfering PNAs. Most PNAs and alkyl hydrocarbons had an R greater than 0.32. The TLC isolate does contain several oxygenated compounds along with NCACs. These are listed in Table III for reference purposes, and are tentatively identified as 9,10-anthraquinone ($M_r = 208$), a 4,5-carbonylphenanthrene ($M_r = 204$), two aceanthrenones ($M_r = 218$), and benzoanthrone ($M_r = 230$). To further characterize these compounds, accurate mass measurements were obtained by capillary GC–MS at 3000 resolution. The elemental compositions thus inferred were consistent with the proposed strutures. In addition, the loss of CO or CHO˙ from $M^{+˙}$ was also confirmed in each case by accurate mass measurement.

TABLE III

OXYGEN-CONTAINING AROMATIC COMPOUNDS FOUND IN THE PREPARATIVE TLC SEPARATION

Compound	M_r	Retention time (min:s)	Confirmed elemental composition
9,10-Anthraquinone or isomer	208	14:01	$C_{14}H_8O_2$
Cyclopentanone[def]phenanthrene or isomer (4,5-carbonylphenantrene)	204	14:39	$C_{15}H_8O$
Aceanthrenone or isomer	218	15:35; 15:44	$C_{16}H_{10}O$
Benzofluorenone, benzanthrone, or isomer	230	17:03	$C_{17}H_{10}O$

Recovery

Recovery studies of the common extraction techniques used for these samples have been published [14]. Recovery of analytes using the HCl fractionation has been shown to be variable but usually within the 50–90% range [2]. Initial experiments within our laboratory indicate that recovery of analytes in both the HCl and neutral fractions can be quantitative (50–90%). Further studies of analyte recovery and of potential surrogates will be published separately.

CONCLUSIONS

NCACs can be isolated and quantitated in soils and sediments using a two-step fractionation scheme based on acid–base partition of basic compounds and prepara-

tive TLC isolation of neutral compounds followed by capillary GC–MS. Co-extractives such as alkyl hydrocarbons and PNAs and effectively removed as interferences from both fractions. Major percentage contribution of reported compounds in the HCl fraction include 7,8-benzoquinoline (12%), acridine (18%), 2-methylquinoline (8%), and azapyrene (6%). With the reported compounds found in the neutral fraction, carbazole constituted 68%; 1-cyanonaphthalene, 7%; and a methylcarbazole, 4%. These compounds are implicated in toxic, teratogenic and carcinogenic effects in fish and mammals.

Future work could be addressed to a more complete investigation of various isomers of azaarenes. The application of solid-phase extraction to simplifying cleanup is also of interest. The use of TLC as a screening method for NCACs is an area largely neglected in environmental analysis. Automated sample appplication and quantitation in TLC are attractive capabilities. Finally, the information provided in this paper should help to define monitoring needed during the cleanup of designated sites by supplying the identities and the quantitative levels of compounds found in creosote-contaminated soil and sediment.

REFERENCES

1 C. W. Wright, D. W. Later and B. W. Wilson, *J. High Resolut. Chromatogr. Chromatogr. Commun.*, 8 (1985) 283–289.
2 F. I. Onuska and K. A. Terry, *J. High Resolut. Chromatogr. Chromatogr. Commun.*, 12 (1989) 362–367.
3 C. A. Krone, D. G. Burrows, D. W. Brown, P. A. Robisch, A. J. Friedman and D. L. Malins, *Environ. Sci. Technol.*, 20 (1986) 1144–1150.
4 A. Bjorseth (Editor), *Handbook of Polycyclic Aromatic Hydrocarbons*, Marcel Dekker, New York, 1983.
5 R. G. Harvey (Editor), *Polycyclic Hydrocarbons and Carcinogenesis (Adv. Chem. Series*, No. 283), American Chemical Society, Washington, DC, 1985.
6 L. B. Ebert (Editor), *Polynuclear Aromatic Compounds (Adv. Chem. Series*, No. 217), American Chemical Society, Washington, DC, 1989.
7 G. R. Southworth, C. C. Keffer, J. J. Beauchamp, *Environ. Sci. Technol.*, 14 (1980) 1529.
8 A. Dipple, in C. E. Searle (Editor), *Chemical Carcinogens (ACS Monograph Series*, No. 173), American Chemical Society, Washington, DC, 1976, pp. 245–313.
9 *Hazardous Waste Site Descriptions, National Priority List*, US Environmental Protection Agency, Washington, DC, HW 8.5, December 1984, and HW 10.145, August 1990.
10 F. H. M. Nestler, *Anal. Chem.*, 46 (1974) 46–53.
11 V. Lopez-Avila, S. Kraska and M. Flanagan, *Intern. J. Environ. Anal. Chem.*, 33 (1988) 91–112.
12 D. W. Later, B. W. Wilson and M. L. Lee, *Anal. Chem.*, 57 (1985) 2979–2984.
13 J. J. Sullivan and B. D. Quimby, *J. High Resolut. Chromatogr. Chromatogr. Commun.*, 12 (1989) 282–286.

14 Test Methods for Evaluating Solid Waste (SW-846), Vol. II3, U.S. Environmental Protection Agency, Washington, DC, November 1986, 3rd ed.

15 G. Zweig and J. Sherma (Editors), *Handbook of Chromatography*, Vol. I, CRC Press, Cleveland, OH, 1972.

16 E. Sawicki, T. W. Stanley, W. C. Elbert and D. Pfaff, *Anal. Chem.*, 36 (1964) 497–502.

17 E. Sawicki, H. Johnson and K. Kosinski, *J. Microchem.*, 10 (1966) 72–102.

18 M. E. Snook, P. J. Fortson and O. T. Chortyk, *Beitr. Tabakforsch. Int.*, 11 (1981) 67–78.

Gas chromatographic determination of the lewisite hydrolysate, 2-chlorovinylarsonous acid, after derivatization with 1,2-ethanedithiol

WILLIAM K. FOWLER*, DOUGLAS C. STEWART and DAVID S. WEINBERG

Southern Research Institute, P.O. Box 55305, Birmingham, AL 35255–5305 (USA)

and

EMORY W. SARVER

US Army Armament, Munitions and Chemical Command, Chemical Research, Development and Engineering Center, Aberdeen Proving Ground, Edgewood Area, MD 21010–5423 (USA)

(First received December 18th, 1990; revised manuscript received May 8th, 1991)

ABSTRACT

The primary hydrolysate of the toxic military agent lewisite (2-chlorovinylarsonous acid, or CVA) can be determined in trace concentrations by gas chromatography with flame-photometric detection after the CVA has been derivatized with 1,2-ethanedithiol to form a stable cyclic disulfide. The method has been shown to be applicable to the analysis of water samples that contain CVA in low ppb (10^9) concentrations. In addition, the method was demonstrated to be at least potentially useful for lewisite vapor determinations in air at sub-ppb levels in situations where any CVA found in the sampler can be assumed to have been formed from lewisite. Relative to the other procedures that are available for determining lewisite or CVA, this procedure is more sensitive, more specific for the analyte or simpler to perform.

INTRODUCTION

The high toxicity of lewisite (2-chlorovinyldichloroarsine) and its potential for use as a military chemical agent have prompted numerous attempts to develop analytical methods for determining this compound at trace levels in environmental matrices. However, lewisite's thermal lability and its nearly instant hydrolysis to the non-volatile 2-chlorovinylarsonous acid (CVA) on contact with moisture virtually preclude the use of gas chromatography for the direct determination of the agent [1].

The hydrolysis of lewisite is complex, involving several products that are in equilibrium with one another [2]. But CVA is always formed rapidly in the first step at pH levels above 1:

$$Cl-CH=CH-AsCl_2 + 2H_2O \underset{}{\overset{(fast)}{\rightleftharpoons}} Cl-CH=CH-As(OH)_2 + 2HCl \qquad (1)$$
$$\text{(lewisite)} \qquad\qquad\qquad \text{(CVA)}$$

$$Cl-CH=CH-As(OH)_2 \underset{\text{(slow)}}{\rightleftharpoons} H_2O + Cl-CH=CH-AsO \underset{\text{(slow)}}{\rightleftharpoons} (Cl-CH=CH-AsO)_x$$

CVA is essentially non-volatile, and its occurrence has never been reported except as a hydrolysis product of lewisite. Indeed, lewisite almost certainly hydrolyzes to CVA rapidly after contract with the human body, so that many (if not most) of the toxic properties associated with lewisite can be presumed to be, in reality, those of CVA. Accordingly, efforts to develop analytical methods for determining "lewisite" are typically based on the detection of either intact lewisite or CVA, whichever is most appropriate to the circumstances at hand.

Waters and Williams [2] found that CVA would decompose in cold caustic alkali as follows:

$$Cl-CH = CH-As(OH)_2 + OH^- \rightarrow As(OH)_3 + Cl^- + C_2H_2 \tag{2}$$

In cold solution (16°C), only alkaline conditions of pH 10.5 or greater would bring about this decomposition, but at 50°C, solutions of pH 9 or greater were effective. Prolonged boiling with water alone brings about some decomposition [2].

Thus, one of the most sensitive and specific methods now available for determining lewisite is an indirect approach based on the gas chromatographic (GC) determination of the acetylene that forms during the alkaline decomposition of CVA [1,3]. However, we have found that quantitative recovery and introduction of the liberated acetylene into a gas chromatograph is difficult. Moreover, the method is not useful for any samples that contain acetylene as a background constituent.

A more rugged and reliable method for determining lewisite is based on the reversed-phase high-performance liquid chromatographic (HPLC) determination of CVA with either electrochemical or ultraviolet (UV) spectrometric detection at 225 nm [4]. The detection limit of this method for CVA, based on a signal-to-noise ratio of 3 ($S/N = 3$), is approximately 2 ng in an injected 100-μl water sample (20 ng/ml) when UV detection is used.

Other less specific methods have been used to determine lewisite and CVA. For example, graphite-furnace atomic absorption spectrometry (GFAAS) provides a sensitive response to decomposed CVA [5], and molybdenum-blue spectrophotometry accurately quantifies the arsenite ion (as arsenate) that is released in the alkaline decomposition of CVA according to reaction 2 above [6]. But these techniques are not applicable to trace determinations when interfering substances are present.

Eagle and Doak [7] reviewed the large amount of work on thioarsenites derived from the reaction of alkyl arsonous oxides and alkyl mercaptan. This reaction is given by reaction 3:

$$RAsO + 2R'SH \rightleftharpoons RAs(SR')_2 + H_2O \tag{3}$$

The analytical method reported here is an indirect GC determination of CVA based on its reaction with 1,2-ethanedithiol (EDT) to form the more stable and volatile cyclic disulfide, 2-(2-chlorovinyl)-1,3,2-dithiarsenoline (CDA) [8]:

$$Cl-CH = CH-As(OH)_2 + HS-CH_2-CH_2-SH \rightarrow$$
$$\text{(CVA)} \qquad\qquad\qquad \text{(EDT)}$$

$$Cl-CH = CH-\overline{As-S-CH_2-CH_2-S} + 2H_2O \tag{4}$$
$$\text{(CDA)}$$
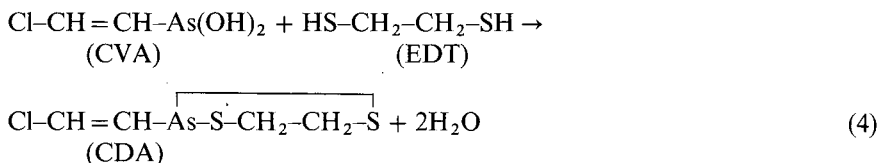
A sulfur-specific flame-photometric detector (FPD) is used to provide a sensitive and selective response to CDA. The detection limit of the method —about 5.5 ng of CVA per milliliter of aqueous sample (based on $S/N = 3$)— is about fourfold lower than that given for the HPLC method. However, the detection limit undoubtedly could be lowered significantly in situations where some loss of precision and accuracy can be tolerated.

EXPERIMENTAL

Neat liquid lewisite was supplied by the US Army as Lot No. L-U-6206-CTF-N; the purity of this material was given as 95.5 wt%. A stock standard solution of lewisite in cyclohexane or isopropanol was prepared by weighing to the nearest 0.1 mg about 40 mg of lewisite in a tared 50-ml volumetric flask and diluting to the mark with the appropriate solvent. Working standard solutions were then prepared as needed by serial dilution from the stock standard solution.

A water sample containing CVA to be used either for calibration of the GC instrument or for test purposes was prepared by injecting a few microliters of a cyclohexane or isopropanol solution of lewisite into a 5.0-ml aliquot of deionized water and agitating the resulting mixture for 15 s on a vortex mixer. During this operation, the mixture was contained in a 125 × 16 mm I.D. glass screw-capped culture tube with a PTFE liner in the cap.

A typical 5.0-ml water sample in a culture tube, fabricated as described above, was treated for analysis as follows. A 0.8-μl aliquot of neat liquid EDT (Aldrich, Milwakee, WI, USA), the purity of which was stated as 99 wt%, was first added to the sample in a fume hood, and the solution was then agitated for 15 s on a vortex mixer. After a 1.0-min waiting period to ensure that the EDT–CVA reaction had gone to completion, a 1.0-ml portion of a 2.0-mg/ml aqueous soltion of AgNO$_3$ (Morton Thiokol, Danvers, MA, USA) was pipetted into the sample solution to precipitate most of the remaining excess EDT. This was followed by another 15-s vortex-mixing step.

Next, a 1.0-ml aliquot of toluene was added to the sample for extraction of the CDA. This mixture was vortex-mixed for 30 s and allowed to equilibrate for an additional 1 min. It was then centrifuged for 2 min in a desk-top centrifuge to separate the aqueous and toluene layers and to settle out a greenish precipitate formed by the reaction between AgNO$_3$ and EDT. Amounts (μl) of the toluene layer were withdrawn by syringe and injected into the GC instrument to carry out the analysis step. The GC conditions are summarized in Table I.

A sample extract prepared in the above manner was analyzed for CDA by injection into a VG 70S GC–mass spectrometry (MS) system. The Hewlett-Packard 5890 GC that was interfaced to the mass spectrometer was equipped with a 25 m × 0.32 mm I.D. DB-5 fused-silica capillary column bearing a 0.52-μm-thick coating of the stationary phase. The injection port and transfer line were both maintained at 150°C. The column temperature was held at 45°C for 3 min, then programmed at 8°C/min to 300°C, where it was held for up to 30 min. The carrier gas (helium) flow-rate was approximately 1 ml/min.

The mass spectrometer was operated in the electron-impact mode at 30 eV. The ion source was maintained at 200°C, and the instrument was set to provide a resolution

TABLE I

GAS CHROMATOGRAPHIC INSTRUMENTAL CONDITIONS FOR DETERMINATION OF
LEWISITE AFTER ITS CONVERSION TO CDA

Instrument	Hewlett-Packard Model 5890, series II
Detector	Flame-photometric detector in the sulfur-specific mode
Column	30 m × 0.53 mm I.D. DB-5 fused-silica capillary column with a 1.5-μm-thick coating of the stationary phase
Temperatures	
Column oven	150°C for 6 min, then ramp at 60°C/min to 300°C, then hold for 3 min
Injection port	225°C
Detector	225°C
Gas flow-rates	
Carrier gas (He)	17 ml/min
Air	97 ml/min
Hydrogen	74 ml/min
Integrator/recorder chart speed	0.5, 1.0 cm/min

of 5000 (based on a 2% valley), although a problem with instrument stability precluded the full attainment of this resolution. Mass spectra were obtained by scanning from m/z 700 to m/z 35 at 1 s/decade with a 0.30-s interscan time. Sample injection volume was 0.3 μl. The original 5-ml water sample had been fortified with 455 μg of lewisite.

To test the proposed method for possible use in determining lewisite vapor collected from air, a four-day test was conducted involving the use of glass impingers (*i.e.*, bubblers) as sampling devices. The reservoir of each bubbler was filled with 5-mm-O.D. glass beads to facilitate mixing of the entrained air with the liquid sample-collection medium. With the glass beads in place, each bubbler reservoir held 15 ml of liquid collection medium.

On each of four days, therefore, each of twelve glass bubblers was charged with 15 ml of deionized water containing 100 mg of ascorbic acid to neutralize any oxidative species that could otherwise interfere with the analyses. The water aliquots had previously been fortified with lewisite to produce duplicate test solutions containing CVA at each of the following six concentrations: 0 (blank), 11.8, 59.1, 89.5, 119 and 178 ng/ml.

Each day, the charged bubblers were immersed in an aqueous ice bath, connected to a suction sampling pump, and permitted to sample room air (free of lewisite) for 12 h at a rate of 1.0 l/min, for a total of 720 l of air. After the sampling period, the bubblers were removed from the ice bath and allowed to equilibrate to room temperature before proceeding with the analysis step. Where necessary, aliquots of bubbler fluid were diluted back to their original volume with deionized water to compensate for evaporative losses during sampling; such corrections were invariably less than 1 ml per bubbler. A 5.0-ml portion of each bubbler aliquot was then taken for analysis by the procedure described above.

During this test, the GC was calibrated daily by analyzing one aqueous lewisite solution at each of the six test concentrations given above and by then performing a linear-regression analysis of the resulting response data. A 2.0-μl sample-injection volume was used throughout the test.

In all of the work reported here, all reagents and solvents were of reagent grade except as otherwise noted.

RESULTS AND DISCUSSION

One of the first tasks in the development of this method was to confirm the presence, identity and elution time of CDA in an extract of a typical lewisite-containing sample that had been treated with EDT as described here. This was accomplished by analyzing a sample extract by GC/MS. The resulting total-ion chromatogram is shown in Fig. 1, where the peaks that appear to be due to the *cis* and *trans* isomers of CDA are identified. The peak at scan No. 541 appears to be the cyclic dimer of EDT ($C_4H_8S_4$).
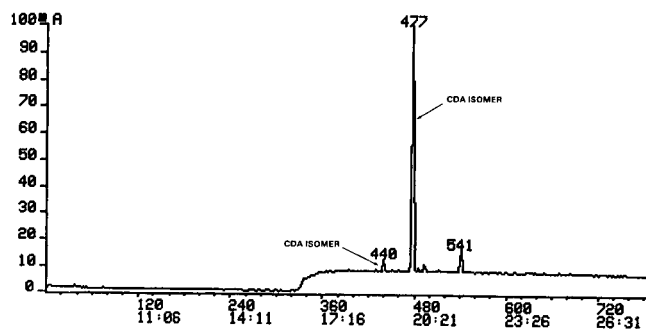
Fig. 1. Total-ion chromatogram for a water-sample extract containing CDA. Ordinate: instrumental response (arbitrary units). Abscissa: upper scale, scan No.; lower scale, time in min:s.

The mass spectra recorded at scan Nos. 440 and 477 (in Fig. 1) are presented in Fig. 2. It is to be noted that the major mass fragments in these spectra are consistent with the postulated fragmentation pattern of Fig. 3. (Although Fig. 3 depicts the *cis* isomer, essentially the same pattern is predicted for either isomer, and there appears to be no basis for identifying the isomers unambiguously from these data.) Further support for the assignments was obtained by checking the isotope peak ratios for conformity with the proposed elemental compositions of the principal ions, as synopsized in Table II.

The GC–MS retention times for the CDA isomers (*ca.* 19–21 min) were much too long for routine GC analyses; accordingly, GC conditions (Table I) were chosen to reduce the CDA retention times to less than about 5 min. This approach also had the desirable effect of merging the *cis* and *trans* isomers into a single peak so that both forms were quantified together. A typical chromatogram from the GC analysis of a lewisite-fortified water sample under the conditions of Table I is shown in Fig. 4. All of the peaks in Fig. 4 except the CDA peak were present in chromatograms obtained from blank (*i.e.*, lewisite-free) water samples. None of these extraneous peaks were identified.

The chromatographic response to residual EDT reagent (Fig. 4) was always very broad, so that the tail of the EDT peak tended to run under the CDA peak. That is, the chromatographic base line beneath the CDA peak was significantly elevated by the tail of the EDT peak. Because the sulfur-specific FPD does not respond linearly to sulfur
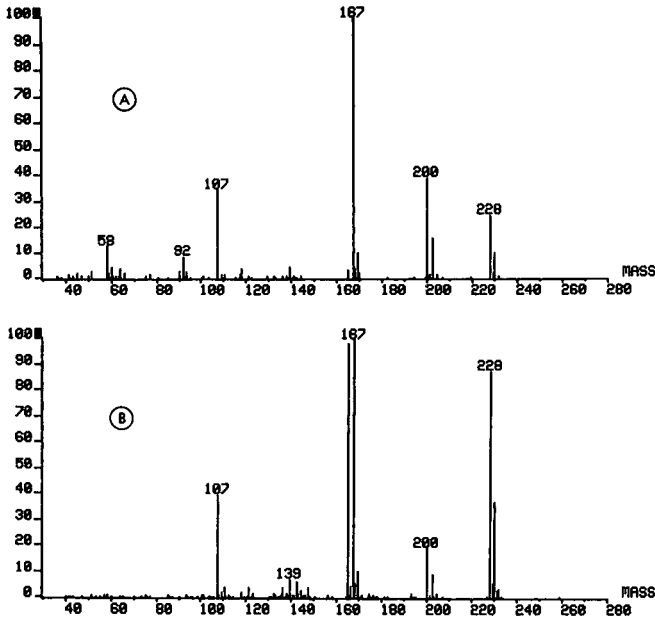
Fig. 2. Mass spectra of sample components corresponding to (A) scan No. 440 and (B) scan No. 477 in the chromatogram of Fig. 1.

compounds, the deconvolution of the CDA response from the EDT response is not a simple subtraction, as would be the case for a linear detector.

Consequently, the CDA peaks must be quantified by computing, for each CDA peak, the quantity $Z = (H_t)^{\frac{1}{2}} - (H_e)^{\frac{1}{2}}$, where H_e is the height of the response or upward baseline displacement due to EDT at the retention time of CDA and H_t is the sum of H_e and the height of the CDA peak above the EDT peak tail. Thus, the analyst must estimate the location of the true chromatographic baseline beneath the CDA peak in each chromatogram. Values of Z are directly proportional to the CDA concentrations
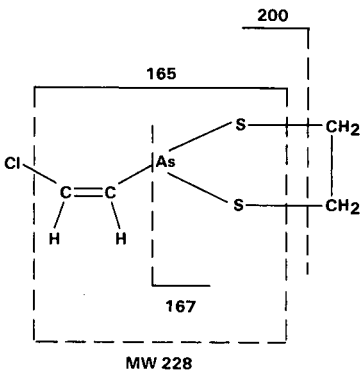
Fig. 3. Mass-spectral fragmentation of CDA. MW = Molecular weight.

TABLE II

ISOTOPE RATIO MEASUREMENTS FOR CDA[a]

Nominal mass	Proposed formulation	Relative intensity	
		Calculated	Found
228	$C_4H_6AsClS_2$	100.00	100.00
229		4.94	5.80
230		40.92	41.5
231		1.83	2.55
232		3.06	3.09
233		0.14	0.092
200	$C_2H_2AsClS_2$	100.00	100.00
201		2.24	3.67
202		40.85	46.6
203		0.92	0.787
204		3.04	5.83
167	$C_2H_4AsS_2$	100.00	100.00
168		2.24	5.16
169		8.87	9.52
170		0.20	0.21
165	$C_2H_2AsS_2$	100.00	100.00
166		2.24	3.94
167		8.87	$(102)^b$

[a] These measurements were taken from the chromatographic peak appearing at scan No. 477 in Fig. 1.
[b] The value in parentheses is high because of interference from other ions.

in the solutions from which they are derived, and only when this procedure is used are data linearity and reproducibility likely to be acceptable at low CVA concentrations. Note also that the tail of the EDT peak probably enhances the instrumental detection limit for CDA to some degree because of the non-linear detector response.

The reaction times for the CVA–EDT reaction and the EDT–AgNO$_3$ reaction were experimentally optimized. For the CVA–EDT reaction, a reaction period of 1 min yielded essentially the same response to spiked lewisite as did reaction periods of 7, 15 and 30 min. Thus, the time allotted for this reaction need not exceed 1 min. The EDT–AgNO$_3$ reaction was optimized by visual observation, since this reaction produces a visible precipitate. Because no further precipitation was observed after the addition of the AgNO$_3$ and the completion of the ensuing 15-s vortex-mixing step (described above), no additional reaction time beyond the mixing step is required.

We found that if a precipitate was not formed on addition of AgNO$_3$ to the sample mixture, then there was not enough EDT in the solution, and neat liquid EDT was therefore added in 0.2-μl increments (with vortex-mixing between increments) until the precipitate was observed. Only when a net stoichiometric excess of EDT was carried into the extraction step was a linear response to the CDA obtained from GC. Furthermore, the precipitate had to be carefully excluded from the syringe whenever an aliquot of the toluene layer was taken for analysis. Otherwise, the resulting response to CDA was found to be excessively variable. This operation was greatly facilitated by
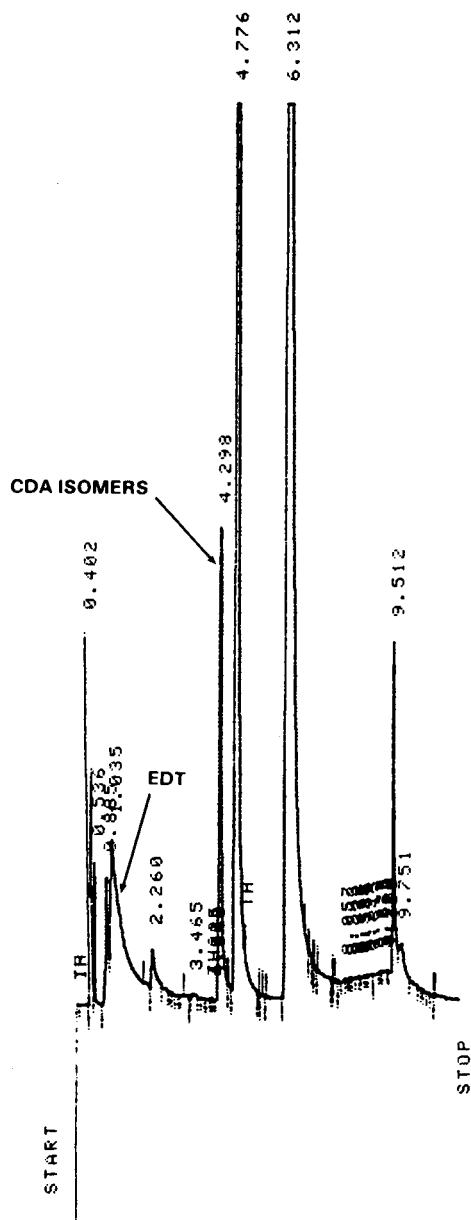
Fig. 4. Typical chromatogram from the GC–FPD analysis of the extract of a lewisite-fortified water sample after conversion of the lewisite to CDA. The lewisite concentration in the water sample was 726 ng/ml. Retention times (in min) are displayed in the chromatogram.

the prior centrifuging step, although the precipitate eventually settled spontaneously if allowed to stand for a day or so.

The efficiency with which the CDA is extracted by toluene was also estimated.

Thus, three 5.0-ml water samples were each spiked with 3.63 μg of lewisite, treated with EDT and AgNO$_3$ as detailed above, combined with 3.0 ml of toluene, and analyzed in the usual way. At the same time, another set of three water samples was treated identically except the volume of toluene was only 1.0 ml. An algebraic evaluation of the resulting GC responses indicated CDA recoveries of 96% for 3.0 ml of toluene and 90% for 1.0 ml of toluene. That the CDA extraction efficiency obtainable with 1.0 ml of toluene is at least 90% was also confirmed by extracting a spiked water sample with two successive 1.0-ml aliquots of toluene and analyzing both extracts for CDA.

In another test, we injected 1-, 2-, 3-, and 4-μl amounts of a CDA-containing toluene extract into the GC system to ascertain the effect of injection volume on the response to CDA. The CDA response per unit volume of injected sample extract was essentially constant over this volume range. Hence, a volume of at least 4 μl could be used if necessary to enhance the method detection limit.

A set of water samples that had been fortified with lewisite at different levels was analyzed by the method, and the resulting response data (Z values) were subjected to linear-regression analysis to obtain an expression for response as a function of CVA concentration. These data were produced by fortifying 5.0-ml aliquots of distilled water with varying amounts of lewisite (including zero lewisite, for use as a blank) in the manner detailed previously. The resulting samples were then analyzed by the recommended procedure. A 1.4-μl injection volume into the GC instrument was used, and all Z values were normalized to a single GC attenuation setting. The non-zero CVA solution concentrations were 28.4, 58.3, 75.6, 89.5, 120, 150 and 298 ng/ml. Moreover, the toluene extract of the sample with a CVA concentration of 120 ng/ml was analyzed eight times over a 3-h period.

The resulting least-squares slope, Y-intercept, and correlation coefficient of the curve were, respectively, 0.0202 mm$^{\frac{1}{2}}$ml/ng, -0.083 mm$^{\frac{1}{2}}$ and 0.99586, where Y was the corrected instrument response (Z value) in units of mm$^{\frac{1}{2}}$. The regression analysis included all eight measurements at 120 ng/ml; the relative standard deviation (R.S.D.) of these replicate measurements was 6.2%. In addition, the sample with the lowest non-zero CVA concentration in the group, i.e., 28.4 ng/ml, yielded an S/N of approximately 10. From this information, the detection limit for CVA in water was computed by extrapolation to $S/N = 3$ (assuming a qadratic response characteristic for the FPD) and found to be 15.6 ng/ml for a 1.4-μl injection volume, or 5.5 ng/ml for a 4.0-μl injection volume. The latter detection limit, when expressed in terms of lewisite rather than CVA, is 6.7 ng/ml.

Fig. 5 displays a chromatogram from the analysis of a water sample that had been spiked with lewisite to produce a 12.3-ng/ml aqueous CVA solution. The analysis was conducted under the conditions of Table I, and a 2.4-μl injection volume was employed. This figure illustrates the low detection limit of the method, as well as the need for correction of the signal for baseline displacement by EDT when the CVA concentration is low.

The results of simulating four days of air sampling with lewisite-fortified bubbler samplers are summarized in Table III. The lewisite recoveries at the lowest non-zero concentration exhibited a consistent positive bias of from 20 to 60%, whereas a generally smaller negative bias occurred at the other non-zero concentrations. The cause of the positive bias at low levels is not known; perhaps the ascorbic acid (which was present in the bubbler fluid but not in the calibration standards) played a role. But
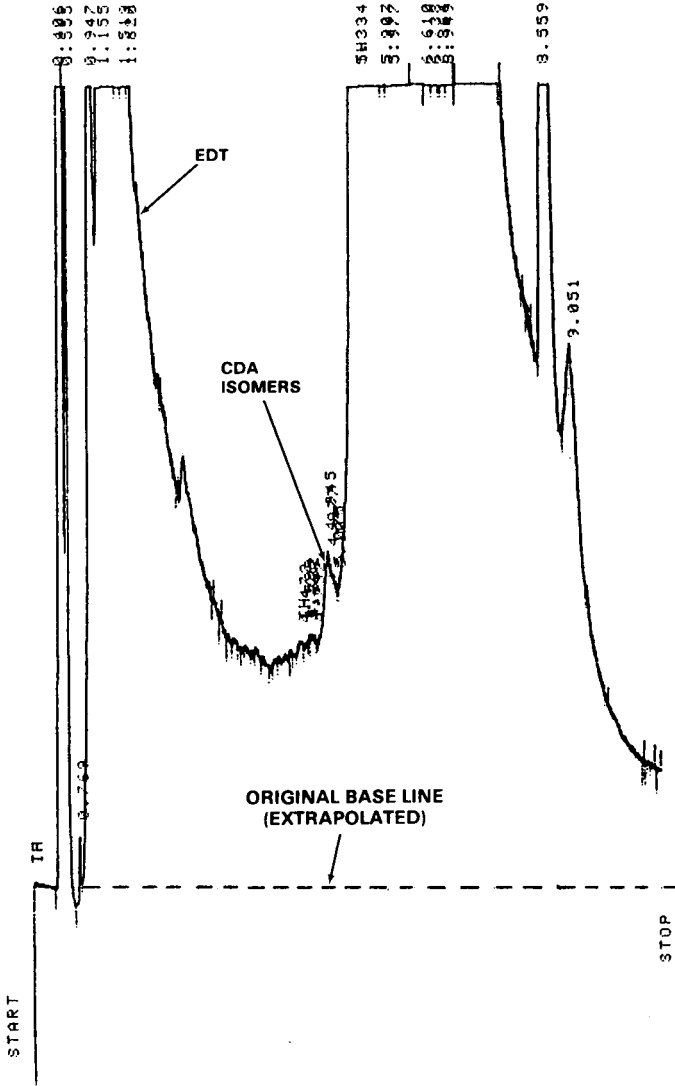
Fig. 5. Chromatogram from the analysis of a water sample that had been fortified with lewisite to produce a CVA concentration of 12.3 ng/ml. The response to the EDT derivative of CVA (*i.e.*, CDA) is indicated in the figure.

note that, because an air volume of 720 l was sampled through each bubbler, the lowest non-zero CVA concentration corresponded to the sampling of lewisite vapor at an average concentration of 0.3 ng/l, or about 35 ppt (10^{12}). For most applications at this rather low concentration level, the observed biases, although quite significant, are likely to be acceptable. Hence, the method appears to have the potential for use in the determination of lewisite vapor at trace concentration levels in air.

TABLE III

RECOVERIES OF ADDED LEWISITE FROM BUBBLERS AFTER DRAWING AIR THROUGH THE BUBBLERS

CVA solution concentration[a] (ng/ml)	Lewisite vapor concentration[b] (ng/l)	Lewisite recovery (%)			
		Day			
		1	2	3	4
0	0	—	—	—	—
0	0	—	—	—	—[c]
11.8	0.30	160	130	140	130
11.8	0.30	150	150	130	120
59.1	1.50	102	82	76	94
59.1	1.50	94	80	80	94
89.5	2.28	100	83	71	97
89.5	2.28	99	92	86	96
119	3.03	105	94	89	91
119	3.03	93	76	85	90
178	4.53	94	95	81	97
178	4.53	93	94	81	93

[a] CVA concentrations in the sample-collection media of the various bubblers.
[b] Lewisite vapor concentrations in air that would have been required in order to have collected the amounts of CVA that were actually present in the bubblers.
[c] The second blank determination on day 4 yielded a very slight non-zero response that corresponded to a CVA solution concentration of about 3 ng/ml. Note, however, that this is well below the estimated detection limit of the method.

The above study was first attempted without the use of ascorbic acid in the bubblers. But the lewisite recoveries in this case were exceedingly low (*ca.* 50%) and variable (*ca.* 25% R.S.D.). Thus, the data demonstrate that the presence of ascorbic acid in the sample-collection fluid does, indeed, improve the recovery of lewisite under these conditions, ostensibly by neutralizing an oxidizing interferant in the atmosphere.

Finally, it should be noted that the excess EDT that remains unneutralized by $AgNO_3$ going into the toluene extraction step eventually fouls the GC syringe after several hours of continuous use, causing a decrease in the GC response to CDA. But the effectiveness of the syringe can be restored by cleaning it thoroughly in a commercial acidic syringe-cleaning solution.

CONCLUSIONS

It was concluded that the method reported here is capable of determining CVA in water with high sensitivity, high specificity and adequate accuracy for most applications. An additional benefit of the method is the relatively low level of operator expertise required to use it effectively. Moreover, because of the facile hydrolysis of lewisite to the non-volatile CVA, air sampling and analysis for lewisite vapor should be possible with the use of an impinger sampler (or bubbler) charged with an aqueous sampling medium.

ACKNOWLEDGEMENTS

REFERENCES

1 Z. Witkiewicz, M. Mazurek and J. Szulc, *J. Chromatogr.*, 503 (1990) 293.
2 W. A. Waters and J. H. Williams, *J. Chem. Soc.*, (1950) 18.
3 R. J. Valis and J. E. Kolakowski, *Development and Application of a Gas Chromatographic Method for Determination of Lewisite Emissions During Incineration of Obsolete Chemical Agent Identification Sets, Technical Report ARCSL-TR-81092*, US Army Chemical Systems Laboratory, Aberdeen Proving Ground (Edgewood Area), MD, 1981.
4 P. C. Bossle, M. W. Ellzy and J. J. Martin, *Determination of Lewisite Contamination in Environmental Waters by High-Performance Liquid Chromatography, Technical Report CRDEC-TR-042*, US Army Chemical Research, Development and Engineering Center, Aberdeen Proving Ground (Edgewood Area), MD, 1989.
5 B. C. Garrett, *Flameless Atomic Absorption Spectrophotometric Analysis for Lewisite (L), Final Technical Report DPG-TR-L145P*, US Army Dugway Proving Ground, Dugway, UT, 1978.
6 W. K. Fowler, T. T. Hancock and J. J. Martin, *Anal. Lett.*, 18A (1985) 2381.
7 H. Eagle and G. Doak, *Pharmacol. Rev.*, 3 (1951) 107.
8 E. W. Sarver, unpublished results, 1974.

Determination of hexahydrophthalic anhydride in air using gas chromatography

B. JÖNSSON*, H. WELINDER and G. SKARPING

Department of Occupational and Environmental Medicine, University Hospital, S-221 85 Lund (Sweden)

(First received January 17th, 1991; revised manuscript received May 1st, 1991)

ABSTRACT

Two methods for the determination of hexahydrophthalic anhydride (HHPA) in air were developed. In a solid sorbent method, HHPA was sampled in Amberlite XAD-2 tubes, eluted in toluene and analysed by gas chromatography with flame ionization detection. The sampling rates were 0.2 and 1.0 l/min. At 15 μg/m^3 (relative humidity <2%) and 27 μg/m^3 (relative humidity 70%) no breakthrough was observed. However, at 160 μg/m^3 (relative humidity <2%), 6% breakthrough was found. The sampling efficiency of the sampling rates 0.2 and 1.0 l/min did not differ. In a bubbler method, HHPA was sampled in bubblers filled with 0.1 M sodium hydroxide solution. The sodium salt of hexahydrophthalic acid was formed. No breakthrough was observed using a sampling rate of 1.0 l/min. The samples were stable during storage for eight weeks in a refrigerator. The HHP acid was esterified with methanol–boron trifluoride and analysed by gas chromatography–flame ionization detection. Apparatus for the generation of standard atmospheres of HHPA, in the range of 10–3000 μg/m^3, was developed using the diffusion principle. For the solid sorbent method the precision (coefficient of variation) of the overall method was 2–7%, and for the bubbler method 3–19% (range 15–160 μg HHPA/m^3; relative humidity = <2–70%). A comparison between the two methods was performed using the standard atmosphere. The concentrations found by the solid sorbent method were 86–98% of those found by the bubbler method (range 15–160 μg HHPA per m^3; relative humidity = <2–70%). In work environment air, 93% was found using the solid sorbent method relative to the bubbler method at a mean concentration of 330 μg/m^3 (coefficient of variation = 39%; range 200–540 μg/m^3). For both methods, concentrations >3 μg/m^3 could be quantified at 60 min sampling with a sampling rate of 1.0 l/min.

INTRODUCTION

Hexahydrophthalic anhydride (HHPA), the saturated analogue of phthalic anhydride (PA), is used as a hardener in epoxy resins. HHPA epoxy resins have good mechanical and electronical insulation properties. Typical products made from HHPA epoxy resins are electrical capacitors and ignition systems.

It has been known for a long time that organic acid anhydrided are irritant to the eyes and to the mucous membranes in the respiratory tract [1]. HHPA has also like several other dicarboxylic anhydrides, been demonstrated to induce allergic rhinitis and asthma [2]. Studies on the chemically related methyltetrahydrophthalic anhydride [3,4] indicate that HHPA may be a sensitizing agent at low concentrations in air.

Organic anhydrides are reactive compounds. Free acids are formed by hydrolysis. The reaction with alcohols and primary and secondary amines results in the formation of esters and amides, respectively. Water is expected to be present in all work environment air. Alcohols and primary and secondary amines may also be present. The reactivity is expected to be strongly influenced by the presence of catalysts such as tertiary amines, which are also expected in the work environment. The toxicity of hexahydrophthalic acid (HHP acid) can be assumed to be low.

Some methods for the determination of acid anhydrides in air have been described in the literature. Most of them describe filter sampling methods of PA [5,6] and trimellitic anhydride [7–9]. The analyses are performed by gas chromatography (GC) or high-performance liquid chromatography (HPLC). PA has been sampled with Tenax as sorbent and analysed by GC with electron-capture detection [10]. Maleic anhydride has been sampled on XAD-2 Amberlite sorbent tubes treated with p-anisidine and analysed by HPLC [11].

Methyltetrahydrophthalic anhydride (MTHPA) has been sampled by two different methods [12]. In the first method, MTHPA was collected on XAD-2 tubes and the anhydride was analysed by GC with flame ionization detection (FID). In the second method, the anhydride was sampled in sodium hydroxide by bubblers and the corresponding acid was analysed by GC–FID, after derivatization with methanol–boron trifluoride.

The serious effects of HHPA generate a requirement for good methods of controlling the work environment. However, to our knowledge no methods of monitoring HHPA in air have been described in the literature. Moller et al. [2] reported that they have measured the concentration of HHPA in air by an impinger method from US National Institute of Occupational Safety and Health, but this method was not described. Pfäffli et al. [13] have monitored HHPA in air by a method used for the determination of PA.

In the present study two methods for the determination of HHPA in air are described and evaluated.

EXPERIMENTAL

Apparatus

For analysis of standard atmosphere samples, a Varian 3500 GC system (Varian, Palo Alto, CA, USA) equipped with a Varian FID system (time constant 50 ms), a Varian 8035 automatic on-column auto-sampler and a temperature-programmable capillary injector was used.The chromatograms obtained were evaluated with a Shimadzu C-R3A integrator (Shimadzu, Kyoto, Japan).

For analysis of work environment samples, a Carlo Erba GC system, Fractovap, Series 4160 (Carlo Erba, Milan, Italy), equipped with an FID system and on-column injector was used. The chromatograms were recorded on a BBS Goerz, Servogor 310 linear recorder.

For identification of hexahydrophthalic acid dimethylester (HHP acid-DME) a Shimadzu GC–MS QP1000 EI/CI quadrupole mass spectrometer connected to a Shimadzu GC 9A GC system was used.

Sampling rates were maintained by portable pumps: GilAir (1.0 l/min; Gilian Instrument, Wayne, NJ, USA) and MSA Model C-210 (0.2 l/min; Mine Safety Applications, Pittsburgh, PA, USA).

Relative humidity (RH) was measured by hygrometer from Solomat (MPM 2000/2013 Thermo Hygro Anemo Tachometer; Solomat, Rowayton, USA). Phase separations were achieved with a Sigma 3E-1 centrifuge (Sigma, Harz, Germany).

Sample tubes and bubblers

For sampling in the solid sorbent method, Amberlite XAD-2 tubes (cat. No. 226-30, SKC, Eigthy Four, PA, USA), and for sampling in the bubbler method 5-ml bubblers equipped with sintered glass filters (cat. No. L.9-751-1, Labglas Service, Stockholm, Sweden), were used.

Columns

Fused-silica capillary columns with chemically bonded stationary phases were used: for standard atmosphere sampling, CP-sil 8 CB (Chrompack, Middelburg, Netherlands) 25 m × 0.25 mm I.D. with a film thickness of 0.25 μm and, for work environment sampling, DB-5 (J & W Scientific, Folsom, CA, USA) 30 m × 0.32 mm I.D. with a film thickness of 1.0 μm.

Chemicals

Ethylacetate, methanol and toluene were from LabScan (Dublin, Ireland). Boron trifluoride, 14% in methanol, was from Sigma (St. Louis, MO, USA). HHPA (>98%), sodium bicarbonate, sulphuric acid, sodium hydroxide and sodium sulphate were from Merck (Darmstadt, Germany). HHP acid-DME was from SyntElec (Lund, Sweden).

Generation of standard atmosphere

HHPA in air was generated by the dynamic generation equipment shown in Fig. 1. Into a 250-ml vessel, placed in a water bath, two 4-ml test tubes containing HHPA were inserted. A stream of HHPA vapour was generated by blowing 2 l/min dried air into the vessel. The outlet was connected to a mixing chamber where the HHPA atmosphere was further diluted with air with a controlled RH. The humid air was generated by mixing dry air with air bubbled through deionized water. The outlet from the mixing chamber was connected to an all-glas 15-l cylinder which then contained the controlled atmosphere of HHPA. The RH was measured by a hygrometer. The cylinder had two outlets for simultaneous sampling. Excess air was removed through a third outlet. All connection tubes were made of PFTE (3.5–7 mm I.D.). All other equipment was glass.

Concentrations in the range 10–3000 μg/m^3 (monitored by the solid sorbent method) were generated by the equipment. The different concentrations were obtained by varying the temperature in the water bath between 35 and 90°C and the flow of dilution air between 0 and 30 l/min. Relative humidity between <2 and 90% could be generated.

Work environment atmosphere

Air samples of HHPA were collected in a plant manufacturing electrical capacitors. Except for HHPA, the plant handled MTHPA, benzyldimethylamine, epoxy resins (epichlorhydrin and bisphenol A/aniline). The RH was 16–44%.
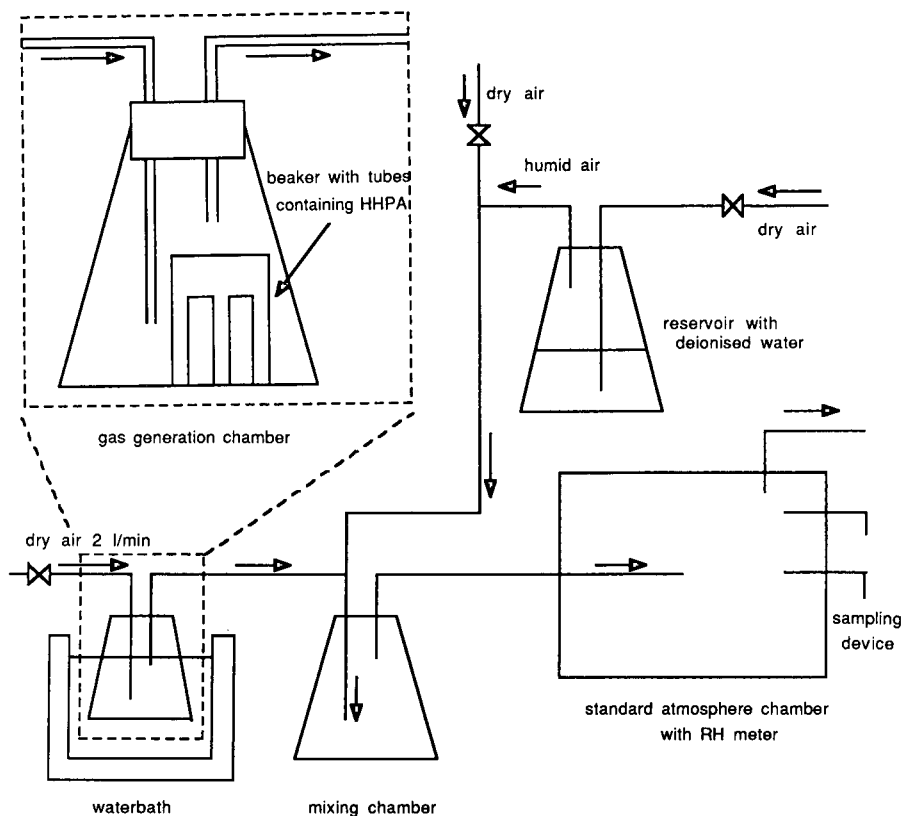
Fig. 1. Equipment for the generation of vaporous HHPA in air.

Procedure in the solid sorbent method

Sampling of HHPA was performed with XAD-2 tubes with one sampling layer and one control layer. The sampling rate was 0.2 l/min or 1.0 l/min.

After sampling, the XAD-2 tubes were sealed with plastic plugs and put into a sealed plastic vessel with a layer of dry silica gel on the bottom. The tubes were stored at −20°C.

Each XAD-2 layer was eluted in 1.0 ml of toluene for 8 min. Thereafter, the toluene was transferred into glass tubes with PFTE screw caps. The solution was analysed immediately after elution.

Procedure in the bubbler method

HHPA was sampled with midget bubblers containing 5 ml of 0.1 *M* sodium hydroxide absorption solution in which HHP acid was formed. The sampling rate was 1.0 l/min.

After sampling, the bubblers were filled with 0.1 *M* sodium hydroxide to the original volume. All solutions were quantitatively transferred into glass tubes with PFTE screw caps and stored at 4°C.

The absorption solutions were acidified with 0.5 ml of 5 M sulphuric acid and extracted with 25 ml (15 ml + 10 ml) of ethylacetate. The ethylacetate was dried overnight with anhydrous sodium sulphate and evaporated to dryness in a stream of dry nitrogen. After evaporation, the residue was dissolved in 1.2 ml of methanol to which 2.0 ml of 14% boron trifluoride in methanol was added. Esterification was performed overnight in glass tubes with PFTE screw caps at 70°C. When the tubes had cooled, 4 ml of saturated sodium bicarbonate was added and the mixtures were extracted with 2 ml of toluene. After centrifugation, the toluene solutions were transferred to glass tubes and dried over anhydrous sodium sulphate. The samples were kept at $-20°C$ until analysis.

Preparations of standard solutions

Standard solutions of HHPA were prepared by dissolving 100 mg of HHPA in 25 ml of toluene. This solution was then further diluted in toluene to appropriate concentrations.

Standard solutions of HHP acid-DME were prepared by reacting 100 mg of HHPA with 25 ml of aqueous 0.1 M sodium hydroxide. The HHP acid was then further diluted in the aqueous sodium hydroxide to appropriate concentrations. The standard solutions were worked up and analysed together with the samples as described above.

To determine the recovery of the work-up procedure of HHP acid-DME, standard solutions of HHP acid-DME were prepared in toluene. A 100-mg aliquot of HHP acid-DME was dissolved in 25 ml of toluene. The solution was then further diluted in toluene to appropriate concentrations.

Analysis

On the Varian equipment, 1.0 μl of the toluene solutions was injected at a rate of 5 $\mu l/s$ into the column. The injector starting temperature was 100°C for 0.2 min, and thereafter the temperature was increased by 50°C/min to a final temperature of 160°C, where it was maintained for 8 min.

The column initial temperature was 100°C for 1 min. Thereafter the temperature was increased by 8°C/min until a final temperature of 135°C, which was maintained for 2 min. When analysing HHP acid-DME, an additional column programming step was added with an increase of the temperature of 40°C/min to a final temperature of 250°C, which was maintained for 2 min.

The detector temperature was 260°C, and the supply of hydrogen and air for the detector was 2 and 280 ml/min, respectively. As make-up gas, helium at a flow-rate of 40 ml/min was used. The gas flow of helium through the column was 2.0 ml/min.

On the Carlo Erba equipment, 1.0 μl of the toluene solution was injected using the cold on-column technique. The column initial temperature was 122°C for 1 min and thereafter the temperature was increased by 10°C/min to the final temperature of 230°C, where it was maintained for 5 min.

The temperature of the detector was 260°C, the supply of hydrogen 12 ml/min and of air 280 ml/min. The flow of helium through the column was 3.0 ml/min.

RESULTS AND DISCUSSION

Standards

The identity of HHP acid-DME was confirmed by GC–mass spectrometry [14]. The purity of HHP acid-DME was checked using GC-FID and found to be *ca.* 97%.

Sampling considerations

Sampling using bubbler has been used for the determination of other anhydrides. The absorbing liquid used was an auqeous solution of sodium hydroxide. In the case of HHPA, the free sodium HHP acid is formed. Sodium HHP acid is expected to be stable in the sampling solution. The relatively fast hydrolysis of HHPA in the bubbler solution minimizes the possible interfering reactions by other co-occurring compounds present. However, a method based on the sampling in alkaline aqueous solutions can not separate HHPA and HHP acid in air. The amounts of HHPA and HHP acid are determined by the subsequent analysis.

Sampling of organic acid anhydrides has also been performed with sorbent tubes containing solid sorbents. With this procedure, the determination of anhydrides is feasible without interference from the possible presence of HHP acid. However, sample losses cannot be disregarded, as HHPA may react with other compounds also present in the sample. HHPA is sampled in a reactive form which may cause sample losses during storage. The subsequent determination ought therefore to be performed reasonably soon after sampling. The method is favoured by the simplicity of sampling, analysis and evaluation of the results.

Procedure in the solid sorbent method

Sampling efficiency. The sampling efficiency for different concentrations of HHPA and different RH in the air was determined by the analysis of the control layer. The results are summarized in Table I. Neither the concentration nor the RH seems seriously to affect the sampling efficiency. The sampling efficiency of the sampling rates 0.2 and 1.0 l/min was investigated. Seven parallel samplings with the different sampling rates were performed. The sampling time was 95 min and RH was <2%. The estimated concentrations found by the different sampling rates were equal (18 $\mu g/m^3$) within the experimental errors.

TABLE I

SAMPLING EFFICIENCY OF THE SOLID SORBENT METHOD FOR DIFFERENT CONCENTRATIONS OF HHPA AND RELATIVE HUMIDITY IN AIR

The sampling rate was 1.0 l/min.

Concentration of HHPA in air ($\mu g/m^3$)	Relative humidity (%)	Sampling volumes (l)	Sampling efficiency[a] (%)	Number of determinations
15	<2	63	>80	7
27	70	59	>90	7
160	<2	51	94	7

[a] Percentage of HHPA in the sampling layer compared with the totally sampled amount.

Recovery. The recovery of HHPA sampled on solid sorbent tubes was initially investigated by the application of 30 μl of a toluene solution containing 0.44 μg/μl on loosely packed Pyrex glass wool. The glass wool was placed in a glass tube in glass to glass connection with a sorbent tube connected to a pump. HHPA was immediately transferred from the glass wool by suction of 6.0 l of air for 30 min. Of the anhydride applied to the glass wool 76% was recovered from the XAD-2. When the glass tube containing the glass wool was shaken in toluene, no HHPA was found. However, when it was instead shaken in sodium hydroxide solution, 9% of the HHPA was found as HHP acid. The recovery was therefore found to be 85% [coefficient of variation (C.V.) 1%; $n = 5$; RH 40%].

Storage. The stability of HHPA on XAD-2 tubes was studied by the simultaneous sampling of pairs of sorbent tubes in the standard atmosphere. On tube of each pair was immediately analysed while the other tubes were kept in a freezer for 20 days until analysis. *Ca.* 10% of the sampled HHPA was lost, and the losses during storage were not influenced by the relative humidity in the sampled air. The RH was <2% ($n = 5$; sampling volume 58 l) and 70% ($n = 6$; sampling volume 60 l). The sampling rate was 1.0 l/min and the concentration *ca.* 20 μg/m^3. When storing HHPA in toluene at microgram per millilitre concentrations degradation of sample was found. At sub-μg/ml concentrations up to 2%/h was lost when kept at room temperature. The loss was influenced by, for example, the condition of the toluene. Samples must therefore be analysed immediately after elution of the solid sorbent tube. When kept in a freezer, standard solutions could be stored up to ten days without noticeable degradation of the sample.

Procedure in the bubbler method

Sampling efficiency. The sampling efficiency was studied by sampling HHPA in the standard atmosphere with two bubblers, containing the alkaline-absorbing solution, coupled in series. All connections were glass to glass. Two different concentrations of HHPA were studied, 21 and 220 μg/m^3 ($n = 8$ for each; sampling volume 120 l; RH <2%). No HHP acid was found in any of the second bubblers.

Storage. No degradation of HHP acid in the absorption solution was found when stored in a refrigerator for eight weeks at concentrations of 0.16 μg/ml ($n = 5$) and 2.5 μg/ml ($n = 5$). Standard solutions of HHP acid-DME in toluene, containing 0.18 μg/ml ($n = 5$) and 2.9 μg/ml (n = 5), kept in a freezer were also stable.

Work-up procedure. The recovery for the work-up of absorbing solution spiked with 1.4 μg of HHPA was 88% (C.V. 4%) and 79% (C.V. 3%) when spiked with 22 μg of HHPA ($n = 10$).

Chromatography

Symmetrical peaks were obtained for HHPA as well as HHP acid-DME in the chromatographic system. No adsorption or decomposition was observed. When analysing the anhydride, no interfering peaks disturbed the evaluation of the chromatograms. When analysing the HHP acid-DME, on peak originating from the esterfication step was eluted with the same retention time; this reduced the detection limit slightly (Fig. 2). A comparison between apolar columns of internal diameter 0.25 mm and a film thickness of 0.25 μm and internal diameter 0.32 mm and a film thickness of 1.0 μm was done. Significantly better resolution relative to the matrix was obtained
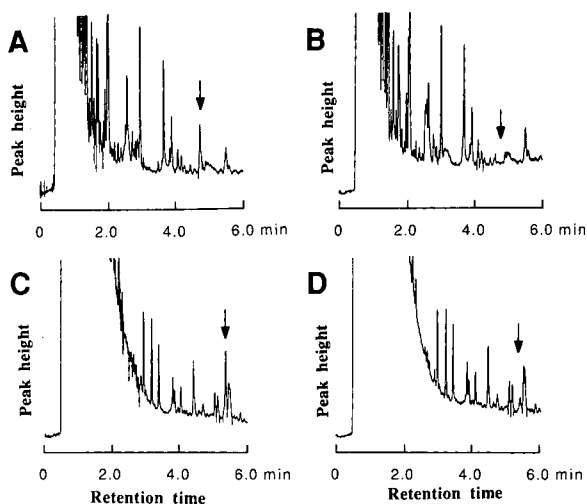
Fig. 2. Chromatograms of (A) 0.1 μg HHPA per millilitre of toluene and (B) blank sample of the solid sorbent method. (C) shows a chromatogram of HHPA-DME (about 0.1 μg/ml in toluene) and (D) a blank sample of the bubbler method.

for the column with the internal diameter of 0.25 mm, which was also the minimal internal diameter of a capillary column that it was possible to use for automatic on-column injections. The on-column injection technique was chosen for the excellent repeatability achieved. At least 1000 injections were possibile without noticeable degradation of the column. The chromatograms were hence easy to evaluate with the integrator.

Detection

Detection of HHPA was performed with FID, photoionization detection (PID) and electron-capture detection (ECD). PID was more than 10 times less sensitive than FID. ECD was much more sensitive than FID. However, ECD is complicated to use, unstable and sensitive to impurites. FID, which is easy to use, relatively sensitive and stable, was therefore chosen. The detection limits for HHPA in toluene using FID and calculated as three times the noise was *ca.* 0.1 μg/ml (Fig. 2). However, owing to the instability of HHPA, concentrations lower than 0.2 μg/ml were not quantified. The practical detection limit is defined by the sampling and the work-up conditions. The detection limit (three times the noise) for HHP acid-DME in toluene is about 0.1 μg of HHPA per millilitre (Fig. 2). Short time sampling (15 min) can be performed down to air concentrations of 13 μg/m³ with both the bubbler and the solid sorbent methods. With 1 h sampling, concentrations >3 μg/m³ can be detected with both methods. For 8 h sampling it is advisable to use the low sampling rate for the solid sorbent method and to change the bubbler or XAD-2 tube at least once during the day.

Quantitative analysis

Calibration graph. Different amounts of HHPA were added to 5 ml of 0.1 *M* aqueous sodium hydroxide and the work-up procedure described above was used.

TABLE II

PRECISION AT DIFFERENT CONCENTRATIONS OF HHPA AND RELATIVE HUMIDITY IN AIR

The sampling rate was 1.01 l/min.

Concentration of HHPA in air (μg/m^3)	Relative humidity (%)	Sampling volumes (l)	Precision of XAD-2 (%)	Precision of bubbler (%)	Number of determinations
15	<2	63	2	12	7
27	70	59	7	19	7[a]
160	<2	51	2	3	7

[a] The precision of the bubbler method was calculated from six determinations.

Single samples at each concentration ($n = 7$) with duplicate injections were made. A linear relation passing through the origin was achieved at the investigated range of 0.6–320 μg of HHPA per sample. The correlation coefficient was 0.9996. HHPA was added to toluene to concentrations in the range of 0.44–440 μg of HHPA per millitre. A linear calibration curve, passing through the origin, was found. The correlation coefficient was 0.9999.

Precision. HHPA was collected in solid sorbent tubes and bubblers for the estimation of the concentration in the standard concentration chamber. The precision of the determinations is presented in Table II. The result at RH = 70% indicates the minor influence of the relative humidity on the precision.

Comparison between the methods. Parallel samples were taken in the standard atmosphere on XAD-2 tubes and bubblers and the work-up procedures were then performed. The correspondence between the results obtained by the two methods was then compared. The low RH (<2%) was chosen to minimize the amount of HHP acid possibly present in the air. With a higher RH, a difference in the concentrations found by the two methods could demonstrate the presence of HHP acid in the air rather than a difference in determination of the anhydride. At 15 μg/m^3 ($n = 7$; sampling volume 63 l; RH <2%) the concentrations found by the solid sorbent method were 93% of those with the bubbler method, and at 160 μg/m^3 ($n = 7$; sampling volume 51 l; RH <2%) 98% and at 27 μg/m^3 ($n = 6$; sampling volume 59 l, RH 70%) 86%. This indicates decreasing recovery with the relative humidity for the solid sorbent method. However, the difference was not statistically significant. A comparison of samples taken simultaneously, by the two methods, in the work environment air was performed. The sampling rate for the solid sorbent tubes was 0.2 ml/min. No breakthrough was observed at any concentration monitored. The concentrations found by the solid sorbent method were 93% of that found by the bubbler method at a mean concentration of 330 μg/m^3 (C.V. = 39%; range 200–540 μg/m^3; sampling volume 19–46 l; $n = 8$). However, the possibility that other factories use other chemicals which can possibly interfere with the HHPA determinations must be considered. The results of the two methods were compared by the paired *t*-test (95% confidence limits; two-tailed). At none of the four conditions was there a significant difference between the methods.

CONCLUSIONS

The two methods for the monitoring of the HHPA in air were found to be reliable with detection limits much below the expected average found in the work environment. The methods were investigated for the concentration range 15–160 $\mu g/m^3$. However the studies in the work environment indicate that they are applicable at least up to 540 $\mu g/m^3$. RH < 70% did not seem to affect the sampling efficiency of the solid sorbent method. The high sampling rate (1.0 l/min) makes it possible to monitor the exposure for relatively short periods. For monitoring for a long time, using the solid sorbent method, a sampling rate of 0.2 l/min is preferable to minimize the breakthrough. The methods showed the same results (within the experimental errors) for the monitoring of HHPA concentration both in the standard atmosphere and when applied in the work environment. However, when both anhydride and acid are present in the air the total is obtained with the bubbler method. The solid sorbent method makes it possible to monitor HHPA as such and it has the advantages of somewhat better precision and a less time-consuming work-up procedure. The sampling solutions obtained for the bubbler method have the obvious advantage of being stable during storage.

ACKNOWLEDGEMENTS

REFERENCES

1 K. M. Venables, *Br. J. Ind. Med.*, 46 (1989) 222.
2 D. R. Moller, J. S. Gallagher, D. I. Bernstein, T. G. Wilcox, H. E. Burroughs and I. L Bernstein, *J. Allergy Clin. Immunol.*, 75 (1985) 663.
3 J. Nielsen, H. Welinder and S. Skerfving, *Scand. J. Work Environ. Health*, 15 (1989) 154.
4 H. Welinder, J. Nielsen, C. Gustavsson, I. Bensryd and S. Skerfving, *Clin. Exp. Allergy*, 20 (1990) 639.
5 R. Geyser and G. A. Saunders, *J. Liq. Chromatogr.*, 9(10) (1986) 2281.
6 J. Nielsen, H. Welinder, A. Schütz and S. Skerfving, *J. Allergy Clin. Immunol.*, 82 (1988) 126.
7 R. Geyer, R. C. Jones and N. Mezin, *J. High Resolut. Chromatogr. Chromatogr. Commun.*, 9 (1986) 308.
8 J. Palassis, J. C. Posner, E. Slick and K. Schulte, *Am. Ind. Hyg. Assoc. J.*, 42 (1981) 785.
9 C. J. Purnell and C. J. Warwick, *J. High Resolut. Chromatogr. Chromatogr. Commun.*, 3 (1980) 482.
10 P. Pfäffli, *Analyst (London)*, 111 (1986) 813.
11 OSHA Analytical Laboratory, Salt Lake City, Utah, U.S., *Method No. 25*, (1981).
12 H. Welinder and C. Gustavsson, *Ann. Occup. Hyg.*, submitted for publication.
13 P. Pfäffli, H. Savolainen and H. Keskinen, *Chromatographia*, 27 (1989) 483.
14 F. Hermann, O. Dufka and J. Churacek, *J. Chromatogr.*, 360 (1986) 79.

Stereoisomeric purity determination of captopril by capillary gas chromatography

DOUGLAS A. BOTH* and MOHAMMED JEMAL

Bristol–Myers Squibb Company, Bristol–Myers Squibb Pharmaceutical Research Institute, P.O. Box 191, 1 Squibb Drive, New Brunswick, NJ 08903–0191 (USA)

(Received March 8th, 1991)

ABSTRACT

The GC method developed for the stereoisomeric purity determination of captopril is based on the combined information derived from the analyses of the captopril sample on two GC systems, one with a chiral and the other with an achiral column. The limit of detection has been determined to be 0.02% (w/w) for (R,S) or (S,R) and 0.03% for (R,R), with corresponding minimum quantifiable levels of 0.08% and 0.09%.

INTRODUCTION

Captopril, 1-[3-mercapto-2-(S)-methyl-1-oxopropyl]-(S)-proline (Fig. 1) is an inhibitor of the angiotensin-converting enzyme and is widely used for the treatment of hypertension and congestive heart failure [1]. Since the compound contains two asymmetric centers, one associated with the proline and the other associated with the 3-mercapto-2-methylpropionic acid side chain, there are three other possible stereoisomers: 1-[3-mercapto-2-(S)-methyl-1-oxopropyl]-(R)-proline, 1-[3-mercapto-2-(R)-methyl-1-oxopropyl]-(S)-proline and 1-[3-mercapto-2-(R)-methyl-1-oxopropyl]-(R)-proline. The production of captopril (S,S) involves the coupling of L-proline with the acid chloride of resolved 3-acetylmercapto-2-(S)-methylpropionic acid. Since both the acid chloride and proline may contain traces of the respective enantiomers, it is possible to form small amounts of each of the three stereoisomers, (R,R), (S,R) and (R,S), which could theoretically be present in the final bulk captopril product. Assuming the unlikely situation where both the proline and the acid chloride meet the
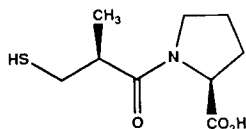

Fig. 1. Chemical structure of captopril.

low end limit of the specifications, 99.5% and 96.0%, respectively, the theoretical amounts of the stereoisomers that can be formed have been computed: 95.5% captopril (S,S), 3.98% (R,S), 0.48% (S,R) and 0.02 (R,R). On the other hand, bulk captopril, which is obtained after extensive purification during routine processing, may not contain any of the stereoisomers. Thus, to ascertain the stereoisomeric purity of captopril (S,S), it was required to develop a method which is capable of quantitating any trace amounts of (R,R), (R,S) and (S,R) in captopril.

Gas chromatography (GC) has been used to resolve enantiomers on chiral columns [2,3] and diastereomers on achiral columns [4,5]. The GC method developed for the stereoisomeric purity determination of captopril is based on the combined information derived from the analyses of the captopril sample on two GC systems, one with a chiral and the other with an achiral column. The limit of detection (LOD) has been determined to be 0.02% (w/w) for (R,S) or (S,R) and 0.03% for (R,R), with corresponding minimum quantifiable levels (MQL) of 0.08% and 0.09%.

EXPERIMENTAL

Reagents and chemicals

Captopril and the other three stereoisomers were characterized products obtained from Bristol–Myers Squibb Pharmaceutical Research Institute (Chemical Process Technology Department, New Brunswick, NJ, USA). Methanol–hydrogen chloride solution (2 M) was prepared by adding dropwise 2.8 ml of acetyl chloride (Applied Science) to 17.2 ml of cold anhydrous methanol (Applied Science) in an ice bath. After removing from the ice bath, the solution is allowed to remain at room temperature for at least 20 minutes prior to use. The reagent is stable for at least two weeks when refrigerated. The other reagents used were pentafluoropropionic anhydride (Pierce), ethyl acetate (Burdick and Jackson, pesticide-residue grade) and *n*-butyl acetate (Burdick and Jackson, pesticide-residue grade).

Sample preparation

Into an autosampler vial containing approximately 5 mg of captopril, 1.0 ml of methanol–hydrogen chloride solution was added. After capping the vial and mixing to aid in dissolution, the solution was heated at 60°C for 30 min. After the samples had cooled, the reagents were removed by evaporation under nitrogen. To the dry residue, 250 μl of ethyl acetate and 250 μl of pentafluoropropionic anhydride were added and the resulting solution was heated at 60°C for 30 min. After cooling, the reagents were removed by evaporation under nitrogen and the dry residue was reconstituted in 0.6 ml of *n*-butyl acetate. A 1.0-μl portion of this solution was then injected into each of the two GC systems described below.

Gas chromatography

A Hewlett-Packard 5890 capillary gas chromatograph, equipped with a split/splitless injection port, a flame ionization detector and 7673A autosampler injector, was used. Injection was in the split mode, with a split flow of 50 ml/min. The split port liner was an unpacked cup splitter (Restek No. 20710). The helium carrier gas head pressure was maintained at 83 kPa (12 p.s.i.g.) and the flow-rate of the helium make-up gas for the flame ionization detector was 30 ml/min. The GC sensitivity was set at

a range of 2^2 and attenuation of 2^2. The analysis was carried out by injecting 1.0 μl of the sample solution into each of the two chromatographic systems, one chiral and the other achiral.

For the achiral column analysis, the column used was Rt_x-1 (100% dimethyl-polysiloxane, Restek Corp.), 30 m × 0.32 mm I.D. and 1.0 μm stationary phase film thickness. The oven temperature was maintained at 170°C for 12 min. The injector and detector temperatures were maintained at 250°C and 300°C, respectively.

For the chiral column analysis, the column used was XE-60–S-valine–S-phen-ylethylamide (Chrompack), 25 m × 0.25 mm I.D. and 0.12 μm stationary phase film thickness. The oven temperature was maintained at 160°C for 15 min. The injector and detector temperatures were maintained at 250°C and 275°C, respectively.

Quantitation

Chiral column. The chiral column system resolves two of the three stereoiso-mers, (S,R) and (R,R), from the main peak, which is due to captopril (S,S). Thus, this system is used to determine the amounts of (S,R) and (R,R) in captopril according to the following equations:

$$\% \text{ of } (S,R) = \frac{A_{SR}}{A_{SR} + A_{RR} + A_{SS+RS}} \cdot 100$$

$$\% \text{ of } (R,R) = \frac{A_{RR}}{A_{SR} + A_{RR} + A_{SS+RS}} \cdot 100$$

where A_{SR} = area of the (S,R) peak; A_{RR} = area of the (R,R) peak; A_{SS+RS} = area of the unresolved peak for captopril and (R,S).

The (R,S), which coelutes with captopril (S,S), is determined by the combina-tion of the results derived from the chiral and achiral systems (see below).

Achiral column. On the achiral column, the four stereoisomers elute as two peaks, composed of the co-elution of (R,S) and (S,R), and the co-elution of (S,S) and (R,R). Thus,

$$\% \text{ of } (S,R) + (R,S) = \frac{A_{SR+RS}}{A_{SR+RS} + A_{SS+RR}} \cdot 100$$

where A_{SR+RS} = the area of the peak representing the co-elution of (S,R) and (R,S); A_{SS+RR} = the area of the peak representing the co-elution of the captopril (S,S) and (R,R).

Using the % of (S,R) calculated from the chiral column data (see above), the % of (R,S) can be determined:

$$\% \text{ of } (R,S) = [\% \text{ of } (S,R) + (R,S)] - [\% \text{ of } (S,R)]$$

RESULTS AND DISCUSSION

    The method developed for the determination of the three stereoisomers, (R,R), (S,R) and (R,S), in captopril, (S,S), is based on a two-step achiral derivatization, methylation of the carboxylic acid followed by the acylation of the sulfhydryl. The resulting product is chromatographed on two separate chromatographic systems, one using an achiral column and the other a chiral column. On the achiral column, the four stereoisomers are resolved into two peaks (Fig. 2), each peak representing a diastereomer and its enantiomer. Thus, (R,S) coelutes with (S,R) and (S,S) coelutes with (R,R). The resolution between the two peaks is 1.8. The chiral column, on the other hand, resolves the components into three peaks (Fig. 3) with the coelution of (S,S) and (R,S). The resolution between the main peak and the (S,R) peak is 1.8, whereas the resolution between the (S,R) and (R,R) peaks is 0.53, which was found to be adequate. On both systems, the minor peaks elute before the main peak, which makes integration of the minor peaks more reliable. The reagent blank chromatogram on each system (Figs. 4 and 5) showed that there were no interfering peaks in the regions of interest. By the combination of the data from the runs obtained on the two chromatographic systems, it is appropriate to determine the levels of the three stereoisomers in captopril.

    The accuracy of the method was established by analyzing captopril samples spiked with varying amounts of each of the three stereoisomers. As shown in Table I, added stereoisomer was quantitatively recovered. The table also shows that precision of replicate injections is excellent. Excellent precision was also obtained for replicate preparations of captopril spiked with the stereoisomers (Table II). The data in Table II were also used to estimate the LOD and MQL of the method, by utilizing the formulae LOD = 3 × standard deviation of replicate sample preparations and
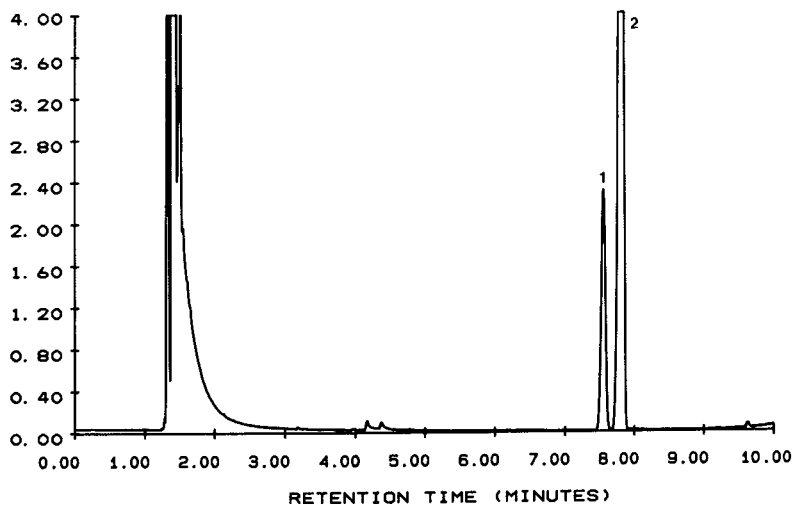
Fig. 2. Achiral column chromatogram of a solution prepared from 5 mg of captopril, (S,S), spiked with 0.5 mg of each of the three stereoisomers, (R,R), (R,S) and (S,R). Peaks: 1 = (R,S) + (S,R) (7.55 min); 2 = captopril + (R,R) (7.82 min). The resolution between the two peaks is 1.8.
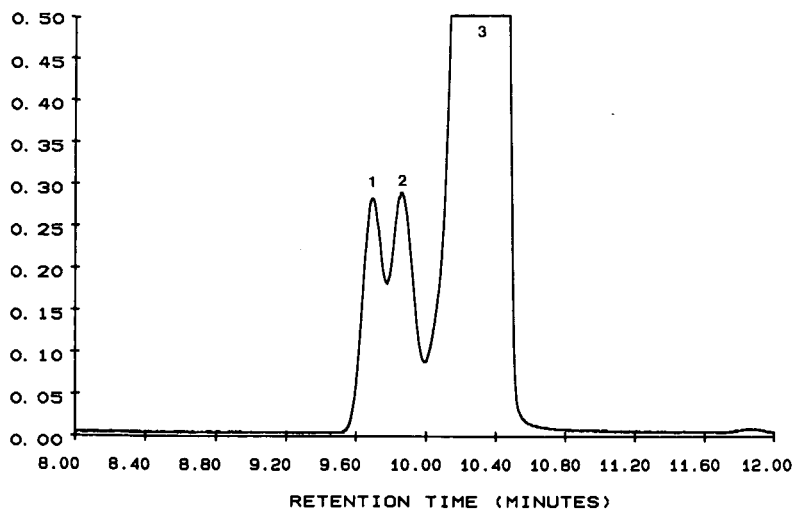
Fig. 3. Chiral column chromatogram of a solution prepared from 5 mg of captopril, (S,S), spiked with 0.5 mg of each of the three stereoisomers, (R,R), (R,S) and (S,R). Peaks: 1 = (S,R) (9.71 min); 2 = (R,R) (9.87 min); 3 = captopril + (R,S). The resolution between peaks 1 and 2 is 0.53; the resolution between peaks 1 and 3 is 1.8.

MQL = 10 × standard deviation of replicate sample preparations. Thus, the LOD is estimated to be 0.02% for (R,S) or (S,R) and 0.03% for (R,R), with corresponding MQL values of 0.08 and 0.09% (w/w).

Analyses of a large number of different batches of captopril showed that little or no stereoisomers are present in captopril. The largest level found was for the (R,S)
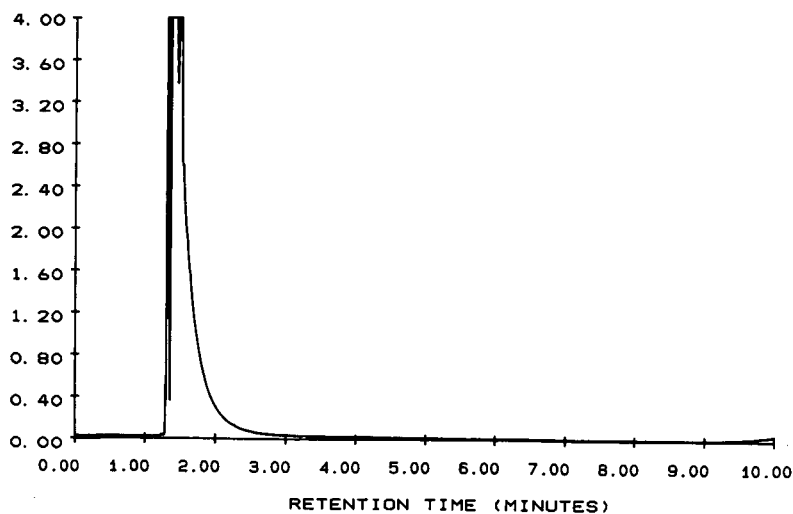
Fig. 4. Chromatogram of a reagent blank corresponding to Fig. 2.
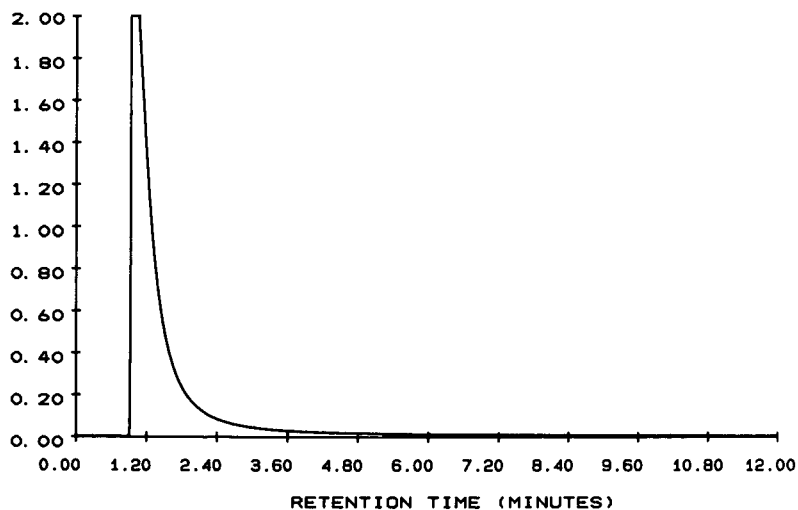
Fig. 5. Chromatogram of a reagent blank corresponding to Fig. 3.

TABLE I

RECOVERY OF THE STEREOISOMERS ADDED TO CAPTOPRIL

The four values shown for each level of a stereoisomer represent replicate injections of the same solution.

Added (%, w/w)	(R,S) Stereoisomer recovered (%, w/w)	(S,R) Stereoisomer recovered (%, w/w)	(R,R) Stereoisomer recovered (%, w/w)
4.4	4.9, 4.9, 4.9, 4.9	4.3, 4.4, 4.4, 4.4	4.9, 4.9, 4.9, 4.9
0.97	1.1, 1.1, 1.1, 1.0	0.99, 0.97, 0.95, 0.98	1.2, 1.2, 1.2, 1.2
0.49	0.54, 0.53, 0.52, 0.54	0.49, 0.52, 0.52, 0.52	0.49, 0.57, 0.54, 0.48
0.20	0.22, 0.23, 0.25, 0.22	0.22, 0.24, 0.22, 0.24	0.22, 0.21, 0.22, 0.16
0.10	0.10, 0.10, 0.12, 0.10	0.13, 0.12, 0.13, 0.12	0.10, 0.087, 0.082, 0.10

TABLE II

REPRODUCIBILITY OF REPLICATE PREPARATIONS OF CAPTOPRIL SPIKED WITH 0.1% (w/w) OF THE STEREOISOMERS

S.D. = Standard deviation; R.S.D. = Relative standard deviation.

Replicate No.	(R,S) Stereoisomer recovered (%, w/w)	(S,R) Stereoisomer recovered (%, w/w)	(R,R) Stereoisomer recovered (%, w/w)
1	0.11	0.10	0.084
2	0.11	0.12	0.081
3	0.11	0.11	0.094
4	0.11	0.12	0.076
5	0.12	0.11	0.10
6	0.12	0.12	0.083
7	0.11	0.11	0.095
8	0.13	0.11	0.081
Mean	0.12	0.11	0.086
S.D.	0.0076	0.0071	0.0084
R.S.D.(%)	6.6	6.3	9.7

stereoisomer as expected, but the level was lower than the MQL even for this stereoisomer.

Before the adoption of the method described here, several different investigations were undertaken. The resolution obtained on the chiral column after just methylation, without subsequent acylation, was not satisfactory. The use of another amino acid-based chiral column, Chiralsil-VAl III, did not give the resolution obtained on the XE-60-S-valine-S-phenylethylamide column.

The method described above could be cleanly accomplished by mutidimensional GC. The sample would first be injected into the achiral column which separates the four compounds into two components, (R,S) and (S,R) coeluting first, and (S,S) and (R,R) coeluting next. The two peaks would then be directed separately to the chiral column, with each producing two peaks on the chiral column. Thus, the first peak from the achiral column will produce two peaks on the chiral column, that of (S,R) eluting first and (R,S) eluting next, well separated from each other.

ACKNOWLEDGEMENTS

REFERENCES

1 D. W. Cushman, H. S. Cheung, E. F. Sabo and M. A. Ondetti, in Z. P. Horovitz (Editor) *Angiotensin-Converting Enzyme Inhibitors*, Urban and Schwarzenberg, München, 1981, pp. 3–25.
2 W. A. Konig, I. Benecke, N. Lucht, E. Schmidt, J. Schulze and S. Sievers, *J. Chromatogr.*, 279 (1983) 555.
3 M. Jemal and A. I. Cohen, *J. Chromatogr.*, 392 (1987) 442.
4 B. Halpern, in K. Blau and G. S. King (Editors), *Handbook of Derivatives for Chromatography*, Heyden, London, 1977, p. 457.
5 M. Jemal and A. I. Cohen, *J. Chromatogr.*, 394 (1987) 388.

Isolation of erythromycin A N-oxide and pseudoerythromycin A hemiketal from fermentation broth of *Saccharopolyspora erythraea* by thin-layer and high-performance liquid chromatography

M. BERAN*, V. PŘIKRYLOVÁ, P. SEDMERA, J. NOVÁK, J. ZIMA and M. BLUMAUEROVÁ

Institute of Microbiology, Czechoslovak Academy of Sciences, 142 20 Prague 4 (Czechoslovakia)
and
T. Kh. TODOROV

Institute of Microbiology, Bulgarian Academy of Sciences, 1113 Sofia (Bulgaria)
(First received October 30th, 1990; revised manuscript received April 30th, 1991)

ABSTRACT

Erythromycin A N-oxide and pseudoerythromycin A hemiketal, accompanying erythromycin A and erythronolide B, were isolated from the fermentation broth of *Saccharopolyspora erythraea* by combination of thin-layer chromatography on silica gel and reversed-phase high-performance liquid chromatography. Their identification is based on the mass and ^1H and ^{13}C NMR spectrometric results.

INTRODUCTION

During the monitoring of erythromycin A (EA) production in a cultivation of mixed culture of *Saccharopolyspora erythraea* mutants 5002 and 5005 blocked at different steps of erythromycin biosynthesis, two biologically inactive substances were produced in large amounts, simultaneously with the production of biologically active EA and erythronolid B (ELB) [1]. Before suppressing their formation, it was necessary to identify them. These substances were isolated from the liquid part of fermentation broth separated by centrifugation. Extraction and a combination of thin-layer chromatography (TLC) on silica gel and reversed-phase high-performance liquid chromatography (HPLC) were used for their isolation (Fig. 1). The substances were identified as erythromycin A N-oxide (EANO) and pseudoerythromycin A hemiketal (psEAHK) by spectroscopic means. ^1H and ^{13}C NMR spectra of EANO and psEAHK are reported here to facilitate the future identification of these compounds. ELB and EA were also isolated from the same source. The structures are depicted in Fig. 2.

EANO has already been isolated from commercial EA by classical column chromatography on silica gel with TLC monitoring [2] and psEAHK was described as a product of the reaction of EA with diethylamine and glacial acetic acid [3].

Fermentation broth (4200 ml)
     (liquid part)

|
                    alkalinization with Na_2CO_3 to pH 9.7
                    extraction with EtOAc (2x3000 ml)
                    evaporation to 500 ml

Aqueous Phase   **EtOAc Phase**

                                     extraction with H_2O; pH 4.5
                                     (1x400 ml)

         Aqueous Phase   **EtOAc Phase**

         alkalinization with   evaporation
         Na_2CO_3 to pH 9.7   prep. TLC
         extract. with EtOAc   crystallization
              (2x300 ml)
                                     ELB (25 mg)

Aqueous Phase   **EtOAc Phase**

                                evaporation

                    Light yellow residue

                                prep. TLC

Fraction 1   **Fraction 2**   **Fraction 3**
(92 mg)   (15 mg)   (73 mg)

     HPLC   HPLC   HPLC
     evaporation   evaporation   evaporation
     crystallization   crystallization   crystalliz.

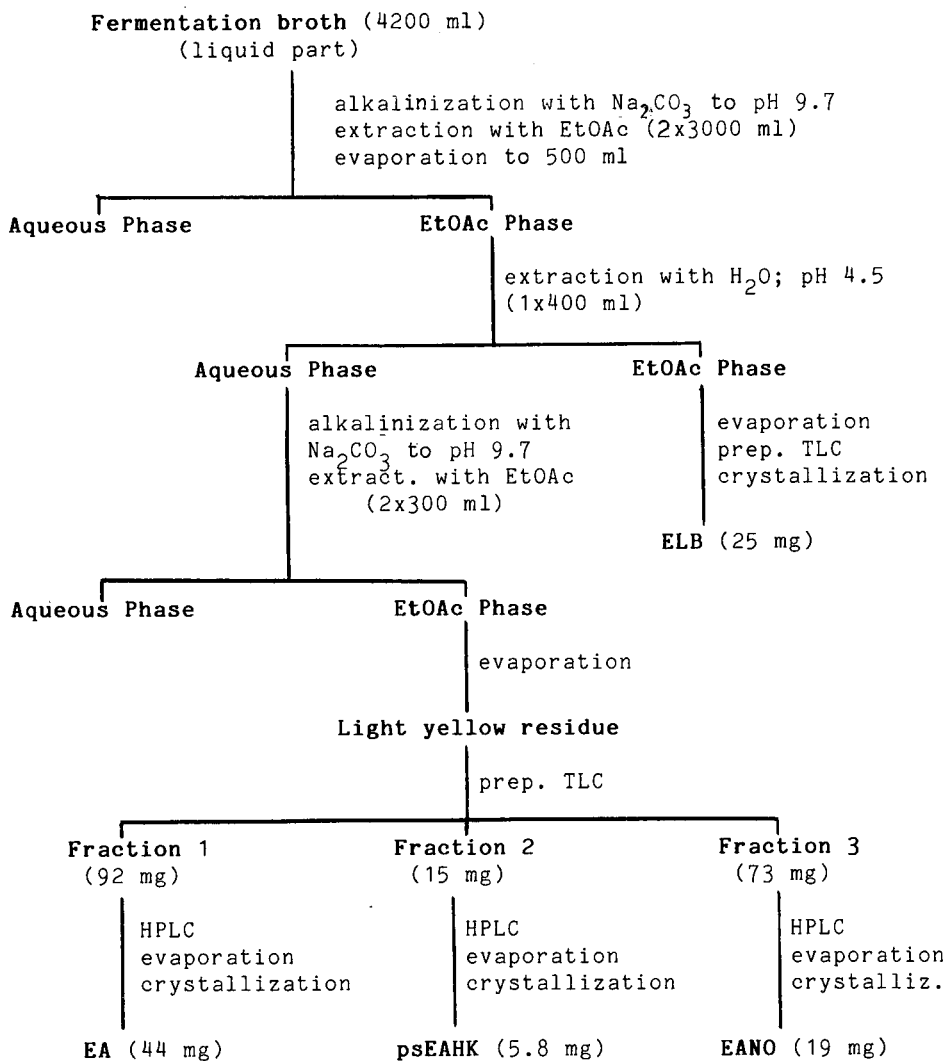**EA** (44 mg)   **psEAHK** (5.8 mg)   **EANO** (19 mg)

Fig. 1. Isolation scheme. EtOAc = Ethyl acetate.

EXPERIMENTAL

Chemicals
     Ethyl acetate, chloroform, methanol, ammonia solution and sodium carbonate
were of analytical-reagent grade (Lachema, Brno, Czechoslovakia). All solvents were
distilled before use. A standard of EA was obtained from Upjohn (Kalamazoo, MI,
USA).
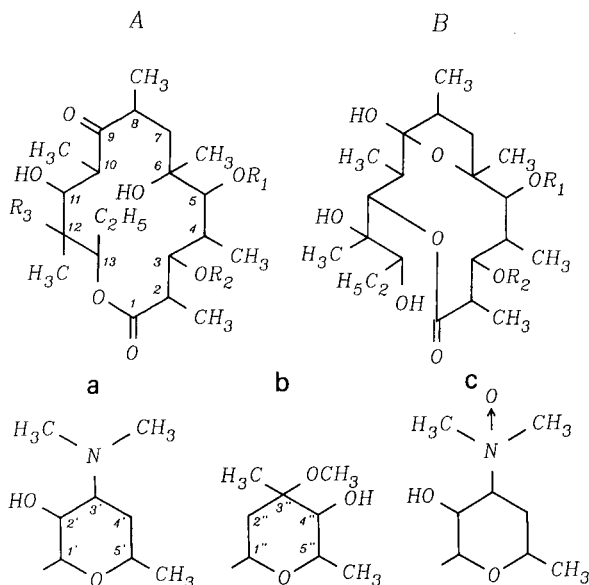
Fig. 2. Structure of isolated erythromycins: erythronolide B (ELB), erythromycin A (EA), erythromycin A N-oxide (EANO) and pseudoerythromycin A hemiketal (psEAHK).

Compound	Aglycone	R_1	R_2	R_3
ELB	A	H	H	H
EA	A	a	b	OH
EANO	A	c	b	OH
psEAHK	B	a	b	—

Samples

Samples suitable for TLC and HPLC analysis were prepared from fermentation broth according to the procedure described in Fig. 1.

Preparative TLC

Preparative TLC was performed on DC-Alufolien Kieselgel 60 ready-made silica gel plates (Merck, Darmstadt, Germany) without prior activation. The mobile phase was chloroform–methanol–ammonia solution (90:10:1, v/v/v). The plates were developed at room temperature over a distance of 17 cm in chromatographic tanks lined with filterpaper, which had been saturated for at least 2 h. The plates were then dried at room temperature. The left and right margins of the TLC plates were cut off and sprayed with a solution of anisaldehyde–sulphuric acid–95% ethanol (1:1:9, v/v/v) and heated in hot air (100°C). Positions of substances of interest were interpolated in the middle part of the preparative TLC plates using marginal strips. Three fraction (1, 2, and 3, R_F ranges 0.1–0.2, 0.2–0.3 and 0.3–0.5, respectively) were obtained after scraping, eluting with chloroform–methanol (2:1, v/v), filtration and evaporation (Fig. 1).

TABLE I

EXPERIMENTAL CONDITIONS FOR PREPARATIVE HPLC

Column	250 × 8 mm I.D.
Stationary phase[a]	Separon SGX C_{18}, 7 μm
Mobile phase	Methanol–water–ammonia solution 850:150:0.6 (pH = 10)
Flow-rate	3 ml min^{-1}
Injection volume	100 μl
Sample amount per run[b]	8 mg
Detection	Refractive index

[a] Tessek, Prague, Czechoslovakia.
[b] Sample dissolved in methanol.

Preparative HPLC

A Model SP 8000B high-performance liquid chromatograph (Spectra-Physics, Santa Clara, CA, USA) with an RIDK 101 differential refractometer (Laboratorní přístroje, Prague, Czechoslovakia) was used. Chromatograms were recorded on a strip-chart recorder at a chart speed of 0.25 cm min^{-1} and a setting of 10 mV. Experimental conditions described in ref. 4 were modified to suit our purpose using EA standard and are summarized in Table I.

Nuclear magnetic resonance

^{1}H and ^{13}C NMR spectra (400 and 100 MHz, respectively) were measured in deuterochloroform at 25°C with a Varian VXR-400 spectrometer. Reported assignments are based on various two-dimensional NMR experiments.

Mass spectrometry

Mass spectral data were measured on a MAT 90 double-focusing mass spectrometer (Finnigan MAT). Samples were studied in the electron impact ionization mode under the following conditions: direct inlet, 150–250°C; electron energy, 70 eV; ion-source temperature, 225°C; total pressure, 2 · 10^{-7} Torr; and emission current, 1 mA. Raw spectral data were recorded with a scan speed of 10 s per decade.
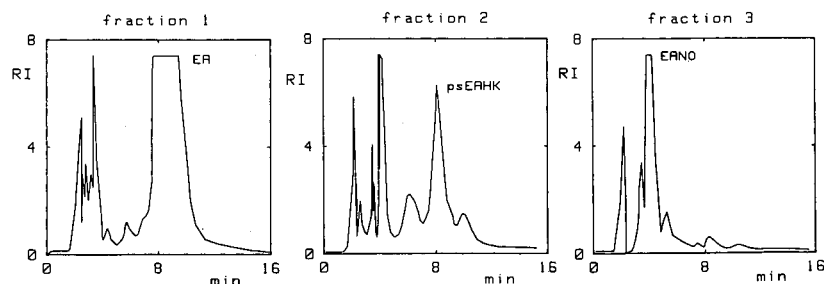

Fig. 3. Typical chromatograms of fractions 1–3 obtained by preparative HPLC. EA = erythromycin A; EANO = erythromycin A N-oxide; psEAHK = pseudoerythromycin A hemiketal. RI = Refractive index.

RESULTS AND DISCUSSION

Extraction, preparative TLC and HPLC

Fermentation broth was separated into liquid and mycelium part by centrifugation. Mycelium was discarded and the fermentation broth filtrate (liquid part) was

TABLE II

^{13}C NMR DATA (CHEMICAL SHIFT, ppm) FOR ERYTHROMYCIN A (EA), ERYTHROMYCIN A N-OXIDE (EANO) AND PSEUDOERTHROMYCIN A HEMIKETAL (psEAHK)

Carbon	EA [7]	EANO	psEAHK [3]	psEAHK
Aglycone				
1	176.30	175.87	176.70	176.95
2	45.02	45.19	46.90	47.04
3	80.30	80.02	80.30	80.94
4	39.50	39.43	39.90	38.33
5	84.00	83.85	85.90	85.78
6	74.78	74.78	84.10	84.39
7	38.54	38.54	40.90	41.09
8	44.93	44.81	37.50	37.76
9	221.90	222.09	106.60	106.84
10	38.10	37.33	38.10	38.31
11	68.76	68.92	72.90	72.92
12	74.45	74.62	76.50	77.20
13	77.10	76.82	77.70	78.00
14	21.16	21.06	22.90	23.03
15	10.70	10.63	11.60	11.90
16	15.90	15.97	14.00	14.22
17	9.20	9.05	10.30	10.50
18	26.50	26.92	29.70	29.95
19	18.40	18.28	11.90	11.90
20	12.00	12.03	10.00	10.25
21	16.20	16.14	17.10	17.09
Desosamine				
1'	103.30	102.68		105.35
2'	71.10	72.62		70.30
3'	65.30	67.08		65.20
4'	29.20	34.80		28.93
5'	68.81	76.20		69.26
6'	21.35	21.17		21.10
7'	40.30^a	52.13^a		40.38^a
8'	40.30^a	58.54^a		40.38^a
Cladinose				
1''	96.50	96.25		96.69
2''	35.00	34.99		35.32
3''	72.70	76.62		72.42
4''	77.90	77.95		78.21
5''	65.70	65.64		65.56
6''	18.46	18.64		17.49
7''	21.43	21.84		21.46
8''	49.50	45.59		49.15

^{a} Signals in the same column can be interchanged.

TABLE III

^{1}H NMR DATA FOR ERYTHROMYCIN A (EA), ERYTHROMYCIN A N-OXIDE (EANO) AND PSEUDOERYTHROMYCIN A HEMIKETAL (psEAHK)[a]

Atom	Multiplicity[b]	Chemical shift (ppm)			Coupling constant (Hz)		
		EA [7]	EANO	psEAHK	EA [7]	EANO	psEAHK
Aglycone							
H-2	dq	2.87	2.900	2.734	9.5,7.1	9.3,7.1	10.1,6.3
H-3	dd	3.99	3.988	3.950	9.4,1.4	9.3,1.5	10.1,0.7
H-4	ddq	1.97	1.914	2.180	7.5,1.5,7.5	n.d.	10.7,11.1,1.7
OH-5	d	3.56	3.559	3.472	7.8	7.8	11.1
H-7^{ax}	dd	1.93	1.957	2.310	14.9,11.9	n.d.	n.d
H-7^{eq}	ddd	1.74	1.654	2.383	14.9,8.4,1.0	14.8,2.0,0.6	n.d.
H-8	ddq	2.68	2.684	2.289	11.4,2.3,7.0	11.5,2.2,7.1	n.d.
H-10	dq	3.08	3.087	2.044	1.4,6.9	1.4,6.9	2.3,7.0
H-11	dbr	3.82	3.842	5.863	1.2	1.4	2.3
11-OH	sbr	3.95	1.281	—	—	—	—
12-OH	sbr	3.13	n.o.	n.o.	—	—	—
H-13	dd	5.03	5.026	2.376	11.0,2.3	10.0,2.3	n.d.
H-14^{eq}	ddq	1.91	1.910	1.683	14.2,2.4,7.5	14.2,2.3,7.4	n.d.
H-14^{ax}	ddq	1.475	1.478	1.356	14.3,11.0,7.3	14.2,11.2,7.4	n.d.
H-15	t	0.84	0.841	0.995	7.4	7.4	7.3
H-16	dbr	1.175	1.192	1.216	7.8	7.1	6.3
H-17	d	1.10	1.108	1.092	7.4	7.4	7.0
H-18	sbr	1.46	1.129	1.378	—	—	—
H-19	d	1.15	1.170	0.952	7.1	7.1	6.3
H-20	d	1.13	1.147	1.146	6.9	6.9	7.0
H-21	sbr	1.12	1.453	1.224	—	—	—
Desosamine							
H-1'	d	4.40	4.531	4.173	7.2	7.0	7.3
H-2'	dq	3.21	3.752	3.304	10.3,7.3	10.1,7.0	10.3,7.3
H-3'	ddd	2.43	3.462	2.545	12.3,10.2,3.9	10.1,12.7,7.4	12.2,10.3,3.7
H-4'^{eq}	ddd	1.66	2.010	1.661	2.2,3.9	n.d.	n.d
H-4'^{ax}	ddd	1.22	1.573	1.278	n.d.	n.d.	n.d.
H-5'	ddq	3.48	3.630	3.482	10.8,2.1,6.1	10.4,1.7,6.3	10.8,2.1,6.2
H-6'	d	1.22	1.267	1.210	6.1	6.2	6.2
H-7'	s	2.29	3.213	2.306	—	—	—
H-8'	s	2.29	3.347	2.306	—	—	—
Cladinose							
H-1''	dbr	4.88	4.888	4.765	4.5	4.9,0.8	4.2
H-2''^{eq}	dd	2.35	2.375	2.354	15.2,0.8	15.0,0.8	15.4,0.7
H-2''^{ax}	dd	1.56	1.567	1.531	15.1,5.0	15.0,4.9	15.4,4.6
4''-OH	d	2.23	n.o.	—	—	—	—
H-4''	dd	3.00	3.025[c]	3.002[c]	9.7,9.7	9.3	9.4
H-5''	dq	3.99	4.012	4.061	9.7,6.2	9.3,6.6	9.4,6.3
H-6''	d	1.27	1.282	1.260	6.2	6.6	6.3
H-7''	s	1.23	1.247	1.155	—	—	—
H-8''	s	3.31	3.213	3.239	—	—	—

[a] n.o. = Not observed; n.d. = not determined.

[b] Multiplicity of ^{1}H resonance. s = Singlet; d = doublet; t = triplet; q = quartet; br = broad.

[c] Additional signal: 10-OH,3.168.

made alkaline (pH 9.7) with sodium carbonate and extracted with ethyl acetate. The extract was reduced in volume and washed with acidified water (pH 4.5). After evaporation of the ethyl acetate ELB was isolated by preparative TLC. The aqueous phase was made alkaline (pH 9.7) with sodium carbonate and again extracted with ethyl acetate. The solvent was evaporated *in vacuo* and the light-yellow residue was separated by preparative TLC.

The three fractions obtained were further purified by preparative HPLC. The respective chromatograms are shown in Fig. 3. Peaks were collected according to the detector response, the solvent was evaporated and the compounds were crystallized. The yields are given in Fig. 1.

Mass spectrometry and nuclear magnetic resonance

ELB, isolated by preparative TLC, was identified using mass and NMR spectra (Tables II–IV). Later we found that fractions 1, 2 and 3 contained as the major components EA, EANO and psEAHK, respectively. Other peaks were not identified owing to the lack of sufficient material or its insufficient purity.

The mass spectrum of EANO closely resembles that of EA, and it was identical with that of authentic EANO prepared as described [5]. The absence of a molecular peak in the mass spectrum agrees with the known behaviour of N-oxides [6]. The similarity of the ^{13}C and ^{1}H NMR spectra (Tables II and III) confirms the presence of erythronolide A and cladinose in the molecule. The 4,6-dideoxyhexose attached to C-5 of the aglycone has the same configuration at C-2′ and C-3′ as desosamine (Table III), but is clearly different. The six-proton singlet of the NMe_2 group is replaced by

TABLE IV

MASS SPECTROMETRIC DATA FOR ERYTHROMYCIN A (EA), ERYTHROMYCIN A N-OXIDE (EANO) AND PSEUDOERYTHROMYCIN A HEMIKETAL (psEAHK)

m/z	Relative intensity (%)		
	EA	EANO	psEAHK
733	1.5	0.3	0.4
716	9.6	–	–
715	1.8	5.1	7.2
657	–	–	1.8
656	–	–	1.8
559	3.6	–	–
558	11.9	1.3	1.1
557	–	–	1.0
382	–	–	1.7
365	1.3	–	–
175	3.0	12.0	15.2
174	3.8	4.0	6.6
159	21.9	26.5	28.8
158	100.0	100.0	100.0
127	11.3	10.7	11.5
115	34.9	25.6	21.0
109	3.3	5.7	5.0
100	3.3	6.6	9.8

two methyls (δ_H 3.213, 3.347; δ_C 52.13, 58.54 ppm). These signals deceptively suggest the presence of the methoxyl groups, but this hypothesis has to be rejected on the basis of results of elemental analysis (1.82% N) and high-resolution measurement of the m/z 158 ion ($C_8H_{16}NO_2$). Another explanation of these signals requires a charge on the nitrogen atom. NMR spectra of both canditates, EA hydrochloride and EANO, were compared with those of our compound and the latter was found to be identical with EANO.

Comparison of the NMR spectra of psEAHK and EA confirms the presence of desosamine and cladinose in the molecule. The most downfield proton in ^{1}H NMR spectrum belongs to an OCHCH(CH_3) spin system and was therefore assigned to H-11. This finding, together with chemical shifts of H-13 and -14 (Table III), indicates a lactone ring closed to C-11. The signal of the C-9 carbonyl in the ^{13}C NMR spectrum is missing and a new signal appearing at 106.81 ppm points to ketal formation. As the distribution of methyl types is unchanged, the ketal is formed between C-6 and C-9. The ^{13}C NMR (Table II) and mass spectrometric data (Table IV) agree well with those published for psEAHK [3].

ACKNOWLEDGEMENTS

REFERENCES

1 M. Blumauerová, V. Přikrylová, Z. Stoycheva, N. Vesselinova and T. Kh. Todorov, *Folia Microbiol.*, 36 (1991) in press.
2 Th. Cachet, E. Roets, J. Hoogmartens and H. Vanderhaeghe, *J. Chromatogr.*, 403 (1987) 343.
3 I. O. Kibwage, R. Busson, G. Janssen, J. Hoogmartens, H. Vanderhaeghe and J. Bracke, *J. Org. Chem.*, 52 (1987) 990.
4 G. Pellegatta, G. P. Carugati and G. Coppi, *J. Chromatogr.*, 269 (1983) 33.
5 E. H. Flynn, M. V. Sigal Jr., P. F. Wiley and K. Gerzon, *J. Am. Chem. Soc.*, 76 (1954) 3121.
6 H. Budzikiewicz, C. Djerassi and D. H. Williams, *Mass Spectrometry of Organic Compounds*, Holden-Day, San Francisco, 1967, p. 328.
7 J. R. Everett and J. W. Tyler, *J. Chem. Soc., Perkin Trans. 1*, (1985) 2599.

Comparison of high-performance liquid chromatography with capillary gel electrophoresis in single-base resolution of polynucleotides

YOSHINOBU BABA*, TOSHIKO MATSUURA, KYOKO WAKAMOTO and MITSUTOMO TSU-HAKO

Kobe Women's College of Pharmacy, Kitamachi, Motoyama, Higashinada-ku, Kobe 658 (Japan)

(First received March 7th, 1991; revised manuscript received April 8th, 1991)

ABSTRACT

High-resolution separations of polynucleotides were performed using capillary gel electrophoresis (cGE) and high-performance liquid chromatography (HPLC) with reversed-phase, ion-exchange and mixed-mode columns. Electropherograms showing cGE separations of single-stranded homopolynucleotides were presented and compared with HPLC separations according to the chain length of the polynucleotides. The resolving power of cGE is much higher than that of any HPLC mode. The chain length limits for complete separation within 60 min by cGE, reversed-phase, ion-exchange and mixed-mode HPLC are *ca.* 250, 30, 40 and 40 nucleotides, respectively. The plate number which is achieved for cGE of $3 \cdot 10^6$–$7 \cdot 10^6$ plates/m is about ten times larger than those of all HPLC modes of $4 \cdot 10^4$–$8 \cdot 10^5$ plates/m. The reproducibility of the migration time in cGE (2–4%) is comparable to those of retention times in HPLC in several separation modes (1–3%).

INTRODUCTION

Analytical biotechnology [1,2] is an expanding field covering in the analytical chemistry of biopolymers such as peptides, proteins, oligonucleotides, RNA and DNA. Rapid analytical techniques with high resolution and sensitivity are required for biopolymer analysis [3]. The largest biological project, the human genome project [4,5], and RNA engineering initiated after Cech's discovery of ribozyme [6] have also led to the investigation of more rapid DNA and RNA analyses. These projects all require the achievement of single-base resolution of polynucleotides from both analytical and preparative points of views.

Chromatography [7] and electrophoresis [8] have both been recognized as the main techniques for the analysis of polynucleotides, RNA and DNA in analytical biotechnology. More recently, high-performance liquid chromatography (HPLC) [9–11] and capillary electrophoresis [12] have been developing rapidly. In HPLC separations, several novel packing materials have been developed for the separation of oligonucleotides and polynucleotides [13–31]. The packing materials developed for HPLC can be classified into four groups: ion-exchange [13–25], reversed-phase [13,26,27], mixed-mode [28–30] and hydroxyapatite [31]. Microparticulate ($< 5 \ \mu$m)

ion exchangers based on polymers [21–25] and mixed-mode packing materials [28–30] have led to high resolving powers of polynucleotides for single-base resolution. Reversed-phase packing materials [13,26,27] have provided an excellent means of rapidly and efficiently purifying synthetic oligonucleotides from crude reaction mixtures. In capillary electrophoretic separations, Karger and co-workers [32,33] first demonstrated the ultra-high resolving power of capillary gel electrophoresis (cGE) using polyacrylamide gel-filled capillaries for the separation of polynucleotides. Several research groups have also been investigating cGE for the single-base resolution of polynucleotides [34–40] and applied it to rapid DNA sequencing [34–36].

In this paper, HPLC and cGE are compared with respect to their performance in the single-base resolution of polynucleotides. First, we examined critically the resolving power of HPLC and cGE, i.e., how wide a range of chain length of polynucleotides can be separated with high resolution. For this purpose, we investigated the suitability of a laboratory-made polyacrylamide gel-filled capillary [40] for cGE and four commercially available columns for HPLC, namely (1) a TSK gel OligoDNA RP conventional silica-based ODS reversed-phase column [27], (2) a TSK gel DEAE-NPR novel microparticulate non-porous polymer-based ion-exchange column [23,24], (3) a Shim-pack WAX-1 silica-based ion-exchange column [20] and (4) a Neosorb-LC-N-7R RPC-5 type column [30]. Binary gradient elution was used for HPLC separations of polynucleotides and the gradient was optimized by using computer-assisted retention prediction and the HPLC computer simulation system reported previously [41–43]. We used commercial homooligodeoxynucleotides of specified chain length an polyadenylic acids digested enzymatically to study the limits of resolution for these systems. In addition, the reproducibility of both techniques was studied. The advantages and limitations of each technique are discussed on the basis of our own experience in the laboratory. The resolving powers of HPLC columns that have been reported previously [13–31] were also compared with that of cGE.

EXPERIMENTAL

Chemicals ·

Polyadenylic acid [poly(A)] was obtained from Yamasa Shoyu (Chiba, Japan), polydeoxyadenylic acid [poly(dA)] from Sigma (St. Louis, MO, USA) and Pharmacia LKB (Uppsala, Sweden), polydeoxyadenylic acids of chain length from the 12mer to 18mer [poly(dA)$_{12-18}$] and from the 40mer to 60mer [poly(dA)$_{40-60}$] and polyadenylic acids of chain length from the 12mer to 18mer [poly(A)$_{12-18}$] from Pharmacia and nuclease P1 from Yamasa Shoyu. All other chemicals were of analytical-reagent or electrophoretic grade from Wako (Osaka, Japan). The concentrations of samples were 2.5 units per 100 μl for poly(dA)$_{12-18}$, 5 units per 100 μl for poly(dA)$_{40-60}$ and 5 units per 100 μl for poly(A)$_{12-18}$. These polynucleotide samples were stored at −18°C until used.

Preparation of poly(A) and poly(dA) enzymatic partial hydrolysates

Oligoadenylate fragments from poly(A) were prepared by enzymatic hydrolysis of poly(A) with nuclease P1 [44]. An aliquot (200 μl) of an aqueous solution of poly(A) (15 mg/ml) was mixed with 200 μl of 0.3 M citrate buffer solution (pH 6). An aliquot (2 μl) of an aqueous solution of nuclease P1 (50 μg/ml) was added to the buffered

solution of poly(A) and the resulting solution was allowed to react at 40°C for 20 min. Oligodeoxyadenylate fragments from poly(dA) were prepared in the similar manner by using nuclease P1. A 20-μl volume of an aqueous solution of poly(dA) (5 units per 20 μl) was mixed with 20 μl of 0.3 M citrate buffer (pH 5.3), 3 μl of an aqueous solution of nuclease P1 (50 μg/ml) was added to the buffered solution of poly(dA) and the resulting solution was allowed to react at 40°C for 40 min. These polynucleotide samples were stored at -18°C until used.

HPLC equipment

A Tri-Rotar VI HPLC system (Jasco, Tokyo, Japan) and an LC-800 HPLC system (Jasco) were used for the separation of oligonucleotides. Both HPLC systems were equipped with a microcomputer-based gradient controller. All gradients were performed with a binary gradient elution technique. Sample solution (5–20 μl) was injected into the column and chromatographed at a flow-rate of 1.0 ml/min. The column temperature was kept at 40°C. Oligonucleotides were detected at 260 nm.

Columns and eluents

Four different types of columns were used: (1) TSKgel OligoDNA RP (TOSOH, Tokyo, Japan) [27], (2) TSKgel DEAE-NPR (TOSOH) [23,24], (3) Shim-pack WAX-1 (Shimadzu, Kyoto, Japan) [20] and (4) Neosorb-LC-N-7R (Nishio, Tokyo, Japan) [30].

The TSKgel OligoDNA RP column (150 mm × 4.6 mm I.D.) is a reversed-phase column based on a silica support, having a particle diameter of 5 μm and a pore size of 250 Å. Octadecyl groups were chemically bonded to the silica support. Eluents for this column were (A) 5% acetonitrile containing 0.1 M ammonium acetate and (B) 25% acetonitrile containing 0.1 M ammonium acetate.

The TSKgel DEAE-NPR column (35 mm × 4.6 mm I.D.) is an anion-exchange column based on a non-porous polymer support, having a particle diameter of 2.5 μm. Diethylaminoethyl groups were chemically bonded to the non-porous polymer support. Eluents for this column were (A) 0, 0.1 or 0.25 M sodium chloride in 20 mM tris(hydroxymethyl)aminomethane (Tris)–HCl buffer (pH 9.0) and (B) 1 M sodium chloride in 20 mM Tris–HCl buffer (pH 9.0).

The Shim-pack WAX-1 column (50 mm × 4 mm I.D.) is an anion-exchange column based on a spherical silica support, having a particle diameter of 3 μm and a pore size of 100 Å. Tertiary amino groups were chemically bonded to the silica support. Eluents for this column were (A) 0.01 M phosphate buffer (pH 6.8) containing 20% of acetonitrile and (B) 0.3 M phosphate buffer (pH 6.8) containing 20% of acetonitrile.

The Neosorb-LC-N-7R column (250 mm × 4 mm I.D.) is a mixed-mode column (RPC-5 type) based on a polychlorotrifluoroethylene support, having a particle diameter of 7 μm. The support was coated with trioctylmethylammonium chloride. Eluents for this column were (A) 0.01 M sodium perchlorate–Tris–acetate buffer (pH 7.5)–1 mM EDTA and (B) 0.15 M sodium perchlorate–Tris–acetate buffer (pH 7.5)–1 mM EDTA.

Capillary electrophoresis

cGE separations were carried out by using an Applied Biosystems (ABI, Foster

City, CA, USA) Model 270A capillary electrophoresis system. Polyimide-coated fused-silica capillaries (375 μm O.D., 100 μm I.D.) (GL Sciences, Tokyo, Japan) of effective length 30 cm and total length 50 cm were used without pretreatment. Polyacrylamide gel-filled capillaries were prepared according to the method reported previously [40] as follows: (1) a buffered solution of acrylamide is prepared, (2) catalysts [N,N,N',N'-tetramethylethylenediamine (TEMED) and ammonium peroxodisulphate] are added to the solution of acrylamide, (3) polymerizing solution is quickly injected into the capillary by means of a vacuum injection system and (4) acrylamide is polymerized in the capillary for 1 h at room temperature. The reproducibility and stability of gel-filled capillaries were discussed in a previous paper [40]; the gel-filled capillaries typically gave only a 10% decrease in the number of theoretical plates after 50 injections. The buffer solution was a mixture of 0.1 M Tris and 0.1 M boric acid with 7 M urea (pH 8.8). The sample solution was introduced into the capillary electrophoretically (1 s at 5 kV). Gel-filled capillaries were run with buffer solution at 10 kV (200 V/cm, 9–11 μA) at 30°C. Polynucleotides were detected at 260 nm.

RESULTS AND DISCUSSION

Enzymatic digestion of poly(A) described under Experimental gave a mixture of polyadenylates containing 5'-terminal phosphate in their chain from the monomer to 300mer [40]. Poly(A) enzymatic partial hydrolysate is advantageous as a model substrate to demonstrate the resolving power of HPLC and cGE compared with poly(A) alkaline partial hydrolysate and poly(dA)$_{40-60}$, which are widely used as model substrates for HPLC and cGE. The reason is that enzymatic digestion of poly(A) produced a poly(A) mixture containing a wide chain length range in addition to single species in each chain length. In contrast, poly(dA)$_{40-60}$ has a narrow chain length range and alkaline hydrolysis of poly(A) gave double poly(A) containing 2'- or 3'-terminal phosphate in each chain length [15]. HPLC separation of poly(A) alkaline partial hydrolysate, therefore, gave a doublet peak in each chain length for small-size poly(A) and, further, high-molecular-weight poly(A) became poorer resolved [15,42]. We first examined the resolving power of cGE and HPLC with several types of columns by separating poly(A) enzymatic partial hydrolysate. In order to compare cGE and HPLC directly, identical samples were analysed.

cGE separation of poly(A) digested by nuclease P1
Fig. 1 shows an electropherogram for mixtures of poly(A) separated by cGE with a polyacrylamide gel (5% T and 5% C)^a-filled capillary at 200 V/cm. To determine the chain length of poly(A) for each band, poly(A)$_{12-18}$ was co-injected with poly(A) mixtures. Consequently, peaks with a migration time of *ca.* 20 min are assigned to poly(A) from the 12mer to 18mer. The large peak at 17 min would correspond to unseparated oligoadenylates from the monomer to 5mer. Fig. 1, therefore, clearly demonstrates that polynucleotides of different chain length are baseline resolved within the poly(A) series in the chain length range from the 6mer to 255mer under the conditions given, and yet the separation was completed in less than 62 min. The resolution, R_s, of each band pair was more than 1.5.

---

^{a} C = g N,N'-methylenebisacrylamide (Bis)/%T; T = g acrylamide + g Bis per 100 ml of solution.
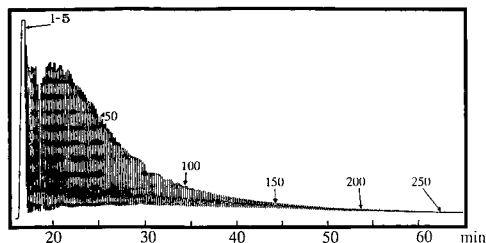
Fig. 1. cGE separation of poly(A) enzymatic partial hydrolysate. Capillary, 100 μm I.D., 375 μm O.D., length 50 cm, effective length 30 cm; running buffer, 0.1 M Tris–0.1 M boric acid–7 M urea (pH 8.8); gel matrix, 5% T and 5% C; field, 200 V/cm; current, 10 μA; injection, 5 kV for 1 s; detection, 260 nm.

The plate number of each peak was estimated to be $2.3 \cdot 10^6$ ($7 \cdot 10^6$/m) for peak 30, $1.5 \cdot 10^6$ ($5 \cdot 10^6$/m) for peak 50 and $9.6 \cdot 10^5$ ($3 \cdot 10^6$/m) for peak 100. The run-to-run reproducibility of the migration time was in the range 2–4% relative standard deviation (R.S.D.) ($n = 5$).

HPLC separations of poly(A) digested by nuclease P1

Figs. 2–5 demonstrate the separations of poly(A) enzymatic partial hydrolysate by HPLC in the reversed-phase (Fig. 2), ion-exchange (Figs. 3 and 4) and mixed modes (Fig. 5). All separations were performed by utilizing gradient elution techniques, the gradients being optimized by HPLC computer simulations [41–43]. The chain length of poly(A) was determined by co-elution of poly(A)$_{12-18}$.

Fig. 2 shows the chromatogram of mixtures of poly(A) separated by reversed-phase HPLC (TSKgel OligoDNA RP column). Poly(A) up to the 30mer were
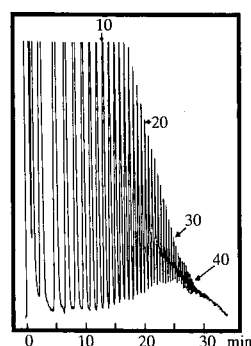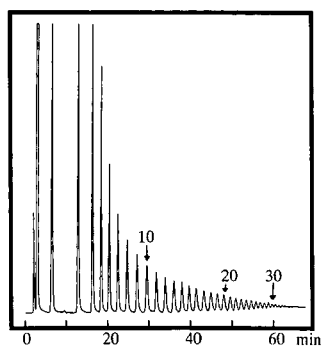

Fig. 2. Reversed-phase HPLC separation of poly(A) enzymatic partial hydrolysate. Column, TSKgel OligoDNA RP (150 mm × 4.6 mm I.D.); eluent, (A) 5% acetonitrile containing 0.1 M ammonium acetate and (B) 25% acetonitrile containing 0.1 M ammonium acetate; gradient programme, 0–10 min from 0 to 18% B, 10–30 min from 18 to 26% B, 30–100 min from 26 to 45% B at 40°C; flow-rate, 1.0 ml/min.

Fig. 3. Anion-exchange HPLC separation of poly(A) enzymatic partial hydrolysate. Column, TSKgel DEAE-NPR (35 mm × 4.6 mm I.D.). Eluent, (A) 0.25 M sodium chloride in 20 mM Tris–HCl buffer (pH 9.0) and (B) 1 M sodium chloride in 20 mM Tris–HCl buffer (pH 9.0); linear gradient from 0 to 100% B in 60 min at 40°C, flow-rate, 1.0 ml/min.
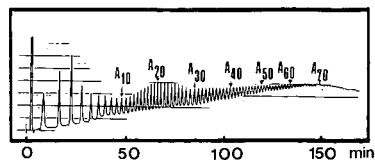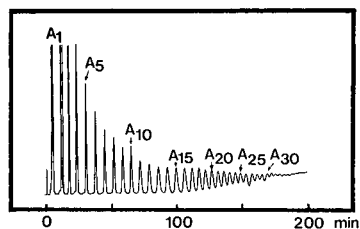
Fig. 4. Anion-exchange HPLC separation of poly(A) enzymatic partial hydrolysate. Column, Shim-pack WAX-1 (50 mm × 4 mm I.D.); eluent, (A) 0.01 M phosphate buffer (H 6.8) containing 20% of acetonitrile and (B) 0.3 M phosphate buffer (pH 6.8) containing 20% of acetonitrile; the convex gradient described previously [42] was used, from 0 to 100% B in 240 min; flow-rate, 1.0 ml/min.

Fig. 5. Mixed-mode HPLC separation of poly(A) enzymatic partial hydrolysate. Column, Neosorb-LC-N-7R (250 mm × 4 mm I.D.); eluent, (A) 0.01 M sodium perchlorate–Tris–acetate buffer (pH 7.5)–1 mM EDTA and (B) 0.15 M sodium perchlorate–Tris–acetate buffer (pH 7.5)–1 mM EDTA; linear gradient from 0 to 100% B in 150 min; flow-rate, 1.0 ml/min.

successfully separated in less than 60 min. The resolution was in the range $R_s = 1.0$–1.5. Such HPLC separations exhibited plate numbers of 80 000 which, with a column length of 15 cm, corresponds to $5 \cdot 10^5$ plates/m. The reproducibility of the retention time was in the range 1–2% R.S.D. ($n = 5$).

Figs. 3 and 4 show the separations of a mixture of poly(A) oligonucleotides by ion-exchange chromatography. The non-porous polymer-based ion exchanger TSKgel DEAE-NPR was used in Fig. 3 and the porous silica-based ion exchanger Shim-pack WAX-1 in Fig. 4. Baseline resolutions were obtained for up to the 20mer, and peaks appeared for up to about the 40mer (Fig. 3) and 35mer (Fig. 4). The chromatographic pattern in Fig. 4 is similar to that in Fig. 3, although the separation time in Fig. 4 was much longer than that in Fig. 3.

The plate numbers were 28 000 ($8 \cdot 10^5$ plates/m) with the TSKgel DEAE-NPR column and 13 000 ($3 \cdot 10^5$ plates/m) with the Shim-pack WAX-1 column. The resolutions for both columns were calculated to be in the range $R_s = 0.8$–1.5. The reproducibility of the retention time for each oligonucleotide was 1–3% R.S.D. ($n = 5$) for both columns.

The chromatogram shown in Fig. 5 was obtained with a mixed-mode column in which the matrix contains sites for both ionic and hydrophobic interactions [28–30]. The resolution possible using this mixed-mode matrix is illustrated by the resolution of a poly(A) enzymatic hydrolysate, which could be separated up to at least the 70mer in less than 150 min. The plate number estimated for each peak was 10 000 ($4 \cdot 10^4$ plates/m) and the resolution for each band pair was in the range $R_s = 0.6$–1.5. The reproducibility of the retention time was 1–2% R.S.D. ($n = 5$).

The performances of cGE and HPLC in the various separation modes as described above are summarized in Table I. Comparison of the resolving powers and analysis time of the four HPLC columns confirms that within a series of poly(A) the TSKgel DEAE-NPR column is the most suitable for the complete and rapid separation of polynucleotides according to chain length.

TABLE I

PERFORMANCE OF cGE AND HPLC IN THE SEPARATION OF POLYNUCLEOTIDES

Method	Plate number (N)	Separated poly(A)	Analysis time (min)	Resolution, R_s	R.S.D. (%)
cGE					
100 μm I.D.;					
5% T and 5% C[a]	2 300 000 (7 · 10^6/m)	6–255mer	62	1.5–1.7	2–4
HPLC					
TSKgel OligoDNA RP[b]	80 000 (5 · 10^5/m)	1–30mer	60	1.0–1.5	1–2
TSKgel DEAE-NPR[c]	28 000 (8 · 10^5/m)	1–40mer	27	0.8–1.5	1–3
Shim-pack WAX-1[d]	13 000 (3 · 10^5/m)	1–30mer	160	0.8–1.5	1–3
Neosorb-LC-N-7R[e]	10 000 (4 · 10^4/m)	1–70mer	150	0.6–1.5	1–2

[a] Gel-filled capillary as in Fig. 1.
[b] Reversed-phase column as in Fig. 2.
[c] Ion-exchange colomn as in Fig. 3.
[d] Ion-exchange column as in Fig. 4.
[e] Mixed-mode column as in Fig. 5.

cGE and HPLC separations of poly(dA) standards and poly(dA) digested by nuclease P1

We next examined the resolving power of cGE and HPLC in the separation of polydeoxyadenylates, poly(dA). The model solutes used were commercially available homooligodeoxyadenylates of specified chain length and poly(dA) enzymatic partial hydrolysate obtained by the method described under Experimental. The electrophoretic conditions were almost the same as described in the previous section. For the HPLC separation of poly(dA), a TSKgel DEAE-NPR column was selected because of its superior resolving power and speed compared with the other columns described. Poly(dA) was separated by gradient-elution chromatography, the gradients being optimized by HPLC computer simulations [41–43].

Fig. 6 shows separations of a mixture of poly(dA) oligonucleotides which
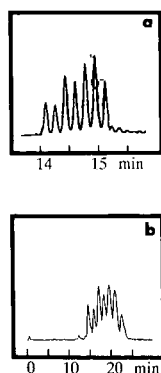

Fig. 6. (a) cGE and (b) anion-exchange HPLC separations of poly(dA)$_{12-18}$. Gel electrophoretic conditions as in Fig. 1. Chromatographic conditions as in Fig. 3 except for eluent and gradient programme. Eluent, (A) 0.1 *M* sodium chloride in 20 m*M* Tris–HCl buffer (pH 9.0) and (B) as in Fig. 3; gradient programme, 0–3 min from 0 to 8% B, 3–15 min from 8 to 18% B, 15–50 min from 18 to 35% B at 40°C.
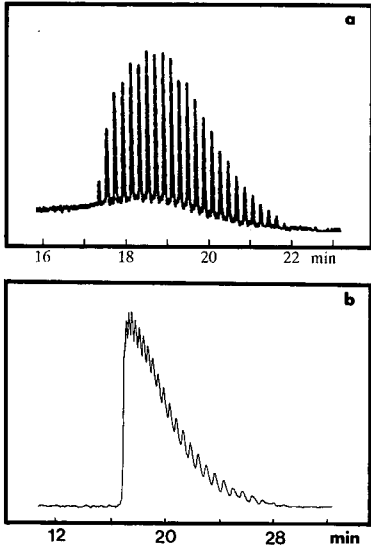
Fig. 7. (a) cGE and (b) anion-exchange HPLC separations of poly(dA)$_{40-60}$. Gel electrophoretic conditions as in Fig. 1 except for gel matrix (7% T and 5% C). Chromatographic conditions as in Fig. 3 except for eluent and gradient programme. Eluent, (A) 0.1 M sodium chloride in 20 mM Tris–HCl buffer (pH 9.0) and (B) as in Fig. 3; gradient programme, 0–4 min from 0 to 20% B, 4–12 min from 20 to 40% B, 12–55 min from 40 to 55% B at 40°C.
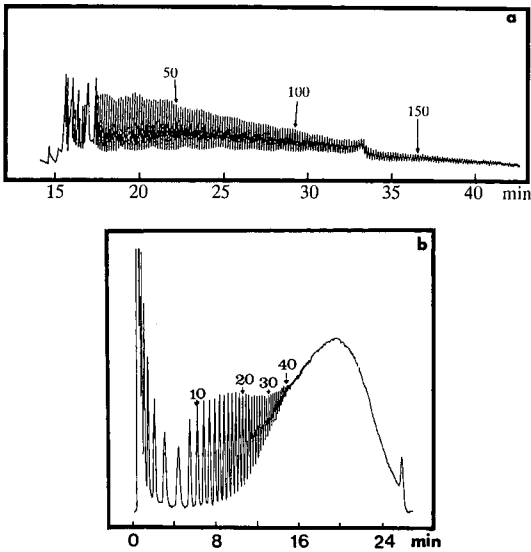

Fig. 8. (a) cGE and (b) anion-exchange HPLC separations of poly(dA) enzymatic partial hydrolysate. Gel electrophoretic conditions as in Fig. 1. Chromatographic conditions as in Fig. 3.

contains 12–18 bases [poly(dA)$_{12-18}$] according to the supplier. All components were completely separated in the cGE separation (Fig. 6a) and HPLC separation (Fig. 6b) illustrated that poly(dA)$_{12-18}$ was well resolved. The analysis time of cGE was shorter than that of HPLC.

Fig. 7 shows separations of poly(dA)$_{40-60}$ by cGE (Fig. 7a) and HPLC (Fig. 7b). In the cGE separation, all poly(dA) polynucleotides were baseline resolved within only 22 min. On the other hand, HPLC failed to resolve each component of poly(dA). We tried to improve the resolution of poly(dA)$_{40-60}$ by changing the HPLC separation conditions, but dit not achieve a better resolution. These results clearly illustrate that the resolving power of cGE is much hihger than that of HPLC in the separation of relatively high-molecular-weight poly(dA), whereas the difference in the resolving powers of the two techniques is not obviously distinguishable in the separation of relatively shorter poly(dA), as shown in Fig. 6.

Separations of poly(dA) enzymatic partial hydrolysate were performed by use of cGE (Fig. 8a) and HPLC (Fig. 8b). Fig. 8a clearly demonstrates that ultra-high resolution of poly(dA) is achieved by using cGE; 180 bands of poly(dA) were completely resolved within only 42 min, whereas baseline resolution was obtained for up to only the 20mer by HPLC as shown in Fig. 8b and peaks appeared for up to about the 40mer. Comparison of the results shows that cGE gave a superior resolution to HPLC. The number of poly(dA) bands that appeared in the cGE separation (Fig. 8a) is smaller than that of poly(A) bands in Fig. 1, because the poly(dA) sample prior to digestion has an approximate average chain length of 290 according to the supplier but the chain length of poly(A) prior to digestion is much larger than that of poly(dA).

Comparison of resolving power and reproducibility of the two techniques

We compared with the utility of cGE and HPLC with four different columns for the separation of homopolynucleotides according to their chain length. The results show that within a series of homopolynucleotides all systems lead to the reliable separation of small-sized poly(A) according to chain length but only the cGE system makes it possible to separate completely higher polynucleotides such as the 250mer.

To evaluate the potential of cGE for single-base resolution of polynucleotides, the performance of cGE was compared with that of HPLC as indicated in Table I. Table I shows a ten times higher plate number for cGE of $7 \cdot 10^6$ plates/m than those for all modes of HPLC of $4 \cdot 10^4$–$8 \cdot 10^5$ plates/m. The chain length limit by cGE, which is 255 nucleotides, is 4–8 times larger than those given by reversed-phase, non-porous polymer-based ion-exchange, porous silica-based ion-exchange and mixed mode HPLC, which are 30, 40, 30 and 70 nucleotides, respectively. cGE separated 40 bands of poly(A) in 10 min, whereas HPLC separated only fifteen bands (TSKgel DEAE-NPR) or two bands (Shim-pack WAX-1) in 10 min. Additionally, each component was resolved completely in cGE but later eluted components in HPLC showed poorer resolution. The resolution values obtained for cGE ranged from $R_s = 1.5$–1.7, which compare favourably with those for HPLC of $R_s = 0.6$–1.5. The reproducibility (2–4% R.S.D.) of the migration time in cGE is comparable to those of the retention times in HPLC in the various modes (1–3% R.S.D.). These results show that the cGE technique gave a superior performance to the HPLC techniques.

To examine the performance of cGE in more detail, we selected high-resolution HPLC and cGE separations of polynucleotides reported in the literature, as listed in

TABLE II

PERFORMANCE OF HPLC AND cGE REPORTED IN THE LITERATURE

Method	Separated polynucleotides	Analysis time (min)
Ion-exchange HPLC		
Partisil SAX [13]	1–30mer	50
Laboratory-made column [15]	4–35mer	300
Nucleogen-DMA-60 [18]	1–37mer	110
MonoQ [19]	1–27mer	15
Gen-Pak FAX [22]	40–60mer	39
TSKgel DEAE-NPR [23]	20–70mer	17
Laboratory-made column [25]	1–18mer	4
Reversed-phase HPLC		
Zorbax ODS [13]	2–10mer	25
μBondapak C_{18} [26]	1–19mer	60
Mixed-mode HPLC		
Laboratory-made column [28,29]	4–90mer	1140
Neosorb-LC-N-7R [30]	1–75mer	95
cGE		
cGE [33]	20–160mer	25
cGE [34]	19–330mer	70
cGE [35]	19–300mer	115
cGE [36]	19–340mer	70
cGE [38]	1–430mer	130

Table II. The results obtained by HPLC given in Table II show that mixed-mode HPLC [28–30] can separate polynucleotide mixtures containing a wide range of chain length and HPLC with a non-porous polymer-based ion-exchange column [23,25] achieved a high-speed analysis of polynucleotides. However, the resolving power and separation speed of cGE as presented here is much better than those of the HPLC techniques listed in Table II. For example, Kato *et al.* [23] reported a rapid separation in less than 20 min of oligodeoxyadenylic acids from the 17mer to 70mer by use of a non-porous polymer-based ion-exchange column. Later eluted bands, however, represented a poor resolution, in contrast to the achievement of baseline separations for up to the 32mer as shown in Fig. 3. Other groups [28–30] have demonstrated high resolutions of polynucleotides with relative wide ranges of chain length by use of mixed-mode separation columns, but their separations required long analysis times.

Table II also shows the cGE separations of polynucleotides reported in the literature. These results demonstrate the ultra-high efficiency of cGE in the single-base resolution of polynucleotides and in DNA sequencing. The cGE separation presented in Fig. 1 gave almost the same efficiency with the respect to resolution and speed as those listed in Table II.

In conclusion, our results suggest that cGE and HPLC are equally effective for the separation of small-sized polynucleotides, whereas for longer polynucleotides cGE is superior to HPLC with respect to resolving power, speed and efficiency. The only disadvantage is that cGE is not suitable for large-scale preparative separations of

polynucleotides. Therefore, for preparative work with small-sized polynucleotides, HPLC is the only choice. Micropreparative analysis of large polynucleotides, however, is realized only by cGE [33]. For high-speed separations of larger polynucleotides there is as yet no alternative to cGE.

REFERENCES

1 Cs. Horváth and J. G. Nikelly (Editors), *Analytical Biotechnology: Capillary Electrophoresis and Chromatography (ACS Symposium Series*, No. 434), American Chemical Society, Washington, DC, 1990.
2 R. L. Garnick, N. J. Solli and P. A. Papa, *Anal. Chem.*, 60 (1988) 2546.
3 D. C. Warren, *Anal. Chem.*, 56 (1984) 1528A.
4 G. L. Trainor, *Anal. Chem.*, 62 (1990) 418.
5 National Institutes of Health and Department of Energy (Editors), *Understanding Our Genetic Inheritance: the U.S. Human Genome Project: The First Five Years, 1991–1995*, U.S. Department of Health and Human Services and U.S. Department of Energy, Springfield, 1990.
6 T. R. Cech, *Angew. Chem., Int. Ed. Engl.*, 29 (1990) 759.
7 A. M. Krstulović (Editor), *CRC Handbook of Chromatography, Nucleic Acids and Related Compounds*, Vol. 1, Parts A and B, CRC Press, Boca Raton, FL, 1987.
8 D. Rickwood and B. D. Hames (Editors), *Gel Electrophoresis of Nucleic Acids —a Practical Approach*, IRL Press, Oxford, 2nd ed., 1990.
9 P. R. Brown, *Anal. Chem.*, 62 (1990) 995A.
10 L. W. McLaughlin and R. Bischoff, *J. Chromatogr.*, 418 (1987) 51.
11 R. Hecker and D. Riesner, *J. Chromatogr.*, 418 (1987) 97.
12 B. L. Karger, A. S. Cohen and A. Guttman, *J. Chromatogr.*, 492 (1989) 585.
13 W. Haupt and A. Pingoud, *J. Chromatogr.*, 260 (1983) 419.
14 W. Müller, *Eur. J. Biochem.*, 155 (1986) 203.
15 J. D. Pearson and F. E. Regnier, *J. Chromatogr.*, 255 (1983) 137.
16 R. R. Drager and F. E. Regnier, *Anal. Biochem.*, 145 (1985) 47.
17 Y. Kato, M. Sasaki, T. Hashimoto, T. Murotsu, S. Fukushige and K. Matsubara, *J. Chromatogr.*, 265 (1983) 342.
18 M. Colpan and D. Riesner, *J. Chromatogr.*, 296 (1984) 339.
19 A. Yu. Tsygankov, Yu. A. Motorin, A. D. Wolfson, D. B. Kirpotin and A. F. Orlovsky, *J. Chromatogr.*, 465 (1989) 325.
20 T. Ueda and Y. Ishida, *J. Chromatogr.*, 386 (1987) 273.
21 D. J. Stowers, J. M. B. Keim, P. S. Paul, Y. S. Lyoo, M. Merion and R. M. Benbow, *J. Chromatogr.*, 444 (1988) 47.
22 W. Warren and M. Merion, *BioChromatography*, 3 (1988) 118.
23 Y. Kato, T. Kitamura, A. Mitsui, Y. Yamasaki, T. Hashimoto, T. Murotsu, S. Fukushige and K. Matsubara, *J. Chromatogr.*, 447 (1988) 212.
24 Y. Kato, Y. Yamasaki, A. Onaka, T. Kitamura, T. Hashimoto, T. Murotsu, S. Fukushige and K. Matsubara, *J. Chromatogr.*, 478 (1989) 264.
25 Y.-F. Maa, S.-C. Lin, Cs. Horváth, U.-C. Yang and D. M. Crothers, *J. Chromatogr.*, 508 (1990) 61.
26 G. D. McFarland and P. N. Borer, *Nucleic Acids Res.*, 7 (1979) 1067.
27 H. Moriyama and Y. Kato, *J. Chromatogr.*, 445 (1988) 225.
28 L. W. McLaughlin, *Chem. Rev.*, 89 (1989) 309.
29 R. Bischoff and L. W. McLaughlin, *Anal. Biochem.*, 151 (1985) 526.
30 H. Sawai, *J. Chromatogr.*, 481 (1989) 201.
31 Y. Yamasaki, A. Yokoyama, A. Ohnaka, Y. Kato, T. Murotsu and K. Matsubara, *J. Chromatogr.*, 467 (1989) 299.
32 A. S. Cohen, D. R. Najarian, A. Paulus, A. Guttman, J. A. Smith and B. L. Karger, *Proc. Natl. Acad. Sci. U.S.A.*, 85 (1988) 9660.
33 A. Guttman, A. S. Cohen, D. N. Heiger and B. L. Karger, *Anal. Chem.*, 62 (1990) 137.
34 J. A. Luckey, H. Drossman, A. J. Kostichka, D. A. Mead, J. D'Cunha, T. B. Norris and L. M. Smith, *Nucleic Acids Res.*, 18 (1990) 4417.
35 H. Swerdlow and R. Gesteland, *Nucleic Acids Res.*, 18 (1990) 1415.

36 A. S. Cohen, D. R. Najarian and B. L. Karger, *J. Chromatogr.*, 516 (1990) 49.
37 A. Paulus and J. I. Ohms, *J. Chromatogr.*, 507 (1990) 113.
38 H.-F. Yin, J. A. Lux and G. Schomburg, *J. High Resolut. Chromatogr.*, 13 (1990) 624.
39 Y. Baba, M. Tsuhako, S. Enomoto, A. M. Chin and R. S. Dubrow, *J. High Resolut. Chromatogr.*, 14 (1991) 204.
40 Y. Baba, T. Matsuura, K. Wakamoto and M. Tsuhako, *Chem. Lett.*, (1991) 371.
41 Y. Baba, in J. L. Glajch and L. R. Snyders (Editors), *Computer-Assisted Method Development for High-Performance Liquid Chromatography*, Elsevier, Amsterdam, 1990, pp. 143–168; *J. Chromatogr.*, 485 (1989) 143.
42 Y. Baba, M. Fukuda and N. Yoza, *J. Chromatogr.*, 458 (1988) 385.
43 Y. Baba and M. K. Ito, *J. Chromatogr.*, 485 (1989) 647.
44 M. Fujimoto, A. Kuninaka and Y. Yoshino, *Agric. Biol. Chem.*, 38 (1974) 1555.

CHROM. 23 427

Synthesis of a new acrylamido buffer (acryloylhistamine) for isoelectric focusing in immobilized pH gradients and its analysis by capillary zone electrophoresis

MARCELLA CHIARI, MARIA GIACOMINI, CLAUDIA MICHELETTI and PIER GIORGIO RIGHETTI*

Chair of Biochemistry and Department of Biomedical Sciences and Technologies, University of Milan, Via Celoria 2, Milan 20133 (Italy)

ABSTRACT

By reacting acryloyl chloride with histamine a weakly basic acrylamido buffer for use in isoelectric focusing in immobilized pH gradients, acryloylhistamine [2-(4-imidazolyl)ethylamine-2-acrylamide], with a pK of 7.0 (25°C) was synthesized. Even though this compound has the same pK value as the commercially available pK 7.0 Immobiline, it has some interesting features: (a) it is strongly resistant to hydrolysis, in contrast to the pK 7.0 and 6.2 species; (b) it is hydrophilic; and (c) owing to its heteroaromatic ring, its amino groups are resistant to oxidation. The above properties (degradation kinetics, hydrophilicity, proneness to oxidation) were established in a quantitative manner by capillary zone electrophoresis analysis.

INTRODUCTION

Isoelectric focusing (IEF) in immobilized pH gradients (IPG) represents perhaps the most powerful development in electrokinetic separations, with an unrivalled resolving power and a very high load ability in preparative runs [1]. The power and the precision of IPG rely on the quality of the buffers used to generate and maintain the pH gradient in the electric field. Unlike conventional IEF, where the pH gradient is obtained by electrophoretic sorting of a vast number of soluble amphoteric buffers, called carrier ampholytes [2], the IPG technique uses a set of a few, well defined chemicals available commercially as crystalline powders or liquids, under the trade name Immobiline. We have recently described the structure and given the formulae of the acidic [3] and basic [4] Immobiline chemicals. In addition, we have proposed over the years a number of additional compounds for expanding the fractionation ability of IPGs: both more acidic [5,6] and more alkaline [7] compounds have been produced in our laboratory. We have also synthesized analogues of the weakest Immobiline bases (the morpholino derivatives, with pK values of 6.2 and 7.0): by introducing a thiomorpholino ring, the pK values of these compounds have been increased to 6.6 and 7.4, respectively, thus offering additional species buffering around neutrality, *i.e.*,

in a region which normally lacks suitable buffering groups and where the bulk water conductivity reaches a minimum [8]. A new, hydrophilic Immobiline with a pK 8.05 has also been synthesized recently, in order to close the gap in the pH 7.0–8.5 region [9]. Thus, the family of acrylamido buffers is expanding: we have described now a total of fourteen monoprotic compounds and there is a report on a biprotic species, itaconic acid [10]. Nevertheless, we have continued the search for new chemicals, especially for compounds buffering around neutrality, so as to increase the versatility and flexibility of the IPG technique.

    We report here the synthesis of a new, weakly basic acrylamido buffer, acryloylhistamine [2-(4-imidazolyl)ethylamine-2-acrylamide], having pK = 7.0. Although this compound has the same pK as the commercially available species (3-morpholinopropylacrylamide, pK 7.0), nevertheless it exhibits some interesting properties: (a) it is strongly resistant to hydrolysis, (b) it is as hydrophilic as the pK 7 Immobiline and (c) owing to the presence of an imidazole moiety, it is resistant to oxidation by peroxodisulphate.

EXPERIMENTAL

    Commercial Immobilines, Repel- and Bind-silane, Gel Bond PAG, the Multiphor II chamber, Multitemp thermostat, the Macrodrive power supply and Pharmalyte carrier ampholytes of pH 4–6 and 6–8 were purchased from Pharmacia-LKB Biotechnology (Bromma, Sweden). Non-commercial acrylamide weak acids and bases were synthesized in our laboratory as reported [5–9]. Acrylamide, N,N'-methylenebisacrylamide (Bis), TEMED, ammonium peroxodisulphate and Coomassie Brilliant Blue R-250 were obtained from Bio-Rad Labs. (Richmond, CA, USA). Acryloyl chloride and histamine were from Fluka (Buchs, Switzerland); the former was distilled just prior to use. Control and oxidized bovine serum albumin (BSA) were a gift from Professor Colonna, University of Milan. Mandelic acid, used as an internal standard in capillary zone electrophoresis (CZE) runs, was purchased from Aldrich (Steinheim, Germany).

Alkaline hydrolysis

    All Immmobiline buffers were dissolved (20 mM each) in 0.1 M sodium hydroxide solution and incubated at 70°C, under a nitrogen atmosphere, for up to 6 h. At 30-min intervals aliquots were collected and diluted in 0.1 M borate buffer (pH 9.0) to 2.5 mM. After adding mandelic acid (2.50 mM) as an internal standard, the samples were analysed by CZE.

Capillary zone electrophoresis

    CZE was performed in a Beckman (Palo Alto, CA, USA) instrument (P/ACE System 2000) equipped with a 50 cm × 50 μm I.D. capillary. Runs were performed at 25°C in a thermostated environment in 0.1 M borate (pH 9.0), except for the oxidation products (see Fig. 7), which were analysed in 50 mM phosphate (pH 7.0). In all instances the migration direction was toward the negative electrode, which means that the acidic species (mandelic acid) is transported there by electroosmosis, as it migrates electrophoretically toward the positive electrode. The samples were injected into the capillary by pressure (800 kPa), usually for 10 s. A calibration graph for each

acrylamido derivative analysed was costructed with a Beckman integration system Gold, with concentration points 0.25, 0.50, 1.00, 1.25, 2.00, 2.50 and 3.50 mM. In each run mandelic acid (2.50 mM) was used as an internal standard.

Thin-layer chromatography (TLC)

TLC was performed on silica gel 60F$_{254}$ plates from Merck (Darmstadt, Germany), using chloroform–methanol (7:3, v/v) as eluent. The spots were revealed either with 3.5% molybdophosphoric acid in ethanol or with ninhydrin.

## Nuclear magnetic resonance (NMR) spectroscopy

NMR analyses were carried out for solutions in deuterated methanol, using tetramethylsilane (TMS) as internal standard, with a Model EM-360 L 60-MHz spectrometer from Varian (Palo Alto, CA, USA).

Isoelectric focusing (IEF) in immobilized pH gradients (IPG)

IEF in IPG was performed in a 4% T, 4% C^a polyacrylamide gel, in the pH range 4–8. The recipe for this IPG interval, utilizing both the commercially available Immobilines or the new species (acryloylhistamine), was as described previously [11]. The gel, after polymerization, washing and drying [1], was reswollen in 0.5% Pharmalyte (pH 4–8). Protein samples (20 μg each) were applied at the anodic gel side. Each run was for 2 h at 400 V, followed by 4 h at 2000 V, at 10°C. The gels were stained with Coomassie Brilliant Blue R-250 in Cu^{2+}.

Synthesis of acryloylhistamine

Histamine (3 g; 0.016 mol) was dissolved into 12 ml of 4 M sodium hydroxide solution and acryloyl chloride (700 μl, 0.008 mol) was added dropwise at 0°C. After stirring for 1 h, the solution was titrated to pH 8.5 and then extracted three times with chloroform. The organic phase was dried with sodium sulphate. After removing the organic solvent *in vacuo*, 250 mg of product were recovered. The material was subsequenty purified by silica gel chromatography (product-to-silica ratio 1:60, w/w) and eluted with chloroform–methanol (8:2). The recovery of the purified product was 198 mg (15% yield). ^{1}H NMR (CH$_3$O^{2}H): δ 2.8 (2H, =C–CH$_2$–, t), 3.6 (2H, –CH$_2$–NH, m), 5.6 (1H, –CH=, m), 6.35 (2H, =CH$_2$, d), 6.9 (1H, NH–CH–CH, s), 7.6 ppm (1H, HN–CH=N, s). The structure of the novel acrylamido buffering compound is thus
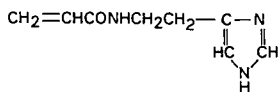
Synthesis of Immobiline analogues

In order to study the proneness of the acrylamido buffers to peroxodisulphate oxidation, analogues lacking the double bond were prepared, so that exposure to peroxodisulphate would not produce concomitantly a gel phase. Two such analogues were prepared: acetylhistamine [a saturated analogue of the pK 7$_{AH}$ (see below) species] and acetylmorpholine (morpholinopropylacetamide, a saturated analogue of the pK 7 species). Both species were prepared essentially as described previously [12], except

---

^{a} C = g N,N'-methylenebisacrylamide (Bis)/% T; T = g acrylamide + g Bis per 100 ml of solution.

that acetic anhydride (in pyridine as solvent) was used for the synthesis instead of acryloyl chloride.

Spectrophotometric analyses

In order to study the potential formation of N-oxides on exposure to peroxodisulphate, the two Immobiline analogues described above were subjected to UV–VIS spectrophotometry with a Cary 219 instrument (Varian). Solutions of 10 mM of each analogue were prepared in 100 mM borate buffer (pH 9) and brought to a 2% final concentration of ammonium peroxodisulphate from a stock 40% solution. Formation of N-oxides was monitored by both the spectra in the 250–450-nm range and by following the absorbance increments with time at a fixed wavelength (280 nm).

Potentiometric titration

The new acrylamido buffer was titrated manually under nitrogen at 25°C. A 10-ml volume of a 10 mM acryloylhistamine solution was titrated with 10 ml of 10 mM hydrochloric acid. The pK value was independently assessed also by measuring the pH of a 2:1 molar solution of buffer/titrant, which, by definition, should correspond to its pK value.

Partition coefficient

In order to establish a hydrophobicity scale, the new compound (acryloyl-histamine, referred to as pK 7$_{AH}$) and Immobilines of pK 6.2, 7.0, 7.4, 8.5 and 9.3 were subjected to partitioning in 1-octanol–water as described by Purcell et al. [13]. The partition coefficient, P, is defined as the ratio of the molarity of a given compound in the organic phase to that in the aqueous phase. Partitioning is performed under conditions in which the alkaline Immobilines are fully deprotonated.

RESULTS

Fig. 1 shows the titration curve of the new, weakly basic acrylamido buffer: as the precursor was histamine, we had hoped to obtain a weakly basic buffer. The aim
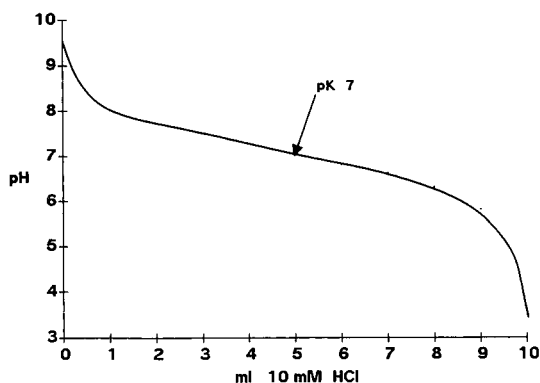

Fig. 1. Titration curve of acryloylhistamine. A 10-ml aliquot of a 10 mM solution of the acrylamido buffer was titrated with 10 ml of 10 mM HCl at 25°C under a nitrogen atmosphere. The pK value was determined to be 7.0.
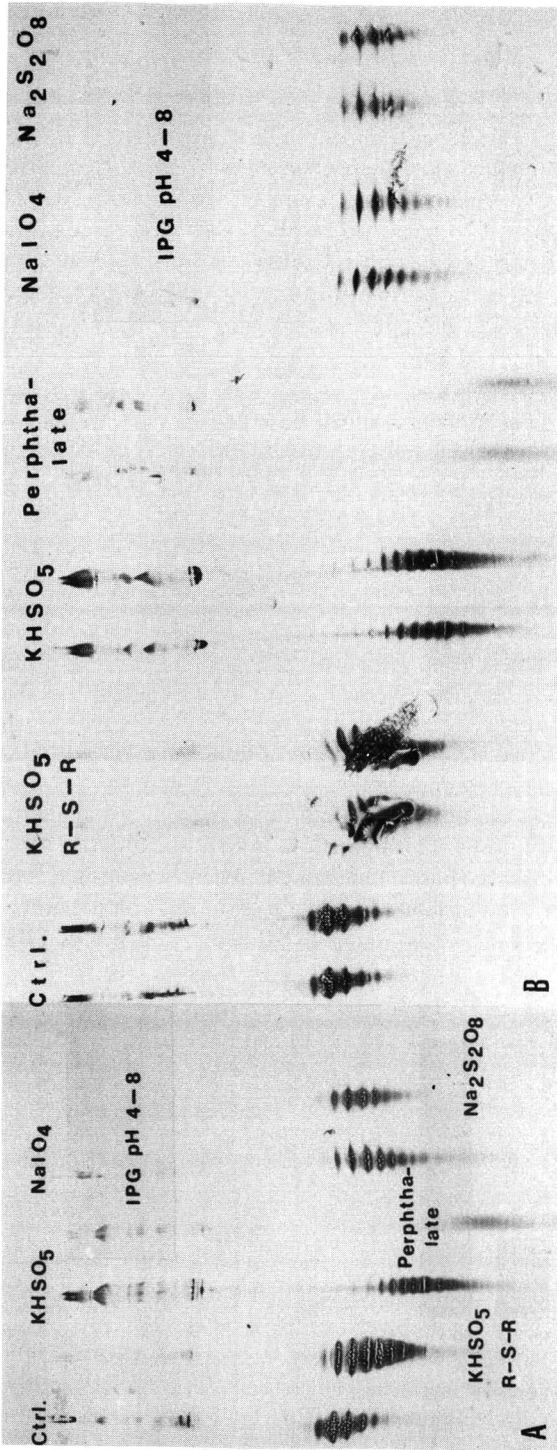
Fig. 2. Analytical IEF gel in the IPG pH 4–8 interval. The gel was a 4% T, 4% C polyacrylamide matrix, reswollen in 0.5% Pharmalyte (pH 4–8). Left side (A): formulation containing the pK 7$_{AH}$ compound; right side (B): recipe with the pK 7.0 Immobiline buffer. Samples: Ctrl. = control bovine serum albumin (BSA); $KHSO_5$ + R-S-R = BSA oxidized by peroxymonosulphate in the presence of a sulphide compound; $KHSO_5$ = BSA oxidized by peroxymonosulphate; perphthalate = BSA oxidized by perphthalate; $NaIO_4$ = BSA oxidized by periodate; $Na_2S_2O_8$ = BSA oxidized by peroxodisulphate. All samples loaded in a 20-μg amount at the anodic gel side. Run: 2 h at 400 V followed by 4 h at 2000 V. Stain: Coomassie Brilliant Blue R-250 in Cu^{2+}.
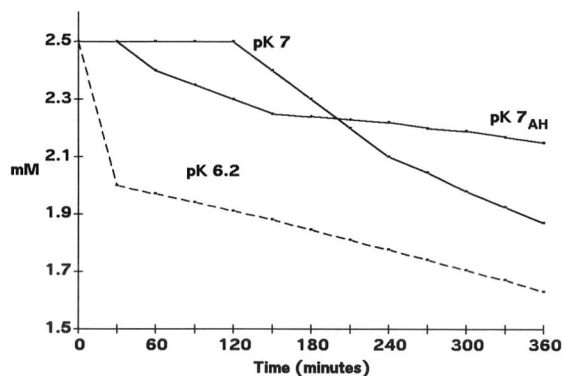
Fig. 3. CZE analysis of Immobiline hydrolytic products. CZE run in a Beckman P/ACE 2000 with a 50 cm ×
50 μm I.D. capillary. Run at 15 kV, 25°C in 0.1 M borate buffer (pH 9). All migrations toward the cathode.
Detection at 214 nm. Mandelic acid (2.5 mM) was used in all runs as an internal standard. Degradation
kinetics of the pK 7.0 and 6.2 commercial Immobilines as compared with the new pK 7$_{AH}$ species. The
quantitative data were obtained by integrating the CZE peaks with the Beckman system Gold.

was in fact to close the gap between the weakest of the acidic (pK 4.6) and the weakest
of the basic (pK 6.2) Immobilines. In reality, we obtained a new species having a pK
essentially identical with that of the commercially available pK 7 compound
(3-morpholinopropylacrylamide). This is also confirmed by Fig. 2: in a pH 4–8 IPG
range, obtained either with the pK 7 or with the pK 7$_{AH}$ compounds, identical pH
ranges and protein patterns were obtained. The good alignment of the protein bands in
the two gels suggests also that the two pK 7 compounds should have very similar
incorporation efficiencies in the polyacrylamide gel.

    One of the main problems with the alkaline Immobilines is their proneness to
hydrolysis when stored in aqueous solutions. This hydrolysis is an autocatalytic event,
because these chemicals are supplied as free bases. One remedy recently proposed is to
store them in n-propanol [14]. Over the years, we have been searching for structures
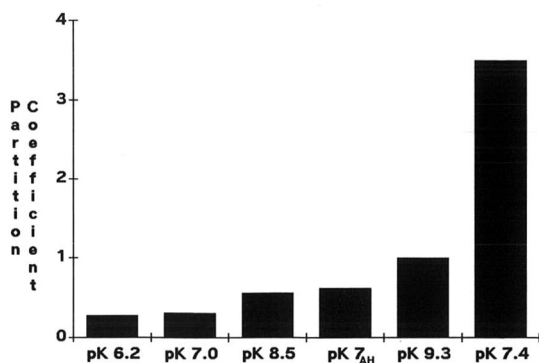that would be more resistant to hydrolysis, so as to improve the reproducibility of the

Fig. 4. Partition coefficients (P) of different alkaline Immobilines in 1-octanol–water. The P values were
assessed by partitioning the different bases in the fully deprotonated form. The molarity ratios in the two
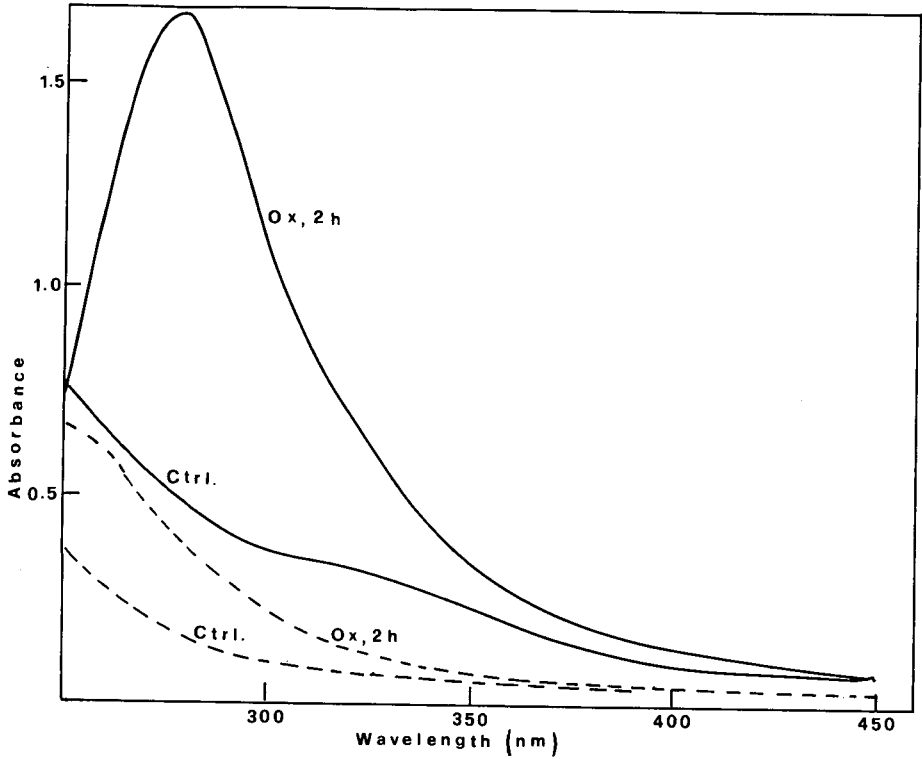phases were measured by absorbance readings at 214 nm in a spectrophotometer.

Fig. 5. UV–VIS spectrophotometry with a Cary 219 instrument of peroxodisulphate oxidation of Immobiline analogues. Solutions of 10 mM of each analogue were prepared in 100 mM borate buffer (pH 9) and with 40% ammonium peroxodisulphate added to a 2% final concentration. Note the strong chromophore at 280 nm for the acetylmorpholine derivative. —— = pK 7.0, morpholine; – – – = pK 7$_{AH}$, histamine.
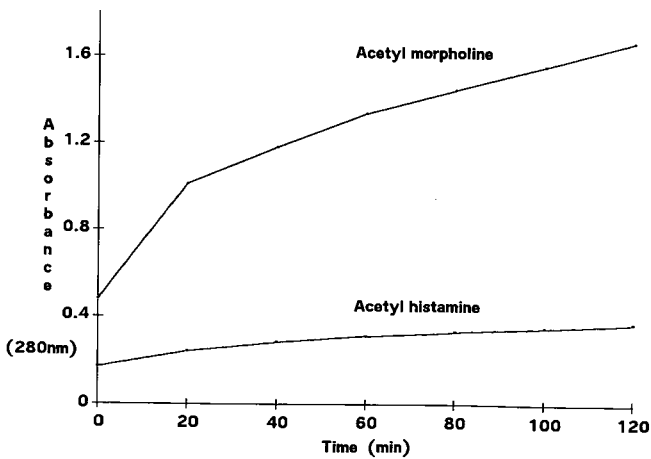

Fig. 6. Kinetics of Immobiline oxidation. Experimental conditions as in Fig. 5, except that the appearance of the chromophore was monitored at a constant wavelength (280 nm).

IPG technique. We therefore subjected the pK 7_{AH} compound and commercial Immobilines with neighbouring pK values (the pK 7.0 and 6.2 species) to forced ageing and measured the extent of hydrolysis by CZE. As shown in Fig. 3, the new pK 7_{AH} compound exhibits much better resistance to hydrolysis than the other two species.

Another desirable property of the Immobiline buffers is their hydrophilicity: hydrophobic interactions are usually deleterious during electrophoresis, as the analyte proteins could bind to the grafted buffers and give pronounced smearing. We have thus created a hydrophobicity scale of several of the basic acrylamido buffers that we had available by partitioning them in 1-octanol–water. The results are shown in Fig. 4: it is seen that most Immobilines are hydrophilic, the hydrophobicity increasing with increasing chain length (thus reaching a higher value with the pK 9.3 buffer). However, a huge hydrophobicity increment is obtained when the oxygen of the morpholino ring in the pK 7 buffer (3-morpholinopropylacrylamide) is replaced with a sulphur atom (pK 7.4, 3-thiomorpholinopropylacrylamide).

A third problem with the Immobiline buffers is their proneness to oxidation during the peroxodisulphate-induced polymerization process [14–16]. In order to quantify this phenomenon, two analogues (acetylmorpholine and acetylhistamine of
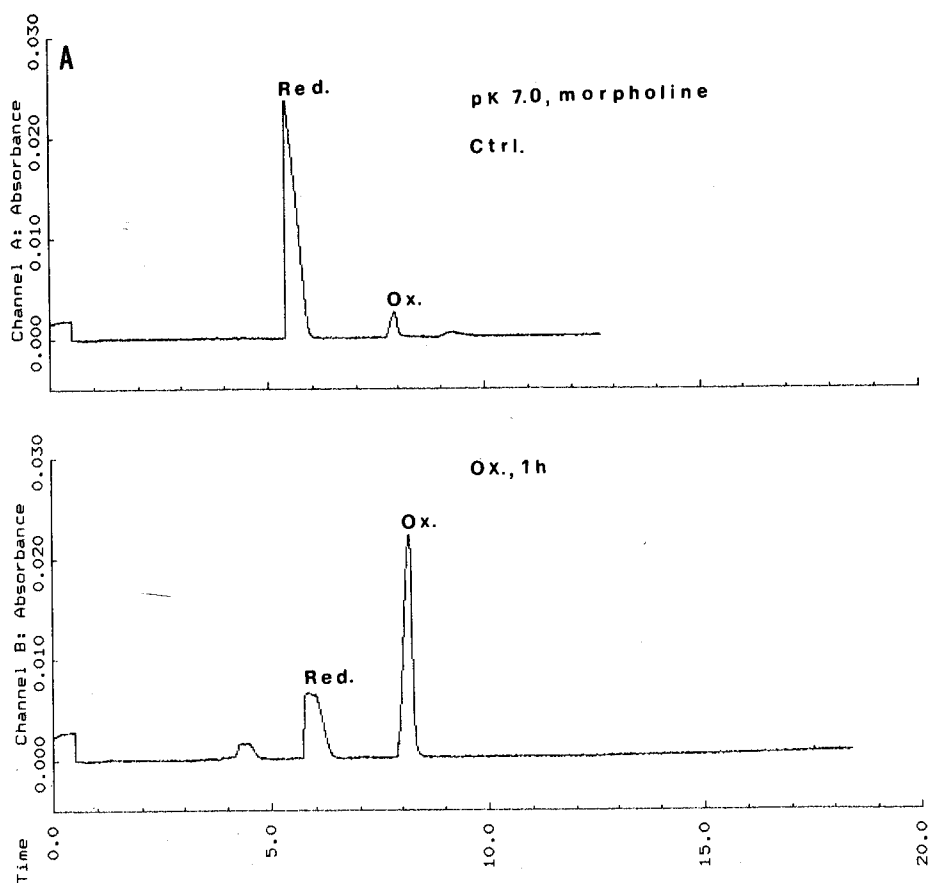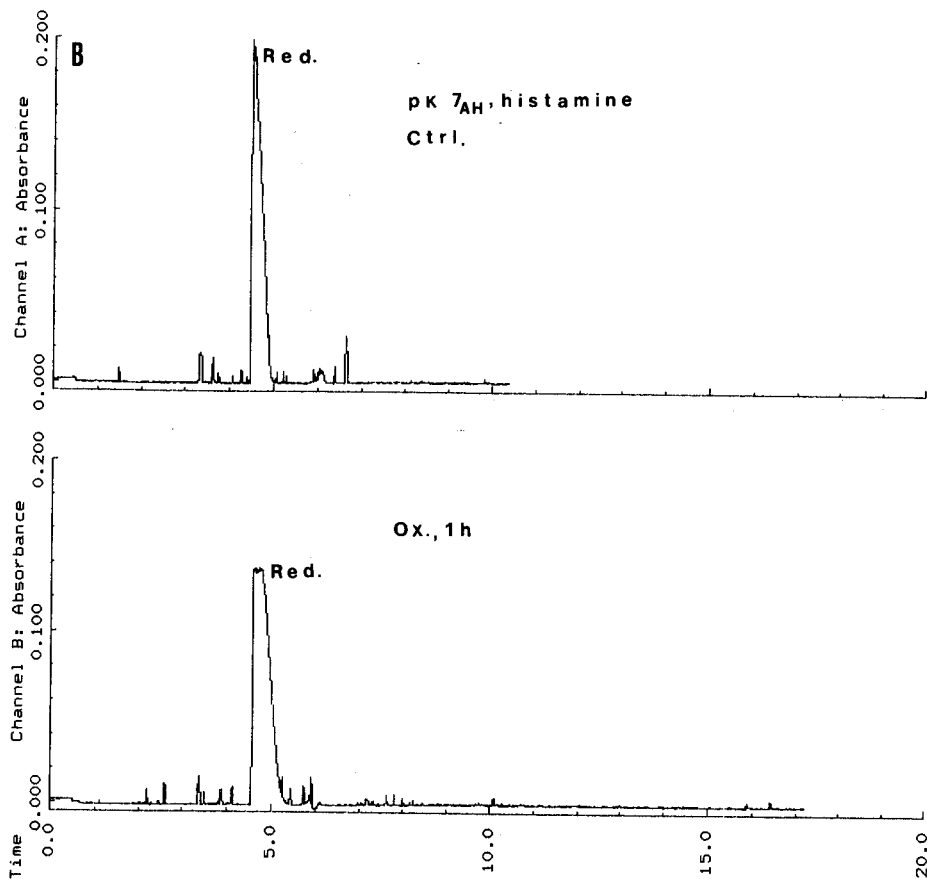

Fig. 7.

Fig. 7. CZE analysis of Immobiline oxidation by peroxodisulphate. The two Immobiline analogues [acetylhistamine (B) and acetylmorpholine (A)] were incubated with 2% peroxodisulphate at room temperature for 1 h and then analysed by CZE in 50 mM phosphate buffer (pH 7). CZE run in a Beckman P/ACE 2000 with a 50 cm × 50 μm I.D. capillary at 15 kV, 25°C. All migrations toward the cathode. Detection at 280 nm. Mandelic acid (2.5 mM) was used in all runs as an internal standard. The quantitative data were obtained by integrating the CZE peaks with the Beckman system Gold. The slow-migrating peak with acetylmorpholine is assumed to be the N-oxide, as such a species can no longer be protonated. Time in min.

the two pK 7 buffers) were incubated in a spectrophotometric cell with 2% peroxodisulphate and spectra recorded at different time intervals up to 2 h. As shown in Fig. 5, while the commercial pK 7 Immobiline is strongly oxidized, with the appearance of a marked chromophore at 280 nm, little modification is seen with the acetylhistamine derivative. The kinetics of such an oxidative process (followed on the 280-nm chromophore) is shown in Fig. 6: at the end of a 2-h period, it is seen that the pK 7$_{AH}$ species has undergone only a very modest oxidation in comparison with the commercial derivative. These data, however, do not allow us to have a quantitative picture of the phenomenon, as the molar absorptivity of the putative oxidation product is not known. CZE has been instrumental in such an assessment: as shown in

Fig. 7, when the analogue of the commercial pK 7 species is analysed at pH 7 (where it would be 50% protonated), it is easily separated from the oxidized form, as the latter cannot be protonated. After incubation for 1 h in peroxodisulphate, as much as 50% of the acetylmorpholine appears to be oxidized. Note that, owing to its proneness to oxidation, even the control contains a small amount (5%) of N-oxide. Conversely, with the new compound proposed here, hardly any modification by peroxodisulphate can be detected (Fig. 7B).

DISCUSSION

Starting from the original set of six acrylamido buffers, commercially available as Immobilines (two acids, with pK 3.6 and 4.6, and four bases, with pK 6.2, 7.0, 8.5 and 9.3), we have developed, over the years, a considerable number of new acrylamido buffers and titrants, covering the pH interval 1–12. With the experience we have accumulated in this period, we are now able to define the desirable properties of ideal buffers for use in the IPG technique. They are essentially three: (a) resistance to chemical degradation (especially spontaneous hydrolysis in solution); (b) hydrophilicity (so as to minimize hydrophobic interaction with proteins under analysis); and (c) resistance to oxidation by peroxodisulphate.

The pK 7_{AH} species described here fulfils most of these requirements. It is clearly more resistant to hydrolysis than the two Immobiline species with similar pK values. At the end of the 6-h degradation period, the pK 6.2 has degraded as much as 35%, the pK 7.0 30% and the pK 7_{AH} only 15%. As all three of them are monosubstituted amides, this resistance to hydrolysis might not be due so much to steric protection of the amido bond, but rather to electronic factors.

The pK 7_{AH} species is also hydrophilic: although, in the hydrophobicity scale of Fig. 4, it is located between the pK 8.5 and 9.3 derivatives, its partition coefficient (0.6) is so close to that of the commercial pK 7.0 compound (0.4) that they can be considered equivalent. In fact, it was surprising to us that the P value should be slightly higher, considering that the substituent chain on the amido group is shorter by two carbon atoms compared with the pK 7.0 compound. Conversely, a huge hydrophobicity increment is noted when the oxygen in the morpholino ring of the pK 7.0 Immobiline is replaced with a sulphur atom (pK 7.4 compound, 3-thiomorpholinopropylacrylamide).

Another desirable property of alkaline Immobilines is their resistance to potential oxidation by peroxodisulphate during the polymerization process. We have recently found that, by contact with peroxodisulphate, the alkaline Immobilines, when deprotonated, are converted into N-oxide derivatives, which are then able to oxidize SH groups in proteins during the focusing process [14–16]. With the pK 7_{AH} species, the fact that the protolytic nitrogen atom is part of a heteroaromatic ring should protect it against potential oxidation processes, as reported in the literature. This appears in fact to be so: as shown in Figs. 5 and 6, little oxidation is seen in the pK 7_{AH} compound on exposure to 2% peroxodisulphate, whereas the corresponding pK 7 commercial species (3-morpholinopropylacrylamide) seems to be substantially modified. Such a phenomenon had been already reported for all Immobiline chemicals [15] and was shown to apply also to the soluble carrier ampholytes used in conventional isoelectric focusing. The presence of such amine oxides ($R_3N^+O^-$) is deleterious to protein

analysis: when focusing proteins in alkaline IPG ranges, free SH groups would be oxidized to S–S bonds by the immobilized N-oxides, generating artefactual, higher pI bands. In a model system, in which free cysteine was incubated anaerobically, at pH 9.0, with a crushed IPG gel, 100% oxidation to cystine was found in a 12-h period [15]. Such oxidation of free SH groups in proteins (e.g., globin α-chains) could be demonstrated even in conventional IEF in the presence of soluble, amphoteric buffers, as the latter also can be oxidized by excess of peroxodisulphate added during the polymerization step. Hence, even when the peroxodisulphate is discharged at the anode in a prefocusing step, a harmful oxidation power remains in the gel in the form of N-oxides of carrier ampholytes [16]. Clearly, the availability of new Immobiline chemicals resistant to peroxodisulphate oxidation would be greatly beneficial to the IPG technique.

ACKNOWLEDGEMENTS

REFERENCES

1 P. G. Righetti, *Immobilized pH Gradients: Theory and Methodology*, Elsevier, Amsterdam, 1990.
2 P. G. Righetti, *Isoelectric Focusing: Theory, Methodology and Applications*, Elsevier, Amsterdam, 1983.
3 M. Chiari, E. Casale, E. Santaniello and P. G. Righetti, *Appl. Theor. Electrophoresis*, 1 (1989) 99–102.
4 M. Chiari, E. Casale, E. Santaniello and P. G. Righetti, *Appl. Theor. Electrophoresis*, 1 (1989) 103–107.
5 E. Gianazza, F. Celentano, G. Dossi, B. Bjellqvist and P. G. Righetti, *Electrophoresis*, 5 (1984) 88–97.
6 P. G. Righetti, M. Chiari, P. K. Sinha and E. Santaniello, *J. Biochem. Biophys. Methods*, 16 (1988) 185–192.
7 C. Gelfi, M. L. Bossi, B. Bjellqvist and P. G. Righetti, *J. Biochem. Biophys. Methods*, 15 (1987) 41–48.
8 M. Chiari, P. G. Righetti, P. Ferraboschi, T. Jain and R. Shorr, *Electrophoresis*, 11 (1990) 617–620.
9 M. Chiari, L. Pagani, P. G. Righetti, T. Jain, R. Shorr and T. Rabilloud, *J. Biochem. Biophys. Methods*, 21 (1990) 165–172.
10 R. Charlionet, R. Sesboüé and C. Davrinche, *Electrophoresis*, 5 (1984) 176–178.
11 E. Gianazza, F. Celentano, G. Dossi, B. Bjellqvist and P. G. Righetti, *Electrophoresis*, 5 (1984) 88–97.
12 P. G. Righetti, M. Chiari, E. Casale and C. Chiesa, *Appl. Theor. Electrophoresis*, 1 (1989) 115–121.
13 W. P. Purcell, G. E. Bass and J. M. Clayton (Editors), *Strategy of Drug Design: a Guide to Biological Activity*, Wiley-Interscience, New York, 1973, pp. 126–143.
14 B. M. Gåveby, P. Petterson, J. Andrasko, L. Ineva-Flygare, U. Johannesson, A. Görg, W. Postel, A. Domscheit, P. L. Mauri, P. Pietta, E. Gianazza and P. G. Righetti, *J. Biochem. Biophys. Methods*, 16 (1988) 141–164.
15 M. Chiari, C. Chiesa, P. G. Righetti, M. Corti, T. Jain and R. Shorr, *J. Chromatogr.*, 499 (1990) 699–711.
16 G. Cossu, M. G. Pirastru, M. Satta, M. Chiari, C. Chiesa and P. G. Righetti, *J. Chromatogr.*, 475 (1989) 283–292.

Short Communication

High-performance liquid chromatographic analysis of flavonol glycosides of *Solidago virgaurea*

PIERGIORGIO PIETTA* and CLAUDIO GARDANA
Università degli Studi di Milano, Via Celoria 2, 20133 Milan (Italy)
and
PIERLUIGI MAURI and LUIGI ZECCA
Istituto Tecnologie Biomediche Avanzate–CNR, Via Ampere 56, 20131 Milan (Italy)
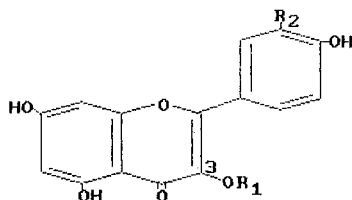(First received February 22nd, 1991; revised manuscript received May 23rd, 1991)

ABSTRACT

Solidago virgaurea flavonols were separated by reversed-phase high-performance liquid chromatography (RPLC) on a C_8 column using 2-propanol–water (14:86) as eluent in the isocratic mode. The presence of rutin, kaempferol-3-O-rutinoside, kaempferol-3-O-robinobioside and isorhamnetin-3-O-rutinoside was confirmed. The identity of kaempferol-3-O-robinobioside was proved by acid hydrolysis followed by determination of kaempferol and rhamnose/galactose and mass spectrometry. A rapid isocratic separation of the flavonol aglycones obtained by acid hydrolysis of the *Solidago virgaurea* extract is also described.

INTRODUCTION

Solidago virgaurea herb is used in folk medicine for its diuretic [1] and hypotensive [2] properties. It has been reported that chlorogenic acid, caffeic acid, rutin (**I**), quercitrin (**II**), astragalin (**III**), kaempferol-3-rutinoside (**IV**), kaempferol-3-O-robinobioside (**V**) and isorhamnetin-3-O-rutinoside (**VI**) are the most representative phenolic compounds [3,4] (Fig. 1). Although thin-layer chromatographic methods have been described [5,6] for the identification of some of these substances, so far no high-performance liquid chromatographic (HPLC) method has been applied to *Solidago virgaurea*.

Owing to the great potential of reversed-phase HPLC in separating complex mixtures of phenolic compounds, we applied a recently reported technique [7] based on C_8 columns coupled with aqueous 2-propanol to evaluate *Solidago virgaurea* extracts. By this approach a valuable HPLC "fingerprint" of *Solidago virgaurea* has been obtained. In this paper we also describe an efficient HPLC procedure for the

Rutin	(I)	R_1 =rutinose ; R_2 = OH
Quercitrin	(II)	R_1 =rhamnose ; R_2 = OH
Astragalin	(III)	R_1 =glucose ; R_2 = H
Kaempferol-3-O-rutinoside	(IV)	R_1 =rutinose ; R_2 = H
Kaempferol-3-O-robinobioside	(V)	R_1 =robinobiose ; R_2 = H
Isorhamnetin-3-O-rutinoside	(VI)	R_1 =rutinose ; R_2 = OCH_3

Fig. 1. Structures of *Solidago virgaurea* flavonol glycosides.

isolation of kaempferol-3-O-robinobioside (**V**), and its characterization by mass spectrometry and acid hydrolysis combined with chromatographic determination of the resulting aglycone and sugars.

EXPERIMENTAL

Materials

 Solidago virgaurea herb was obtained from different commercial sources (Milanfarma, Milan, Italy; Birkenweg, Kleinostheim/Main, Germany; Galke, Gittelde/Harz, Germany). Quercetin-3-O-rhamnoglucoside (rutin, **I**), quercetin-3-O-rhamnoside (quercitrin, **II**), kaempferol-3-O-rhamnoglucoside (kaempferol-3-O-rutinoside, **IV**) and isorhamnetin-3-O-rhamnoglucoside (isorhamnetin-3-O-rutinoside, **VI**) were purchased from Extrasynthese (Genay, France). Kaempferol-3-O-rhamnogalactoside (kaempferol-3-O-robinobioside, **V**) was obtained in our laboratory from *Solidago virgaurea* by semi-preparative HPLC. 2-Propanol and water were of HPLC grade (Chromasolv; Riedel de Haën, Hannover, Germany).

Chromatographic conditions

 Chromatographic analyses were performed on a system consisting of a Model 510 pump equipped with a Model U6K universal injector (Waters Assoc., Milford, MA, USA) and a Model HP 1040 A photodiode-array detector (DAD) (Hewlett-Packard, Waldbronn, Germany). Chromatographic runs were performed on a 7-μm spherical Aquapore C_8 column (250 × 4.6 mm I.D.) from Brownlee Labs. (Santa Clara, CA, USA). A semi-preparative 7-μm C_8 column (250 × 7.0 mm I.D.) was also supplied by Brownlee Labs. The eluent was 2-propanol–water (14:86) at a flow-rate of 1.8 ml/min. The eluent for the aglycones was 1-propanol–tetrahydrofuran–0.6% citric acid (12.5:7.5:80) at a flow-rate of 2 ml/min. The peaks were monitored at 254

nm and the UV spectra acquired for each peak were computer normalized and the plots superimposed.

Sample preparation

Solidago virgaurea powdered samples (1 g) were treated with ethanol–water (50:50) (50 ml) at 70°C for 60 min. After filtration, the solution was concentrated, then extracted with ethyl acetate (3 × 20 ml). The combined extracts were dried over sodium sulphate, filtered and evaporated to dryness *in vacuo*. The residue was dissolved in methanol (3 ml).

Acid hydrolysis

A 0.5-ml volume of the sample solution was refluxed with 5 ml of methanol and 10 ml of 2 M hydrochloric acid for 30 min. The reaction mixture was then diluted to 25 ml with methanol. A 10-μl aliquot of the filtered solution (Spartan 13 filters, 0.45 μm; Schleicher and Schüll, Dassel, Germany) was injected into the HPLC system.

Isolation of kaempferol-3-O-rhamnogalactoside (V)

Aliquots of 50 μl of the sample solution were chromatographated on the semi-preparative column using 2-propanol–water (14:86) at a flow-rate of 4 ml/min. Peak V was collected by means of a Gilson Model 201 fraction (Biolabo Instruments, Milan, Italy) and the combined fractions were freeze-dried. This compound was hydrolysed with 2 M hydrochloric acid–methanol, (1:1) at 100°C for 10 min. Galactose and rhamnose were detected by gas chromatography as acetyl derivatives [8]. Kaempferol was detected by HPLC as described under *Chromatographic conditions* for aglycones.

Mass spectrometry

Fast atom bombardament (FAB) mass spectra were obtained on a VG Analytical Model 70-70 EQ instrument, employing argon atoms with kinetic energy 7 keV. Recordings in the negative-ion mode were taken at a resolution of 3000, with a speed of 20 s per decade. Data were processed with a Digital PDP 8/A computer system.

RESULTS AND DISCUSSION

Preliminary experiments using C_{18} columns showed that a methanol–water–acetic acid mobile phase in the isocratic mode would not provide the optimum peak shape and separation of *Solidago virgaurea* flavonols. On the other hand, a short analysis time (14 min) with good peak resolution was obtained by isocratic elution on a C_8 column using 2-propanol–water (14:86) as the mobile phase (Fig. 2). Four major flavonoids were present (peaks I, IV, VI and V), while the previously reported [2] quercitrin (**II**) was present only in a trace amount and astragalin (retention time *ca.* 25 min) was absent. Peaks I, II, IV and VI were identified by co-chromatography with standards. In addition, the identity of peaks I, IV and VI was confirmed by comparing their UV spectra with those of corresponding standards. Peak II was small, and its spectrum was not significant.

The spectrum of peak V with diode-array detection presented a slope of the maximum in the short-wavelength region typical of kaempferol derivatives (Fig. 3).
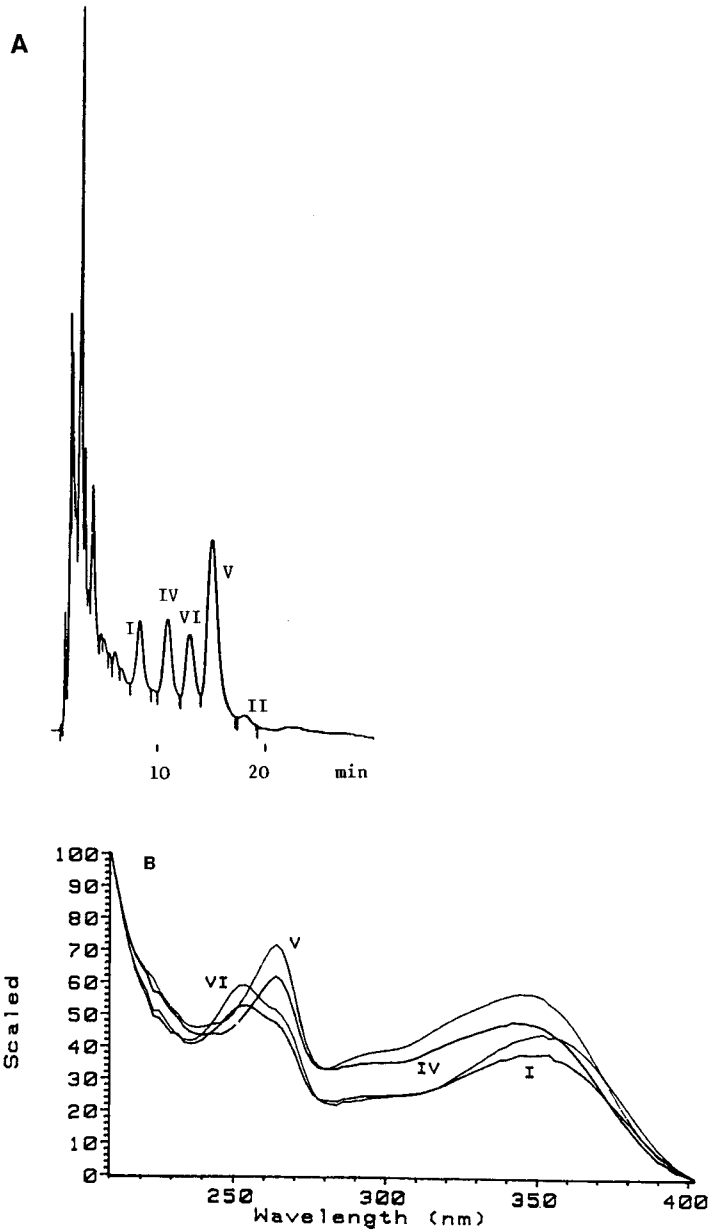
Fig. 2. (A) Typical chromatogram of a *Solidago virgaurea* extract. Peak numbers correspond to compound numbers in Fig. 1. Column, C$_8$ Aquapore RP 300; eluent, 2-propanol–water (14:86); flow-rate, 1.8 ml/min; UV detection at 254 nm. (B) Spectra obtained with diode-array detection. Numbers on lines correspond to compound numbers in Fig. 1.
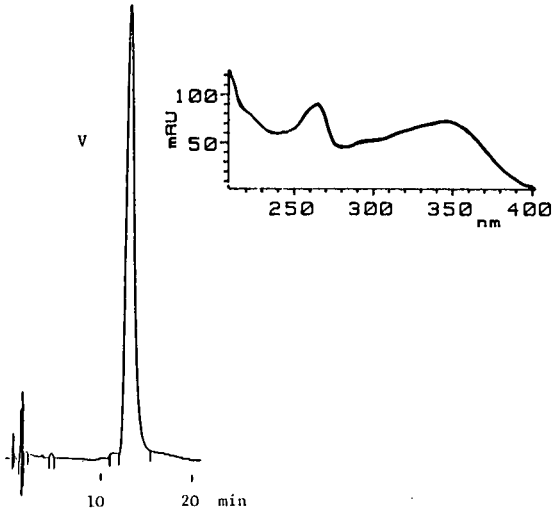
Fig. 3. HPLC and spectrum obtained with diode-array detection of compound V purified from peak V.

On acid hydrolysis of the isolated compound, kaempferol was obtained from V; in addition, galactose and rhamnose in the ratio 1:1 were detected. The negative-ion mass spectrum (Fig. 4) of V showed a deprotonated molecular ion at m/z 593 and an abundant fragment ion at m/z 285. The latter corresponds to the aglycone kaempferol originating from the molecular ion by loss of a rhamnosylgalactose residue. These data represent further positive evidence that peak V was the previously reported [4] kaempferol-3-O-rhamnogalactoside (V).
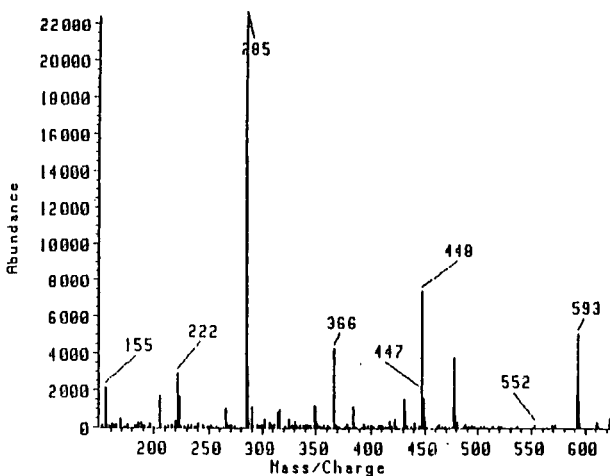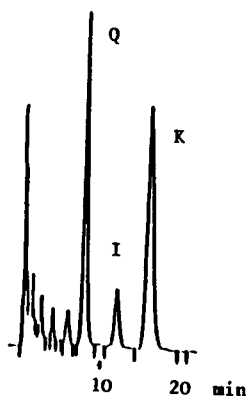

Fig. 4. Mass spectrum of V.

Fig. 5. Typical chromatogram of acid-hydrolysed *Solidago virgaurea* extract. Q = Quercetin; I = isorhamnetin; K = kaempferol.

During this study a rapid procedure for the determination of quercetin, isorhamnetin and kaempferol was also elaborated. *Solidago virgaurea* extract was hydrolysed under acid conditions, and the resulting aglycones were directly separated in the isocratic mode (Fig. 5). This procedure represents an improvement over the gradient approach [9], and it may be usefully applied to the determination of these widespread flavonol aglycones.

ACKNOWLEDGEMENTS

REFERENCES

1 H. Schilcher, *Z. Phytother.*, 8 (1987) 141.
2 J. Metzner, R. Hirschelmann and K. Hiller, *Pharmazie,* 39 (1984) 369.
3 H. Schilcher, *Naturwissenschaften*, 51 (1964) 636.
4 J. Budzianowski, L. Skzypczak and M. Wesolowska, *Sci. Pharm.*, 58 (1990) 15.
5 L. Skrzypczakowa, *Acta Pol. Pharm.*, 19 (1962) 481.
6 H. Schilcher and U. Bornschein, *Dtsch. Apoth.-Ztg.*, 40 (1986) 1377.
7 P. G. Pietta, P. L. Mauri, E. Manera and P. L. Ceva, *J. Chromatogr.*, 513 (1990) 397.
8 P. Albersheim, D. J. Nevins, P. D. English and A. Karr, *Carbohydr. Res.*, 5 (1967) 340.
9 H. Wagner, S. Bladt, U. Hartmam and A. Daily, *Dtsch. Apoth.-Ztg.*, 45 (1989) 2421.

Short Communication

Chromatographic determination of citric acid for monitoring the mould process

ZBIGNIEW J. WODECKI

Department of Organic Chemistry, Technical University of Gdańsk, 80-952 Gdańsk (Poland)

BOGUMIŁ TORŁOP

Citric Acid Factory, 81-130 Pelpin (Poland)

and

MAREK ŚLEBIODA*

Department of Organic Chemistry, Technical University of Gdańsk, 80-952 Gdańsk (Poland)

(First received February 22nd, 1991; revised manuscript received May 2nd, 1991)

ABSTRACT

A reliable method for monitoring the mould citric acid production process is presented. The method is based on in-line sample work-up and high-performance liquid chromatographic determination of citric acid with ultraviolet detection. It provides good precision (better than 1% in the range of 0–150 g dm^{-3}) and requires no special equipment.

INTRODUCTION

Citric acid is today the most widely used organic acid in the food and pharmaceutical industries. All the commercial methods of production of citric acid involve the conversion of inexpensive sources of glucose or sucrose, such as treated beet molasses, by selected strings of *Aspergillus niger*. It is important to monitor the mould process by determining the concentration of citric acid in the biosynthetic reaction mixture. From among the several high-performance liquid chromatographic (HPLC) methods of determination of carboxylic acids [1] we chose solvophobic chromatography for its simplicity and for the durability of the octadecyl silica columns. In this method the retention of carboxylic acids is the result of hydrophobic interactions of the hydrocarbon moiety of the solute with the octadecyl chains of the stationary phase, after suppression of ionization of the acidic functional groups by addition of acids or acidic buffers to the mobile phase.

EXPERIMENTAL

Instrumentation

An HP 1090 Hewlett-Packard liquid chromatograph equipped with a C_{18} guard column (25 × 4.6 mm I.D.), a column-switching valve, a Nucleosil ODS 100-5 analytical column (250 × 4.6 mm I.D.) and a autosampler were used. UV-detection at 210 nm was accomplished with the HP 1040 diode-array detector. The column was operated at temperature of 55°C. The mobile phase flow-rate was maintained at 1.00 cm^3 min^{-1}.

Reagents

Water used as the mobile phase component and as a solvent was freshly redistilled from glass apparatus. Methanol and ethanol (POCH, Poland) p.a. were used as obtained. Orthophosphoric acid (0.1%) (POCH, Poland) p.a. in water was used as a mobile phase for HPLC analysis.

Procedure

Samples taken from the the shell pan citric acid production process were stabilized by the addition of 96% ethanol, in order to obtain a final concentration of 30%, and stored refrigerated. They had a very complex matrix; besides citric acid there were sugars, proteins and enzymes. To avoid the analytical column deterioration caused by strongly retained substances, a sample clean-up step prior to the analysis was necessary. It was done using solid-phase extraction. During off-line as well as on-line work-up procedures the interfering substances were retained on a C_{18} cartridge or guard column, while citric acid was not retained.

Off-line work-up procedure. A solid-phase extraction C_{18} column (SOPHEX, DHN, Poland) was preconditioned by passing through it 2 · 1.0 cm^3 of methanol and 3 · 1.0 cm^3 of water. The sample (0.10 cm^3) was subsequently introduced and the carboxylic acid fraction was eluted with 3 · 1.0 cm^3 of water into a weighed polyethylene vial. The vial was stoppered, weighed again and the content was analysed for citric acid using an HPLC system analogous to that described above but without the guard column in-line.

In-line work-up procedure. The sample (1 mm^3) was injected into the chromatographic system. After the analysis was completed (10 min), the column-switching valve was activated and the guard column was washed with methanol (5 min) to elute substances which previously had been retained and then with the mobile phase (10 min). The column-switching valve was subsequently deactivated and the entire system was washed with the mobile phase (2 min).

Precipitation method (standard industrial method for the determination of citric acid). The sample (10 cm^3) was neutralized with a 1 M solution of sodium hydroxide in water and heated on a steam bath. Then a 10% (w/v) solution of calcium chloride (15 cm^3) was added and the precipitate was collected. The filter paper containing the precipitate was ashed in an electric oven (800°C), and the residue was dissolved in 1 M hydrochloric acid. The acid was back-titrated with a 1 M solution of sodium hydroxide.
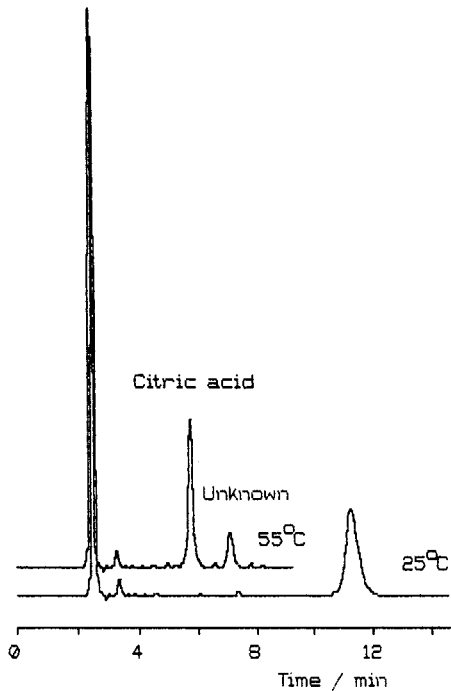
Fig. 1. Effect of temperature on the separation of components of sample taken from the shell pan citric acid production process. For chromatographic conditions see the Experimental section.

RESULTS AND DISCUSSION

The applied chromatographic conditions provided good separation of citric acid from substances eluting close to the void volume, but examination of the UV spectrum of the citric acid peak revealed that an unknown substance present in the sample co-eluted with citric acid. This can be easily avoided by raising the temperature to 55°C (Fig. 1). Because of the very complex matrix, a sample clean-up step prior to the analysis was necessary, otherwise the analytical column deteriorated and interference with the analysis resulted. Usually this is done off-line using solid-phase extraction cartridges. To override this time-consuming and potentially error-causing step, we employed an in-line chromatographic system.

The precision of the in-line HPLC method was estimated to be $\pm$ 1.1 mg cm^{-3} (about $\pm$ 0.9% for the sample containing 100–150 mg cm^{-3} citric acid). The results obtained using both the off-line and in-line work-up procedures were in a good agreement with the results obtained using a standard precipitation method for citric acid determination (within 1.2% at about the 100 mg cm^{-3} level). The method proposed can be a reliable analytical tool for monitoring the biosynthetic production of citric acid.

ACKNOWLEDGEMENT

REFERENCE

1 R. Schwarzenbach, *J. Chromatogr.*, 251 (1982) 339.

Short Communication

Effect of derivatization of steroids on their retention behaviour in inclusion chromatography using cyclodextrin as a mobile phase additive

KAZUTAKE SHIMADA*, TOMOYUKI OE and MITSUAKI SUZUKI

Faculty of Pharmaceutical Sciences, Kanazawa University, Kanazawa 920 (Japan)

(First received March 27th, 1991; revised manuscript received May 28th, 1991)

ABSTRACT

The effect of derivatization of steroids on their retention behaviour in high-performance liquid chromatography using cyclodextrin as a mobile phase additive was examined by using as model compounds four 17-ketosteroids and twenty derivatives substituted at the 3- or 17-position with p-nitrobenzoyl chloride, p-nitrobenzoyl azide, 1-anthroyl azide, p-nitrophenylhydrazine and O-p-nitrobenzylhydroxylamine. The results suggested that separation reflecting the chemical structures of the steroid moieties is obtained by derivatizing a functional group which is located near the isomeric position, and derivatives having more hydrogen-bonding sites show greatly changed chromatographic behaviour.

INTRODUCTION

In recent years, considerable attention has been focused on inclusion chromatography using cyclodextrin (CD) as a mobile phase additive or stationary phase in high-performance liquid chromatography (HPLC) [1]. This type of chromatography is often preferable to conventional techniques for the separation of optical, geometric and structural isomers [2,3].

In previous papers we reported the use of CD as a mobile phase additive, which is of great advantage in the separation of isomeric steroids (oestrogens [4], bile acids [5], cardiac steroids [6,7]) in reversed-phase HPLC. The method was also applied to the separation of fluorescent derivatives. Bile acids derivatized with 1-anthroyl cyanide [8] or bromoacetylpyrene [9] showed a similar chromatographic behaviour to that of the underivatized compounds and satisfactory separation was also obtained by this mode of chromatography. However, the effect of the derivatization of steroids on their retention behaviour in this type of chromatography has not been examined fully.

In this work, the retention behaviour of four 17-ketosteroids [androsterone (**Ia**), epiandrosterone (**Ib**), etiocholanolone (**Ic**) and epietiocholanolone (**Id**)] and twenty

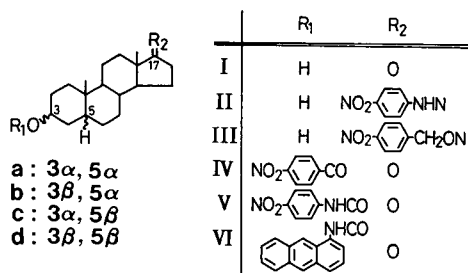|	R_1	R_2
I	H	O
II	H	NO_2-⟨ ⟩-NHN
III	H	NO_2-⟨ ⟩-CH_2ON
IV	NO_2-⟨ ⟩-CO	O
V	NO_2-⟨ ⟩-NHCO	O
VI	⟨anthryl⟩-NHCO	O

a : 3α, 5α
b : 3β, 5α
c : 3α, 5β
d : 3β, 5β

Fig. 1. Structures of 17-ketosteroids and their derivatives.

derivatives substituted at the 3- or 17-position (Fig. 1) were examined from the standpoints of structures of the steroids, derivatized position, derivatized form and mobile phase additive in order to obtain information on the appropriate methods for the derivatization of steroids in this type of chromatography.

EXPERIMENTAL

Materials

CDs and 17-ketosteroids were kindly supplied by Nihon Shokuhin Kako (Tokyo, Japan) and Teikoku Hormone (Tokyo, Japan), respectively. *p*-Nitrophenyl-hydrazine and O-*p*-nitrobenzylhydroxylamine · HCl were purchased from Nacalai Tesque (Kyoto, Japan) and *p*-nitrobenzoyl chloride from Tokyo Kasei Kogyo (Tokyo, Japan). *p*-Nitrobenzoyl azide was prepared from *p*-nitrobenzoyl chloride by a conventional method with sodium azide, and 1-anthroyl azide was synthesized according to the procedure described by Fujino *et al.* [10].

Apparatus

HPLC was carried out on a Shimadzu (Kyoto, Japan) LC-6A chromatograph equipped with a Shimadzu SPD-6AV ultraviolet (UV) detector at a flow-rate of 1.0 ml/min. A YMC-GEL CN (5 μm) column (15 cm × 0.4 cm I.D.) (YMC, Kyoto, Japan) was used at ambient temperature. The void volume was determined by the use of sodium nitrate. Proton nuclear magnetic resonance (^{1}H NMR) spectra were obtained with a JEOL (Tokyo, Japan) JNM-FX 100S spectrometer at 100 MHz.

Derivatized 17-ketosteroids

The 17-ketosteroids 17-(*p*-nitrophenylhydrazone) (**II**), 17-(O-*p*-nitrobenzyl-oxime) (**III**), 3-(*p*-nitrobenzoate) (**IV**), 3-(N-*p*-nitrophenylcarbamate) (**V**) and 3-(N-1-anthrylcarbamate) (**VI**) were synthesized from the corresponding 17-ketosteroids (**I**) by using *p*-nitrophenyhydrazine, O-*p*-nitrobenzylhydroxylamine · HCl, *p*-nitro-benzoyl chloride, *p*-nitrobenzoyl azide and 1-anthroyl azide, respectively, by conventional methods. Although the *syn* and *anti* conformers were formed, the main product was used as the authentic sample in the case of hydrazone (**II**) and oxime (**III**) derivatives, which were obtained by purification by recrystallization and preparative thin-layer chromatography, respectively. All these structures were confirmed by the ^{1}H NMR spectra.

TABLE I

THE CAPACITY FACTORS OF 17-KETOSTEROIDS AND THEIR DERIVATIVES

The numbering corresponds to that in Fig. 1. Mobile phase, methanol–water: I, 2:3, t_0 0.82 min; II–V, 3:2, t_0 0.78 min; VI, 13:7; t_0 0.80 min. Detection, UV: I, 210 nm; II–IV, 254 nm; V, 280 nm; VI, 254 nm.

No.	a	b	c	d
I	14.1	11.7	12.5	11.2
II	15.5	14.7	14.6	13.5
III	9.6	8.9	8.6	9.3
IV	11.7	16.9	12.3	16.0
V	15.0	17.7	15.7	16.0
VI	6.7	12.6	10.3	10.1

RESULTS AND DISCUSSION

It is necessary to use a mobile phase containing water in inclusion chromatography using CD as a mobile phase additive in reversed-phase HPLC [1]. Steroids were eluted much earlier from a CN-coated than from an alkyl-coated column using the same solvent system in reversed-phase HPLC. It is possible for a CN-coated column to elute steroids with a mobile phase containing a large proportion of water [7]. According to these data, all the experiments were done with a YMC-GEL CN column.

The capacity factors (k') of all the compounds examined obtained without CD are listed in Table I, in which more than 35% of water was used in the mobile phase. The relative k' values obtained with the addition of 2 mM of β- or γ-CD are reported in Fig. 2. Although the data are not shown, α-CD had little effect on the k' values of any of the compounds examined as reported previously for other steroids [4–9]. On the contrary, the k' values of all these compounds decreased with increasing concentration of β- or γ-CD in the mobile phase. This effect can be explained by the cavity size of the CD, that of α-CD being too small to include these compounds.

	a	b	c	d
	β*/γ	β/γ	β/γ	β/γ
I	27**/26	14/25	40/26	31/14
II	80/53	72/51	71/44	82/30
III	81/63	63/60	82/58	77/36
IV	92/85	23/66	36/64	67/45
V	85/75	16/63	22/38	82/41
VI	98/93	35/77	58/61	97/59

Fig. 2. Relative capacity factors of 17-ketosteroids and their derivatives. * Added CD (2 mM). ** Relative identification value (the identification value obtained without CD was taken as 100).

Effect of CD on the retention of 17-ketosteroids

Regarding the 5-position isomers, the k' value of the 5α-isomer (**Ia, b**) was influenced more than that of the 5β-isomer (**Ic, d**) with the addition of 2 mM β-CD. Although the relative k' values of **Ia** and **Ic** were the same (26), that (14) of the 5β-isomer (**Id**) was influenced more than that (25) of the 5α-isomer (**Ib**) with the addition of 2 mM γ-CD. The effect is more clearly observed with 3β-hydroxy compounds (**Ib, d**) than the corresponding 3α-isomers (**Ia, c**) (Fig. 2). These findings agree with our previous results obtained with cardiac steroids [6].

Effect of CD on the retention of derivatized 17-ketosteroids

The effect of derivatization at the 17-position on the retention behaviour was examined as above and similar results were observed with both hydrazone (**II**) and oxime (**III**) derivatives (Fig. 2), that is, the k' values of all these derivatives decreased more with the addition of γ-CD than β-CD. In 3β-hydroxy compounds, the k' value of the 5α-isomer (**IIb, IIIb**) was influenced more than that of the 5β-isomer (**IId, IIId**) with the addition of β-CD. In contrast, the relative k' value of the 5β-isomer (**IId, IIId**) became smaller than that of the 5α-isomer (**IIb, IIIb**) with the addition of γ-CD. This effect was also observed with 3α-hydroxy compounds (**IIa** *vs.* **IIc**; **IIIa** *vs.* **IIIc**), except for **IIa** (80) *vs.* **IIc** (71) with β-CD as mobile phase additive.

Next, the effect of derivatization at the 3-position was examined and the following results reflecting the chemical structures of steroid moiety were obtained (Fig. 2). The k' values of the 3α,5α-series (**IVa–VIa**) are least influenced in each instance moiety by either CD. In contrast, those of the 3α,5β-series (**IVc–VIc**) were substantially decreased with the addition of either CD. The k' value of the 5α- (**IVb–VIb**) or 5β-isomer (**IVd–VId**) of the 3β-series was decreased more than that of the 5β- or 5α-isomer with the addition of β- or γ-CD, respectively. The addition of β-CD decreased the k' values of compounds having a 3-equatorial substituent (**IVb,c–VIb,c**) more than those of the corresponding isomer (**IVa,d–VIa,d**). On the other hand, γ-CD decreased the k' values of derivatives having an A/B *cis* ring junction (**IVc,d–VIc,d**) more than those of the derivatives having an A/B *trans* ring junction (**IVa,b–VIa,b**).

These results indicate that β- and γ-CD distinguish substituents at the 3-position and the A/B ring junction, respectively. It may be difficult for the former host compound to include an axial substituent [3α,5α (a); 3β,5β (d) series]. Although a few exceptions have been observed, with respect to the structures of the derivatizing moiety, the k' values of the derivatives having more hydrogen bonding sites (**II, V**) are more influenced in most instances than the other derivatives (**III, IV**). Also, the k' values of the derivative having a larger substituent (**VI**) are smaller than those of the corresponding derivative having a smaller substituent (**V**).

CONCLUSIONS

The retention behaviour of four 17-ketosteroid isomers and twenty derivatives was demonstrated by HPLC using CD as a mobile phase additive. Compounds derivatized at the 3-position showed greater variations in chromatographic behaviour reflecting their configurational changes at the 3- and 5-positions than compounds derivatised at the 17-position. The results suggested that the separation reflecting the chemical structures of steroid moieties is obtained by derivatizing the functional

groups which are located near the isomeric position, and derivatives having more hydrogen-bonding sites show greatly changed chromatographic behaviour in this type of chromatography. These results should be helpful in choosing a derivatization method for steroids in this type of chromatography, and in identifying the peaks in chromatograms of biological samples.

Further investigations of the chromatographic behaviour of derivatized steroids in inclusion chromatography are being made in comparison with the conventional method [11].

ACKNOWLEDGEMENTS

REFERENCES

1 W. L. Hinze, *Sep. Purif. Methods*, 10 (1981) 159, and references cited therein.
2 D. W. Armstrong, W. DeMond, A. Alak, W. L. Hinze, T. E. Riehl and K. H. Bui, *Anal. Chem.*, 57 (1985) 234.
3 M. Gazdag, G. Szepesi and K. Mihalyti, *J. Chromatogr.*, 450 (1988) 145.
4 K. Shimada, T. Masue, K. Toyoda, M. Takani and T. Nambara, *J. Liq. Chromatogr.*, 11 (1988) 1475.
5 K. Shimada, Y. Komine and T. Oe, *J. Liq. Chromatogr.*, 12 (1989) 491.
6 K. Shimada, T. Oe, Y. Hirose and Y. Komine, *J. Chromatogr.*, 478 (1989) 339.
7 K. Shimada, Y. Kurata and T. Oe, *J. Liq. Chromatogr.*, 13 (1990) 493.
8 K. Shimada, Y. Komine and K. Mitamura, *J. Chromatogr. Sci.*, 28 (1990) 331.
9 K. Shimada, Y. Komine and K. Mitamura, *J. Chromatogr.*, 565 (1991) 111.
10 H. Fujino, M. Hidaka and S. Goya, *Yakugaku Zasshi*, 109 (1989) 606.
11 E. Heftmann and J.-T. Lin, *J. Liq. Chromatogr.*, 5 (1982) 121.

Short Communication

High-performance liquid chromatographic detection of enantiomeric amino alcohols after derivatization with *o*-phthaldialdehyde and various thiosugars

ALEXANDR JEGOROV*

Institute of Entomology, Czechoslovak Academy of Sciences, Branišovská 31, 370 05 České Budějovice (Czechoslovakia)

TOMÁŠ TRNKA

Department of Organic Chemistry, Charles University, Albertov 6, 128 40 Prague (Czechoslovakia)

and

JOSEF STUCHLÍK

Galena Co., 147 70 Opava, Komárov (Czechoslovakia)

(First received February 13th, 1991; revised manuscript received May 22nd, 1991)

ABSTRACT

A series of thiosugars are described as the new pre-column derivatization agents for chiral resolution of 2-amino-1-alcohols. The isoindole derivatives were formed by reaction of 2-amino-1-alcohols with *o*-phthaldialdehyde and thiosugars in aqueous solution and at a mildly basic pH. The reaction was complete within 1 min. The diastereomers formed can efficiently be resolved on conventional reversed-phase columns and measured with a fluorescence detector which provides detection limits of less than 10 pmol per 10-μl injection.

INTRODUCTION

Amino alcohols are present as a terminal group in some fungal metabolites, *e.g.* in peptide antibiotics (peptaibols) [1,2], as well as in various natural compounds produced by other organisms [3]. Amino alcohols are also used as chiral synthones for the preparation of a number of biologically active compounds, *e.g.* ergot alkaloids such as ergometrin or methylergometrin [4,5], which are nowadays produced synthetically. In both cases, an appropriate analytical method is necessary to identify or to control the enantiomeric purity of either natural or synthetic compounds, as it is well known that compounds constituted from different enantiomers usually possess different biological activity.

Whereas a number of liquid chromatographic methods have been described for

the resolution of amino acid enantiomers, apparently little attention has been paid to the resolution of amino alcohols. Resolution of some amino alcohols was recently achieved after derivatization with various chiral isocyanates or isothiocyanates [6,7]. Another method, which was primarily developed for the analysis of amino acid enantiomers, is based on the pre-column derivatization of amino groups with *o*-phthaldialdehyde (OPA) and chiral thiols. Compared with other reagents, the analysis of amino compounds after derivatization with the OPA–thiol reagents is quick, convenient and relatively independent of the presence of impurities in the sample. Diastereomeric isoindole derivatives thus formed are easily separable on a reversed-phase high-performance liquid chromatographic (HPLC) column and can be easily detected using fluorimetry. Boc-L-cysteine, N-acetyl-L-cysteine and N-acetyl-penicill-amine were used also for the derivatization of amino alcohols, and good resolution was obtained for all amino alcohols tested with at least one chiral reagent [8]. Since no reagent has general applicability, we describe here an alternative method for the resolution of amino alcohol enantiomers, which is based on their derivatization with *o*-phthaldialdehyde and various thiosugars.

EXPERIMENTAL

Reagents and chemicals

The sodium salts of 1-thio-β-D-glucose [9], 1-thio-β-D-galactose [10] and 1-thio-β-D-mannose [11] were prepared as described previously; OPA (Calbiochem, Los Angeles, CA, USA), amino alcohol enantiomers (Fluka, Buchs, Switzerland and Sigma, St. Louis, MO, USA), methanol, boric acid, potassium hydroxide and sodium acetate (Lachema, Brno, Czechoslovakia) were used.

Chromatographic systems

A Varian Vista 5500 liquid chromatographic system equipped with a Fluorichrom filter fluorescence detector was used. The excitation wavelength has a maximum at 360 nm, while the emission wavelength has a bandpass above 420 nm. The analytical column used was a Separon SGX C_{18}, 7 μm (250 × 4 mm I.D.) from Tessek (Prague, Czechoslovakia). Solvent A was 0.1 M sodium acetate (pH 7.3, adjusted with dilute acetic acid) and solvent B was a 1:9 mixture of sodium acetate (pH 7.3) and methanol, respectively. A linear gradient elution of 30–70% B over 40 min was used. A constant flow-rate of 1 ml/min was maintained during the analysis. A back-pressure terminator (Varian, Sunnyvale, CA, USA), set at 0.6 MPa, was used to prevent formation of bubbles. Stability studies were performed with a Bio-Rad AS-100 HRLC automatic sampling system (Richmond, CA, USA) and a Hypersil ODS, 3 μm (60 × 4.6 mm I.D.) column from Hewlett Packard (Amstelveen, Netherlands) under isocratic elution with 0.1 M sodium acetate (pH 7.2)–methanol (6:4, v/v); the flow-rate was 1.0 ml/min, and evaluation was based on comparison of peak areas of baseline-separated peaks.

Derivatization procedure

Stock solutions were prepared weekly with 50 mg of sodium salts of thiosugars in 1 ml of water, 50 mg of OPA in 1.25 ml of methanol and amino alcohols (4 mM in water). Borate buffer was prepared by dissolving 0.50 g of boric acid in 19 ml of water

and adjusting the pH to 9.30 (8.20 or 10.00) with potassium hydroxide solution (45 g of potassium hydroxide in 100 ml of water). A 10-μl sample of the amino alcohol solution, 100 μl of the borate buffer 50 μl of the thiosugar solution and 50 μl of the OPA solution (thiosugar/OPA ratio = 2.2) were introduced consecutively into a small glass vessel, and the mixture was stirred. After 60 s, a 10-μl aliquot was ana-lysed. For the studies of fluorescence response, both racemic mixtures and individual enantiomers were used.

RESULTS AND DISCUSSION

We have recently shown that thiosugars can be employed for the chiral resolu-tion of amino acids [12,13]. By analogy with the reactions of other thiols [14–16], 1-isoindolyl-(1-thio-β-D-glycosides) are assumed to be formed in the course of a reac-tion of an amino acid with OPA and a thiosugar. This type of derivatization can possibly be applied to all kinds of primary amines and to a wide range of mercaptans. Accordingly, all amino alcohols reacted with OPA and thiosugars in alkaline condi-tions yield highly fluorescent isoindole derivatives. The reactions occurred rapidly and quantitatively at ambient temperature, reaching their maximum fluorescence within 1 min (Fig. 1). In the course of the reaction, only one highly fluorescent derivative was formed with each amino alcohol enentiomer. Similarly, as in the case of OPA–2-mercaptol derivatives [17–20], thiosugar-substituted isoindoles are unsta-ble (Fig. 1). Their stability was found to decrease with decreasing pH. The stability of OPA–thiosugar mixtures themselves is also limited, hence the use of separate stock solutions is recommended. Solutions of sodium salts of thiosugars are stable for months with the exception of the sodium salt of 1-thio-β-D-mannose, a fresh solution of which should be prepared every day.
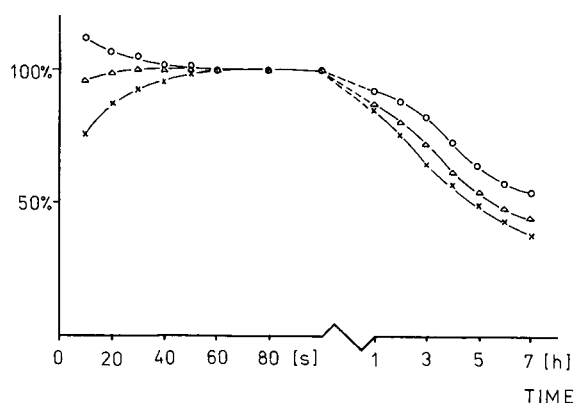

Fig. 1. Fluorescence response of the OPA–1-thio-β-D-galactose derivatization as a function of reaction time and pH [($\times$) 8.2, ($\triangle$) 9.3, ($\bigcirc$) 10.0] and stability of the selected derivative in the borate buffer at 20°C [mixture: 10 μl of 3 mM (S)-(+)-2-amino-1-butanol, 200 μl of borate buffer, 30 μl of thiosugar solution, 30 μl of OPA solution]; relative percentages refer to the area of the chromatographic peak obtained by the analysis of the reaction mixture injected after 60 s (100%). Conditions: Hypersil ODS, 3 μm (60 × 4.6 mm I.D.) column, isocratic elution with 0.1 M sodium acetate (pH 7.2)–methanol (6:4, v/v), flow-rate 1.0 ml/min.

TABLE I

RESOLUTION AND RETENTION TIMES OF VARIOUS OPA–THIOSUGAR DERIVATIVES

Column: Separon SGX C_{18}, 7 μm (250 × 4 mm, I.D.), for elution conditions see the Experimental section; $t_0 = 1.1$ min. Resolution $R = (t_{R_2} - t_{R_1})/(w_1 - w_2)$ where w_1 and w_2 are the peak width at half height of the first and the second eluted peaks, respectively. t_R values corresponding to derivatives with fluorescence response higher from the enantiomeric couple are underlined.

| Sample	Derivatization reagent OPA–thiosugar											
	1-Thio-β-D-glucose				1-Thio-β-D-galactose				1-Thio-β-D-mannose			
	t_{r1}	t_{r2}	R	Elution order	t_{r1}	t_{r2}	R	Elution order	t_{r1}	t_{r2}	R	Elution order
2-Amino-1-propanol	9.8		0	–	8.8		0	–	12.1	_12.9_	0.53	R, S
2-Amino-1-butanol	_16.5_	18.4	1.50	S, R	_15.0_	16.2	0.87	S, R	17.5	_19.8_	1.36	R, S
2-Amino-1-pentanol	_23.4_	25.5	1.60	S, R	_21.9_	23.3	1.02	S, R	24.1	_26.4_	1.34	R, S
2-Amino-1-hexanol	_29.3_	31.5	1.56	S, R	_28.1_	29.6	1.02	S, R	30.1	_32.2_	1.24	R, S
Valinol	_21.2_	23.0	1.47	S, R	_20.3_	21.8	1.19	S, R	21.5	_23.6_	1.52	R, S
Leucinol	_29.0_	31.4	1.61	S, R	_27.8_	29.6	1.27	S, R	29.1	_31.1_	1.20	R, S
α-Phenylglycinol	_23.4_	25.9	2.18	S, R	_23.5_	25.0	1.00	S, R	23.7		0	–
Phenylalaninol	_23.8_	27.4	3.20	S, R	_23.6_	27.1	2.10	S, R	_22.6_	24.3	1.29	S, R
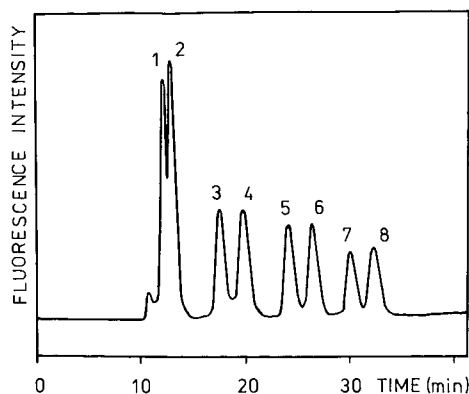
Fig. 2. Separation of amino alcohol enantiomers after pre-column derivatization with OPA–1-thio-β-D-mannose. Column, Separon SGX C$_{18}$, 7 μm (250 × 4 mm I.D.); mobile phase A, 0.1 M sodium acetate (pH 7.3); mobile phase B, 0.1 M sodium acetate–methanol (1:9, v/v); gradient 30–70% B in 40 min; flow-rate, 1.0 ml/min. Peaks: 1, 2 = (R)-, (S)-2-amino-1-propanol; 3, 4 = (R)-, (S)-2-amino-1-butanol; 5, 6 = (R)-, (S)-2-amino-1-pentanol; 7,8 = (R)-, (S)-2-amino-1-hexanol.

Fig. 2 shows an example of the separation of four amino alcohols derivatized with OPA–1-thio-β-D-mannose. Resolution and elution orders of other derivatives are given in Table I. As for the role of individual thiosugars, elution orders obtained with 1-thio-β-D-mannose were mostly reversed compared with that of 1-thio-β-D-glucose or 1-thio-β-D-galactose. This indicates that the configuration of the OH group at the C-2 atom plays an important role in the interaction between the sugar moiety and OH group of an amino alcohol. As is evident from Table I, as well as from, for example, space models of the isoindole, the OH group at the C-4 atom (glucose $vs.$ galactose) could not participate in this case. However, this remote OH group might participate in chiral recognition if suitable polar groups are present on the side chain of an amino compound, as was documented, for example, in the differential resolution of Lys, Asp and Glu [21].

The relative sample standard deviations of retention times were 1.5% [1-thio-β-D-glucose-(S)-(+)-2-amino-1-pentanol, n = 6] for the gradient method (Fig. 2) or 1.4% [1-thio-β-D-galactose-(R)-(−)-2-amino-1-butanol, n = 24, within 2 days] for the isocratic method (Fig. 3). The average relative deviation of the peak area for individual derivatives was less than 4% for between-day assays and less than 3% for within-days assays, which shows that the present system is reproducible. The detection limit for (S)-(+)-2-amino-1-butanol, based on a signal-to-noise ratio of 2, was less than 10 pmol. The analysis of amino alcohols after conversion to isoindoles is relatively easy when large samples are available (> 100 pmol), which is the case for most analysis of enantiomeric purity of synthetic chemicals. Problems associated with the analysis increase with diminishing sample size and are largely due to impurities in reagent and the inherent lack of chemical stability of the isoindoles examined in the reaction. Much of this background interference was shown to derive from OPA contaminants and old samples of thiosugar solutions.

As in the case of other chiral thiols, individual enantiomers formed derivatives having slightly different specific fluorescence intensity (Table I). In this particular
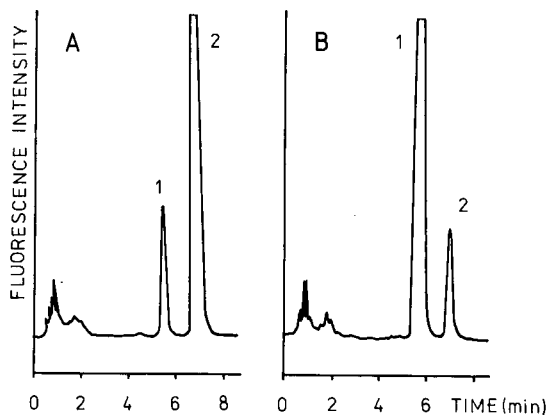
Fig. 3. Separation of 2-amino-1-butanol derivatized with OPA–1-thio-β-D-glucose. Conditions: Hypersil ODS, 3 μm (60 × 4.6 mm I.D.) column, isocratic elution with 0.1 M sodium acetate (pH 7.2)–methanol (6:4, v/v), flow-rate 1.0 ml/min. (A) (S)-(+)-2-Amino-1-butanol (3 mM) with 1% (R)-(−)-2-amino-1-butanol impurity; (B) (R)-(−)-2-amino-1-butanol (3 mM) with 1% (S)-(+)-2-amino-1-butanol impurity Peaks: 1, 2 = (S)-, (R)-2-amino-1-butanol; column efficiency = 81 200 plates/m [plate number = 5.54 $(t_{r2}/w)^2$] for peak 2.

case, (S)-enantiomers formed derivatives whose chromatographic peaks had about 5–20% greater area regardless of whether they were eluted first or second in the enantiomeric pair. Since derivatives of quite different amino compounds possess almost identical absorbance and fluorescence spectra and usually also exhibit comparative fluorescence responses [14,15], differences in the fluorescence intensity of various enantiomers seem likely to originate from the local arrangement of substituents around the isoindole moiety.

Most of the amino alcohols showed sufficient resolution with each of the three derivatization reagents. Baseline separation usually allowed simultaneous determination of trace impurities of one enantiomer in the other with one thiosugar (Fig. 3). For a particular case, separation can alternatively be achieved using isocratic elution. Resolution is fairly dependent on the quality of the column used; in our experience, poorly end-capped or old columns usually suffer particularly from loss of resolution. As the buffer–methanol mixture causes relatively high back-pressure on reversed-phase columns, the use of short-length columns seems to be reasonable.

REFERENCES

1 H. Brückner, G. Jung and M. Przybylski, *Chromatographia*, 17 (1983) 679.
2 H. Brückner and M. Przybylski, *Chromatographia*, 19 (1984) 188.
3 N. K. Gulavita and P. J. Scheuer, *J. Org. Chem.*, 54 (1989) 366.
4 A. Stall and A. Hofmann, *Helv. Chim. Acta*, 26 (1943) 944.
5 R. Paul and G. W. Anderson, *J. Am. Chem. Soc.*, 82 (1960) 4596.
6 K. J. Miller, J. Gal and M. M. Ames, *J. Chromatogr.*, 307 (1984) 335.
7 J. Gal and A. J. Sedman, *J. Chromatogr.*, 314 (1984) 275.
8 R. H. Buck and K. Krummen, *J. Chromatogr.*, 387 (1987) 255.
9 M. Černý and J. Pacák, *Collect. Czech. Chem. Commun.*, 26 (1961) 2084.
10 M. Černý, J. Staněk and J. Pacák, *Monatsh. Chem.*, 94 (1963) 290.
11 J. Hykl, *Thesis*, Charles University, Prague, 1988.

12 A. Jegorov, J. Tříska, T. Trnka and M. Černý, *J. Chromatogr.*, 434 (1988) 417.
13 A. Jegorov, V. Maťha, T. Trnka and M. Černý, *J. High Resolut. Chromatogr.*, 13 (1990) 718.
14 S. S. Simons, Jr. and D. F. Johnson, *Anal. Biochem.*, 99 (1978) 705.
15 S. S. Simons, Jr. and D. F. Johnson, *J. Org. Chem.*, 43 (1978) 2886.
16 G. Morineau, M. Azoulay and F. Frappier, *J. Chromatogr.*, 467 (1989) 209.
17 B. N. Jones, in E. Shively (Editor), *Methods of Protein Microcharacterization*, Humana Press, Clifton, NJ, Jersey, 1986, p. 121.
18 J. C. Hodgin, P. Y. Howard, D. M. Ball, C. Cloete and L. De Jager, *J. Chromatogr. Sci.*, 21 (1983) 503.
19 W. A. Jacobs, *J. Chromatogr.*, 392 (1987) 435.
20 B. J. Micallef, B. J. Shelp and R. O. Ball, *J. Liq. Chromatogr.*, 12 (1989) 1281.
21 A. Jegorov, J. Tříska, T. Trnka and M. Černý, *Chirality*, in press.

CHROM. 23 495

Short Communication

Purification of common bean chloroplast DNA by DEAE cellulose column chromatography

O. CARELSE*, C. J. CHETSANGA and M. V. MUBUMBILA

Department of Biochemistry, University of Zimbabwe, P.O. Box MP 167, Mount Pleasant, Harare (Zimbabwe)

(First received September 10th, 1990; revised manuscript received May 6th, 1991)

ABSTRACT

DEAE cellulose column chromatography has been used for the purification of chloroplast DNA. This technique is more time-efficient than the caesium chloride gradient method. It is a reliable tool and yields a high concentration of double-stranded DNA molecules. The chloroplast DNA obtained after DEAE cellulose chromatography is sensitive to different restriction endonucleases and can be used for DNA fragment cloning and sequencing.

INTRODUCTION

Chloroplast DNA (cpDNA) has been purified on caesium chloride gradients from a variety of plant species after RNase T1 treatment [1]. In general the caesium chloride gradient technique is excellent for the preparation of small amounts of DNA. However, this method is expensive, time-consuming and yields DNA containing considerable amounts of caesium chloride.

RNase T1 treatment is an important step in several methods used in DNA preparation [1,2]. This treatment destroys RNA contaminants but often presents a risk of DNase 1 contamination, which can digest the DNA molecules.

The diethylaminoethyl (DEAE) anion exchanger has been used in the nucleogen–DEAE form as a column support for high-performance liquid chromatography isolation of plasmid DNA [3]. DNA cellulose has also been used for isolating lambda phage [4,5], proteins [6] and tRNA [7,8].

These earlier observations have been used to develop a procedure for purifying chloroplast DNA by DEAE cellulose column chromatography. The chromatographic conditions used here make it possible to separate DNA from RNA in a given chloroplast nucleic acid preparation. The DNA was analysed by endonuclease digestion and agarose gel electrophoresis.

EXPERIMENTAL

Materials

   Bean culture was performed either outside or in a greenhouse. Young bean leaves of *Phaseolus vulgaris*, variety Saxa, were harvested after 15 days for chloroplast preparation and nucleic acid extraction.

Chemicals and reagents

   DEAE cellulose, DNase 1, RNase T1, proteinase K and the restriction endonucleases BamHI and XhoI were obtaiend from Sigma (St. Louis, MO, USA). All the reagents used were of analytical-reagent grade and all solutions were made with sterile distilled water.

Chromatographic conditions

   The DEAE cellulose was pre-cycled before use according to the instructions of the manufacturer [9]. Dried DEAE cellulose (10 g) was first suspended in 0.5 M hydrochloric acid, for 30 min, then subjected to several washes with water, to adjust the solution to pH 7.0 and to remove the fines by decanting. The DEAE cellulose was treated with 0.5 M sodium hydroxide and again washed to pH 7.0. The DEAE cellulose was stored in buffer A (0.2 M sodium chloride, 0.05 M Tris–HCl, pH 7.5) at 4°C.

   About 5 ml of the DEAE cellulose were packed into a 20-ml syringe plugged with sterile glass wool and equilibrated with buffer A.

Preparation of chloroplasts

   Chloroplasts and chloroplast nucleic acids were prepared by a previously described procedure [10] with some modifications. The following steps were performed at 4°C. Briefly, 1 kg of bean leaves was homogenised in a Waring blender with 2000 ml of a solution containing 5 mM Tris–HCl (pH 8.0), 25 mM ethylenediaminetetraacetic acid (EDTA), 1.25 M sodium chloride, 0.01% bovine serum albumin (BSA) and 7 mM 2-mercaptoethanol. The extract was first filtered through one layer of cheesecloth followed by a 50-μm nylon mesh and finally through a 25-μm nylon mesh (Lockertex, Warrington, UK). After centrifuging for 1 min at 3000 g, the chloroplasts were recovered in pellet form and stored at -20°C or used immediately for DNA extraction.

Preparation of chloroplast nucleic acids

   About 10 g of chloroplasts were suspended in 100 ml of a solution of 10 mM Tris–HCl (pH 8.0), 10 mM sodium chloride, 1% sodium dodecyl sulphate and 5 mg of proteinase K. The mixture was incubated at 37°C for 12 h.

   The suspension was extracted with an equal volume of phenol saturated with $T_{10}E_{10}$ buffer [10 mM Tris–HCl (pH 8.0), 10 mM EDTA] and the nucleic acids were recovered in the aqueous phase after centrifuging for 20 min at 12 000 g. A one tenth volume of 3 M sodium acetate (pH 5.4) was added to the aqueous phase and the nucleic acids were precipitated with two volumes of cold 95% ethanol.

   The precipitated nucleic acids were recovered in pellet form after centrifuging for 10 min at 10 000 g, resuspended in 2 ml of $T_{10}E_1$ buffer [10 mM Tris–HCl (pH 7.5), 1 mM EDTA] and dialysed.

After dialysis against water for 24 h at 4°C, a one tenth volume of 3 M sodium acetate (pH 5.4) was added to the nucleic acid solution and the nucleic acids were reprecipitated with two volumes of ethanol. After centrifugation, the pellet was re-suspended in 2 ml of buffer A.

Chromatography of chloroplast nucleic acids

The nucleic acid solution, containing 50 mg of nucleic acids, was loaded onto the DEAE cellulose column and the column was washed with buffer A to remove unbound material which was collected in 2-ml fractions. The UV absorption at 260 nm (A_{260}) of each fraction was measured; peak I was observed, and elution continued until all A_{260} absorbing material had been removed from the column, which required 24 ml of buffer A.

The column-bound nucleic acids were eluted with buffer B [1.0 M sodium chloride, 0.05 M Tris–HCl (pH 7.5)]. A second A_{260} peak (peak II) was obtained and elution continued until all A_{260} absorbing material had been removed from the column.

The fractions under peaks I and II were pooled, giving volumes of 8 and 14 ml, respectively. Each set of pooled fractions was precipitated with two volumes of ethanol. Each precipitate was washed twice with 70% ethanol to remove NaCl, and the air-dried pellet was dissolved in 0.5 ml of $T_{10}E_1$ buffer (pH 7.5).

The nucleic acids recovered from the DEAE cellulose column were initially characterised by recording the absorption spectrum in the range 220–300 nm on a Shimadzu UV-VIS recording spectrophotometer (Model UV-160A).

Nucleic acid analysis

Both nucleic acids were treated with either DNase 1, RNase T1 or proteinase K. To three Eppendorf tubes the following reagents were added: 10 μl of one of the nucleic acid samples, 2 μl of a 10 × digestion buffer (100 mM Tris–HCl pH 7.5, 100 mM magnesium chloride, 100 μg/ml BSA, 1000 mM sodium chloride) and 6 μl of sterile distilled water. Into tube 1 were added 2 μl of DNase 1 (0.1 μg/μl), tube 2 2 μl of RNase T1 (1U/μl) and tube 3 2 μl of proteinase K (0.05 μg/μl). Tube 1 was incubated at 0°C while tubes 2 and 3 were incubated at 37°C. The tubes were all incubated for 2 h.

DNA was digested with restriction endonucleases. The reaction medium contained 10 μl of cpDNA (0.5 μg/μl), 5 μl of the 10 × digestion buffer, 1 U of either BamHI or XhoI enzyme per μg of cpDNA and sterile distilled water to bring the volume to 50 μl. After incubating the mixture for 3 h at 37°C the DNA fragments were separated by gel electrophoresis in 1% agarose. The bands were visualised after ethidium bromide staining.

RESULTS AND DISCUSSION

The chloroplast extract purified on a DEAE cellulose column contained two different types of nucleic acids, as shown by their chromatographic migration (Fig. 1).

The identification of chloroplast nucleic acid components was obtained after analysis of the nucleic acids peaks and their fractionation on agarose gel electrophoresis. Upon electrophoresis, the large DNA molecules moved more slowly than the
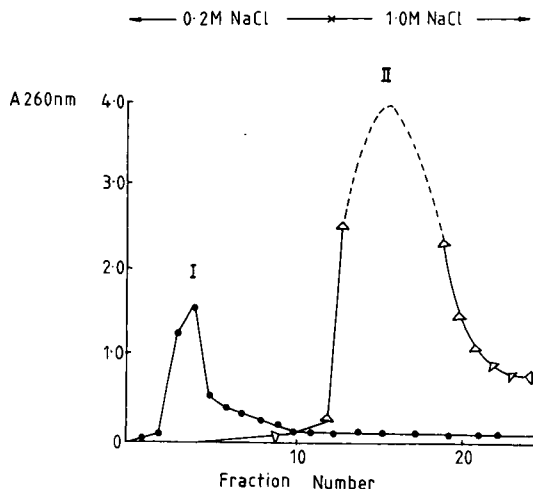
Fig. 1. Elution profile of chloroplast nucleic acids on DEAE cellulose column chromatography. Each fraction has a volume of 2 ml. Peak I is DNA and peak II RNA.

smaller RNA molecules. This indicated that peak I contained only intact DNA while peak II contained RNA and degraded DNA. The RNA, which are tRNA molecules, may be easily purified by polyacrylamide gel electrophoresis with the removal of the degraded DNA fragments [7,8].

The DNA was not tightly bound to DEAE cellulose and was eluted with the 0.2 M sodium chloride buffer (Fig. 1, peak I). The more tightly bound RNA was eluted with the 1.0 M sodium chloride buffer (Fig. 1, peak II). The DNA and RNA peaks were confirmed by degradation with DNase 1 and RNase T1, respectively. They were not affected by proteinase K treatment.

The sum of the molecular weights of the DNA fragments after XhoI digestion was estimated to be 150 kbp. This value is identical to that reported for common bean chloroplast DNA on a caesium chloride gradient [8,11].

In this work a yield of 50 mg of chloroplast nucleic acids was obtained from 1 kg of common bean leaves. The chloroplast nucleic acids were separated into their two major types, DNA (5 mg) and RNA (30 mg), by DEAE cellulose column chromatography. In deriving these estimates of yield, the relationship whereby one absorbance unit at 260 nm is equivalent to 50 $\mu g/ml$ DNA and 40 $\mu g/ml$ RNA was used [2,6]. The A_{260}/A_{280} ratio was about 1.80. This indicates that the recovered DNA and RNA are reasonably pure.

This separation technique has the advantages of being fast, cheap and easy to perform. The DNA recovery is five times higher than that reported for the same weight of higher plant leaves [10].

ACKNOWLEDGEMENTS

REFERENCES

1 H. J. Bohnert, E. J. Crouse and J. M. Schmitt, in B. Parthier and D. Boulter (Editors), *Encyclopedia of Plant Physiology, New Series*, Vol. 14B, Springer-Verlag, Berlin, 1982, pp. 475–530.
2 T. Maniatis, E. F. Fritsh and J. Sambrook, *Molecular Cloning*, Cold Spring Harbor Laboratory, Cold Spring Harbor, CA, 1982.
3 R. Hecker, M. Colpan and D. Riesner, *J. Chromatogr.*, 326 (1985) 251–261.
4 M. V. Olson, *Biotechniques*, Jan/Feb (1985) 8.
5 S. A. Benson and R. K. Taylor, *Biotechniques*, May/June (1984) 126–127.
6 D. T. Plummer, *An Introduction to Practical Biochemistry*, McGraw-Hill, Maidenhead, 1987.
7 G. Burkard, A. Steinmetz, M. Keller, M. Mubumbila, E. J. Crouse and J.-H. Weil, in M. Edelman, R. B. Hallick and N. H. Chua (Editors), *Methods in Chloroplast Molecular Biology*, Elsevier, Amsterdam, 1982, pp. 347–357.
8 M. Mubumbila, K. H. J. Gordon, E. J. Crouse, G. Burkard and J.-H. Weil, *Gene*, 21 (1983) 257–266.
9 *Improved Techniques with Advanced Ion Exchange Celluloses, Publication*, 607 Whatman, Springfield Mill, 1989, p. 5.
10 R. G. Herrmann, H. J. Bohnert, K. V. Kowallik and J. M. Schmitt, *Biochim. Biophys. Acta*, 378 (1975) 305–317.
11 J. D. Palmer, *Nature (London)*, 301 (1983) 92–93.

CHROM. 23 503

Short Communication

Immobilization method for polyethylene glycol using a cross-linking co-agent

YOSHIKUNI YAKABE, YOSHIHISA SUDOH and YASUYO TAKAHATA*

Department of Research and Development, Chemicals Inspection and Testing Institute, 1-1, Higashimukoji-ma 4-chome, Sumida-ku, Tokyo 131 (Japan)

ABSTRACT

A cross-linking co-agent was used in the immobilization of polyethylene glycol (PEG) 20M peroxide to produce a capillary column for gas chromatography. The co-agent promoted the immobilization of PEG 20M and the concentrations of peroxide necessary to achieve over 80% non-extractability decreased from 15% for PEG 20M immobilization by the peroxide alone to 5 and 3% for PEG 20M immobilization using 3 and 5% of the co-agent in PEG 20M, respectively. The use of the co-agent suppressed the decrease in column efficiency and the increase in column polarity which occur in immobilization using the peroxide alon. The co-agent also increased the thermostability of the column. The mechanism of the participation of the co-agent in the immobilization of PEG 20M is discussed.

INTRODUCTION

The immobilization of the stationary phase is an important process in the preparation of capillary columns for gas chromatography as it makes the stationary phase film both stable and durable [1].

Methyl silicone stationary phases such as SE-30 can easily be immobilized by cross-linking the methyl side-chains of the stationary phase with peroxides such as dicumyl peroxide (DCUP). However, polyethylene glycol (PEG), which is an important stationary phase owing to its unique separation characteristics, is not easy to immobilize with peroxide alone [2–8].

Bystricky [8] reported that with 20% (w/w) of the DCUP of PEG 20M, only 65% of Carbowax 20M could be immobilized on a glass capillary column under optimum conditions. Double the amount of peroxide and a 20°C higher temperature are necessary to achieve immobilization greater than 90°C. Several alternative immobilization methods specific to PEG have been developed [4,7].

In the peroxide cross-linking of rubber or plastics, a cross-linking co-agent is

used to enhance the extent of cross-linking and consequently to improve the phys-icochemical properties, such as thermostability, of the rubber or plastics.

In this study, the use of a cross-linking co-agent in the immobilization of PEG 20M on a glass capillary column was investigated. Triallyl isocyanurate (TAIC) was used as the cross-linking co-agent because it is typically used in the peroxide cross-linking of rubber and plastics [10].

EXPERIMENTAL

PEG 20M was purchased from Gaskuro Kogyo. DCUP was kindly supplied by Nippon Oil and Fats. TAIC of extra pure grade was purchased from Tokyo Kasei Kogyo and used without further purification. All other chemicals were of guaranteed reagent grade and were used without further purification.

Capillaries of 1.2 mm I.D. were drawn from Pyrex glass tubes with a Shimadzu GDM-18 glass drawing machine, which was partially modified. This inner diameter was chosen as it allows the column to be easily attached to a conventional gas chromatograph for packed columns without any alterations.

After the capillary had been treated with 6 M hydrochloric acid for 1 h and rinsed successively with water and methanol, it was statically coated with a solution of PEG 20M in methylene chloride containing DCUP and TAIC in various amounts. The column was flused with nitrogen gas for 1 h, sealed at both ends and was then cured at 160°C for 1 h. After cutting both ends of the column to give a length of 40 m, the fused-silica capillaries (30 cm $\times$ 250 μm) were attached to both ends of the column through stainless-steel connectors and the column was mounted on a gas chromatograph through the ends of other fused-silica capillaries. The column was then conditioned at 180°C for 1 h and its performance was tested with standard chemicals. The column was rinsed with methylene chloride and then the column performance was tested again to determine the non-extractability of PEG 20M. The column temperature was then raised to 250°C at a rate of 5°C/min and was held at 250°C for 84 h; the performance was tested to determine the thermostability of the column.

The non-extractability and thermostability of the PEG-20M film were estimated from the changes in capacity factor of the naphthalene peak after rinsing with methylene chloride and heating the column at 250°C for 84 h, respectively.

The Kováts retention indices for benzene, butan-1-ol, pentan-2-one, nitropropane and pyridine were measured at 80°C and were summed to estimate the polarity of the column.

RESULTS AND DISCUSSION

Fig. 1 shows the variation in extraction with DCUP concentration for the column immobilized with DCUP alone and with TAIC concentration for the columns immobilized with both DCUP and TAIC. The non-extractability increased with increasing concentration of DCUP, and a DCUP concentration greater than 15% of the weight of PEG 20M was required to achieve more than 80% immobilization with DCUP alone.

The addition of TAIC greatly enhanced the immobilization of PEG 20M on the
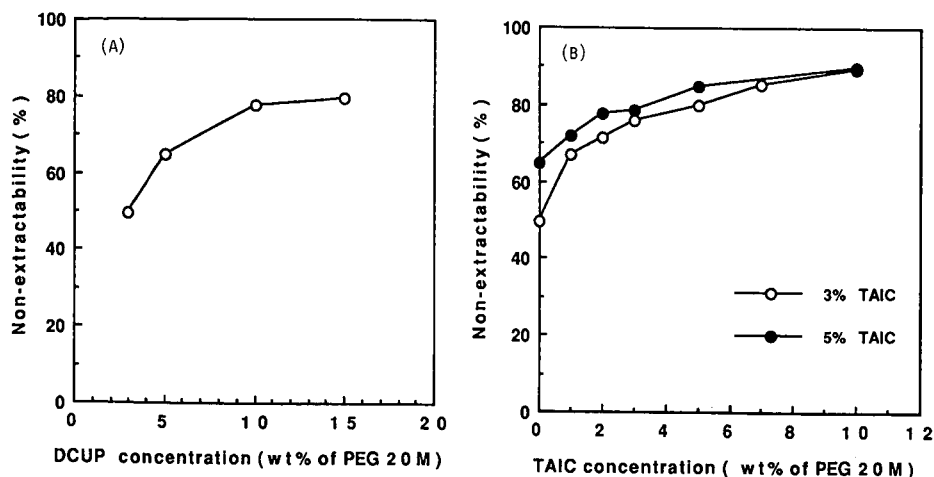
Fig. 1. Variation of non-extractability (A) with DCUP concentration for the column immobilized with (A) DCUP alone and (B) with TAIC concentration for the columns immobilized using both TAIC and DCUP. Concentrations are expressed as percentage of weight of PEG 20M.

glass capillary. For example, the addition of only 1% (w/w) TAIC increased the non-extractability from 49.4 to 67.1% with 3% (w/w) DCUP. The non-extractability increased with increasing concentration of TAIC, but the addition of an excess of TAIC (10% of the weight of PEG 20M) resulted in the tailing of all peaks tested. On the addition of 3 and 5% TAIC, the DCUP concentration required to achieve more than 80% immobilization was lowered from 15 to 5 and 3% of the weight of PEG 20M, respectively.

To examine the effect of the cross-linking co-agent on column performance, coating efficiency and thermostability, the Kováts retention indices were measured for columns with similar extractabilities prepared under three different conditions and a column which had not been immobilized.

Fig. 2 shows the Van Deemter curves for the naphthalene peak of these columns and Table I compares the performances of these columns. The optimum flow-

TABLE I

COMPARISON OF THE PERFORMANCES OF SIMILAR COLUMNS PREPARED UNDER VARIOUS CONDITIONS

Column No.	Curing conditions (%)		Non-extractability (%)	Coating efficiency (%)	$\Delta\Sigma RI^a$	Δk^b (%)
	DCUP	TAIC				
1	–	–	–	82.8	–	–
2	15	–	79.6	67.5	65	10.2
3	3	5	80.0	74.9	27	6.5
4	5	5	84.8	71.5	37	5.4

[a] $\Delta\Sigma RI$ = Deviation of the sum of the Kováts retention indices for five reference compounds from that of a non-immobilized column.

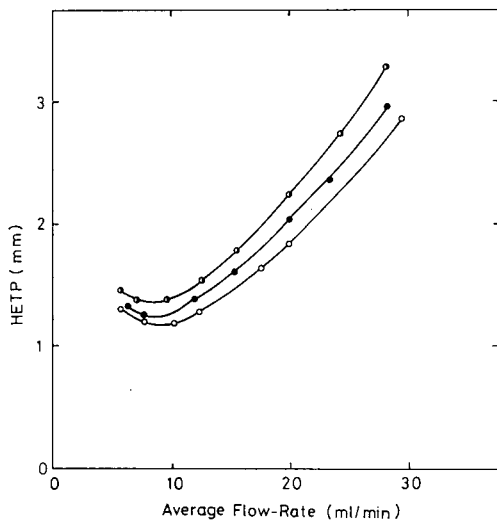[b] Δk = Percentage decrease of the capacity factor for naphthalene after heating at 250°C for 84 h.

Fig. 2. Van Deemter curves of the naphthalene peak at 140°C for columns prepared under various conditions. Film thickness = 1 μm; length = 40 m. (○) Non-immobilized column; (◑) column immobilized with 15% DCUP; (●) column immobilized with 3% DCUP and 5% TAIC.
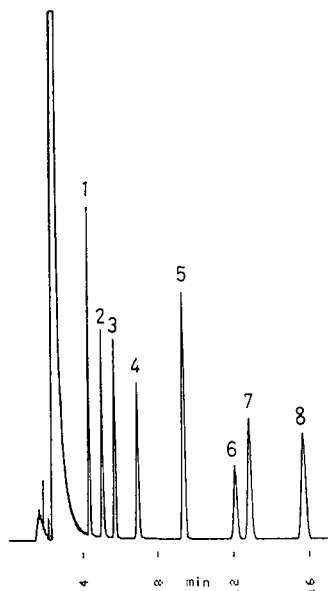

Fig. 3. Gas chromatogram of a test mixture on the column immobilized with 3% DCUP and 5% TAIC (expressed as percentage of weight of PEG 20M). Film thickness = 1 μm; length = 40 m; column temperature = 140°C; flow-rate = 20 ml/min. Peaks: 1 = pentadecane; 2 = octan-1-ol; 3 = methylcaprate; 4 = dicyclohexylamine; 5 = naphthalene; 6 = caproic acid; 7 = 2,6-dimethylaniline; 8 = 2,6-dimethylphenol.

rate was about 8 ml/min for the 1.2 mm I.D. column. The column efficiency at the optimum flow-rate decreased with the immobilization of the stationary phase, but the magnitude of the decrease was smaller for the columns immobilized using TAIC than for those immobilized using DCUP alone.

The column was heated at 250°C for 84 h and the change in capacity factor for the naphthalene peak was measured to evaluate the thermostability of the column. For the non-immobilized column, the stationary phase formed droplets during heating and the column efficiency decreased significantly. For the immobilized columns, no changes in the appearance of the stationary phase, peak shapes of standard chemicals nor column efficiency were observed, except for the decrease of the capacity factor. The use of TAIC reduced the decrease in the capacity factor for the naphthalene peak on heating at 250°C for 84 h to about 60% of that for the column immobilized with DCUP alone. This corresponds to the extension of the column lifetime from 540 to 940 h during one half-life.

The use of TAIC also depressed the increase in column polarity, which was frequently observed in the immobilization of PEG with peroxide and caused changes in the separation pattern of complex mixtures such as polyunsaturated fatty acids [4,5,9]. Table I shows the deviations of the sum of Kováts retention indices for five reference compounds for columns with very similar non-extractabilities from that of a non-immobilized column. The deviations for the columns immobilized using both TAIC and DCUP were less than 50% of the value for the column immobilized with DCUP alone.

Fig. 3 shows a chromatogram of the test mixture containing various types of compounds. All the peaks were symmetrical and no tailing was observed for the peaks of acidic or basic compounds, which indicates that the column was deactivated satisfactorily.

In conclusion, the use of a cross-linking co-agent in the immobilization of PEG 20M increases the efficiency and thermostability of the column and decreases the change in column polarity caused by the immobilization. The column is deactivated satisfactorily and can be used for the determination of various types of compounds.

REFERENCES

1 L. Blomberg, J. Buijten, K. Markides and T. Wännman, *J. Chromatogr.*, 279 (1983) 9–20.
2 R. C. M. de Nijs and J. de Zeeuw, *J. High Resolut. Chromatogr. Chromatogr. Commun.*, 5 (1982) 501–503.
3 H. Traitler, L. Kolarovic and A. Sorio, *J. Chromatogr.*, 279 (1983) 69–73.
4 J. Buijten, L. Blomberg, K. Markides and T. Wännman, *J. Chromatogr.*, 268 (1983) 387–394.
5 V. Martinez de la Gándara, J. Sanz and I. Martinez-Castro, *J. High Resolut. Chromatogr. Chromatogr. Commun.*, 7 (1984) 44–45.
6 M. V. Russo, G. C. Goretti and A. Liberti, *J. High Resolut. Chromatogr. Chromatogr. Commun.*, 8 (1985) 535–538.
7 M. Horka, V. Kahle, K. Janak and K. Tesařik, *J. High Resolut. Chromatogr. Chromatogr. Commun.*, 8 (1985) 259–263.
8 L. Bystricky, *J. High Resolut. Chromatogr. Chromatogr. Commun.*, 9 (1986) 240–241.
9 J. K. G. Kramer, R. C. Fouchard and K. J. Jenkins, *J. Chromatogr. Sci.*, 23 (1985) 54–56.
10 W. Hofmann, *Vulcanisation and Vulcanising Agents*, Maclaren, London, 1967.

Short Communication

Rapid identification of microbial starch degradation products from a complex nutrient medium by a thin-layer chromatographic method

LJUBICA VRBAŠKI* and ŽIKA LEPOJEVIĆ
Department of Pharmaceutical Technology, Faculty of Technology, 21000 Novi Sad (Yugoslavia)
(First received January 3rd, 1991; revised manuscript received May 21st, 1991)

ABSTRACT

An improved thin-layer chromatographic method has been established for the rapid identification of microbial starch degradation products from a complex nutrient medium. The method is based on spotting 10 μl of a diluted liquid starch medium containing microorganism cells on high-performance liquid chromatography plates precoated with silica gel 60 with a concentration zone for nano-thin-layer chromatography. The mobile phase is chloroform–glacial acetic acid–water (3:6:1, v/v/v). After the first development the plates were dried and again developed. The separated carbohydrates were detected with a 50% (w/v) solution of sulphuric acid in ethanol after heating at 150°C for 10 min. The duration of the assay was less than 2 h.

INTRODUCTION

With the progress of biotechnology it becomes important to have an effective method for screening strains of microorganisms with desired characteristics. Many of the problems associated with these studies arise from the difficulty of obtaining rapid, accurate and reproducible measurements, particularly from complex media. It is known that nutrient media contain a large number of organic and inorganic compounds of low, intermediate and high molecular mass that can interfere with each other and mask the desired metabolite. In such circumstances a variety of methods have been used for sample purification.

The microbiological problem of screening starch-positive strains of microorganisms requires the development of an adequate methodology, although numerous assays for the measurement of starch degradation products exists and the modern instrumental methods of chemical analysis are used. These methods are often technically difficult, time-consuming and do not permit use of a small volume of samples containing the microorganism cells.

The determination of products of metabolically degraded starch is of interest for

many reasons, especially in monitoring the action under usual and unusual conditions of strains of microorganisms that can hydrolyse starch. A microbiological test for starch hydrolysis is afforded by flooding the plate with dilute (Lugol's) iodine after inoculation and growth. Absence of the bluish-purple colour characteristic of the starch–iodine complex indicates hydrolysis. For different microorganism strains the area of hydrolysis is of different width and colour. Problems occur when it is necessary to identify and determine the products of metabolically degraded starch and their relative proportions. It is generally agreed that thin-layer chromatography (TLC) offers the best potential for application in this microbiological analysis. Advantages include easy manipulation, shorter analysis times and use of small volumes of sample.

Over the past years a very large number of articles have been published on the chromatography of carbohydrates, among them two recent reviews [1,2]. However, from the microbiological point of view there are more articles dealing with separation of individual carbohydrates from model solutions than from complex culture media.

The method described in the present report is an adaptation of the procedure previously described [3] for the chromatographic separation of carbohydrates as possible products of starch metabolism. This paper [3] also describes the separation of individual carbohydrates from model solution. The principal advantage of the present procedure over those previously described is rapid identification of microbial starch degradation products together with a complex nutrient medium containing the cells of microorganisms. In addition, it is possible to obtain the spectra of carbohydrates after enzymatic hydrolysis of starch.

EXPERIMENTAL

Chemicals
All chemicals were of analytical-reagent grade. Glucose, soluble starch, acetone, chloroform and glacial acetic acid were purchased from Kemika (Zagreb, Yugoslavia) and maltose, raffinose and trehalose from Merck (Darmstadt, Germany). α-Cyclodextrin was acquired from Fluka (Buchs, Switzerland) and β-cyclodextrin from Chinoin (Budapest, Hungary).

Standards
The following standards were used: 1 mg/ml glucose, maltose, raffinose, trehalose, α- and β-cyclodextrin and soluble starch, separately and in a mixture containing 1 mg/ml of each.

Microorganisms
For this study four strains of bacteria were used as producers of various width and colour of zone hydrolysis on starch agar media, independently of their taxonomic status.

Medium and culture condition
One loopful of physiologically young cells was inoculated into a 100-ml Erlenmeyer flask containing 30 ml of nutrient broth: peptone 1-Torlak, 15 g/l; meat extract-Torlak, 3 g/l; sodium chloride, 5 g/l; dipotassium hydrogenphosphate 0.3 g/l (Torlak, Belgrade, Yugoslavia) with 10 g/l soluble starch, cultured at 25°C for 2 days.

Sample preparation

In the first experiment culture broth samples were deproteinized by adding 4 ml of acetone to 2 ml of broth. The mixture was held in the cold ($4 \pm 1°C$) for 24 h, and then centrifuged for 10 min (1600 g). The supernatant was evaporated *in vacuo* (27°C). The remaining solid was redissolved in 2 ml of double-distilled water and applied as sample. In the second experiment culture broth containing cells of microorganisms was diluted with double-distilled water in the ratio 1:1.

Thin-layer chromatography

High-performance thin-layer chromatographic (HPTLC) plates precoated with silica gel 60 (10 × 20 cm) with a concentration zone (2.5 × 20 cm) for nano-TLC (Merck) were used. From the prepared samples and standards, 10 μl of each were spotted onto the plate. After the samples had been added and dried, the plate was placed onto a chromatographic chamber (Desaga, Heidelberg, Germany) with 70 ml of chloroform–glacial acetic acid–water (3:6:1, v/v/v) in the bottom. The chamber was covered with a lid, and solvent allowed to move up the plate. When the solvent reached the top, the plate was removed and dried for 10 min under hot air. The plate was returned to the chamber and ascent made on fresh solvent of the same composition. The dried plate was sprayed with a 50% (w/v) solution of sulphuric acid in ethanol and heated at 105°C, which allowed the coloured spots to develop in about 10 min.

RESULTS AND DISCUSSION

It is accepted [4–7] that proteins in nutritive media interfere with direct determination of carbohydrate. Therefore the optimal conditions for their elimination were investigated, the best results being obtained under the conditions described above. Results given by this method are shown in Fig. 1.

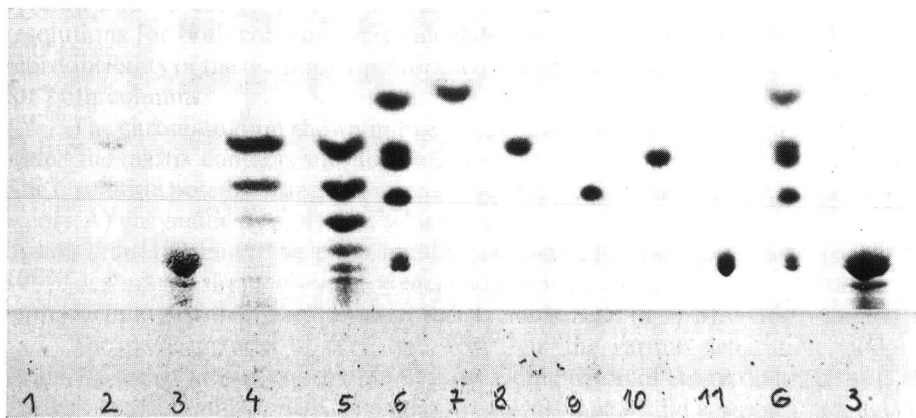Separation of carbohydrates from microbial starch degradation products

Fig. 1. TLC of carbohydrates after deproteinization of the starch nutrient medium. Spots: 1 = nutrient medium; 2 = strain of bacterium a_5; 3 = strain of bacterium a_6; 4 = strain of bacterium a_{12}; 5 = strain of bacterium a_{952}; 6 = mixture of carbohydrate, 10 μl; 7 = glucose, 10 μl; 8 = maltose, 10 μl; 9 = raffinose, 10 μl; 10 = trehalose, 10 μl; 11 = α- + β-cyclodextrin, 10 μl. For conditions see Experimental section.
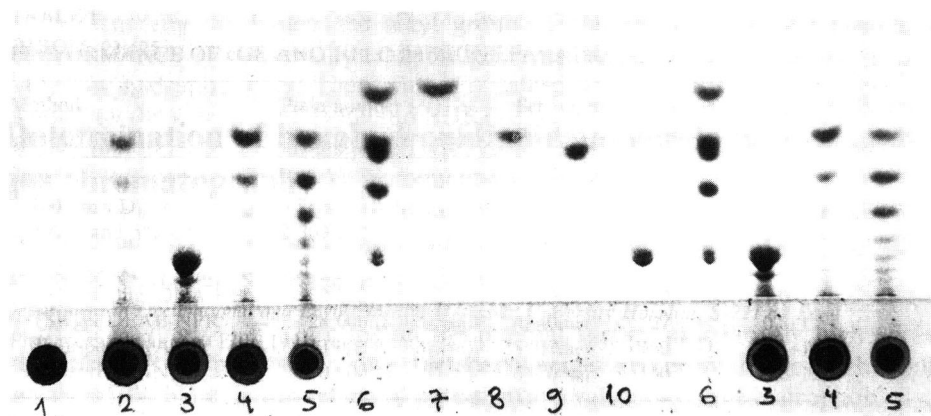
Fig. 2. TLC of carbohydrates a diluted starch medium. Spots: 1 = nutrient medium; 2 = strain of bacterium a_5; 3 = strain of bacterium a_6; 4 = strain of bacterium a_{12}; 5 = strain of bacterium a_{952}; 6 = mixture of carbohydrate, 10 μl; 7 = glucose, 10 μl; 8 = maltose, 10 μl; 9 = trehalose, 10 μl; 10 = α- + β-cyclodextrin, 10 μl. For conditions see Experimental section.

proved to be comparable to that of the components of the standard mixture-Maltotriose in standard mixture was substituted by raffinose, as, according to the experimental conditions, they have the same R_F values [3]. The purification period is too long, so that a relatively small number of samples could be analysed in a normal working day. This initiated the idea of spotting the plates with nutritive media that contained the microorganism cells. The first results indicated that the media should be diluted, the best dilution being in the ratio 1:1. Results are shown in Fig. 2. In this case raffinose was not used as a standard.

When the results obtained after deproteinization (Fig. 1) are compared with the results obtained on the plate with cell sample (Fig. 2), it can be seen that the spots clearer in the second case, that is when sample contains the cells. It seems that some loss occurred in the course of purification.

The advantage of this method, in our opinion, is that the spots of carbohydrates from the nutritive media containing bacteria cells are clear and distinctly separated (Fig. 2). It is quite easy to determine the number of starch metabolic products and thus to characterize the particular strain. The results are reproducible when conducted

TABLE I

R_F VALUES OF CARBOHYDRATES ON HPTLC PLATES ($n = 5$)

Carbohydrate	$R_F \times 100$
Glucose	62
Maltose	51
Trehalose	49
Raffinose	39
α-Cyclodextrin	24
β-Cyclodextrin	23

repeatedly under the same experimental conditions. A particular strain will give the same number of spots with the same R_F values. This fact has not yet been reported in the accessible literature.

As from the aspect of biotechnology it is extremely important to obtain a very large quantity of material, the sensitivity of the proposed method was not important in the present investigation.

R_F values for the pure substances used as standards for products of metabolically degraded starch are given in Table I. R_F values were determined from the arithmetic means of five runs.

CONCLUSION

Advantages of the method described in this paper include the simplicity of the procedure, the short chromatographic run time and full reproducibility for small samples. The assay does not require time-consuming purification or extraction procedures. The method can also be recommended as a valuable screening procedure for detection of desired microbial starch degradation products from a complex nutrient medium.

ACKNOWLEDGEMENT

REFERENCES

1 A. M. Siouffi, E. Mincsovics and E. Tyihak, *J. Chromatogr.*, 492 (1989) 471.
2 S. C. Churms, *J. Chromatogr.*, 500 (1990) 555.
3 Lj. Vrbaški and Ž. Lepojević, *Zb. Prir. Nauk Matica Srpska*, 77 (1989) 129.
4 G. Zweig and J. Sherma (Editors), *Handbook of Chromatography*, Vol. 2, CRC Press, Cleveland, OH, 1972, p. 204.
5 J. A. DePinto and L. L. Campbell, *Science*, 146 (1964) 1064.
6 J. A. DePinto and L. L. Campbell, *Arch. Biochem. Biophys.*, 125 (1964) 1064.
7 R. D. McDowall, *J. Chromatogr.*, 492 (1989) 3.

PUBLICATION SCHEDULE FOR 1991

Journal of Chromatography and Journal of Chromatography, Biomedical Applications

MONTH	D 1990– M 1991	J	J	A	S	O	N	D
Journal of Chromatography	Vols. 535–545/1	545/2 546/1 + 2 547/1 + 2	548/1 + 2 549/1 + 2 550/1 + 2	552/1 + 2 553/1 + 2 554/1 + 2 555/1 + 2	556/1 + 2 557/1 + 2 558/1	558/2 559/1 + 2		
Cumulative Indexes, Vols. 501–550				551/1 + 2				
Bibliography Section	560/1	560/2			561/1			561/2
Biomedical Applications	Vols. 562–566	567/1	567/2 568/1	568/2	569/1 + 2 570/1	570/2	571/1 + 2	572/1 + 2

INFORMATION FOR AUTHORS

(Detailed *Instructions to Authors* were published in Vol. 522, pp. 351–354. A free reprint can be obtained by application to the publisher, Elsevier Science Publishers B.V., P.O. Box 330, 1000 AH Amsterdam, The Netherlands.)

Types of Contributions. The following types of papers are published in the *Journal of Chromatography* and the section on *Biomedical Applications:* Regular research papers (Full-length papers), Review articles and Short Communications. Short Communications are usually descriptions of short investigations, or they can report minor technical improvements of previously published procedures; they reflect the same quality of research as Full-length papers, but should preferably not exceed six printed pages. For Review articles, see inside front cover under Submission of Papers.

Submission. Every paper must be accompanied by a letter from the senior author, stating that he/she is submitting the paper for publication in the *Journal of Chromatography*.

Manuscripts. Manuscripts should be typed in double spacing on consecutively numbered pages of uniform size. The manuscript should be preceded by a sheet of manuscript paper carrying the title of the paper and the name and full postal address of the person to whom the proofs are to be sent. As a rule, papers should be divided into sections, headed by a caption (*e.g.*, Abstract, Introduction, Experimental, Results, Discussion, etc.). All illustrations, photographs, tables, etc., should be on separate sheets.

Introduction. Every paper must have a concise introduction mentioning what has been done before on the topic described, and stating clearly what is new in the paper now submitted.

Abstract. All articles should have an abstract of 50–100 words which clearly and briefly indicates what is new, different and significant.

Illustrations. The figures should be submitted in a form suitable for reproduction, drawn in Indian ink on drawing or tracing paper. Each illustration should have a legend, all the *legends* being typed (with double spacing) together on a *separate sheet*. If structures are given in the text, the original drawings should be supplied. Coloured illustrations are reproduced at the author's expense, the cost being determined by the number of pages and by the number of colours needed. The written permission of the author and publisher must be obtained for the use of any figure already published. Its source must be indicated in the legend.

References. References should be numbered in the order in which they are cited in the text, and listed in numerical sequence on a separate sheet at the end of the article. Please check a recent issue for the layout of the reference list. Abbreviations for the titles of journals should follow the system used by *Chemical Abstracts*. Articles not yet published should be given as "in press" (journal should be specified), "submitted for publication" (journal should be specified), "in preparation" or "personal communication".

Dispatch. Before sending the manuscript to the Editor please check that the envelope contains four copies of the paper complete with references, legends and figures. One of the sets of figures must be the originals suitable for direct reproduction. Please also ensure that permission to publish has been obtained from your institute.
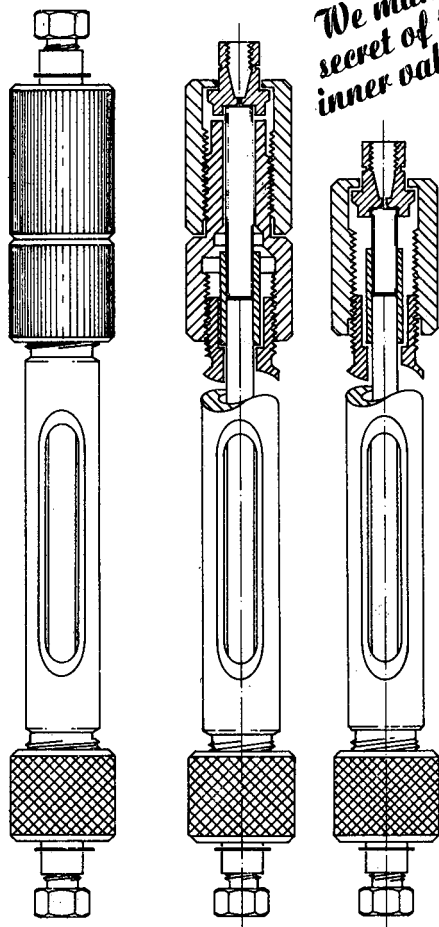
Proofs. One set of proofs will be sent to the author to be carefully checked for printer's errors. Corrections must be restricted to instances in which the proof is at variance with the manuscript. "Extra corrections" will be inserted at the author's expense.

Reprints. Fifty reprints of Full-length papers and Short Communications will be supplied free of charge. Additional reprints can be ordered by the authors. An order form containing price quotations will be sent to the authors together with the proofs of their article.

Advertisements. Advertisement rates are available from the publisher on request. The Editors of the journal accept no responsibility for the contents of the advertisements.